SYNTHETIC AND MECHANISTIC STRATEGIES TO ACHIEVE UNCONVENTIONAL SITE-SELECTIVITY IN CROSS-COUPLINGS OF DIHALO-HETEROARENES

by

Jacob Patrick Norman

A dissertation submitted in partial fulfillment
of the requirements for the degree

of

Doctor of Philosophy

in

Chemistry

MONTANA STATE UNIVERSITY
Bozeman, Montana

May 2024

©COPYRIGHT

by

Jacob Patrick Norman

2024

All Rights Reserved

DEDICATION

I dedicate this work to Wyatt Josiah Norman, my beloved brother (January 4, 1998—November 6, 2020). My brother loved mathematics, history, philosophy, theology, and the natural sciences. He was a renaissance man who exemplified scholarship. His many wholesome attributes, including his humor, playfulness, and creativity are dearly missed. May this dissertation serve as a living tribute to his memory.

Although it was hard-won, I would not hesitate to trade my PhD and all it has taught me for another day with you.

ACKNOWLEDGEMENTS

I owe much of my success in graduate school to the community of professionals I have been surrounded with and their spirit of cooperation. I must thank Nathaniel Larson who has contributed enormously to the present work, and who ranks among the most reliable and intelligent individuals I have known. I thank other members and alumni of the Neufeldt Group, including Emily Elias (née Reeves) and Steven Rehbein who provided excellent training in the laboratory, Matthew Kania, Oliver Jackson, Aaron Morrenzin, Emily Entz, John Russell, Grace Ibsen, Albert Reyes, Collin Stein, Vitor H. Menezes da Silva, Olivia Bauman, Amberlie Kuglin, and Marie Dominick for lending their insight, ensuring the smooth operation of our lab, and abiding my particular brand of madness for many years. I am grateful to my committee members, Mary Cloninger, Thomas Livinghouse, Michael Mock, and Garrett Moraski, whose words of encouragement have propped me up and whose expertise in chemistry has dispensed with many problems which would have been difficult to solve alone. I thank Brian Tripet for his assistance with NMR, and Doreen Brown, a steadfast ally who has done so much to ease my journey through the PhD program. I express my deep gratitude to Sharon Neufeldt, my advisor and mentor, who has been a model for excellence in scientific thinking, writing, and presentation. I have been inspired by her unyielding pursuit of perfection in science and her interrogating thought process. As a mentor, she has demanded continuous improvement, yet in five years, I have never found cause to question her compassion or empathy. I am deeply grateful to my grandfather, Merton Norman, for his generous financial support. I thank the NIH, the NSF, and the American taxpayer, whose compulsory support will not be forgotten. Finally, I am eternally grateful to my wife, Autumn Norman, who has sacrificed much and with whom I share this accomplishment.

ABSTRACT

Pd-catalyzed cross-couplings rank among the most powerful methods for constructing substituted biaryls, polyaryls, and heteroarenes. Frequently, di- or polyhalogenated (hetero)arenes are employed as starting materials in cross-couplings to access products with increased structural complexity via multiple cross-coupling or substitution steps. N-heteroarenes bearing multiple reactive handles—such as halides, are of particular interest as starting materials since their cross-coupled products can be medicinally relevant. Non-symmetrical dihalogenated N-heteroarenes typically exhibit a site-selectivity bias for C—X bonds which are adjacent to at least one heteroatom in Pd-catalyzed cross-couplings. However, some Pd catalysts—particularly those with hindered ligands, promote atypical selectivity at distal C—X bonds of 2,X-dichloropyridines and related heterocycles during the selectivity-determining oxidative addition step. This dissertation explores the mechanistic origins of these ligand trends and emphasizes the critical importance of Pd's ligation state—either *mono* (PdL) or *bis* (PdL_2), in controlling the site of oxidative addition. Ligation state is also relevant when selecting for the products of mono- vs difunctionalization in cross-couplings of dihalogenated substrates, since bisligated 14 e^- Pd dissociates quickly from the monofunctionalized intermediate after an initial cross-coupling cycle, whereas monoligated 12 e^- Pd is slow to dissociate and may "ring-walk" to the remaining reactive site(s). Additionally, this dissertation explores alternative methods to access minor regioisomers in cross-couplings of dichloro-azines. One approach involves ligand-free conditions where atypical site-selectivity at dichloropyridines and dichloropyrimidines arises from a change in Pd's speciation from mono- to multinuclearity. Another approach employs a thiolation/Liebeskind-Srogl arylation sequence to achieve site-selectivity which is orthogonal to that of Suzuki-Miyaura couplings.

TABLE OF CONTENTS

1. INTRODUCTION 1

1.1 Fundamentals of Pd-Catalyzed Cross-Couplings 1
1.2 A Dichotomy of Ligands in Pd-Catalyzed Cross-Couplings 3
1.3 Cross-Couplings of (Hetero)arene Electrophiles with Multiple Reactive Sites 8
1.4 Focuses of this Work 15
1.5 References 17

2. UNCONVENTIONAL SITE-SELECTIVITY IN PALLADIUM-CATALYZED CROSS-COUPLINGS OF DICHLOROHETEROARENES UNDER LIGAND-CONTROLLED AND LIGAND-FREE SYSTEMS.

2.1 Author Contributions 21
2.2 Manuscript Information 22
2.3 Abstract 23
2.4 Introduction 24
2.5 Results and Discussion 27
2.6 Conclusion 38
2.7 References 39

3. DIFFERENT OXIDATIVE ADDITION MECHANISMS FOR 12- AND 14-ELECTRON PALLADIUM(0) EXPLAIN LIGAND-CONTROLLED DIVERGENT SITE SELECTIVITY.

3.1 Author Contributions 42
3.2 Manuscript Information 43
3.3 Abstract 44
3.4 Introduction 44
3.5 Results and Discussion 46
3.6 Conclusion 54
3.9 References 56

4. THIOLATION/LIEBESKIND-SROGL COUPLING SEQUENCE ENABLES ATYPICAL SELECTIVITY IN C—C COUPLINGS OF HETEROARYL HALIDES

4.1 Introduction 60
4.2 Diverse Cross-Coupling Conditions Result in C4-Selectivity. 65
4.3. C—S Bond Activation Enables Arylation at C2 68

TABLE OF CONTENTS CONTINUED

4.4 Conclusion 75
4.5 References 77

5. A MECHANISTIC BASIS FOR LIGAND EFFECTS ON PALLADIUM RING-WALKING IN SUZUKI-MIYAURA COUPLINGS

5.1 Introduction 80
5.2 Results and Discussion 84
5.3 Conclusion 97
2.4 References 99

APPENDICES 102

APPENDIX A: SUPPORTING INFORMATION (Chapter 2) 124
APPENDIX B: SUPPORTING INFORMATION (Chapter 3) 191
APPENDIX C: CHAPTER FOUR EXPERIMENTAL 237
APPENDIX D: CHAPTER FIVE EXPERIMENTAL 244
APPENDIX E: SPECTRAL DATA 252

LIST OF TABLES

Table Page

1.1 Carbonylative Amidation of Vinyl Chloride (Nicholas 1987) 5

2.1 Optimization of the Pd/NHC-Catalyzed C4- Selective Suzuki−Miyaura Coupling 28

2.2 Optimization of the Ligand-Free C4-Selective Suzuki Coupling 36

3.1 Evaluation of Monodentate Ligands for the Suzuki—Miyaura Coupling Using $Pd(OAc)_2$ 47

4.1 Evaluation of Site-Selectivity in Pd-Catalyzed Suzuki-Miyaura Couplings of 2,4-Dichloropyrimidine 67

4.2 Selected Entries from the C2-Selective Liebeskind-Srogl Optimization (Series 1) 70

4.3 Selected Entries from the C2-Selective Liebeskind-Srogl Optimization (Series 2) 72

5.1 Difunctionalization of 2,4-Dichloropyridines Correlated with Ligand Sterics, Substrate Sterics, and Substrate Concentration 83

5.2 Effects of Coordinating Additives on Diarylation Selectivity 90

5.3 Effects of Coordinating Aromatic Solvents on Diarylation Selectivity 91

5.4 Effect of Molarity on Diarylation Selectivity 92

5.5 Effects of Precatalyst Identity and Arene Additives 94

LIST OF SCHEMES

Scheme Page

1.1 Seminal Iron-Catalyzed Cross-Coupling Reported by Kochi (1971) 1

1.2 Relationship between a Ligand's Minimum % Buried Volume, Ligation State, and Reactivity 7

1.3 Ligand-Controlled Chemodivergent Suzuki Coupling of a Chloroaryl Triflate (Fu 2000) 9

1.4 (A) Pd-Catalyzed Cross-Coupling of Dihalo-Heteroarenes with Non-Identical Halogens (B) Chemoselective Strategies are Limited by the Cost of Starting Materials 11

1.5 Ligation State-Controlled Regiodivergent Cross-Couplings of 2,X-Dichloroazines 15

1.6 C2-Arylation of 2,4-Dichloropyrimidine via a C2-Sective Thiolation/C—S Bond Activation Sequence 16

1.7 Ligand-Controlled Selectivity for Mono- vs. Difunctionalization of Dichloro-(hetero)arenes 16

2.1 Graphical abstract for the *J. Org. Chem.* manuscript 23

2.2 Ligand Effects on the Cross-Coupling Selectivity of 2,4-Dichloropyridines 25

2.3 Scope of C4-Selective Suzuki−Miyaura Cross-Couplings Catalyzed by Pd/IPr 30

2.4 C4-Selective Negishi and Kumada Couplings of 2,4-Dichloropyridine and 2,4-Dichloroquinoline 32

2.5 Sequential C4-Selective Cross-Coupling and S_NAr Enable Access to a Challenging Substitution Pattern 33

2.6 Previously Reported C4-Selective Cross-Coupling that is Not Under Ligand Control 35

2.7 Scope of C4-Selective Suzuki-Miyaura Cross-Couplings Under Ligand-Free Catalysis 37

3.1 Graphical abstract for the *ACS Catal.* manuscript 44

LIST OF SCHEMES CONTINUED

Scheme Page

3.2 Ligands that Give Unconventional Selectivity 45

3.3 (A) Influence of 6-Substituent on the Selectivity of Cross-Coupling Catalyzed by Pd/IMes; (B) Influence of Substrate Concentration on the Selectivity of Cross-Coupling Catalyzed by Pd/IMes; and (C) with Pd/IPr, Selectivity Trends with Difference in LUMO Coefficients. 54

4.1 (A) Synthesis and Reactivity of 2,4-Dichloropyrimidine (B) Bond Dissociation Energies of C_2—Cl and C_4—Cl from Ref. 7 and LUMO of 2,4-Dichloropyrimidine 61

4.2 Proposed Advantages of Regio-inversion: (A) Regiocontrol improves step-economy during parallel synthesis programs (B) Regiocontrol enables synthetic flexibility during the assembly of structures with sensitive functional groups 62

4.3 Preparation of 4-chloro-2-halopyrimidines for Use in Halide-Selective Cross-Coupling Reactions 63

4.4 Synthetic Approaches to C2-Substituted 4-Chloropyrimidines 64

4.5 Preparation of 4-chloro-2-alkylthiopyrimidines 68

4.6 Generic Mechanism of the Pd-Catalyzed Liebeskind-Srogl Cross-Coupling 69

4.7 Scope of C2-Selective Liebeskind-Srogl Couplings Catalyzed by Pd/IPent 73

4.8 C2-Selective Arylation via a Thiolation/C—S Bond Activation Sequence 74

4.9 (A) Cu-Catalyzed Aerobic Liebeskind-Srogl coupling of Thioesters with Boronic Acids (B) Proposed Synthetic Route to C2-Functionalized 4-Chloropyrimidines Under Catalytic Reaction Conditions 76

5.1 Synthetic Applications for Ring-Walking Catalysts: (A) Generic Mechanism of Catalyst-Transfer Polycondensations (B) First Pd(NHC)-Catalyzed CTP with Pd-PEPPSI-IPr (C) Selective Diamination of Tetrabromo-Spirobifluorenes with Pd-PEPPSI-IPr 81

5.2 Relationship between Ligand Sterics and Mono- vs Diarylation Selectivity over Time 85

LIST OF SCHEMES CONTINUED

Scheme Page

5.3 Intermolecular Competition Study between a Dichloroarene and its Monoarylated Product....86

5.4 Proposed Mechanisms for the Formation of Mono- and Diarylated Products 88

5.5 Selectivity vs Conversion for Reactions with Variable Phenylboronic Acid Equivalents....93

5.6 Monoarylation/Starting Material (**64a**/**64**) Ratio vs Diarylation/Monoarylation (**64b**/**64a**) Ratio as Suzuki-Miyaura Reactions Progress....95

5.7 Effect of Varied C5-Substituents on Selectivity for SMCs with 1,3-Dichlorobenzenes....96

LIST OF FIGURES

Figure Page

1.1 Generic Mechanism of Pd-Catalyzed C—C Cross-Coupling Reactions 3

1.2 The Preferred Site of Oxidative Addition to Palladium is Typically α to the Heteroatom 12

1.3 Electrophilicity of C—Br Bonds is Positively Correlated with ^{1}H NMR shifts (ppm) in the Unsubstituted Heteroarene Structure 12

1.4 (A) Activation Energy for Oxidative Addition Derived from Distortion ($\Delta E^{\ddagger}_{dist}$) and Interaction Energies ($\Delta E^{\ddagger}_{int}$) (B) Conventional Site of Oxidative Addition to Palladium and Bond Dissociation Energies (BDEs) Calculated Using B3LYP/6-31G(d) 13

3.1 Calculated transition structures for oxidative addition of chlorobenzene at (A) $Pd(PMe_3)$ and (B) $Pd(PMe_3)_2$. Differences in Gibbs free energies of activation are listed in units of kcal mol^{-1} relative to the lowest-energy structure in each set (defined as $\Delta\Delta G^{\ddagger} = 0.0$). (C) Key frontier molecular orbitals of the relevant species, where $Pd(PMe_3)_2$ is distorted into a bent geometry as adopted in the arene—$Pd(PMe_3)_2$ pre-oxidative addition π-complex 28

3.2 Calculated free energy diagrams illustrating the oxidative addition of 2,4-dichloropyridine at Pd(NHC) or Pd(NHC)(**1**), where NHC = IPr (A) or IMes (B) 51

4.1 (A) Selected Therapeutic Agents Containing 2,4-Disubstituted Pyrimidines (B) 2,4-Disubstituted Pyrimidines Represented in the Nitrogenous Nucleobases 60

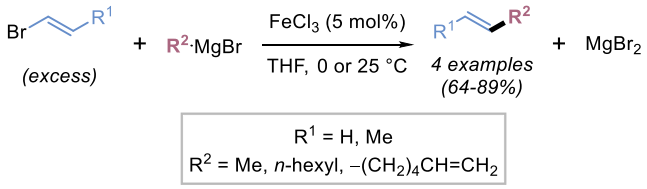
CHAPTER ONE

INTRODUCTION

1.1 Fundamentals of Pd-Catalyzed Cross-Coupling

In 1971, Kochi reported a C—C bond-forming reaction between alkenyl halides and Grignard reagents in the presence of an iron catalyst.[1] His report was among the first[2] to describe what we now refer to as cross-coupling. In the decades preceding this discovery, related reactions catalyzed by salts of Cr, Fe, Co, Ni, or Cu, which enabled the "homocoupling" of Grignard reagents in the presence of an oxidant, had stimulated great interest among the synthetic community as a carbon-carbon bond-forming method.[3] And yet, by definition, metal-catalyzed homocoupling offered no means of preparing non-symmetrical products. Unsymmetrical biaryls were particularly challenging to prepare by existing methods, which were largely restricted to radical processes like the Gomberg-Bachmann reaction[4] and the photolysis of aryl iodides[5] or aryl thallium reagents,[6] often resulting in unpredictable regioselectivity. For the first time, the reaction reported by Kochi provided a method for coupling distinct fragments—an electrophile and nucleophile, resulting in non-symmetrical products joined by a new carbon-carbon bond (Scheme 1.1).

Scheme 1.1. Seminal Iron-Catalyzed Cross-Coupling Reported by Kochi (1971).



Cross-coupling research flourished in the 1970s, and soon iron catalysts were supplanted by palladium in state-of-the-art C—C bond-forming reactions which included the Mizoroki-Heck,[7] Kumada-Corriu,[8] Sonogashira,[9] Murahashi,[10] Migita-Stille,[11] Negishi,[12] and Suzuki-Miyaura[13] cross-couplings. The distinction between each of these named reactions, fundamentally, is the identity of the nucleophile which undergoes coupling with an organo-halide electrophile. For C—C bond-forming reactions, the ideal nucleophile is usually an organometallic reagent,[14] and these range from highly reactive organo-lithium (Murahashi) and -magnesium (Kumada-Corriu) reagents to milder organo-stannane (Migita-Stille) and -boron (Suzuki-Miyaura) coupling partners which are more broadly tolerant of functional groups. Many of these Pd-catalyzed processes involve a catalytic cycle consisting of three steps: oxidative addition, transmetalation, and reductive elimination (Figure 1.1). During oxidative addition, a nucleophilic Pd(0) catalyst adds into the C—X bond of an organohalide, generating a Pd(II) intermediate. During transmetalation, the nucleophilic coupling partner replaces the halide at the metal center, forming a new Pd(II) intermediate where both coupling partners are bonded to the metal center. Finally, during reductive elimination, Pd undergoes a two-electron reduction to reform the active Pd(0) catalyst, concomitant with the formation of a new C—C bond between the two organic fragments. A variety of C—heteroatom bond-forming processes, such as the Buchwald-Hartwig aryl-amination, are also possible and proceed through mechanisms similar to that in Figure 1.1. However, in contrast to C—C bond-forming processes, these reactions do not involve a formal transmetalation step; instead, a primary amine, secondary amine, alcohol, or thiol, etc., becomes bound to the Pd center through the action of a base. Subsequent reductive elimination of Pd(II) results in the formation of the C—heteroatom bond and regeneration of the Pd(0) catalyst.

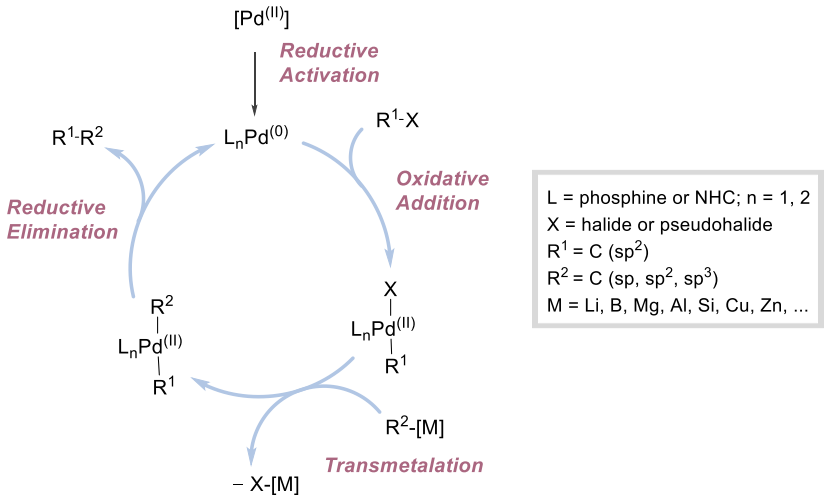


Figure 1.1. Generic Mechanism of Pd-Catalyzed C—C Cross-Coupling Reactions.

To the synthetic chemist, Pd-catalyzed cross-couplings presented an irresistible set of methods for forging diverse bonds, including C—C bonds with sp^2-sp, sp^2-sp^2, and sp^2-sp^3 hybridization. In 2010, the Nobel Prize in Chemistry was awarded to Richard Heck, Ei-ichi Negishi,[15] and Akira Suzuki[16] for their contributions to the field of Pd-catalyzed cross-coupling, and in 2011, cross-couplings had grown to encompass an astonishing 61% of all carbon-carbon bond-forming reactions carried out in the pursuit of drug candidates, and the Suzuki-Miyaura coupling alone accounted for 66% of these.[17] In fact, the general trend of "flattening" modern medicinal molecules can be largely attributed to the simplifying power of cross-couplings during the assembly of π-conjugated planar molecules.[18]

1.2 A Dichotomy of Ligands in Pd-Catalyzed Cross-Couplings

Featured in the seminal publications of Heck, Migita and Stille, Kumada, Negishi, Suzuki, and Sonogashira, triphenylphosphine had earned its reputation as the quintessential cross-coupling ligand. Despite the enormous advantages that triphenylphosphine-ligated Pd (e.g., $Pd(PPh_3)_4$)

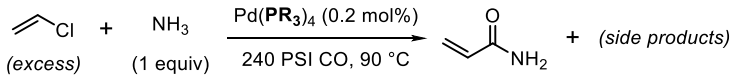
offered over simple Pd(II) salts,[7] cross-coupling faced several critical limitations during the late 20th century. Broadly, these included (1) limitations to the scope of starting materials which could be coupled and (2) the incidence of competing side reactions mediated by Pd.[19] In retrospect, both of these apparent limitations can be attributed to the limited variety of ligands used during the early years of cross-coupling research.

With respect to the scope of electrophiles employed in cross-coupling, the ubiquitous but inert aryl chlorides presented a glaring limitation: the oxidative addition of aryl chlorides to Pd was generally considered infeasible in the absence of forcing conditions or electron withdrawing-groups on the chloroarene.[20] At the temperatures required for aryl chloride activation, most mononuclear Pd catalysts decompose to less reactive Pd aggregates,[21] which limited catalyst selection to those few which are thermally stable.[22] While palladium aggregation can be suppressed by use of excess ligand, this practice commonly results in catalyst "poisoning" where the Pd center becomes coordinatively saturated and inactive.

The solution to breaking incalcitrant aryl chloride bonds emerged in 1987 when Nicholas reported the carbonylative amidation of vinyl chloride with ammonia under carbon monoxide: for this transformation, the ligand P^tBu_3 significantly outperformed PPh_3 (Table 1.1), while bidentate phosphines were essentially inactive.[23] However, bulky trialkylphosphine ligands such as PCy_3 and P^tBu_3, did not find mainstream use until the late 90's, which witnessed milestone publications by Hartwig,[24] Nishiyama,[25] and Fu.[26] Thereafter, the use of hindered alkyl phosphine ligands became common practice in cross-coupling reactions of "deactivated" aryl chlorides such as α-arylation, Suzuki-,[27] Stille-,[28] and Heck couplings.[29] Notably, early works by Nolan[30] as well as Caddick and Cloke[31] highlighted similar capabilities of hindered N-heterocyclic carbene (NHC) ligands, which had recently emerged as "phosphine mimics" in Pd catalysis. The commonality

among these reports was the use of ligands which are both sterically hindered and electron-rich (σ-donating).

Table 1.1 Carbonylative Amidation of Vinyl Chloride (Nicholas 1987).



R =	Time (min) to 80% conv.[a]
phenyl	170
p-tolyl	102
tert-butyl [b]	38

[a] Conversion measured by consumption of NH_3. [b] $Pd(P^tBu_3)_n$ was prepared *in situ* from free phosphine and Pd^0/dibenzylideneacetone.

For one thing, the relative instability of unbound trialkylphosphines or NHCs makes them less likely to dissociate from metals than triaryl phosphines, suppressing the formation of catalytically inactive Pd aggregates. However, the vital distinction between these sterically demanding ligands versus triphenylphosphine is their ability to promote low-coordinate, "monoligated" Pd intermediates where only one phosphine or NHC is bound to Pd instead of two.[32]

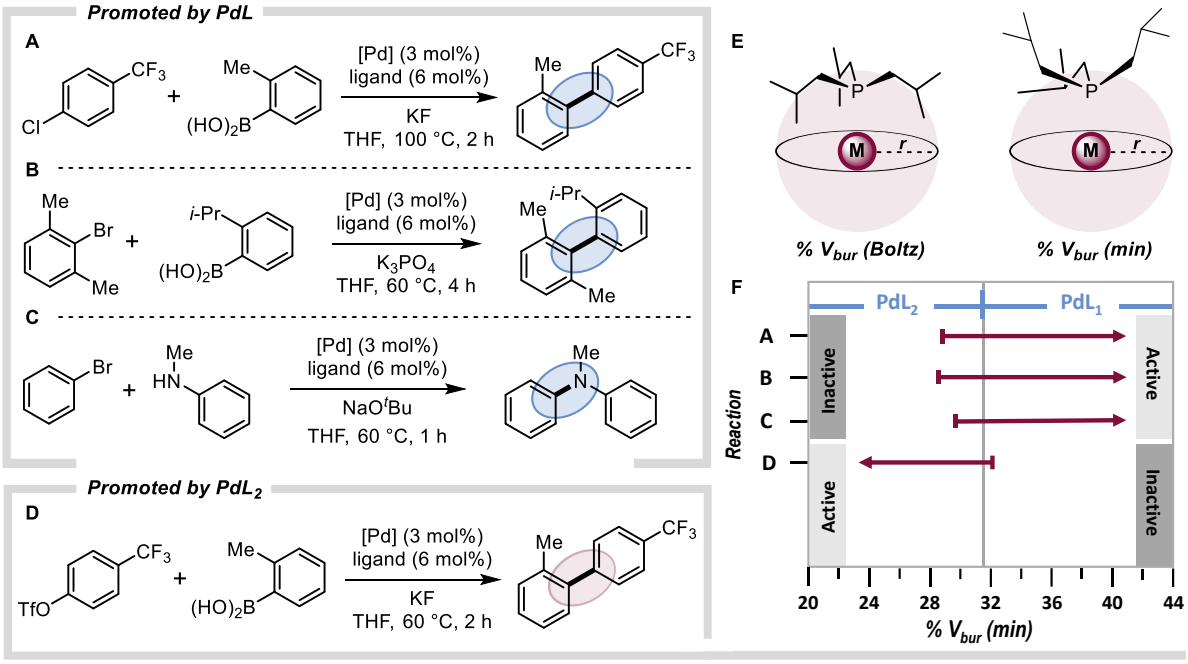
The practical advantages of controlling a metal's ligation state extend well beyond activation of stubborn aryl halide bonds. Arguably, the steric hindrance of an ancillary NHC or phosphine ligand is the most impactful reaction parameter during the optimization of Pd-catalyzed cross-couplings where conditions would otherwise be considered typical. Sigman and Doyle recently classified reactivity patterns of phosphine ligands using *minimum percent buried volume* [% V_{bur} (min)] as a steric descriptor. Percent buried volume describes the percentage of volume within an imaginary sphere surrounding the coordinated metal and occupied by the ligand's structure; the metal is positioned at the center of this sphere which has an assigned radius of 3.5

Å. *Minimum* percent buried volume is a related metric, but refers specifically to the smallest percent buried volume among all energetically accessible ligand conformers (Scheme 1.2.E).[33] Critically, this descriptor enables one to reliably predict whether mono- or bisligation will be favored at a metal center at various stages of a catalytic cycle. For example, values less than 29% favor the coordination of two phosphines during oxidative addition, whereas values greater than 32% favor coordination of a single phosphine. For ligands with % V_{bur} (min) values between 29% and 32%, both mono- and bisligated states are possible.

While a large variety of cross-coupling reactions can be performed successfully using either mono- or bis-ligated Pd, there are also many examples in which ligation state has proven critical to a reaction's success. In an evaluation of 56 sterically diverse phosphine ligands, Sigman and Doyle highlighted several cases in which monoligated Pd is required to achieve high yields: these include various cross-couplings of aryl chloride electrophiles[34] (including the reaction in Scheme 1.2.A), a Suzuki-Miyaura reaction involving hindered, *ortho*-substituted coupling partners (Scheme 1.2.B), a Heck coupling,[35] and a Buchwald Hartwig aryl-amination (Scheme 1.2.C). On the other hand, bisligated Pd was necessary to achieve adequate conversion in the Suzuki-Miyaura coupling of an aryl triflate (Scheme 1.2.D). Regarding Pd-catalyzed cross-couplings of aryl chlorides, the positive correlation between increasing % V_{Bur} (min) values for phosphine ligands and improved reaction yields reflects the superiority of monoligated Pd compared to bisligated Pd during oxidative addition at Ar—Cl bonds, as discussed above. However, the requirement for hindered ligands during both the Buchwald-Hartwig aryl amination of bromobenzene and the Suzuki coupling between a hindered, *ortho*-substituted boronic acid and 2,6-dimethyl-bromobenzene suggest the relevance of ligation state during other elementary steps of the catalytic cycle.[36] For example, during aryl amination, an amine cannot associate to Pd(II) unless a vacant

coordination site is available. Likewise, transmetalation of a sterically encumbered nucleophile will be slow at crowded or saturated Pd(II) intermediates.

Scheme 1.2. Relationship between a Ligand's Minimum % Buried Volume, Ligation State, and Reactivity *(adapted from Ref. 33).*



(**A**-**C**) Pd-catalyzed cross-couplings promoted by monoligated Pd (**D**) Pd-catalyzed cross-coupling promoted by bisligated Pd (**E**) *Left:* Depiction of percent buried volume using the Boltzmann-weighted average of ligand conformers; *Right:* Depiction of minimum percent buried volume; r = 3.5 Å (**F**) Overview of % V_{bur} (min) reactivity thresholds for 56 phosphine ligands screened in reactions A-D; PdL vs PdL_2; Ligation states were determined spectroscopically.

In summary, our ability to access multiple ligation states—particularly monoligated Pd with use of increasingly hindered ligands, has significantly broadened the perceived capabilities of Pd-catalyzed cross-couplings over time. Nevertheless, small triaryl phosphines and bisphosphines continue to play a central role in modern cross-coupling applications, and often exhibit reactivity biases which complement those of hindered monophosphines or NHCs. Moreover, as this thesis shall describe, bisligated Pd catalysts can also exhibit regiochemical

preferences which are orthogonal to those of monoligated Pd, and typically disfavor unwanted over-functionalization of multiply halogenated (hetero)arenes.

1.3 Cross-Couplings of (Hetero)arene Electrophiles with Multiple Reactive Sites

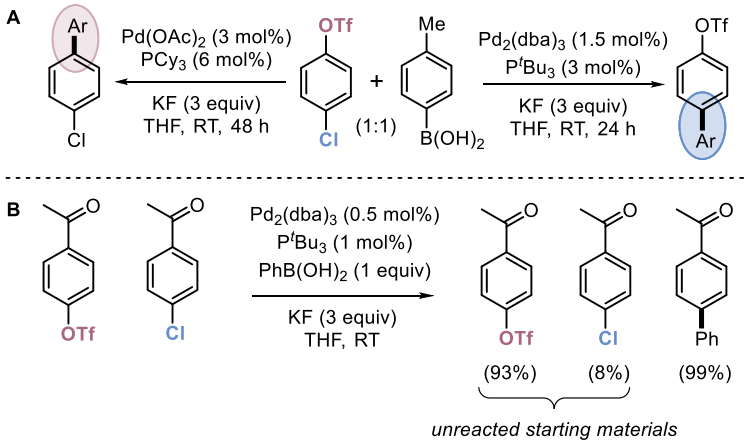
In cross-couplings of di- or polyhalogenated heteroarenes where multiple products of cross-coupling are possible, regioselectivity and chemoselectivity are generally dictated by characteristics of substrate, such as C—X bond strength. For example, it is well established that aryl iodides are more reactive toward oxidative addition at Pd than aryl bromides, which are, in turn, more reactive than aryl chlorides. This reactivity trend is primarily a result of relative C—X bond strengths which differ dramatically among the halogens. With few exceptions,[37] this order of reactivity is dependable when planning synthetic routes which involve substrates bearing multiple reactive halides. By comparison, there are relatively few examples where chemoselectivity is controlled by changes to the catalyst or other reaction conditions, rather than the innate reactivity of the substrate.[38]

1.3.1 Chemodivergent Cross-Couplings of Chloroaryl Triflates

The first example of switchable chemoselectivity under catalyst control was demonstrated by Fu in the Suzuki coupling of chloroaryl triflates.[39] Triflates, classified as 'pseudohalides,' exhibit similar reactivity to halides when utilized as leaving groups in cross-coupling reactions. By convention, aryl triflates are substantially more reactive toward oxidative addition at Pd than aryl chlorides. In keeping with this established order, Fu described a triflate-selective Suzuki-Miyaura arylation of chloroaryl triflates promoted by a Pd/PCy_3 catalyst. Yet, in the same report, Fu also described a chloride-selective arylation mediated by P^tBu_3, which left the triflate intact, contrary

to convention (Scheme 1.3.A). Additionally, in an intermolecular competition between an aryl chloride and an aryl triflate, P^{t}Bu$_3$ exhibited the same preference for reaction at chloride (Scheme 1.3.B). The ratio of phosphine to Pd was also relevant to the reaction outcome: the ligand PCy$_3$ exhibits a preference for C—OTf oxidative addition when PCy$_3$ is used in a 2:1 ratio with Pd, however, selectivity for triflate is diminished when PCy$_3$ is used in a 1.2:1 ratio with Pd. In contrast, P^{t}Bu$_3$ furnishes high chloride selectivity independent of the phosphine-palladium ratio.

Scheme 1.3. Ligand-Controlled Chemodivergent Suzuki Coupling of a Chloroaryl Triflate (Fu 2000).



In 2010, Houk and Schoenebeck revisited Fu's finding, and provided computational evidence that the divergent chemoselectivity preferences exhibited by PCy$_3$ versus P^{t}Bu$_3$ can be attributed to the valency of palladium during oxidative addition: P^{t}Bu$_3$ is sufficiently hindered to preclude ligation of a second phosphine during oxidative addition, whereas PCy$_3$ is less hindered, thus its ligation state during oxidative addition (mono or bis) depends upon the Pd/phopshine ratio employed.[40] According to Houk and Schoenebeck, selectivity for oxidative addition at C—OTf versus C—Cl can be explained in terms of distortion and interaction energies: for oxidative addition at monovalent Pd(PR$_3$), C—Cl is more easily distorted into the required transition state

geometry. On the other hand, divalent $Pd(PR_3)_2$ is more electron-rich, and therefore *interacts* more favorably with the most electropositive ring carbon at the triflate site. Multiple studies of cross-coupling selectivity with chloroaryl triflates have since corroborated this correlation between chemoselectivity and the ligation state of palladium, including contributions by Manabe,[41] Sigman,[42] Neufeldt,[43] and So.[44] Thus, low-valent Pd catalysts have challenged the very conception that chemoselectivity is dictated by an immutable order of (pseudo)halide reactivity.

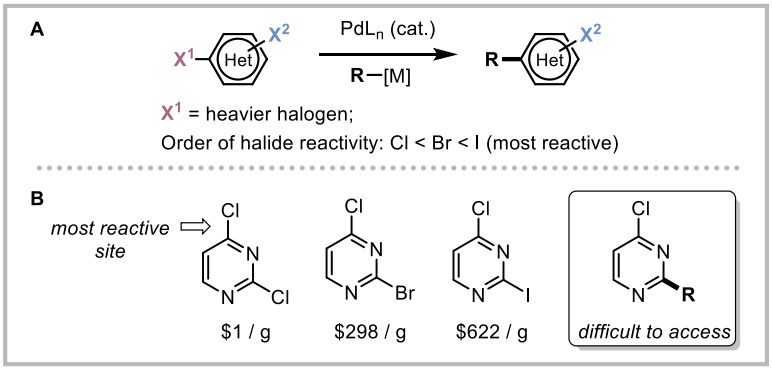
1.3.2 Site-Selective Cross-Couplings of Dihalo(hetero)arene Electrophiles

Aromatic nitrogen-heterocycles are ubiquitous among metabolites, therapeutics, agrichemicals, and functional materials. Synthetic methods for the derivatization of heteroaromatic scaffolds include metalation, nucleophilic aromatic substitution (S_NAr), electrophilic aromatic substitution (EAS), C—H activation, and cross-coupling. Frequently, these methods are employed in sequence with one another to access novel substitution patterns within chemical discovery programs and process chemistry.[45] Owing to their robustness and synthetic versatility, cross-coupling reactions have proven quite popular in this regard,[46] and the sub-disciplines of heterocyclic chemistry, medicinal chemistry, and cross-coupling methodology frequently intersect.

In an ideal scenario, two or more cross-coupling reactions may be performed using a single heteroarene substrate bearing non-identical halogens, such that the reaction proceeds with predictable chemoselectivity (at the heavier halogen first) and with minimal "over-functionalization" resulting from reaction at multiple sites. In such a scenario, the remaining halide(s) might then be functionalized via a second substitution method—whether cross-coupling or another reaction—or perhaps be left intact as a design element in the final target structure. However, heteroarene starting materials bearing mixed halogens are far less accessible than their

analogues bearing identical halogens, often differing by an order of magnitude in price (Scheme 1.4). For this reason, technologies enabling the prediction and control of *site-selectivity* in cross-couplings of (non-symmetric) dihalogenated heteroarenes—especially dichloroheteroarenes, are in great demand.[47]

Scheme 1.4. (A) Pd-Catalyzed Cross-Coupling of Dihalo-Heteroarenes with Non-Identical Halogens (B) Chemoselective Strategies are Limited by the Cost of Starting Materials *(chemical prices were sourced from Ambeed.com; accessed 31 Oct. 2023).*



When two identical halides occupy non-equivalent positions on a heteroarene, oxidative addition to Pd normally takes place at the halide adjacent to at least one heteroatom. Simple resonance analysis of pyridine indicates that the most reactive ring positions are situated *ortho* and *para* to the heteroatom: besides its neutral structure, the most stable resonance contributors of pyridine place a formally negative charge on nitrogen, pyridine's most electronegative atom (Figure 1.2). Therefore, the carbon atoms in the 2-, 4-, and 6-positions are more electropositive than those in the 3- or 5-positions and are best suited to interact with a reductant such as Pd(0) during the oxidative addition step. However, for pyridine and related azines, C—X bonds α to nitrogen are weaker due to the proximity of nitrogen's lone pair which is coplanar with the C2—X bond.

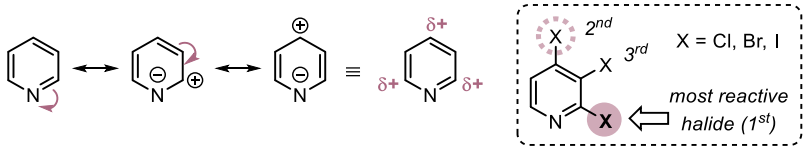


Figure 1.2. The Preferred Site of Oxidative Addition to Palladium is Typically α to the Heteroatom.

Generally, regiochemical outcomes for cross-couplings of dihalogenated heteroarenes can be predicted on the basis of ^{1}H NMR shifts by analysis of the non-halogenated parent structure (Figure 1.3). The most deshielded proton of the parent heteroarene is the one α to at least one heteroatom and usually corresponds to the preferred site of oxidative addition at the analogous dihaloheteroarene.[48] However, there are notable exceptions to this trend. For example, 2,4-dichloropyrimidine and 2,4-dibromopyrimidine react at the C4-site, yet the most deshielded proton of the parent structure is located at C2.[49]

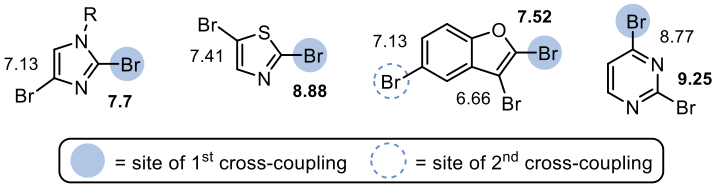


Figure 1.3. Electrophilicity of C—Br Bonds is Positively Correlated with ^{1}H NMR shifts (ppm) in the Unsubstituted Heteroarene Structure.

Houk and Merlic applied the distortion-interaction model[50] (also referred to as an activation-strain model),[51] to describe the origin of site selectivity computationally. The activation energy for oxidative addition at a C—X bond is equal to the distortion energy plus the interaction energy (Figure 1.4.A). *Distortion* is related to bond dissociation energies (BDEs) and refers to the energy required to distort the reactants into the transition state geometry. Oxidative addition is generally favored at weaker C—X bonds which are easier to distort (Figure 1.4.B, *left*). However,

exceptions to this trend were observed in specific situations. Oxidative addition took place at the stronger C—X bond in certain cases where (1) both C—X bonds have almost identical bond dissociation energies (BDEs), (2) the weaker C—X bond is located on a fused carbocycle rather than on the heterocycle, and (3) the halides are situated on a substituted ring and are each adjacent to different heteroatoms (Figure 1.4.B, *right*). In these instances, site selectivity is better explained in terms of frontier molecular orbital distribution and the *interaction* between Pd's HOMO and the substrate LUMO. Oxidative addition can still take place at stronger C—X bonds if the LUMO coefficient is larger at these sites. For instance, despite a lower BDE for C—Br at the C5 site, a 2,5-dibromobenzoxazole exhibits a stronger interaction between Pd and C2 of the substrate, which can be attributed to the significantly larger LUMO contribution at C2 versus C5.

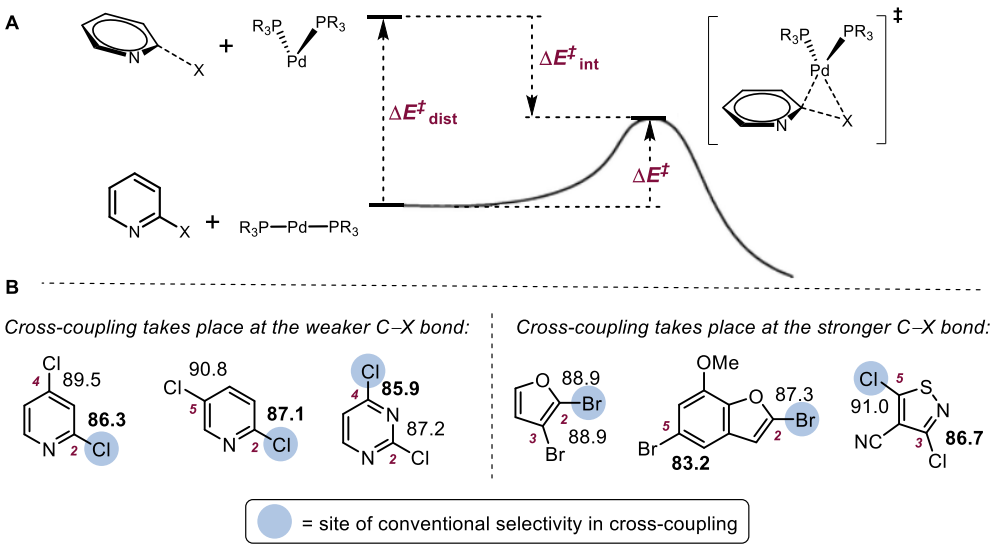


Figure 1.4. (A) Activation Energy for Oxidative Addition Derived from Distortion ($\Delta E^{\ddagger}_{dist}$) and Interaction Energies ($\Delta E^{\ddagger}_{int}$) (B) Conventional Site of Oxidative Addition to Palladium and Bond Dissociation Energies (BDEs) Calculated Using B3LYP/6-31G(d) *(adapted from Ref. 50).*

More recently, Leitch developed a structure-reactivity model to quantitatively predict relative rates for oxidative addition of (hetero)aryl-chloride, -bromide, and -triflate electrophiles

to $Pd(PCy_3)_2$.[52] Leitch concluded that descriptors of C—X bond strength, including intrinsic bond strength index (IBSI) and leaving group stability, are insufficient to model the rate of oxidative addition. Rather, the most relevant molecular descriptors are the electrostatic potential (ESP) at the *ipso* (C—X) carbon, followed by the ESP at ring atoms *ortho* to the leaving group—where more positive *ipso* carbon atoms and more negative *ortho* atoms both accelerate oxidative addition. The ESP of Pd is also consequential, with a more negative metal center resulting in an increased rate of oxidative addition. By using these molecular descriptors to calculate relative oxidative addition barriers, site selectivity could be accurately predicted with a wide array of dihalogenated heteroarenes. Nevertheless, like prior models, this framework manifests limitations in its predictive capacity; for instance, dichloroisothiazoles exhibit a regiochemical preference which is contrary to prediction.

Beyond empirically catalogued examples of site-selective cross-coupling, the models put forth by Handy, Houk, and Leitch provide the current basis for site-selectivity predictions in cross-couplings of dihalogenated azines and other heteroarenes. Nevertheless, these models are not without limitations. By design, these frameworks largely or completely emphasize aspects of substrate control, such as C—X bond strengths, LUMO distribution, ESP, and steric repulsive effects, while placing little emphasis on ligand identity or catalyst speciation. For Houk's distortion-interaction model, 25 dihaloheteroarenes were surveyed computationally, but all transition structures were calculated using the small model $Pd(PH_3)_2$ where the Pd catalyst is bisligated. Likewise, Leitch modeled site selectivity trends for 28 dihaloheteroarenes, but parameterization was predicated on empirically derived reaction rates using only $Pd(PCy_3)_2$ in THF. Neither model is expected to be reliable when dramatic changes are made with regard to catalyst speciation, ligand structure, or catalyst ligation state. Additionally, while these models are

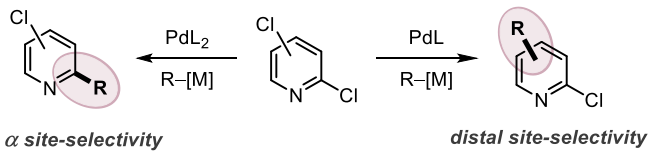
of great relevance in predicting the initial site of reaction, they are unable to predict selectivity for mono- versus difunctionalization (reaction at both halides), which varies widely depending on ligand identity.

In unusual instances, the site-selectivity of cross-coupling departs from the conventional pattern, occurring at C—X bonds positioned distal to heteroatoms.[53] A Scifinder search indicates that, for the majority of dihalogenated N-heteroarene substrate classes, fewer than 8% of cross-coupling reactions lead to "atypical" site-selectivity.[54] Nevertheless, these exceptions point to limitations in our existing predictive models. Most significantly, the lack of mechanistic explanations for atypical site selectivity hinders the development of strategies to deliberately invert it.

1.4 Focuses of this Work

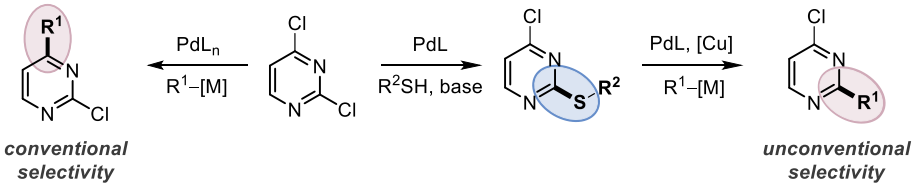
As discussed above, cross-couplings of dihalogenated N-heteroarenes normally proceed with predictable site selectivity for halides positioned α to nitrogen. Thus, minor regioisomers are challenging to prepare, impeding synthetic strategies to access polysubstituted azines. Chapters 2 and 3 will focus on catalyst-controlled approaches where changes to Pd's ligation state or speciation can invert site-selectivity in Pd-catalyzed cross-couplings of dichlorinated pyridines, pyridazines, pyrimidines, and quinolines. The synthetic opportunities offered by regio-inversion shall also be discussed.

Scheme 1.5. Ligation State-Controlled Regiodivergent Cross-Couplings of 2,X-Dichloroazines.



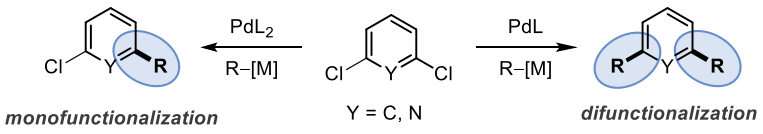
Unlike 2,4-dichloropyridine, 2,4-dichloro*pyrimidine* proves impervious to catalyst-controlled approaches aimed at inverting the site preference in catalytic C—C bond-forming processes. Chapter 4 describes a two-step synthetic strategy to achieve selective C2-arylation of 2,4-dichloropyrimidines.

Scheme 1.6. C2-Arylation of 2,4-Dichloropyrimidine via a C2-Sective Thiolation/C—S Bond Activation Sequence.



A third challenge, broadly applicable to cross-couplings with dihalogenated electrophiles, is the ability to control mono- versus difunctionalization. Some catalysts are known to "ring-walk" across π-conjugated systems, resulting in reaction at both halides instead of one, despite the use of nucleophile in sub-stoichiometric quantity. Chapter 5 will provide a mechanistic basis for ligand effects on Pd ring-walking and strategies to minimize over-functionalization of dichloroarenes and dichloropyridines.

Scheme 1.7. Ligand-Controlled Selectivity for Mono- vs. Difunctionalization of Dichloro-(hetero)arenes.



1.5 References

1. Tamura, M.; Kochi, J. K. Vinylation of Grignard Reagents. Catalysis by Iron. *J. Am. Chem. Soc.* **1971**, *93*, 1487−1489.

2. Vavon and Mottez, *Bull. Soc. Chim.,* **1994**, *5*, 11, 196.

3. Kharasch, M. S.; Reinmuth, O. *Grignard Reactions of Nonmetallic Substances*; Constable: London, 1954.

4. Gomberg, M.; Bachmann, W. E. *J. Am. Chem. Soc.* **1924**, *46*, 10, 2339–2343.

5. (a) Wolf, W.; Kharasch, N. *J. Org. Chem.* **1965**, *30*, 8, 2493—2498 (b) Bunnett, J. F.; Wamser, C. C. *J. Am. Chem. Soc.* **1966**, *88*, 23, 5534-5537.

6. Taylor, E. C.; Kienzle, F.; McKillop, A. *J. Am. Chem. Soc.* **1970**, *92*, 20, 6088—6089.

7. Dieck, H. A.; Heck, R. F. *J. Am. Chem. Soc.* **1974**, *96*, 4, 1133—1136.

8. Tamao, K.; Minato, A.; Miyake, N.; Matsuda, T.; Kiso, Y.; Kumada, M. *Chem. Lett.* **1975**, *4*, 133– 136.

9. Sonogashira, K.; Tohda, Y.; Hagihara, N. *Tetrahedron Lett.* **1975**, *16*, 4467–4470.

10. Murahashi, S.; Yamamura, M.; Yanagisawa, K.; Mita, N.; Kondo, K. *J. Org. Chem.* **1979**, *44*, 2408—2417.

11. (a) Kosugi, M.; Sasazawa, K.; Shikizu, Y.; Migita, T. *Chem. Lett*., **1977**, *6*, 301–302. (b) Kosugi, M.; Shimizu, Y.; Migita, T. *J. Organomet. Chem.*, **1977**, *129*, C36-C38. (c) Milstein, D.; Stille, J. K. *J. Am. Chem. Soc.*, **1978**, *100*, 3636–3638.

12. King, A. O.; Okukado, N.; Negishi, E. *J. Chem. Soc.*, *Chem. Commun.* **1977**, 683– 684.

13. Miyaura, N.; Yanagi, T.; Suzuki, A. *Synth. Commun.* **1981**, *11*, 513—519.

14. Not all Pd-catalyzed C—C bond-forming reactions require an organometallic nucleophile. For instance, the Mizoroki-Heck reaction enables cross-coupling of alkenes with aryl halide electrophiles and does not involve a transmetalation step.

15. For Nobel Lecture, see: E. Negishi, *Angew. Chem.* **2011**, *123*, 6870–6897; *Angew. Chem. Int. Ed.* **2011**, *50*, 6738–6764.

16. A. Suzuki, *Angew. Chem.* **2011**, *123*, 6854–6869; *Angew. Chem. Int. Ed*. **2011**, *50*, 6722–6737.

17. Roughley, S. D.; Jordan, A. M. *J. Med. Chem.* **2011**, *54*, 3451– 3479.

18. Lovering, F.; Bikker, J.; Humblet, C. *J. Med. Chem.* **2009**, *52*, 6752– 6756.

19. Campeau, J.-L.; Hazari, N. *Organometallics* **2019**, *38*, 3– 35.

20. (a) Farina, V.; Krishnamurthy, V.; Scott, W. *J. Org. React.* **1997**, *50*, 1-652. (b) Mitchell, T. N. In *Metal-catalyzed Cross-coupling Reactions*; Diederich, F., Stang, P. J., Eds.; Wiley-VCH: New York, 1998; Chapter 4. (c) Gribble, G. W. *Palladium in Heterocyclic Chemistry*; Pergamon: New York, 2000.

21. (a) van Leeuwen, P. W. N. M. *Appl. Catal., A* **2001**, *212*, 61−81. (b) Widegren, J. A.; Finke, R. G. J. *Mol. Catal. A* **2003**, *198*, 317−341. (c) de Vries, J. G. When Does Catalysis with Transition Metal Complexes Turn into Catalysis by Nanoparticles? In *Selective Nanocatalysts and Nanoscience*; Zecchina, A., Bordiga, S., Groppo, E., Eds.; Wiley-VCH, 2011; pp 73−103.

22. Beller, M.; Fischer, H.; Herrmann, W. A.; Öfele, K.; Brossmer, C. *Angew. Chem., Int. Ed.* **1995**, *34*, 1848– 1849.

23. Nicholas, P. P. *J. Org. Chem.* **1987**, *52* (23), 5266– 5272.

24. F. Paul, J. Pratt, J. F. Hartwig, *J. Am. Chem. Soc*. **1994**, *116*, 5969 – 5970. (b) J. F. Hartwig, F. Paul, *J. Am. Chem. Soc.* **1995**, *117*, 5373 – 5374. (c) J. F. Hartwig, *Angew. Chem.* **1998**, *110*, 2154 –2177; *Angew. Chem. Int. Ed.* **1998**, *37*, 2046 – 2067.

25. (a) Nishiyama, M.; Yamamoto, T.; Koie, Y. *Tetrahedron Lett.* **1998**, *39*, 617– 620. (b) Yamamoto, T.; Nishiyama, M.; Koie, Y. *Tetrahedron Lett.* **1998**, *39*, 2367.

26. G. C. Fu, *Acc. Chem. Res.* **2008**, *41*, 1555 – 1564, and references cited therein.

27. Shen, W. *Tetrahedron Letters*, **1997**, *38*, 32, 5575-5578.

28. Littke, A. F.; Schwarz, L.; Fu, G. C. *J. Am. Chem. Soc.* **2002**, *124*, 6343-6348.

29. Stürmer, R. *Angew. Chem. Int. Ed.* **1999**, *38*, 22, 3307-3308.

30. (a) Huang, J.; Grasa, G. *Org. Lett.*, **1999** *1*, 8, 1307-1309. (b) Grasa, G. A.; Nolan, S. P. *Org. Lett.*, **2001**, *3*, 1, 119-122.

31. Caddick, S.; Cloke, F. G. N.; Hitchcock, P. B.; Leonard, J.; Lewis, A. K. d. Ks.; McKerrecher, D.; Titcomb, L. R. *Organometallics* **2002**, *21*, 4318– 4319. (b) Lewis, A. K.; Caddick, S.; Cloke, F. G.; Billingham, N. C.; Hitchcock, P. B.; Leonard, J. *J. Am. Chem. Soc.* **2003**, *125*, 10066–10073.

32. (a) Christmann, U.; Vilar, R. *Angew. Chem. Int. Ed.* **2005**, *44*, 366 –374. (b) Molander, G. A.; Canturk, B. *Angew. Chem. Int. Ed.* **2009**, *48*, 9240 – 9261.

33. Newman-Stonebraker, S. H.; Smith, S. R.; Borowski, J. E.; Peters, E.; Gensch, T.; Johnson, H. C.; Sigman, M. S.; Doyle, A. G. *Science* **2021**, *374* (6565), 301– 308.

34. See also: Zhao, S.; Gensch, T.; Murray, B.; Niemeyer, Z. L.; Sigman, M. S.; Biscoe, M. R. *Science* **2018**, *362*, 670– 674.

35. See: Stambuli, J. P.; Stauffer, S. R.; Shaughnessy, K. H.; Hartwig, J. W. *J. Am. Chem. Soc.* **2001,** *123*, 2677-2678.

36. Borowski, J. E.; Newman-Stonebraker, S. H.; Doyle, A. G. *ACS Catal*. **2023**, *13*, 7966– 7977.

37. For selected exceptions where chemoselective cross-coupling results at the site of a smaller halide, see: (a) Cheng, J.; Trudell, M. L. *Org. Lett.* **2001**, *3*, 1371–1374. (b) Ji, J.; Bunnelle, W. H. *Org. Lett.* **2003**, *5*, 4611–4614. (c) Keylor, M. G.; Niemeyer, Z. L.; Sigman, M. S.; Tan, K. L. *J. Am. Chem. Soc.* **2017**, *139*, 10613–10616. (d) Qiu, Y. L.; Wang, C.; Peng, X.; Cao, H.; Ying, L.; Gao, X.; Wang, B.; Or, Y. S. WO2013052369 A1, **2013**. (e) Ashcroft, C. P.; Fussell, S. J.; Wilford, K. *Tetrahedron Lett.* **2013**, *54*, 4529–4532. (f) Ishikawa, S.; Manabe, K.; *Tetrahedron* **2011**, *67*, 10156–10163.

38. (a) Reeves, E. K.; Entz, E. D.; Neufeldt, S. R. *Chem. Eur. J.* **2021**, *27*, 6161– 6177 (b) Ng, S. S.; Pang, W. H.; Yuen, O. Y.; So, C. M. *Org. Chem. Front.*, **2023**, *10*, 4408-4436.

39. Littke, A. F.; Dai, C. Y.; Fu, G. C. *J. Am. Chem. Soc.* **2000**, *122*, 4020–4028.

40. Schoenebeck, F.; Houk, K. N. *J. Am. Chem. Soc.* **2010**, *132*, 2496–2497.

41. Manabe, K.; Ohba, M.; Matsushima, Y. *Org. Lett.* **2011**, *13*, 2436–2439.

42. Niemeyer, Z. L. ; Milo, A.; Hickey, D. P.; Sigman, M. S. *Nature Chem.* **2016**, *8*, 610–617.

43. Reeves, E. K. ; Humke, J. J.; Neufeldt, S. R. *J. Org. Chem.* **2019**, *84*, 11799–11812.

44. (a) Chen, Z.; Gu, C.; Yuen, O. Y.; So, C. M. *Chem. Sci.* **2022**, *13*, 4762– 4769. (b) Wang, M.; Yuen, O. Y.; So, C. M. *Chin. J. Chem*. **2023**, *41*, 909—914.

45. Cardoza, S.; Shrivash, M. K.; Das, P.; Tandon, V. *J. Org. Chem.*, **2021**, *86*, 1330—1356.

46. (a) Colacot, T. J. Platinum Met. Rev. 2011, 55, 84–90. (b) Johansson Seechurn, C. C. C.; Deangelis, A.; Colacot, T. J.; Introduction to *New Trends in Cross Coupling, Theory and Applications*; RSC Catalysis Series *No. 21*; Colacot, T. J.; The Royal Society of Chemistry: Cambridge, UK, 2015; pp. 1-19

47. For reviews on site-selectivity in cross-couplings of multiply halogenated heteroarenes, see: (a) Schröter, S.; Stock, C.; Bach, T. *Tetrahedron* **2005**, *61*, 2245−2267. (b) Fairlamb, I. J. S. *Chem. Soc. Rev.* **2007**, *36*, 1036−1045. (c) Bellina, F.; Rossi, R. Adv. Synth. Catal. 2010, 352, 1223−1276. (d) Rossi, R.; Bellina, F.; Lessi, M. 2012, 354, 1181−1255. (e) Manabe, K.; Yamaguchi, M. *Catalysts* **2014**, *4*, 307−320. (f) Kapdi, A. R.; Prajapati, D. *RSC Adv.* **2014**, *4*, 41245−41259. (g) Almond-Thynne, J.; Blakemore, D. C.; Pryde, D. C.; Spivey, A. C. *Chem. Sci.* **2017**, *8*, 40−62. (h) Palani, V.; Perea, M. A.; Sarpong, R. *Chem. Rev.* **2022**, *122*, 10126−10169.

48. (a) Handy, S. T.; Zhang, Y. *Chem. Commun.* **2006**, *3*, 299−301. See also (b) Zhang, Y.; Handy, S. T. *Open Org. Chem. J.* **2008**, *2*, 58−64. (c) Kashihara, M.; Gordon, C. P.; Copéret, C. *Org. Lett.* **2020**, *22*, 8910−8915.

49. Abraham, R. J.; Reid, M. ^{1}H chemical shifts in NMR. Part 18. Ring currents and p-electron effects in hetero-aromatics. *J. Chem. Soc., Perkin Trans. 2* **2002**, 1081−1091.

50. (a) Legault, C. Y.; Garcia, Y.; Merlic, C. A.; Houk, K. N. *J. Am. Chem. Soc.* **2007**, *129*, 12664−12665. (b) Garcia, Y.; Schoenebeck, F.; Legault, C. Y.; Merlic, C. A.; Houk, K. N. *J. Am. Chem. Soc.* **2009**, *131*, 6632−6639.

51. (a) de Jong, G. T.; Bickelhaupt, F. M. *ChemPhysChem* **2007**, *8*, 1170—1181. (b) de Jong, G. T.; Bickelhaupt, F. M. *J. Chem. Theory Comput.* **2007**, *3*, 514—529.

52. Lu, J.; Donnecke, S.; Paci, I.; Leitch, D. C. *Chem. Sci.* **2022**, *13*, 3477−3488.

53. For noteworthy examples of unconventional site-selectivity, see: (a) Strotman, N. A.; Chobanian, H. R.; He, J.; Guo, Y.; Dormer, P. G.; Jones, C. M.; Steves, J. E. *J. Org. Chem.* **2010**, *75*, 1733−1739. (b) Dai, X.; Chen, Y.; Garrell, S.; Liu, H.; Zhang, L.-K.; Palani, A.; Hughes, G.; Nargund, R. *J. Org. Chem.* **2013**, *78*, 7758−7763. (c) Fowler, J. M.; Britton, E.; Pask, C. M.; Willans, C. E.; Hardie, M. J. *Dalton Trans.* **2019**, *48*, 14687−14695. (d) Palani, V.; Hugelshofer, C. L.; Kevlishvili, I.; Liu, P.; Sarpong, R. *J. Am. Chem. Soc.* **2019**, *141*, 2652–2660 (e) Yang, M.; Chen, J.; He, C.; Hu, X.; Ding, Y.; Kuang, Y.; Liu, J.; Huang, Q. *J. Org. Chem.* **2020**, *85*, 6498−6508. (f) Scott, N. W. J.; Ford, M. J.; Jeddi, N.; Eyles, A.; Simon, L.; Whitwood, A. C.; Tanner, T.; Willans, C. E.; Fairlamb, I. J. S. *J. Am. Chem. Soc.* **2021**, *143*, 9682−9693. (g) Norman, J. P.; Larson, N. G.; Entz, E. D.; Neufeldt, S. R. *J. Org. Chem.* **2022**, *87*, 7414−7421. (h) Kim, G.; Lee, G.; Kim, G.; Seo, Y.; Jarhad, D. B.; Jeong, L. S. *Org. Chem. Front.* **2022**, *9*, 5536– 5543.

54. Norman, J. P.; Neufeldt, S. R. *ACS Catal.* **2022**, *12*, 12014– 12026.

CHAPTER TWO

UNCONVENTIONAL SITE SELECTIVITY IN PALLADIUM-CATALYZED CROSS-COUPLINGS OF DICHLOROHETEROARENES UNDER LIGAND-CONTROLLED AND LIGAND-FREE SYSTEMS

2.1 Contribution of Authors and Co-Authors

Manuscript in Chapter 2

Author: Jacob P. Norman

Contributions: Performed experimental work, writing/editing of the manuscript, and wrote sections of the supporting information (Appendix A).

Co-Author: Nathaniel G. Larson

Contributions: Performed experimental work and wrote sections of the SI (Appendix A).

Co-Author: Emily D. Entz

Contributions: Performed experimental work.

Co-Author: Sharon R. Neufeldt

Contributions: Wrote sections of the manuscript and edited both the manuscript and SI (Appendix A).

2.2 Manuscript Information

Jacob P. Norman, Nathaniel G. Larson, Emily D. Entz, Sharon R. Neufeldt

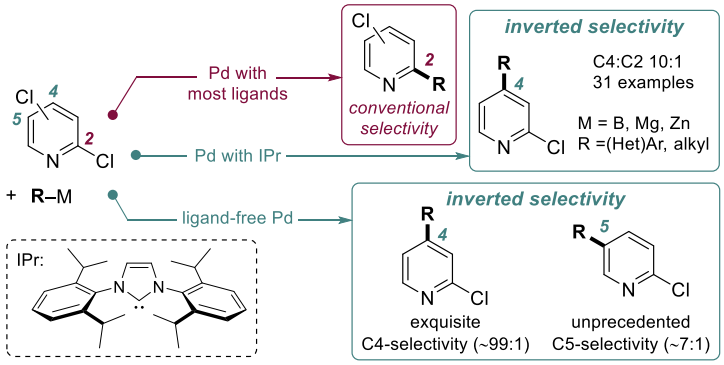
The Journal of Organic Chemistry

Status of Manuscript:
____ Prepared for submission to a peer-reviewed journal
____ Officially submitted to a peer-reviewed journal
____ Accepted by a peer-reviewed journal
_X_ Published in a peer-reviewed journal

American Chemical Society
J. Org. Chem. **2022**, *87*, 11, 7414–7421.
DOI: 10.1021/acs.joc.2c00665

2.3 Abstract

Halides adjacent to nitrogen are conventionally more reactive in Pd-catalyzed cross-couplings of dihalogenated N-heteroarenes. However, a very sterically hindered N-heterocyclic carbene ligand is shown to promote room-temperature cross-coupling at C4 of 2,4-dichloropyridines with high selectivity (~10:1). This work represents the first highly selective method with a broad scope for C4-coupling of these substrates where selectivity is clearly under ligand control. Under the optimized conditions, diverse substituted 2,4-dichloropyridines and related compounds undergo cross-coupling to form C4−$C_{(sp2)}$ and C4−$C_{(sp3)}$ bonds using organoboron, -zinc, and -magnesium reagents. The synthetic utility of this method is highlighted in multistep syntheses that combine C4-selective cross-coupling with subsequent nucleophilic aromatic substitution reactions. The majority of the products herein (71%) have not been previously reported, emphasizing the ability of this methodology to open up underexplored chemical space. Remarkably, we find that ligand-free "Jeffery" conditions enhance the C4 selectivity of Suzuki coupling by an order of magnitude (>99:1). These ligand-free conditions enable the first C5-selective cross-couplings of 2,5-dichloropyridine and 2,5-dichloropyrimidine.



Scheme 2.1. Graphical abstract for the *J. Org. Chem.* manuscript.

2.4 Introduction

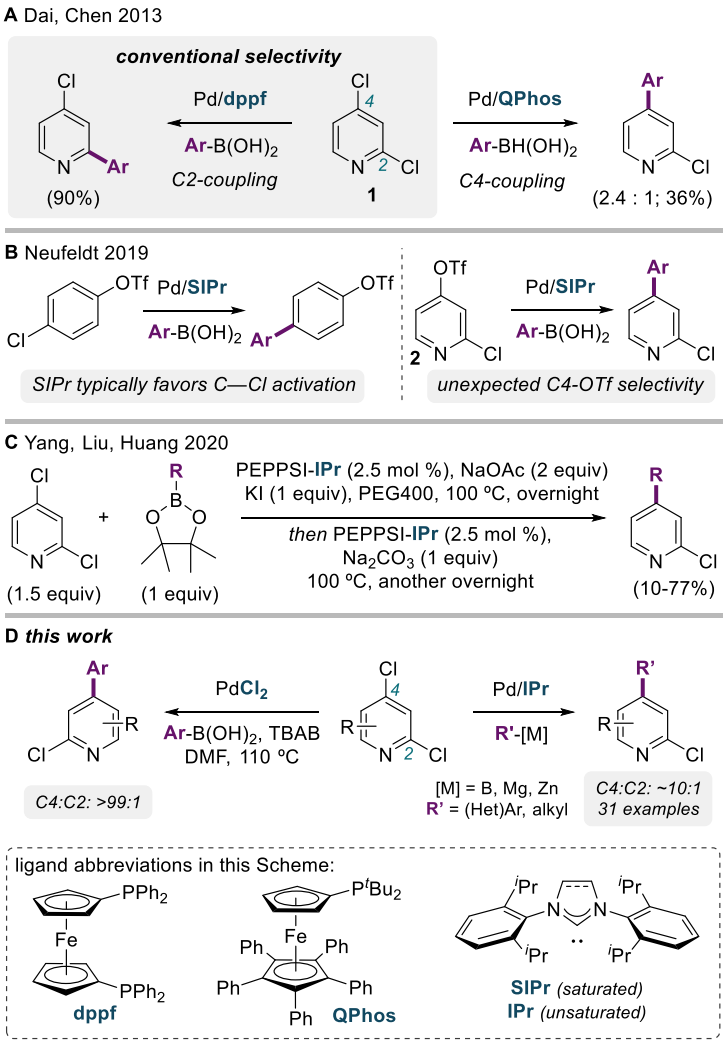
Nitrogen-containing heterocycles are privileged scaffolds in discovery-oriented synthesis such as medicinal chemistry. Heteroaromatic cores can be elaborated through cross-coupling reactions, which are among the most widely used methods in organic synthesis.[1] Heteroarene starting materials containing multiple halogen-leaving groups are practical building blocks since cross-coupling often occurs with predictable selectivity to give a product that retains one halide. Halides, especially chlorides, are valuable structural features of drug-like molecules. In fact, 15% of the unique small-molecule drugs approved by the FDA from 1994 to 2012 are chlorinated.[2] For six-membered nitrogen-containing heteroarenes, cross-coupling typically takes place at a C−X bond adjacent to nitrogen, if present.[3] It is generally very challenging to invert the conventional site preference to react at a C−X bond distal to nitrogen. As such, innate substrate biases leave significant chemical space underexplored by organic synthesis.

Like other nitrogen-containing heterocycles, 2,4-dichloro-pyridines nearly always undergo cross-coupling adjacent to nitrogen (at C2, example in Scheme 2.2.A, left).[4–7] Houk and Merlic explained this selectivity based on a distortion−interaction model: the C2−Cl bond is weaker and is therefore easier to distort into the transition-state geometry.[8] C2 is also more positively charged due to its proximity to nitrogen, which may enhance attractive interactions with a reductant such as Pd(0). Preferential cross-coupling at C4 to leave a C2-chloride intact is possible if C4 is substituted by bromide or iodide, but heteroarenes containing mixed halogens are often much less accessible than dichlorinated substrates.

Dai, Chen, and co-workers provided the first evidence that “innate” selectivity could be inverted by judicious ligand choice.[9] In the presence of bulky monophosphine QPhos, **1** undergoes

Suzuki−Miyaura cross-coupling preferentially at C4, albeit with modest selectivity and yield (Scheme 2.2.A). In contrast, the diphosphine dppf promotes conventional selectivity, leading exclusively to the C2-coupled product. In 2019, we reported that the room-temperature Pd/SIPr-catalyzed cross-coupling of **2** gives exclusive reaction at the C4-triflate (Scheme 2.2.B, right).[10]

Scheme 2.2. Ligand Effects on the Cross-Coupling Selectivity of 2,4-Dichloropyridines.



This result was surprising not only because the C2 site of di(pseudo)halogenated pyridines is normally more reactive toward cross-coupling but also because Pd/SIPr is usually *chemoselective* for chloride over triflate (Scheme 2.2.B, left). Based on the anomalous selectivity for the reaction of **2** in Scheme 2.2.B, we began exploring the use of the N-heterocyclic carbene (NHC) ligand SIPr and its unsaturated analogue IPr for C4-selective cross-coupling of dichloropyridines. During the course of our investigations, Yang and coworkers reported the use of a Pd(PEPPSI)(IPr) catalyst for C4-selective Suzuki−Miyaura cross-coupling of 2,4-dichloropyridines.[11] A series of standard optimization reactions using **1** at 60−100 °C revealed that the Pd(PEPPSI)(IPr) catalyst provides C4 selectivity ranging from 2.5:1 to 10.4:1, varying with solvent and base. Intriguingly, a 10-fold improvement in selectivity was found upon switching to unusual conditions that employ KI, NaOAc, and PEG400, together with the addition of a second batch of Pd(PEPPSI)(IPr) and a second base (Na_2CO_3) after ∼12 h (Scheme 2.2.C).

Here, we report that the use of IPr under mild conditions (often room temperature) enables a broader scope of C4-selective cross-couplings of 2,4-dichloropyridines and related substrates (Scheme 2.2.D, left). Control studies demonstrate that site selectivity is ligand-controlled under the conditions that we report. However, we further disclose that ligand is not necessary to achieve high C4 selectivity under some high-temperature conditions, including those previously reported by Yang et al. We find that ligand-free conditions analogous to those used in the Jeffery−Heck reaction lead to much higher C4 selectivity than can be achieved under ligand control (∼99:1 vs ∼10:1 for reactions of **1**, Scheme 2.2.D, right). These ligand-free conditions enable unprecedented C5 selectivity in the cross-coupling of 2,5-dichloropyridine and 2,5-dichloropyrimidine. At present, the ligand-free conditions are less general than the ligand-controlled system. Preliminary

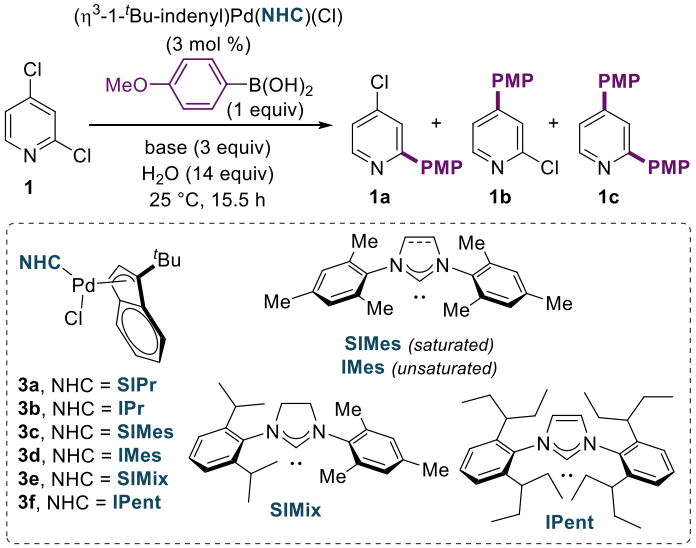
evidence suggests that the unprecedented selectivity in the absence of strongly coordinating ligands (e.g., phosphines or NHCs) may be a consequence of multinuclear Pd species.

2.5 Results and Discussion

2.5.1 Initial Discovery of C4-Selective Suzuki Coupling

The unexpected C4-OTf selectivity shown in Scheme 2.2.B led us to apply our previously reported reaction conditions[10] to the Suzuki−Miyaura cross-coupling of 2,4-dichloropyridine (**1**). The Hazari precatalyst (η^3-1-^{t}Bu-indenyl)Pd(SIPr)(Cl)[12] (**3a**) was used with KF as a base in THF at room temperature (Table 2.1, entry 1). Gratifyingly, these conditions afforded **1b** as the major product, resulting from reaction at C4. The crude ratio of **1a**/**1b** = 1:8 reflects much higher C4 selectivity than had been previously reported with QPhos (Scheme 2.2.A) and is similar to the selectivity later reported by Yang et al. during most of their optimization studies.[11] The yield of **1b** increased when K_2CO_3 was used as the base (entry 2), and selectivity and yield improved slightly upon switching to catalyst **3b** containing the unsaturated analogue IPr (entry 3). Similar results were obtained in benzene (entry 5), but the polar solvents DMF and propylene carbonate led to an erosion of selectivity (entries 6−7).[13] The steric bulk of IPr appears to be important for selectivity: when using the smaller ligands SIMes and IMes, much more cross-coupling at C2 was observed (entries 9−10). Interestingly, the unsaturated ligand IMes is slightly more selective than its saturated analogue, SIMes. This observation parallels the trend seen with IPr versus SIPr (compare entries 5 and 8). Use of a ligand whose sterics are intermediate between SIPr and SIMes (SIMix) affords intermediate selectivity (entry 11). Finally, the ligand IPent, which bears longer alkyl ortho-substituents, promotes over-arylation, leading to a mixture of products **1b** and **1c** (entry 12).[14] None of **1b** and only trace **1a** was detected when the ligand was omitted (entries 4 and 13),

Table 2.1. Optimization of the Pd/NHC-Catalyzed C4- Selective Suzuki−Miyaura Coupling.



entry	NHC	solvent	**1a** (%)	**1b** (%)	**1c** (%)	1a : 1b
1[b]	SIPr	THF	5	39	5	1 : 8
2	SIPr	THF	7	66	10	1 : 9
3	IPr	THF	7	69	8	1 : 10
4[c]	--	THF	1	<1	0	--
5	IPr	C_6H_6	8	70	6	1 : 9
6	IPr	DMF	8	47	15	1 : 6
7	IPr	PC[d]	9	45	17	1 : 5
8	SIPr	C_6H_6	9	64	8	1 : 7
9	SIMes	C_6H_6	24	35	3	1 : 1.5
10	IMes	C_6H_6	23	40	3	1 : 1.7
11	SIMix	C_6H_6	8	34	2	1 : 4
12	IPent	C_6H_6	1	34	23	1 : 34
13[e]	--	C_6H_6	2	0	0	--

[a]GC yields calibrated against undecane as the internal standard. Average of two trials. PMP = *para*-methoxyphenyl. [b]KF was used instead of K_2CO_3. [c]No NHC ligand; Pd source was $PdCl_2$ (3 mol %). [d]PC = propylene carbonate. [e]No NHC ligand; Pd source was (η^3-1-^{t}Bu-indenyl)$_2$(m-Cl)$_2$Pd$_2$ (1.5 mol %).

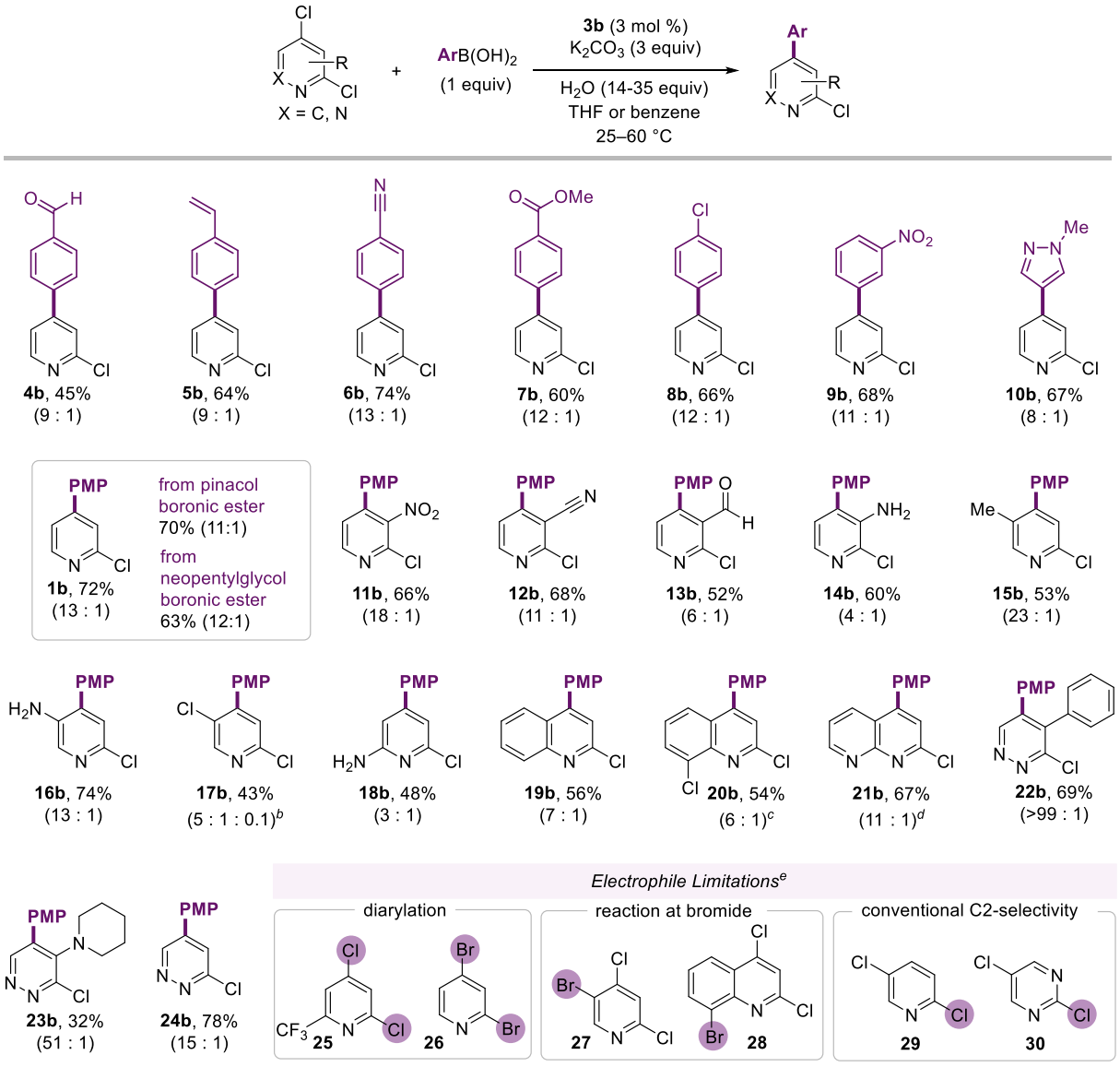
demonstrating the critical role of the NHC ligand in both the selectivity and reactivity of the catalyst under these conditions. The mechanistic origin of the observed ligand-controlled selectivity is the topic of further study in our group and will be reported in the near future. In brief, our mechanistic studies indicate that IPr favors oxidative addition at 12e− Pd(0), whereas reaction at 14e− Pd(0) is more prominent with other ligands.

Scope of the C4-Selective Suzuki Coupling

With optimized conditions in hand (Table 2.1, entries 3 and 5), we next examined the scope of aryl boronic acids in the Suzuki coupling. Substrate **1** undergoes Pd/IPr-catalyzed cross-coupling with diverse arylboronic acids (Scheme 2.3), affording the C4-coupled products in moderate to good isolated yields. Boronic esters are also competent cross-coupling partners in the reaction to form **1b**. The conditions are tolerant to aldehyde, nitrile, and alkene functional groups on the boronic acid coupling partner (**4b**−**6b**). Using 4-chlorophenylboronic acid, the major product **8b** results from the reaction of 4-pyridyl chloride, leaving both 2-pyridyl and the aryl chloride intact. Pyrazoleboronic acid reacts well (**10b**), but poor conversions were observed with other heteroarylboron reagents (see Appendix A). This limitation may be addressed through the use of heteroarylzinc or magnesium reagents instead of boronic acids (*vide infra*).

The optimized conditions enable Suzuki−Miyaura coupling of 2,4-dichloropyridines with diverse substituents at the 3-, 5-, and 6-positions. Aldehyde, nitrile, and unprotected amines are well tolerated, and no competing amination products were detected in the reactions of aminopyridines. Interestingly, the C4 selectivity is eroded when there is an amino substituent at the 3- or 6-position (**14b** and **18b**), but high selectivity is retained when the amino group is at the 5-position (**16b**). This observation suggests that the ability of substituents to coordinate to

Scheme 2.3. Scope of C4-Selective Suzuki−Miyaura Cross-Couplings Catalyzed by Pd/IPr.



[a] Isolated yields of products shown. Ratios are the crude ratio of C4:C2-coupled product prior to purification based on GC signal integrations. ~5− 20% diarylation was observed in all cases unless otherwise indicated (see the Appendix A for isolated yields when available). Reactions were conducted at room temperature unless otherwise indicated. [b] Reaction conducted at 75 °C. [c] Reaction conducted at 60 °C. [d] Ratio represents C4:C2:C5-coupled products. [e] No cross-coupling at C8 was detected. [f] **3f** (3 mol %) was used as the catalyst instead of **3b**. [g] See Appendix A for details.

palladium might play a role in the observed site selectivity. A limitation of this method is the substrate with a 6-trifluoromethyl group (**25**). Whereas diarylation is seen in ~5−20% yield for most of the other reactions in Scheme 2.3, the major product of the reaction of 25 corresponds to diarylation, despite the use of only 1 equiv of arylboronic acid (see Appendix A).

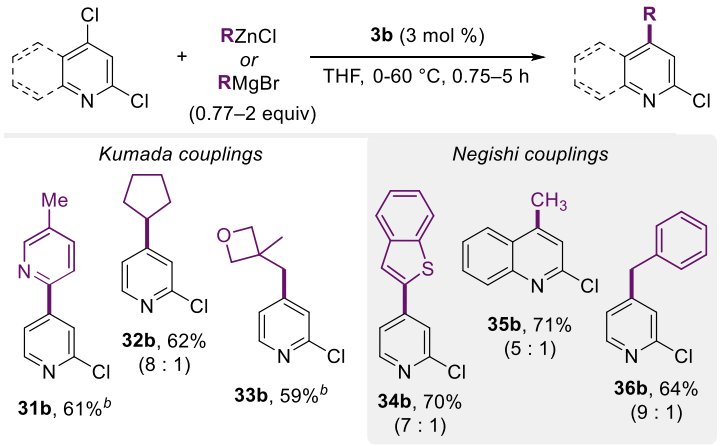
In addition to dichloropyridines, the analogous 2,4-dichloroquinoline and 2,4-dichloro-1,8-naphthyridine substrates undergo C4-selective coupling (**19b** and **21b**). These conditions are also effective for cross-coupling at the conventionally disfavored C5-site of 3,5-dichloropyridazines (**22b**−**24b**).[9] Additional chloride substituents at less electrophilic sites are well tolerated, including at the 5-position of pyridine and at the 8-position of quinoline (**17b** and **20b**). However, bromide substituents react more quickly than C4- chloride (**27**−**28**). 2,4-Dibromopyridine (**26**) does not display the same behavior as its dichloro- analogue; **26** leads to both C4-arylated and diarylated compounds as major products. Finally, these conditions are not effective for cross-coupling distal to nitrogen using substrates **29** or **30**. With these substrates, the major product results from reaction at C2−Cl, representing conventional selectivity.

C4-Selective Kumada and Negishi Couplings

The Pd/IPr catalytic system is also effective for promoting C4-selective cross-coupling with organozinc and organomagnesium nucleophiles. Although the Suzuki coupling is mostly limited to arylboronic acids, Negishi and Kumada conditions enable installation of heteroaryl and alkyl groups in good yield (Scheme 2.4). For example, a 2-pyridyl group was introduced at the C4 position of **1** using the corresponding Grignard reagent (product **31b**); this group is notoriously challenging to install through Suzuki coupling methods.[15] Secondary and primary alkyl Grignard reagents were effective coupling partners (**32b** and **33b**), and C4-methylation and benzylation

could be achieved using zinc reagents (**35b** and **36b**). Interestingly, the selectivity of these reactions appears to be influenced by the identity of the coupling partner. **31b** and **33b** were the only products observed by GCMS from their respective reactions, whereas the C2-coupled compounds were minor products in the other reactions. This phenomenon may reflect decomposition of some C2-coupled products, leading to artificially high C4:C2 ratios (see Appendix A).

Scheme 2.4. C4-Selective Negishi and Kumada Couplings of 2,4-Dichloropyridine and 2,4-Dichloroquinoline. [a]

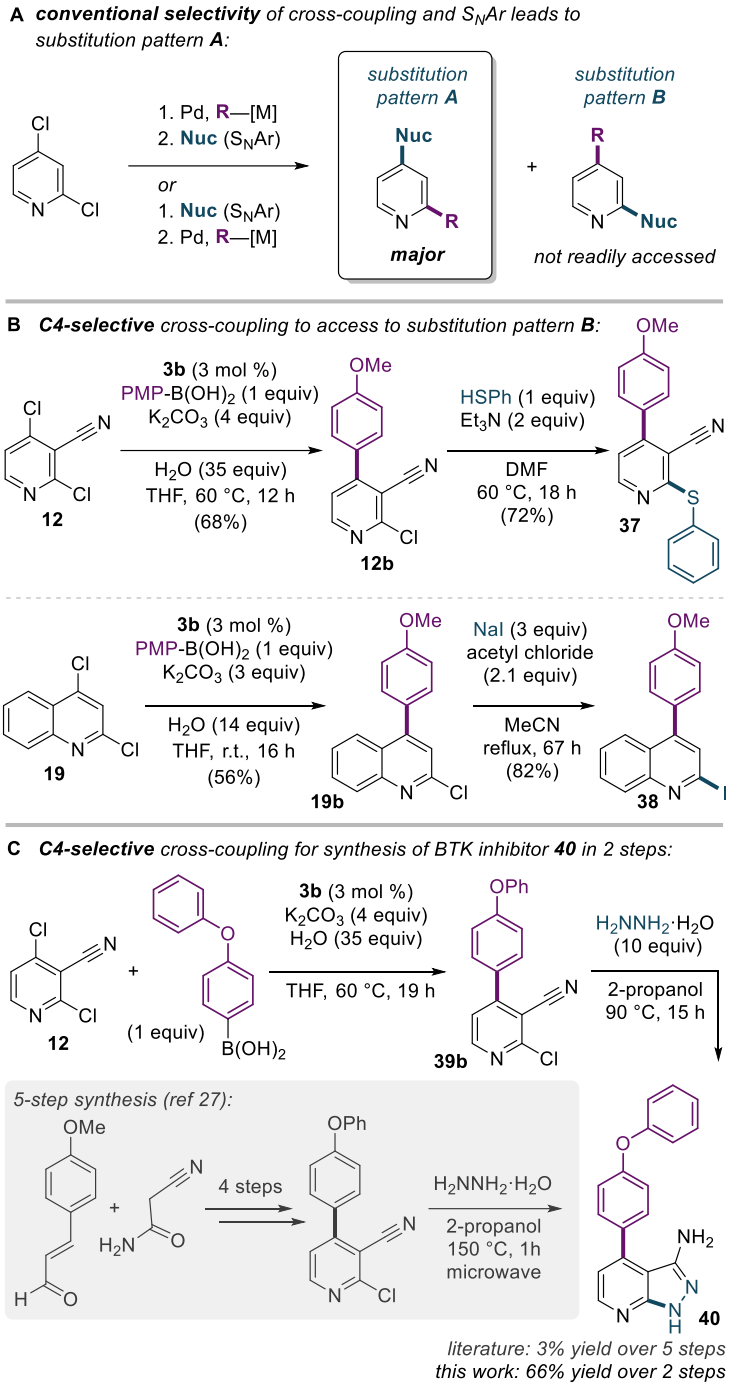


[a] Isolated yields of product shown. Ratios are the crude ratio of C4:C2-coupled product prior to purification, based on GC signal integrations. [b] Product shown was the only product observed.

Application to Multistep Syntheses

We envisioned that the C4-selective cross-coupling methods could be particularly useful for accessing pyridine motifs with a C−C bond at C4 and a C−heteroatom bond at C2 (″substitution pattern B″, Scheme 2.5.A). Nucleophilic aromatic substitution (SNAr) reactions are a commonly used strategy for introducing heteroatom substituents onto pyridine. For 2,4-dihalopyridines, transition metal-free S_NAr reactions tend to proceed at C4.[16] Conversely, as discussed above, the conventional site for cross-coupling reactions of these substrates is C2. As such, sequential cross-

Scheme 2.5. Sequential C4-Selective Cross-Coupling and S_NAr Enable Access to a Challenging Substitution Pattern. [a]



coupling and S_NAr reactions are useful for generating products with substitution pattern A based on typical selectivity, independent of the order of these steps. However, the complementary pattern B is not generally accessible by conventional methods.

Three compounds with substitution pattern B were prepared by Pd/IPr-catalyzed C4-selective cross-coupling, followed by S_NAr reactions. The use of thiolate and iodide nucleophiles for the S_NAr steps enabled the synthesis of products **37** and **38** (Scheme 2.5.B). We were also able to apply this strategy to a novel synthesis of the Bruton's tyrosine kinase inhibitor **40**. The previously reported synthesis of this compound required five synthetic steps providing an overall yield of 3%.[17] However, our two-step synthesis enables access to **40** in 66% overall yield.

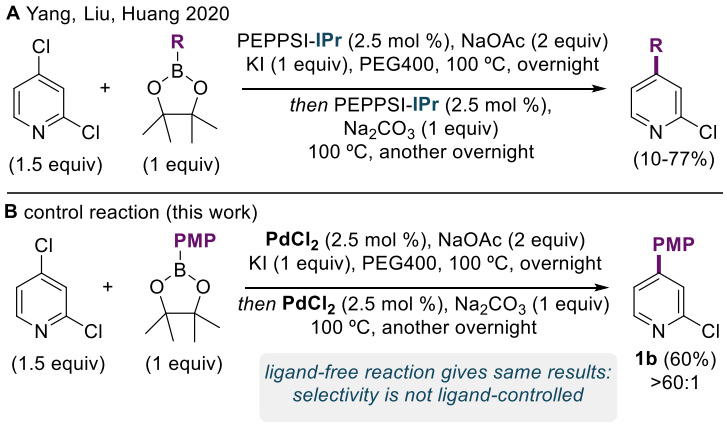
Role of Catalyst Speciation in C4 Selectivity

We were intrigued by the exceptional ~99:1 selectivity achieved under Yang et al.'s unusual conditions, as our own experience suggested that this high selectivity was uncharacteristic of a Pd/IPr catalyst. We hypothesized that selectivity might not be under ligand control under the final optimized conditions that were previously reported.

Upon conducting ligand-free control reactions, we found that IPr is not necessary for the C4 selectivity in the system reported by Yang et al. (Scheme 2.6.B). The C4-coupled product is formed in excellent selectivity using $PdCl_2$ in the absence of added ligands. As such, the selectivity in Yang's high-temperature reaction is not controlled by IPr and its mechanistic origin is not the same as that of the room-temperature Pd/IPr-catalyzed conditions that we report here. Yang et al. suggest that KI might initially react with **1** to form 2-chloro-4-iodopyridine, which then undergoes selective cross-coupling at C4−I. However, inspired by recent reports by Fairlamb,[18,19] we were intrigued by the possibility that the high C4 selectivity in the Yang system might be attributed to a

change in catalyst speciation from mono- to multinuclearity. Thus, we turned to alternative cross-coupling conditions that have been well established to promote formation of palladium nanoparticles by applying "Jeffery−Heck" conditions toward the Suzuki coupling of **1** (Table 2.2). These so-called "Jeffery" conditions are characterized by the use of simple palladium salts, inorganic bases, and tetraalkylammonium additives.[20,21]

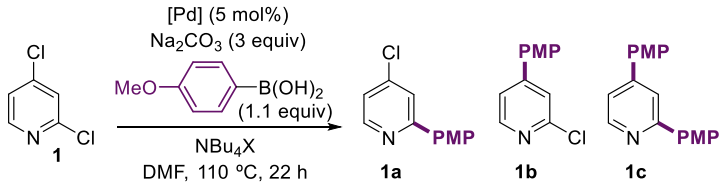
Scheme 2.6. Previously Reported C4-Selective Cross-Coupling that is Not Under Ligand Control.



Gratifyingly, ligand-free Jeffery-type conditions using $PdCl_2$, Na_2CO_3, and 3−5 equiv of NBu_4Br were found to afford remarkable C4 selectivity for the Suzuki−Miyaura coupling of **1** (Table 2.2, entries 1−2, **1a**/**1b** = 1:>99 by GC analysis). Comparable selectivity but somewhat lower conversion was observed with $Pd(OAc)_2$ or Pd_2dba_3 (entries 3 and 4). Similar results were obtained using NBu_4Cl instead of the bromide salt (compare entries 1 and 5), indicating that selectivity cannot be explained by initial Cl/Br exchange at C4. The use of only 1 equiv of NBu_4Br (entry 6), replacing the halide with a noncoordinating anion such as PF_6 (entry 7) or complete omission of the quaternary ammonium salt (entries 8−9) results in diminished selectivity and yield of **1b**, consistent with the known roles of both coordinating anions and non-coordinating cations

on stabilizing nanoparticles.[22] Added water has a marginally detrimental effect on selectivity when using 3 equiv of NBu_4Br (entries 10−11), but the combination of H_2O (5 equiv) and NBu_4Br (5 equiv, entry 14) appeared to improve conversion for some of the reactions in Scheme 2.7. Finally, lower catalyst loading (entry 12) or lower temperature (entry 13) adversely affect selectivity and yields of **1b**.

Table 2.2. Optimization of the Ligand-Free C4-Selective Suzuki Coupling. [a]

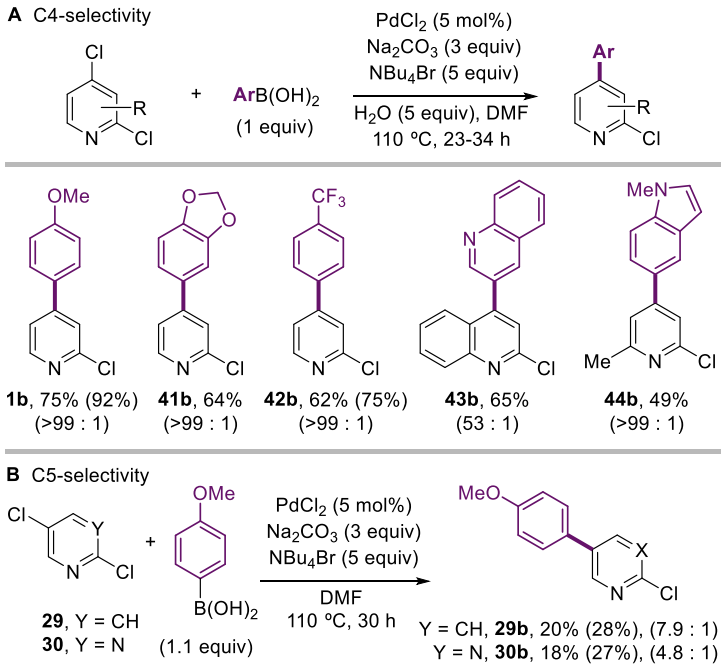


entry	[Pd]	NBu_4X (equiv)	**1a** (%)	**1b** (%)	**1c** (%)	1a : 1b
1	$PdCl_2$	Br (3)	0.5	81	0.4	1 : >99
2	$PdCl_2$	Br (5)	0.5	84	0.4	1 : >99
3	$Pd(OAc)_2$	Br (3)	0.7	73	0.4	1 : >99
4	Pd_2dba_3	Br (3)	0.5	57	0.2	1 : >99
5	$PdCl_2$	Cl (3)	1.1	72	0.5	1 : 65
6	$PdCl_2$	Br (1)	1.2	69	0.7	1 : 58
7	$PdCl_2$	PF_6 (3)	3.0	48	3.1	1 : 16
8	$PdCl_2$	--	3.5	56	3.1	1 : 16
9[b]	$PdCl_2$	--				
10[c]	$PdCl_2$	Br (3)	0.9	79	0.6	1 : 88
11[d]	$PdCl_2$	Br (3)	1.1	83	0.7	1 : 75
12[e]	$PdCl_2$	Br (3)	0.8	45	0.5	1 : 56
13[f]	$PdCl_2$	Br (3)	0.3	9	0.5	1 : 29
14[c]	$PdCl_2$	Br (5)	0.8	85	0.5	1 : >99

[a] GC yields calibrated against undecane as the internal standard. Average of two trials. [b] With KBr (3 equiv). [c] With H_2O (5 equiv). [d] With H_2O (10 equiv). [e] With 1 mol % of $PdCl_2$. [f] Reaction run at 25 °C.

The optimized Jeffery-type ligand-free conditions are general to coupling of **1** and **19** with boronic acids bearing both electron-donating and electron-withdrawing functional groups (Scheme 2.7). In all cases, C2- and diarylation products were absent or observed in only trace quantities. As such, product purification is more facile compared to the Pd/IPr conditions. Remarkably, 2,5-dichloropyridine and 2,5-dichloropyrimidine undergo preferential coupling at C5 to afford products **29b** and **30b**. This selectivity is unprecedented: all previously reported cross-couplings of these substrates with spectroscopically supported structural assignments proceed through C2−Cl cleavage.[23–25] Yields are only modest with these substrates as well as with many substituted 2,4-dichloropyridines and related electrophiles. Current work in our group aims to uncover the

Scheme 2.7. Scope of C4-Selective Suzuki-Miyaura Cross-Couplings Under Ligand-Free Catalysis. [a]



[a] Isolated yields are reported. Yields in parentheses are the calibrated GC yields of the indicated product prior to purification. Ratios are the crude ratio of C4:C2- or C5:C2-coupled products prior to purification, based on GC signal integrations.

mechanistic origin of the unique selectivity under ligand-free conditions. We anticipate that mechanistic insights will enable improvements to the reaction scope.

2.6 Conclusions

Ligand-controlled selectivity is demonstrated with a Pd/IPr catalytic system. This system is effective for C4-selective Suzuki, Kumada, and Negishi cross-couplings of a variety of substituted 2,4-dichloropyridines and related substrates. This methodology allows installation of aryl, heteroaryl, and alkyl groups at the C4 position of pyridine while retaining a chloride substituent at C2. If desired, the chloride can subsequently be replaced with a different heteroatom through an S_NAr reaction. This synthetic sequence comprising C4-selective cross-coupling followed by S_NAr provides products with a substitution pattern that can be challenging to access through more conventional methods. The mechanistic origin of ligand-controlled inversion of typical site selectivity is the focus of an upcoming report. Intriguingly, ligand-free "Jeffery" conditions are found to increase the C4 selectivity in a Suzuki coupling of 2,4-dichloropyridine by an order of magnitude. For the first time, C5-selective cross-coupling of 2,5-dichloropyridine and 2,5-dichloropyrimidine is achieved through the use of these ligand-free conditions. By analogy to the Jeffery−Heck reaction, it is likely that palladium nanoparticles are involved under these ligand-free conditions. Ongoing work in our group examines the mechanistic basis for this atypical selectivity.

2.7 References

1. Roughley, S. D.; Jordan, A. M. *J. Med. Chem.* **2011**, *54*, 3451.

2. Smith, B. R.; Eastman, C. M.; Njardarson, J. T. *J. Med. Chem.* **2014**, *57*, 9764−9773.

3. Reviews: (a) Schröter, S.; Stock, C.; Bach, T. *Tetrahedron* **2005**, *61*, 2245− 2267. (b) Fairlamb, I. J. S. *Chem. Soc. Rev.* **2007**, *36*, 1036−1045. (c) Manabe, K.; Yamaguchi, M. *Catalysts* **2014**, *4*, 307− 320. (d) Almond-Thynne, J.; Blakemore, D. C.; Pryde, D. C.; Spivey, A. C. *Chem. Sci.* **2017**, *8*, 40−62. (e) Palani, V.; Perea, M. A.; Sarpong, R. *Chem. Rev.* **2021**, DOI: 10.1021/acs.chemrev.1c00513

4. Cross-coupling examples of 2,4-dichloropyridines: (a) Cruskie, M. P. J., Jr.; Zoltewicz, J. A.; Abboud, K. A. *J. Org. Chem.* **1995**, *60*, 7491−7495. (b) Norman, M. H.; Chen, N.; Chen, Z.; Fotsch, C.; Hale, C.; Han, N.; Hurt, R.; Jenkins, T.; Kincaid, J.; Liu, L.; Lu, Y.; Moreno, O.; Santora, V. J.; Sonnenberg, J. D.; Karbon, W. *J. Med. Chem.* **2000**, *43*, 4288−4312. (c) Murray, J. I.; Woscholski, R.; Spivey, A. C. *Chem. Commun*. **2014**, *50*, 13608−13611. (d) Young, I. S.; Glass, A.-L.; Cravillion, T.; Han, C.; Zhang, H.; Gosselin, F. *Org. Lett.* **2018**, *20*, 3902−3906.

5. Cross-coupling examples of 2,4-dichloroquinoline: (a) Shiota, T.; Yamamori, T. *J. Org. Chem.* **1999**, *64*, 453−457. (b) Legros, J.-Y.; Primault, G.; Fiaud, J.-C. *Tetrahedron* **2001**, *57*, 2507−2514.

6. Cross-coupling example with 3,5-dichloropyridazine, which also favors reaction adjacent to nitrogen at C3: Blaise, E.; Kümmerle, A. E.; Hammoud, H.; de Araujo-Ju´ nior, J. X.; Bihel, F.; Bourguignon, J.-J.;´ Schmitt, M. *J. Org. Chem.* **2014**, *79*, 10311−10322.

7. Isolated reports of exceptions to C2-selectivity: (a) Dai, Y.; Hartandi, K.; Ji, Z.; Ahmed, A. A.; Albert, D. H.; Bauch, J. L.; Bouska, J. J.; Bousquet, P. F.; Cunha, G. A.; Glaser, K. B.; Harris, C. M.; Hickman, D.; Guo, J.; Li, J.; Marcotte, P. A.; Marsh, K. C.; Moskey, M. D.; Martin, R. L.; Olson, A. M.; Osterling, D. J.; Pease, L. J.; Soni, N. B.; Stewart, K. D.; Stoll, V. S.; Tapang, P.; Reuter, D. R.; Davidsen, S. K.; Michaelides, M. R. *J. Med. Chem.* **2007**, *50*, 1584−1597. (b) Khoje, A. D.; Gundersen, L.-L. Reactivity and regioselectivity in Stille couplings of 3-substituted 2,4-dichloropyridines. *Tetrahedron Lett.* **2011**, *52*, 523− 525.

8. (a) Legault, C. Y.; Garcia, Y.; Merlic, C. A.; Houk, K. N. *J. Am. Chem. Soc.* **2007**, *129*, 12664−12665. (b) Garcia, Y.; Schoenebeck, F.; Legault, C. Y.; Merlic, C. A.; Houk, K. N. *J. Am. Chem. Soc.* **2009**, *131*, 6632−6639.

9. Dai, X.; Chen, Y.; Garrell, S.; Liu, H.; Zhang, L.-K.; Palani, A.; Hughes, G.; Nargund, R. *J. Org. Chem.* **2013**, *78*, 7758−7763.

10. Reeves, E. K.; Humke, J. N.; Neufeldt, S. R. *J. Org. Chem.* **2019**, *84*, 11799−11812.

11. Yang, M.; Chen, J.; He, C.; Hu, X.; Ding, Y.; Kuang, Y.; Liu, J.; Huang, Q. *J. Org. Chem.* **2020**, *85*, 6498−6508.

12. Melvin, P. R.; Nova, A.; Balcells, D.; Dai, W.; Hazari, N.; Hruszkewycz, D. P.; Shah, H. P.; Tudge, M. T. *ACS Catal.* **2015**, *5*, 3680−3688.

13. We hypothesize that polar solvents can promote a more polar "displacement" mechanism for oxidative addition, compared to a 3-centered mechanism in nonpolar solvents. These two different mechanisms are biased toward C2 versus C4 selectivity, respectively (a detailed mechanistic study is forthcoming).

14. Pd/IPent has been shown to promote exhaustive arylation in other contexts. Although the origin of IPent's effect has not been studied, it is likely that its steric bulk disfavors dissociation of Pd from the product after reductive elimination: Groombridge, B. J.; Goldup, S. M.; Larrosa, I. *Chem. Commun.* **2015**, *51*, 3832−3834.

15. Cook, X. A. F.; Gombert, A.; McKnight, J.; Pantaine, L. R. E.; Willis, M. C. *Angew. Chem., Int. Ed.* **2021**, *60*, 11068− 11091.

16. Examples: (a) Banks, R. E.; Burgess, J. E.; Cheng, W. M.; Haszeldine, R. N. 93. Heterocyclic polyfluoro-compounds. Part IV. Nucleophilic substitution in pentafluoropyridine: the preparation and properties of some 4-substituted 2,3,5,6-tetrafluoropyridines. *J. Chem. Soc.* **1965**, 575−581. (b) Mittelbach, M. *Synthesis* **1988**, *1988*, 479−480. (c) Schlosser, M.; Rausis, T.; Bobbio, C. *Org. Lett*. **2005**, *7*, 127−129. (d) Schlosser, M.; Bobbio, C.; Rausis, T. *J. Org. Chem.* **2005**, *70*, 2394−2502.

17. Duan, J.; Jian, B.; Lu, Z. Azaindoles as BTK Kinase Modulators and Use Thereof. WO 2011019780 A1, February 17, 2011; pp 63− 64.

18. (a) Scott, N. W. J.; Ford, M. J.; Jeddi, N.; Eyles, A.; Simon, L.; Whitwood, A. C.; Tanner, T.; Willans, C. E.; Fairlamb, I. J. S. A *J. Am. Chem. Soc.* **2021**, *143*, 9682−9693. (b) Appleby, K. M.; Dzotsi, E.; Scott, N. W. J.; Dexin, G.; Jeddi, N.; Whitwood, A. C.; Pridmore, N. E.; Hart, S.; Duckett, S. B.; Fairlamb, I. J. S. *Organometallics* **2021**, *40*, 3560−3570.

19. Fairlamb's conditions employ PPh_3 in a low ligand:Pd ratio, which promote formation of clusters and nanoparticles. These conditions were shown to effect C4-selective cross-coupling of 2,4-dibromopyridine (C2/C4 ∼ 1:10). Notably, Fairlamb's conditions are not effective for C4-selective cross-coupling of 2,4-dichloropyridine (see Appendix A).

20. (a) Jeffery, T. *J. Chem. Soc., Chem. Commun.* **1984**, 1287−1289. (b) Jeffery, T. *Tetrahedron Lett.* **1985**, *26*, 2667− 2670. (c) Jeffery, T. *Tetrahedron* **1996**, *52*, 10113−10130.

21. Chernyshev, V. M.; Khazipov, O. V.; Eremin, D. B.; Denisova, E. A.; Ananikov, V. P. *Coord. Chem. Rev.* **2021**, *437*, 213860.

22. de Vries, J. G. When Does Catalysis with Transition Metal Complexes Turn into Catalysis by Nanoparticles?. *Selective Nanocatalysts and Nanoscience*, 2011; Wiley:VCH, pp 73−103.

23. For selected examples of typical selectivity with 2,5- dihalopyrimidine see: (a) Hughes, G.; Wang, C.; Batsanov, A. S.; Fern, M.; Frank, S.; Bryce, M. R.; Perepichka, I. F.; Monkman, A. P.; Lyons, B. P. *Org. Biomol. Chem.* **2003**, *1*, 3069−3077. (b) Malik, I.; Ahmed, Z.; Reimann, S.; Ali, I.; Villinger, A.; Langer, P. *Eur. J. Org. Chem.* **2011**, *2011*, 2088−2093.

24. For selected examples of typical selectivity with 2,5- dichloropyridines see: (a) Brumfield, S.; Matasi, J. J.; Tulshian, D.; Czarniecki, M.; Greenlee, W.; Garlisi, C.; Qiu, H.; Devito, K.; Chen, S.-C.; Sun, Y.; Bertorelli, R.; Ansell, J.; Geiss, W.; Le, V.-D.; Martin, G. S.; Vellekoop, S. A.; Haber, J.; Allard, M. L. *Bioorg. Med. Chem. Lett.* **2011**, *21*, 7287−7290. (b) Curreli, F.; Ahmed, S.; Benedict Victor, S. M.; Iusupov, I. R.; Belov, D. S.; Markov, P. O.; Kurkin, A. V.; Altieri, A.; Debnath, A. K. *J. Med. Chem*. **2020**, *63*, 1724−1749.

25. For reported exceptions to conventional selectivity of 2,5-dichloropyridine and -pyrimidine in direct arylations and Sonogashira couplings, albeit without spectroscopic support for structural assignment of the products, see (a) Zheng, L.-L.; Yin, B.; Tian, X.- C.; Yuan, M.-Y.; Li, X.-H.; Gao, F. *Tetrahedron Lett.* **2019**, *60*, 151316. (b) Al-Khawaldeh, I.; Al Yasiri, M. J.; Aldred, G. G.; Basmadjian, C.; Bordoni, C.; Harnor, S. J.; Heptinstall, A. B.; Hobson, S. J.; Jennings, C. E.; Khalifa, S.; Lebraud, H.; Martin, M. P.; Miller, D. C.; Shrives, H. J.; de Souza, J. V.; Stewart, H. L.; Temple, M.; Thomas, H. D.; Totobenazara, J.; Tucker, J. A.; Tudhope, S. J.; Wang, L. Z.; Bronowska, A. K.; Cano, C.; Endicott, J. A.; Golding, B. T.; Hardcastle, I. R.; Hickson, I.; Wedge, S. R.; Willmore, E.; Noble, M. E. M.; Waring, M. J. *J. Med. Chem*. **2021**, *64*, 10001−10018.

CHAPTER THREE

DIFFERENT OXIDATIVE ADDITION MECHANISMS FOR 12- AND 14-ELECTRON PALLADIUM(0) EXPLAIN LIGAND-CONTROLLED DIVERGENT SITE SELECTIVITY

3.1 Contribution of Authors and Co-Authors

Manuscript in Chapter 3

Author: Jacob P. Norman

Contributions: Performed experimental work, edited the manuscript, and wrote sections of the supporting information (Appendix B).

Co-Author: Nathaniel G. Larson

Contributions: Performed experimental work, edited the manuscript, and wrote sections of the supporting information (Appendix B).

Co-Author: Sharon R. Neufeldt

Contributions: Performed DFT calculations, wrote the manuscript, and edited the supporting information in Appendix B.

3.2 Manuscript Information

Jacob P. Norman, Nathaniel G. Larson, Sharon R. Neufeldt

ACS Catalysis

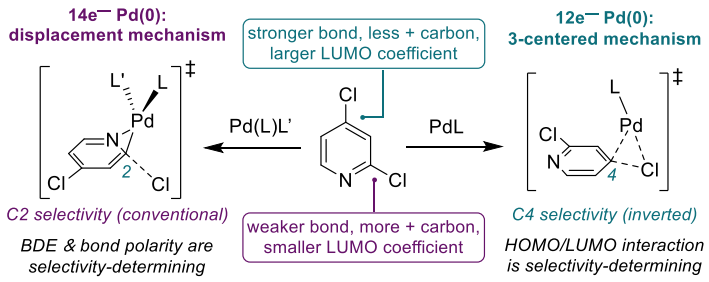
Status of Manuscript:
____ Prepared for submission to a peer-reviewed journal
____ Officially submitted to a peer-reviewed journal
____ Accepted by a peer-reviewed journal
_X_ Published in a peer-reviewed journal

American Chemical Society
ACS Catal. **2022**, *12,* 15, 8822–8828.
DOI: 10.1021/acscatal.2c01698

3.3 Abstract

In cross-coupling reactions, dihaloheteroarenes are usually most reactive at C–halide bonds adjacent to a heteroatom. This selectivity has been previously rationalized. However, no mechanistic explanation exists for anomalous reports in which specific ligands effect inverted selectivity with dihalopyridines and -pyridazines. Here we provide evidence that these ligands uniquely promote oxidative addition at 12e⁻ Pd(0). Computations indicate that 12e⁻ and 14e⁻ Pd(0) can favor different mechanisms for oxidative addition due to differences in their HOMO symmetries. These mechanisms are shown to lead to different site preferences, where 12e⁻ Pd(0) can favor oxidative addition at an atypical site distal to nitrogen.

Scheme 3.1. Graphical abstract for the *ACS Catal.* manuscript.

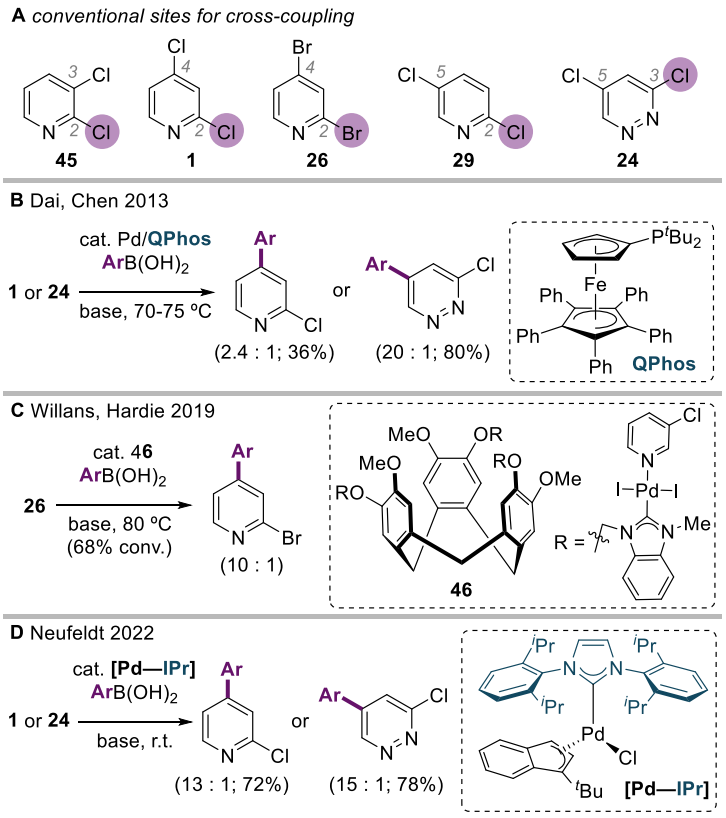


3.4 Introduction

Heteroarenes are common motifs in high-value small molecules such as pharmaceutical drugs and agrichemicals.[1] A popular method for their elaboration involves employing halogenated heteroarene substrates in cross-coupling reactions. Dihaloheteroarenes bearing two identical halides typically react with predictable selectivity at a C−X bond α to a heteroatom, when present (Scheme 3.2.A).[2] However, the ability to invert selectivity can open up underexplored synthetic

space. Because of the importance of dihaloheteroarene cross-coupling reactions, the origin of their innate selectivity has been thoroughly studied. Houk and Merlic rationalized the typical selectivity with a distortion-interaction model.[3] Relevant to the current work, oxidative addition of 6-membered nitrogen-containing dihaloheteroarenes takes place at the weaker C−X bond, which is the bond adjacent to nitrogen. Because this bond is weaker, it is easier to distort into the transition state geometry. Leitch et al. recently demonstrated that conventional selectivity is also correlated with more positive electrostatic potentials at the *ipso* carbon and with more negative potentials at an *ortho* atom.[4]

Scheme 3.2. Ligands that Give Unconventional Selectivity.

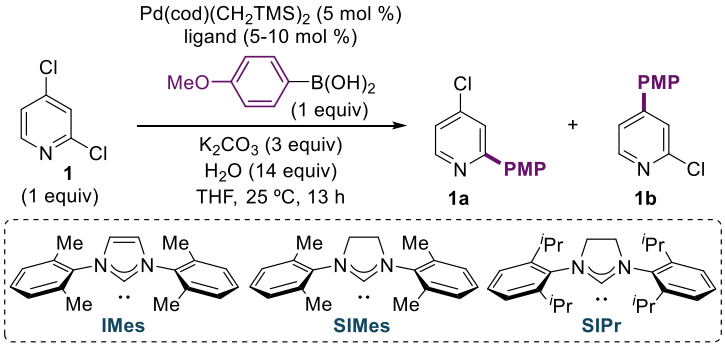


Although current models explain the conventional selectivity of 6-membered dihaloheteroarenes, there exist rare reports in which the use of specific ligands leads to inverted selectivity, resulting in cross-coupling at a site distal to nitrogen. The use of QPhos gives modest C4-selectivity with **1** and high C5- selectivity with **24** (Scheme 3.2.B).[5] Bulky NHC ligands (**46** and IPr) can promote C4-selectivity with **1** and **26** and C5- selectivity with **24** (Scheme 3.2.C,D).[6–9] There is currently no mechanistic rationale for these ligand-controlled deviations from the conventional selectivity.[10] The absence of mechanistic understanding precludes rational catalyst design, and thus, cross-coupling reactions at distal C−X bonds remain unexplained curiosities. Here, we communicate the key discovery that two competing mechanisms for oxidative addition display different site preferences. Due to its HOMO π-symmetry, 14e− Pd(0) prefers to react with halogenated heteroarenes through a nucleophilic displacement mechanism at an α C−Cl bond. Conversely, 12e− Pd(0) prefers a concerted three-centered transition state due to its HOMO σ-symmetry, and this mechanism is biased toward a distal C−Cl bond. As such, accessing 12e− Pd(0) is critical to achieving oxidative addition at the atypical site.

3.5 Results and Discussion

The reported C4- and C5-cross-couplings of **1**, **26**, and **24** employ very sterically hindered electron-rich monodentate ligands.[5–7] To further evaluate ligand effects, we screened a number of monodentate phosphines and NHC ligands for the Suzuki coupling of **1** using $Pd(cod)(CH_2SiMe_3)_2$ (Table 3.1).[11] There is a clear correlation between ligand sterics and the C4:C2 ratio for triarylphosphines (entries 1−4), alkylphosphines (entries 5−13), and NHCs (entries 14−18). Bulky alkyl phosphines are more C4-selective than bulky triaryl phosphines, and unsaturated NHC ligands are more selective than their saturated analogues. On the basis of these trends, we

Table 3.1. Evaluation of Monodentate Ligands for the Suzuki—Miyaura Coupling Using $Pd(OAc)_2$.



entry	ligand (mol %)	%V_{bur} (min)[b]	**1a** (%)	**1b** (%)	1a : 1b
1	PPh_3 (5)	(28.2)	84.2	0.6	>99 : 1
2	PPh_3 (10)		81.6	0.4	>99 : 1
3	P(*o*-tol)$_3$ (5)	(34.4)	42.0	21.5	2.0 : 1
4	P(*o*-tol)$_3$ (10)		30.3	17.0	1.8 : 1
5	PMe_3 (5)	(22.1)	18.5	2.2	8.4 : 1
6	PMe_3 (10)		9.9	0.9	11.0 : 1
7	P(*n*-Bu)$_3$ (5)	(24.2)	20.0	7.6	2.6 : 1
8	P(*n*-Bu)$_3$ (10)		0.8	0.3	3.2 : 1
9	PCy_3 (5)	(30.2)	27.9	44.9	1 : 1.6
10	PCy_3 (10)		27.2	39.9	1 : 1.5
11	PAd_2(*n*-Bu) (5)	(32.8)	24.1	51.8	1 : 2.2
12	P^{t}Bu$_3$ (5)	(36.3)	27.0	47.3	1 : 1.8
13	Q-Phos (5)	(47.6)	24.1	50.1	1 : 2.1
14	IMes (5)	36.5	32.5	52.0	1 : 1.6
15	SIMes (5)	36.9	27.9	22.0	1.3 : 1
16	IPr (5)	44.5	9.5	66.8	1 : 7.0
17	IPr[c]		6.6	68.4	1 : 10.4
18	SIPr (5)	47.0	9.5	36.4	1 : 3.8

[a] GC yields calibrated against undecane as the internal standard. Average of two trials. 0–6.5% diarylation observed in all entries (see Appendix B). PMP = *p*-methoxyphenyl. [b] Values in parentheses are minimum percent buried volumes obtained from the Kraken database.[12] Percent buried volumes of NHCs reported for LAuCl complexes at a L–Au distance of 2.00 Å from reference.[13] [c] With (η^3-1-^{t}Bu-indenyl)Pd(IPr)(Cl) (3 mol %) as catalyst, 15.5 h.

hypothesized that sterically hindered strong σ-donor ligands favor unconventional selectivity by promoting oxidative addition at a low-coordinate species (i.e., 12e− PdL). Smaller ligands or ones that are better π-acceptors, such as PAr_3 and saturated NHCs, would be more likely to favor coordination of a second ligand.[14–16] Notably, among trialkylphosphines, selectivity switches near the $\%V_{bur}$(min) threshold that was previously reported to determine whether PdL or PdL_2 dominates as the active species for oxidative addition.[17,18] Nevertheless, it was unclear why 12e− PdL might react at the stronger C4−Cl bond. To evaluate this question, we used density functional theory (DFT) calculations to closely examine the mechanisms of oxidative addition at 12e− and 14e− Pd(0) using a simple model system comprising PhCl and $Pd(PMe_3)_n$ (n = 1 or 2). Three oxidative addition transition structures were located with $Pd(PMe_3)$ (Figure 3.1A). Two of these (**TS7a** and **TS7b**) represent classic 3-centered concerted mechanisms, wherein Pd simultaneously interacts with the *ipso* carbon and the chloride. The third structure is better described as a nucleophilic displacement mechanism (**TS7c**). In this mechanism, Pd interacts with both the *ipso* and the *ortho* carbons of the aromatic ring, as evidenced by the short C_{ortho}− Pd distance (2.49 Å). Conversely, the long Pd−Cl distance indicates that there is no significant interaction between Pd and Cl. This type of mechanism has also been referred to as a nucleophilic substitution (S_NAr-type) mechanism[19] or a dissociative process.[20]

For monoligated $Pd(PMe_3)$, the lowest-energy transition structure is the concerted mechanism **TS7a.** In contrast, a nucleophilic displacement mechanism (**TS8b**) is favored over a concerted mechanism (**TS8a**) for bisligated $Pd(PMe_3)_2$ (Figure 3.1B).[23–25] This difference in the preferred mechanisms for PdL and PdL_2 may be explained by frontier molecular orbital interactions. The HOMO of $Pd(PMe_3)$ is a σ-type orbital, so its symmetry is suited to the concerted mechanism in which Pd donates only into the *ipso* carbon (via overlap with chlorobenzene's

lowest-energy unoccupied orbital without a node through the *ipso* carbon, LUMO + 1).[26] In contrast, the HOMO of $Pd(PMe_3)_2$ has π-symmetry (Figure 3.1C) and, thus, can backbond into two carbons of PhCl during oxidative addition via a displacement mechanism. Notably, simple model ligands like PMe_3 are not always adequate for describing the behavior of more complex ligands.[27] Furthermore, Maseras and co-workers have shown that ligand identity and solvent can influence the predicted mechanism of oxidative addition at 14e− PdL_2 with the substrate bromobenzene.[19,28]

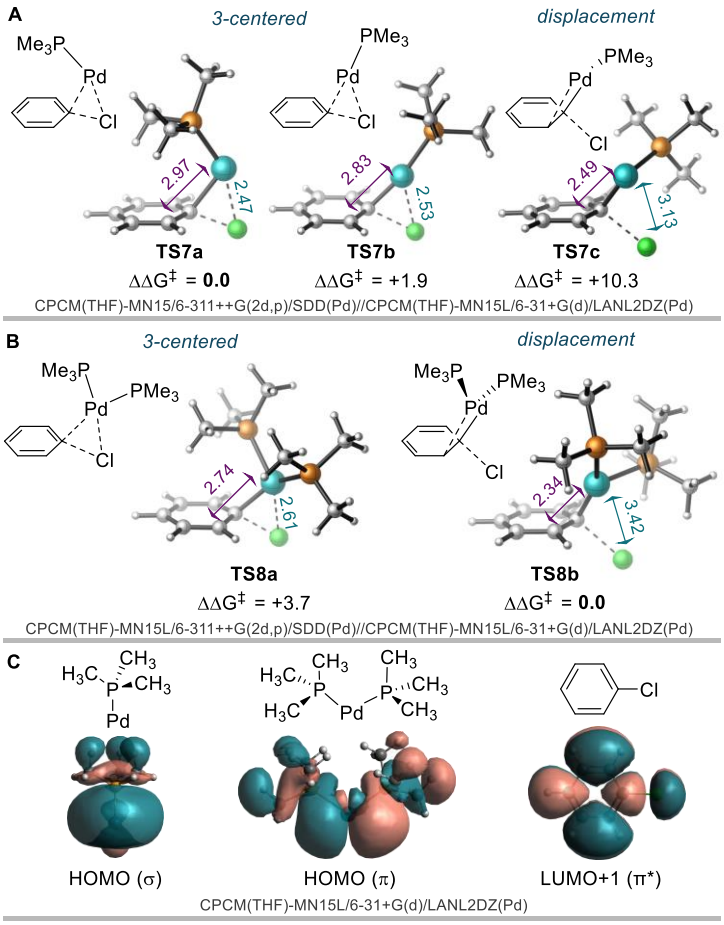


Figure 3.1. Calculated transition structures for oxidative addition of chlorobenzene at (A) $Pd(PMe_3)$ and (B) $Pd(PMe_3)_2$. Differences in Gibbs free energies of activation are listed in units of kcal mol^{-1} relative to the lowest-energy structure in each set (defined as $\Delta\Delta G^{\ddagger} = 0.0$).[21] (C) Key frontier molecular orbitals of the relevant species, where $Pd(PMe_3)_2$ is distorted into a bent geometry as adopted in the arene—$Pd(PMe_3)_2$ pre-oxidative addition π-complex.[22]

However, in this case, our calculations using $Pd(PMe_3)_n$ and PhCl prove to be consistent with those obtained using Pd(IPr) and 2,4-dichloropyridine (**1**).

The LUMO of 2,4-dichloropyridine has π-symmetry, with nodal planes on either side of nitrogen and of C4 (Figure 3.2, inset). The LUMO coefficient at C4 is substantially larger than at C2, with C4 accounting for 26% of the LUMO density and C2 contributing only 8%. Thus, it becomes apparent why PdL_2 and PdL might exhibit different site-selectivity. Because the π-type HOMO of PdL_2 would donate into two atoms of the pyridine ring during a nucleophilic displacement mechanism, strong orbital overlap can be achieved during reaction at C2 despite the small LUMO coefficient at that carbon, and bond dissociation energies and electrostatic potentials become more important to selectivity. However, the σ-type HOMO of PdL can only donate into one atom of the pyridine ring. As such, the larger LUMO coefficient at C4 versus C2 is important during the reaction of PdL because it dictates the strength of the $HOMO_{(Pd)}/LUMO_{(substrate)}$ overlap.

Using monoligated Pd(IPr), a 3-centered mechanism for oxidative addition at C2 (**TS10a-IPr**, Figure 3.2A) is preferred over a displacement mechanism (see Appendix B). Only a 3-centered mechanism could be located for oxidative addition at C4 (**TS10b-IPr**). DFT predicts that reaction at C4 via **TS10b-IPr** should be favored over C2 by 1.7 kcal/mol (C4:C2 = 18:1) using Pd(IPr). This prediction is in good agreement with the experimentally reported C4-selectivity with IPr (typically ∼10:1)[7] and stands in stark contrast to the prediction with bisligated Pd(IPr)(L). Unsurprisingly, considering the sterics of IPr, we were unable to find transition structures involving $Pd(IPr)_2$. However, nucleophilic displacement transition structures were located with bisligated Pd(IPr)(L) where L is a second substrate molecule (**1**).[29] With the bisligated complex, C2−Cl via **TS13a-IPr** is strongly favored over reaction at C4 (**TS13b-IPr**). Overall, the lowest-energy path

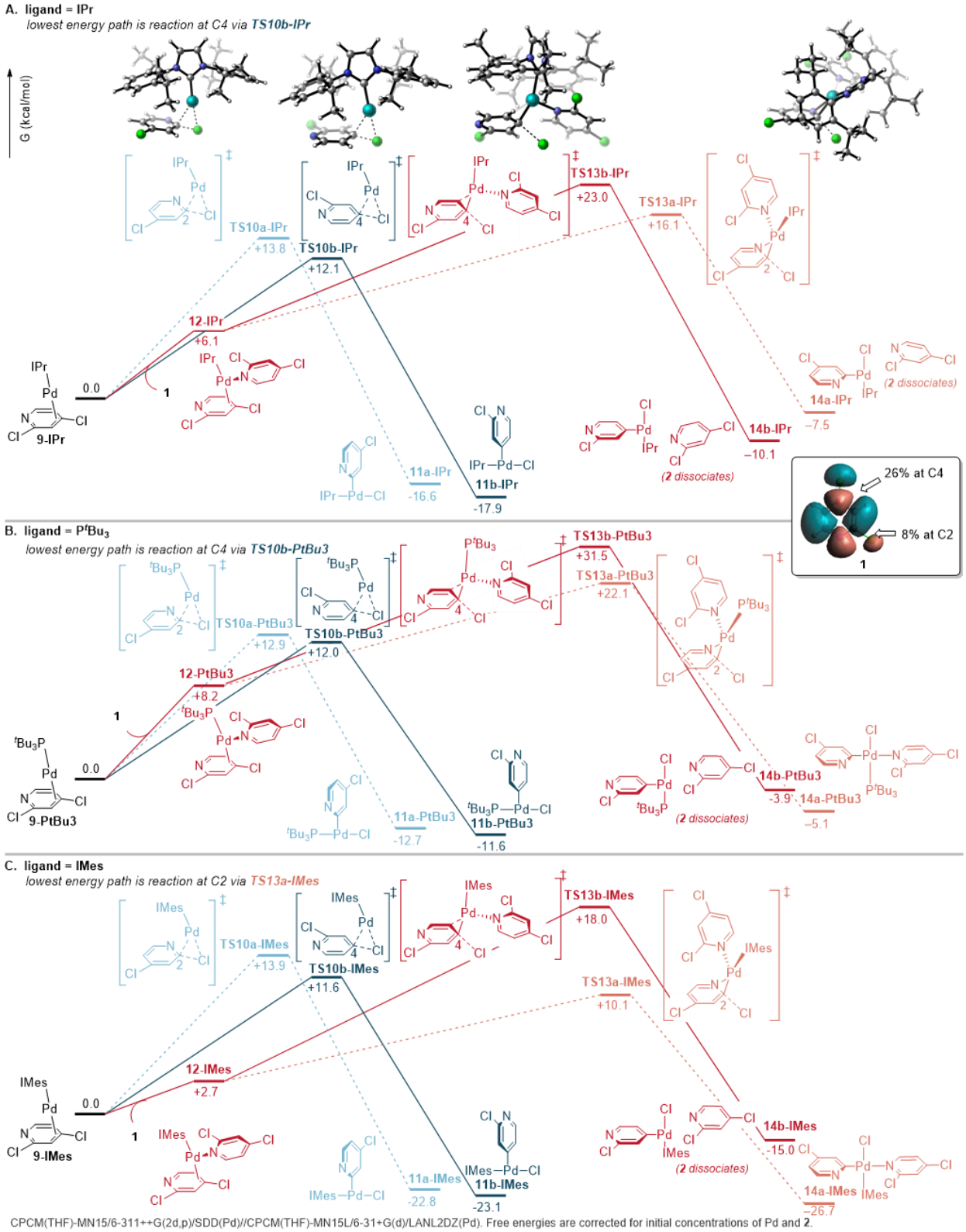


Figure 3.2. Calculated free energy diagrams illustrating the oxidative addition of 2,4-dichloropyridine at Pd(NHC) or Pd(NHC)(**1**), where NHC = IPr (A) or IMes (B). [21,22,34]

in Figure 3.2.A is C4-oxidative addition at monoligated Pd(IPr) via **TS10b-IPr**, consistent with experimental selectivity with this ligand.

For comparison, analogous DFT calculations were performed with P^{t}Bu$_3$, another bulky monodentate ligand that favors reaction at C4 but to a lesser extent than IPr (see Table 3.1, entry 12). Consistent with experiment, the DFT calculations predict worse C4-selectivity with Pd(P^{t}Bu$_3$) (Figure 3.2.B, predicted C4:C2 = 5:1, experimental C4:C2 = 2:1). The enhanced selectivity of IPr compared to P^{t}Bu$_3$ is likely due to the stronger σ-donation by IPr,[14d,30] which could enhance the PdL(HOMO) → **1**(LUMO) interaction (see Appendix B for further discussion). Like IPr, P^{t}Bu$_3$ is too bulky for a bisligated transition state to contribute significantly to the reaction mechanism.

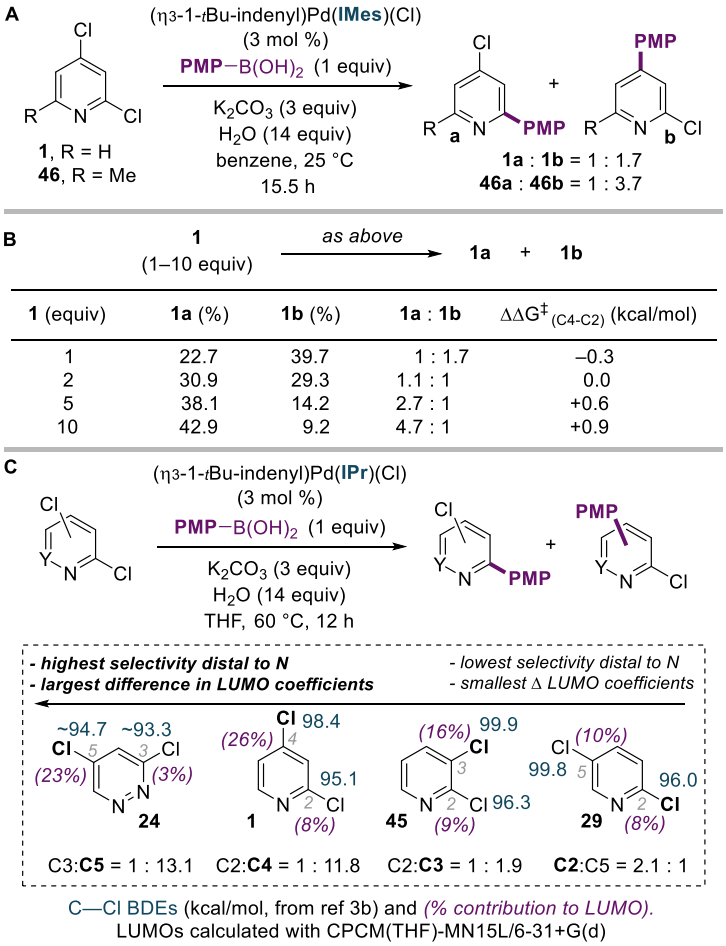
DFT calculations with IMes reveal similar trends as seen with IPr: PdL favors reaction at C4 (Figure 3.2.C, **TS10b-IMes**), while PdL$_2$ favors reaction at C2 (**TS13a-IMes**). However, unlike IPr, the calculations with IMes predict that the bisligated path via **TS13a-IMes**, involving oxidative addition at C2, is energetically competitive with the monoligated path (C4:C2 = 1:13 based on **TS10b-IMes** and **TS13a-IMes**). This prediction is consistent with the experimental observation that IMes is much less C4-selective than IPr and supports the hypothesis that smaller ligands lead to a higher proportion of bisligated active catalyst. The calculations do not quantitatively reproduce the experimentally observed 1.6:1 selectivity with IMes (Table 3.1, entry 14). However, the energy of the crowded transition structure **TS13a-IMes** was found to be extremely sensitive to the DFT method (see Appendix B), likely due in part to differences in how dispersion interactions are handled. This suggests the possibility of considerable error in quantitative analysis when comparing mono- to bisligated structures. Furthermore, these calculations cannot take into account the ability of **1** to coordinate to other acids that are present in higher concentrations than Pd under the catalytic conditions (e.g., boron, K+ , H$_2$O). Equilibria

involving coordination of **1** to these species would detract from the overall concentration of Pd(IMes)(**1**).

The calculations suggest that IMes gives worse C4-selectivity than IPr due to a higher proportion of bisligated active catalyst. Experimental data support the hypothesis that an N-bound dichloropyridine group could serve as the second ligand on Pd in Suzuki couplings catalyzed by Pd/IMes. C4-selectivity is significantly enhanced for **46** compared to **1** (Scheme 3.3.A), where **46** should be a worse ligand for Pd due to sterics.[31] Furthermore, increased reaction is observed at C2 at higher substrate concentrations (Scheme 3.3.B). The increased C2- selectivity at high [**1**] is consistent with a higher probability for reaction at bisligated Pd(IMes)(**1**).

On the basis of the calculations, we anticipated that, under conditions that promote oxidative addition at 12e− PdL using IPr, selectivity should trend with the difference between LUMO coefficients at the two sites of a dihaloheteroarene. Indeed, this prediction bears out for the substrates in Scheme 3.3.B. The best selectivity for the site remote to nitrogen is achieved with the substrate displaying the largest difference in LUMO coefficients (**24**), while preferential reaction at C2 is observed when the two sites have nearly identical LUMO coefficients (**29**).[32,33] To our knowledge, this is the first report of C3-favored cross-coupling of **45** supported by spectroscopic characterization, although diarylation is competitive with monoarylation (see Appendix B).

Scheme 3.3. (A) Influence of 6-Substituent on the Selectivity of Cross-Coupling Catalyzed by Pd/IMes; (B) Influence of Substrate Concentration on the Selectivity of Cross-Coupling Catalyzed by Pd/IMes; and (C) with Pd/IPr, Selectivity Trends with Difference in LUMO Coefficients.



3.6 Conclusion

This work shows that 12- and 14-electron Pd(0) can favor different mechanisms for oxidative addition due to differences in their HOMO symmetries. The HOMO σ-symmetry of 12e− PdL means that LUMO coefficients at individual sites of dihaloheteroarenes are particularly important for determining selectivity. Conversely, the HOMO π-symmetry of 14e− PdL_2 enables

Pd to backbond into two atoms of the substrate during oxidative addition, rendering LUMO coefficients at individual atoms less important, and allowing selectivity to be dominated by other factors including C−X bond strengths. This work has implications for understanding oxidative addition reactivity trends and for rational design of site-selective catalysts. A systematic evaluation of the factors influencing the preferred mechanisms of oxidative addition will be reported in due course.

3.7. References

1. Pennington, L. D.; Moustakas, D. T. *J. Med. Chem.* **2017**, *60*, 3552−3579.

2. For reviews, see: (a) Schröter, S.; Stock, C.; Bach, T. *Tetrahedron* **2005**, *61*, 2245−2267. (b) Fairlamb, I. J. S. *Chem. Soc. Rev.* **2007**, *36*, 1036−1045. (c) Manabe, K.; Yamaguchi, M. *Catalysts* **2014**, *4*, 307−320. (d) Almond-Thynne, J.; Blakemore, D. C.; Pryde, D. C.; Spivey, A. C. *Chem. Sci.* **2017**, *8*, 40−62. (e) Palani, V.; Perea, M. A.; Sarpong, R. *Chem. Rev.* **2022**, *122*, 10126−10169.

3. (a) Legault, C. Y.; Garcia, Y.; Merlic, C. A.; Houk, K. N. *J. Am. Chem. Soc.* **2007**, *129*, 12664−12665. (b) Garcia, Y.; Schoenebeck, F.; Legault, C. Y.; Merlic, C. A.; Houk, K. N. *J. Am. Chem. Soc.* **2009**, *131*, 6632−6639.

4. Lu, J.; Donnecke, S.; Paci, I.; Leitch, D. C. *Chem. Sci.* **2022**, *13*, 3477−3488.

5. Dai, X.; Chen, Y.; Garrell, S.; Liu, H.; Zhang, L.-K.; Palani, A.; Hughes, G.; Nargund, R. *J. Org. Chem.* **2013**, *78*, 7758−7763.

6. Fowler, J. M.; Britton, E.; Pask, C. M.; Willans, C. E.; Hardie, M. J. *Dalton Trans.* **2019**, *48*, 14687−14695.

7. Norman, J. P.; Larson, N. G.; Entz, E. D.; Neufeldt, S. R. *J. Org. Chem.* **2022**, *87*, 7414−7421.

8. Yang, M.; Chen, J.; He, C.; Hu, X.; Ding, Y.; Kuang, Y.; Liu, J.; Huang, Q. *J. Org. Chem.* **2020**, *85*, 6498−6508.

9. (a) The precatalysts used in ref 7 are of the type (η^3-1-^{t}Bu-indenyl)Pd(NHC)(Cl) and were designed to release monoligated PdL: Melvin, P. R.; Nova, A.; Balcells, D.; Dai, W.; Hazari, N.; Hruszkewycz, D. P.; Shah, H. P.; Tudge, M. T. *ACS Catal.* **2015**, *5*, 3680−3688. (b) Espinosa, M. R.; Doppiu, A.; Hazari, N. *Adv. Synth. Catal.* **2020**, *362*, 5062−5078.

10. (a) Multinuclear clusters are implicated in C4-selective cross-coupling of 2,4-dibromopyridine at low ligand loadings in a Pd/PPh_3 system, although the reason for a C4-preference of multinuclear clusters is not yet known: Scott, N. W. J.; Ford, M. J.; Jeddi, N.; Eyles, A.; Simon, L.; Whitwood, A. C.; Tanner, T.; Willans, C. E.; Fairlamb, I. J. S. *J. Am. Chem. Soc.* **2021**, *143*, 9682−9693. (b) Appleby, K. M.; Dzotsi, E.; Scott, N. W. J.; Dexin, G.; Jeddi, N.; Whitwood, A. C.; Pridmore, N. E.; Hart, S.; Duckett, S. B.; Fairlamb, I. J. S. *Organometallics* **2021**, *40*, 3560−3570.

11. (a) For examples of the use of Pd(cod)(CH_2SiR_3)$_2$ + free ligand "L" as a precursor to putative PdL_n see: Fors, B. P.; Watson, D. A.; Biscoe, M. R.; Buchwald, S. L. *J. Am. Chem. Soc.* **2008**,

130, 13552−13554. (b) Watson, D. A.; Su, M.; Teverovskiy, G.; Zhang, Y.; Garcia-Fortanet, J.; Kinzel, T.; Buchwald, S. L. Formation of ArF from LPdAr(F): Catalytic Conversion of Aryl Triflates to Aryl Fluorides. *Science* **2009**, *325*, 1661−1664. (c) Sergeev, A. G.; Schulz, T.; Torborg, C.; Spannenberg, A.; Neumann, H.; Beller, M. *Angew. Chem.*, *Int. Ed.* **2009**, *48*, 7595−7599. (d) Larini, P.; Kefalidis, C. E.; Jazzar, R.; Renaudat, A.; Clot, E.; Baudoin, O. *Chem.−Eur. J.* **2012**, *18*, 1932−1944. (e) Andersen, T. L.; Friis, S. D.; Audrain, H.; Nordeman, P.; Antoni, G.; Skrydstrup, T. *J. Am. Chem. Soc.* **2015**, *137*, 1548−1555. (f) Milner, P. J.; Yang, Y.; Buchwald, S. L. *Organometallics* **2015**, 34, 4775−4780. (g) Elias, E. K.; Rehbein, S. M.; Neufeldt, S. R. *Chem. Sci.* **2022**, *13*, 1618−1628.

12. Gensch, T.; dos Passos Gomes, G.; Friederich, P.; Peters, E.; Gaudin, T.; Pollice, R.; Jorner, K.; Nigam, A.; Lindner-D'Addario, M.; Sigman, M. S.; Aspuru-Guzik, A. *J. Am. Chem. Soc.* **2022**, *144*, 1205−1217.

13. Clavier, H.; Nolan, S. P. *Chem. Commun.* **2010**, *46*, 841−861.

14. (a) Vummaleti, S. V. C.; Nelson, D. J.; Poater, A.; Gómez-Suárez, A.; Cordes, D. B.; Slawin, A. M. Z.; Nolan, S. P.; Cavallo, L. *Chem. Sci.* **2015**, *6*, 1895−1904. (b) Lummiss, J. A. M.; Higman, C. S.; Fyson, D. L.; McDonald, R.; Fogg, D. E. *Chem. Sci.* **2015**, *6*, 6739−6746. (c) Back, O.; Henry-Ellinger, M.; Martin, C. D.; Martin, D.; Bertrand, G. *Angew. Chem., Int. Ed.* **2013**, *52*, 2939−2943. (d) Morán-González, L.; Pedregal, J. R.-G.; Besora, M.; Maseras, F. *App. Eur. J. Inorg. Chem.* **2022**, No. e202100932.

15. (a) For examples of nitrogen-containing substrates/products acting as ligands for Pd during cross-couplings, see: Alcazar-Roman, L. M.; Hartwig, J. F.; Rheingold, A. L.; Liable-Sands, L. M.; Guzei, I. A. *J. Am. Chem. Soc.* **2000**, *122*, 4618−4630. (b) Singh, U. K.; Strieter, E. R.; Blackmond, D. G.; Buchwald, S. L. *J. Am. Chem. Soc.* **2002**, *124*, 14104−14114. (c) Jutand, A.; Négri, S.; Principaud, A. *Eur. J. Inorg. Chem.* **2005**, *2005*, 631−635. (d) Tougerti, A.; Negri, S.; Jutand, A. *Chem. -Eur. J.* **2007**, *13*, 666−676. (e) Perego, L. A.; Grimaud, L.; Bellina, F. *Adv. Synth. Catal.* **2016**, *358*, 597−609.

16. (a) Evidence has been reported for oxidative addition of aryl halides at both bisligated $Pd(PPh_3)_2$ and monoligated $Pd(PPh_3)$: Amatore, C.; Jutand, A.; Khalil, F.; M'Barki, M. A.; Mottier, L. *Organometallics* **1993**, *12*, 3168−3178. (b) Joshi, C.; Macharia, J. M.; Izzo, J. A.; Wambua, V.; Kim, S.; Hirschi, J. S.; Vetticatt, M. J. *ACS Catal.* **2022**, *12*, 2959− 2966.

17. Newman-Stonebraker, S. H.; Smith, S. R.; Borowski, J. E.; Peters, E.; Gensch, T.; Johnson, H. C.; Sigman, M. S.; Doyle, A. G. *Science* **2021**, *374*, 301−308.

18. (a) Evidence suggests that PCy_3 can support oxidative addition at both $Pd(PCy_3)$ and $Pd(PCy_3)_2$: Mitchell, E. A.; Jessop, P. G.; Baird, M. C. *Organometallics* **2009**, *28*, 6732−6738. (b) Barrios-Landeros, F.; Carrow, B. P.; Hartwig, J. F. *J. Am. Chem. Soc.* **2009**, *131*,

8141−8154. (c) McMullin, C. L.; Jover, J.; Harvey, J. N.; Fey, N. *Dalton Trans.* **2010**, *39*, 10833−10836.

19. (a) Portnoy, M.; Milstein, D. *Organometallics* **1993**, *12*, 1665−1673. (b) Maes, B. U. W.; Verbeeck, S.; Verhelst, T.; Ekomie, A.; von Wolff, N.; Lefevre, G.; Mitchell, E. A.; Jutand, A. *Chem. Eur. J.* **2015**, *21*, 7858−7865. (c) Besora, M.; Maseras, F. *Dalton Trans.* **2019**, *48*, 16242−16248.

20. Senn, H. M.; Ziegler, T. *Organometallics* **2004**, *23*, 2980−2988.

21. Relative free energies are reported after applying Cramer and Truhlar's quasi-harmonic approximation to vibrational entropy: Ribeiro, R. F.; Marenich, A. V.; Cramer, C. J.; Truhlar, D. G. *Phys. Chem. B* **2011**, *115*, 14556−14562.

22. (a) 3D images of optimized structures were generated with CYLview: Legault, C. Y. CYLview20; Universitéde Sherbrooke, 2020 (http://www.cylview.org). (b) 3D images of molecular orbitals were generated with Avogadro: Hanwell, M. D; Curtis, D. E; Lonie, D. C; Vandermeersch, T.; Zurek, E.; Hutchison, G. R Avogadro: An advanced semantic chemical editor, visualization, and analysis platform. *J. Cheminformatics* **2012**, *4*, 17.

23. For previous experimental studies supporting a displacement mechanism for PdL_2 during reaction of PhCl, see ref 19a.

24. For previous computational studies showing that PdL and PdL_2 can favor different mechanisms during reaction with PhBr, see ref 19c.

25. (a) For seminal examples of computational studies showing a 3-centered concerted mechanism for oxidative addition of ArCl at PdL (L = P^tBu_3), see: Ahlquist, M.; Norrby, P.-O. *Organometallics* **2007**, *26*, 550−553. (b) Schoenebeck, F.; Houk, K. N. *J. Am. Chem. Soc.* **2010**, *132*, 2496−2497.

26. The LUMO and LUMO + 1 of PhCl are nearly isoenergetic (∼1 kcal/mol difference). In contrast, the LUMO and LUMO + 1 of **1** differ by about 9 kcal/mol.

27. Entz, E. D.; Russell, J. E. A.; Hooker, L. V.; Neufeldt, S. R. *J. Am. Chem. Soc.* **2020**, *142*, 15454−15463.

28. We also find that the preferred mechanism of oxidative addition of the C4−Cl bond of 2,4-dichloropyridine at PdL_2 depends on L. Ligand-dependent mechanistic differences might explain the variable magnitude of C2-selectivity with small triaryl vs trialkyl phosphines (see Appendix B).

29. For prior evidence supporting a displacement mechanism for PdL_2 (L = PPh_3) during reaction of 2-chloropyridine, see ref 19b.

30. (a) Huang, J.; Schanz, H.-J.; Stevens, E. D.; Nolan, S. P. *Organometallics* **1999**, *18*, 2370−2375. (b) Hopkinson, M. N.; Richter, C.; Schedler, M.; Glorius, F. *Nature* **2014**, *510*, 485−496.

31. A recent publication demonstrates that a C6-substituent can also slow the rate of oxidative addition at C2 due to sterics, although the effect of C6-sterics on C4−X oxidative addition was not examined: see ref 4.

32. Notably, LUMO differences are not the only variable that trends with selectivity. The most selective substrate (pyridazine) also has the smallest difference in bond dissociation energies. Additionally, pyridazines are worse ligands than pyridines, which could further disfavor bisligated Pd.

33. With 2,4-dibromopyridine **26**, over-arylation is observed (see ref 7).

34. All thermodynamic quantities were computed with the GoodVibes code (298.15 K) applying corrections for initial concentrations ([Pd] = 0.0075 M and [2] = 0.25 M): Luchini, G.; Alegre-Requena, J. V.; Funes-Ardoiz, I.; Paton, R. S. GoodVibes: Automated Thermochemistry for Heterogeneous Computational Chemistry Data. F1000Research **2020**, *9*, 291.

CHAPTER FOUR

THIOLATION/LIEBESKIND-SROGL COUPLING SEQUENCE ENABLES ATYPICAL SELECTIVITY IN C—C COUPLINGS OF HETEROARYL HALIDES

4.1 Introduction

Pyrimidines—especially 2,4-disubstituted pyrimidines, are of immense relevance to biology and the development of biologically active molecules.[1] Of the top 100 small molecule drugs by retail sales in 2022, 20% contained at least one 2,4-disubstituted pyrimidine.[2] Commonly, these are represented in tyrosine kinase inhibitors such as imatinib, nilotinib, pralsetinib, and osimertinib used in the treatment of cancers. Other life-saving medications, including the statin drug rosuvastatin, the antimalarial pyrimethamine, the HIV treatment rilpivirine, and antibacterial sulfa drugs such as sulfamethazine and sulfamerazine feature 2,4-disubstituted pyrimidines in their

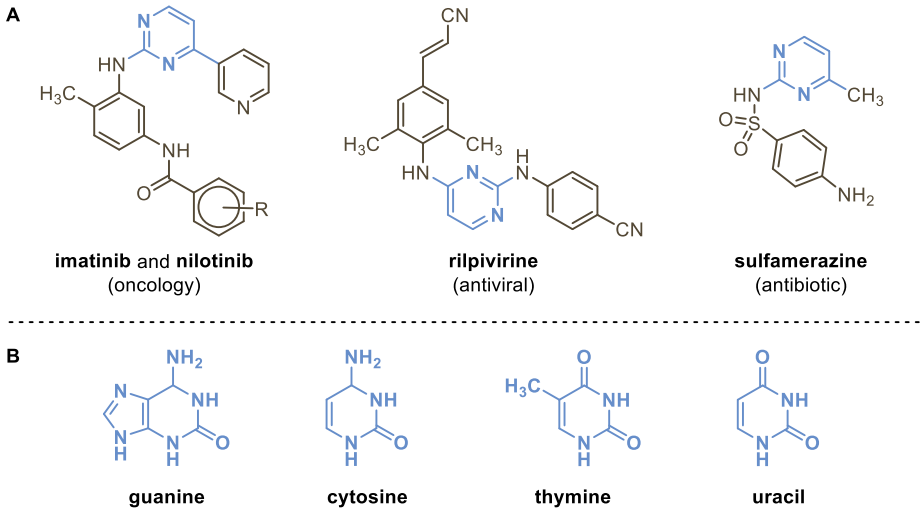
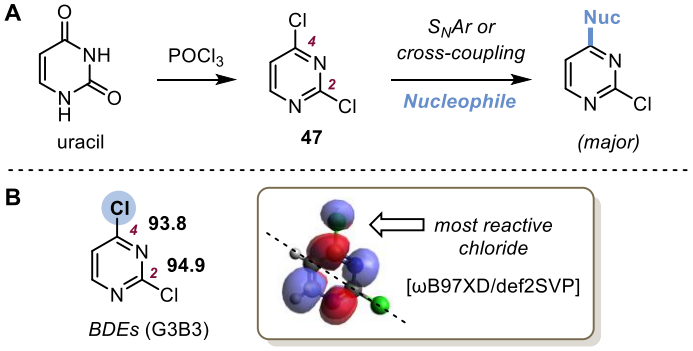


Figure 4.1. (A) Selected Therapeutic Agents Containing 2,4-Disubstituted Pyrimidines (B) 2,4-Disubstituted Pyrimidines Represented in the Nitrogenous Nucleobases.

structures. Moreover, four of the canonical nucleobases—guanine, thymine, cytosine, and uracil, which constitute the fundamental units of genetic code—are themselves 2,4-disubstituted pyrimidines. In total, the relevance of this structural pattern to the fields of biology and medicine as we know them, is difficult to overstate.

Scheme 4.1. (A) Synthesis and Reactivity of 2,4-Dichloropyrimidine (B) Bond Dissociation Energies of C_2—Cl and C_4—Cl from Ref. 7 and LUMO of 2,4-Dichloropyrimidine *(calculated by Sharon Neufeldt).*

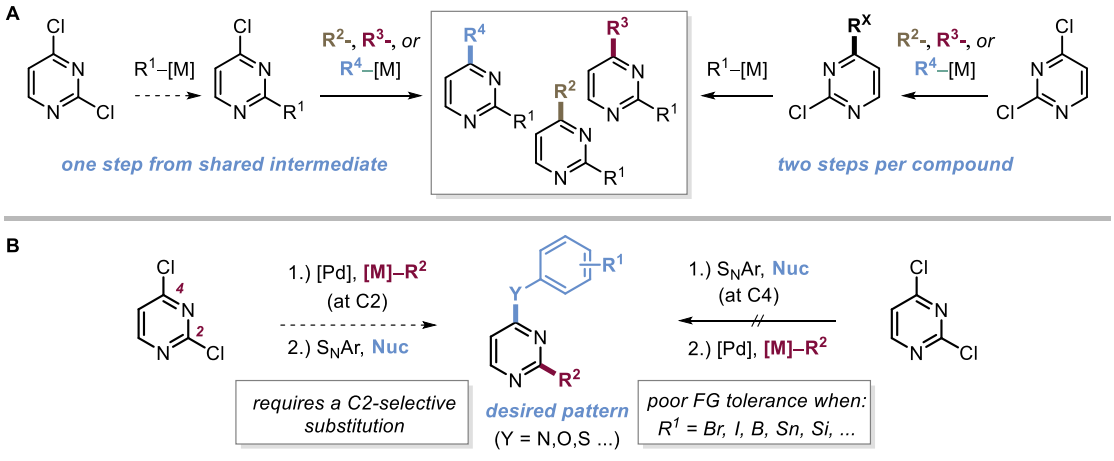


The inexpensive 2,4-dichloropyrimidine (**47**) offers a practical starting point to access more elaborate 2,4-disubstituted pyrimidine scaffolds via nucleophilic aromatic substitution (S_NAr) or cross-coupling at the chloride sites and can be prepared in one step by the dehydrohalogenation of uracil (Scheme 4.1A).[3] In both S_NAr and cross-coupling reactions, **47** exhibits a regiochemical preference for reaction at its "C4-site" which is α to only a single nitrogen.[4] Counterintuitively, the C2-site, which is flanked by two α-nitrogen ring members, is significantly less reactive.[5] A recent literature analysis by Norman and Neufeldt, surveying 1,284 Pd-catalyzed cross-couplings of **47**, indicates that >99% of these reactions proceed with C4-selectivity. The <1% of ostensibly C2-selective reactions are not supported by structural

characterization.[6] A few molecular descriptors of **47** may explain its invariable regiochemical preference for reaction at C4: The C4—Cl bond has a marginally smaller BDE (93.8) than C2—Cl (94.9),[7] and critically, the LUMO of **47** is characterized by a node which bisects C2 (Scheme 4.1B). Thus, a more favorable interaction between the HOMO of PdL_n and the LUMO at C4 is reasonable to expect.

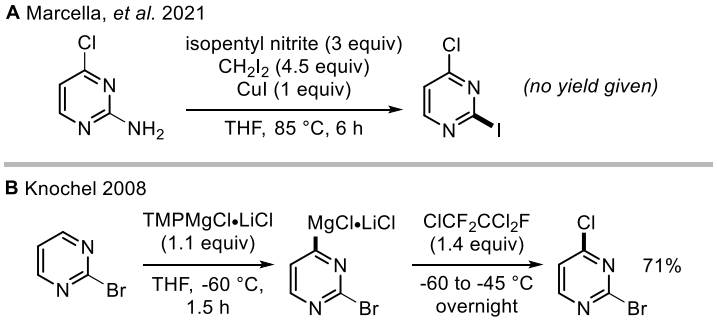
By necessity, 2,4-disubstituted pyrimidines are prepared by first reacting at the C4-site of 2,4-dichloropyrimidine, followed by the C2-site.[8] Notably, this order of site-substitution is limiting in some scenarios. For one thing, step-economy suffers during parallel synthesis programs where a large selection of substituents are varied at the C4-position while holding the C2-substituent constant: in such programs, each compound requires a minimum of two synthetic steps instead of a single step involving a common C2-substituted precursor (Scheme 4.2A.) Secondly, inherent C4-

Scheme 4.2. Proposed Advantages of Regio-inversion: (A) Regiocontrol improves step-economy during parallel synthesis programs (B) Regiocontrol enables synthetic flexibility during the assembly of structures with sensitive functional groups.



selectivity is limiting if a Pd-sensitive group is first installed at C4 (e.g., via S_NAr) prior to coupling at C2—such groups might include aryl halides, aryl boronates, or strongly coordinating functional groups which can act as catalyst poisons (Scheme 4.2B.). Thus, it would be ideal to install such nucleophiles at the desired C4-site *after* completing the cross-coupling step at C2. Finally, the inherent order of site reactivity prevents one from accessing simple C2-substituted products in which the C4-chloride is preserved.

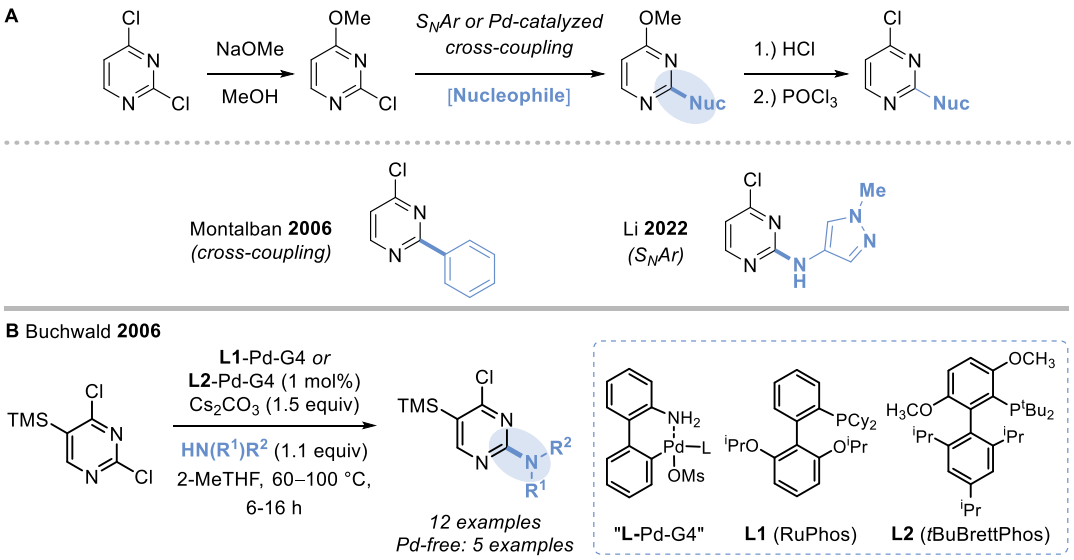
Scheme 4.3. Preparation of 4-chloro-2-halopyrimidines for Use in Halide-Selective Cross-Coupling Reactions.



Adding to the difficulty, starting materials of the formula 4-chloro-2-X-pyrimidine where X = Br, or I, are challenging to access on scale. For instance, 4-chloro-2-iodopyrimidine is prepared via a Sandmeyer reaction from 2-amino-4-chloropyrimidine (Scheme 4.3A.).[9] Alternatively, Knochel has described a C4-selective magnesiation of 2-bromo-pyrimidine with TMPMgCl·LiCl (Scheme 4.3B.). Trapping Knochel's metalated intermediate with an electrophilic chlorine source yields 2-bromo-4-chloropyrimidine.[10] However, Knochel's protocol is performed at -60 °C and is thus largely restricted to laboratory-scale applications. Therefore, traditional chemoselective

strategies, in which a more reactive halide is positioned at the less reactive C2-site, are limited by the commercial availability of starting materials.

Scheme 4.4. Synthetic Approaches to C2-Substituted 4-Chloropyrimidines.



At present, there are two notable synthetic workarounds that provide access to 2-substituted-4-chloropyrimidines. The first strategy involves "protecting" the C4-site via nucleophilic methoxylation, followed by substitution at C2 with the desired nucleophile (Scheme 4.4A.). The C4-methoxy group can then be returned to a chloride functionality via a two-step demethylation/dehydro-chlorination protocol. This method of substitution has been demonstrated with Pd-catalyzed cross-coupling[11] and more recently with S_NAr[12] at the C2-site. Nevertheless, this approach employs reaction conditions which are poorly tolerant of functional groups during both the protection and deprotection steps. An alternative approach, demonstrated by Buchwald, employs a trimethylsilyl directing group at C5 (Scheme 4.4.B).[13] In the presence of a bulky C5-

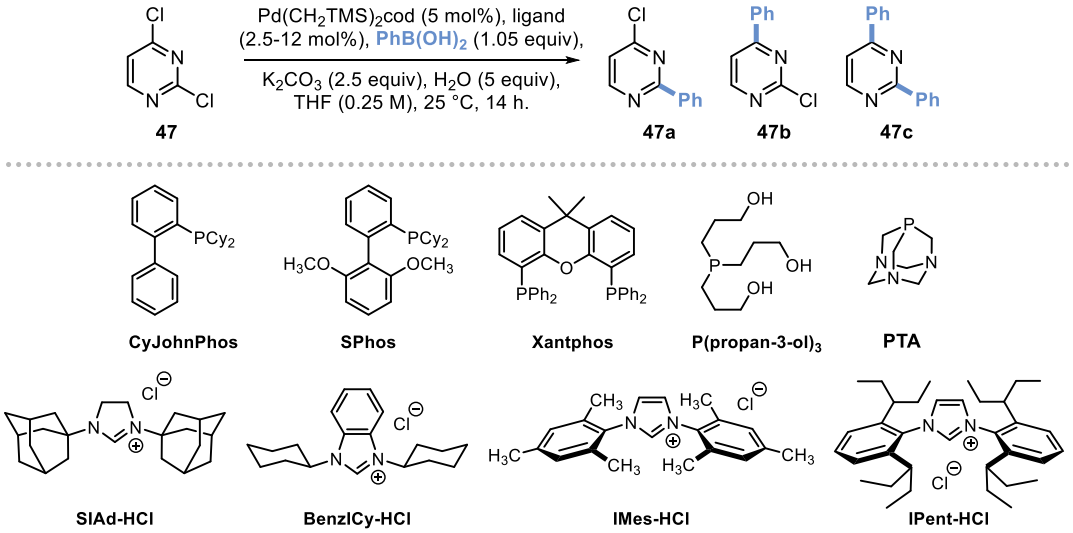
substituent, both metal-catalyzed and metal-free aminations take place at C2. The TMS group may later be removed through treatment with a strong acid. Despite the importance of both synthetic routes outlined in Scheme 4.4., each suffers from issues related to functional group tolerance and step-economy, requiring three or four steps to achieve what might ideally be accomplished in one.

4.2 Diverse Cross-Coupling Conditions Result in C4-Selectivity.

Considering the large body of literature describing invariable C4-selectivity in Pd-catalyzed cross-couplings of 2,4-dichloropyrimidines, it seemed unlikely that C2-coupling could be achieved under standard Suzuki-Miyaura conditions. However, the literature as a whole is largely biased toward the use of select few ligands—especially PPh_3 and dppf,[6] whereas the regioselectivity preferences of some less common ligands are undocumented. To evaluate regioselectivity trends, we surveyed 13 ligands under typical SMC conditions and confirmed that product **47b** was major in all cases where good conversion was achieved, regardless of a ligand's structural characteristics (Table 4.1). In some cases, **47a** was detected as a minor product, as in entries 6 and 7 which employ trialkyl phosphines. As discussed in the previous chapters, hindered N-heterocyclic carbenes are known to invert the typical site preference for 2,4-dichloropyridine and some related azines—however, each of the NHCs surveyed here resulted in high selectivity for the conventional C4-site of **47**. Strotman, et al. report the use of the ligand PTA (phosphatriazaadamantane) to facilitate atypical C2-selectivity in the SMC of N-methyl-2,4-dibromoimidazole.[14] However, this too promotes formation of **47b** in the SMC of 2,4-dichloropyrimidine. We speculated that a multifunctional ligand, such as *tris*-(3-hydroxypropyl)phosphine, employed in entries 13 and 14, might promote C2-selectivity through one or more hydrogen-bonding interactions with the

nitrogen ring members either during or leading up to oxidative addition, but the desired C2-regioisomer was formed in only trace yield (entry 14). Finally, a phosphine- and NHC-free reaction employing $Pd(CH_2TMS)_2cod$ as the catalyst led exclusively to the **47b** and in relatively low yield (entry 15).

Table 4.1. Evaluation of Site-Selectivity in Pd-Catalyzed Suzuki-Miyaura Couplings of 2,4-Dichloropyrimidine.



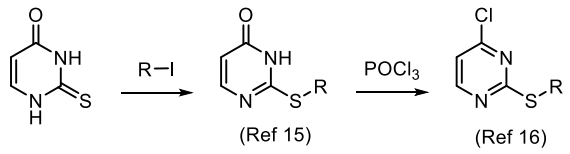
entry	Ligand	Pd:L	T °C	**47** (%)	**47a** (%)	**47b** (%)	**47c** (%)
1	PPh_3	1 : 2.4	25	0	0	85	0
2	CyJohnPhos	1 : 1	25	0	2	94	13
3	SPhos	1 : 1.3	25	34	0	51	9
4	Xantphos	1 : 1	25	18	1	66	0
5[b,c]	DPPP	1 : 1	60	71	0	0	0
6[b]	PCy_3	1 : 2	60	21	5	40	1
7	$P(^tBu)_3$	1 : 1	25	4	5	81	4
8	IMes-HCl	1 : 1	25	36	2	42	0
9	SIAd-HCl	1 : 1	25	65	0	18	0
10[d]	BenzICy-HCl	1 : 1	25	19	0	44	0
11[d]	IPent-HCl	1 : 1	25	30	1	38	0
12[b]	PTA	1 : 2	60	33	0	17	0
13	$P(propan\text{-}3\text{-}ol)_3$	2 : 1	25	0	0	75	17
14	$P(propan\text{-}3\text{-}ol)_3$	1 : 1	25	0	2	68	3
15	None	--	25	58	0	11	0

[a] GC yields of 2,4-dichloropyrimidine (**47**) are calibrated. GC yields of cross-coupling products are uncalibrated and based on peak integrations relative to a dodecane internal standard. GC yields are rounded to the nearest integer. [b] Reaction at 60 °C instead of 25 °C, and K_3PO_4 instead of K_2CO_3. [c] DPPP = 1,3-*bis*(diphenylphosphino)propane. [d] 21.5 h reaction.

4.3 C—S Bond Activation Enables Arylation at C2.

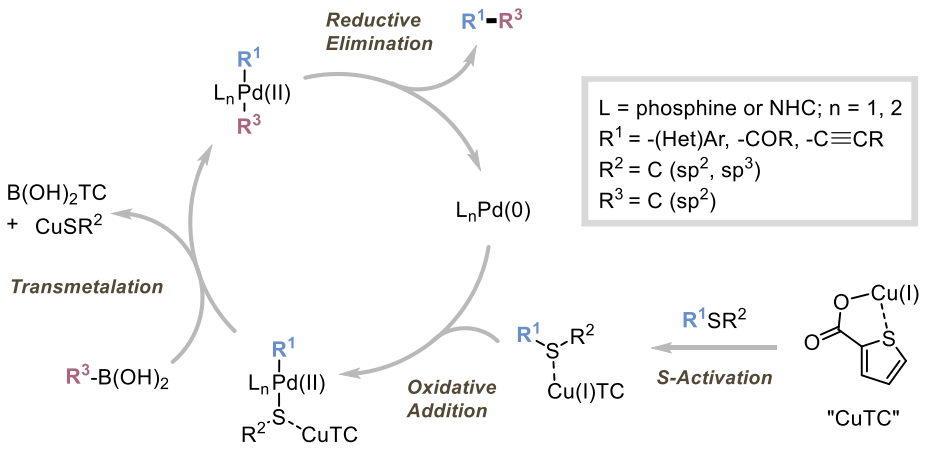
Given that direct C2-substitution of **47** via SMC appeared to be intractable, we turned our attention toward alternative synthetic strategies employing leaving groups other than Cl at the less reactive C2-position. As discussed above, 4-chloro-2-X-pyrimidines are challenging to access where X = Br or I. Similarly, there are no direct methods by which the C2-chloride can be converted into a C—O pseudohalide such as a triflate or oxyphosphonium (-OPR_3^+ X^-) leaving group. On the other hand, 4-chloro-2-alkylthiopyrimidines are readily prepared in two steps from 2-thiouracil (Scheme 4.5).[15,16]

Scheme 4.5. Preparation of 4-chloro-2-alkylthiopyrimidines



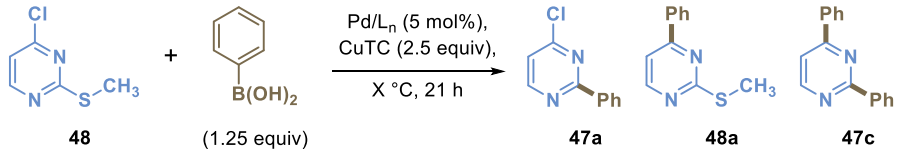
While alkyl sulfides are non-traditional leaving groups in cross-coupling, the C—S bond can be activated toward oxidative addition at Pd by the action of a thiophilic cocatalyst. For example, use of a Cu(I)-carboxylate enables the Pd-catalyzed Liebeskind-Srogl coupling (LSC) between aryl thioethers and various nucleophiles. The mechanism of the archetypal LSC involves oxidative addition of a C—S bond to Pd(0), followed by transmetalation with an arylboron species which displaces the sulfur leaving group. Reductive elimination results in a new C—C bond and regeneration of the Pd(0) catalyst.[17] The Cu(I)-carboxylate also functions as a thiolate scavenger and is typically used in excess for this purpose.

Scheme 4.6. Generic Mechanism of the Pd-Catalyzed Liebeskind-Srogl Cross-Coupling.



The LSC is a unique Pd-catalyzed process in that (hetero)aryl chlorides and most aryl bromides are left untouched during the reaction; instead, oxidative addition results selectively at the aryl sulfide Ar—SR' bond (or alternatively, at a thioester RC(O)—SR' bond) which is weakened via a dative interaction between the S atom and the thiophilic Cu(I) species.[18] For this reason, the LSC is sometimes described as *orthogonal* to the Suzuki-Miyaura Coupling which takes place at aryl halide sites but tolerates thioethers and thioesters. Considering the halide tolerance of the LSC and the straightforward preparation of 4-chloro-2-alkylthiopyrimidines, we speculated that C2-selective LSCs of 2-(alkylthio)-4-chloropyrimidines could be a general solution to access C2-substituted 4-arylpyrimidines. To our knowledge, this approach has only been evaluated once in the literature. Pujol and Guillaumet described a C2-selective thiolation of 4-chloro-2-(methylthio)-pyrrolo[2,3-d]pyrimidine catalyzed by $Pd(PPh_3)_4$ but encountered difficulty during purification.[19] Thus, we determined that a thorough exploration of catalysts, reaction conditions, and scope would shed light on the viability of this approach.

Table 4.2. Selected Entries from the C2-Selective Liebeskind-Srogl Optimization (Series 1).



Entry	Catalyst	T °C	Solvent (M)	**48** (%)	**47a** (%)	**48a** (%)	**47c** (%)
1[b,c]	$Pd(PPh_3)_4$	100	dioxane (.13)	0	37	0	4
2[c,d]	$Pd(PPh_3)_4$	25	THF (.13)	60	23	4	1
3[c,d]	$Pd(PPh_3)_4$	40	THF (.13)	38	40	4	2
4[c,d]	$Pd(PPh_3)_4$	60	THF (.13)	16	54	1	3
5[c,d]	$Pd(PPh_3)_4$	75	MeCN (.13)	21	3	2	<1
6	$Pd(PPh_3)_4$	65	THF (.25)	9	47	1	3
7	$Pd(PPh_3)_4$	65	EtOH (.25)	6	40	1	3
8	$Pd(PPh_3)_4$	65	PhMe (.25)	32	31	3	1
9[e]	$Pd(PPh_3)_4$	65	PC (.25)	12	37	1	2
10	$Pd(PPh_3)_4$	65	sulfolane (0.25)	0	34	0	12
11	$Pd(PCy_3)_2$	65	THF (.25)	16	58	0	<1
12	$Pd(P^tBu_3)_2$	65	THF (.25)	5	61	0	3
13[f]	Pd(IPent)	65	THF (.25)	15	62	0	1
14[g]	Pd / MePhos	65	THF (.25)	20	55	0	1
15[g]	Pd / Xantphos	65	THF (.25)	19	60	0	<1
16	None	65	THF (.25)	77	10	0	0

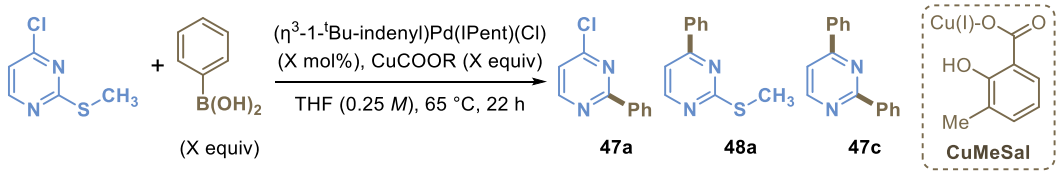
[a] Yields are calibrated GC yields calculated using an *n*-undecane internal standard. Yields are rounded to the nearest integer; yields <1 are less than <0.5 %. In most reactions, unidentified side products were detected, which are reflected in lower mass balances. [b] 36 h reaction time, 1.5 equiv aryl boronic acid. [c] 3.0 equiv. CuTC (copper(I) thiophene-2-carboxylate). [d] 17 h reaction time. [e] PC = propylene carbonate. [f] Pd(IPent) = (η^3-1-^{t}Bu-indenyl)Pd(IPent)(Cl). [g] 5 mol% $Pd(CH_2TMS)_2cod$ was used as a Pd source in a 1:1 molar ratio with ligand.

Initially, several reaction parameters in the LSC of 4-chloro-2-(methylthio)pyrimidine (**48**) with phenylboronic acid were evaluated—including solvent, temperature, and catalyst (Table 4.2). When $Pd(PPh_3)_4$ is used as the catalyst in the presence of excess Cu(I)-thiophene-2-carboxylate

(CuTC), yields are optimal in THF near 60—65 °C. Yields are adversely affected by inadequate heating, excessive heating (e.g., at 100 °C), and the use of acetonitrile as the solvent. Throughout the literature, $Pd(PPh_3)_4$ is regularly conscripted as the default catalyst in LSCs.[20] However, trialkyl monophosphines (entries 11 and 12) and the hindered NHC ligand IPent (entry 13) outperform PPh_3 in terms of both selectivity and yield of **47a**. Other ligands, such as the biarylphosphine MePhos and the bisphosphine Xantphos are similarly effective in this transformation. Notably, conversion is low in the absence of Pd catalysts, indicating the limited ability of simple Cu(I) species to mediate the reaction (entry 16).

Further optimization experiments for the LSC of **48** marked a 33 % increase in the yield of **47a** when the phenylboronic acid loading was increased from 1.25 to 2.0 equivalents (Table 4.3., entries 1-3, and entry 7). Reaction outcomes were indistinguishable when either CuTC or CuMeSal—the Cu(I) carboxylate derived from salicylic acid, were used as the Cu(I) source (compare entries 4 and 5). However, conversion was significantly diminished when CuTC was replaced with Cu(I) acetate (entries 4-6). High yields of the C2-phenylated product **47a** were maintained when CuTC equivalents were decreased from 2.5 to 2.0, but the yield of product **47a** suffered when fewer than 2.0 equivalents of Cu(I) were included (entries 8-10). Finally, under the optimal reaction conditions, Pd loadings with the catalyst (η^3-1-^{t}Bu-indenyl)Pd(IPent)(Cl) were reduced from 5 mol% to 0.5 mol% without adversely impacting the yield of **47a** (entries 7 vs. 8, and 9 vs. 12).

Table 4.3. Selected Entries from the C2-Selective Liebeskind-Srogl Optimization (Series 2).



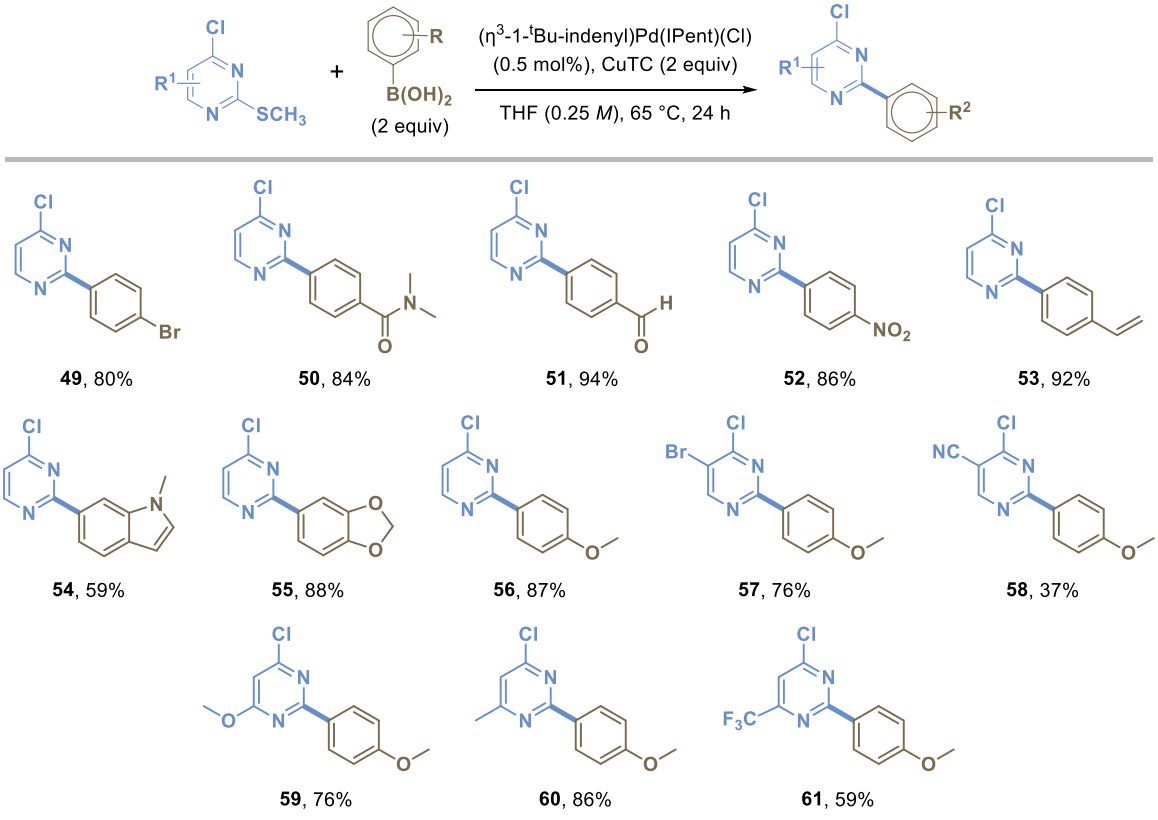
Entry	mol% Pd	Cu(I) (equiv)	BA[f] equiv	**48** (%)	**47a** (%)	**48a** (%)	**47c** (%)
1[b,c]	5	CuTC (2.5)	1.25	13	63	0	1
2[c]	5	CuTC (2.5)	1.5	8	71	0	1
3[c]	5	CuTC (2.5)	1.75	7	82	0	1
4	5	CuTC (2.3)	1.75	0	83	0	1
5	5	CuMeSal (2.3)	1.75	0	83	0	3
6	5	CuOAc (2.3)	1.75	43	28	1	3
7	5	CuTC (2.5)	2	0	96	0	1
8[d]	1	CuTC (2.5)	2	0	94	0	1
9	1	CuTC (2)	2	3	97	0	<1
10	1	CuTC (1.8)	2	7	87	0	1
11	0.5	CuTC (2)	2	5	93	0	<1
12[e]	0.5	CuTC (2)	2	0	96	0	1
13	0.1	CuTC (2)	2	24	70	0	<1

[a] Yields are calibrated GC yields calculated using an *n*-undecane internal standard. Yields are rounded to the nearest integer; yields <1 are less than <0.5 %. In some reactions, unidentified side products were detected, which are reflected in lower mass balances. [b] Average of three trials. [c] 34 h reaction time. [d] 24 h reaction time. [e] Duplicate of previous entry. [f] BA = $PhB(OH)_2$.

The optimized, C2-selective reaction conditions are general to a broad selection of arylboronic acids and substituted 4-chloro-2-methylthiopyrimidines (Scheme 4.4). Notably, aryl bromides are tolerated when present on both nucleophilic and electrophilic coupling partners (products **49** and **57**), exemplifying the thioselectivity of the LSC. Moreover, these reaction conditions are tolerant of amide (**50**), aldehyde (**51**), nitrile (**58**), ether (**55-61**), and alkene (**53**)

functionalities each of which are sensitive to strong acids or harsh halogenation reagents, such as phosphorous(IV) oxychloride ($POCl_3$). Both HCl and $POCl_3$ are required in earlier synthetic routes to produce 2-aryl-4-chloropyrimidines (as mentioned above: Scheme 4.4A), preventing direct access to most of products in Scheme 4.7 due to functional group incompatibility. Nevertheless, the low yield of product **58** indicates these reaction conditions may be poorly tolerant of nitriles

Scheme 4.7. Scope of C2-Selective Liebeskind-Srogl Couplings Catalyzed by Pd/IPent.

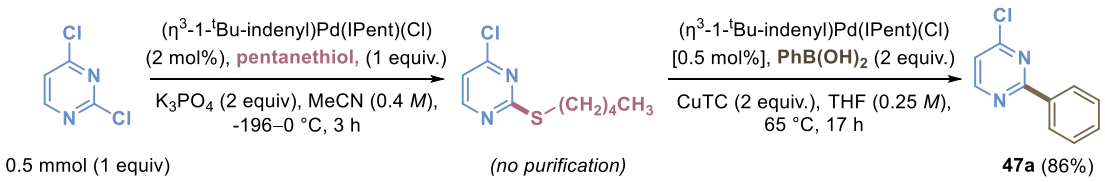


[a] 0.1 mmol reactions took place in sealed 1-dram reaction vials under N_2. CuTC = Cu(I) thiophene-2-carboxylate. ^{1}H NMR yields are the average of two trials based on aromatic signal integrations using 1,3,5-trimethoxybenzene as an internal standard; range of reaction yields = 3.5% (on average; see Appendix C).

compared to other substituents, possibly due to competitive coordination of the cyano- nitrogen to Pd or Cu. This observation aligns with the finding that this reaction does not progress in acetonitrile (refer to Table 4.2, entry 5).

Recently, our research group developed a Pd-catalyzed C2-selective thiolation of **47**, representing the first documented example of a C2-selective cross-coupling with this substrate.[21] The mechanistic cause of C2-selectivity is a topic of ongoing study in our group. Notably, the atypical site selectivity of this reaction is specific to sulfur nucleophiles, whereas carbon nucleophiles (e.g., Grignard reagents) undergo cross-coupling at the C4-position under otherwise identical reaction conditions. Nevertheless, the site-selective thiolation complements the method described above and suggests the possibility of a two-step procedure—a C2-thiolation followed by LSC, which enables the C2-arylation of **47** with boronic acids (Scheme 4.8.). Fortuitously, C2-selectivity and yields are optimal with the precatalyst (η^3-1-^{t}Bu-indenyl)Pd(IPent)(Cl) in both procedural steps, eliminating the need to isolate the sulfide intermediate (see Appendix C).

Scheme 4.8. C2-Selective Arylation via a Thiolation/C—S Bond Activation Sequence.



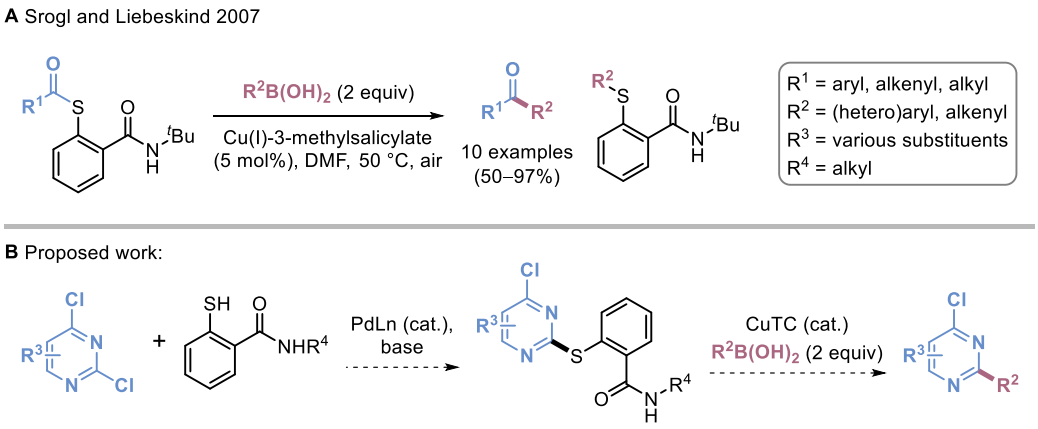
[a] The calibrated GC yield of **47a** was calculated using peak integrations based on an undecane internal standard (average of two trials = 84%, 88%). See Appendix C for a description of the two-step protocol.

4.4 Conclusion

In summary, an expedient and versatile synthetic route to 2-aryl-4-chloropyrimidines is demonstrated via a C2-selective Liebeskind-Srogl Coupling of 4-chloro-2-(alkylthio)pyrimidines. The protocol is characterized by high yields (usually ≥80%) and broad functional group tolerance. Importantly, this method contrasts previous synthetic strategies to prepare 2-aryl-4-chloropyrimidines which involved the use of protecting groups, corrosive acids, and harsh halogenation reagents. Finally, the C—S selective LSC may be used in sequence with a C2-selective thiolation (recently developed by the Neufeldt group) to arylate the 2-position of 2,4-dichloropyrimidine.

A notable drawback of the seminal LSC is its dependence on stoichiometric copper. Since then, Srogl and Liebeskind have introduced multiple iterations of their eponymous reaction,[22] including a Cu-catalyzed, aerobic variation.[23] The Cu-catalyzed reaction is specific to thioesters which possess a chelating pendant group—such as an *ortho*-phenylcarboxamide (Scheme 4.9A). Future work could focus on developing an improvement to the two-step thiolation/C—S activation protocol where use of a chelating thiophenol in the first step renders the second step catalytic with respect to Cu (Scheme 4.9B). Without the need for stoichiometric Cu, this modified two-step protocol would be amenable to applications in process development, while expediting the synthesis of structures containing 2,4-disubstituted pyrimidines.

Scheme 4.9. (A) Cu-Catalyzed Aerobic Liebeskind-Srogl coupling of Thioesters with Boronic Acids (B) Proposed Synthetic Route to C2-Functionalized 4-Chloropyrimidines Under Catalytic Reaction Conditions.



4.5. References

1. For selected examples of 2,4-disubstituted pyrimidines in medicinal chemistry, see: (a) Manley, P. J.; Balitza, A. E.; Bilodeau, M. T.; Coll, K. E.; Hartman, G. D.; McFall, R. C.; Rickert, K. W.; Rodman, L. D.; Thomas, K. A. *Bioorg. Med. Chem. Lett.* **2003**, *13*, 1673–1677. (b) Mohamed, T.; Rao, P. P. *Bioorg. Med. Chem. Lett.* **2010**, *20*, 3606– 3609. (c) Mohamed, T.; Zhao, X.; Habib, L. K.; Yang, J.; Rao, P. P. N. *Bioorg. Med. Chem.* **2011**, *19*, 2269– 2281. (d) Mohamed, T.; Yeung, J. C. K.; Vasefi, M. S.; Beazely, M. A.; Rao, P. P. N. *Bioorg. Med. Chem. Lett.* **2012**, *22*, 4707– 4712. (e) Mukherjee, P.; Li, H.; Sevrioukova, I.; Chrei, G.; Marta, P.; Roman, L. J.; Poulos, T. L.; Silverman, R. B. *J. Med. Chem.* **2015**, *58*, 3, 1067– 1088. (f) Kim, J.; Kim, Y. J.; Londhe, A. M.; Pae, A. N.; Choo, H.; Kim, H. J.; Min, S. J. *Molecules* **2019**, *24.* (g) Hopfner, S. M.; Lee, B. S.; Kalia, N. P.; Miller, M. J.; Pethe, K.; Moraski, G. C. *Applied Sciences* **2021**, *11*, 19, 9092. DOI:10.3390/app11199092. (h) Zhang, X.; Wang, J.; Xu, J.; Pang, Q.; Liu, D.; Zhang, G. *J. Org. Chem.* **2023**, *88*, 10266−10276. (i) Kim, G.; Hou, X.; Byun, W. S.; Kim, G.; Jarhad, D. B.; Lee, G.; Hyun, Y. E.; Yu, J.; Lee, C. S.; Qu, S.; Warnick, E.; Gao, Z.-G.; Kim, J. Y.; Ji, S.; Shin, H.; Choi, J.-R.; Jacobson, K. A.; Lee, H. W.; Lee, S. K.; Jeong, L. S. *J. Med. Chem.* **2023**, *66*, 17, 12249–12265.

2. Williams, R. E.; Top 200 Small Molecule Drugs by Retail Sales in 2022; https://njardarson.lab.arizona.edu/sites/njardarson.lab.arizona.edu/files/NjardarsonGroup2022SmallMoleculeTopPosterV3.pdf (poster accessed online November 28, 2023); *see:* McGrath, N. A.; Brichacek, M.; Njardarson, J. T. *J. Chem. Educ*. **2010**, *87*, 12, 1348–1349.

3. (a) Singh, K.; Kaur, H.; Smith, P.; de Kock, C.; Chibale, K.; Balzarini, J. *J. Med. Chem.* **2014**, *57*, 435– 448. (b) Gehringer, M.; Forster, M.; Pfaffenrot, E.; Bauer, S. M.; Laufer, S. A. *Chemmedchem* **2014**, *9*, 11, 2516– 2527. (c) Manzoor, S.; Gabr, M. T.; Rasool, B.; Pal K.; Hoda, N. *Bioorg. Chem.*, **2021**, *116*, 105354.

4. Almond-Thynne, J.; Blakemore, D. C.; Pryde, D. C.; Spivey, A. C. *Chem. Sci.* **2017**, *8*, 40−62., See also: reference 6.

5. Dvorak, C.A. (**2008**). 2,4-Dichloropyrimidine. In Encyclopedia of Reagents for Organic Synthesis, (Ed.). https://doi.org/10.1002/047084289X.rn00879

6. Norman, J. P.; Neufeldt, S. R. *ACS Catal.* **2022**, *12*, 12014– 12026

7. F Garcia, Y.; Schoenebeck, F.; Legault, C. Y.; Merlic, C. A.; Houk, K. N. *J. Am. Chem. Soc.* **2009**, *131*, 6632– 6639.

8. For selected examples of C4- followed by C2-substitution, see: (a) Solberg, J.; Undheim, K. *Acta Chem. Scand.* **1989**, *43*, 62–68. (b) Mangalagiu, I.; Benneche, T.; Undheim, K. *Acta Chem. Scand.* **1996**, *50*, 914. (c) Duan, S.; Widlicka, D. W.; Burns, M. P.; Kumar, R.; Hotham,

I.; Desrosiers, J. N.; Bowles, P.; Jones, K. N.; Nicholson, L. D.; Buetti-Weekly, M. T.; Han, L.; Steflik, J.; Hansen, E.; Hayward, C. M.; Strohmeyer, H.; Monfette, S.; Sutton, S. C.; Morris, C. *Org. Process Res. Dev.* **2022**, *26*, 3, 879– 890.

9. Marcella, B. P.; Housseman, C. G.; Daugan, A.; Dumoulin, A.; Laugeois; M.; Denis; A.; Faucher, N.; Botez, I.; Le Tiran, A.; Christensen K.; Lamotte, Y. New Macrocyclic LRRK2 Kinase Inhibitors. WO 2021/224320, November 11, 2021, A1;—pp 284.

10. (a) Mosrin, M.; Petrera, M.; Knochel, P. *Synthesis* **2008**, 3697– 3702. (b) Mosrin, M.; Knochel, P. *Org. Lett.* **2008**, *10*, 12, 2497–2500.

11. Ceide, S. C.; Montalban, A. G. *Tetrahedron Lett.* **2006**, *47*, 4415– 4418.

12. Li, C.; Haeffner, F.; Wang, S.; Yuan, C.; Shang, D.; Shi, X.; Ma, B.; Hopkins, B. T.; OBrien, E. M. *Org. Process Res. Dev.* **2022**, *26*, 137– 143.

13. Smith, S. M.; Buchwald, S. L. *Org. Lett.* **2016**, *18*, 9, 2180– 2183.

14. Strotman, N. A.; Chobanian, H. R.; He, J.; Guo, Y.; Dormer, P. G.; Jones, C. M.; Steves, J. E. *J. Org. Chem.* **2010**, *75*, 1733−1739.

15. (a) Abdel-Rahman, A. A. H.; Abdel-Megied, A. E. S.; Goda, A. E. S.; Zeid, I. F.; El Ashry, E. S. H. *Nucleosides Nucleotides* **2003**, *22*, 2027. (b) Tibiletti, F.; Simonetti, M.; Nicholas, K. M.; Palmisano, G.; Parravicini, M.; Imbesi, F.; Tollari, S.; Penoni, A. *Tetrahedron* **2010**, *66*, 1280– 1288. (c) Werner, M.; Pampel, J.; Pham, T. L.; Thomas, F. *Chem. Eur. J.* **2022**, *28*, e202201339.

16. Davey, D. D.; Adler, M.; Arnaiz, D.; Eagen, K.; Erickson, S.; Guilford, W.; Kenrick, M.; Morrissey, M. M.; Ohlmeyer, M.; Pan, G.; Paradkar, V. M.; Parkinson, J.; Polokoff, M.; Saionz, K.; Santos, C.; Subramanyam, B.; Vergona, R.; Wei, R. G.; Whitlow, M.; Ye, B.; Zhao, Z.; Devlin, J. J.; Phillips, G. *J. Med. Chem.* **2007**, *50*, 1146– 1157. (b) Abdel-Mohsen, H. T.; Omar, M. A.; El Kerdawy, A. M.; Mahmoud, A. E. E.; Ali, M. M.; El Diwani, H. I. *Eur. J. Med. Chem.* **2019**, *179*, 707– 722.

17. (a) Liebeskind, L. S.; Srogl, J. *J. Am. Chem. Soc*. **2000**, *122*, 45, 11260–11261. (b) Liebeskind, L. S.; Srogl, J. *Org. Lett.* **2002**, *4*, 6, 979–981. (c) Djamaladdin G. Musaev and Lanny S. Liebeskind. *Organometallics* **2009**, *28*, 16, 4639-4642.

18. For examples of chemoselective LSCs where aryl chlorides or bromides are tolerated, see: (a) Kusturin, C.; Liebeskind, L. S.; Rahman, H.; Sample, K.; Schweitzer, B.; Srogl, J.; Neumann, W.; *Org. Lett.* **2003**, *5*, 4349-4352. (b) Fausett, B. W.; Liebeskind, L. S.; *J. Org. Chem.* **2005**, *69*, 4851-4853. (c) Mehta, V. P.; Sharama, A.; Van der Eycken, E. *Org. Lett.* **2008**, *10*, 1147-1150. (c) Mehta, V. P.; Modha, S. G.; Van der Eycken, E.; *J. Org. Chem*. **2009**, *74*, 6870-6873.

(d) Creech, G. S.; Kwon, O. *Chem. Sci.*, **2013**, *4*, 2670–2674. (e) Quan, Z. J.; Lv, Y.; Jing, F. Q.; Jia, X. D.; Huo, C. D.; Wang, X. C. *Adv. Synth. Catal.* **2014**, *356*, 325-332.

19. Prieur, V.; Pujol, M. D.; Guillaumet, G.; *Eur. J. Org. Chem.* **2015**, 6547-6556.

20. Cheng, H.-G.; Chen, H.; Liu, Y.; Zhou, Q. *Asian J. Org. Chem.* **2018**, *7*, 490.

21. Jackson, O. D.; Reyes, A.; Stein, C. D.; Andrews, C. T.; Neufeldt, S. R. C2-Selective Palladium-Catalyzed C—S Cross-Coupling of 2,4-Dihalopyrimidines [manuscript in preparation].

22. Zhang, Z.; Lindale, M. G.; Liebeskind, L. S. *J. Am. Chem. Soc.* **2011**, *133*, 6403– 6410.

23. (a) Villalobos, J. M.; Srogl, J.; Liebeskind, L. S. *J. Am. Chem. Soc.* **2007**, *129*, 15734– 15735. (b) Adrián Varela-Álvarez, Lanny S. Liebeskind, and Djamaladdin G. Musaev *Organometallics* **2012**, *31*, 22, 7958-7968.

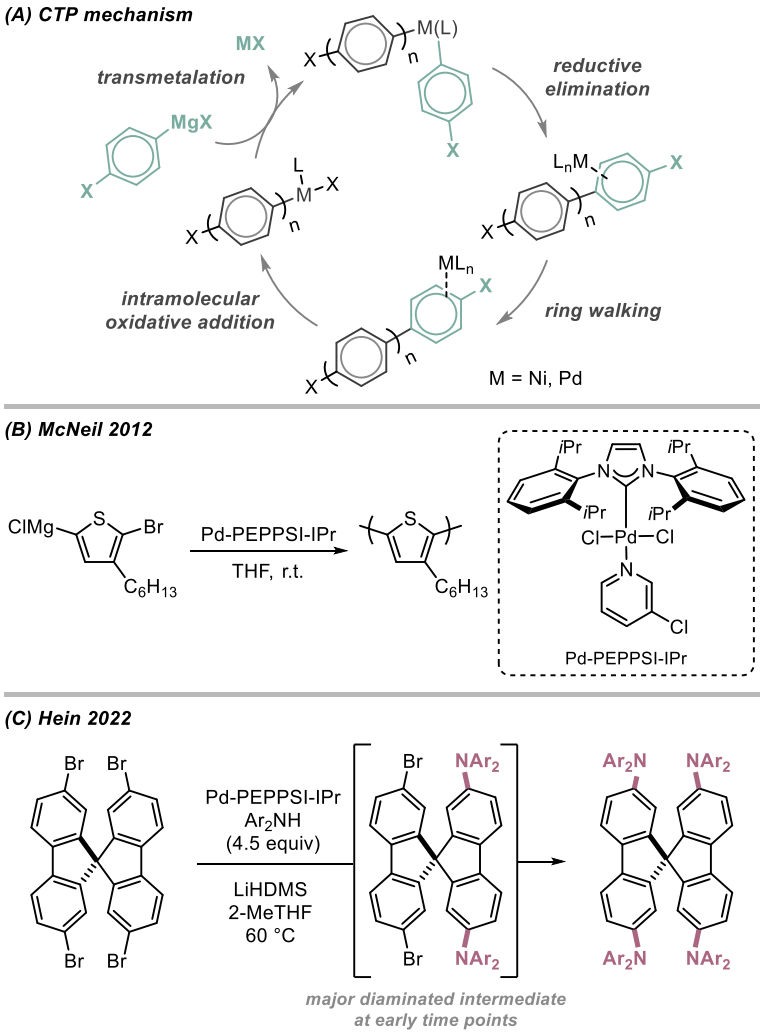
CHAPTER FIVE

A MECHANISTIC BASIS FOR LIGAND EFFECTS ON PALLADIUM RING-WALKING IN SUZUKI-MIYAURA COUPLINGS OF DICHLORO(HETERO)ARENES

5.1 Introduction

The previous chapters have described the utility and popularity of di- and polyhalogenated (hetero)arenes during the construction of bioactive compounds or functional materials. Commonly, these multiply halogenated (hetero)arenes are selected as starting materials when multiple halide substitutions are to be made in a stepwise fashion.[1] In Pd-catalyzed cross-couplings of dihalo(hetero)arenes bearing chemically equivalent halides, the products of mono- versus disubstitution may be differentiated by judicious choice of catalyst[2] or modifications to coupling partner stoichiometry. Traditional catalysts—such as $Pd(PPh_3)_4$ or Pd/dppf, generally favor the product of monosubstitution, leaving one halide intact.[3,4] However, a minor product often results from disubstitution regardless of catalyst choice—unless the nucleophile is used in deficit.[5] In contrast to PPh_3 and dppf, some sterically hindered phosphine and NHC ligands, including P^tBu_3,[6] RuPhos,[7] SIPr,[8] IPr,[9] and IPent,[10] are known to promote a non-statistical distribution of products where difunctionalization is major, despite manipulation of reactant stoichiometry. In many of these instances, Pd migrates in an intramolecular fashion from the new bond in the product of the first cross-coupling to the next reactive site, commonly referred to as "ring-walking."[11]

Scheme 5.1. Synthetic Applications for Ring-Walking Catalysts: (A) Generic Mechanism of Catalyst-Transfer Polycondensations (B) First Pd(NHC)-Catalyzed CTP with Pd-PEPPSI-IPr (C) Selective Diamination of Tetrabromo-Spirobifluorenes with Pd-PEPPSI-IPr.

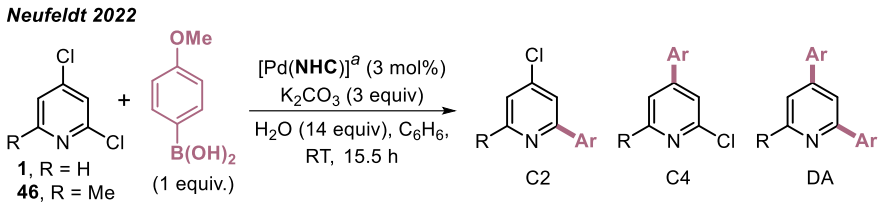


Notably, some practical applications of cross-coupling are also predicated on a catalyst's ability to ring-walk.[12] Catalyst-transfer polycondensations (CTPs)—as the name implies, require an *intramolecular* catalyst transfer along a single growing polymer, intermittent with cross-coupling cycles which enchain new monomeric units (X-Ar-[M]) at the C-X terminus (Scheme

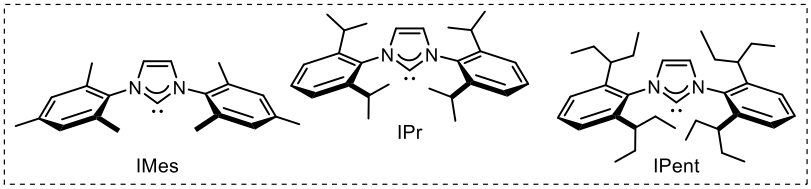
5.1.A).[13] This process is typically described as a "chain growth" mechanism, contrasting the conventional "step-growth" mechanism which does not involve ring-walking.[14] In 2012, McNeil reported the first Pd(NHC)-catalyzed CTP to proceed via a chain growth mechanism, facilitated by the hindered ligand IPr (Scheme 5.1.B).[15] Since then, IPr and the hindered monophosphine P^tBu_3, have comprised the vast majority of ancillary ligands to be successfully employed in Pd-catalyzed CTPs.[16] The unique reactivity of these hindered ligands contrasts that of smaller or bidentate phosphines which are known to favor the step-growth mechanism in Pd-catalyzed polymerizations.[17] A second application of hindered, ring-walking catalysts was recently featured by Hein et al., who demonstrated the selective diamination of tetrabromo-spirobifluorenes using Pd-PEPPSI-IPr (Scheme 5.1.C).[18]

However, when monosubstitution of a dihaloarene is the desired outcome, the propensity of a catalyst to favorably associate with and traverse a π-conjugated system is disadvantageous, and the use of precatalysts which are desirable for their reactivity or air-stability may be impracticable because of their tendency toward over-functionalization. In Chapter 2, which investigates the relationship between NHC ligand sterics and the site selectivity of cross-couplings with 2,4-dichloropyridines, we described an intriguing ligand trend where both selectivity for the unconventional C4-site *and* selectivity for diarylation increased concurrently with increasingly hindered NHC ligands (Table 5.1, entries 1-3).[19] In our study, the use of sterically demanding NHCs such as IPr and IPent were shown to improve selectivity for the atypical C4-regioisomer, but yields were diminished due to a corresponding increase in diarylated side product. Chapter 3 explained that the inversion of typical site selectivity (C4 vs C2) results from a change in Pd's

Table 5.1. Difunctionalization of 2,4-Dichloropyridines Correlated with Ligand Sterics, Substrate Sterics, and Substrate Concentration.



entry	NHC	**1** or **46** (equiv)	R	C2 (%)	C4 (%)	DA (%)	(C2 + C4) : DA
1	IMes	1	H	23	40	3	21 : 1
2	IPr	1	H	8	70	6	13 : 1
3	IPent	1	H	1	34	23	1.5 : 1
4	IMes	2	H	31	29	1	67 : 1
5	IMes	5	H	38	14	1	75 : 1
6	IPr	2	H	10	73	2	42 : 1
7	IMes	1	Me	15	56	5	14 : 1
8[b]	IPr	1	Me	3	45	21	2.3 : 1



[a] Pd(NHC) = (η^3-1-^{t}Bu-indenyl)Pd(NHC)(Cl); [b] Reaction time = 13 h. (For experimental details for entries 1-3, see Appendix A; For entries 4-8, see Appendix B).

ligation state during oxidative addition, where more hindered ligands promote monoligation (and reaction at C4), while smaller or bidentate ligands favor bisligation (and reaction at C2),[20] In keeping with this hypothesis, we discovered that increased concentrations of 2,4-dichloropyridine marked a return to conventional C2 site selectivity as well as a decrease in the yield of diarylated product (Table 5.1, compare entries 4-6 with entries 1 and 2). Finally, we found that the introduction of a methyl group α to the pyridyl nitrogen, resulted in a noticeable increase in diarylated product, suggesting that the ability of a substrate to participate in ligand substitutions

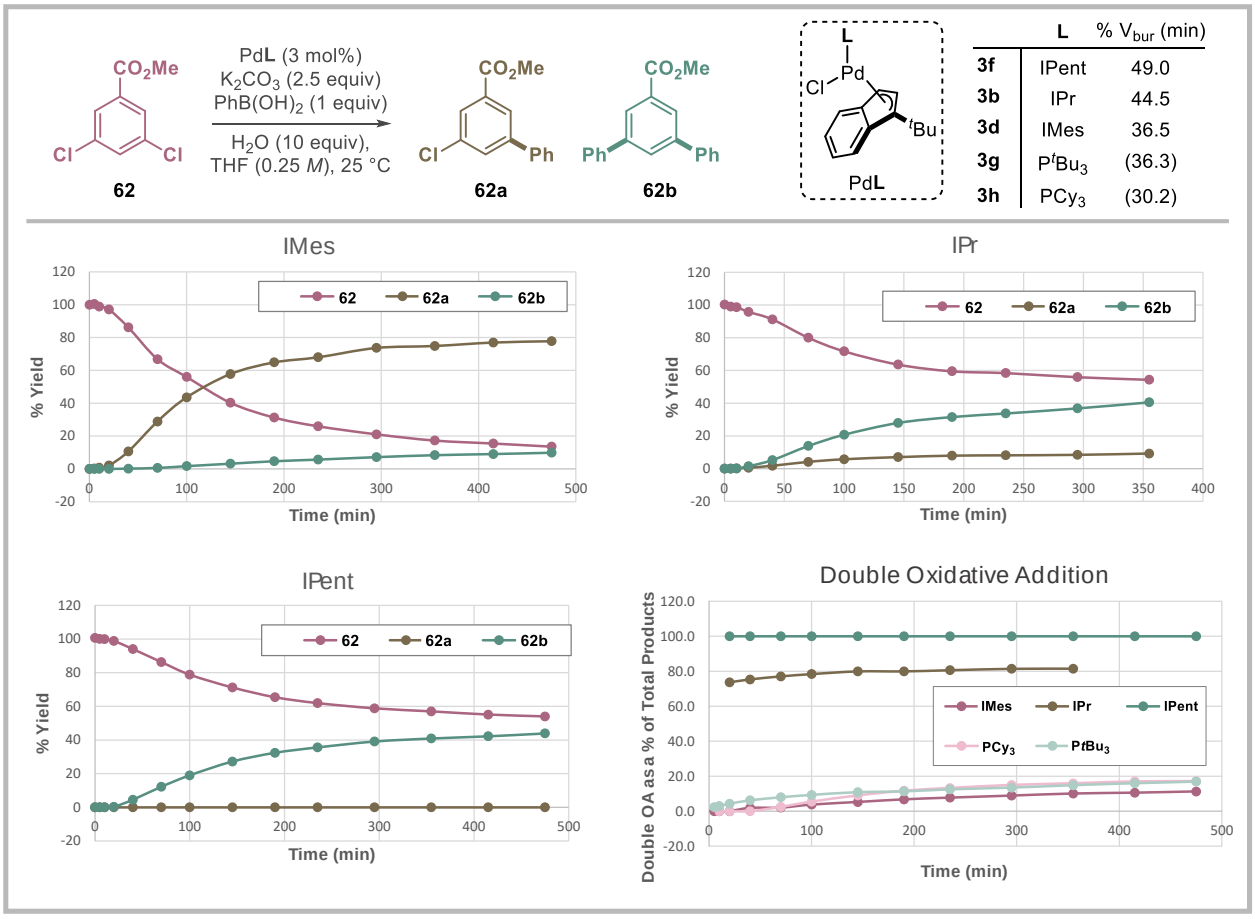
might inhibit over-arylation normally (Table 5.1, compare entries 7 and 8 to 1 and 2). Taken together, these findings pointed to the possibility that variations in selectivity for mono- vs difunctionalization also result from differences in catalyst ligation state.

Despite an obvious correlation between ligand sterics and the ring-walking ability of Pd catalysts in the literature, the mechanistic basis for this relationship remains unexplained. The term "diffusion control" is sometimes invoked by authors who have described ring-walking processes,[21] yet the mechanism by which diffusion (of the catalyst from substrate) takes place is rarely discussed. Currently, the cross-coupling community lacks guiding principles which could inform multiparameter optimizations of small molecule cross-couplings with dihalogenated heteroarenes as well as CTPs. Herein, we explore the hypothesis that selectivity for mono- vs difunctionalization is linked to Pd's coordination number and is therefore governed by several steric factors including the size of the ancillary NHC or phosphine ligand.

5.2 Results and Discussion:

We began our investigation by evaluating a series of NHC and phosphine ligands in the SMC of dichloroarene **62** with phenylboronic acid by monitoring their reactions over time. Based on literature precedent and our prior experience with Pd-catalyzed cross-couplings of dichloropyridines, we anticipated that the product of monoarylation, **62a**, would be favored by smaller NHC or phosphine ligands, while the product of diarylation, **62b**, would be favored by more hindered ones. Consistent with our previous findings, we found that the ligand IMes promoted monoarylated product **62a** predominantly, with minimal accumulation of **62b** as the

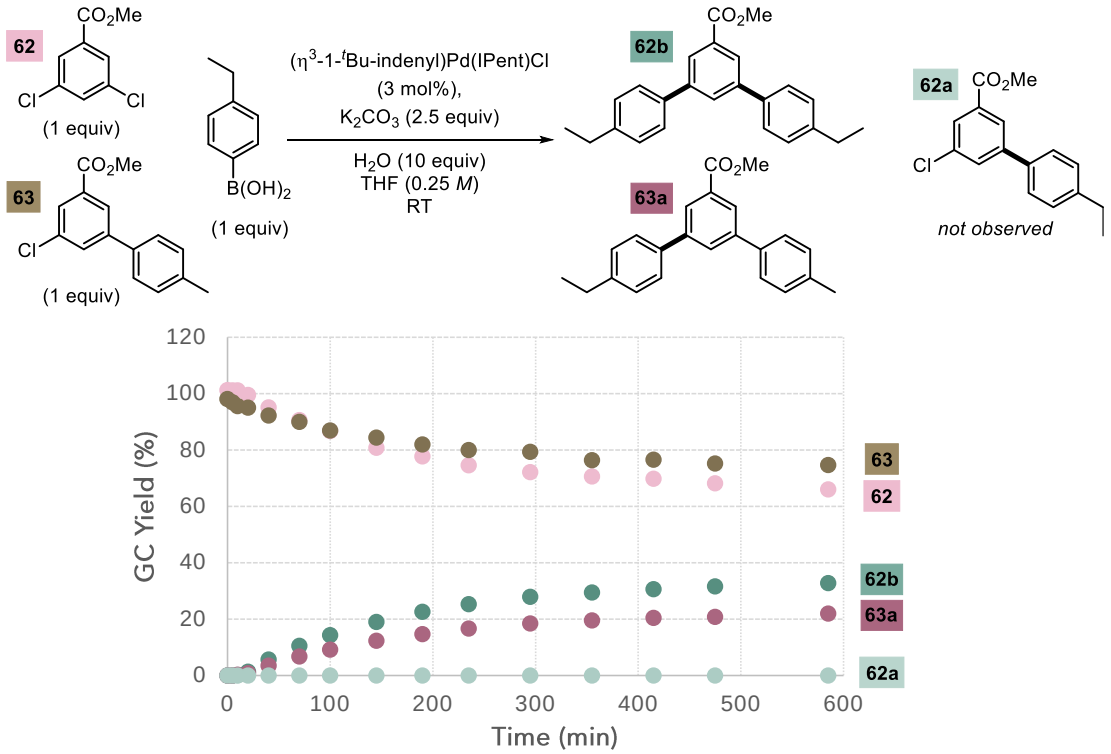
Scheme 5.2. Relationship between Ligand Sterics and Mono- vs Diarylation Selectivity over Time. *(Results by Nathaniel Larson)*



reaction progressed. Remarkably, and in stark contrast to IMes, monoarylated product **62a** was never observed in the reaction mediated by IPent. Instead, **62** is converted directly to **62b**, consistent with a ring-walking mechanism of diarylation. With the ligand IPr, **62b** predominates but is not exclusive, marking a shift in mechanism related directly to steric effects. Like IMes, trialkylphosphines PCy_3 and P^tBu_3 favor monoarylation under these conditions, and the ratio of observed products is inconsistent with a ring-walking mechanism. In terms of percent buried volume, the steric demands of P^tBu_3 are comparable to those of IMes—a similarity which is

seemingly reflected in their reaction profiles. Evidently, the proclivity of a catalyst to promote diarylation via an intramolecular catalyst transfer (i.e., by ring-walking between reactive sites) can be predicted on the basis of percent buried volume, with a numerical cutoff within the range of 36.5—44.5 % for the reaction in Scheme 5.2. The stark contrast in selectivity exhibited by IPr and IPent versus IMes, P^tBu_3, and PCy_3 is reminiscent of the "reactivity cliff" described by Sigman and Doyle[22] during their evaluation of steric descriptors which can predict both the ligation state and reactivity of phosphine ligands.

Scheme 5.3. Intermolecular Competition Study between a Dichloroarene and its Monoarylated Product.



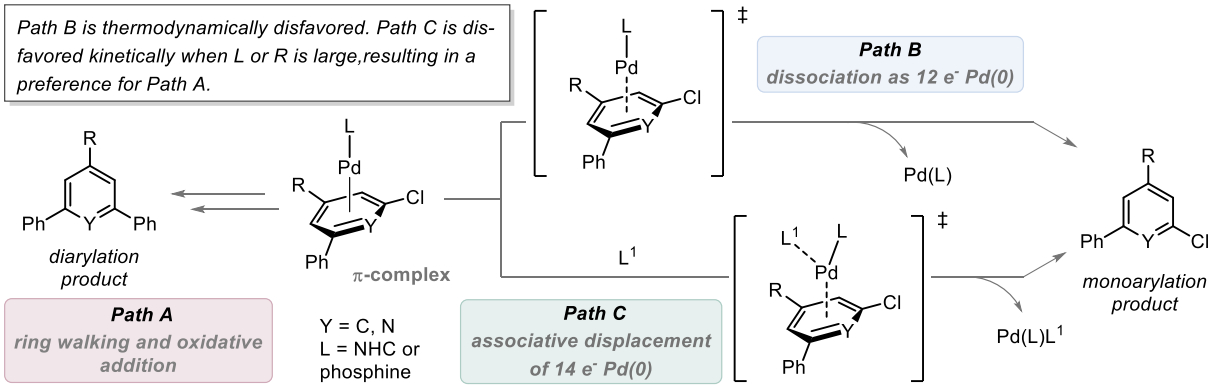
[a] Reactions were monitored by taking aliquots for GC analysis; yields are calibrated against undecane as the internal standard. **62a**, the monoarylated product of **62**, was not detected at any time point. *(Experimental contributions made by Nathaniel Larson)*

McNeil and others have noted that selective diarylation rarely, yet sometimes results from an *inter*molecular catalyst transfer (as opposed to ring-walking) if the monosubstituted intermediate is significantly more reactive than the dihaloarene which precedes it.[23] To evaluate this possibility, we designed an intermolecular competition study between **62** and its monoarylated product **63** (Scheme 5.3), mediated by Pd(IPent) (**3f**). While rates of conversion were similar for both starting materials, the dichloride **63** was consumed more rapidly than the monoarylated intermediate **63**, confirming that diarylation results from an *intra*molecular catalyst transfer rather than an *inter*molecular process. Intriguingly, the similarity in reaction rates between **62** with its two reactive sites, and **63** with its one reactive site, is inconsistent with a turnover-limiting oxidative addition, transmetalation, or reductive elimination step. Rather, the comparable rates of conversion for **62** vs **63** point to dissociation of the diarylated product from the catalyst as the turnover-limiting step.

On the basis of observed ligand steric trends (Scheme 5.2), previous data relating selectivity to the coordinating ability of a substrate (Table 5.1), and the evidence for turnover-limiting dissociation of catalyst from substrate (Scheme 5.3), we proposed the following mechanistic hypothesis depicted in Scheme 5.4: Initially, Pd completes one catalytic cycle at the first reactive site of the dichloroarene, which culminates in a reductive elimination step to form the first C—C bond. If Pd is bisligated during reductive elimination, PdL_2 will dissociate from the monofunctionalized product spontaneously as a 14 e^- species.[24] However, if Pd is monoligated, a Pd-arene π-complex results from reductive elimination, such that the intermediacy of 12 e^- Pd is avoided. After π-complexation, Pd may traverse the π-system and undergo a second oxidative addition at the remaining C—Cl bond (Path A). Operating under the assumption that dissociation

of 12 e$^-$ PdL from the substrate (Path B) is disfavored thermodynamically, the complexed substrate must be displaced by an incoming ligand for substrate turnover to occur (Path C).[12a] If ligand exchange is slow relative to ring-walking and oxidative addition, a second catalytic cycle will take place; however, if the rate of ligand exchange outcompetes that of ring-walking and oxidative addition, then separation of catalyst from the monoarylated product will result. Accordingly, ligands with a greater % V_{Bur} (min), which are able to promote low-coordinate Pd during reductive elimination, will result in stable Pd(L)(arene) π-complexes. Finally, when additional substituents larger than H ("R" in Scheme 5.4) are present on the arene, the intermediate Pd(L)(arene) π-complex will be slow to participate in ligand exchange, and a second oxidative addition event may result.

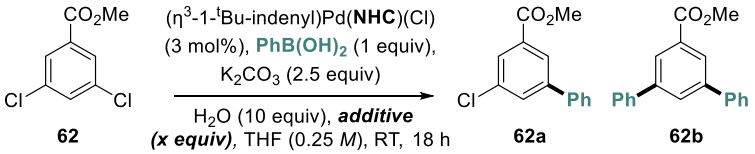
Scheme 5.4. Proposed Mechanisms for the Formation of Mono- and Diarylated Products.



To evaluate this hypothesis, we first surveyed a selection of small, coordinating additives which could, in principle, participate in ligand exchange (Path C). Under typical cross-coupling conditions, the NHC ligand IPr promotes formation of **62b** in a ratio of 4.2:1 with **62a** (mono-).

Remarkably, as little as 10 mol% of either indene or pyridine is sufficient to induce a selectivity switch in favor of monoarylation. However, this effect is markedly diminished when lutidine or tert-butylindene, are used in place of their non-alkylated analogues. As a coordinating additive, DMSO is particularly effective (4:1), and the magnitude of this effect increases with DMSO loading, albeit at the expense of conversion over time. Unlike DMSO, the addition of sulfolane did not significantly impact selectivity, indicating that DMSO inverts selectivity by virtue of its coordinating ability. Finally, an excess of acetonitrile also causes a selectivity switch. By comparison to IPr, the ligand IPent is resistant to the impact of coordinating additives—although, at 10 mol% DMSO, selectivity for **1b** is no longer exclusive, and **1a** becomes favored when DMSO is present in large excess. Taken together, the entries in Table 1 strongly support the notion that variations in the ratio of arylated products, **1a** vs **1b**, arise from the competition between mechanistic Pathways A and C (Scheme 5.4).

Table 5.2. Effects of Coordinating Additives on Diarylation Selectivity.



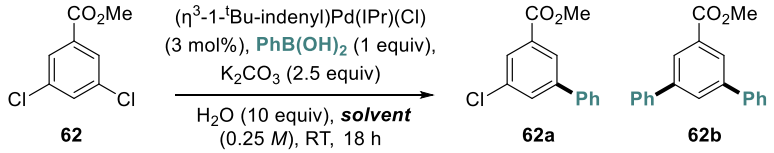
entry	NHC	additive (equiv)	**62a** (%)	**62b** (%)	**62a : 62b**
1	IPr	--	10	41	1 : 4.2
2	IPent	--	0	45	1 : >99
3	IPr	pyridine (0.1)	44	29	1.5 : 1
4	IPr	lutidine (0.1)	36	34	1.1 : 1
5	IPr	indene (0.1)	59	21	2.8 : 1
6	IPr	1-^{t}Bu-indene (0.1)	23	39	1 : 1.7
7	IPr	DMSO (0.1)	63	15	4.2 : 1
8	IPr	DMSO (1)	79	11	7.2 : 1
9	IPr	DMSO (10)	79	11	7.2 : 1
10	IPr	sulfolane (10)	11	41	1 : 3.7
11	IPent	DMSO (0.1)	3	41	1 : 15
12	IPent	DMSO (10)	32	28	1.1 : 1
13	IPr	MeCN (10)	58	20	2.9 : 1

[a] GC yields are calibrated against undecane as an internal standard. Average of two trials.
(Experimental contributions made by Nathaniel Larson)

Given the profound effect of π-accepting coordinators on selectivity in our system, we considered that solvent molecules may also participate in ligand exchange at the metal center. Indeed, when THF is replaced with benzene as the reaction solvent, selectivity reverses in favor of monoarylation. Moreover, selectivity is correlated with the coordinating ability of the solvent, with anisole marking a decrease in monoarylation compared to benzene, while benzotrifluoride marks an increase (compare entries 2-4). Methylated aromatic solvents such as toluene, xylenes, and mesitylene, favor an increase in diarylation corresponding with their degree of methylation

(entries 5-7), reiterating the importance of steric effects during the ligand exchange step. Significantly, arylated products are observed in a ratio of only 1:1, with use of mesitylene as the solvent.

Table 5.3. Effects of Coordinating Aromatic Solvents on Diarylation Selectivity.



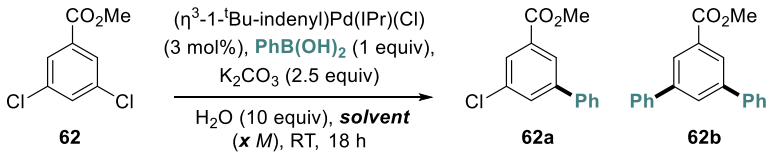
entry	solvent	**62a** (%)	**62b** (%)	**62a** : **62b**
1	THF	10	41	1 : 4.2
2	benzene	60	17	3.6 : 1
3	$PhCF_3$	66	16	4.2 : 1
4	anisole	45	23	1.9 : 1
5	PhMe	53	18	3.0 : 1
6	xylenes	36	13	2.8 : 1
7	mesitylene	25	28	1 : 1.1

[a]GC yields are calibrated against undecane as the internal standard and are the average of two trials (see Appendix D).

The observed additive and solvent trends in the SMC mediated by Pd-IPr or -IPent are consistent with the hypothesis outlined in Scheme 5.4. And yet, given that IPr promotes a mixture of products **62a** and **62b**, we were curious which coordinating species participate in ligand exchange processes under typical reaction conditions that omit exogenous additives. We considered whether THF might facilitate ligand exchange, only to lesser effect than benzene, when used as the solvent. Upon inspection, we discovered a correlation between solvent volume and selectivity where more dilute reactions led to an increase in difunctionalized product (Table 5.4,

entries 1-4). However, variations in molarity had no effect when benzene was used as the solvent (entries 5-8). From these data we concluded that the coordinator which promotes ligand exchange under typical conditions is not THF itself, but rather a solute. Benzene, on the other hand, is capable of associating to Pd and outcompetes coordination of solute(s) when present in excess. Returning to the proposed mechanistic pathways for catalytic turnover outlined in Scheme 5.4, the selectivity-determining steps of both Pathways A and B are unimolecular processes, and their rates will not be affected by concentration. Conversely, Path C involves a bimolecular ligand exchange where the rate is dependent upon [L^1] and [Pd(L)(arene)]. Since monoarylation selectivity improves under more concentrated conditions in THF, we may also infer that Path C is the favored mechanism by which monoarylated product is liberated, whereas Path B is inoperative.

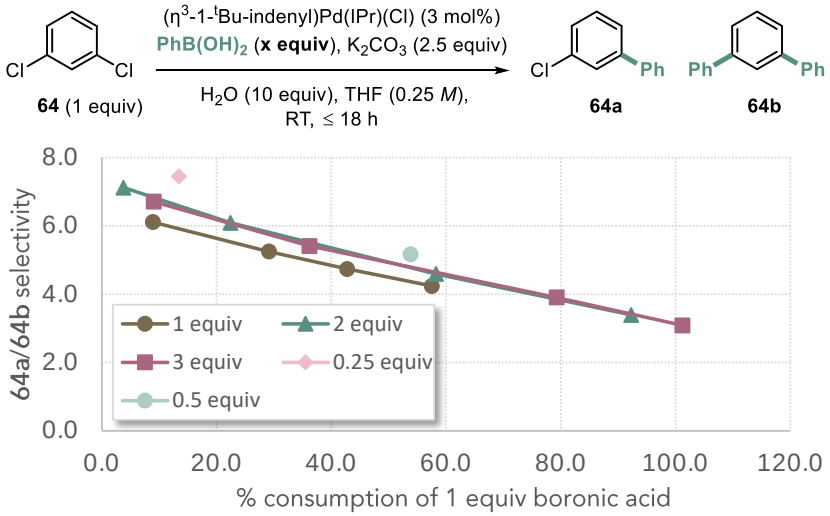
Table 5.4. Effect of Molarity on Diarylation Selectivity.



entry	solvent	molarity	MA (%)	DA (%)	MA : DA
1	THF	0.4	14	38	1 : 2.6
2	THF	0.25	10	41	1 : 4.2
3	THF	0.2	8	39	1 : 5
4	THF	0.16	6	37	1 : 6.2
5	benzene	0.4	61	17	3.6 : 1
6	benzene	0.25	60	17	3.6 : 1
7	benzene	0.2	60	17	3.5 : 1
8	benzene	0.16	59	17	3.6 : 1

[a]GC yields are calibrated against undecane as the internal standard and are the average of two trials (see Appendix D).

Scheme 5.5. Selectivity vs Conversion for Reactions with Variable Phenylboronic Acid Equivalents.[a]



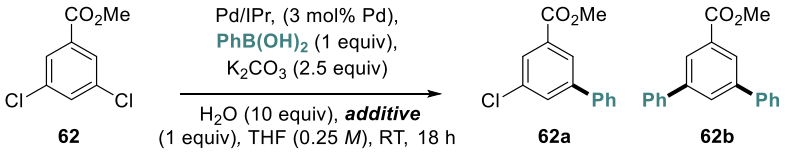
[a] Each data point represents an aliquot taken at intervals from one of five reactions in which boronic acid equivalents were varied. Single data points were collected for reactions with sub-stoichiometric boronic acid loadings. Selectivity and conversion were calculated using calibrated GC yields based on an *n*-undecane internal standard.

Having ruled out THF-mediated turnover at the intermediate π-complex, we turned our attention to π-acceptors present in the reaction which include phenylboronic acid, indene byproducts of precatalyst activation, and the dichloroarene itself (and its arylated products). Conceivably, each of these species could disrupt ring-walking by assuming the role of L^1 in Scheme 5.4, preceding the association of an unreacted substrate to Pd via ligand exchange. Since phenylboronic acid is the least hindered of these π-acceptors, association of its phenyl ring to the intermediate Pd π-complex seemed plausible. Nevertheless, we found that the stoichiometry of phenylboronic acid had no effect on the ratio of arylated products with respect to boronic acid conversion (Scheme 5.5). Rather, each reaction conformed to a linear trend wherein selectivity drifted from ~ 7:1 (MA/DA) to ~ 3:1 during the reaction window where one equivalent of boronic

acid was consumed, independent of the boronic acid loading. From these data we may conclude that phenylboronic acid does not meaningfully impact the distribution of products by participating in ligand exchange reactions.

Having previously identified indene as a competent coordinator able to invert selectivity at sub-stoichiometric loadings (*vide supra*), we considered the possibility that a byproduct of precatalyst activation, such as 1-*tert*-butyl-3-phenylindene,[25] could promote Path C under typical reaction conditions. To evaluate this possibility, we compared (η^3-1-^{t}Bu-indenyl)Pd(NHC)(Cl) to $[Pd(IPr)Cl_2]_2$ which lacks a "throw-away" ligand,[26] but found no difference in selectivity or yield (Table 5.5, compare entries 1 and 2), allowing us to rule out coordination of *tert*-butylindene byproducts.

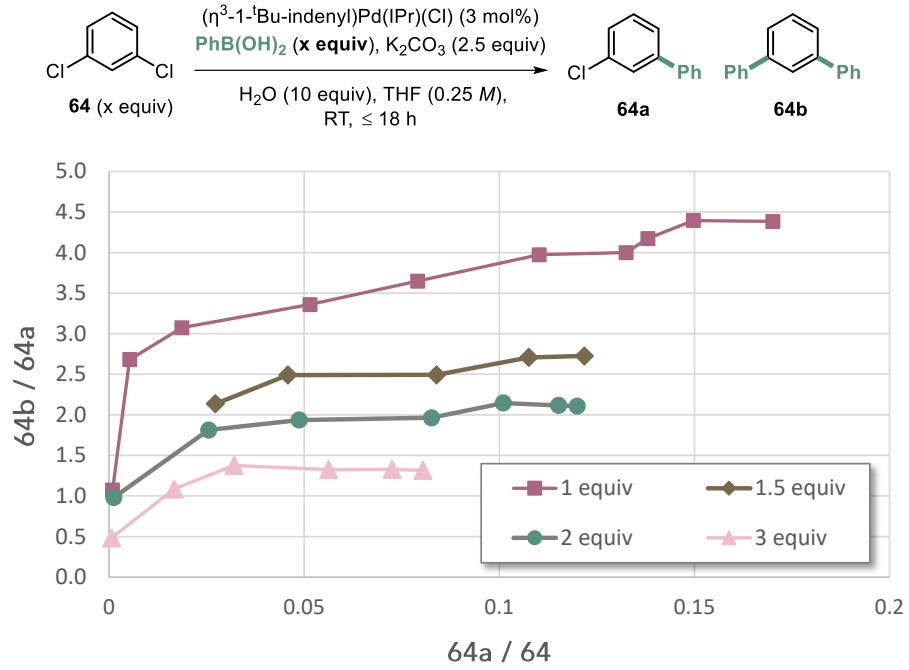
Table 5.5. Effects of Precatalyst Identity and Arene Additives.



entry	precatalyst	**62a** (%)	**62b** (%)	**62a** : **62b**
1	(η^3-1-^{t}Bu-indenyl)Pd(NHC)(Cl)	10	41	1 : 4.2
2	$[Pd(IPr)Cl_2]_2$	10	40	1 : 4

[a]GC yields are calibrated against undecane as the internal standard. Average of two trials.

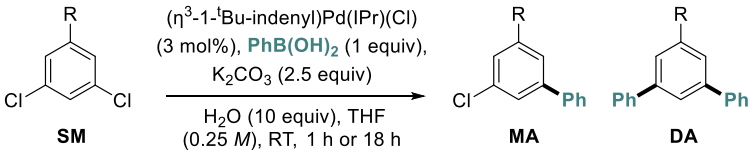
Scheme 5.6. Monoarylation/Starting Material (**64a**/**64**) Ratio vs Diarylation/Monoarylation (**64b**/**64a**) Ratio as Suzuki-Miyaura Reactions Progress *(Results by Nathaniel Larson).*

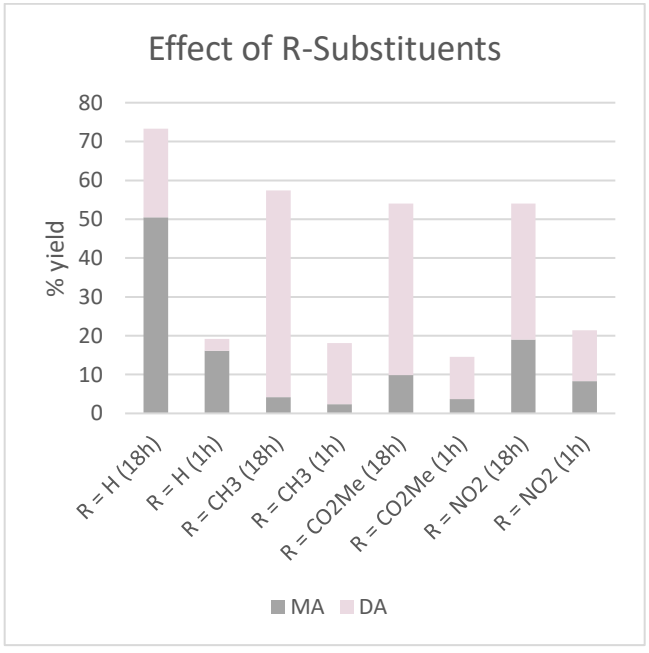


Having carefully evaluated the effects of other potential coordinators in the SMC, we concluded that catalytic turnover most likely takes place via an associative ligand exchange where an unreacted dichloroarene replaces the arylated product bound to Pd. To test this hypothesis, it was necessary to correlate the concentration of a dichloroarene substrate, such as **64**, with selectivity for its products (**64a**/**64b**). However, experiments which modify [**64**] are likely to alter the product distribution for at least two reasons: (1) by modifying [L^1] in Path C, and (2) by biasing the intermolecular competition between chloroarene reactants **64** and **64a** which are both precursors to **64b**. To differentiate these possibilities, we plotted the ratio of reactants (**64a**/**64**) against the ratio of arylated products (**64b**/**64a**) and discovered an inverse correlation between increasing [**64**] and diarylation selectivity (**64b**/**64a**), irrespective of the reactant distribution

(Scheme 5.6). From these data we may infer that in the absence of exogenous coordinating additives or solvents, the mechanism by which Pd(IPr) moves from one substrate to the next is in fact the simplest one, wherein **64** replaces **64a** or **64b** directly in an associative ligand exchange step. For processes which involve Pd ring-walking, the distribution of products **64a** versus **64b** reflects the rate of ligand exchange relative to the rate of oxidative addition from the preceding π-complex intermediate.

Scheme 5.7. Effect of Varied C5-Substituents on Selectivity for SMCs with 1,3-Dichlorobenzenes. *(Results by Nathaniel Larson).*





Substrate Steric Effects: Having determined the identity of L^1 in path C, we speculated that dichloroarenes with additional substituents (i.e., dichloroarenes which are more hindered) may be slower to undergo ligand exchange, leading to an increase in diarylation from Path A. Scheme 5.7 demonstrates that substrates with C3-substituents larger than H are biased toward the product of diarylation, in line with our expectation. Interestingly, this observation holds true independent of electron-donating or -withdrawing effects conferred by the substituent.

5.3 Conclusion

Bulky N-heterocyclic carbene or phosphine ligands are known to promote selective difunctionalization in Pd-catalyzed cross-couplings of dihalo(hetero)arenes via an intramolecular catalyst transfer or "ring-walking" mechanism. This work demonstrates that Pd's ability to ring-walk over π-conjugated systems is a unique attribute of low-valent PdL which forms stable $14e^-$ π-complexes with dihaloarene electrophiles. Conversely, ring-walking is not observed with bisligated Pd, since PdL_2 can readily dissociate from the π-system, whereas PdL cannot.[27] Bulky NHC ligands such as IPr and IPent promote low-coordinate Pd complexes and thereby facilitate ring-walking and difunctionalization, while smaller or bidentate ligands result in monoarylation. Under conditions which employ hindered, low-valent Pd catalysts, the typical mechanism of catalytic turnover involves an associative ligand exchange at the 14e- Pd π-complex, where an unreacted dichloroarene displaces the product of cross-coupling. The rate of associative ligand exchange—and therefore selectivity, is highly sensitive to steric factors, including sterics imposed by the ancillary NHC (or phosphine) ligand, the incoming coordinator, and the coordinated substrate.

In practice, these findings enable one to control selectivity for mono- vs diarylation of dichloro(hetero)arenes in many scenarios. Selectivity for monoarylation may be improved by (1) selecting smaller or bidentate ligands instead of hindered ones when possible or, if bulky ligands are necessary, (2) including a coordinating additive to facilitate ligand exchange at Pd. If exhaustive arylation is the desired outcome, IPent is especially effective for this purpose, and polar, non-coordinating solvents such as THF are preferable to coordinating, aromatic solvents such as toluene. Moreover, in planning synthetic routes, one should expect that highly substituted (or sterically hindered) dihaloarenes will exhibit more difunctionalization—particularly in cross-couplings involving monoligated Pd. Finally, this work explains the exclusivity of highly hindered NHC and phosphine ligands in Pd-mediated applications which benefit from ring-walking, such as catalyst-transfer polycondensations.[28]

5.4 References

1. For selected examples of stepwise functionalization of polyhalo(hetero)arenes, see: (a) Garg, N. K., Sarpong, R. and Stoltz, B. M. *J. Am. Chem. Soc.* **2002**, *124*, 131794 (b) Fisher, T. J.; Dussault, P. H. *Eur. J. Org. Chem.* **2012**, 2831–2836 and references therein. (b) Ceide, S. C.; Montalban, A. G. *Tetrahedron Lett.* **2006**, *47*, 4415– 4418. (c) Young, I. S.; Glass, A.-L.; Cravillion, T.; Han, C.; Zhang, H.; Gosselin, F. *Org. Lett.* **2018**, *20*, 3902– 3906.

2. Prajapati, D.; Schulzke, C.; Kindermann, M. K.; Kapdi, A. R. *RSC Adv.* **2015**, *5*, 53073−53085.

3. Examples of monosubstitution with traditional catalysts and symmetrical substrates: (a) Bunz, U. H. F.; Roidl, G.; Adams, R. D. *J. Organometallic Chem.* **2000**, *600*, 56-62. (b) Guillén, E.; Hirrezuelo, J.; Martínez-Mallorquín, R.; López-Romero, J. M.; Rico, R. *Tetrahedron* **2011**, *67*, 2555– 2561. Doebelin, C.; Wagner, P.; Bertin, I.; Simonin, F.; Schmitt, M.; Bihel, F.; Bourguignon, J.-J. *RSC Adv.* **2013**, *3*, 10296– 10300.

4. For PPh_3, examples of selective diarylation are largely limited to diiodoarenes: (a) Tsvetkov, A. V.; Latyshev, G. V.; Lukashev, N. V.; Beletskaya, I. P. *Tetrahedron Lett*. **2000**, *41*, 3987-3990. (b) Sinclair, D. J.; Sherburn, M. S. J. *Org. Chem.* **2005**, *70*, 9, 3730–3733.

5. See ref. 2a. Note, in some scenarios, difunctionalization cannot be mitigated by using an excess of dihaloarene: Tietze, L. F.; Nordmann, G. *Synlett* **2001**, 337-340.

6. (a) Dong, C.-G.; Hu, Q.-S. *J. Am. Chem. Soc.* **2005**, *127,* 28, 10007. (b) Weber, S. K., Galbrecht, F., and Scherf, U. *Org. Lett*. **2006**, *8*, 4039– 4041.

7. For examples of difunctionalization or polymerization with RuPhos, see: (a) Dai, X.; Chen, Y.; Garrell, S.; Liu, H.; Zhang, L.-K.; Palani, A.; Hughes, G.; Nargund, R. *J. Org. Chem.* **2013**, *78*, 7758−7763, see Table 1, entry 16. (b) Lee, J.; Park, H.; Hwang, S.-H.; Lee, I.-H.; Choi, T.-L. *Macromolecules* **2020**, *53*, 3306– 3314. (c) Lee, J. Ryu, H.; Park, S.; Cho, M.; Choi, T.-L. *J. Am. Chem. Soc*. **2023**, *145,* 28, 15488-15495.

8. For an example of difunctionalization with the ligands SIPr, IPr, and IPent, see: Norman, J. P.; Larson, N. G.; Entz, E. D.; Neufeldt, S. R. *J. Org. Chem.* **2022**, *87*, 7414−7421.

9. Zhu, Y. X.; Li, E. C.; Shen, K.; Hang, X.; Bonnesen, P. V.; Hong, K.; Zhang, H. H.; Huang, W. Intramolecular Catalyst Transfer over Sterically Hindered Arenes in Suzuki Cross-Coupling Reactions, *Asian J. Org. Chem.*, **2019**, *8* , 1506 —1512. See also: ref. 18.

10. Groombridge, B. J.; Goldup, S. M.; Larrosa, I. Selective and general exhaustive cross-coupling of dichloroarenes with a deficit of nucleophiles mediated by a Pd–NHC complex. *Chem. Commun.* **2015**, *51*, 3832– 3834.

11. Leone, A. K.; Goldberg, P. K.; McNeil, A. J. Ring-Walking in Catalyst-Transfer Polymerization. *J. Am. Chem. Soc*. **2018**, *140,* 25, 7846– 7850.

12. (a) Strawser, D.; Karton, A.; Zenkina, O. V.; Iron, M. A.; Shimon, L. J. W.; Martin, J. M. L.; van der Boom, M. E. *J. Am. Chem. Soc*. **2005**, *127*, 9322– 9323, DOI: 10.1021/ja050613h (b) Zenkina, O. V.; Karton, A.; Freeman, D.; Shimon, L. J. W.; Martin, J. M. L.; van der Boom, M. E. *Inorg. Chem.* **2008**, *47*, 5114– 5121, DOI: 10.1021/ic702289n (c) Sontag, S. K.; Bilbrey, J. A.; Huddleston, N. E.; Sheppard, G. R.; Allen, W. D.; Locklin, J. *J. Org. Chem*. **2014**, *79*, 1836– 1841, DOI: 10.1021/jo402259z (d) Smith, J. A.; Schouten, A.; Wilde, J. H.; Westendorff, K. S.; Dickie, D. A.; Ess, D. H.; Harman, W. D. *J. Am. Chem. Soc.* **2020**, *142*, 16437– 16454, DOI: 10.1021/jacs.0c08032.

13. (a) Sheina, E. E.; Liu, J.; Iovu, M. C.; Laird, D. W.; McCullough, R. D. Chain Growth Mechanism for Regioregular Nickel-Initiated Cross-Coupling Polymerizations. *Macromolecules* **2004**, *37*, 3526−3528. (b) Yokoyama, A.; Miyakoshi, R.; Yokozawa, T. *Macromolecules* **2004**, *37*, 1169−1171. (c) Yokoyama, A.; Yokozawa, T. *Macromol. Rapid Commun*. **2004**, *25*, 1663−1666. For notable papers describing CTP mechanism, see: (d) Zhao, Y.; Nett, A. J.; McNeil, A. J.; Zimmerman, P. M *Macromolecules* **2016**, *49*, 7632– 7641.

14. (a) Adachi, I.; Miyakoshi, R.; Yokoyama, A.; Yokozawa, T. *Macromolecules*, **2006**, *39*, 7793-7795. Yokozawa, T.; Ohta, Y. *Chem. Rev.* **2016**, *116*, 1950−1968.

15. Bryan, Z. J.; Smith, M. L.; McNeil, A. J. *Macromol. Rapid Commun.* **2012**, *33*, 842– 847, DOI: 10.1002/marc.201200096

16. Leone, A. K.; Mueller, E. A.; McNeil, A. J. *J. Am. Chem. Soc.* **2018**, *140*, 15126– 15139, DOI: 10.1021/jacs.8b09103

17. (a) Mao, Y.; Wang, Y.; Lucht, B. L. *J. Polymer Sci.: Part A: Polymer Chem.* **2004**, *42*, 5538 –5547 (b) Bhatt, M. P.; Magurudeniya, H. D.; Sista, P.; Sheina, E. E.; Jeffries-EL, M.; Janesko, B. G.; McCullough, R. D.; Stefan, M. C. *J. Mater. Chem. A* **2013**, *1*, 12841– 12849.

18. Deem, M. C.; Derasp, J. S.; Malig, T. C.; Legard, K.; Berlinguette, C. P.; Hein, J. E. *Nat. Commun*. **2022**, *13*, 2869, DOI: 10.1038/s41467-022-30255-1

19. Norman, J. P.; Larson, N. G.; Entz, E. D.; Neufeldt, S. R. *J. Org. Chem.* **2022**, *87*, 7414−7421.

20. Norman, J. P.; Larson, N. G.; Neufeldt, S. R. *ACS Catal*. **2022**, *12*, 15, 8822–8828.

21. Larrosa, I.; Somoza, C.; Banquy, A.; Goldup, S. M. *Org. Lett.* **2011**, *13*, 1, 146-149. *See also: Ref 18 and 9.*

22. Newman-Stonebraker, S. H.; Smith, S. R.; Borowski, J. E.; Peters, E.; Gensch, T.; Johnson, H. C.; Sigman, M. S.; Doyle, A. G. *Science* **2021**, *374*, 301−308.

23. Bryan, Z. J.; Hall, A. O.; Zhao, C. T.; Chen, J.; McNeil, A. J. *ACS Macro Lett*. **2016**, *5*, 69–72.

24. Mikami, K.; Nojima, M.; Masumoto, Y.; Mizukoshi, Y.; Takita, R.; Yokozawa, T.; Uchiyama, M. *Polym. Chem*. **2017**, *8*, 1708– 1713, DOI: 10.1039/C6PY01934J

25. 1-*tert*-butyl-3-phenylindene was detected in the product mixture by GCMS. Formation of this byproduct by reduction of (η^3-1-^{t}Bu-indenyl)Pd(NHC)(Cl) has been reported previously: Melvin, P. R.; Balcells, D.; Hazari, N.; Nova, A. *ACS Catal*. **2015**, *5*, 5596– 5606, DOI: 10.1021/acscatal.5b01291

26. Reduction of $[Pd(IPr)Cl_2]_2$ by phenylboronic acid generates biphenyl which is arguably a (weak) "throw-away" ligand in this context.

27. For the dissociation of Pd(IPr)(**62a**) → Pd(IPr) + **62a**, DFT calculations indicate the products are 20 kcal/mol higher in energy than the reactant: Larson, N. G.; Norman, J. P.; Neufeldt, S. R. (manuscript in preparation).

28. Note that unlike PdL_2, NiL_2 is well known for its ability to ring-walk, thus the mechanistic findings of this study do not apply to Ni-catalyzed processes.

APPENDICES

APPENDIX A

SUPPORTING INFORMATION

for

CHAPTER TWO

A1. General Materials and Methods

NMR spectra were recorded at 298 K on a Bruker DRX 500 MHz (500.233 MHz for ^{1}H, 125.795 MHz for ^{13}C, 470.639 MHz for ^{19}F), a Bruker Avance III 600 MHz (600.130 MHz for ^{1}H or 150.903 MHz for ^{13}C) spectrometer, or a Bruker Ascend 400 MHz (400.130 MHz for ^{1}H NMR, 100.613 for ^{13}C). ^{1}H and ^{13}C NMR chemical shifts are reported in parts per million (ppm) relative to TMS, with the residual solvent peak used as an internal reference [^{1}H NMR: $CHCl_3$ (7.26 ppm), C_6D_5H (7.16 ppm), DMSO-d_5 (2.50 ppm); ^{13}C NMR: $CDCl_3$ (77.16 ppm), ^{13}C NMR: C_6D_6 (128.06 ppm), DMSO-d_6 (39.52 ppm)]. Multiplicities are reported as follows: singlet (s), broad singlet (br s) doublet (d), doublet of doublets (dd), doublet of doublets of doublets (ddd), triplet (t), quartet (q), and multiplet (m). GC data were collected using a Shimadzu GC-2010 Plus with a flame ionization detector equipped with a SH-Rxi-5ms capillary column (15 m x 0.25 mm ID x 0.25 µm df). GCMS data were collected with a Shimadzu GC-2030 paired with a Shimadzu GCMS-QP2020 NX and equipped with a SH-Rxi-5ms capillary column (30 m x 0.25 mm ID x 0.25 µm df). LC-MS analyses were performed on either an Agilent 6538 Q-TOF MS or a Bruker micro-TOF MS, both coupled to an Agilent 1290 Infinity UHPLC system. A 50 mm long Eclipse Plus C18 column (Agilent Technologies, Santa Barbara, CA; i.d. 2.1 mm, 1.8 µm particle size) was used for separation. A 6-minute gradient was used at a flow rate of 0.6 mL/min: 0-1 min 95% buffer A (100% H2O with 0.1% formic acid), followed by a gradient from 1-4 minutes of 5-95% buffer B (100% acetonitrile with 0.1% formic acid), 1 minute 95% buffer B, and returning to 95% buffer A for 1 minute. The mass spectrometers were operated in positive-ion mode with electrospray ionization. All reactions that require heating were conducted in aluminum single-size

vial reaction blocks (Chemglass) fitted to an IKA stirring hot plate equipped with a temperature probe.

Unless otherwise noted below, all commercially-obtained chemicals were used as received. PEPPSI-SIPr and PEPPSI-IPr were obtained from Sigma Aldrich. (η^3-1-^{t}Bu-indenyl)$_2$(μ-Cl)$_2$Pd$_2$, (η^3-1-^{t}Bu-indenyl)Pd(IPr)(Cl), and (η^3-1-^{t}Bu-indenyl)Pd(IPent)(Cl) were obtained from Umicore. Other (η^3-1-^{t}Bu-indenyl)Pd(NHC)(Cl) precatalysts were prepared from the corresponding *N*-heterocyclic carbene ligands IMes, SIMes, SIMix, or SIPr (each obtained from Strem Chemicals or Sigma Aldrich) according to a literature procedure.[1] Unless otherwise noted, dichloroheteroarenes and arylboronic acid starting materials were obtained from Oakwood Chemical. 4,5-Dichloro3(2H)-pyridazinone (**A45**)[2] and 3,4,5-trichloropyridazine (**A46**)[3] were prepared according to literature procedures. Potassium fluoride, 1,4-dioxane, benzyl bromide, iodine, potassium *tert*-butoxide, tetrabutylammonium hexafluorophosphate, and palladium (II) chloride were obtained from Acros Organics. Potassium carbonate, methylmagnesium bromide, triphenylphosphine, tri-*tert*-butylphosphine, 4-vinylphenylboronic acid, 2,4-dichloro3-cyanopyridine, and 2,4-dichloro-5-methylpyridine were obtained from Alfa Aesar. 2,4-dichloro-5-nitropyridine and 3,3'-bromomethyloxetane were obtained from Combi-Blocks. 2,4-Dichloro-1,8-naphthyridine and 3-amino2,4-dichloropyridine were obtained from Millipore Sigma. 3-Amino-2,4-dichloropyridine was obtained from Synthonix. Sodium carbonate, THF, toluene, and methanol were obtained from Fisher Scientific. Magnesium turnings, *tert*-butyl bromide, cyclopentyl bromide, benzothiophene (thianaphthene), 2-bromo-5-methylpyridine, lithium chloride, tetrabutylammonium bromide and chloride, tris(dibenzylideneacetone)dipalladium(0), diphenylphosphinoferrocene, tri-*o*-tolylphosphine, and tricyclohexylphosphine were obtained

from Oakwood chemical. Diisobutylaluminum hydride (DIBAL), magnesium bromide diethyl etherate, propylene carbonate, potassium bromide, and *n*-butyllithium were obtained from Sigma-Aldrich. Palladium (II) acetate, trimethyl phosphine, Q-Phos, and CataCXium A were obtained from Strem Chemical. 2,4-Dichloroquinoline, zinc dichloride, and $Pd(PPh_3)_4$ were obtained from TCI Chemicals. Benzene was obtained from Beantown Chemical. For the purposes of Kumada or Negishi cross-couplings or for preparation of Grignard reagents, THF was purified on a JC Meyer solvent dispensing system and stored under N_2 prior to use. For the purpose of Suzuki-Miyaura cross-couplings, THF was used as received from Fisher Scientific. For the purpose of Suzuki-Miyaura cross-couplings under ligand-free reaction conditions, DMF was purified on a JC Meyer solvent dispensing system and stored under N_2 prior to use. 1,4-Dioxane required for Pd/dppf-mediated Suzuki-Miyaura cross-couplings was used as received from Acros Organics but kept under N_2 prior to and during use. Grignard reagents were titrated according to a literature procedure.[4]

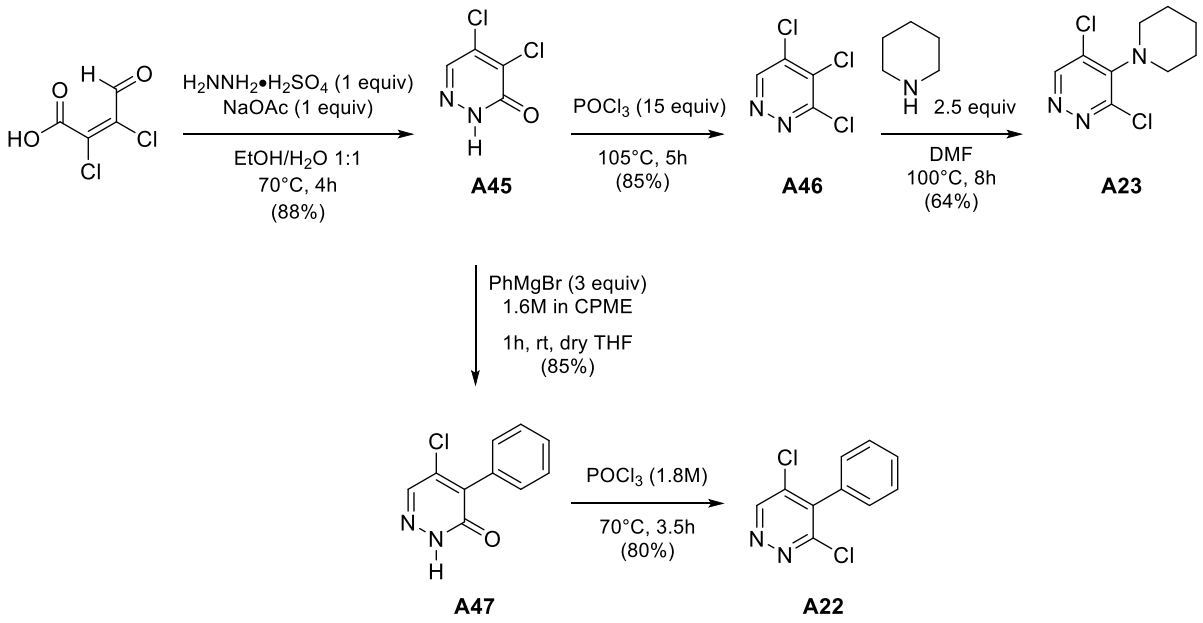
Deuterated solvents ($CDCl_3$, C_6D_6, DMSO-d_6) were obtained from Cambridge Isotopes and stored over molecular sieves. Manual flash column chromatography was performed on SiliCycle silica gel 60 (40-63 μm particle size) and thin layer chromatography was performed on SiliCycle TLC plates pre-coated with extra hard silica gel 60 F_{254}. Automated flash column chromatography was performed with a Biotage Selekt equipped with Biotage Sfär silica flash cartridges (20 μm particle size; 50 Å pore width) for normal phase separations, or Silica C18 cartridges (30 μm particle size; 100 Å pore width) for reversed phase separations.

A2. Synthesis and Characterization of Reagents

Chlorinated Heteroarenes

3-Amino-4,6-dichloropyridine (**A16**): Glacial acetic acid (14.2 mL) was heated to 60 °C in a round-bottom flask equipped with a Vigreux reflux condenser and stir bar. Iron powder (4.175 g, 74.8 mmol, 3.5 equiv) and 2,4-dichloro-5-nitropyridine (4.122 g, 21.36 mmol, 1.0 equiv) were added to the flask consecutively while stirring. The mixture was allowed to stir at 60 ºC for 2.5 h. Partway through the reaction time, the mixture thickened such that stirring was encumbered, so an additional 8 mL glacial acetic acid was added to the flask. The resulting suspension was vacuum-filtered through Celite and the filter cake was washed thoroughly with ethyl acetate. Solvent was removed from the filtrate under reduced pressure, and the resulting solids were taken up in ethyl acetate. The organic solution was washed with saturated aqueous sodium bicarbonate, deionized water (3x), and brine. The organic layer was dried over magnesium sulfate, filtered, and concentrated under reduced pressure. The resulting white solid was dried under vacuum overnight, affording **A16** as a very pale pink solid (2.030 g, 58% yield). ^{1}H NMR (500 MHz, $CDCl_3$, δ): 7.88 (s, 1H), 7.21 (s, 1H), 4.16 (br s, 2H); ^{13}C{1H} NMR (126 MHz, $CDCl_3$, δ): 139.7, 139.3, 136.2, 129.7, 123.9

Scheme A1. Dichloropyridazines Synthetic Map.



5-Chloro-4-phenyl-3(2H)-pyridazinone (**A47**): Compound **A47** was prepared according to a procedure adapted from the literature.5 4,5-Dichloro-3(2H)-pyridazinone (**A45**)[2] (1.2 g, 7.27 mmol, 1.0 equiv) was added to an oven-dried 50 mL Schlenk flask equipped with a stir bar. The flask was fitted with a rubber septum, the septum was secured with copper wire, and the flask was evacuated and backfilled with N_2 (3x). Dry THF (12 mL) was transferred into the flask by cannula. The flask was cooled in an ice bath, and a solution of phenylmagnesium bromide (1.6 *M* in CPME, 13.6 mL, 21.82 mmol, 3.0 equiv) was added dropwise over 10 min by cannula. The flask was removed from the ice bath and the reaction was stirred at room temperature for 1 h. The flask was returned to the ice bath, opened to air, and quenched by the slow addition of aqueous NH_4Cl (12 mL; 100 g/L). The resulting mixture was partitioned between deionized water and ethyl acetate. The aqueous layer was extracted with ethyl acetate (2x). The combined organic fractions were

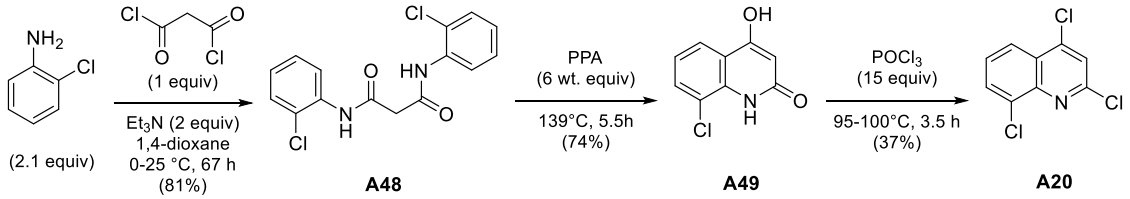
washed with brine, dried over magnesium sulfate, filtered, and concentrated under reduced pressure. The resulting solids were triturated in hexanes, filtered, and dried under vacuum to afford **A47** as a white solid (1.277 g, 85% yield). ^{1}H NMR (500 MHz, DMSO-d_6, δ): 13.40 (br s, 1H), 8.03 (s, 1H), 7.47-7.40 (multiple overlapping signals, 5H). Spectral data are consistent with the literature report.[5]

3,5-Dichloro-4-phenylpyridazine (**A22**): Phosphorous(V) oxychloride (3.4 mL) and **A47** (1.266 g, 6.127 mmol, 1.0 equiv) were combined in an oven-dried round-bottom flask equipped with a stir bar. The flask was then fitted with a Vigreux reflux condenser and sealed with a rubber septum fastened with copper wire. An outgassing line, which was assembled with PVC tubing, a needle adapter, and a needle, was routed from the condenser through a mineral oil bubbler, which was in turn routed through an aqueous KOH trap. An in-gas needle was introduced to the condenser, and the system was purged with N_2. The in-gas line was closed off such that hydrogen chloride evolution could be monitored visually. The reaction mixture was heated to 70 °C and stirred for 3.5 h. Stirring was continued while the reaction cooled to ambient temperature. The reaction was quenched by slow, dropwise addition of aqueous NaOH (5 mol % in water) while stirring until bubbling ceased. The mixture was diluted with water and filtered affording a brown solid. The wet solid was taken up in benzene, and then concentrated under reduced pressure; this process was repeated once. The resulting solids were dried under vacuum overnight to afford **A22** as a brown solid (1.109 g, 80% yield). ^{1}H NMR (500 MHz, DMSO-d_6, δ): 9.54 (s, ^{1}H), 7.58-7.51 (multiple overlapping signals, 3H), 7.46-7.43 (m, 2H); ^{13}C{^{1}H} NMR (126 MHz, DMSO-d_6, δ): 155.6,

151.6, 138.8, 137.9, 131.7, 129.7, 128.71, 128.68. HRMS (ESI Q-TOF) m/z: [M]+ Calcd for $C_{10}H_6Cl_2N_2$ 223.9908; Found 223.9896.

3,5-Dichloro-4-(1-piperidinyl)-pyridazine (**A23**): 3,4,5-Trichloropyridazine (**A46**)[3] (550.3 mg, 3.0 mmol, 1.0 equiv) was combined with DMF (9.38 mL) and a stir bar in a 5-dram vial. The vial was fitted with a septum and placed under an atmosphere of N_2 gas. Piperidine (744 µL, 7.5 mmol, 2.5 equiv) was added dropwise through the septum via a 100 µL syringe to the stirring solution, resulting in rapid evolution of HCl gas and increased turbidity. The reaction was stirred at ambient temperature for 1 h. DMF was removed under vacuum, and the residue was purified by flash column chromatography on silica gel in 10% acetone in hexanes (R_f = 0.22). The combined fractions were dried under vacuum to afford **A23** as a white solid with minor brown discoloration (445 mg, 64% yield). ^{1}H NMR (500 MHz, $CDCl_3$, δ): 8.68 (s, ^{1}H), 3.36-3.34 (m, 4H), 1.77-1.64 (multiple overlapping signals, 6H); $^{13}C\{^1H\}$ NMR (126 MHz, $CDCl_3$, δ): 155.5, 148.0, 143.1, 123.9, 50.6, 25.6, 23.7. HRMS (ESI Q-TOF) m/z: [M]+ Calcd for $C_9H_{11}Cl_2N_3$ 231.0330; Found 231.0326.

Scheme A2. Synthesis of 2,4,8-Trichloroquinoline (**A20**).



***N*^{1},*N*^{3}-Bis(2-chlorophenyl)-propanediamide** (**A48**): Compound **A48** was prepared according to a modified literature procedure.[6] Malonyl dichloride was purified by simple vacuum distillation

prior to use; triethylamine was distilled from calcium hydride, sparged with N_2, and stored over 4 Å molecular sieves prior to use. 2-Chloroaniline (2.679 g, 21 mmol, 2.1 equiv) was weighed into a 100-mL round bottom flask, followed by dry 1,4-dioxane (24 mL) and a stir bar. The flask was fitted with a rubber septum and the septum was secured with copper wire. An ingas needle and smaller diameter outgassing needle were introduced through the septum, and the contents of the flask were sparged with N_2 for 15 min. Dry triethylamine (2 equiv, 20 mmol, 2.8 mL) was added through the septum via 1-mL syringe, and the sealed flask was cooled in an ice bath. Under N_2, a solution of malonyl dichloride (973 µL, 10 mmol, 1 equiv) in dry 1,4-dioxane (28.5 mL) was added dropwise to the cooled stirring solution through the septum via a 10-mL syringe over 20 min. The solution became bright yellow and evolution of HCl gas was observed. The flask was removed from the ice bath and stirred at ambient temperature for 67 h. The flask was opened to air and the bright yellow mixture was poured into a 500-mL beaker. While stirring, aqueous HCl (2 *M*, 36 mL) was added slowly to the mixture. The mixture was stirred for an additional 30 min, resulting in precipitation of yellow solids. The solids were collected by vacuum filtration, washed with water, and dried under vacuum, affording **A48** as a yellow powder (2.6132 g, 81% yield). A minor dioxane impurity (3 mol%, 0.8% by mass) was detected by ^{1}H-NMR analysis. ^{1}H NMR (500 MHz, DMSO-d_6, δ): 10.04 (s, 2H), 7.90 (dd, J = 8.3, 1.3 Hz, 2H), 7.51 (dd, J = 8.0, 1.3 Hz, 2H), 7.43 (ddd, J = 8.7, 8.0, 1.3, 2H) 7.19 (ddd, J = 8.7, 8.0, 1.3, 2H), 3.75 (s, 2H). Spectral data are consistent with the literature.[6]

8-Chloro-4-hydroxy-2(1H)-quinolinone (**A49**): N^1,N^3-Bis(2-chlorophenyl)-propanediamide (**A48**) (1.661 g, 5.14 mmol, 1.0 equiv) and polyphosphoric acid (9.965 g, 6.0 wt. equiv) were

measured into a round-bottom flask equipped with stir bar. The flask was fitted with a water-cooled coil-type jacketed condenser fitted with a rubber septum secured by copper wire. The system was placed under an atmosphere of N_2 gas, and the mixture was heated to 139 °C for 5.5 h. The system was allowed to cool to handling temperature and the mixture was poured into ice water, inducing precipitation and hardening of the tar-like mixture. The transfer was completed with alternating washes of ethyl acetate and water. The resulting slurry was stirred overnight to break up the tar, resulting in a suspension of precipitated fine solids. The suspension was decanted from residual tar and the precipitate was collected by filtration, washed with water, and dried under vacuum to afford **A49** as a pale brown powder (737 mg, 74% yield). ^{1}H NMR (500 MHz, DMSO-d_6, δ): 11.61 (br s, 1H), 10.37 (br s, 1H), 7.78 (dd, J = 7.9, 1.3 Hz, 1H), 7.66 (dd, J = 7.9, 1.3 Hz, 1H), 7.17 (t, J = 7.9 Hz, 1H), 5.81 (s, 1H). Spectral data are consistent with the literature.[7]

2,4,8-Trichloroquinoline (**A20**): 8-Chloro-4-hydroxy-2(1H)-quinolinone (**A49**) (737.4 mg, 3.77 mmol, 1.0 equiv) and phosphorous(V) oxychloride ($POCl_3$) (5.3 mL, 56.6 mmol, 15.0 equiv) were combined in a round-bottom flask equipped with a stir bar. The flask was fitted with a water-cooled coil-type jacketed condenser fitted with a rubber septum secured by copper wire. The system was placed under an atmosphere of N_2 and heated at 95-100°C for 3.5 h. Evolving hydrogen chloride gas was routed through a mineral oil bubbler and then through an aqueous KOH trap using PVC tubing. Excess $POCl_3$ was removed by short-path vacuum distillation. Residual $POCl_3$ was quenched by dropwise addition of aqueous NaOH (5 mol %) then diluted with deionized water, inducing precipitation. The dark brown precipitate was filtered, washed with water, triturated in hexanes by sonication, and vacuum filtered through Celite. The filtrate was concentrated under

reduced pressure, but excessive residual water was observed by ^{1}H NMR. The solids were redissolved in chloroform, and the solution was washed with brine (2x), passed through a plug of magnesium sulfate, and concentrated under reduced pressure. The resulting solids were dried under vacuum overnight to afford **A20** as a pale yellow solid (324 mg, 37% yield). ^{1}H NMR (500 MHz, $CDCl_3$, δ): 8.13 (dd, *J* = 8.5, 1.3 Hz, 1H), 7.90 (dd, *J* = 7.6, 1.3 Hz, 1H). 7.58 (s, 1H), 7.57 (dd, *J* = 8.5, 7.6 Hz, 1H). ^{13}C{^{1}H} NMR (126 MHz, $CDCl_3$, δ): 151.0, 144.9, 144.8, 133.4, 131.8, 127.8, 126.7, 123.4, 123.2. HRMS (TOF MS ESI+) m/z: [M]+ Calcd for $C_9H_4Cl_3N$ 230.9409; Found 230.9471.

8-Bromo-2,4-dichloroquinoline (**28**): Compound **28** was prepared according to a modified literature procedure.[8] 2-Bromoaniline (230 µL, 1 mmol, 1.0 equiv), malonic acid (208 mg, 2 mmol, 2 equiv) and phosphorous(V) oxychloride ($POCl_3$) (2.0 mL) were combined in a 10 mL oven-dried Schlenk flask equipped with a stir bar. The flask was fitted with a water-cooled coil-type jacketed condenser equipped with a rubber septum secured by copper wire. The system was placed under an atmosphere of N_2 and heated at 100 °C for 6 h. Evolving hydrogen chloride gas was routed through a mineral oil bubbler and then through an aqueous KOH trap using PVC tubing. The reaction mixture was allowed to cool to room temperature and was subsequently poured onto crushed ice with stirring. The resulting mixture was extracted with excess dichloromethane and washed with sat. $NaHCO_3$ (aq) until the aqueous layer was slightly basic (pH 8). The layers were separated, and the organic layer was dried over anhydrous $MgSO_4$, filtered, and concentrated under reduced pressure. The crude residue was purified by flash column chromatography (R_f = 0.58 in 98:2 hexanes:EtOAc). ^{1}H NMR (400 MHz, $CDCl_3$ δ): 8.18 (dd, *J* = 8.4, 1.2 Hz, ^{1}H), 8.12 (dd, *J* =

7.6, 1.2 Hz, 1H), 7.58 (s, 1H), 7.50 (dd, *J* = 8.4, 7.6 Hz, 1H). $^{13}C\{^{1}H\}$ NMR (101 MHz, $CDCl_3$ δ): 150.9, 145.5, 144.7, 135.3, 128.1, 126.5, 124.13, 124.05, 123.0. HRMS (ESI+) m/z: [M]+: Calcd for $C_9H_4Cl_2BrN$ 274.8904; Found 274.8904.

Grignard Reagents

5-Methyl-2-pyridylmagnesium bromide (**A50**): Compound **A50** was prepared according to a modified literature procedure.[9] To an oven-dried 25 mL Schlenk flask equipped with a stir bar, under N_2, was added freshly crushed magnesium turnings (80.2 mg, 3.3 mmol, 1.1 equiv), dry degassed THF (6.0 mL), dry lithium chloride (127.2 mg, 3 mmol, 1.0 equiv), and diisobutylaluminum hydride (30 µL of a 1.0 *M* solution in THF, 0.03 mmol, 0.01 equiv). The reaction mixture was stirred for 5 min, followed by the dropwise addition of a solution of 2-bromo-5-methylpyridine (516.1 mg, 3.0 mmol, 1.0 equiv) in dry degassed THF (3.0 mL). The reaction was stirred at 23 ºC for 1 h, resulting in a dark red solution that was used without further purification.

Cyclopentylmagnesium bromide (**A51**): To an oven-dried 25 mL Schlenk flask equipped with a stir bar, under N_2, was added freshly crushed magnesium turnings (53.5 mg, 2.2 mmol, 1.1 equiv) and dry degassed THF (6.7 mL). Cyclopentyl bromide (475 µL, 4 mmol, 1.0 equiv) was then added dropwise to the reaction mixture. The reaction mixture was heated to reflux for 3 h, resulting in a light brown solution that was used without further purification.

3,3'-Methyloxetanylmagnesium bromide (**A52**): To an oven-dried 25 mL Schlenk flask equipped with a stir bar, under N_2, was added freshly crushed magnesium turnings (106.9 mg, 4.4

mmol, 1.1 equiv), dry degassed THF (6.0 mL), and diisobutylaluminum hydride (40 µL of a 1.0 *M* solution in THF, 0.04 mmol, 0.01 equiv). The reaction mixture was stirred for 5 min, followed by the dropwise addition of a solution of 3-bromomethyl-3-methyloxetane (462 µL, 4.0 mmol, 1.0 equiv) in dry degassed THF (7 mL). The reaction mixture was heated to reflux for 2.5 h resulting in a colorless solution containing a white precipitate. This mixture was used without further purification.

2-Benzothiophenylmagnesium bromide (**A53**): Compound **A53** was prepared according to a modified literature procedure.[7] To an oven-dried 25 mL Schlenk flask ("Flask A") equipped with a stir bar, under N_2, was added benzothiophene (1.073 g, 8 mmol, 1 equiv) and dry degassed THF (13 mL). The resulting solution was cooled to -84 ºC. *n*-BuLi (3.2 mL of a 2.5 *M* solution in hexanes, 8 mmol, 1.0 equiv) was added dropwise, and the mixture was stirred for 2 h while warming to 0 ºC. In a separate 50 mL Schlenk flask ("Flask B") equipped with a stir bar, under nitrogen, was added magnesium bromide ethyl etherate (2.066 g, 3.0 mmol, 1.0 equiv) and dry degassed THF (14 mL). The cold contents of Flask A were added to the slurry in Flask B. The reaction mixture was stirred at 23 ºC until all solids were dissolved, resulting in a rusty colored solution that was used without further purification.

Benzylmagnesium bromide (**A54**): To an oven-dried 25 mL Schlenk flask equipped with a stir bar, under N_2, was added freshly crushed magnesium turnings (106.9 mg, 4.4 mmol, 1.1 equiv), dry degassed THF (6.0 mL), and diisobutylaluminum hydride (40 µL of 1.0 *M* solution in THF, 0.04 mmol, 0.01 equiv). The resulting mixture was stirred for 5 min, followed by the dropwise addition of benzyl bromide (475µL, 4 mmol, 1.0 equiv) in dry degassed THF (7 mL). The reaction

mixture was heated to reflux for 3 h, resulting in a clear solution containing a small quantity of white crystals. This mixture was used without further purification.

A3. Suzuki Cross-Couplings with Pd/IPr

General Procedures

GC-Scale Reactions: The specified solids required in the Suzuki-Miyaura reactions were added to a 1-dram reaction vial in order of increasing mass: palladium catalyst (palladium source and free ligand) or precatalyst, the specified dihalopyridine substrate if solid (0.08 mmol, 1 equiv), arylboronic acid (0.08 mmol, 1.0 equiv), potassium carbonate or cesium carbonate, and then a stir bar. Liquid reagents were pre-measured by syringe and added in quick succession: benzene, THF, or 1,4-dioxane (0.32 mL, 0.25 *M*) via 1-mL syringe, followed by N_2-sparged deionized water via 50-µL syringe. Note: dihalopyridine substrates were added last if liquid, via microliter syringe. A septum cap equipped with an N_2-ingas and outgassing needle was fastened to the 1-dram reaction vial and the headspace was sparged for 30-45 seconds. With continuous sparging, the vial was unscrewed from the septum cap and lowered while the cap was replaced with a PTFE-lined cap. The reaction was stirred vigorously at the specified temperature for the specified duration.

Scaled-Up Reactions for Product Isolation: Precatalyst (η^3-1-^{t}Bu-indenyl)Pd(IPr)Cl (8.4 mg, 0.012 mmol, 3.0 mol%) was weighed into a 1-dram vial followed by solid substrate, if applicable (2,4-dichloropyridine, quinoline, or 3,5-dichloropyridazine, 0.4 mmol, 1 equiv), arylboronic acid (0.4 mmol, 1.0 equiv), potassium carbonate, and a stir bar. Liquid reagents were pre-measured by syringe and added in quick succession: benzene or THF (1.6 mL, 0.25 *M*) via a

1-mL syringe followed by N_2-sparged deionized water via a 100-µL or 250-µL syringe. In cases where the substrate was a liquid, the substrate was added last via microliter syringe (0.4 mmol, 1 equiv). A septum cap equipped with an N_2-ingas and outgassing needle was fastened to the 1-dram reaction vial and the mixture was sparged for 30-45 seconds. With continuous sparging, the vial was unscrewed from the septum cap and lowered while the cap was replaced with a PTFE-lined cap. The reaction was stirred vigorously at the specified temperature for the specified duration. The cap was removed, the reaction mixture was diluted in ethyl acetate then filtered through a plug of Celite. The reaction outcome was assessed by GC and TLC (isomeric ratios were determined by GC). The mixture was purified by flash column chromatography or crystallization under the specified conditions, and the product was dried under vacuum.

Conditions A: potassium carbonate (221.1 mg, 1.6 mmol, 4.0 equiv), deionized water (250 µL, 13.8 mmol, 34.6 equiv), THF, 60 °C.

Conditions B: potassium carbonate (165.8 mg, 1.2 mmol, 3.0 equiv), deionized water (100 µL, 5.53 mmol, 13.8 equiv), THF, 25 °C.

Conditions C: potassium carbonate (165.8 mg, 1.2 mmol, 3.0 equiv), deionized water (100 µL, 5.53 mmol, 13.8 equiv), benzene, 25 °C.

Optimization (Table 1)

Table A1. Optimization of the C4-Selective Suzuki-Miyaura Coupling with Pd/IPr.[a]

entry	trial	NHC	base	solvent	additive (equiv)	**1a** (%)	**1b** (%)	**1c** (%)	**1a** : **1b**
1	1	SIPr	KF	THF	--	4	35	4	1 : 8.8
2	2	SIPr	KF	THF	--	5	44	5	1 : 8.8
3	Average	SIPr	KF	THF	--	5	39	5	1 : 7.8
4	1	SIPr	K_2CO_3	THF	--	7.4	67.7	9.1	1 : 9.1
5	2	SIPr	K_2CO_3	THF	--	6.2	63.0	10.3	1 : 10.1
6	Average	SIPr	K_2CO_3	THF	--	6.8	65.4	9.7	1 : 9.6
7	1	IPr	K_2CO_3	THF	--	6	69	8	1 : 11.5
8	2	IPr	K_2CO_3	THF	--	7	68	7	1 : 9.7
9	Average	IPr	K_2CO_3	THF	--	7	69	8	1 : 9.9
10	1	IPr	K_2CO_3	C_6H_6	--	8	69	6.0	1 : 8.6
11	2	IPr	K_2CO_3	C_6H_6	--	8	70	6.4	1 : 8.8
12	Average	IPr	K_2CO_3	C_6H_6	--	8	70	6.2	1 : 8.8
13	1	IPr	K_2CO_3	$PhCH_3$	--	8	75	4	1 : 9.4
14	2	IPr	K_2CO_3	$PhCH_3$	--	8	72	4	1 : 9.0
15	Average	IPr	K_2CO_3	$PhCH_3$	--	8	74	4	1 : 9.2
16	1	IPr	K_2CO_3	DMF	--	8	46	17	1 : 5.8
17	2	IPr	K_2CO_3	DMF	--	8	48	14	1 : 5.9
18	Average	IPr	K_2CO_3	DMF	--	8	47	15	1 : 5.9
19	1	IPr	K_2CO_3	PC[b]	--	9	43	16	1 : 4.8
20	2	IPr	K_2CO_3	PC[b]	--	9	46	18	1 : 5.1
21	Average	IPr	K_2CO_3	PC[b]	--	9	45	17	1 : 5.0
22[c]	1	--	K_2CO_3	C_6H_6	--	2	<1	n.d.	--
23[c]	2	--	K_2CO_3	C_6H_6	--	1	<1	n.d.	--
24[c]	Average	--	K_2CO_3	C_6H_6	--	2	<1	n.d.	--
25[d]	1	--	K_2CO_3	THF	--	2	1	n.d.	--
26[d]	2	--	K_2CO_3	THF	--	1	<1	n.d.	--
27[d]	Average	--	K_2CO_3	THF	--	1	<1	n.d.	--
28	1	SIPr	K_2CO_3	C_6H_6	--	9	61	8	1 : 6.8
29	2	SIPr	K_2CO_3	C_6H_6	--	9	66	7	1 : 7.3
30	Average	SIPr	K_2CO_3	C_6H_6	--	9	64	8	1 : 7.1
31	1	SIMes	K_2CO_3	C_6H_6	--	21	30	3	1 : 1.4
32	2	SIMes	K_2CO_3	C_6H_6	--	27	39	3	1 : 1.4
33	Average	SIMes	K_2CO_3	C_6H_6	--	24	35	3	1 : 1.5
34	1	IMes	K_2CO_3	C_6H_6	--	21	35	3	1 : 1.6
35	2	IMes	K_2CO_3	C_6H_6	--	24	44	3	1 : 1.7
36	Average	IMes	K_2CO_3	C_6H_6	--	23	40	3	1 : 1.7
37	1	SIMix	K_2CO_3	C_6H_6	--	8	36	2	1 : 4.5
38	2	SIMix	K_2CO_3	C_6H_6	--	8	31	2	1 : 3.9
39	Average	SIMix	K_2CO_3	C_6H_6	--	8	34	2	1 : 4.3
40	1	IPent	K_2CO_3	C_6H_6	--	1	31	21	1 : 31
41	2	IPent	K_2CO_3	C_6H_6	--	1	37	24	1 : 37
42	Average	IPent	K_2CO_3	C_6H_6	--	1	34	23	1 : 34
43	1	IPr	K_2CO_3	THF	NBu_4Br (1)	<1	3	n.d.	--
44	2	IPr	K_2CO_3	THF	NBu_4Br (1)	1	4	n.d.	--

Table A1 Continued

45	Average	IPr	K_2CO_3	THF	NBu_4Br (1)	<1	3	n.d.	--
46	1	IPr	K_2CO_3	THF	NBu_4Br (3)	<1	2	n.d.	--
47	2	IPr	K_2CO_3	THF	NBu_4Br (3)	<1	2	n.d.	--
48	Average	IPr	K_2CO_3	THF	NBu_4Br (3)	<1	2	n.d.	--
49	1	IPr	K_2CO_3	THF	NBu_4Cl (3)	<1	1	n.d.	--
50	2	IPr	K_2CO_3	THF	NBu_4Cl (3)	<1	<1	n.d.	--
51	Average	IPr	K_2CO_3	THF	NBu_4Cl (3)	<1	1	n.d.	--
52	1	IPr	K_2CO_3	THF	NBu_4OH (3)[e]	1	4	n.d.	--
53	2	IPr	K_2CO_3	THF	NBu_4OH (3)[e]	1	4	n.d.	--
54	Average	IPr	K_2CO_3	THF	NBu_4OH (3)[e]	1	4	n.d.	--
55	1	IPr	K_2CO_3	dioxane	--	6.7	77.1	7.6	1 : 12
56[f]	1	IPr	K_2CO_3	dioxane	--	2.8	43.0	25.4	1 : 15
57	1	IPr	K_2CO_3	toluene	--	8.8	78.2	4.8	1 : 9
58[f]	1	IPr	K_2CO_3	toluene	--	8.5	44.6	15.4	1 : 5

[a]Reactions were conducted according to the General Procedure for GC-scale reactions. GC yields calibrated against undecane as an internal standard. Calculated yield values were rounded to the nearest integer. Entries reported as <1 indicate a calibrated GC yield less than 0.5%; nd = not detected. [b]PC = propylene carbonate. [c]No NHC ligand; Pd source was (η^3-1-^{t}Bu-indenyl)$_2$(μ-Cl)$_2$Pd$_2$ (1.5 mol %). [d]No NHC ligand; Pd source was $PdCl_2$ (3 mol %). [e]NBu_4OH was added as a solution in water (156 µL of a 40% aqueous solution, 3 equiv) added; no additional water added to the reaction. [f]Reaction was conducted at 100 °C.

Discussion: Unlike our optimized ligand-free conditions (*vide infra*), the addition of tetraalkylammonium salts to the Pd/IPr catalytic conditions inhibits cross-coupling (Table A1, entries 43-54). The use of high temperatures in the Pd/IPr conditions does not lead to significant improvements in C4-selectivity (compare entry 55 to 56, and entry 57 to 58), indicating that the high-temperatures used in ligand-free conditions are not solely responsible for the greatly enhanced selectivity under 'Jeffery' conditions.

Isolation and Characterization of Products (Table 2.1 and Scheme 2.3)

4-Chloro-2-(4-methoxyphenyl)pyridine (1a). Compound **1a** was prepared according to a modified literature procedure.[10] $Pd(OAc)_2$ (33.7 mg, 0.15 mmol, 5 mol %), 1,1'-*bis*-(diphenylphosphino)ferrocene (109.8 mg, 0.15 mmol, 5 mol %), Cs_2CO_3 (2.44 g, 7.5 mmol 2.5 equiv) and *p*-methoxyphenylboronic acid (455.8 mg, 3 mmol, 1 equiv) were added to an oven-

dried 5-dram vial in a N_2-filled glovebox. The vial was sealed with a septum and removed from the glovebox, and 2,4-dichloropyridine (**1,** 322 µL, 3 mmol, 1 equiv), deionized water (378 µL, 21 mmol, 7 equiv), and 1,4-dioxane (12 mL) were added through the septum. The reaction was allowed to stir at 70 ºC for 19 h. Purification via flash column chromatography (R_f = 0.50 in 20% ethyl acetate in hexanes) yielded **1a** as an off-white solid (504 mg, 76% yield). Spectral data are consistent with the literature.[11]

2-Chloro-4-(4-methoxyphenyl)pyridine (1b). Compound **1b** was prepared according to the general procedure using Conditions B and 2,4-dichloropyridine (43.2 µL, 0.4 mmol, 1.0 equiv) with stirring for 16.5 h. Three separate reactions were performed using *p*-methoxyphenylboronic acid (60.8 mg, 0.4 mmol, 1.0 equiv), *p*-methoxyphenylboronic acid pinacol ester (93.6 mg, 0.4 mmol, 1.0 equiv), or *p*-methoxyphenylboronic acid neopentyl glycol ester (88.0 mg, 0.4 mmol, 1.0 equiv). Purification by flash column chromatography on silica gel (R_f = 0.29 in 10% acetone in hexanes) provided **1b** and other isolated side products as white solids with varying degrees of brown discoloration. *p*-Methoxyphenylboronic acid method: (63.3 mg, 72% yield); *p*-methoxyphenylboronic acid pinacol ester method: (61.5 mg, 70% yield; diarylated side product **1c**: 15.2 mg, 13% yield); *p*-methoxyphenylboronic acid neopentyl glycol ester method: (55.4 mg, 63% yield; diarylated side product **1c**: 10.5 mg, 9% yield). **1b**: ^{1}H NMR (600 MHz, $CDCl_3$, δ): 8.36 (d, *J* = 5.2 Hz, 1H), 7.6-7.5 (m, 2H), 7.48 (d, *J* = 1.1 Hz, 1H), 7.37 (dd, *J* = 1.6, 5.3 Hz, 1H), 7.01-6.98 (m, 2H), 3.85 (s, 3H). Spectral data are consistent with the literature.[12] 2,4-bis(4-methoxyphenyl)pyridine (**1c**): ^{1}H NMR (600 MHz, $CDCl_3$, δ): 8.65 (d, *J* = 5.2 Hz, 1H), 8.00 (m,

2H), 7.83 (s, 1H), 7.65 (m, 2H), 7.35 (dd, J = 5.2, 1.4 Hz, 1H), 7.04-7.01 (multiple peaks, 4H), 3.88 (coincidentally overlapping singlets, 6H). Spectral data are consistent with the literature.[13]

Larger-Scale Preparation of 1b: Compound **1b** was prepared according to the general procedure using Conditions B with 2,4-dichloropyridine (216 µL, 2.0 mmol, 1.0 equiv) and *p*-methoxyphenylboronic acid (303.9 mg, 2.0 mmol, 1.o equiv) with stirring for 27 h. Purification by flash column chromatography on silica gel (R_f = 0.29 in 10% acetone in hexanes) provided **1b** as a white solid with slight yellow discoloration (265.8 mg, 61% yield). Spectral data are consistent with the literature.[12]

4-(2-Chloro-4-pyridinyl)benzaldehyde (4b). Compound **4b** was prepared according to the general procedure using Conditions B, 2,4-dichloropyridine (43.2 µL, 0.4 mmol, 1.0 equiv) and *p*-formylphenylboronic acid (60.0 mg, 0.4 mmol, 1.0 equiv) with stirring for 16 h. Purification by flash column chromatography on silica (R_f = 0.22 in 10% acetone in hexanes) provided **4b** as a white solid (38.8 mg, 45% yield). ^{1}H NMR (500 MHz, $CDCl_3$, δ): 10.08 (s, 1H), 8.48 (d, J = 5.2 Hz, 1H), 8.01-7.99 (m, 2H), 7.78-7.76 (m, 2H), 7.57 (d, J = 1.5 Hz, 1H), 7.46 (dd, J = 5.2, 1.5 Hz, 1H). Spectral data are consistent with the literature.[14] The C2-mononarylated isomer **A4a** was isolated as a minor product in low purity (7.5 mg, <9% yield). ^{1}H NMR (600 MHz, $CDCl_3$, δ): 10.9 (s, 1H), 8.64 (d, J = 5.3 Hz, 1H), 8.17-8.15 (m, 2H), 8.01-7.99 (m, 2H), 7.18 (d, J = 1.8 Hz, 1H), 7.32 (dd, J = 1.8, 5.3 Hz, 1H). The minor product of diarylation **4c** was also isolated (8.3 mg, 7% yield). ^{1}H NMR (600 MHz, $CDCl_3$, δ): 10.12 (s, 1H), 10.11 (s, 1H), 8.84 (d, J = 5.0 Hz, 1H), 8.26-8.24 (m, 2H), 8.05-8.02 (multiple peaks, 5H), 7.88-7.86 (m, 2H), 7.55 (dd, J = 1.6, 5.0 Hz, 1H).

2-Chloro-4-(4-vinylphenyl)pyridine (5b). Compound **5b** was prepared according to the general procedure using Conditions B, 2,4-dichloropyridine (43.2 μL, 0.4 mmol, 1.0 equiv) and *p*-vinylphenylboronic acid (60.0 mg, 0.4 mmol, 1.0 equiv) with stirring for 16.5 h. Purification by flash column chromatography on silica (R_f = 0.21 in 2.5% acetone in hexanes) provided **5b** as an off-white solid (55.7 mg, 65% yield). ^{1}H NMR (600 MHz, $CDCl_3$, δ): 8.39 (d, *J* = 5.2 Hz, 1H), 7.56-7.55 (m, 2H), 7.51-7.49 (multiple overlapping signals, 3H), 7.39 (d, *J* = 5.2 Hz, 1H), 6.74 (dd, *J* = 17.6, 10.9 Hz, 1H), 5.83 (d, *J* = 17.6 Hz, 1H), 5.34 (d, *J* = 10.9 Hz, 1H). ^{13}C{^{1}H} NMR (126 MHz, $CDCl_3$, δ): 152.3, 151.0, 150.1, 139.1, 135.9 (two signals are coincidentally overlapping), 127.2, 127.1, 121.7, 120.2, 115.5. HRMS (ESI Q-TOF) m/z: [M]+ Calcd for $C_{13}H_{10}ClN$ 215.0502; Found 215.04922.

4-(2-Chloro-4-pyridinyl)benzonitrile (6b). Compound **6b** was prepared according to the general procedure using Conditions B, 2,4-dichloropyridine (43.2 μL, 0.4 mmol, 1.0 equiv) and *p*-cyanophenylboronic acid (58.8 mg, 0.4 mmol, 1.0 equiv) with stirring for 16.5 h. Purification by flash column chromatography on silica (R_f = 0.19 in 10% acetone in hexanes) provided **6b** as a white crystalline solid (60.3 mg, 70% yield); ^{1}H NMR (600 MHz, $CDCl_3$, δ): 8.47 (d, *J* = 5.2 Hz, 1H), 7.78-7.77 (m, 2H), 7.71-7.70 (m, 2H), 7.52 (d, *J* = 1.1 Hz, 1H), 7.42 (dd, *J* = 5.2, 1.1 Hz, 1H). The spectral data are consistent with the literature.[15] The C2-mononarylated isomer **A6a** was isolated as a minor product in low purity (7.8 mg, <9% yield). ^{1}H NMR (600 MHz, $CDCl_3$, δ): 8.63 (d, *J* = 5.2 Hz, 1H), 8.11-8.10 (m, 2H), 7.78-7.77 (multiple overlapping signals, 3H), 7.33 (dd, *J* = 5.2, 1.8 Hz, 1H). The minor product of diarylation **A6c** was also isolated (14.3 mg, 13%

yield). ^{1}H NMR (600 MHz, $CDCl_3$, δ): 8.84 (d, J = 5.0 Hz, 1H), 8.19-8.18 (m, 2H), 7.94 (s, 1H), 7.83-7.79 (multiple overlapping signals, 6H), 7.52 (dd, J = 5.0, 1.3 Hz, 1H).

4-(2-Chloro-4-pyridinyl)benzoic acid methyl ester (7b). Compound **7b** was prepared according to the general procedure using Conditions B, 2,4-dichloropyridine (43.2 µL, 0.4 mmol, 1.0 equiv) and *p*-(methoxycarbonyl)phenylboronic acid (72.0 mg, 0.4 mmol, 1.0 equiv) with stirring for 16 h. Purification by flash column chromatography on silica (R_f = 0.24 in 5% acetone in hexanes) provided **7b** as a white microcrystalline solid (59.8 mg, 60% yield). ^{1}H NMR (600 MHz, $CDCl_3$, δ): 8.43 (d, J = 4.9 Hz, 1H), 8.138.12 (m, 2H), 7.65-7.64 (m, 2H), 7.53 (s, 1H), 7.42 (d, J = 4.9 Hz, 1H), 3.93 (s, 3H). Spectral data are consistent with the literature.[15]

2-Chloro-4-(4-chlorophenyl)pyridine (8b). Compound **8b** was prepared according to the general procedure using Conditions B, 2,4-dichloropyridine (43.2 µL, 0.4 mmol, 1.0 equiv) and *p*-chlorophenylboronic acid (62.5 mg, 0.4 mmol, 1.0 equiv) with stirring for 16 h. Purification by flash column chromatography on silica (R_f = 0.25 in 5% THF in hexanes) resulted in partial separation of **8b** from the C2-monoarylated isomer. Coeluted fractions were purified by evaporative crystallization from acetone and water, providing **8b** as an off-white solid (59 mg, 66% yield). ^{1}H NMR (500 MHz, $CDCl_3$, δ): 8.43 (d, J = 5.2 Hz, 1H), 7.55-7.52 (m, 2H), 7.50 (d, J= 1.6 Hz, 1H), 7.47-7.45 (m, 2H), 7.38 (dd, J = 5.2, 1.6 Hz, 1H). Spectral data are consistent with the literature.[15]

2-Chloro-4-(3-nitrophenyl)pyridine (9b). Compound **9b** was prepared according to the general procedure (except on the 1.0 mmol scale) using Conditions B, 2,4-dichloropyridine (108.0 µL, 1.0

mmol, 1.0 equiv) and *m*-nitrophenylboronic acid (166.9 mg, 1.0 mmol, 1.0 equiv) with stirring for 16 h. Purification by flash column chromatography on silica (R_f = 0.24 in 10% acetone in hexanes) provided **9b** as a white crystalline solid (156.7 mg, 67% yield); mp 159-161 °C [uncorrected, measured against benzoic acid (113-117 °C)]. ^{1}H NMR (600 MHz, $CDCl_3$, δ): 8.52 (dd, *J* = 5.2, 0.5 Hz, 1H), 8.48 (dd, *J* = 1.8, 1.8 Hz, 1H), 8.33 (ddd, *J* = 8.0, 1.9, 0.9 Hz, 1H), 7.95 (ddd, *J* = 8.0, 1.9, 0.9 Hz, 1H), 7.71 (dd, *J* = 8.0, 8.0 Hz, 1H), 7.60 (dd, *J* = 1.9, 0.8 Hz, 1H), 7.48 (dd, *J* = 5.2, 1.8 Hz, 1H). ^{13}C{^{1}H} NMR (126 MHz, $CDCl_3$, δ): 152.9, 150.7, 149.1, 149.0, 138.8, 133.0, 130.6, 124.4, 122.3, 122.2, 120.5. HRMS (ESI Q-TOF) m/z: [M]+ Calcd for $C_{11}H_7ClN_2O_2$ 234.0196; Found 234.0193.

2-Chloro-4-(1-methyl-1H-pyrazol-4-yl)pyridine (10b). Compound **10b** was prepared according to the general procedure using Conditions B, with the modification that the reaction was heated to 75 °C, and with 2,4-dichloropyridine (43.2 μL, 0.4 mmol, 1.0 equiv) and (1-methyl-1*H*-pyrazol-4-yl)boronic acid (75.5 mg, 0.6 mmol, 1.5 equiv) with stirring for 35 h. Products were purified via flash column chromatography using a step gradient: 0.75% methanol in CH_2Cl_2 until elution of the C2-monoarylated product **A10a**, 3% methanol in CH_2Cl_2 until elution of **10b**, 5% methanol in CH_2Cl_2 until elution of the diarylated product **A10c** (R_f values in 0.75% methanol/CH_2Cl_2: C2-monoarylated isomer **A10a** = 0.17, C4-monoarylated isomer **10b** = 0.31, diarylated product **A10c** = 0.09). Product **10b** was isolated as an off-white solid (52 mg, 67% yield). ^{1}H NMR (500 MHz, $CDCl_3$, δ): 8.27 (d, *J* = 5.3 Hz, 1H), 7.80 (s, 1H), 7.72 (s, 1H), 7.34 (d, *J* = 1.3 Hz, 1H), 7.22 (dd, *J* = 5.3, 1.3 Hz, 1H), 3.94 (s, 3H). ^{1}H NMR (500 MHz, DMSO-d_6, δ): 8.43 (s, 1H), 8.30 (dd, *J* = 5.3, 0.6 Hz, 1H), 8.12 (d, *J* = 0.6 Hz, 1H), 7.71 (dd, *J* = 1.5, 0.6 Hz, 1H), 7.57 (dd, *J* = 5.3, 1.5

Hz, 1H), 3.88 (s, 3H). Spectral data are consistent with the literature.[16] The C2-mononarylated isomer (**A10a**) was isolated as a minor product in low purity (10 mg, <13% yield). ^{1}H NMR (500 MHz, $CDCl_3$, δ): 8.42 (d, *J* = 5.4 Hz, 1H), 7.93 (s, 1H), 7.92 (s, 1H), 7.44 (d, *J* = 1.9 Hz, 1H), 7.10 (dd, *J* = 5.4, 1.9 Hz, 1H), 3.95 (s, 3H). The minor product of diarylation (**A10c**) was also isolated (9 mg, 9% yield). ^{1}H NMR (500 MHz, $CDCl_3$, δ): 8.48 (dd, *J* = 5.2, 0.7 Hz, 1H), 7.97 (s, 1H), 7.95 (s, 1H), 7.87 (d, *J* = 0.7 Hz, 1H), 7.76 (s, 1H), 7.50 (dd, *J* = 1.7, 0.7 Hz, 1H), 7.15 (dd, *J* = 5.2, 1.7 Hz, 1H), 3.97 (s, 3H), 3.96 (s, 3H).

2-Chloro-4-(4-methoxyphenyl)-3-nitropyridine (11b). Compound **11b** was prepared according to the general procedure using Conditions A, 2,4-dichloro-3-nitro-pyridine (77.2 mg, 0.4 mmol, 1.0 equiv) and *p*-methoxyphenylboronic acid (60.8 mg, 0.4 mmol, 1.0 equiv) with stirring for 9 h. Purification by flash column chromatography on silica gel in 10-15% acetone/hexanes (R_f = 0.25 in 10% acetone in hexanes) provided **11b** as a colorless crystalline solid (70.3 mg, 66% yield), with evidence of yellow impurity (^{1}H NMR shows there is a 6% impurity comprising C2-monoarylated isomer **A11a**); mp 110-113 °C [uncorrected, measured against benzoic acid (110-113 °C)]. ^{1}H NMR (500 MHz, $CDCl_3$, δ): 8.49 (d, *J* = 5.1 Hz, 1H), 7.36-7.33 (multiple peaks, 3H), 6.99-6.97 (m, 2H), 3.85 (s, 3H). ^{13}C{^{1}H} NMR (126 MHz, $CDCl_3$, δ): 161.5, 150.0, 145.1 (this small quaternary peak was selected from among impurity peaks based on comparison with an ACD labs simulated spectrum), 144.3, 142.3, 129.2, 125.0, 124.3, 115.0, 55.5. HRMS (ESI Q-TOF) m/z: [M]+ Calcd for $C_{12}H_9ClN_2O_3$ 264.0302; Found 264.0298.

2-Chloro-4-(4-methoxyphenyl)-3-pyridinecarbonitrile (12b). Compound **12b** was prepared according to the general procedure using Conditions A, 2,4-dichloro-3-cyano-pyridine (69.2 mg,

0.4 mmol, 1.0 equiv) and *p*-methoxyphenylboronic acid (60.8 mg, 0.4 mmol, 1.0 equiv) with stirring for 12 h. Purification by flash column chromatography on silica gel (R_f = 0.21 in 10% acetone in hexanes) provided **12b** as a colorless crystalline solid (66.4 mg, 68% yield). ^{1}H NMR (500 MHz, $CDCl_3$, δ): 8.52 (d, *J* = 5.3 Hz, 1H), 7.60-7.57 (m, 2H), 7.36 (d, *J* = 5.3 Hz, 1H), 7.07-7.04 (m, 2H), 3.88 (s, 3H). Spectral data are consistent with the literature.[17] The minor product of diarylation (**A12c**) was also isolated (4.4 mg, 3% yield; R_f = 0.10 in 10% acetone in hexanes). ^{1}H NMR (600 MHz, $CDCl_3$, δ): 8.77 (d, *J* = 5.1 Hz, 1H), 7.91-7.90 (m, 2H), 7.62-7.58 (m, 2H), 7.31 (d, *J* = 5.1 Hz, 1H), 7.07-7.04 (multiple peaks, 4H), 3.89 (coincidentally overlapping singlets, 6H).

2-Chloro-4-(4-methoxyphenyl)-3-pyridinecarboxaldehyde (13b). Compound **13b** was prepared according to the general procedure using Conditions C, 2,4-dichloro-3-pyridinecarboxaldehyde (70.4 mg, 0.4 mmol, 1.0 equiv) and *p*-methoxyphenylboronic acid (60.8 mg, 0.4 mmol, 1.0 equiv) with stirring for 12 h. Purification by flash column chromatography on silica gel (R_f = 0.21 in 10% acetone in hexanes) provided **13b** as a yellow solid (51.4 mg, 52% yield). ^{1}H NMR (600 MHz, $CDCl_3$, δ): 10.14 (s, 1H), 8.49 (d, *J* = 5.1 Hz, 1H), 7.31 (d, *J* = 5.1 Hz, 1H), 7.29-7.26 (m, 2H), 7.02-7.00 (m, 2H), 3.87 (s, 3H). ^{13}C{^{1}H} NMR (126 MHz, $CDCl_3$, δ): 190.3, 161.0, 154.4, 151.5, 151.1, 130.8, 128.1, 127.6, 124.8, 114.5, 55.5. HRMS (ESI Q-TOF) m/z: [M]+ Calcd for $C_{13}H_{10}ClNO_2$ 247.0400; Found 247.0385. The C2-mononarylated isomer **A13a** was isolated as a minor product in low purity (9.9 mg, <10% yield). ^{1}H NMR (600 MHz, $CDCl_3$, δ): 9.97 (s, 1H), 8.65 (d, *J* = 5.3 Hz, 1H), 7.51-7.49 (m, 2H), 7.38 (d, *J* = 5.3 Hz, 1H), 7.03-7.02 (m, 2H), 3.88 (s, 3H).

2-Chloro-4-(4-methoxyphenyl)-3-pyridinamine (14b). Compound **14b** was prepared according to the general procedure using Conditions C, 3-amino-2,4-dichloro-pyridine (65.2 mg, 0.4 mmol, 1.0 equiv) and *p*-methoxyphenylboronic acid (60.8 mg, 0.4 mmol, 1.0 equiv) with stirring for 18.5 h. Purification by flash column chromatography on silica gel (R_f = 0.42 in 25% ethyl acetate in hexanes) provided **14b** as a white crystalline solid (56.7 mg, 60% yield); mp 113-116 °C [uncorrected, measured against benzoic acid (111-113 °C)]. ^{1}H NMR (500 MHz, $CDCl_3$, δ): 7.79 (d, J = 4.8 Hz, 1H), 7.38-7.35 (m, 2H), 7.01-6.98 (m, 2H), 6.95 (d, J = 4.8 Hz, 1H), 4.19 (br s, 2H), 3.85 (s, 3H). ^{13}C{^{1}H} NMR (126 MHz, $CDCl_3$, δ): 159.9, 138.1, 137.6, 137.3, 135.2, 129.6, 128.7, 124.2, 114.7, 55.5. HRMS (ESI Q-TOF) m/z: [M]+ Calcd for $C_{12}H_{11}ClN_2O$ 234.0560; Found 234.0557. The C2-monoarylated isomer **A14a** was isolated as a minor product (12.2 mg, 13% yield). ^{1}H NMR (500 MHz, $CDCl_3$, δ): 7.98 (d, J = 5.2 Hz, 1H), 7.62-7.59 (m, 2H), 7.15 (d, J = 5.2 Hz, 1H), 7.02-7.00 (m, 2H), 4.23 (br s, 2H), 3.86 (s, 3H). The minor product of diarylation **A14c** was also isolated (16.7 mg, 14% yield). ^{1}H NMR (500 MHz, $CDCl_3$, δ): 8.13 (d, J = 4.9 Hz, 1H), 7.68-7.66 (m, 2H), 7.46-7.44 (m, 2H), 7.03-7.00 (multiple peaks, 4H), 6.98 (d, J = 4.9 Hz, 1H), 3.90 (br s, 2H), 3.864 (s, 3H), 3.859 (s, 3H).

2-Chloro-4-(4-methoxyphenyl)-5-methylpyridine (15b). Compound **15b** was prepared according to the general procedure using Conditions B, 2,4-dichloro-5-methylpyridine (64.8 mg, 0.4 mmol, 1.0 equiv) and *p*-methoxyphenylboronic acid (60.8 mg, 0.4 mmol, 1.0 equiv) with stirring for 18.5 h. Purification by flash column chromatography on silica gel (R_f = in 5% acetone in hexanes) resulted in partial purification of the C4-monoarylated isomer. One fraction containing coeluted monoarylated isomers and diarylated product was purified further by preparatory TLC in

the same eluent. Product **15b** was extracted from the silica gel with acetone and combined with remaining **15b** fractions obtained from flash column chromatography, providing an off-white solid (49.9 mg, 53% yield). ^{1}H NMR (500 MHz, $CDCl_3$, δ): 8.24 (s, 1H), 7.26-7.24 (m, 2H), 7.19 (s, 1H), 7.00-6.98 (m, 2H), 3.86 (s, 3H), 2.25 (s, 3H). $^{13}C\{^{1}H\}$ NMR (151 MHz, $CDCl_3$, δ): 159.9, 152.1, 150.9, 149.2, 130.3, 129.91, 129.87, 124.2, 114.2, 55.5, 17.0. HRMS (ESI Q-TOF) m/z: [M]+ Calcd for $C_{13}H_{12}ClNO$ 233.0607; Found 233.0603. The minor product of diarylation **A15c** was also isolated (21.8 mg, 18% yield). ^{1}H NMR (500 MHz, $CDCl_3$, δ): 8.52 (s, 1H), 7.96-7.94 (m, 2H), 7.52 (s, 1H), 7.33-7.31 (m, 2H), 7.01-7.98 (multiple peaks, 4H), 3.87 (s, 3H), 3.86 (s, 3H), 2.30 (s, 3H).

6-Chloro-4-(4-methoxyphenyl)-3-pyridinamine (16b). Compound **16b** was prepared according to the general procedure using Conditions C, 5-amino-2,4-dichloropyridine (78.2 mg, 0.48 mmol, 1.2 equiv) and *p*-methoxyphenylboronic acid (60.8 mg, 0.4 mmol, 1.0 equiv) with stirring for 21 h. Purification was performed by reversed phase flash column chromatography with a 12 g C18 silica column, using an initial automated program comprising of a flow rate of 36 mL/min of water:acetonitrile (98:2 to 6:94) over 30 column volumes. When the product began eluting, the program was paused and reset to elute the analyte at 50-53% MeCN in water. After the elution, the initial program was resumed. The C4 monoarylated product **16b** coeluted with the C2 monoarylated isomer **A16a** at 52-53% MeCN. Fractions containing **16b** were partitioned between dichloromethane and saturated brine. The organic layers were combined and dried over magnesium sulfate and solvent was removed under reduced pressure affording a mixture of the product isomers. Further purification attempts were unsuccessful, and the final product **16b** was

obtained as a rust colored solid in 94% purity (74.4 mg, 74% yield based on 94% purity). ^{1}H NMR (400 MHz, C6D6, δ): 7.55 (s, 1H), 6.55-7.00 (m, 2H), 6.90 (s, 1H), 6.66-6.71 (m, 2H), 3.28 (s, 3H), 2.88 (br s, 2H). ^{13}C{^{1}H} NMR (100 MHz, C6D6, δ): 160.6, 141.5, 139.9, 137.5, 136.9, 130.1, 124.6, 125.3, 115.1, 55.2. HRMS (ESI+) m/z: [M]+: Calcd for $C_{12}H_{11}ClN_2O$ 234.0560; Found 234.0562

2,5-Dichloro-4-(4-methoxyphenyl)pyridine (17b). Compound **17b** was prepared according to the general procedure using Conditions C, 2,4,5-trichloropyridine (73.0 mg, 0.4 mmol, 1.0 equiv) and *p*-methoxyphenylboronic acid (60.8 mg, 0.4 mmol, 1.0 equiv) with stirring for 21 h. Purification was performed by reversed phase flash column chromatography with a 12 g C18 silica column, using an initial automated program comprising a flow rate of 30 mL/min of water:methanol (98:2 to 0:100) over 40 column volumes. When the product began eluting, the program was paused and reset to elute the analyte at 65-60% MeOH in water. After the elution, the initial program was resumed. The C4 monoarylated product eluted at 67% MeOH. Fractions containing product **17b** were partitioned between ethyl acetate and saturated brine. The organic layers were combined and dried over magnesium sulfate and solvent was removed under reduced pressure affording an off-white solid (44.0 mg, 43% yield). ^{1}H NMR (500 MHz, C_6D_6, δ): 8.16 (s, 1H), 6.94-7.02 (m, 2H), 6.87 (s, 1H), 6.66-6.71 (m, 2H), 3.26 (s, 3H). ^{13}C{^{1}H} NMR (150 MHz, C_6D_6, δ): 160.5, 149.9, 149.51, 149.46, 130.2, 128.9, 128.0, 125.3, 113.8, 54.5 ppm. HRMS (ESI+) m/z: [M]+: Calcd for $C_{12}H_9Cl_2NO$ 253.0061; Found 253.0073.

6-Chloro-4-(4-methoxyphenyl)-2-pyridinamine (18b). Compound **18b** was prepared according to the general procedure using Conditions C, 2-amino-4,6-dichloro-pyridine (65.2 mg, 0.4 mmol,

1.0 equiv) and *p*-methoxyphenylboronic acid (60.8 mg, 0.4 mmol, 1.0 equiv) with stirring for 25.5 h. Purification by flash column chromatography on silica gel (R_f = 0.22 in 25% ethyl acetate in hexanes) provided **18b** as a colorless crystalline solid with minor brown discoloration (45.1 mg, 48% yield); mp 167-172 °C [uncorrected, measured against benzoic acid (115-118 °C)]. ^{1}H NMR (500 MHz, $CDCl_3$, δ): 7.51-7.49 (m, 2H), 6.96 (m, 2H), 6.86 (d, *J* = 1.3 Hz, 1H), 6.53 (d, *J* = 1.3 Hz, 1H), 4.61 (br s, 2H), 3.85 (s, 3H). ^{13}C{^{1}H} NMR (126 MHz, $CDCl_3$, δ): 160.8, 158.8, 152.6, 150.2, 130.0, 128.2, 114.6, 111.5, 103.8, 55.5. HRMS (ESI QTOF) m/z: [M]+ Calcd for $C_{12}H_{11}ClN_2O$ 234.0560; Found 234.0551. The C2-monoarylated isomer **A18a** was isolated as a minor product (R_f = 0.30 in 25% ethyl acetate in hexanes; 12.6 mg, 13% yield). ^{1}H NMR (500 MHz, $CDCl_3$, δ): 7.88-7.86 (m, 2H), 7.03 (d, *J* = 1.5 Hz, 1H), 6.97-6.95 (m, 2H), 6.40 (d, *J* = 1.5 Hz, 1H), 4.57 (br s, 2H), 3.85 (s, 3H). The column eluent was modified to 5% methanol in CH_2Cl_2 to elute the diarylated product **A18c**, isolated in low purity (R_f = 0.02 in 25% ethyl acetate in hexanes; 19.7 mg, <16% yield). ^{1}H NMR (500 MHz, $CDCl_3$, δ): 7.94-7.91 (m, 2H), 7.60-7.57 (m, 2H), 7.22 (d, *J* = 1.3 Hz, 1H), 7.00-6.96 (multiple peaks, 4H), 6.58 (d, *J* = 1.3 Hz, 1H), 4.62 (br s, 2H), 3.859 (s, 3H), 3.856 (s, 3H).

2-Chloro-4-(4-methoxyphenyl)quinoline (19b). Compound **19b** was prepared according to the general procedure using Conditions B on a 3.0 mmol scale using 2,4-dichloroquinoline (**19**, 594.2 mg, 3.0 mmol, 1.0 equiv) and *p*-methoxyphenylboronic acid (455.9 mg, 3.0 mmol, 1.0 equiv) with stirring for 19 h. The product mixture was diluted in ethyl acetate, filtered through Celite, and solvent was removed under reduced pressure (as described in the general procedure) Purification method 1: The concentrated residue was dissolved in excess acetone in a conical flask, then water was added until the solution appeared to become saturated. Slow evaporation of the acetone/water

solution from the flask induced crystallization. Yellow-tinted crystals were collected from three crops, separated from solvent, and dried in air to provide product **19b** (454 mg, 56% yield). Purification method 2: The concentrated residue was purified on a Biotage Selekt automated column using 100 grams of high-capacity silica (*see General Materials and Methods*), a linear gradient of 2-20% acetone in hexanes over 12 column volumes, at a flow rate of 120 mL/min (R_f = 0.60 in 10% acetone in hexanes. GC analysis indicated coelution of the C2- and C4-monoarylated isomers (**A19a** and **19b**); however, large colorless crystals of **19b** formed selectively within the fractions and were collected in two separate crops and dried under air to provide product **19b** (403.2 mg, 50% yield); mp 152-154 °C [uncorrected, measured against benzoic acid (113-117 °C)]. ^{1}H NMR (500 MHz, $CDCl_3$, δ): 8.08 (d, *J* = 8.4 Hz, 1H), 7.93 (d, *J* = 8.4 Hz, 1H), 7.73 (ddd, *J* = 8.4, 7.0, 1.3 Hz, 1H), 7.51 (ddd, *J* = 8.4, 7.0, 1.2 1H), 7.46-7.43 (m, 2H), 7.32 (s, 1H), 7.08-7.05 (m, 2H), 3.91 (s, 3H). ^{13}C{^{1}H} NMR (126 MHz, $CDCl_3$, δ): 160.4, 151.5, 150.5, 148.6, 130.9, 130.5, 129.15, 129.12, 126.9, 126.1, 125.9, 122.1, 114.3, 55.6. HRMS (ESI Q-TOF) m/z: [M]+ Calcd for $C_{16}H_{12}ClNO$ 269.0607; Found 269.0606.

2,8-Dichloro-4-(4-methoxyphenyl)quinoline (20b). Compound **20b** was prepared according to the general procedure using Conditions C, 2,4,8-trichloroquinoline (102.3 mg, 0.44 mmol, 1.1 equiv) and *p*-methoxyphenylboronic acid (60.8 mg, 0.4 mmol, 1.0 equiv) with stirring for 15.5 h. The product was purified by reversed phase flash column chromatography with a 12 g C18 silica column, using an initial automated program utilizing a flow rate of 13 mL/min of water:acetonitrile (98:2 to 5:95) over 30 column volumes. When the product began eluting, the program was paused and reset to elute the analyte at 61-70% MeCN in water. After the elution, the initial program was resumed. The C4 monoarylated product **20b** eluted cleanly at 65-67% MeCN, but the C2-

monoarylated isomer **A20a** and the 2,4-diarylated product **A20c** subsequently coeluted with each other. Fractions containing **20b** were partitioned between ethyl acetate and saturated brine. The organic layers were combined and dried over magnesium sulfate, concentrated, and dried furnishing **20b** as a white solid (65.9 mg, 54% yield). ^{1}H NMR (500 MHz, $CDCl_3$, δ): 7.86 (dd, *J* = 1.8, 1.4 Hz, 1H), 7.84 (dd, *J* = 3.0, 1.4 Hz, 1H), 7.43-7.40 (multiple peaks, 3H), 7.38 (s, 1H), 7.087.05 (m, 2H), 3.90 (s, 3H). ^{13}C{^{1}H} NMR (126 MHz, $CDCl_3$, δ): 160.6, 152.1, 151.5, 145.0, 133.1, 130.9, 130.6, 128.9, 127.5, 126.7, 125.3, 123.2, 114.4, 55.6. HRMS (ESI Q-TOF) m/z: [M]+ Calcd for $C_{16}H_{11}Cl_2NO$ 303.0218; Found 303.0217. The minor products **A20a** and **A20c** were further purified by (normal-phase) flash column chromatography in 5-20% acetone in hexanes. The C2-monoarylated isomer **A20a** was isolated as a minor product in low purity (4.0 mg, <3% yield). ^{1}H NMR (500 MHz, $CDCl_3$, δ): 8.24-8.22 (m, 2H), 8.13 (dd, *J* = 8.4, 1.3 Hz, 1H), 8.01 (s, 1H), 7.87 (dd, *J* = 7.5, 1.3 Hz, 1H), 7.48 (dd, *J* = 8.4, 7.5 Hz, 1H), 7.07-7.04 (m, 2H), 3.90 (s, 3H). The minor product of 2,4-diarylation **A20c** was also isolated in low purity (7.3 mg, <5% yield). ^{1}H NMR (500 MHz, $CDCl_3$, δ): 8.30-8.27 (m, 2H), 7.83-7.81 (multiple peaks, 3H), 7.49-7.46 (m, 2H), 7.33 (dd, *J* = 8.4, 7.5 Hz, 1H), 7.09-7.07 (m, 2H), 7.07-7.04 (m, 2H), 3.92 (s, 3H), 3.89 (s, 3H).

2-Chloro-4-(4-methoxyphenyl)-1,8-naphthyridine (21b). Compound **21b** was prepared according to the general procedure using Conditions B, with the modification that catalyst **3f** (9.8 mg, 0.012 mmol, 3.0 mol%) was used instead of **3b**, 2,4-dichloro-1,8-naphthyridine (79.6 mg, 0.4 mmol, 1.0 equiv) and *p*-methoxyphenylboronic acid (60.8 mg, 0.4 mmol, 1.0 equiv) with stirring for 12 h. Purification by flash column chromatography on silica gel (R_f = 0.22 in 20% pyridine in hexanes) provided **21b** as a white solid (72.1 mg, 67% yield). ^{1}H NMR (600 MHz, $CDCl_3$, δ): 9.04

(dd, J = 4.3, 1.7 Hz, 1H), 8.28 (dd, J = 8.3, 1.7 Hz, 1H), 7.42 (dd, J = 8.3, 4.3 Hz, 1H), 7.38-7.37 (multiple peaks, 3H), 7.05-7.03 (m, 2H), 3.86 (s, 3H). $^{13}C\{^{1}H\}$ NMR (151 MHz, $CDCl_3$, δ): 160.7, 156.1, 154.0, 153.7, 152.3, 135.6, 130.8, 127.8, 123.0, 122.2, 120.6, 114.5, 55.5. HRMS (TOF MS ESI+) m/z: [M]+ Calcd for $C_{15}H_{11}ClN_2O$ 270.0560; Found 270.0567.

3-Chloro-5-(4-methoxyphenyl)-4-phenylpyridazine (22b). Compound **22b** was prepared according to the general procedure using Conditions A, 3,5-dichloro-4-phenylpyridazine (**A22**, 135.0 mg, 0.6 mmol, 1.5 equiv) and *p*-methoxyphenylboronic acid (60.8 mg, 0.4 mmol, 1.0 equiv) with stirring for 22 h. Product **22b** was purified on an automated column using 10 grams of high-capacity silica, a linear gradient of 5-40% acetone in hexanes over 11 column volumes (R_f = 0.36 in 20% acetone in hexanes). Product **22b** was isolated as a white solid (81.5 mg, 69% yield). ^{1}H NMR (500 MHz, $CDCl_3$, δ): 9.12 (s, 1H), 7.34-7.33 (m, 3H), 7.15-7.14 (m, 2H), 7.03-7.01 (m, 2H), 6.77-6.75 (m, 2H), 3.74 (s, 3H). $^{13}C\{^{1}H\}$ NMR (126 MHz, $CDCl_3$, δ): 160.3, 157.0, 151.6, 140.5, 137.7, 133.4, 130.9, 129.7, 128.9, 128.6, 126.0, 114.3, 55.3. HRMS (ESI Q-TOF) m/z: [M]+ Calcd for $C_{17}H_{13}ClN_2O$ 296.0716; Found 296.0706. The minor product of diarylation **A22c** was also isolated in low purity (10.1 mg, <7% yield, R_f = 0.15 in 20% acetone in hexanes). ^{1}H NMR (500 MHz, $CDCl_3$, δ): 9.15 (s, 1H), 7.28-7.26 (m, 2H), 7.21-7.17 (m, 3H), 7.03-7.01 (m, 2H), 6.93-6.91 (m, 2H), 6.79-6.75 (multiple peaks, 4H), 3.782 (s, 3H), 3.778 (s, 3H).

3-Chloro-5-(4-methoxyphenyl)-4-(1-piperidinyl)pyridazine (23b). Compound **23b** was prepared according to the general procedure using Conditions A, modified to heat at 66 °C instead of 60 °C, with 3,5-dichloro-4-(1-piperidinyl)-pyridazine (**A23**, 92.8 mg, 0.4 mmol, 1.0 equiv), and *p*-methoxyphenylboronic acid (60.8 mg, 0.4 mmol, 1.0 equiv) with stirring for 8 days (however, yields were comparable when the reaction was run for only 3 days). Product **23b** was purified on

an automated column using 10 grams of high-capacity silica, a linear gradient of 5-40% acetone in hexanes over 11 column volumes (although **23b** eluted after 13 column volumes) at a flow rate of 40 mL/min (R_f = 0.21 in 20% acetone in hexanes), providing **23b** as a red-brown solid (38.7 mg, 32% yield). ^{1}H NMR (500 MHz, $CDCl_3$, δ): 8.74 (s, 1H), 7.28-7.26 (m, 2H), 7.00-6.98 (m, 2H), 3.85 (s, 3H), 2.99-2.97 (m, 4H), 1.51-1.47 (m, 2H), 1.43-1.39 (m, 4H). ^{13}C{^{1}H} NMR (126 MHz, $CDCl_3$, δ): 159.8, 156.5, 149.3, 143.0, 130.7, 126.4, 126.3, 114.4, 55.4, 50.2, 25.5, 23.8. HRMS (ESI Q-TOF) m/z: [M]+ Calcd for $C_{16}H_{18}ClN_3O$ 303.1138; Found 303.1129.

3-Chloro-5-(4-methoxyphenyl)pyridazine (24b). Prior to the reaction, 3,5-dichloropyridazine (purchased as a reddish brown solid) was purified by trituration in pentanes and filtration through a sintered funnel; the filtrate was concentrated and dried furnishing 3,5-dichloropyridazine starting material as a white solid (70% recovery). Compound **24b** was prepared according to the general procedure using Conditions A, purified 3,5-dichloropyridazine (59.6 mg, 0.4 mmol, 1.0 equiv) and *p*-methoxyphenylboronic acid (60.8 mg, 0.4 mmol, 1.0 equiv) with stirring for 6 h. Purification by flash column chromatography on silica gel (R_f = 0.22 in 15% acetone in hexanes) provided **24b** as a white crystalline solid with minor red-brown discoloration (68.8 mg, 78% yield); mp 94–97 °C [uncorrected, measured against benzoic acid (113-117 °C)]. ^{1}H NMR (600 MHz, $CDCl_3$, δ): 9.24 (d, J = 1.5 Hz, 1H), 7.55-7.54 (multiple peaks, 3H), 6.97 (d, J =7.4 Hz, 2H), 3.80 (s, 3H). ^{13}C{^{1}H} NMR (151 MHz, $CDCl_3$, δ): 161.9, 157.2, 148.5, 140.7, 128.6, 125.0, 123.6, 115.2, 55.5. HRMS (ESI Q-TOF) m/z: [M]+ Calcd for $C_{11}H_9ClN_2O$ 220.0403; Found 220.0403.

2,4-Bis-(4-methoxyphenyl)-6-(trifluoromethyl)pyridine (A25c). Compound **A34c** was prepared according to the general procedure using Conditions B, 2,4-dichloro-6-(trifluoromethyl)pyridine (86.4 mg, 0.4 mmol, 1.0 equiv) and *p*-methoxyphenylboronic acid (60.8 mg, 0.4 mmol, 1.0 equiv) with stirring for 12 h. Purification by flash column chromatography on silica (R_f = 0.34 in 7% acetone in hexanes) provided **A25c** as a white crystalline solid (61.8 mg, 43% yield); mp 95-98 °C [uncorrected, measured against benzoic acid (109-111 °C)]. ^{1}H NMR (500 MHz, $CDCl_3$, δ): 8.09-8.06 (m, 2H), 7.96 (d, J = 1.3 Hz, 1H), 7.70 (d, J = 1.3 Hz, 1H), 7.67-7.64 (m, 2H), 7.06-7.00 (multiple peaks, 4H), 3.88 (s, 3H), 3.87 (s, 3H). ^{13}C{^{1}H} NMR (126 MHz, $CDCl_3$, δ): 161.2, 161.1, 158.1, 150.4, 148.7 (q, J_{CF} = 33.9 Hz), 130.8, 129.9, 128.7, 128.5, 122.0 (q, J_{CF} = 274.5 Hz), 119.4, 115.5 (q, J_{CF} = 2.7 Hz), 114.8, 114.3, 55.54, 55.49. ^{19}F NMR (471 MHz, $CDCl_3$, δ): -68.0.

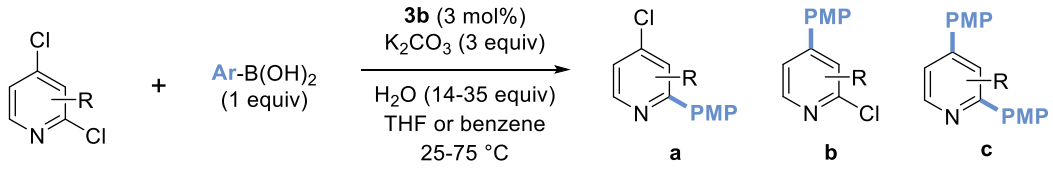
2-Chloro-4-(4-phenoxyphenyl)-3-pyridinecarbonitrile (39b). Compound **39b** was prepared according to the general procedure using Conditions A on a 1.0 mmol scale, 2,4-dichloro-3-cyanopyridine (173.0 mg, 1.0 mmol, 1.0 equiv) and *p*-phenoxyphenylboronic acid (214.0 mg, 1.0 mmol, 1.0 equiv) with stirring for 19 h. Purification by flash column chromatography on silica gel (R_f = 0.26 in 10% acetone in hexanes) provided **39b** as a white solid (188 mg, 61% yield). ^{1}H NMR (500 MHz, $CDCl_3$, δ): 8.52 (d, J = 5.2 Hz, 1H), 8.59-8.56 (m, 2H), 7.41-7.37 (multiple peaks, 3H), 7.20-7.17 (m, 1H), 7.12-7.08 (multiple peaks, 4H). Spectral data are consistent with the literature.[17]

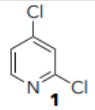
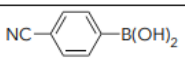
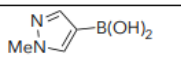
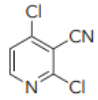
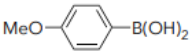
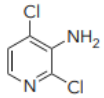
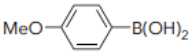
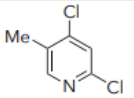
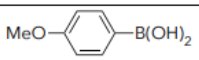
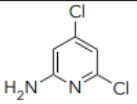
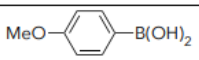
Discussion About Mass Balance

The moderate isolated yields in Scheme 2.3 (ligand-controlled conditions) are generally due to a combination of factors: (1) unreacted starting material, (2) formation of diarylated product,

and (3) material loss during purification of the target product by column chromatography due to partial coelution of regioisomers.

In several examples above, we report isolated yields of the minor regioisomer as well as the diarylated regioisomer. These isolated yields are summarized below. In some cases, the mass balances are above 90%. In cases with lower mass balance, there was significant material loss during isolation of products.



Substrate	$ArB(OH)_2$	estimated unreacted substrate based on crude GC (uncalibrated, %)[a]	**a** (%)	**b** (%)	**c** (%)	Sum of substrate + **a** + **b** + **c** (%)
 **1**		6	9	71 (**6b**)	13	99
1		2	13	67 (**10b**)	9	91
		2	6[b]	68 (**12b**)	3	79
		6	13	60 (**14b**)	14	93
		11	2[b]	53 (**15b**)	18	84
		4	13	48 (**18b**)	16	81

[a]Yield calculated by extrapolation from the isolated yield of the C4 product (**b**) and the ratio of C4 product to remaining starting material signals by GC analysis of the crude reaction mixture. [b]Yield calculated by extrapolation from the isolated yield of the C4 product (**b**) and the ratio of C4:C2 product signals by GC analysis of the crude reaction mixture.

The GC chromatograms below illustrate the crude reaction mixtures prior to purification for two of the reactions with lower mass balance (reactions to form **12b** and **18b**). There are no significant unidentified peaks.

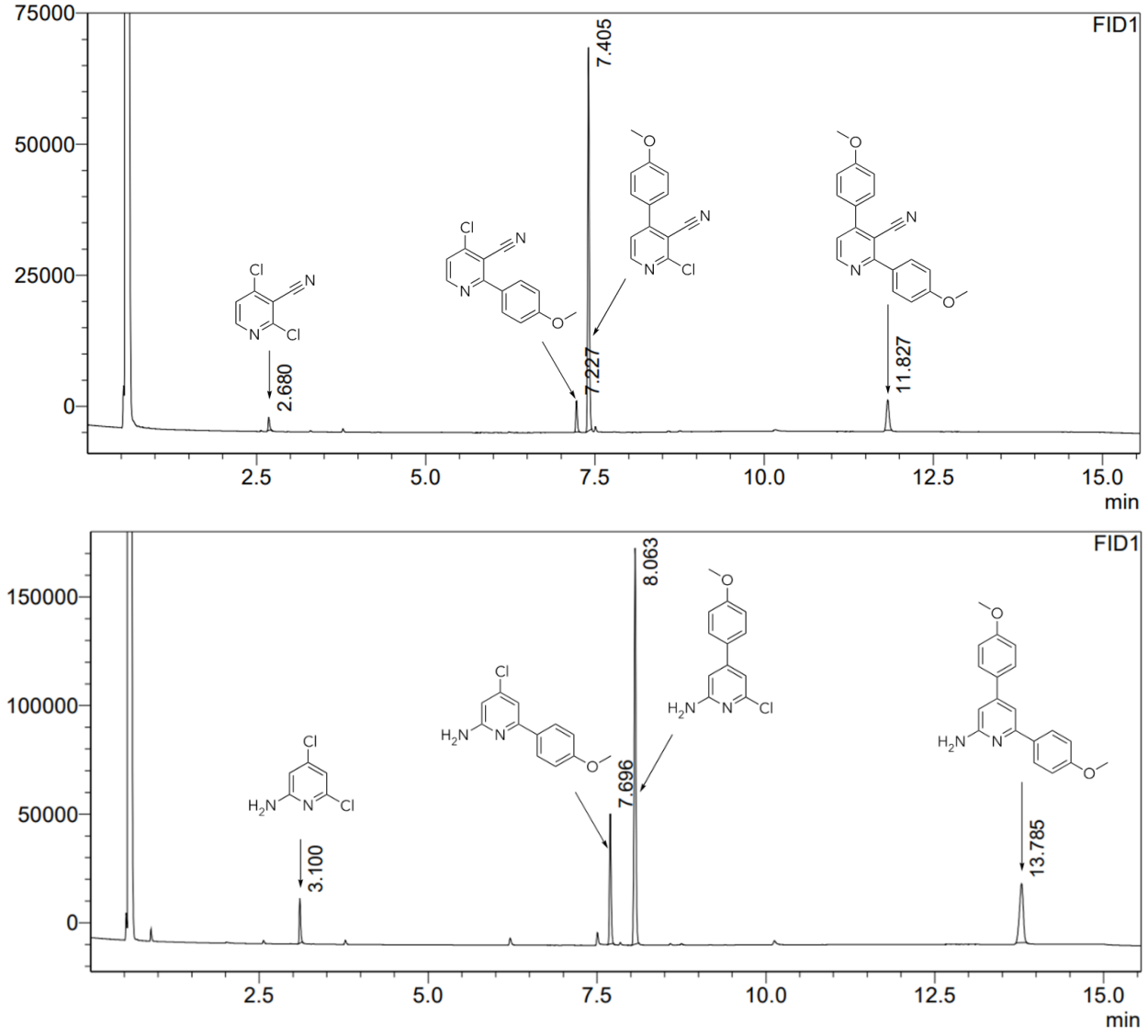
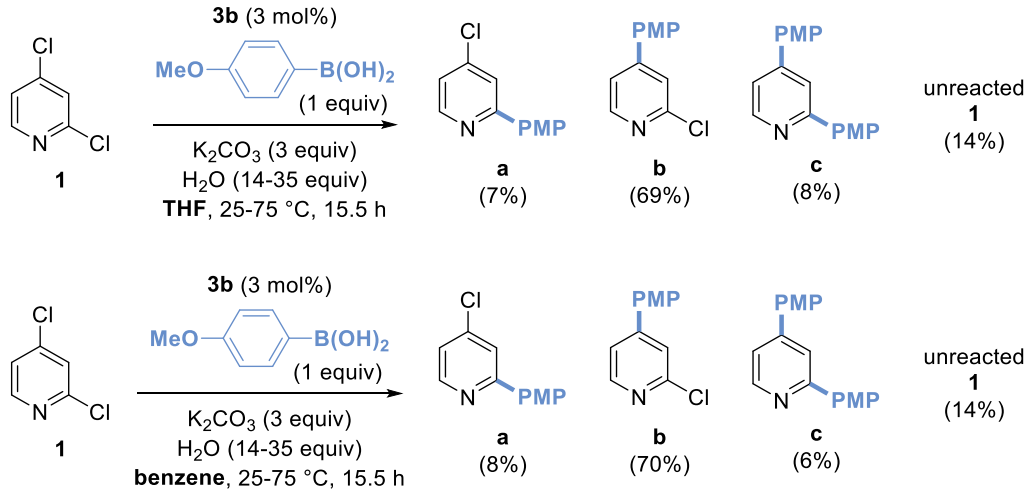


Figure A1. GC Chromatograms of Pd(IPr)-catalyzed Suzuki Couplings with Low Mass Balances.

In the optimization table (Table 2.1), a standard was added to the reactions and calibrated GC yields were obtained. We generally see good mass balance accounted for by major and minor

regioisomers, unreacted starting material, and diarylation products. Examples are illustrated below, corresponding to entries 3 and 5 of Table 2.1.

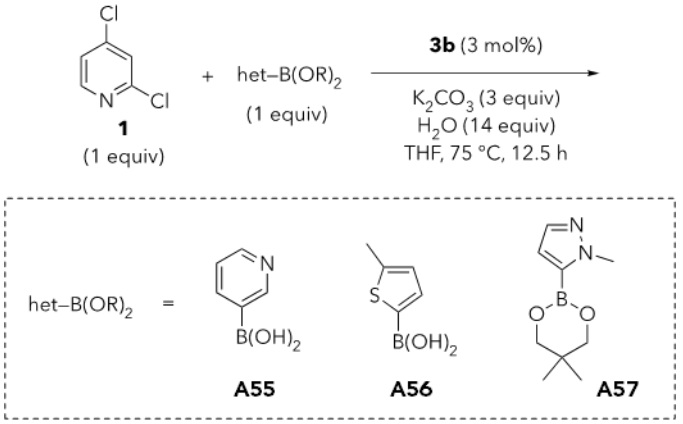
Scheme A3. Yields and Conversion of Reactions in Entries 3 and 5 of Table 2.1.

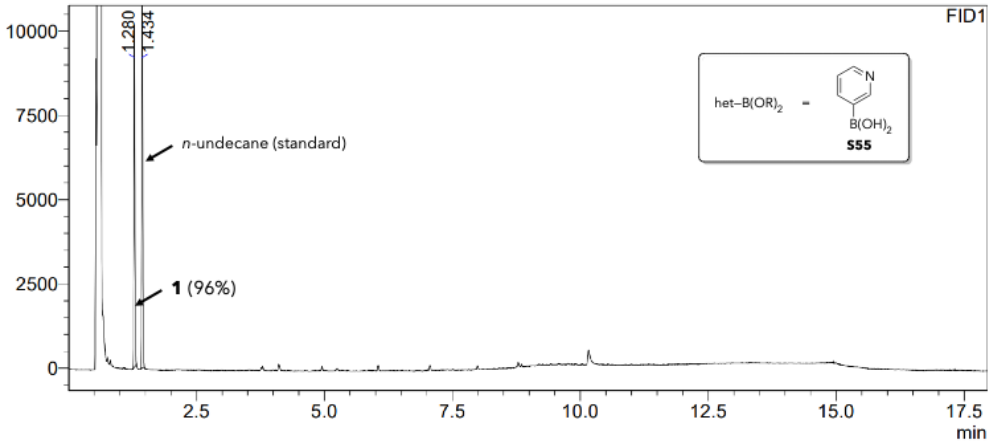


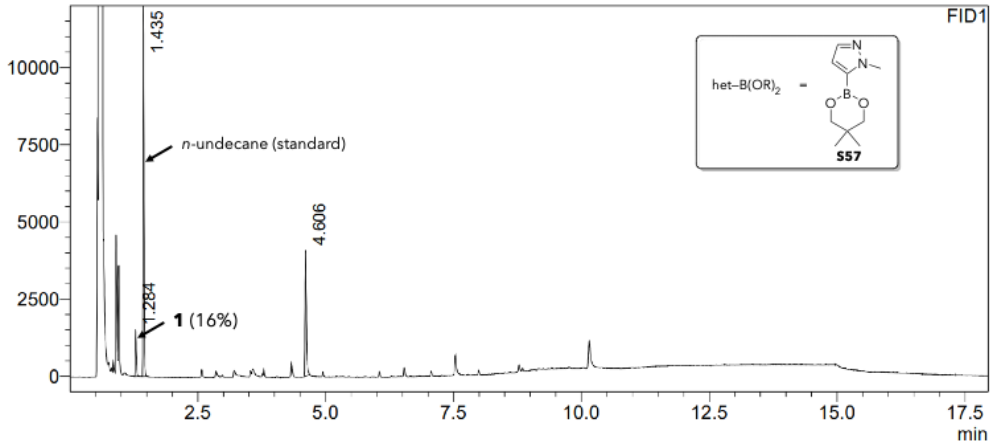
Scope Limitations of the Suzuki Coupling

Boron Nucleophile Limitations: Heteroaryl boronic acids and esters **A55**-**A57** were ineffective in the Suzuki cross-coupling with **1** under the optimized conditions using catalyst **3b** (General Procedure for GC-Scale Reactions) at room temperature or even at a higher temperature (75 ºC, below). For **A55** and **A56**, most of the starting material **1** remained after the reaction time. For **A57**, most of the starting material was consumed, but only small amounts of products were detected by GC. The GC chromatograms of these crude reactions are depicted below.

Scheme A4. Boron Nucleophile Limitations.





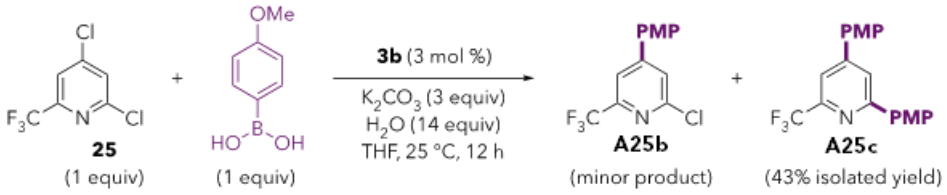


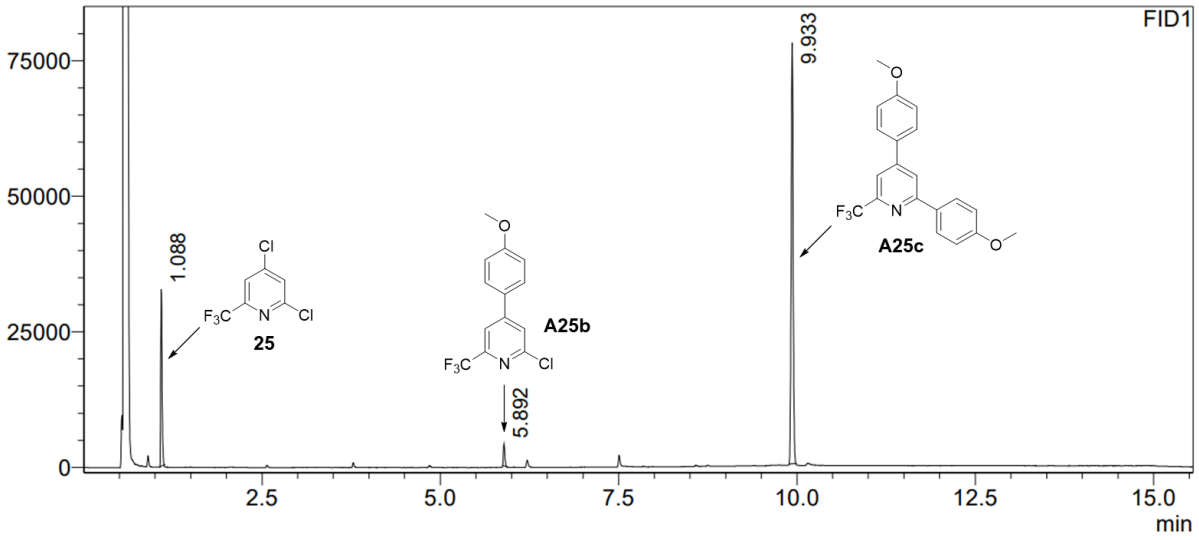
Substrate Limitations Overview. Some substrates did not provide the desired cross-coupling selectivity. These substrates are categorized below as 2,4-dihalopyridines that lead to overarylation (**25** and **26**), brominated 2,4dichloropyridine or quinolines that react at bromide instead of chloride (**27** and **28**), and 2,5-dichloropyridine and pyrimidine (**29** and **30**), substrates for which the Pd/IPr catalytic system provides conventional selectivity next to nitrogen. The reactions below were conducted according to the General Procedure for GC-Scale Reactions.

Substrates Resulting in Overarylation. Reactions of both substrates **25** and **26** afford diarylated product **A25c** and **1c** as the major products by crude GC analysis. For the reaction of **25** with catalyst **3b**, a small amount of C4-monarylated product **A25b** is detected by crude GC, but the major product is **A25c** from diarylation (Scheme A5). Product **A25c** was isolated and characterized (*vide supra*). The monoarylated product was not isolated, but its identity was tentatively assigned on the basis of its mass (by GCMS analysis) and inference based on the usual selectivity exhibited by **3b** (Pd/IPr, which favors reaction at C4 with other 2,4-dichloropyridines) and **3d** (Pd/IMes, which gives nearly a 1:1 mixture of C2- and C4arylated products with other 2,4-dichloropyridines). When **3d** (Pd/IMes) is used as the catalyst for the Suzuki coupling of **25**, much less diarylation is observed, and two monoarylated products are formed in a 1.5:1 ratio (assigned as **A25b** and **A25a**, Scheme A6). Notably, only one of these two monoarylated products is observed in the reaction using catalyst **3b**, and based on the usual selectivity with **3b** we infer that this product is **A25b**. Dibromo substrate **26** undergoes extensive diarylation using catalyst **3b** (Scheme A7). Product **1c** has been isolated and characterized (*vide supra*), and the identities of the minor monoarylated products **A26a** and **A26b** are supported by GCMS analysis. The regiochemistry of **A26a** and **A26b** was inferred based on the usual selectivity exhibited by **3b**

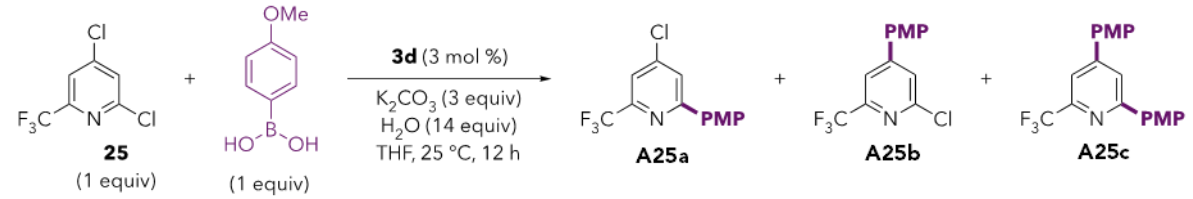
(Pd/IPr, which favors reaction at C4 with 2,4-dichloropyridines) and subsequently confirmed using C4-selective cross-coupling conditions recently reported by Fairlamb[18] (*vide infra).*

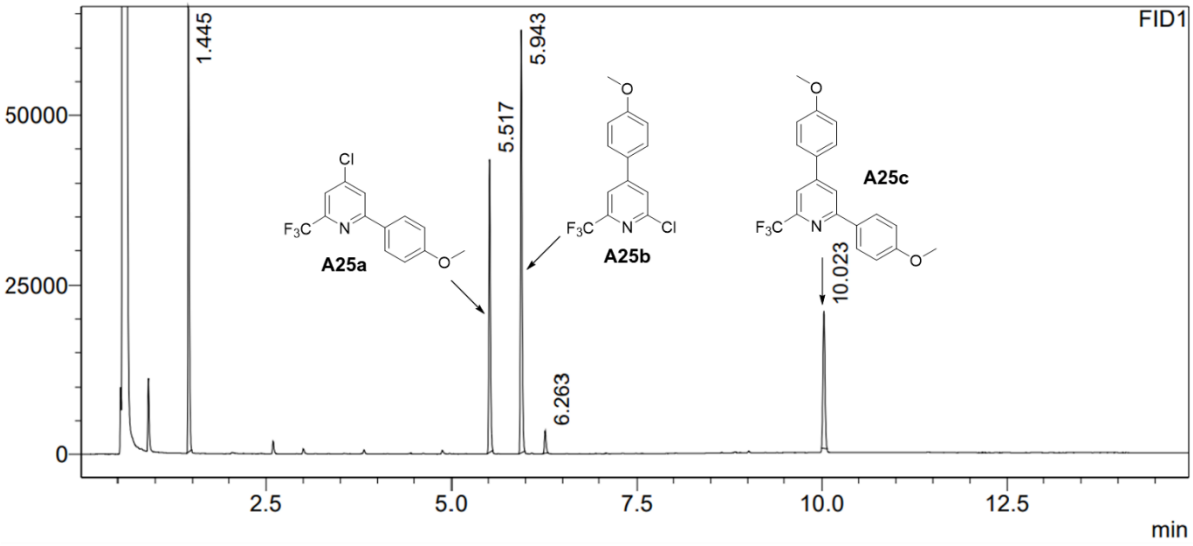
Scheme A5. Suzuki reaction of **25** using Pd/IPr catalyst **3b**.



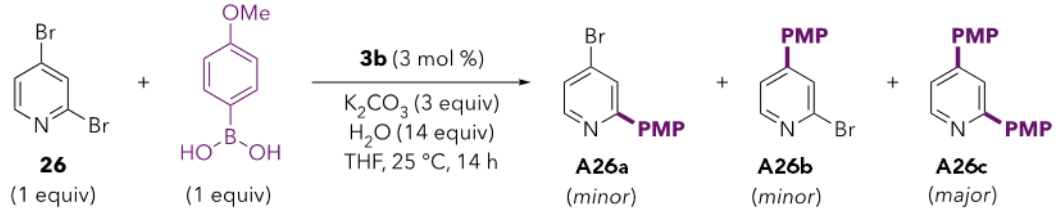


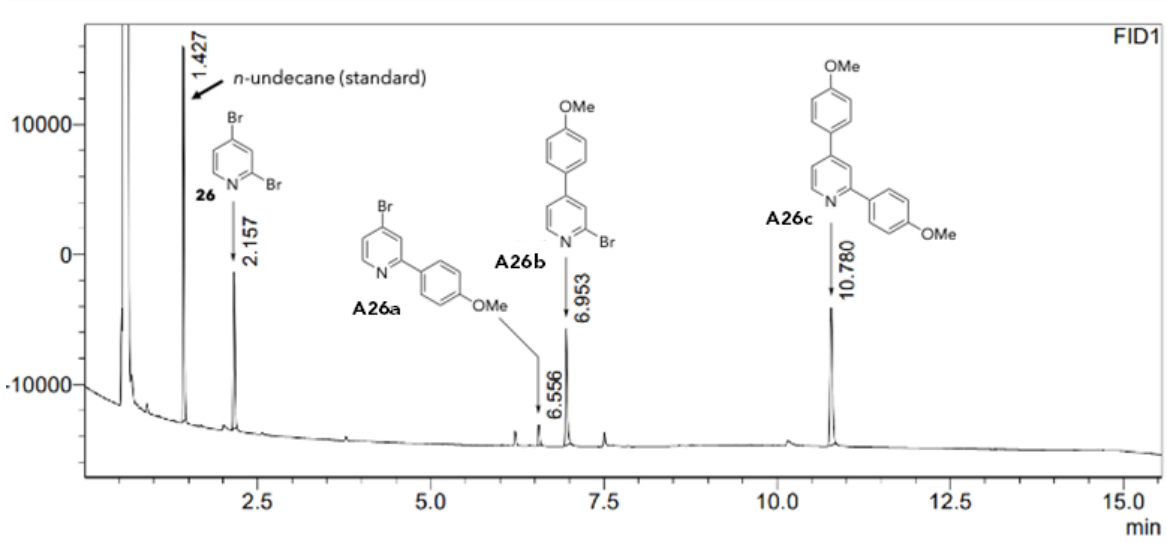
Scheme A6. Suzuki reaction of **25** using Pd/SIMes catalyst **3d**.





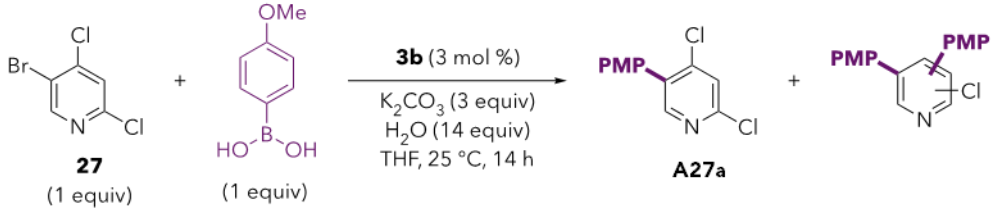
Scheme A7. Suzuki reaction of **26** using Pd/IPr catalyst **3b**.

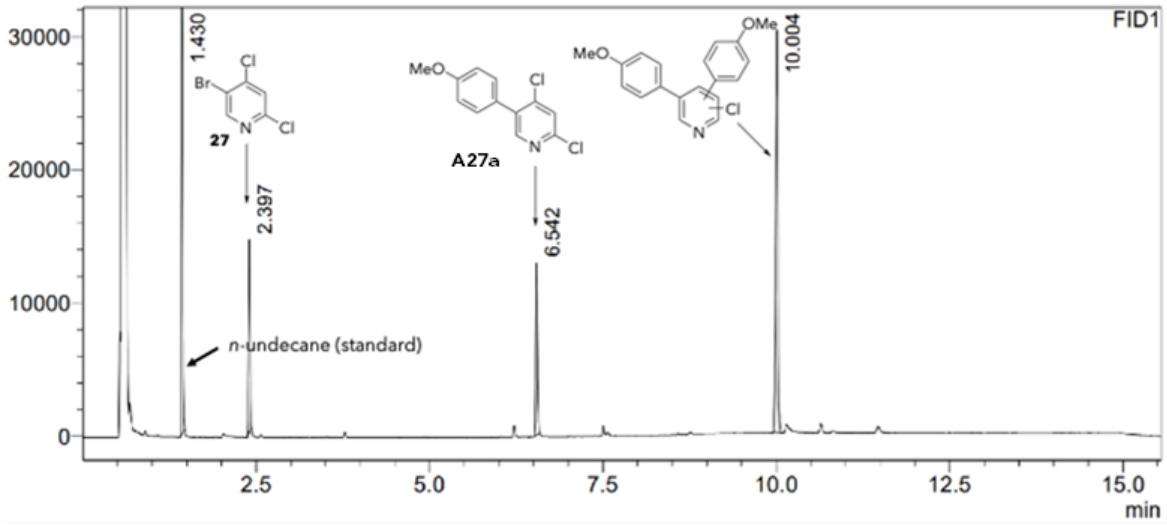




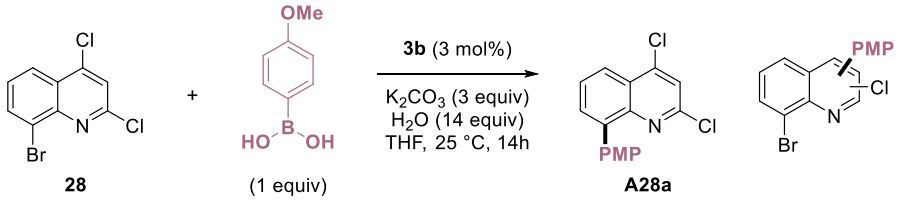
Substrates Resulting in Reaction at Bromide. Substrates **27** and **28** undergo extensive reaction at bromide under the optimized conditions, providing a mixture of dichloro-monoarylated products **A27a** and **A28a** and diarylated products resulting from reaction at bromide and one of the chlorides (Schemes A7-A8). Product identities were assigned based on GCMS analysis.

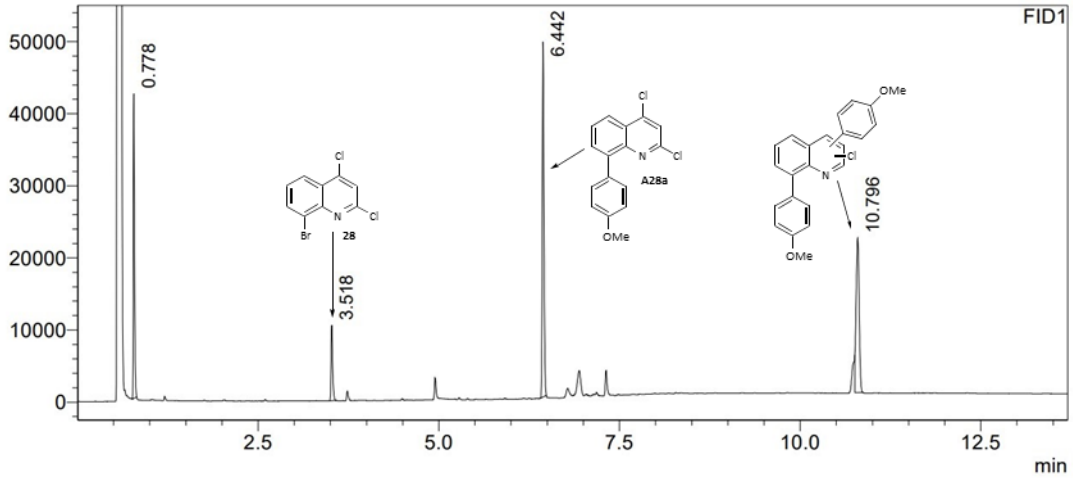
Scheme A8. Suzuki reaction of **27** using Pd/IPr catalyst **3b**.





Scheme A9. Suzuki reaction of **28** using Pd/IPr catalyst **3b**.

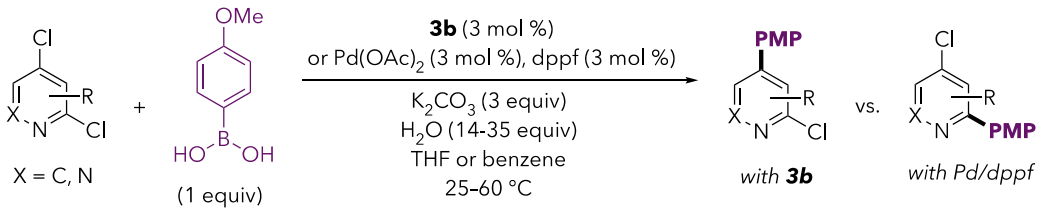




Comparison of Results with IPr (C4-Selective) vs. dppf (C2-Selective)

C4-selectivity remains ligand-controlled for the substrates depicted in Scheme 3.2, as evidenced by the observation of different major products when using catalyst **3b** (ligand = IPr) versus using $Pd(OAc)_2$/dppf (Table A2).

Table A2. Retention time (RT) of major products by GC-FID for reactions catalyzed by **3b** or by $Pd(OAc)_2$/dppf.



entry	substrate	**3b** (min)	Pd/dppf (min)
1	**A20**	7.11	7.21
2	**A22**	7.21	7.16
3	**A23**	7.25	7.02
4	**A24**	6.52	6.68
5	**A25**	7.81	7.88
6	**A27**	8.03	7.69
7	**A30**	7.10	7.20
8	**A31**	6.79	6.48
9	**A32**	7.62	7.98
10	**A33**	7.22	6.62

A4. Kumada Cross Couplings with Pd/IPr

General Procedures

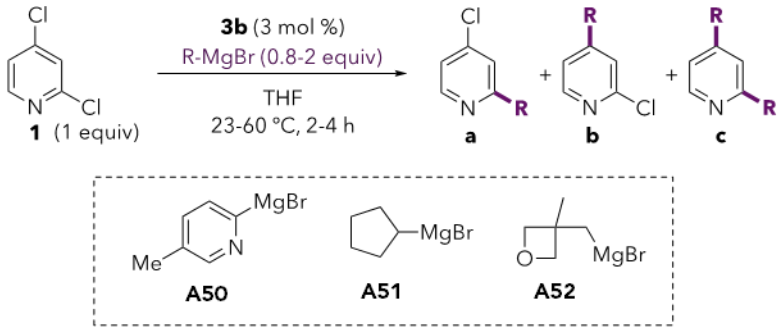
GC-Scale Reactions: The precatalyst **3b** (1.7 mg, 0.0024 mmol, 3.0 mol%) was added to an oven-dried 1-dram vial equipped with a stir bar. The vial was transferred to a N_2 atmosphere glovebox, and the Grignard reagent (0.772 equiv) was added as a solution in THF followed by 2,4-dichloropyridine (0.08 mmol, 1 equiv). The vial was sealed with a PTFE-lined cap and removed from the glovebox. The reaction was stirred for 2-4 hours at 23-60 ºC. The reaction mixture was opened to air and quenched with EtOAc (~3.2 mL), and the internal standard undecane was added (7.5 µL, 0.036 mmol). The vial was shaken to mix the contents, and the mixture was filtered through Celite prior to analysis by GC and GCMS.

Scaled-Up Reactions for Product Isolation: The precatalyst **3b** (8.4 mg, 0.012 mmol, 3.0 mol%) was added to an oven-dried 1- or 5-dram vial equipped with a stir bar. The vial was transferred to a N_2 atmosphere glovebox, and the Grignard reagent (0.77-2 equiv) as a solution in THF was added followed by the addition of 2,4-dichloropyridine (1 equiv). The vial was sealed with a PTFE-lined cap and removed from the glovebox. The reaction was stirred for 2-5 hours at 23 ºC, then the vial was opened to air. The reaction mixture was diluted with EtOAc and washed with sat. aqueous NH_4Cl (3 x 10 mL), sat. aqueous $NaHCO_3$ (3 x 10 mL), and brine (2 x 10 mL) in a separatory funnel. The organic layer was extracted with additional EtOAc (3 x 10 mL) and the combined organic layers were dried over anhydrous $MgSO_4$. The crude reaction mixture was analyzed by GC, concentrated under vacuum, and purified by normal or reversed phase flash column chromatography.

Optimization

Kumada reactions were performed according to the general procedure for GC-scale reactions.

Table A3. Optimization of Kumada Cross-Couplings.



entry	T (°C)	time (h)	R-MgBr (equiv)	**a** : **b** [a]	**1** (%)[b]
1	23	2	**A50** (1)	<1 : 100	16
2[c]	23	2	**A50** (1)	--[d]	100
3[e]	23	2	**A50** (1)	--[d]	72
4	23	3	**A51** (1)	1 : 8	5
5	23	3	**A51** (0.8)	1 : 7	13
6[c]	23	3	**A51** (1)	--[d]	56
7	23	3	**A52** (1)	<1 : 39	30
8	23	3	**A52** (2)	<1 : 60	7
9[c]	23	3	**A52** (1)	--[d]	98
10[f]	60	4	**A52** (1)	--[d]	64

[a] Ratios based on the ratio of signals for **a** and **b** in the GC chromatogram. [b]GC yield of recovered starting material calibrated against undecane. In entry 3, the starting material was 2-bromo-4-chloropyridine instead of **1**. [c]No catalyst (metal free control). [d]"--" means no cross-coupled products **a** or **b** were observed. [e]2-Bromo-4-chloropyridine was used instead of **1** in combination with $Pd(OAc)_2$ (5 mol %) and dppf (5 mol %) as the catalytic system instead of **3b**. [f]$Pd(OAc)_2$ (5 mol %) and dppf (5 mol %) was used as the catalytic system instead of **3b**.

Discussion: Catalyst-free controls using reagents **A50**–**A52** (Table A3, entries 2, 6, 9) show no formation of products **a** or **b**, indicating that there is no background S_NAr reactivity. Entries 1, 5, and 8 represent the optimized conditions that were used for scale-up reactions. Interestingly,

products **a** and **c** were not observed in the cross couplings with **A50** and **A52**. The use of 2-bromo-4-chloropyridine as the substrate for reaction with **A50** (entry 3), a substrate that should be strongly biased toward reaction at C2, also did not lead to any detectable cross-coupled products. Reaction of the pyridyl Grignard **A50** at C2 would lead to a 2,2'-bipyridine derivative which can chelate to Pd or Mg, providing a compound that is insoluble or not volatile and therefore invisible by GC-FID. Similarly in the case of Grignard **A52**, product **a** is not obtained even when using $Pd(OAc)_2$/dppf (entry 10), although considerably more starting material was consumed. It is possible that the C2-functionalized product **a** resulting from reaction of Grignard **A52** is prone to decomposition.

Isolation and Characterization of Kumada Products from Scheme 2.4

2-Chloro-5'-methyl-4,2'-bipyridine (31b). Product **31b** was prepared according to the general procedure using **3b** (8.4 mg, 0.012 mmol, 3 mol %), 5-methyl-2-pyridylmagnesium bromide (**A50**, 1.6 mL of a 0.25 *M* solution in THF, 0.40 mmol, 1.00 equiv), and **1** (43.2 μL, 0.40 mmol, 1.00 equiv). The reaction was stirred at 23 ºC for 2 h. The crude GC chromatogram indicated the presence of unreacted **1**. Purification was performed by flash column chromatography (R_f= 0.46 in 90:10 Hex:EtOAc) yielded a white solid (49.7 mg, 61% yield). ^{1}H NMR (500 MHz, $CDCl_3$, δ): 8.58-8.61 (m, 1H), 8.49 (d, *J* = 5.2 Hz, 1H), 7.967.99 (m, 1H), 7.82 (dd, J= 5.2, 1.5 Hz, 1H), 7.72 (d, *J* = 8.0 Hz, 1H), 7.65 (dd, *J* = 8.0, 1.9 Hz, 1H), 2.44 (s, 3H). ^{13}C{^{1}H} NMR (126 MHz, $CDCl_3$, δ): 152.7, 151.0, 150.8, 149.7, 137.8, 134.6, 121.7, 120.7, 119.8. HRMS (ESI+) m/z: [M]+: Calcd for $C_{11}H_9ClN_2$ 204.0454; Found 204.0455. The C2 monoarylated isomer **A31a** has been reported in previous literature, and the signals for product **31b** are not consistent with those reported for **A31a**.[19]

2-Chloro-4-cyclopentylpyridine (32b). Product **32b** was prepared according to the general procedure using **3b** (8.4 mg, 0.012 mmol, 3 mol %), cyclopentylmagnesium bromide (**A51**, 1.34 mL of a 0.299 ± 0.004 *M* solution in THF, 0.40 mmol, 0.77 equiv), and **1** (56.2 µL, 0.52 mmol, 1.00 equiv). The reaction was stirred at 23 ºC for 4 h. The crude GC chromatogram indicated the presence of unreacted **1**. Purification was performed by reversed phase flash column chromatography with a 12 g C18 silica column, using an initial automated program comprising a flow rate of 30 mL/min of water:acetonitrile (98:2 to 0:100) over 31 column volumes. When the product began eluting, the program was paused and reset to elute the analyte at 58-69% MeCN in water over 11 column volumes. After the elution, the initial program was resumed. The C4 monoarylated product **32b** eluted at 61-64% MeCN. Fractions containing **32b** were partitioned between dichloromethane and saturated brine. The organic layers were combined and dried over magnesium sulfate and solvent was removed under reduced pressure affording **32b** as a light brown oil (50.8 mg, 62% yield). ^{1}H NMR (500 MHz, $CDCl_3$, δ): 8.24 (d, *J* = 5.2 Hz, 1 H), 7.17 (s, 1H), 7.06 (d, *J* = 5.2 Hz, 1H), 2.92-3.01 (m, 1H), 2.02-2.12 (m, 2H), 1.75-1.85 (m, 2H), 1.65-1.75 (m, 2H), 1.51-1.61 (m, 2H). ^{13}C{^{1}H} NMR (126 MHz, $CDCl_3$, δ): 159.3, 151.7. 149.5, 123.1, 121.6, 45.1, 34.0, 25.6. HRMS (ESI+) m/z: [M]+: Calcd for $C_{10}H_{12}ClN$ 181.0658; Found 181.0666.

2-Chloro-4-(3,3'-methyloxetanyl)pyridine (33b). Product **33b** was prepared according to the general procedure using **3b** (8.4 mg, 0.012 mmol, 3 mol %), 3,3'-methyloxetanylmagnesium bromide (**A52**, 5.71 mL of a 0.14 *M* solution in THF, 0.80 mmol, 2.0 equiv), and **1** (43.2 µL, 0.40 mmol, 1.00 equiv). The reaction was stirred at 23 ºC for 3 h. Purification was performed by reversed phase flash column chromatography with a 12 g C18 silica column, using an initial automated program comprising a flow rate of 25 mL/min of water:acetonitrile (98:2 to 8:92) over

21 column volumes. When the product began eluting, the program was paused and reset to elute the analyte at 46-49% MeCN in water. After the elution, the initial program was resumed. The C4 monoarylated product **33b** coeluted with an aliphatic impurity at 49% MeCN. Fractions containing **33b** were partitioned between ethyl acetate and saturated brine. The organic layers were combined and dried over magnesium sulfate and solvent was removed under reduced pressure. The aliphatic impurity was removed *in vacuo* yielding an off white colored solid (46.5 mg, 59% yield). ^{1}H NMR (400 MHz, $CDCl_3$, δ): 8.30 (d, J = 5.0 Hz, 1H), 7.11 (s, 1H), 6.99 (d, J = 5.0 Hz), 4.59 (d, J = 5.8 Hz, 2H), 4.37 (d, J = 5.8 Hz, 2H), 2.96 (s, 2H), 1.28 (s, 3H). $^{13}C\{^{1}H\}$ NMR (101 MHz, $CDCl_3$, δ): 151.8, 150.5, 149.6, 125.0, 123.4, 82.7, 82.1, 43.9, 39.7, 23.3 ppm. HRMS (ESI+) m/z: [M]+: Calcd for $C_{10}H_{12}ClNO$ 197.0607; Found 197.0599.

A5. Negishi Cross-Couplings with Pd/IPr

General Procedures

GC-Scale Reactions. In a glovebox, Grignard reagent (0.77-1 equiv as a solution in THF) and a solution of $ZnCl_2$ in THF (1 *M*, equimolar with the Grignard reagent) were combined in an oven-dried 1-dram vial ("vial A") equipped with a stir bar and stirred for at least 0.5 hours at ambient temperature. Outside of the glovebox, the precatalyst **3b** (1.7 mg, 0.0024 mmol, 3.0 mol %) was added to a separate oven-dried 1-dram vial equipped with a stir bar ("vial B"), and this vial was transferred into the glovebox. The contents of vial A, comprising the organozinc reagent (0.771 equiv), and 2,4-dichloropyridine (0.08 mmol, 1 equiv) were added to vial B. Vial B was sealed with a PTFE-lined cap and removed from the glovebox. Reactions were stirred for 0.75-4 hours at 23-60 ºC. The reaction mixture was opened to air, diluted with ethyl acetate (~3 mL), and

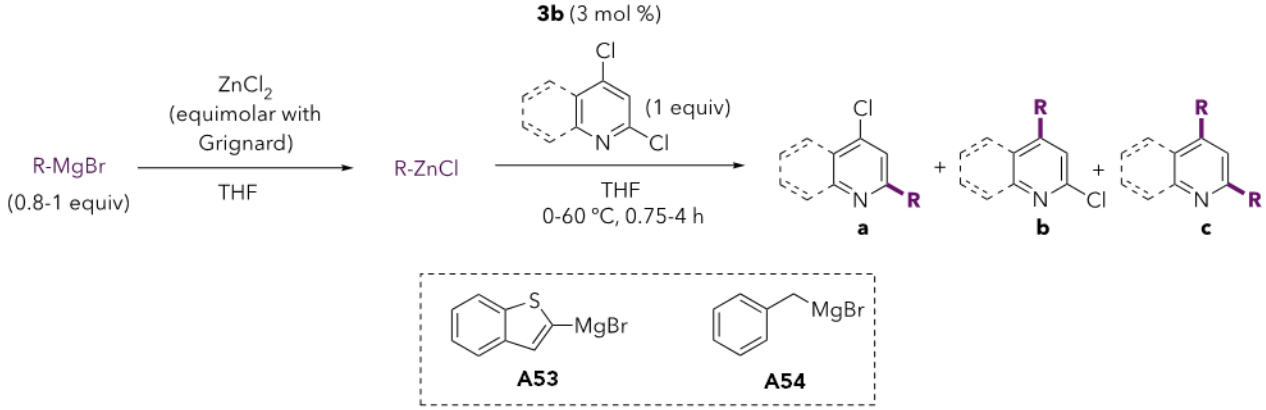
the internal standard undecane was added (7.5 μL, 0.036 mmol). The vial was shaken to mix the contents, and the mixture was filtered through Celite prior to analysis by GC and GCMS.

Scaled-Up Reactions for Product Isolation. In a glovebox, Grignard reagent (0.77-1 equiv as a solution in THF) and a solution of $ZnCl_2$ in THF (1 *M*, equimolar with the Grignard reagent). were combined in an oven-dried 1- or 5-dram vial ("vial A") equipped with a stirbar. The mixture was stirred for 0.5 hours at ambient temperature. Outside of the glovebox, the precatalyst **3b** (8.4 mg, 0.012 mmol, 3.0 mol %) was added to a separate oven-dried 1- or 5-dram vial equipped with a stir bar ("vial B"), and this vial was transferred into the glovebox. The contents of vial A, comprising the organozinc reagent (0.77-1 equiv), and 2,4-dichloropyridine (0.08 mmol, 1 equiv) were added to vial B. Vial B was sealed with a PTFE-lined cap and removed from the glovebox. Reactions were stirred for 45 min at 60 ºC unless otherwise indicated. The reaction mixture was opened to air, diluted with ethyl acetate (~3 mL), and washed with sat. NH_4Cl (3 x 10 mL), sat. $NaHCO_3$ (3 x 10 mL), and brine (2 x 10 mL) in a separatory funnel. The organic layer was extracted with additional ethyl acetate (3 x 10 mL) and the combined organic layers were dried over anhydrous $MgSO_4$. The crude product was analyzed by GC and purified by normal or reversed phase column chromatography.

Optimization

Negishi reactions were performed according to the general procedure for GC-scale reactions. Yield of remaining starting material (**1**) is calibrated against the undecane internal standard. Ratio of products **a** and **b** are assuming equal response factor between the isomers.

Table A4. Optimization of Negishi Cross Couplings.



entry	T (°C)	time (h)	R-MgBr (equiv)	**a** : **b** [a]	**1** (%)[b]
1	60	0.75	**A53** (1)	1 : 68	2
2	60	0.75	**A53** (0.8)	1 : 7.7	33
3[c]	60	0.75	**A53** (1)	--[d]	98
4	60	3	**A54** (1)	<1 : 99	0
5	23	3	**A54** (1)	1 : 45	8
6	0	3	**A54** (1)	1 : 9	21
7[c]	60	3	**A54** (1)	--[d]	96
8	60	2	MeMgBr (1)	<1 : 99	51
9[e]	60	4	MeMgBr (1)	1 : 16	0
10[e]	60	4	MeMgBr (0.8)	1 : 4	0

[a] Ratios based on the ratio of signals for **a** and **b** in the GC chromatograph. [b]All reactions were performed with 2,4-dichloropyridine (**1**) unless otherwise indicated. GC yield of recovered starting material calibrated against undecane. [c]No catalyst (metal free control). [d]"--" means no cross-coupled products **a** or **b** were detected. [e]2,4-Dichloroquinoline (**19**) was used instead of **1**.

Discussion: Catalyst-free controls (Table A4, entries 3 and 7) show no reaction, indicating that there is no background S_NAr reactivity. Entries 2, 6, and 10 represent optimized conditions that were used for scale-up reactions. Although the results of entry 1 appear promising only low yields of product B could be isolated.

Isolation and Characterization of Negishi Products from Scheme 2.4

4-Benzothiophen-2-yl-2-chloropyridine (34b). Product **34b** was prepared according to the general procedure using **3b** (8.4 mg, 0.012 mmol, 3 mol %), benzothiophenylzinc chloride (**A53**, 2.35 mL of a 0.170 ± 0.001 *M* solution in THF, 0.40 mmol, 0.80 equiv), and **1** (54.0 µL, 0.50 mmol, 1.00 equiv). The reaction was stirred at 60 ºC for 0.75 h. Purification was performed by reversed phase flash column chromatography with a 12 g C18 silica column, using an initial automated program comprising a flow rate of 12 mL/min of water:acetonitrile (98:2 to 5:95) over 35 column volumes. When the product began eluting, the program was paused and reset to elute the analyte at 61-70% MeCN in water. After the elution, the initial program was resumed. The C4-monoarylated product **34b** coeluted with the diarylated product at 65-67% MeCN in water. Fractions containing **34b** were partitioned between ethyl acetate and saturated brine. The organic layers were combined and dried over magnesium sulfate and concentrated under reduced pressure. Compound **34b** was further purified by normal phase flash column chromatography (R_f= 0.36 in 80:20 Hex:EtOAc), affording **34b** as an off-white colored solid (68.9 mg, 70% yield). Spectral data are consistent with those previously reported.[20]

2-Chloro-4-methylquinoline (35b). Compound (**35b**) was prepared according to the general procedure using **3b** (8.4 mg, 0.012 mmol, 3 mol %), methylzinc chloride (1.00 mL of 0.67 ± 0.02 *M* solution in THF, 0.40 mmol, 0.77 equiv), and 2,4-dichloroquinoline (103.0 mg, 0.52 mmol, 1.00 equiv). The reaction was stirred at 60 ºC for 4 h. Purification was performed by reversed phase flash column chromatography with a 12 g C18 silica column, using an initial automated program comprising a flow rate of 30 mL/min of water:acetonitrile (98:2 to 6:94) over 35 column volumes. When the product began eluting, the program was paused and reset to elute the analyte

at 56% MeCN in water. After the elution, the initial program was resumed. The C4 monoarylated product eluted at 56% MeCN. Fractions containing **35b** were partitioned between dichloromethane and saturated brine. The organic layers were combined and dried over magnesium sulfate and solvent was removed under reduced pressure affording **35b** as a white solid (50.5 mg, 71% yield). Spectral data are consistent with those previously reported.[21]

4-Benzyl-2-chloropyridine (36b). Compound (**36b**) was prepared according to the general procedure using **3b** (8.4 mg, 0.012 mmol, 3 mol %), benzylzinc chloride (**A54**, 4.82 mL of a 0.083 *M* solution in THF, 0.40 mmol, 1.00 equiv), and 2,4-dichloropyridine (43.2 µL, 0.40 mmol, 1.00 equiv). The reaction was stirred at 0 ºC for 3 h. Purification was performed by reversed phase flash column chromatography with a 12 g C18 silica column, using an initial automated program comprising a flow rate of 35 mL/min of water:acetonitrile (98:2 to 5:95) over 35 column volumes. When the product began eluting, the program was paused and reset to elute the analyte at 70-73% MeCN in water. After the elution, the initial program was resumed. The C4 monoarylated product **36b** eluted at 72-73% MeCN. Fractions containing **36b** were partitioned between dichloromethane and saturated brine. The organic layers were combined and dried over magnesium sulfate and solvent was removed under reduced pressure affording **36b** as a light brown oil (52.3 mg, 64% yield). ^{1}H NMR (500 MHz, C_6D_6, δ): 7.95 (d, J = 5.0 Hz, 1H), 7.00-7.10 (multiple peaks, 3H), 6.75-6.80 (multiple peaks, 3H), 6.33 (dd, J = 5.0, 0.7 Hz, 1H), 3.27 (s, 2H) ppm. ^{13}C{^{1}H} NMR (126 MHz, C_6D_6, δ): 153.4, 152.7, 150.2, 138.8, 129.5, 129.3, 127.3, 124.9, 123.2, 41.0 ppm. HRMS (ESI+) m/z: [M]+: Calcd for $C_{12}H_{11}ClN$ 203.0502; Found 203.0519.

A6. Multistep Syntheses using C4-Selective Cross-Coupling with Pd/IPr (Scheme 2.5)

4-(4-Methoxyphenyl)-2-(phenylthio)-3-pyridinecarbonitrile (37). Thiophenol (40.8 μL, 0.4 mmol, 1.0 equiv) was added dropwise to a stirring solution of 2-chloro-4-(4-methoxyphenyl)-3pyridinecarbonitrile (**12b**, 97.9 mg, 0.4 mmol, 1.0 equiv), triethylamine (111.5 μL, 0.8 mmol, 2.0 equiv), and DMF (0.4 mL) in a 1-dram reaction vial. The vial was sparged with N_2 gas using the technique described in the "general procedure" on page 117, sealed with a PTFE-lined cap, and heated to 60 °C for 18.3 h. After cooling, a crystalline precipitate formed. The mixture was poured into a 125 mL Erlenmeyer flask and diluted with 30 mL of deionized water, inducing precipitation of the desired product and solubilizing byproducts. The precipitate was filtered and saved, and the liquid filtrate was extracted with ethyl acetate. The organic phase was concentrated, affording mixed white and orange solids. The solids were washed with diethyl ether over a fritted funnel until all orange discoloration had passed into the filtrate. The combined organic solids were dried under vacuum furnishing **37** as a colorless crystalline solid with slight yellow discoloration (92.2 mg, 72% yield); mp 156–158 °C [uncorrected, measured against benzoic acid (113-117 °C)]. ^{1}H NMR (500 MHz, C_6D_6, δ): 7.84 (d, J = 5.2 Hz, 1H), 7.59-7.57 (m, 2H), 7.24-7.22 (m, 2H), 7.12-7.04 (multiple peaks, 3H), 7.00-6.67 (m, 2H), 6.29 (d, J = 5.2 Hz, 1H), 3.23 (s, 3H). ^{13}C{^{1}H} NMR (126 MHz, C_6D_6, δ): 164.9, 161.6, 153.4, 151.3, 136.4, 130.3, 129.5, 129.4, 129.3, 119.7, 115.8, 114.6, 105.5, 54.9 (two signals are coincidentally overlapping). ^{13}C{^{1}H} NMR (126 MHz, $CDCl_3$, δ): 164.5, 161.4, 153.7, 151.8, 135.6, 130.1, 129.6, 129.4, 128.8, 127.9, 120.0, 115.9, 114.6, 105.1, 55.6. HRMS (ESI Q-TOF) m/z: [M]+ Calcd for $C_{19}H_{14}N_2OS$ 318.0827; Found 318.0812.

2-Iodo-4-(4-methoxyphenyl)-quinoline (38). Reaction conditions were adapted from a literature procedure describing the di-iodination of 2,4-dichloropyridine.[22] 2-Chloro-4-(4-methoxyphenyl)quinoline (**19b**, 107.9 mg, 0.4 mmol, 1.0 equiv), NaI (179.9 mg, 1.2 mmol, 3.0 equiv), and acetonitrile (0.45 mL) were combined in a 1-dram vial with stir bar. Acetyl chloride (2.1 equiv 0.84 mmol, 59.9 μL) was added dropwise to the stirring mixture. The vial was sparged with N_2 gas using the technique described under "general procedure" on page 117, sealed with a PTFE cap, and heated to reflux for 67 h. TLC analysis indicated complete consumption of quinoline starting material **19b**. The product mixture was quenched by dropwise addition of deionized water (8.5 mL) while stirring. An aqueous solution of 10% K_2CO_3/5% $NaHSO_3$ was added to the mixture, and the mixture was shaken and extracted with $CHCl_3$ (3x). The organic fractions were combined, dried over Mg_2SO_4, filtered, concentrated, and purified by column chromatography on silica (R_f = 0.46 in 10% ethyl acetate in hexanes) to separate product **38** from polar impurities detected by TLC. Product fractions were concentrated and dried affording **38** as a white crystalline solid (119 mg, 82% yield); mp 114-117 °C [uncorrected, measured against benzoic acid (112-114 °C)]. ^{1}H NMR (500 MHz, $CDCl_3$, δ): 8.06 (d, *J* = 8.4 Hz, 1H), 7.88 (d, *J* = 8.4 Hz, 1H), 7.67 (ddd, *J* = 8.4, 6.9, 1.3 Hz, 1H), 7.64 (s, 1H), 7.47 (ddd, *J* = 8.4, 6.9, 1.3 Hz, 1H), 7.40-7.37 (m, 2H), 7.04-7.01 (m, 2H), 3.87 (s, 3H). ^{13}C{^{1}H} NMR (126 MHz, $CDCl_3$, δ): 160.3, 149.97, 149.50, 131.6, 130.8, 130.1, 129.3, 128.6, 127.1, 126.3, 126.2, 119.2, 114.3, 55.5. HRMS (ESI Q-TOF) m/z: [M]+ Calcd for $C_{16}H_{12}INO$ 360.9964; Found 360.9963.

4-(4-phenoxyphenyl)-1H-Pyrazolo[3,4-b]pyridin-3-amine (40).

2-Chloro-4-(4-phenoxyphenyl)-3-pyridinecarbonitrile (**39b**, 122.7 mg, 0.4 mmol, 1.0 equiv), hydrazine-monohydrate (200.2 mg, 4.0 mmol, 10.0 equiv), and *i*PrOH (6.2 mL) were combined

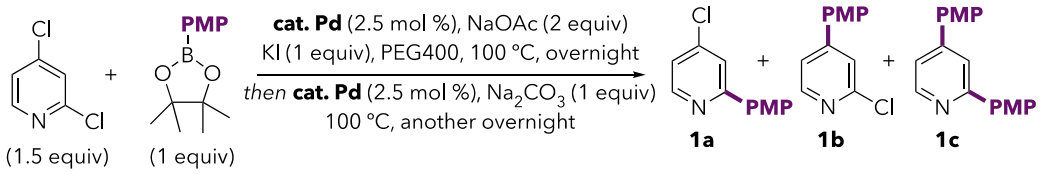
with a stir bar in a 25 mL round-bottom flask equipped with water-cooled jacketed condenser. The condenser was sealed with a rubber septum secured by copper wire, the system was sparged with N_2 gas, and the reaction was heated to 90 °C with stirring for 15 h under an atmosphere of N_2. The mixture was cooled, and trace impurities were detected by TLC. Solvent was removed under reduced pressure, and the solids were columned on silica (R_f = 0.27 in 4.5% methanol in CH_2Cl_2). All rinses and transfers were completed with $CHCl_3$. Solvent was removed under reduced pressure, furnishing a bright yellow solid. Drying under vacuum afforded **40** (119.3 mg, 99% yield). ^{1}H NMR (500 MHz, $CDCl_3$, δ): 10.82 (br s, 1H), 8.50 (d, *J* = 4.8 Hz, 1H), 7.58-7.55 (m, 2H), 7.42-7.39 (m, 2H), 7.20-7.17 (m, 1H), 7.16-7.14 (m, 2H), 7.12-7.10 (m, 2H), 6.95 (d, *J* = 4.8 Hz, 1H), 4.05 (br s, 2H). ^{13}C{^{1}H} NMR (126 MHz, $CDCl_3$, δ): 158.8, 156.3, 153.5, 149.4, 147.5, 145.3, 131.7, 130.4, 130.1, 124.3, 119.8, 118.6, 115.8, 104.1.

A7. Ligand-Free Suzuki Cross-Couplings

Ligand-Free Control Reaction Based on Previously-Reported Conditions (Scheme 2.6b)

Reactions were set up according to the literature procedure[15] (Table A5, entries 1-3) with the indicated modifications (entries 4-12).

Table A5. Analysis of the Role of Ligand in the Previously-Reported Conditions[15] for C4-Selective Suzuki Cross-Coupling.[a]



entry	trial	Pd source	additional ligand (mol %)	**1a** (%)	**1b** (%)	**1c** (%)	**1a** : **1b**
1	1	PEPPSI-IPr	--	<1	80	2	<1 : 80
2	2	PEPPSI-IPr	--	<1	84	2	<1 : 84
3	Average	PEPPSI-IPr	--	<1	82	2	<1 : 82
4	1	**3b**	--	<1	69	1	<1 : 69
5	2	**3b**	--	<1	81	1	<1 : 81
6	Average	**3b**	--	<1	75	1	<1 : 75
7	1	$Pd(OAc)_2$	PPh_3 (5)	28	14	2	1.9 : 1
8	2	$Pd(OAc)_2$	PPh_3 (5)	32	18	2	1.8 : 1
9	Average	$Pd(OAc)_2$	PPh_3 (5)	30	16	2	1.9 : 1
10	1	$PdCl_2$	--	<1	54	1	<1 : 54
11	2	$PdCl_2$	--	<1	66	1	<1 : 66
12	Average	$PdCl_2$	--	<1	60	1	<1 : 60

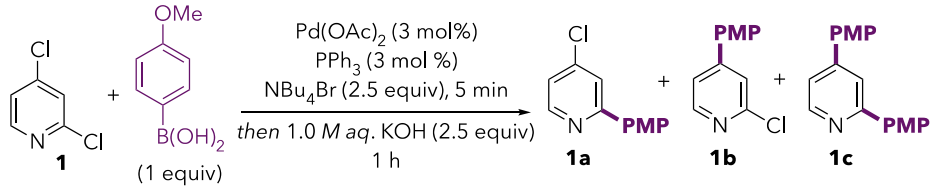
[a]GC yields calibrated against undecane as the internal standard.

Discussion: Selectivity under Yang's high-temperature conditions is significantly better than what is observed under the Pd/IPr-catalyzed room temperature conditions employed in our work. However, ligand-free control reactions using $PdCl_2$ (Table A5, entries 10-12) demonstrate that the same extremely high selectivity is observed in the absence of IPr. The selectivity under the conditions reported in reference 15 is therefore not ligand-controlled. When PPh_3 is used as a ligand in combination with $Pd(OAc)_2$ (entries 7-9, a catalytic system analogous to Fairlamb's work with dibromopyridine),18 the reaction favors C2-arylated product **1a**, but with poor yield. In all other entries, extremely high selectivity for product **1b** is observed.

Coupling of **1** under Fairlamb's Recently Reported Pd/PPh_3 Conditions

The Suzuki coupling in Table A6 was set up according to conditions reported by Fairlamb et al., who observed C4-selective cross-coupling of 2,4-dibromopyridine.[18] Reactions were conducted on a 0.16 mmol reaction scale.

Table A6. Reaction of **1** under Fairlamb's Conditions.



entry	solvent	Temp. (°C)	**1a** (%)	**1b** (%)	**1c** (%)	**1a** : **1b**
1	THF	40	90.6	5.2	4.9	17 : 1
2	dioxane	110	85.4	0.6	12.8	142 : 1

Discussion: Intriguingly, although these conditions promote C4-selective Suzuki coupling of 2,4-di*bromo*pyridine, 2,4-di*chloro*pyridine undergoes preferential C2-coupling.

General Procedures for the Ligand-Free 'Jeffery' Conditions Reported Herein

GC-Scale Reactions. Solids were added to a 1-dram reaction vial in order of increasing mass: palladium catalyst (typically 0.008 mmol, 5 mol %), *p*-methoxyphenylboronic acid (26.7 mg, 0.18 mmol, 1.1 equiv), sodium carbonate (50.9 mg, 0.48 mmol, 3.0 equiv), tetrabutylammonium salt (0-5 equiv), and a stir bar. Inside a nitrogen-atmosphere glovebox, liquid reagents were pre-measured by syringe and added in quick succession: DMF (0.64 mL) via 1-mL syringe, followed by 2,4-dichloropyridine (17.2 µL, 0.16 mmol, 1.0 equiv) via 25-µL syringe. The

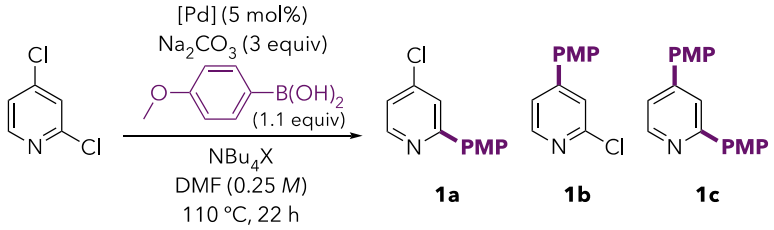
reaction vial was sealed under nitrogen with either a septum screwcap or a solid PTFE-lined screwcap. When indicated, N_2-sparged deionized water was added through the septum cap outside the glovebox via 25- or 50-µL syringe, and the puncture was sealed with electrical tape. The reaction was stirred vigorously at the indicated temperature for 22 h. The reaction vial was opened to air, diluted with ethyl acetate (~ 3 mL), and *n*-undecane (15 µL, 0.44 equiv) was added as an internal standard via 25-µL syringe. An aliquot was filtered through Celite into a separate vial for GC analysis.

Scaled-Up Reactions for Product Isolation. $PdCl_2$ (4.4 mg, 0.025 mmol, 5.0 mol%) was weighed into a 1-dram vial followed by solid substrate if applicable (2,5-dichloropyridine, pyrimidine, or 2,4-dichloroquinoline, 0.5 mmol, 1 equiv), arylboronic acid (0.5 mmol, 1.0 equiv), sodium carbonate (159 mg, 1.5 mmol, 3.0 equiv), tetrabutylammonium bromide (806 mg, 2.5 mmol, 5.0 equiv) and a stir bar. DMF (2 mL) was added inside a nitrogen-atmosphere glovebox and sealed with either a septum screwcap or a solid PTFE-lined screwcap. Unless otherwise indicated, N_2-sparged deionized water (45 µL, 2.5 mmol, 5.0 equiv) was added through the septum cap outside the glovebox via 50-µL syringe (*note: conversion in 0.5 mmol scale reactions was more adversely affected by dry conditions compared to 0.16 mmol scale reactions*), followed by 2,4-dichloropyridine substrate (if liquid), and the puncture was sealed with electrical tape. The reaction was stirred vigorously at 110 °C for the indicated time. After cooling to ambient temperature, the cap was removed, the reaction mixture was diluted with ethyl acetate and, in cases where calibrated GC yields are reported, *n*-undecane (46.9 µL, 0.44 equiv) was added as an internal standard via 50-µL syringe. The reaction mixture was then filtered through a plug of Celite. The reaction outcome was assessed by GC and TLC (isomeric ratios were determined by GC). The

mixture was purified by flash column chromatography and/or reversed phase chromatography as indicated, and the product was dried under vacuum.

Optimization of the Ligand-Free Conditions (Table 2.2)

Table A7. Optimization of Ligand-Free Suzuki Coupling



entry	trial	Pd source	NBu_4X (equiv)	**1a** (%)	**1b** (%)	**1c** (%)	**1a** : **1b**
1	1	$PdCl_2$	Br (3)	0.3	82	0.4	1 : >99
2	2	$PdCl_2$	Br (3)	0.6	80	0.4	1 : >99
3	Average	$PdCl_2$	Br (3)	0.5	81	0.4	1 : >99
4	1	$PdCl_2$	Br (5)	0.4	87	0.4	1 : >99
5	2	$PdCl_2$	Br (5)	0.5	80	0.4	1 : >99
6	Average	$PdCl_2$	Br (5)	0.5	84	0.4	1 : >99
7	1	$Pd(OAc)_2$	Br (3)	0.7	75	0.4	1 : >99
8	2	$Pd(OAc)_2$	Br (3)	0.6	71	0.3	1 : >99
9	Average	$Pd(OAc)_2$	Br (3)	0.7	73	0.4	1 : >99
10	1	Pd_2dba_3	Br (3)	0.4	61	0.2	1 : >99
11	2	Pd_2dba_3	Br (3)	0.5	52	0.2	1 : >99
12	Average	Pd_2dba_3	Br (3)	0.5	57	0.2	1 : >99
13	1	$PdCl_2$	Cl (3)	0.8	72	0.4	1 : 90
14	2	$PdCl_2$	Cl (3)	1.3	72	0.6	1 : 55
15	Average	$PdCl_2$	Cl (3)	1.1	72	0.5	1 : 65
16	1	$PdCl_2$	Br (1)	1.2	67	0.8	1 : 56
17	2	$PdCl_2$	Br (1)	1.2	71	0.6	1 : 59
18	Average	$PdCl_2$	Br (1)	1.2	69	0.7	1 : 58
19	1	$PdCl_2$	PF_6 (3)	2.6	44	2.4	1 : 17
20	2	$PdCl_2$	PF_6 (3)	3.4	52	3.8	1 : 15
21	Average	$PdCl_2$	PF_6 (3)	3.0	48	3.1	1 : 16
22[b]	1	$PdCl_2$	---				
23[b]	2	$PdCl_2$	---				
24[b]	Average	$PdCl_2$	---				
25	1	$PdCl_2$	---	3.3	55	3.0	1 : 17
26	2	$PdCl_2$	---	3.7	58	3.2	1 : 16
27	Average	$PdCl_2$	---	3.5	56	3.1	1 : 16
28	1	$PdCl_2$	Br (1)	1.2	67	0.8	1 : 56
29	2	$PdCl_2$	Br (1)	1.2	71	0.6	1 : 59
30	Average	$PdCl_2$	Br (1)	1.2	69	0.7	1 : 58
31[c]	1	$PdCl_2$	Br (3)	1	80	0.6	1 : 80
32[c]	2	$PdCl_2$	Br (3)	0.8	78	0.5	1 : 98
33[c]	Average	$PdCl_2$	Br (3)	0.9	79	0.6	1 : 88
34[d]	1	$PdCl_2$	Br (3)	1.1	82	0.6	1 : 75
35[d]	2	$PdCl_2$	Br (3)	1.0	84	0.8	1 : 84

Table A7 Continued

36[d]	Average	$PdCl_2$	Br (3)	1.1	83	0.7	1 : 75
37[e]	1	$PdCl_2$	Br (3)	0.8	40	0.5	1 : 50
38[e]	2	$PdCl_2$	Br (3)	0.8	49	0.4	1 : 61
39[e]	Average	$PdCl_2$	Br (3)	0.8	45	0.5	1 : 56
40[f]	1	$PdCl_2$	Br (3)	0.3	8	0.4	1 : 27
41[f]	2	$PdCl_2$	Br (3)	0.3	10	0.5	1 : 33
42[f]	Average	$PdCl_2$	Br (3)	0.3	9	0.5	1 : 29
43[c]	1	$PdCl_2$	Br (5)	0.8	85	0.4	1 : >99
44[c]	2	$PdCl_2$	Br (5)	0.7	84	0.6	1 : >99
45[c]	Average	$PdCl_2$	Br (5)	0.8	85	0.5	1 : >99

[a]Reactions were conducted according to the General Procedure on page 161 for GC-scale reactions. GC yields calibrated against undecane as an internal standard. Calculated yield values were rounded to the nearest integer. [b]With KBr (3 equiv). [c]With H_2O (5 equiv). [d]With H_2O (10 equiv). [e]With 1 mol% $PdCl_2$. [f]Reaction run at 25 °C.

Isolation and Characterization of Cross-Coupled Products
(Scheme 2.7)

2-Chloro-4-(4-methoxyphenyl)pyridine (1b). Compound **1b** was prepared according to the general procedure under ligand-free conditions using 2,4-dichloropyridine (54 µL, 0.5 mmol, 1.0 equiv) and *p*-methoxyphenylboronic acid (83.6 mg, 0.55 mmol, 1.1 equiv) with stirring for 30 h. Purification by flash column chromatography on silica gel in 6-20% ethyl acetate/hexanes (R_f = 0.42 in 15% ethyl acetate in hexanes) provided **1b** as a white solid (82.1 mg, 75% yield). Spectral data are consistent with previously reported data and literature.[12]

Larger-Scale Preparation of 1b: Compound **1b** was prepared according to the general procedure under ligand-free conditions using 2,4-dichloropyridine (270 µL, 2.5 mmol, 1.0 equiv) and *p*-methoxyphenylboronic acid (417.9 mg, 2.75 mmol, 1.1 equiv) with stirring for 40 h. Purification by flash column chromatography on silica gel in 6-20% ethyl acetate/hexanes (R_f = 0.42 in 15% ethyl acetate in hexanes) provided **1b** as a white solid (347 mg, 63% yield). Spectral data are consistent with previously reported data and literature.[12]

4-(1,3-benzodioxol-5-yl)-2-chloro-pyridine (41b). Compound **41b** was prepared according to the general procedure under ligand-free conditions using 2,4-dichloropyridine (54 μL, 0.5 mmol, 1.0 equiv) and 3,4-(methylenedioxy)-benzeneboronic acid (91.3 mg, 0.55 mmol, 1.1 equiv) with stirring for 34 h. Purification by flash column chromatography on silica gel in 2-21% ethyl acetate/hexanes (R_f = 0.35 in 15% ethyl acetate in hexanes) provided **41b** as a white solid (75 mg, 64% yield). ^{1}H NMR (500 MHz, $CDCl_3$, δ): 8.36 (d, J = 5.2 Hz, 1H), 7.44 (d, J = 1.6 Hz, 1H), 7.32 (dd, J = 5.2, 1.7 Hz, 1H), 7.11 (dd, J = 8.1, 1.6 Hz, 1H), 7.06 (d, J = 1.7 Hz, 1H), 6.90 (d, J = 8.1 Hz, 1H), 6.03 (s, 2H). ^{13}C{^{1}H} NMR (126 MHz, $CDCl_3$, δ): 152.3, 151.2, 150.1, 149.2, 148.7, 131.0, 121.7, 121.4, 120.2, 109.1, 107.3, 101.8. HRMS (ESI Q-TOF) m/z: [M]+ Calcd for $C_{12}H_8ClNO_2$ 233.0244; Found 233.0245.

2-Chloro-4-[4-(trifluoromethyl)phenyl]-pyridine (42b). Compound **42b** was prepared according to the general procedure under ligand-free conditions using 2,4-dichloropyridine (54 μL, 0.5 mmol, 1.0 equiv) and *p*-(trifluoromethyl)phenylboronic acid (104.5 mg, 0.55 mmol, 1.1 equiv) with stirring for 23 h. Purification by flash column chromatography on silica gel using a linear gradient of 1-28% ethyl acetate/hexanes over 9 column volumes (R_f = 0.40 in 15% ethyl acetate in hexanes) provided **42b** as a white solid (79.1 mg, 62% yield). ^{1}H NMR (500 MHz, $CDCl_3$, δ): 8.46 (d, J = 5.2 Hz, 1H), 7.76 (d, J = 8.4, 2H), 7.72 (d, J = 8.4 Hz, 2H), 7.55 (d, J = 1.3 Hz, 1H), 7.43 (dd, J = 5.2, 1.3 Hz, 1H). Spectral data are consistent with literature.[23]

2-Chloro-4-(3-quinolinyl)-quinoline (43b). Compound **43b** was prepared according to the general procedure under ligand-free conditions using 2,4-dichloroquinoline (99 mg, 0.5 mmol, 1.0 equiv) and 3-quinolineboronic acid (95.1 mg, 0.55 mmol, 1.1 equiv) with stirring for 27.5 h. Purification by flash column chromatography on silica gel in 20% ethyl acetate/hexanes (R_f = 0.33

in 20% ethyl acetate in hexanes) provided **43b** as a tan solid (94.1 mg, 65% yield). ^{1}H NMR (500 MHz, $CDCl_3$, δ): 9.05 (d, *J* = 1.9 Hz, 1 H), 8.32 (d, *J* = 1.4 Hz, 1 H), 8.24 (d, *J* = 8.5 Hz, 1H), 8.14 (d, *J* = 8.5 Hz, 1H) 7.94 (d, *J* = 8.1 Hz, 1H), 7.83-7.87 (multiple peaks, 3H), 7.68 (dd, *J* = 15.2, 7.4 Hz, 1H), 7.56 (dd, *J* = 15.2, 7.4 Hz, 1H), 7.47 (s, 1H). $^{13}C\{^{1}H\}$ NMR (126 MHz, $CDCl_3$, δ): 150.5, 150.4, 148.6, 148.22, 148.15, 136.7, 131.0, 130.8, 130.0, 129.7, 129.5, 128.3, 127.8, 127.7, 127.6, 125.7, 125.5, 122.9. HRMS (ESI Q-TOF) m/z: [M]+ Calcd for $C_{18}H_{11}ClN_2$ 290.0611; Found 290.0615.

2-Chloro-6-methyl-4-(1-methyl-1H-indol-5-yl)-pyridine (44b). Compound **44b** was prepared according to the general procedure under ligand-free conditions using 2,4-dichloro-6-methylpyridine (81 mg, 0.5 mmol, 1.0 equiv) and 1-methyl-5-indolyl-boronic acid (96.2 mg, 0.55 mmol, 1.1 equiv) with stirring for 30 h. Purification by flash column chromatography on silica gel in 5-20% ethyl acetate/hexanes (*Rf* = 0.45 in 20% ethyl acetate in hexanes) provided **44b** as a white solid (62.2 mg, 49% yield). ^{1}H NMR (500 MHz, $CDCl_3$, δ): 7.88 (m, 1.6 Hz, 1H), 7.45 (dd, *J* = 8.6, 1.6 Hz, 1H), 7.41 (d, *J* = 0.8 Hz, 1H), 7.38 (d, *J* = 8.6 Hz, 1H), 7.33 (d, *J* = 0.8 Hz, 1H), 7.11 (d, *J* = 3.1 Hz, 1H), 6.56 (dd, *J* = 3.1, 0.7 Hz, 1H), 3.81 (s, 3H), 2.58 (s, 3H). $^{13}C\{^{1}H\}$ NMR (126 MHz, $CDCl_3$, δ): 159.3, 153.2, 151.1, 137.4, 130.3, 129.1, 128.4, 120.7, 120.1, 119.9, 119.0, 110.0, 101.9, 33.1, 24.4. HRMS (ESI Q-TOF) m/z: [M]+ Calcd for $C_{15}H_{13}ClN_2$ 256.0767; Found 256.0772.

2-Chloro-5-(4-methoxyphenyl)-pyridine (29b). Compound **29b** was prepared according to the general procedure under ligand-free conditions, with the modification that no water was added. The reaction vial was charged with 2,5-dichloropyridine (74 mg, 0.5 mmol, 1.0 equiv) and *p*-methoxyphenylboronic acid (83.6 mg, 0.55 mmol, 1.1 equiv) and stirred for 30 h. Purification by

flash column chromatography on silica gel in 1-36% ethyl acetate/hexanes (R_f = 0.41 in 15% ethyl acetate in Cl hexanes) resulted in coelution of **29b** and the diarylated product (the estimated crude yield of diarylated product is ~1% based on GC analysis). Further purification was performed using reversed phase flash column chromatography with a 30 g C18 silica column, using an initial automated program comprising a flow rate of 35 mL/min of water:acetonitrile (98:2 to 1:99) over 20 column volumes. When the product began eluting, the program was paused and reset to elute the analyte at 98% MeCN in water. Fractions containing **29b** were partitioned between ethyl acetate and saturated brine. The organic layers were combined and dried over magnesium sulfate and dried *in vacuo* providing **29b** as a white solid (22.4 mg, 20% yield). ^{1}H NMR (500 MHz, $CDCl_3$, δ): 8.57 (dd, J = 2.6, 0.6 Hz, 1H), 7.79 (dd, J = 8.3, 2.6 Hz, 1H), 7.46- 7.51 (m, 2H), 7.36 (dd, J = 8.3, 0.6 Hz, 1H), 6.98-7.03 (m, 2H), 3.86 (s, 3H). The product of C2-arylation was also isolated (4.5 mg, 4%). Spectral data for both monoarylated products are consistent with the literature.[11] Side products resulting from diarylation and homocoupling of **29** (m/z = 224) were each detected by GCMS. These side products, as well as remaining starting material, appears to account for most of the remaining mass balance.

2-Chloro-5-(4-methoxyphenyl)-pyrimidine (30b). Compound **30b** was prepared according to the general procedure under ligand-free conditions with the modification that no water was added. The reaction vial was charged with 2,5-dichloropyrimidine (74.5 mg, 0.5 mmol, 1.0 equiv) and *p*-methoxyphenylboronic acid (83.6 mg, 0.55 mmol, 1.1 equiv) and stirred for 30 h. Purification by flash column chromatography on silica gel in 1-45% ethyl acetate/hexanes (R_f = 0.31 in 15% ethyl acetate in hexanes) resulted in coelution of the C5 isomer and a bipyrimidine side product. Fractions containing product **30b** were combined and solvent was removed under reduced

pressure. Further purification was performed using reversed phase flash column chromatography with a 30 g C18 silica column, using an initial automated program comprising a flow rate of 35 mL/min of water:acetonitrile (98:2 to 1:99) over 20 column volumes. When the product began eluting, the program was paused and reset to elute the analyte at 50-55% MeCN in water. Fractions containing **30b** were partitioned between ethyl acetate and saturated brine. The organic layers were combined and dried over magnesium sulfate and dried *in vacuo* providing **30b** as a white solid (18.5 mg, 17% yield). ^{1}H NMR (500 MHz, $CDCl_3$, δ): 8.78 (s, 2H), 7.46-7.53 (m, 2H), 7.00-7.08 (m, 2H), 3.87 (s, 3H). Spectral data are consistent with the literature.24 The crude reaction mixture was analyzed by GCMS; in addition to remaining starting material, a small amount of C2-arylated product, and trace diarylated product, several small peaks corresponding to unidentified side products were observed.

A8. References

1. Melvin, P. R.; Nova, A.; Balcells, D.; Dai, W.; Hazari, N.; Hruszkewycz, D. P.; Shah, H. P.; Tudge, M. T. *ACS Catal.* **2015**, *5*, 3680−3688.

2. Jiang, X.; Hu, F. *Synlett.* **2018**, *29*, 1207-1210.

3. Baranov, A. B.; Tsypin, V. G.; Malin, A. S.; Laskin, B. M. *Russ. J. Appl. Chem.* **2004**, *77*, 1997-2000.

4. Krasovskiy, A.; Knochel, P. *Synthesis* **2006**, 5, 0890-0891.

5. Tran, T.-A.; Shin, Y.-J.; Kramer, B.; Choi, J.; Zou, N.; Vallar, P.; Martens, P.; Boatman, P. D.; Adams, J. W.; Ramirez, J.; Shi, Y.; Morgan, M.; Unett, D. J.; Chang, S.; Shu, H.-H.; Tung, S.-F.; Semple, G. *Bioorg. Med. Chem. Lett.* **2015,** *25*, 1030–1035.

6. Habash, M.; Taha, M. O. *Bioorg. Med. Chem.* **2011**, *19*, 4746–4771.

7. Yahyazadeh, A.; Yousefi, H. *Spectrochim. Acta A Mol. Biomol. Spectrosc.* **2014**, 1*17*, 696–701.

8. Rossiter, S.; Péron J. M.; Whitfield P. J.; Jones, K.; *Bioorganic Med. Chem Lett.* **2005**, 15, 4806-4808.

9. Su, Z.; Yeagley, A. A.; Su, R.; Peng, L.; Melander, C. *ChemMedChem*. **2012**, 7, 2030-2039.

10. Dai, X.; Chen, Y.; Garrell, S.; Liu, H.; Zhang, L.-K.; Palani, A.; Hughes, G.; Nargund, R. *J. Org. Chem.* **2013**, *78*, 7758– 7763.

11. Reeves, E. K.; Humke, J. N.; Neufeldt, S. R. *J. Org. Chem.* **2019**, *84*, 11799–11812.

12. Thapa, S.; Gurung, S. K.; Dickie, D. A.; Giri, R.; *Angew. Chem. Int. Ed*. **2014**, *53*, 11620−11624.

13. Sicre, C.; Alonso-Gómez, J. L.; Cid, M. M. *Tetrahedron* **2006**, *62*, 11063-11072.

14. Crouse, G. D.; Sparks, T. C.; McLead, C. L.; Demeter, D. A.; Bryan, K.; Brown, A. V.; Dent III W. H.; Cudworth, D. P.; Nugent, J. S.; Hunter R.; Samaritoni, J. G. Pesticidal Compositions. U.S. Patent US 2009/0209476 A1, August 20, **2009**.

15. Yang, M.; Chen, J.; He, C.; Hu, X.; Ding, Y.; Kuang, Y.; Liu, J. Huang, Q. *J. Org. Chem.* **2020**, *85*, 6498–6508.

16. Minxing, X.; Feng, T.; Wei, H.; Jun, W.; Han, S.; Zhaoyu, L.; Chongxing, Tu.; Xinge, Z. Pyrimidinamine and pyridinamine Hedgehog signal conduction inhibitors. International Patent CN103864770 (A), June 18, **2014**. (paragraph 1443).

17. Duan, Jingwu; Jian, Bing; Lu, Zhonghui. Azaindoles as BTK Kinase Modulators and Use Thereof. International Patent WO 2011/019780 A1, February 17, **2011**. (pages 63-64).

18. Scott, N. W. J.; Ford, M. J.; Jeddi, N.; Eyles, A.; Simon, L.; Whitwood, A. C.; Tanner, T.; Willans, C. E.; Fairlamb, I. J. S. *J. Am. Chem. Soc.* **2021**, *143*, 9682-9693.

19. Louërat, F.; Gros, P.C. *Tetrahedron* **2010,** *51*, 3558-3560.

20. Baloch, M.; Roy, D.; Bensaid, S.; Guerchais, V.; Doucet, H. *Eur. J of Inorg. Chem.* **2012**, *28*, 4454-4462.

21. Levy, J. N.; Alegre-Requena, J. V.; Liu, R.; Paton, R. S.; McNally, A. *J. Am. Chem. Soc.* **2020**, *142*, 11295-11305.

22. Corcoran, R. C.; Bang, S. H. *Tetrahedron Lett.* **1990**, *31*, 6757-6758.

23. Gurung, S. K.; Thapa, S.; Vangala, A. S.; Giri, R. *Org. Lett.* **2013**, *15*, 20, 5378-5381.

24. Mosquera, Á.; Riveiros, R.; Sestelo, J. P.; Sarandeses, L. A. *Org. Lett.* **2008** *10*, 17, 3745-3748.

APPENDIX B

SUPPORTING INFORMATION

for

CHAPTER THREE

B1. General Materials and Methods

NMR spectra were recorded at 298 K on a Bruker DRX 500 MHz (500.233 MHz for ^{1}H, 125.795 MHz for ^{13}C, 470.639 MHz for ^{19}F) or a Bruker Ascend 400 MHz (400.130 MHz for ^{1}H NMR, 100.613 for ^{13}C). ^{1}H and ^{13}C NMR chemical shifts are reported in parts per million (ppm) relative to TMS, with the residual solvent peak used as an internal reference [^{1}H NMR: $CHCl_3$ (7.26 ppm), C_6D_5H (7.16 ppm); ^{13}C NMR: $CDCl_3$ (77.16 ppm), ^{13}C NMR: C_6D_6 (128.06 ppm)]. Multiplicities are reported as follows: singlet (s), doublet (d), doublet of doublets (dd), and multiplet (m). GC data were collected using a Shimadzu GC-2010 Plus with a flame ionization detector equipped with a SHRxi-5ms capillary column (15 m x 0.25 mm ID x 0.25 μm df). GCMS data were collected with a Shimadzu GC-2030 paired with a Shimadzu GCMS-QP2020 NX and equipped with a SH-Rxi-5ms capillary column (30 m x 0.25 mm ID x 0.25 μm df). LC-MS analyses were performed on either an Agilent 6538 Q-TOF MS or a Bruker micro-TOF MS, both coupled to an Agilent 1290 Infinity UHPLC system. A 50 mm long Eclipse Plus C18 column (Agilent Technologies, Santa Barbara, CA; i.d. 2.1 mm, 1.8 μm particle size) was used for separation. A 6-minute gradient was used at a flow rate of 0.6 mL/min: 0-1 min 95% buffer A (100% H_2O with 0.1% formic acid), followed by a gradient from 1-4 minutes of 5-95% buffer B (100% acetonitrile with 0.1% formic acid), 1 minute 95% buffer B, and returning to 95% buffer A for 1 minute. The mass spectrometers were operated in positive-ion mode with electrospray ionization.

Unless otherwise noted below, all commercially-obtained chemicals were used as received. (η^3-1-^{t}Buindenyl)Pd(IPr)(Cl) was obtained from Umicore. *N*-heterocyclic carbene ligands IMes, SIMes, IPr, or SIPr were each obtained from Strem Chemicals or Sigma Aldrich. Unless otherwise

noted, dichloro-heteroarenes and arylboronic acid starting materials were obtained from Oakwood Chemical. Arylated pyridines **2a**, **2b**, **B2c**, **B4b**, and **B5b** were prepared as previously reported.[1] 1,4-Dioxane, potassium *tert*-butoxide, and palladium (II) chloride were obtained from Acros Organics. Potassium carbonate, triphenylphosphine, and tri-*tert*-butylphosphine, were obtained from Alfa Aesar. THF, toluene, and methanol were obtained from Fisher Scientific. *tert*-butyl bromide, diphenylphosphinoferrocene, tri-*o*-tolylphosphine, and tricyclohexylphosphine were obtained from Oakwood chemical. Tri-*n*-butylphosphine was obtained from Sigma-Aldrich. Palladium (II) acetate, trimethyl phosphine, QPhos, CyJohnPhos, and CataCXium A were obtained from Strem Chemical. Benzene was obtained from Beantown Chemical. For the purpose of Suzuki-Miyaura cross-couplings, THF was used as received from Fisher Scientific. 1,4-Dioxane required for Pd/dppf-mediated Suzuki-Miyaura cross-couplings was used as received from Acros Organics but kept under N_2 prior to and during use.

Deuterated solvents ($CDCl_3$, C_6D_6) were obtained from Cambridge Isotopes and stored over molecular sieves. Manual flash column chromatography was performed on SiliCycle silica gel 60 (40-63 μm particle size) and thin layer chromatography was performed on SiliCycle TLC plates pre-coated with extra hard silica gel 60 F_{254}. Automated flash column chromatography was performed with a Biotage Selekt equipped with Biotage Sfär silica flash cartridges (20 μm particle size; 50 Å pore width) for normal phase separations, or Silica C18 cartridges (30 μm particle size; 100 Å pore width) for reversed phase separations.

B2. General Procedure for Suzuki Cross-Couplings

The specified solids required in the Suzuki-Miyaura reactions were added to a 1-dram reaction vial in order of increasing mass: palladium catalyst (palladium source and free ligand) or precatalyst, the specified dihalopyridine substrate if solid (0.08 mmol, 1 equiv), arylboronic acid (0.08 mmol, 1.0 equiv), potassium carbonate or cesium carbonate, and then a stir bar. Liquid reagents were pre-measured by syringe and added in quick succession: benzene, THF, or 1,4-dioxane (0.32 mL, 0.25 *M*) via 1-mL syringe, followed by N_2-sparged deionized water via 50-µL syringe. Note: dihalopyridine substrates were added last if liquid, via microliter syringe. A septum cap equipped with an N_2-ingas and outgassing needle was fastened to the 1-dram reaction vial and the headspace was sparged for 30-45 seconds. With continuous sparging, the vial was unscrewed from the septum cap and lowered while the cap was replaced with a PTFE-lined cap. The reaction was stirred vigorously at the specified temperature for the specified duration.

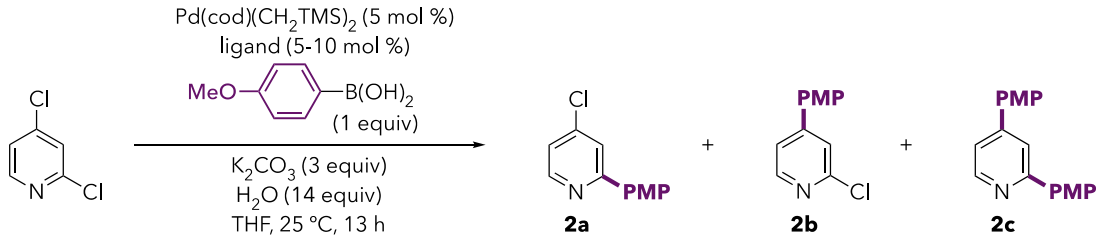
B3. Ligand Screen with (cod)Pd(CH2SiMe3)2 (Table 1), [(η3-1-tBu-indenyl)Pd(Cl)]2, and Pd(OAc)2)

Overview and Discussion

The effect of phosphine sterics was evaluated in reactions in which free phosphine was combined with (cod)Pd(CH_2SiMe_3)$_2$ (as shown in Chapter 3, Table 3.1), [(η^3-1-^{t}Bu-indenyl)Pd(Cl)]$_2$, or Pd(OAc)$_2$. In addition, NHC ligands were evaluated in combination with (cod)Pd(CH_2SiMe_3)$_2$ or Pd(OAc)$_2$, or as part of a pre-formed complex with structure (η^3-1-^{t}Bu-indenyl)Pd(NHC)(Cl). Overall, the steric trends were comparable for all Pd sources. However, in the conditions with Pd(OAc)$_2$, a dependence of selectivity and yield on L:Pd ratio was seen for some ligands that was not seen when using (cod)Pd(CH_2SiMe_3)$_2$. This may reflect the ability of

$Pd(OAc)_2$ to oxidize phosphines,[2] thereby leading to a much lower effective L:Pd ratio and a change in the nature of the active catalyst. Notably, when using PCy_3 in combination with both $Pd(OAc)_2$ and $[(\eta^3\text{-}1\text{-}^t\text{Bu-indenyl})Pd(Cl)]_2$, selectivity switches for L:Pd = 1:1 compared to 2:1. This observation is consistent with prior evidence that PCy_3 can support both mono- and bisligated palladium[3] which are expected to give different selectivities. However, this effect is not seen when using $(cod)Pd(CH_2SiMe_3)_2$, and instead a slight preference for reaction at C4 is observed with both 5 and 10 mol % PCy_3. This observation seems to suggest a higher concentration of monoligated $Pd(PCy_3)$ when using $(cod)Pd(CH_2SiMe_3)_2$ as the palladium source.

Table B1. Ligand Screen with $(cod)Pd(CH_2SiMe_3)_2$ (Table 1).[a]



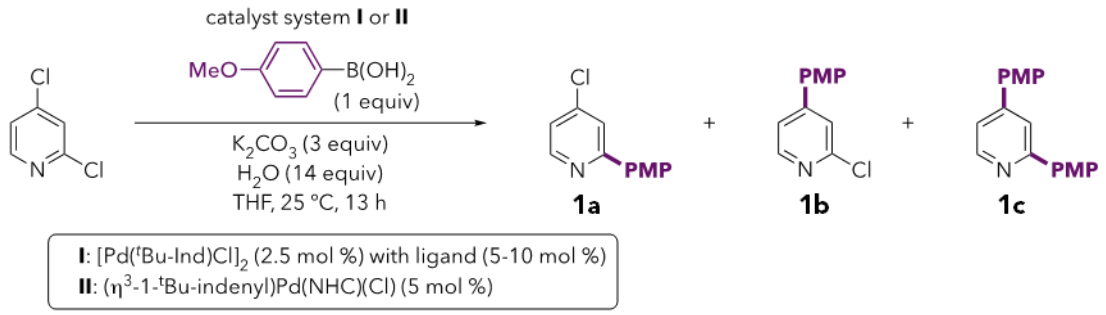
entry	trial	ligand (mol %)	%V_{bur} (min)[b]	**2a** (%)	**2b** (%)	**2c** (%)	**2a** : **2b**
1	1	PPh_3 (5)		83.9	0.5	0.1	>99 : 1
2	2	PPh_3 (5)		84.5	0.6	0.2	>99 : 1
3	Average	PPh_3 (5)	(28.2)	84.2	0.6	0.2	>99 : 1
4	1	PPh_3 (10)		82.8	0.3	0.1	>99 : 1
5	2	PPh_3 (10)		80.3	0.4	0.3	>99 : 1
6	Average	PPh_3 (10)	(28.2)	81.6	0.4	0.2	>99 : 1
7	1	P(*o*-tol)$_3$ (5)		39.1	22.0	4.2	1.8 : 1
8	2	P(*o*-tol)$_3$ (5)		44.8	20.9	3.4	2.1 : 1
9	Average	P(*o*-tol)$_3$ (5)	(34.4)	42.0	21.5	3.8	2.0 : 1
10	1	P(*o*-tol)$_3$ (10)		33.7	18.6	2.2	1.7 : 1
11	2	P(*o*-tol)$_3$ (10)		26.9	15.4	1.1	1.8 : 1
12	Average	P(*o*-tol)$_3$ (10)	(34.4)	30.3	17.0	1.7	1.8 : 1
13	1	PMe_3 (5)		18.8	2.2	0.4	8.5 : 1
14	2	PMe_3 (5)		18.3	2.2	0.4	8.3 : 1
15	Average	PMe_3 (5)	(22.1)	18.5	2.2	0.4	8.4 : 1
16	1	PMe_3 (10)		9.2	0.6	0.3	15.4 : 1
17	2	PMe_3 (10)		10.5	1.1	0.3	9.7 : 1
18	Average	PMe_3 (10)	(22.1)	9.9	0.9	0.3	11.0 : 1
19	1	P(*n*-Bu)$_3$ (5)		21.6	7.4	0.7	2.9 : 1

Table B1 Continued

20	2	P(*n*-Bu)$_3$ (5)		18.4	7.8	0.7	2.4 : 1
21	Average	P(*n*-Bu)$_3$ (5)	(24.2)	20.0	7.6	0.7	2.6 : 1
22	1	P(*n*-Bu)$_3$ (10)		0.8	0.3	0.3	3.2 : 1
23	2	P(*n*-Bu)$_3$ (10)		0.7	0.2	0.3	3.2 : 1
24	Average	P(*n*-Bu)$_3$ (10)	(24.2)	0.8	0.3	0.3	3.2 : 1
25	1	PCy$_3$ (5)		26.3	42.0	4.7	1 : 1.6
26	2	PCy$_3$ (5)		29.4	47.7	5.9	1 : 1.6
27	Average	PCy$_3$ (5)	(30.2)	27.9	44.9	5.3	1 : 1.6
28	1	PCy$_3$ (10)		27.2	39.0	2.6	1 : 1.4
29	2	PCy$_3$ (10)		27.2	40.7	3.6	1 : 1.5
30	Average	PCy$_3$ (10)	(30.2)	27.2	39.9	3.1	1 : 1.5
31	1	PAd$_2$(*n*-Bu) (5)		24.4	53.0	6.5	1 : 2.2
32	2	PAd$_2$(*n*-Bu) (5)		23.7	50.7	10.0	1 : 2.1
33	Average	PAd$_2$(*n*-Bu) (5)	(32.8)	24.1	51.8	8.2	1 : 2.2
34	1	PAd$_2$(*n*-Bu) (10)		26.4	48.6	10.2	1 : 1.8
35	1	P^{t}Bu$_3$ (5)		26.8	46.7	9.6	1 : 1.7
36	2	P^{t}Bu$_3$ (5)		27.1	47.8	11.9	1 : 1.8
37	Average	P^{t}Bu$_3$ (5)	(36.3)	27.0	47.3	10.8	1 : 1.8
38	1	P^{t}Bu$_3$ (10)		27.1	47.5	8.9	1 : 1.7
39	1	IMes (5)		33.9	50.8	4.9	1 : 1.5
40	2	IMes (5)		31.0	53.3	8.1	1 : 1.7
41	Average	IMes (5)	36.5	32.5	52.0	6.5	1 : 1.6
42	1	SIMes (5)		27.2	21.3	0.7	1.3 : 1
43	2	SIMes (5)		28.5	22.6	0.8	1.3 : 1
44	Average	SIMes (5)	36.9	27.9	22.0	0.8	1.3 : 1
45	1	IPr (5)		8.8	65.7	13.8	1 : 7.4
46	2	IPr (5)		10.1	67.9	6.7	1 : 6.7
47	Average	IPr (5)	44.5	9.5	66.8	10.3	1 : 7.0
48	1	SIPr (5)		9.3	35.5	3.5	3.8 : 1
49	2	SIPr (5)		9.6	37.3	3.4	3.9 : 1
50	Average	SIPr (5)	47.0	9.5	36.4	3.5	3.8 : 1

[a] Reactions were conducted according to the General Procedure for GC-scale reactions. GC yields calibrated against undecane as an internal standard. [b]Values in parentheses are minimum percent buried volumes obtained from the Kraken database.[4] Percent buried volumes of NHCs reported for LAuCl complexes at a L–Au distance of 2.00 Å from reference 5.

Table B2. Ligand Screen with [(η^3-1-^{t}Bu-indenyl)Pd(Cl)]$_2$ (**I**) and (η^3-1-^{t}Bu-indenyl)Pd(NHC)-(Cl) (**II**). [a]



entry	trial	Pd source	ligand (mol %)	%V_{bur} (min)[b]	**1a** (%)	**1b** (%)	**1c** (%)	**1a** : **1b**
1	1	**I**	PPh_3 (5)		77.4	0.3	0.1	>99 : 1
2	2	**I**	PPh_3 (5)		74.1	0.4	n.d.	>99 : 1
3	Average	**I**	PPh_3 (5)	(28.2)	75.7	0.4	0.1	>99 : 1
4	1	**I**	PPh_3 (10)		77.7	0.3	0.1	>99 : 1
5	2	**I**	PPh_3 (10)		64.6	0.4	n.d.	>99 : 1
6	Average	**I**	PPh_3 (10)	(28.2)	71.2	0.4	0.1	>99 : 1
7	1	**I**	P(*o*-tol)$_3$ (5)		24.4	13.7	0.9	1.8 : 1
8	2	**I**	P(*o*-tol)$_3$ (5)		28.2	17.1	1.3	1.6 : 1
9	Average	**I**	P(*o*-tol)$_3$ (5)	(34.4)	26.3	15.4	1.1	1.7: 1
10	1	**I**	P(*o*-tol)$_3$ (10)		9.3	6.4	0.1	1.5 : 1
11	2	**I**	P(*o*-tol)$_3$ (10)		17.4	11.9	0.4	1.5 : 1
12	Average	**I**	P(*o*-tol)$_3$ (10)	(34.4)	13.4	9.1	0.3	1.5 : 1
13	1	**I**	PMe_3 (5)		4.7	0.5	n.d.	8.7 : 1
14	2	**I**	PMe_3 (5)		4.4	0.5	n.d.	9.2 : 1
15	Average	**I**	PMe_3 (5)	(22.1)	4.6	0.5	n.d.	9.0 : 1
16	1	**I**	PMe_3 (10)		6.1	0.4	n.d.	16.5 : 1
17	2	**I**	PMe_3 (10)		7.6	0.4	n.d.	21.4: 1
18	Average	**I**	PMe_3 (10)	(22.1)	6.8	0.4	n.d.	18.9 : 1
19	1	**I**	P(*n*-Bu)$_3$ (5)		3.1	0.6	n.d.	5.2 : 1
20	2	**I**	P(*n*-Bu)$_3$ (5)		2.1	0.4	n.d.	5.3: 1
21	Average	**I**	P(*n*-Bu)$_3$ (5)	(24.2)	2.6	0.5	n.d.	5.3 : 1
22	1	**I**	P(*n*-Bu)$_3$ (10)		2.3	0.4	n.d.	5.8 : 1
23	2	**I**	P(*n*-Bu)$_3$ (10)		1.6	0.2	n.d.	6.8 : 1
24	Average	**I**	P(*n*-Bu)$_3$ (10)	(24.2)	2.0	0.3	n.d.	6.7 : 1
25	1	**I**	PCy_3 (5)		13.1	21.8	0.8	1 : 1.7
26	2	**I**	PCy_3 (5)		23.4	37.9	3.5	1 : 1.6
27	Average	**I**	PCy_3 (5)	(30.2)	18.3	29.9	2.2	1 : 1.7
28	1	**I**	PCy_3 (10)		0.4	0.1	n.d.	4.0 : 1
29	2	**I**	PCy_3 (10)		0.4	0.1	n.d.	4.0 : 1
30	Average	**I**	PCy_3 (10)	(30.2)	0.4	0.1	n.d.	4.0 : 1
31	1	**I**	PAd_2(*n*-Bu) (5)		21.4	43.8	4.9	1 : 2.0
32	2	**I**	PAd_2(*n*-Bu) (5)		21.4	46.3	6.0	1 : 2.2
33	Average	**I**	PAd_2(*n*-Bu) (5)	(32.8)	21.4	45.1	5.5	1 : 2.1
34	1	**I**	PAd_2(*n*-Bu) (10)	(32.8)	1.7	2.6	1.4	1 : 1.5
35	1	**I**	P^{t}Bu$_3$ (5)		24.6	43.1	6.2	1 : 1.7
36	2	**I**	P^{t}Bu$_3$ (5)		26.9	46.6	8.0	1 : 1.7
37	Average	**I**	P^{t}Bu$_3$ (5)	(36.3)	25.8	44.9	7.1	1 : 1.7
38	1	**I**	P^{t}Bu$_3$ (10)	(36.3)	18.6	31.4	3.5	1 : 1.7

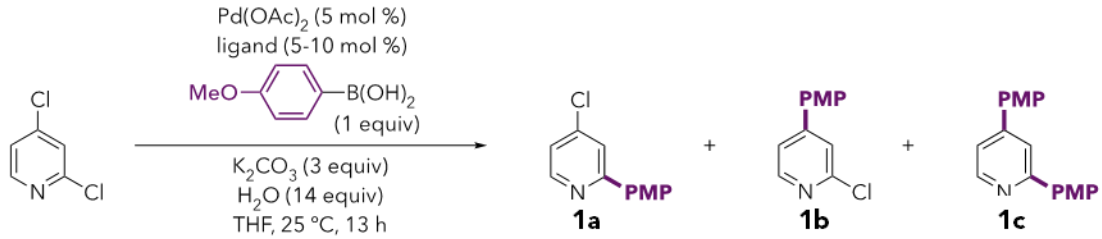
Table B2 Continued

39	1	**I**	Q-Phos (5)		23.0	47.2	5.7	1 : 2.1
40	2	**I**	Q-Phos (5)		23.2	49.4	6.9	1 : 2.1
41	Average	**I**	Q-Phos (5)	(47.6)	23.1	48.3	6.3	1 : 2.1
42	1	**II**	IMes		31.6	39.7	1.7	1 : 1.3
43	2	**II**	IMes		29.7	37.0	1.3	1 : 1.2
44	Average	**II**	IMes	36.5	30.7	38.4	1.5	1 : 1.3
48	1	**II**	SIMes		37.6	36.9	1.4	1.1 : 1
49	2	**II**	SIMes		38.6	38.8	1.3	1 : 1.0
50	Average	**II**	SIMes	36.9	38.1	37.9	1.4	1 : 1.0
51	1	**II**	IPr		6.6	68.8	4.0	1 : 10.4
52	2	**II**	IPr		6.5	70.1	4.3	1 : 10.8
53	Average	**II**	IPr	44.5	6.6	69.5	4.2	1 : 10.6

54	1	**II**	SIPr		7.2	70.9	7.7	1 : 9.8
55	2	**II**	SIPr		6.6	67.7	7.1	1 : 10.2
56	Average	**II**	SIPr	47.0	6.9	69.3	7.4	1 : 10.0

[a] Reactions were conducted according to the General Procedure for GC-scale reactions. GC yields calibrated against undecane as an internal standard. [b]Values in parentheses are minimum percent buried volumes obtained from the Kraken database.[4] Percent buried volumes of NHCs reported for LAuCl complexes at a L–Au distance of 2.00 Å from reference 5.

Table B3. Ligand Screen with $Pd(OAc)_2$[a]



entry	trial	ligand (mol %)	%V_{bur} (min)[b]	**1a** (%)	**1b** (%)	**1c** (%)	**1a** : **1b**
1	1	PPh_3 (5)		5.5	0.9	1.5	6.1 : 1
2	2	PPh_3 (5)		6.4	0.6	1.6	10.7 : 1
3	Average	PPh_3 (5)	(28.2)	6.0	0.7	1.6	8.6 : 1
4	1	PPh_3 (10)		64.6	0.4	n.d.	>99 : 1
5	2	PPh_3 (10)		64.6	0.4	n.d.	>99 : 1
6	Average	PPh_3 (10)	(28.2)	63.3	0.4	n.d.	>99 : 1
7	1	P(*o*-tol)$_3$ (5)		20.8	10.4	1.8	2.0 : 1
8	2	P(*o*-tol)$_3$ (5)		20.5	10.7	1.7	1.9 : 1
9	Average	P(*o*-tol)$_3$ (5)	(34.4)	20.7	10.6	1.8	2.0 : 1
10	1	P(*o*-tol)$_3$ (10)		7.2	4.1	1.0	1.8 : 1
11	2	P(*o*-tol)$_3$ (10)		10.2	5.9	1.7	1.7 : 1
12	Average	P(*o*-tol)$_3$ (10)	(34.4)	8.7	5.0	1.4	1.7 : 1
13	1	PMe_3 (5)		2.8	0.2	n.d.	14.0 : 1
14	2	PMe_3 (5)		6.9	0.8	n.d.	8.6 : 1

Table B3 Continued

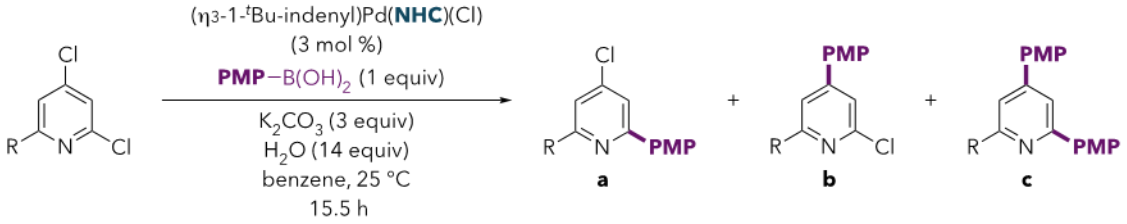
15	Average	PMe_3 (5)	(22.1)	4.9	0.5	n.d.	9.8 : 1
16	1	PMe_3 (10)		8.3	0.9	n.d.	9.2 : 1
17	2	PMe_3 (10)		6.9	0.6	n.d.	11.5 : 1
18	Average	PMe_3 (10)	(22.1)	7.6	0.8	n.d.	9.5 : 1
19	1	P(*n*-Bu)$_3$ (5)		6.3	1.0	n.d.	6.3 : 1
20	2	P(*n*-Bu)$_3$ (5)		9.0	2.2	n.d.	4.1 : 1
21	Average	P(*n*-Bu)$_3$ (5)	(24.2)	7.7	1.6	n.d.	4.8 : 1
22	1	P(*n*-Bu)$_3$ (10)		5.1	0.7	n.d.	7.3 : 1
23	2	P(*n*-Bu)$_3$ (10)		6.3	1.0	n.d.	6.3 : 1
24	Average	P(*n*-Bu)$_3$ (10)	(24.2)	5.7	0.9	n.d.	6.3 : 1
25	1	PCy_3 (5)		11.5	16.0	2.0	1 : 1.4
26	2	PCy_3 (5)		9.6	15.7	1.6	1 : 1.6

27	Average	PCy_3 (5)	(30.2)	10.6	15.9	1.8	1 : 1.5
28	1	PCy_3 (10)		2.6	1.2	2.3	2.2 : 1
29	2	PCy_3 (10)		2.9	0.8	1.2	3.6 : 1
30	Average	PCy_3 (10)	(30.2)	2.7	1.0	1.8	2.7 : 1
31	1	CyJohnPhos (5)		28.9	15.9	3.7	1.8 : 1
32	2	CyJohnPhos (5)		26.5	14.0	3.0	1.9 : 1
33	Average	CyJohnPhos (5)	(31.8)	27.7	14.9	3.3	1.9 : 1
34	1	PAd_2(*n*-Bu) (5)		17.6	33.0	3.0	1 : 1.9
35	2	PAd_2(*n*-Bu) (5)		21.8	43.5	3.9	1 : 2.0
36	Average	PAd_2(*n*-Bu) (5)	(32.8)	19.7	38.3	3.4	1 : 1.9
37	1	PAd_2(*n*-Bu) (10)	(32.8)	21.6	45.6	7.1	1 : 2.1
38	1	P^tBu_3 (5)		26.9	44.3	8.7	1 : 1.7
39	2	P^tBu_3 (5)		22.1	33.7	4.3	1 : 1.5
40	Average	P^tBu_3 (5)	(36.3)	24.5	39.0	6.5	1 : 1.6
41	1	P^tBu_3 (10)	(36.3)	27.7	39.7	7.7	1 : 1.4
42	1	Q-Phos (5)		22.8	40.5	4.2	1 : 1.8
43	2	Q-Phos (5)		22.9	41.1	4.7	1 : 1.8
44	Average	Q-Phos (5)	(47.6)	22.9	40.8	4.4	1 : 1.8
45	1	Q-Phos (10)	(47.6)	24.2	45.8	6.7	1 : 1.9
46	1	IMes (5)		26.6	27.1	2.5	1 : 1
47	2	IMes (5)		25.9	26.3	2.5	1 : 1
48	Average	IMes (5)	36.5	26.2	26.7	2.5	1 : 1
49	1	SIMes (5)		8.5	7.3	1.5	1.2 : 1
50	2	SIMes (5)		13.2	10.6	2.0	1.2 : 1
51	Average	SIMes (5)	36.9	10.8	8.9	1.8	1.2 : 1
52	1	IPr (5)		4.3	22.8	3.4	1 : 5.3
53	2	IPr (5)		5.2	37.2	5.2	1 : 7.2
54	Average	IPr (5)	44.5	4.8	30.0	4.3	1 : 6.3
55	1	SIPr (5)		2.9	4.9	1.5	1 : 1.7
56	2	SIPr (5)		4.9	7.7	2.1	1 : 1.6
57	Average	SIPr (5)	47.0	3.9	6.3	1.8	1 : 1.6

[a] Reactions were conducted according to the General Procedure for GC-scale reactions. GC yields calibrated against undecane as an internal standard. [b]Values in parentheses are minimum percent buried volumes obtained from the Kraken database.[4] Percent buried volumes of NHCs reported for LAuCl complexes at a L–Au distance of 2.00 Å from reference 5.

B4. Influence of 6-Substituent on Selectivity with IMes (Scheme 3.3A) and IPr

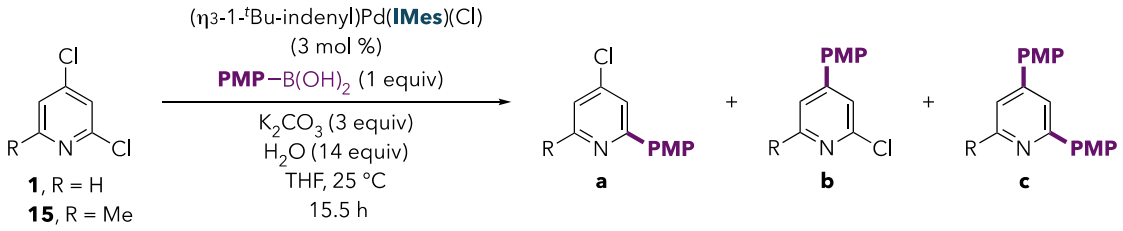
Table B4. Effect of 6-Substituent on Selectivity in Benzene (Scheme 3.3A).[a]



entry	trial	NHC	-R	**a** (%)	**b** (%)	**c** (%)	**a** : **b**
1	1	IMes	H	21	35	3	1 : 1.7
2	2	IMes	H	25	44	3	1 : 1.8
3	Average	IMes	H	23	40	3	1 : 1.7
4	1	IMes	Me	15	55	4	1: 3.7
5	2	IMes	Me	15	57	6	1 : 3.8
6	Average	IMes	Me	15	56	5	1 : 3.7
7	1	IPr	H	8	69	6	1 : 8.6
8	2	IPr	H	8	72	5	1 : 9.0
9	Average	IPr	H	8	71	6	1 : 8.8
10[b]	1	IPr	Me	3	45	21	1 : 15

[a]Reactions were conducted according to the General Procedure for GC-scale reactions. GC yields calibrated against undecane as an internal standard. [b]Reaction run for 13 h.

Table B5. Effect of 6-Substituent on Selectivity in THF.[a]



entry	trial	-R	**a** (%)	**b** (%)	**c** (%)	**a** : **b**
1	1	H	36	47	4	1 : 1.3
2	2	H	49	38	5	1.3 : 1
3	Average	H	43	43	4	1 : 1
4[b]	1	CF_3	34	56	11	1 : 1.5
5[b]	2	CF_3	34	60	14	1 : 1.8
6[b]	Average	CF_3	34	58	12	1: 1.7
7	1	Me	23	56	11	1 : 2.4
8	2	Me	21	55	11	1 : 2.6
9	Average	Me	22	56	11	1 : 2.5

[a]The General Procedure was used for GC-scale reactions. Unless otherwise noted, yields are GC yields calibrated against undecane as an internal standard. [b]Uncalibrated GC yields.

B5. Influence of [**1**] on Selectivity with IMes (Scheme 3.3B), IPr, and P^{t}Bu$_3$

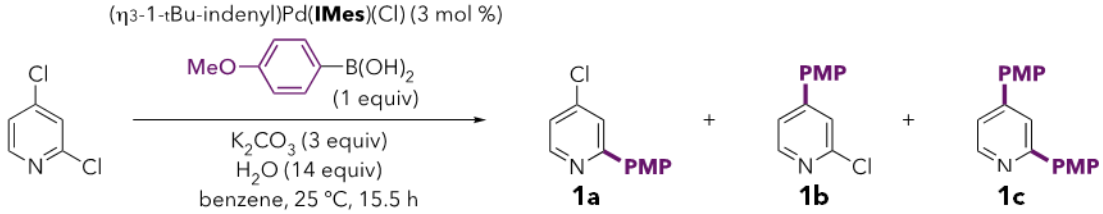
Overview and Discussion

The selectivity of (η^3-1-^{t}Bu-indenyl)Pd(IMes)(Cl) is sensitive to the concentration of substrate **1** (Table B7). At higher [**1**], more reaction at C2 is seen, consistent with greater availability of **1**

that can coordinate to Pd(IMes) leading to preferential reaction at C2 through a bisligated transition state **TS13a-IMes**.

For comparison, no change or only a slight change in selectivity is seen in analogous experiments using (η^3-1-^{t}Bu-indenyl)Pd(**IPr**)(Cl) (Table B7) and (cod)Pd(CH_2SiMe_3)$_2$/**P^{t}Bu$_3$** (Table B8). With both catalytic systems, DFT calculations predict that reaction at C4 is favored through monoligated PdL, but that *if* bisligated PdL(**1**) could react, it would prefer C2. For the former catalytic system, reaction of C2—Cl at Pd(IPr)(**1**) (**TS13a-IPr**) is calculated to be disfavored over the monoligated TS for reaction at C4 (**TS10b-IPr**) by 4.0 kcal/mol. In the latter system, reaction at C2 at Pd(P^{t}Bu$_3$)(**1**) is disfavored by 10.1 kcal/mol (see Figure 3.1 in the manuscript, compare **TS13a-P^{t}Bu$_3$** to **TS10b-P^{t}Bu$_3$**). These trends are consistent with the very slight sensitivity of the Pd/IPr system to [**1**], and the nonexistent sensitivity of the Pd/P^{t}Bu$_3$ system to [**1**].

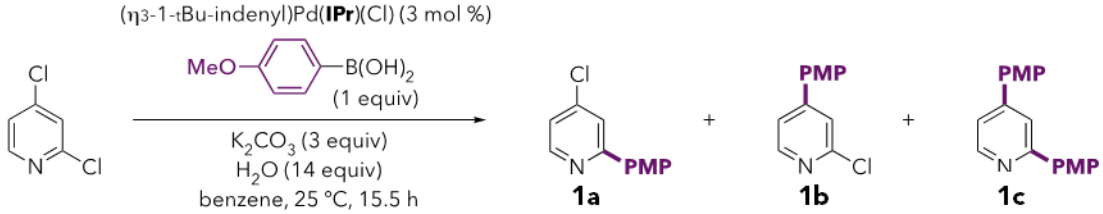
Table B6. Influence of [**1**] on Selectivity with IMes (Scheme 3.2B)[a]



entry	Trial	**1** (equiv)	**1a** (%)	**1b** (%)	**1c** (%)	1a : 1b	$\Delta\Delta G^{\ddagger}_{(C4\text{-}C2)}$ (kcal/mol)[b]
1	1	1	21.1	35.3	2.7	1 : 1.7	-0.3
2	2	1	24.3	44.0	3.0	1 : 1.8	-0.3
3	Average	1	22.7	39.6	2.9	1 : 1.7	-0.3
4	1	2	28.6	27.5	0.8	1 : 1.0	0.0
5	2	2	33.2	31.1	1.0	1.1 : 1	0.0
6	Average	2	30.9	29.3	0.9	1.1 : 1	0.0
7	1	5	32.3	10.4	0.7	3.1 : 1	+0.7
8	2	5	43.8	17.9	0.6	2.4 : 1	+0.5
9	Average	5	38.1	14.2	0.7	2.7 : 1	+0.6
10	1	10	42.0	8.8	0.9	4.8 : 1	+0.9
11	2	10	43.8	9.6	0.4	4.6 : 1	+0.9
12	Average	10	42.9	9.2	0.7	4.7 : 1	+0.9

[a]Reactions were conducted according to the General Procedure for GC-scale reactions. GC yields calibrated against undecane as an internal standard. [b]Difference in free energies of activation for reaction at C4 versus C2 calculated from the experimental product ratios using the Eyring equation at 298.15 K.

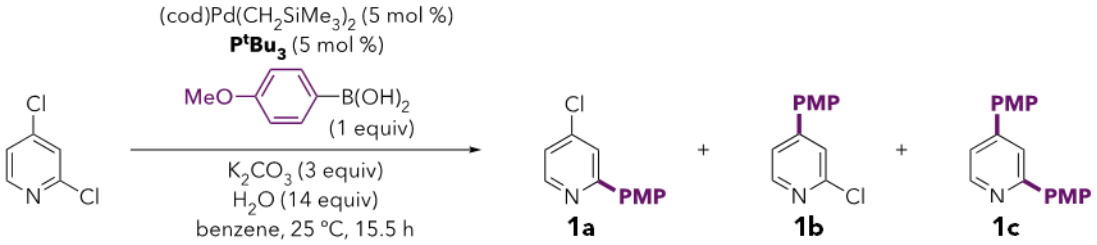
Table B7. Influence of [**1**] on Selectivity with IPr.[a]



entry	Trial	**1** (equiv)	**1a** (%)	**1b** (%)	**1c** (%)	1a : 1b	$\Delta\Delta G^{\ddagger}_{(C4\text{-}C2)}$ (kcal/mol)[b]
1	1	1	8.1	69.0	6.0	1 : 8.5	-1.3
2	2	1	8.6	70.5	6.4	1 : 8.2	-1.3
3	Average	1	8.3	69.7	6.2	1 : 8.4	-1.3
4	1	2	10.0	75.2	1.9	1 : 7.5	-1.2
5	2	2	9.1	70.1	1.7	1 : 7.7	-1.2
6	Average	2	9.6	72.6	1.8	1 : 7.6	-1.2
7	1	5	9.9	68.9	0.8	1 : 7.0	-1.2
8	2	5	9.8	70.9	0.8	1 : 7.2	-1.2
9	Average	5	9.9	69.9	0.8	1 : 7.1	-1.2
10	1	10	12.2	74.8	0.6	1 : 6.1	-1.1
11	2	10	10.2	65.7	0.6	1 : 6.4	-1.1
12	Average	10	11.2	70.3	0.6	1 : 6.3	-1.1

[a]Reactions were conducted according to the General Procedure for GC-scale reactions. GC yields calibrated against undecane as an internal standard. [b]Difference in free energies of activation for reaction at C4 versus C2 calculated from the experimental product ratios using the Eyring equation at 298.15 K.

Table B8. Influence of [**1**] on Selectivity with P^{t}Bu$_3$[a]



entry	Trial	**1** (equiv)	**1a** (%)	**1b** (%)	**1c** (%)	1a : 1b	$\Delta\Delta G^{\ddagger}_{(C4\text{-}C2)}$ (kcal/mol)[b]
1	1	1	29.3	49.0	14.4	1 : 1.7	-0.3
2	2	1	29.3	46.6	12.7	1 : 1.6	-0.3
3	Average	1	29.3	47.8	13.6	1 : 1.7	-0.3
4	1	2	31.9	50.8	4.8	1 : 1.6	-0.3
5	2	2	38.1	60.5	5.3	1 : 1.6	-0.3
6	Average	2	35.0	55.7	5.1	1 : 1.6	-0.3
7	1	5	39.1	62.0	1.9	1 : 1.6	-0.3
8	2	5	37.0	61.5	1.4	1 : 1.7	-0.3
9	Average	5	38.1	61.8	1.7	1 : 1.7	-0.3
10	1	10	37.1	63.4	1.0	1 : 1.7	-0.3
11	2	10	36.8	58.9	1.1	1 : 1.6	-0.3
12	Average	10	37.0	61.2	1.1	1 : 1.7	-0.3

[a]Reactions were conducted according to the General Procedure for GC-scale reactions. GC yields calibrated against undecane as an internal standard. [b]Difference in free energies of activation for reaction at C4 versus C2 calculated from the experimental product ratios using the Eyring equation at 298.15 K.

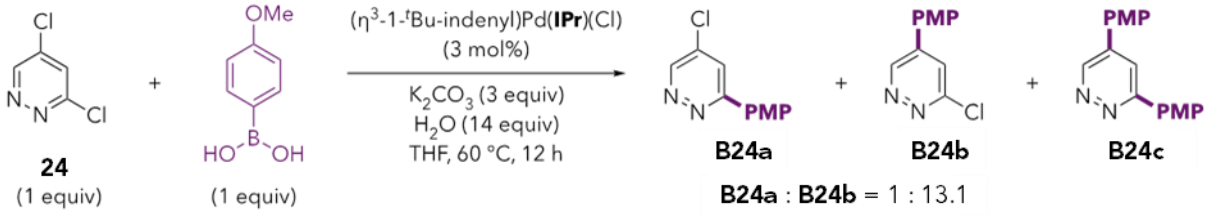
B6. Selectivity Analysis of Substrates in Scheme 3.2C

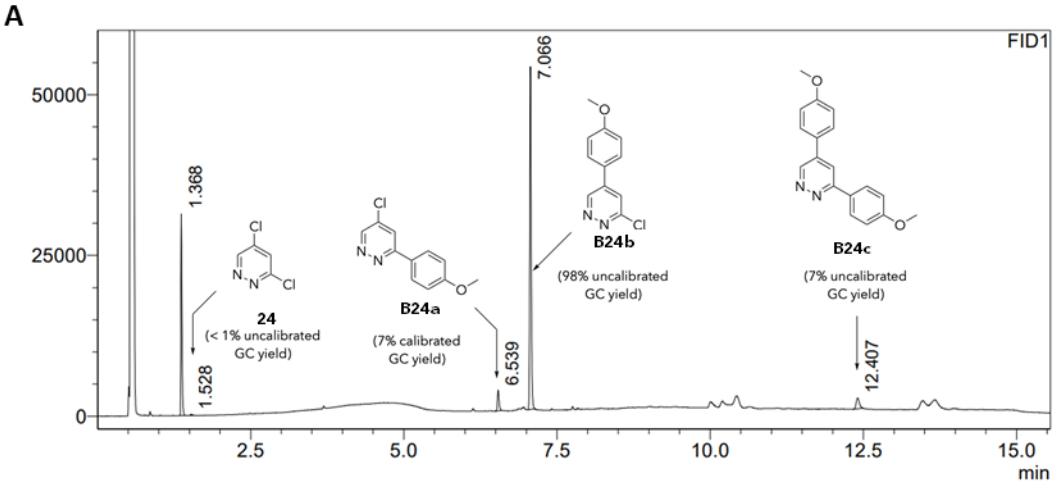
Cross-coupling reactions of the substrates in Scheme 3.2C were set up according to the General Procedure for GC-scale reactions using (η^3-1-^{t}Bu-indenyl)Pd(IPr)(Cl) (3 mol%), K_2CO_3 (3 equiv), and deionized H_2O (14 equiv) at 60 °C in THF with stirring for 12 h. Reaction outcomes were analyzed by GC and GCMS using *n*-undecane as an internal standard. Solvent was removed from the reaction vials under vacuum, then the crude solids were redissolved in $CDCl_3$ or C_6D_6, filtered through Celite, and analyzed by ^{1}H NMR. The unconventional monoarylated products of each reaction in Scheme 3.2C were isolated and fully characterized as described below in Section G, or they were isolated and characterized previously.[1] GC and ^{1}H NMR signals present in the crude

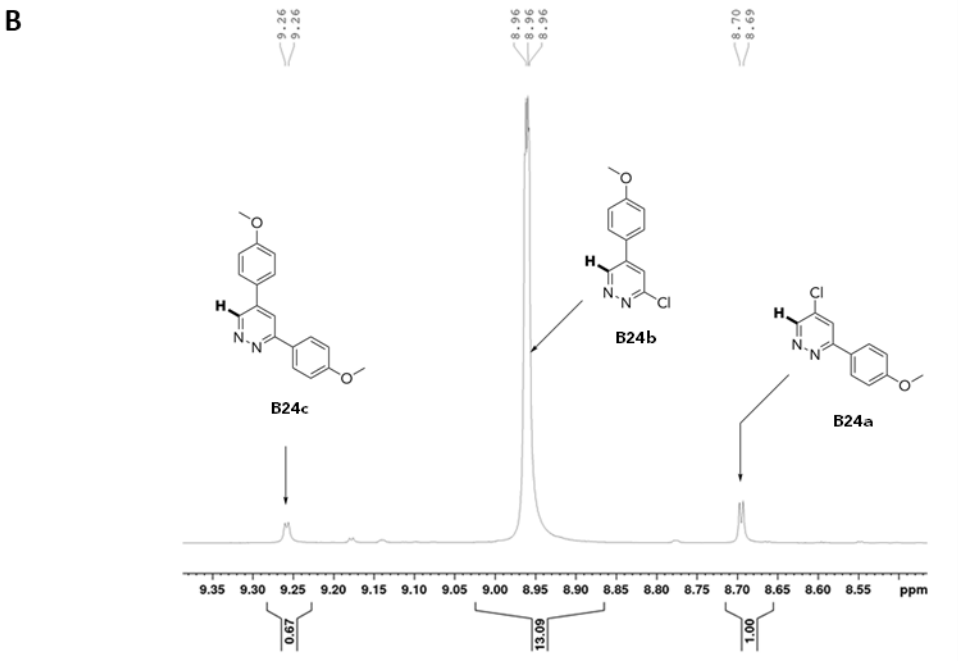
reaction mixtures were identified based on comparison to those of the isolated products. The GC retention times of the diarylated products were assigned based on their mass values obtained by GCMS analysis. Where relevant, NMR yields of minor products were calculated from NMR signal ratios relative to the major product, whose yield was determined by calibrated GC analysis.

The Pd/IPr-catalyzed Suzuki cross-coupling of 3,5-dichloropyridazine (**24**) favors reaction at C5 according to crude GC, GCMS, and ^{1}H NMR analyses (ratio of **B24a** and **B24b** = 1 : 13.1 based on the ratio of signal integrations by ^{1}H NMR (C_6D_6, 500 MHz, Scheme B1.B). As discussed in Chapter 3, the difference in LUMO coefficient between C3 and C5 is substantial, consistent with high selectivity for the C5-site.

Scheme B1. Suzuki reaction of 5 using a Pd/IPr catalyst. (A) GC chromatogram of the crude reaction mixture. (B) Relevant region of the ^{1}H NMR spectrum of the crude reaction mixture.

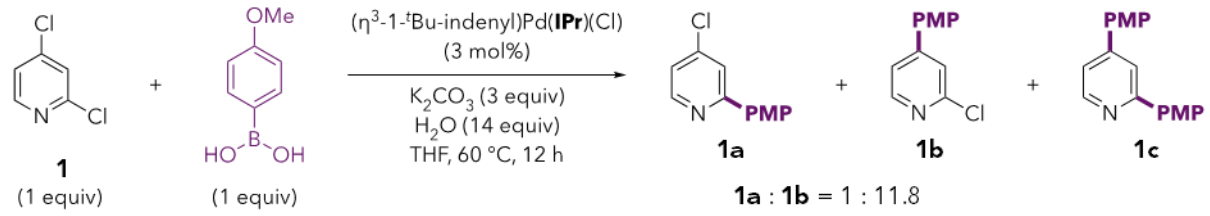




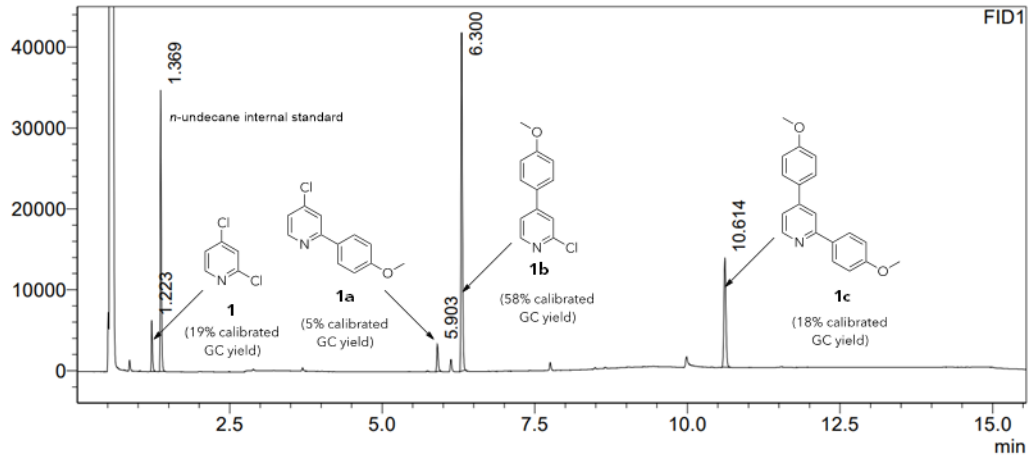


The Pd/IPr-catalyzed Suzuki cross-coupling of 2,4-dichloropyridine (**1**) favors reaction at C4 according to crude GC, GCMS, and ^{1}H-NMR analyses (ratio of **1a** and **1b** = 1 : 11.78 based on the ratio of signal integrations by ^{1}H-NMR ($CDCl_3$, 400 MHz, Scheme B2.B), and 1 : 11.82 based on the ratio of calibrated signal integrations by GC, Scheme B2.A). As discussed in the manuscript, the difference in LUMO coefficient between C2 and C4 is substantial, consistent with high selectivity for the C4-site.

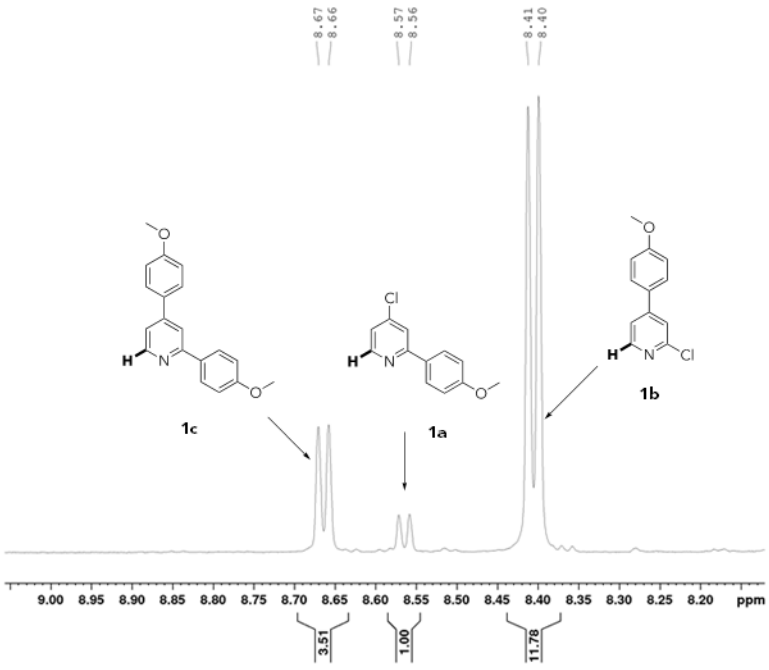
Scheme B2. Suzuki reaction of **1** using a Pd(IPr) catalyst.



A

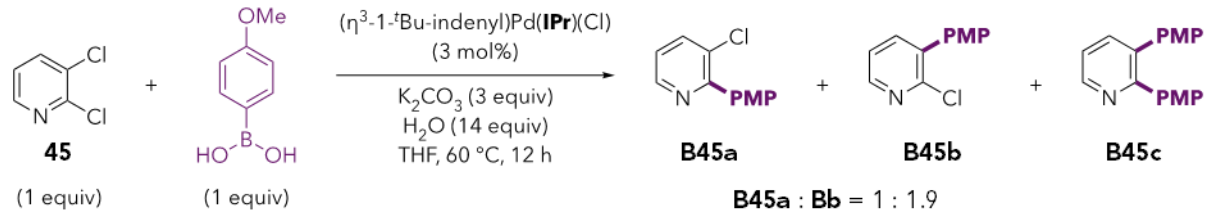


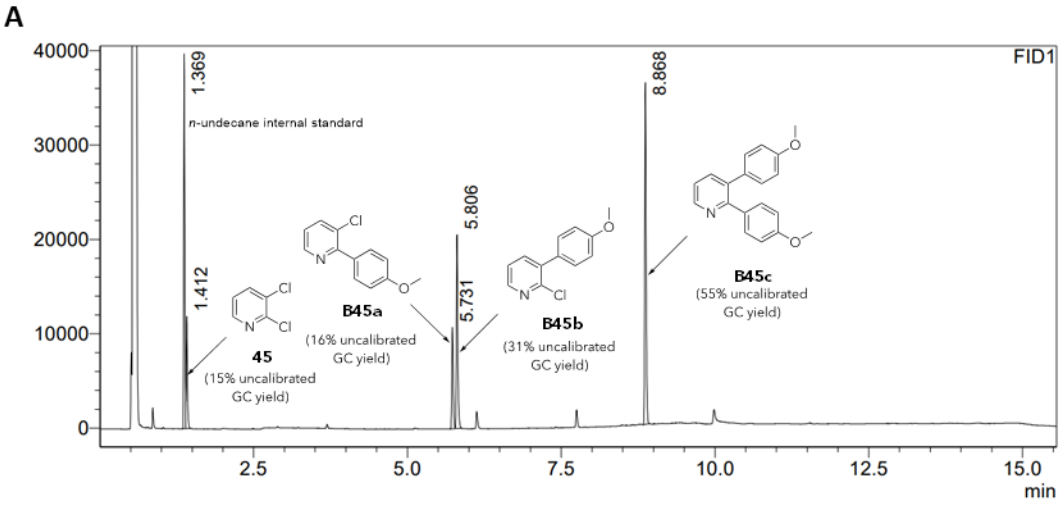
B

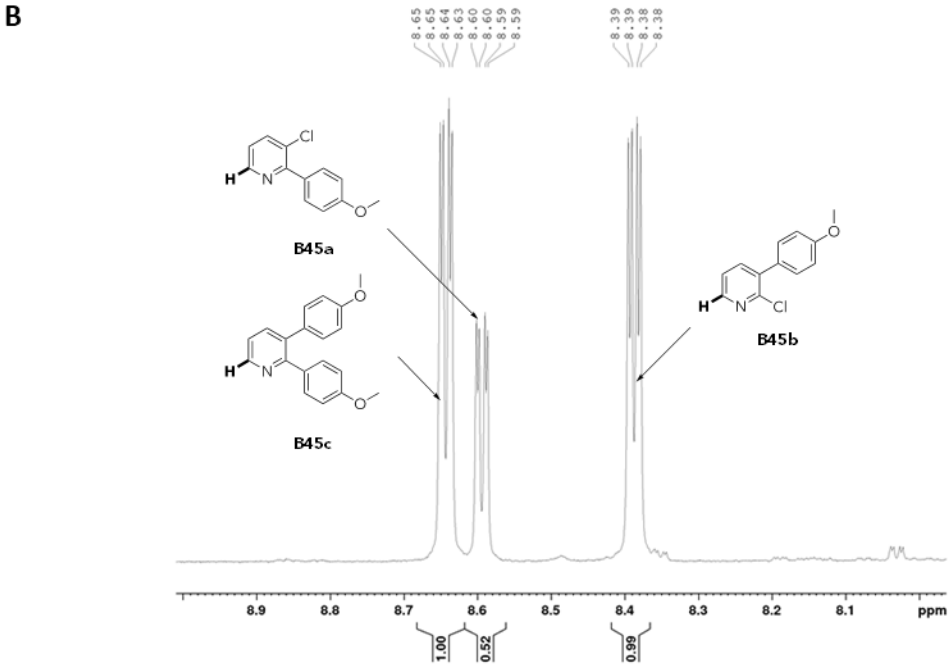


The Pd/IPr-catalyzed Suzuki cross-coupling of 2,3-dichloropyridine (**45**) favors reaction at the unconventional site C3 under the optimized system according to crude GC and GCMS analysis (ratio of **B45a** and **B45b** = 1 : 1.9 based on the ratio of signal integrations by ^{1}H-NMR ($CDCl_3$, 400 MHz, Scheme B3B). As such, the use of (η^3-1-^{t}Bu-indenyl)Pd(IPr)(Cl) promotes reaction at the site distal to nitrogen, albeit in low selectivity. As discussed in the Chapter 3, the difference in LUMO coefficient between C2 and C3 is modest, thus the reaction is not as selective as the reactions of 2,4-dichloropyridine or 3,5-dichloropyridazine.

Scheme B3. Suzuki reaction of **45** using a Pd(IPr) catalyst.

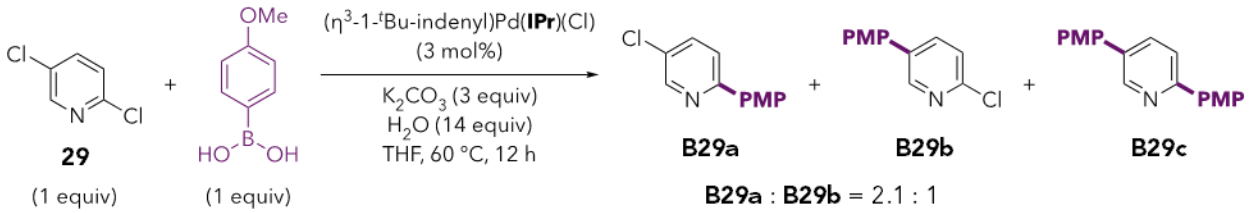


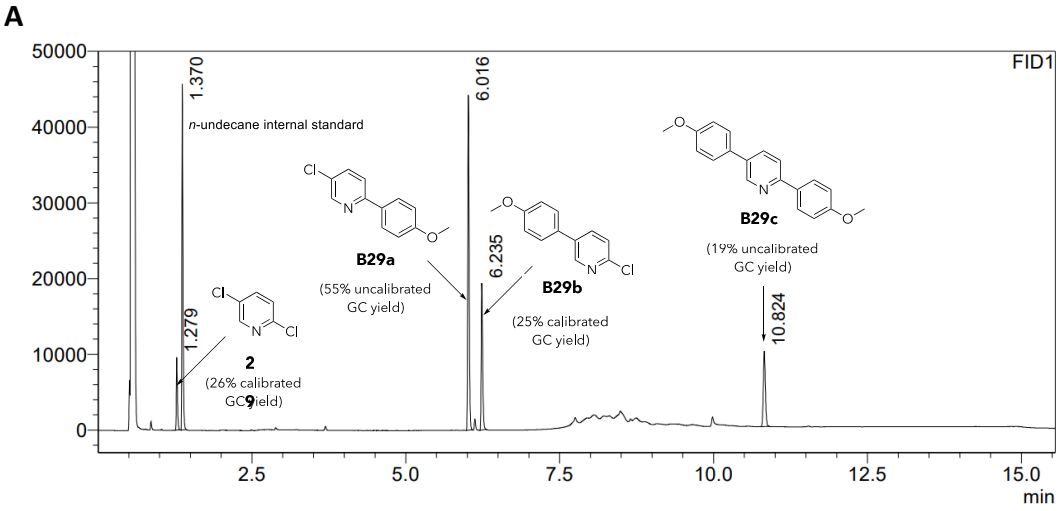


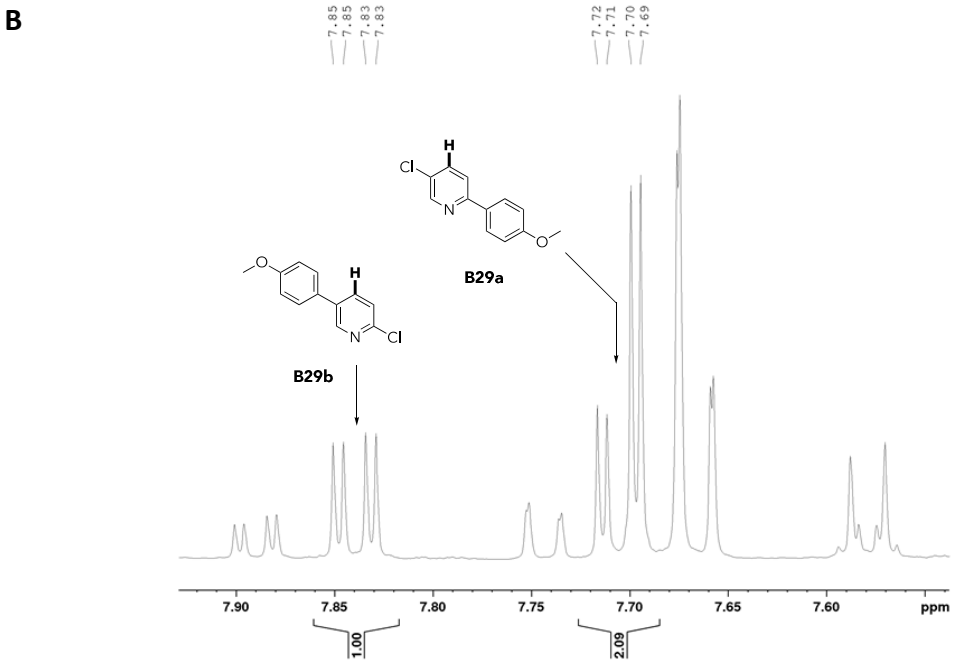


2,5-Dichloropyridine (**29**) favors reaction at C2 under the optimized system according to crude GC and GCMS analysis (ratio of **B29b** to **B29a** = 1 : 2.1 based on the ratio of signal integrations by ^{1}H-NMR ($CDCl_3$, 400 MHz, Scheme B4B). As such, the use of (η^3-1-^{t}Bu-indenyl)Pd(IPr)(Cl) does not enable unconventional selectivity with this substrate. As discussed in the manuscript, the difference in LUMO coefficient between C2 and C5 is very small (8% C2 and 10% C5), and thus it is likely that palladium is more strongly influenced by bond dissociation energies (which favor reaction at C2) than by LUMO coefficients.

Scheme B4. Suzuki reaction of **29** using a Pd(IPr) catalyst.







B7. Isolation and Characterization of Cross-Coupled Products (Table 3.1 and Scheme 3.3)

4-Chloro-2-(4-methoxyphenyl)-6-methylpyridine (46a). Compound **46a** was prepared according to a modified literature procedure.[6] Palladium(II) acetate (4.5 mg, 0.02 mmol, 5 mol %), 1,1'-bis(diphenylphosphino)ferrocene (14.8 mg, 0.2 mmol, 5 mol %), cesium carbonate (325.8 mg, 1 mmol 2.5 equiv) and *p*-methoxyphenylboronic acid (60.8 mg, 0.4 mmol, 1 equiv) were added to an oven-dried 1-dram vial in a N_2-filled glovebox. The vial was sealed with a septum, removed from the glovebox, and 2,4-dichloro-6-methylpyridine (**46**, 64.8 mg, 0.4 mmol, 1 equiv), deionized water (50 µL, 2.8 mmol, 7 equiv), and 1,4-dioxane (1.6 mL) were added through the septum. The reaction was allowed to stir at 70 ºC for 21 h. Purification by flash column chromatography (R_f = 0.63 in 20% ethyl acetate in hexanes) provided a pure fraction of **46a** that was used for characterization and for preparing GC calibration curves. ^{1}H NMR (500 MHz, $CDCl_3$, δ): 7.91-7.95 (m, 2H), 7.46 (d, *J* = 1.4 Hz, 1H), 7.05 (d, *J* = 1.4 Hz, 1H), 6.96-7.01 (m, 2H), 3.86 (s, 3H), 2.58 (s, 3H). ^{13}C{^{1}H} NMR (126 MHz, $CDCl_3$, δ): 161.0, 159.9, 158.2, 144.7, 131.3, 128.6, 121.1, 117.3, 114.4, 55.6, 24.8. HRMS (ESI Q-TOF) m/z: [M]+ Calcd for $C_{13}H_{12}ClNO$ 233.0607; Found 233.0615.

2-Chloro-4-(4-methoxyphenyl)-6-methylpyridine (46b). Compound **46b** was prepared according to the general procedure. An oven dried 1-dram vial was charged with a stir bar, (η^3-1-^{t}Bu-indenyl)Pd(IPr)Cl (8.4 mg, 0.012 mmol, 3.0 mol%), *p*-methoxyphenylboronic acid (60.8 mg, 0.4 mmol, 1 equiv), and potassium carbonate (165.8 mg, 1.2 mmol, 3 equiv). Dry degassed THF (1.6 mL), deionized water (100 µL, 5.6 mmol, 14 equiv), and 2,4-dichloro-6-methylpyridine (**46**, 64.8 mg, 0.4 mmol, 1 equiv) were added and the reaction mixture was sparged with N_2. The reaction was allowed to stir at 25 ºC for 20 h. Purification was performed by reversed phase flash

column chromatography with a 12 g C18 silica column, using an initial automated program comprising of a flow rate of 30 mL/min of water:acetonitrile (98:2 to 2:98) over 30 column volumes. When the product began eluting, the program was paused and reset to elute the analyte at 63% MeCN in water. After the elution, the initial program was resumed. Pure fractions containing **46b** were partitioned between dichloromethane and saturated brine. The organic layers were combined, dried over magnesium sulfate, and solvent was removed under reduced pressure affording a pure fraction of **46b** that was used for characterization and for preparing GC calibration curves. ^{1}H NMR (500 MHz, $CDCl_3$, δ): 7.52-7.59 (m, 2H), 7.31 (d, J = 0.8 Hz, 1H), 7.24 (d, J = 0.8, 1H), 6.97- 7.02 (m, 2H), 3.87 (s, 3H), 2.57 (s, 3H) ^{13}C{^{1}H} NMR (126 MHz, $CDCl_3$, δ): 161.0, 159.6, 151.4, 151.3, 129.5, 128.4, 119.5, 118.5, 114.7, 55.6, 24.4. HRMS (ESI Q-TOF) m/z: [M]+ Calcd for $C_{13}H_{12}ClNO$ 233.0607; Found 233.0643.

2,4-Bis(4-methoxyphenyl)-6-methylpyridine (46c). Compound **46c** was prepared according to a modified literature procedure.[7] An oven dried 1-dram vial was charged with a stirbar, (η^3-1-^{t}Bu-indenyl)Pd(IPent)Cl (9.8 mg, 0.012 mmol, 3.0 mol%), *p*-methoxyphenyl-boronic acid (121.6 mg, 0.8 mmol, 2 equiv), and potassium carbonate (165.8 mg, 1.2 mmol, 3 equiv). Benzene (1.6 mL), water (100 µL, 5.6 mmol, 14 equiv), and 2,4-dichloro-6-methylpyridine (**46**, 64.8 mg, 0.4 mmol, 1 equiv) was added quickly and the vial was sparged with N_2. The reaction was allowed to stir at 25 ºC for 20 h. Purification by flash column chromatography (R_f = 0.29 in 20% ethyl acetate in hexanes) afforded **46c** as a white solid (86.6 mg, 64% yield). ^{1}H NMR (500 MHz, $CDCl_3$, δ): 8.02-7.97 (m, 2H), 7.64–7.58 (multiple peaks, 3H), 7.21 (d, J = 1.2 Hz, 1H), 7.03-6.99 (m, 4H), 3.88 (s, 3H), 3.87 (s, 3H), 2.66 (s, 3H). Spectral data are consistent with those previously reported.[7]

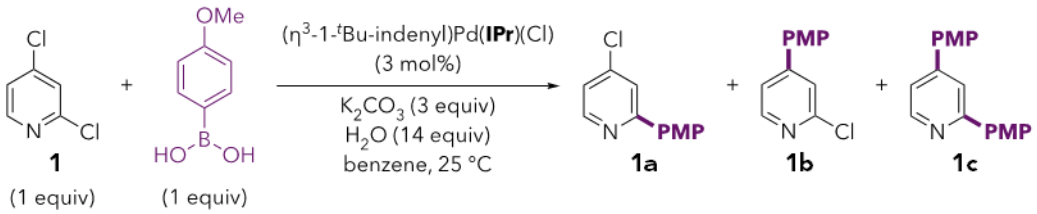
2-Chloro-3-(4-methoxyphenyl)pyridine (B45b). Compound **B45b** was prepared according to the general procedure. An oven dried 1-dram vial was charged with a stir bar, (η^3-1-^{t}Bu-indenyl)Pd(IPr)Cl (8.4 mg, 0.012 mmol, 3.0 mol%), 2,3-dichloropyridine (**45**, 59.2 mg, 0.4 mmol, 1.0 equiv), *p*-methoxyphenylboronic acid (60.8 mg, 0.4 mmol, 1.0 equiv), and potassium carbonate (165.8 mg, 1.2 mmol, 3 equiv). Benzene (1.6 mL) and water (100 µL, 5.6 mmol, 14 equiv) were added and the reaction was allowed to stir for 16 h. Purification by flash column chromatography on silica (R_f = 0.42 in 20% ethyl acetate in hexanes) provided **B45b** as white solid (21.9 mg, 25% yield). ^{1}H NMR (400 MHz, $CDCl_3$, δ): 8.36 (dd, *J* = 4.8, 1.9 Hz, 1H), 7.65 (dd, *J* = 7.6, 1.9 Hz, 1H), 7.41-7.37 (m, 2H), 7.29 (dd, *J* = 7.6, 4.8 Hz, 1H), 7.01-6.96 (m, 2H), 3.86 (s, 3H). ^{13}C{^{1}H} NMR (101 MHz, $CDCl_3$, δ): 159.8, 150.0, 148.2, 139.8, 136.9, 130.7, 130.0, 122.7, 114.0, 55.5. HRMS (ESI Q-TOF) m/z: [M]+ Calcd for $C_{12}H_{10}ClNO$ 219.0451; Found 219.0454. The other regioisomer (the C2 monoarylated isomer **B45a**) has been previously reported,[8] and its spectral data are distinct from those of product **B45b** reported here.

B8. Time Trial for Suzuki Reaction of **1**

The Pd/IPr-mediated coupling of 2,4-dichloropyridine and *p*-methoxyphenyl boronic acid was monitored over a period of 155 min. Two identical reactions were set up in parallel according to the General Procedure for GC-scale reactions using 1-dram reaction vials with the following modifications. Each reaction was run on a 0.6 mmol scale with respect to the limiting reagents (2,4-dichloropyridine and *p*-methoxyphenylboronic acid). One vial was designated as a "control" (sealed with a PTFE-lined cap, no aliquots removed), and the other was equipped with a septum cap. An *n*-undecane internal standard was added to both vials prior to stirring and both were sparged with N_2 prior to stirring. Aliquots were withdrawn from the second vial by syringe, diluted

in ethyl acetate, and analyzed quantitatively by GC. The final aliquot at t = 155 min gave results comparable to the control vial (entries 5-6 in Table B9), demonstrating that the periodic removal of aliquots did not significantly alter the course of the reaction.

Table B9. Product Formation Over Time Using the Pd/IPr Conditions for the SMC of **1**.



entry	time (min)	**1** (%)	**1a** (%)	**1b** (%)	**1c** (%)	**1a** : **1b**
1	5	93	trace	3	2	--
2	15	80	2	12	4	1 : 6
3	35	53	5	37	4	1 : 8
4	75	26	8	63	6	1 : 8
5	155	16	9	75	8	1 : 8
6	155 (control)	15	9	75	8	1 : 8

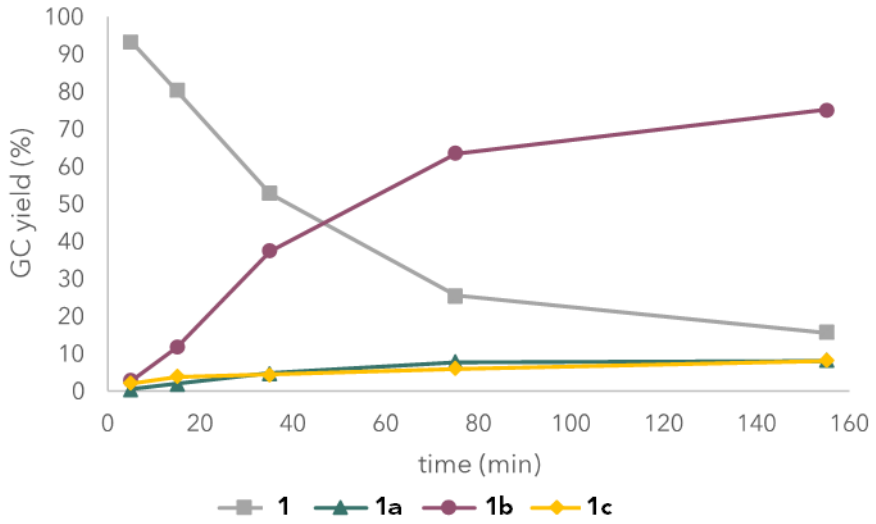


Figure B1. Visual representation of product formation over time using Pd/IPr conditions for the Suzuki coupling of **1**.

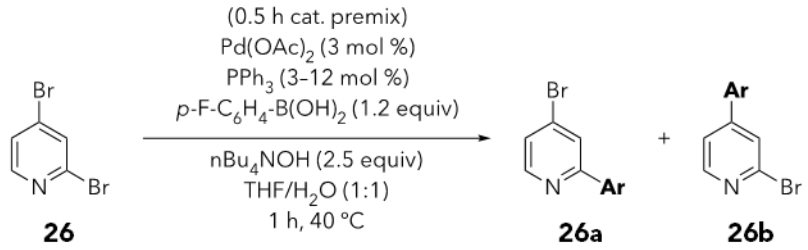
Discussion: C4 over C2-selectivity remains constant after the first 15 minutes (Table B9 and Figure B1). The C2-monoarylated isomer **1a** might be somewhat more likely to undergo a second arylation than the C4-monoarylated isomer **1b** when a 1:1 ratio of electrophile and nucleophile is used. Both chloride and arylated pyridines (potential ligands for Pd) build up throughout the reaction, yet these factors are not expected to improve C4-selectivity based on our mechanistic understanding of selectivity. Although aliquot removal may alter the ratio of homogeneous to heterogeneous material within the reaction vial, the control vial closely resembles the second vial after 155 min indicating that this effect was not significant.

B9. Evidence Against Multinuclear Speciation

Effect of Pd:L ratio

Fairlamb et al. recently found that the selectivity of Pd/PPh_3-catalyzed cross-coupling of 2,4-dibromopyridine is sensitive to the ratio of Pd:PPh_3.[9] This was interpreted as a change in catalyst speciation depending on the amount of ligand [i.e., predominantly mononuclear Pd at high [PPh_3] (2-4 equiv relative to Pd) and multinuclear Pd at low [PPh_3] (<2 equiv relative to Pd)]. Fairlamb's results are summarized below (ratios approximated from Figure 1 of ref 9a). To highlight the significant effect of stoichiometry in Fairlamb's system, the differences in free energies of activation are also listed below. This value ($\Delta\Delta G‡$) represents the difference in the free energy barrier for reaction at C4 vs. C2 based on the reported experimental selectivity and was derived with the Eyring equation at 40 ºC (Fairlamb's reaction temperature).

Table B10. Influence of Pd:L Ratio on Selectivity in Fairlamb's System[a]

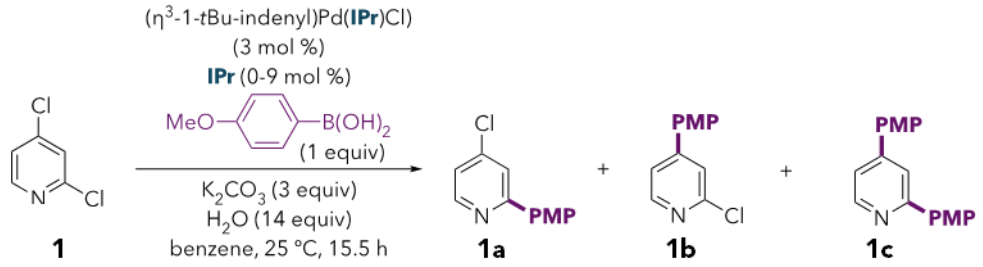


entry	$Pd:PPh_3$	**26a** (%)	**26b** (%)	26a : 26b	$\Delta\Delta G^{\ddagger}_{(C4\text{-}C2)}$ (kcal/mol)[b]
1	1 : 1	6	79	1 : 13	-1.6
2	1 : 1.5	8	78	1 : 9.8	-1.4
3	1 : 2	10	76	1 : 7.6	-1.3
4	1 : 2.5	7	24	1 : 3.4	-0.8
5	1 : 4	10	5	2 : 1	+0.4

[a]Product yields are estimated from Figure 1 of ref 9a. [b]Difference in free energies of activation for reaction at C4 versus C2 calculated from the estimated experimental product ratios using the Eyring equation at 313.15 K.

In contrast, we observe a negligible effect of metal to ligand ratio when additional free IPr or IMes is added to the reactions with (η^3-1-^{t}Bu-indenyl)Pd(NHC)(Cl). In contrast to Fairlamb's system, the results in our system suggest that there is not a catalyst speciation change upon changing ligand quantity.

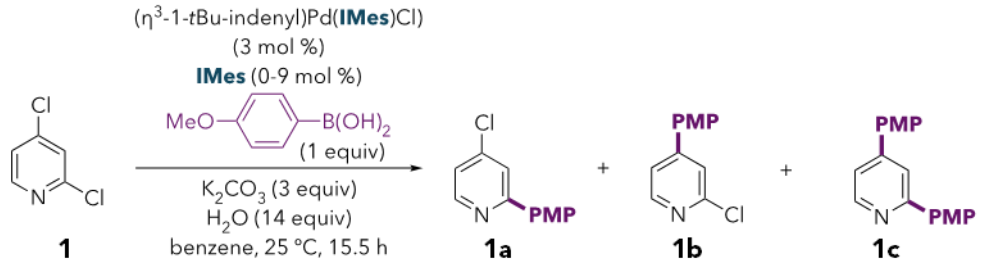
Table B1. Influence of Pd:L Ratio on Selectivity in Our System with L = IPr[a]



entry	trial	Added IPr (mol %)	Pd:IPr	**1a** (%)	**1b** (%)	**1c** (%)	**1a** : **1b**	$\Delta\Delta G^{\ddagger}_{(C4\text{-}C2)}$ (kcal/mol)[b]
1	1	0	1 : 1	8.1	69	6	1 : 8.1	-1.2
2	2	0	1 : 1	8.6	70.5	6.4	1 : 8.6	-1.3
3	Average	0	1 : 1	8.4	69.8	6.2	1 : 8.3	-1.3
4	1	1.5	1 : 1.5	7.9	77.3	6.8	1 : 9.7	-1.3
5	2	1.5	1 : 1.5	7.6	70.9	6.6	1 : 9.3	-1.3
6	Average	1.5	1 : 1.5	7.8	74.1	6.7	1 : 9.5	-1.3
7	1	3.0	1 : 2	7.9	75.3	8.8	1 : 9.6	-1.3
8	2	3.0	1 : 2	8.0	74.5	5.7	1 : 9.3	-1.3
9	Average	3.0	1 : 2	8.0	74.9	7.2	1 : 9.4	-1.3
10	1	4.5	1 : 2.5	8.0	77.8	4.3	1 : 9.7	-1.3
11	2	4.5	1 : 2.5	8.5	79.4	4.1	1 : 9.3	-1.3
12	Average	4.5	1 : 2.5	8.3	78.6	4.2	1 : 9.5	-1.3
13	1	9.0	1 : 4	8.4	79.8	4.0	1 : 9.5	-1.3
14	2	9.0	1 : 4	8.6	78.7	4.9	1 : 9.1	-1.3
15	Average	9.0	1 : 4	8.5	79.3	4.5	1 : 9.3	-1.3

[a]Reactions were conducted according to the General Procedure for GC-scale reactions. GC yields calibrated against undecane as an internal standard. [b]Difference in free energies of activation for reaction at C4 versus C2 calculated from the experimental product ratios using the Eyring equation at 298.15 K.

Table B2. Influence of Pd:L Ratio on Selectivity in Our System with L = IMes[a]



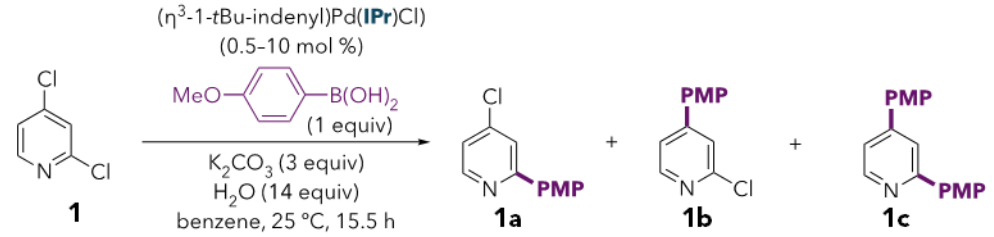
entry	trial	Added IMes (mol %)	Pd:IMes	**1a** (%)	**1b** (%)	**1c** (%)	**1a** : **1b**	$\Delta\Delta G^{\ddagger}_{(C4\text{-}C2)}$ (kcal/mol)[b]
1	1	0	1 : 1	21.1	35.3	2.7	1 : 1.7	-0.3
2	2	0	1 : 1	24.3	44.0	3.0	1 : 1.8	-0.3
3	Average	0	1 : 1	22.7	39.7	2.9	1 : 1.7	-0.3
4	1	1.5	1 : 1.5	26.3	54.0	4.9	1 : 2.1	-0.4
5	2	1.5	1 : 1.5	26.5	55.5	5.6	1 : 2.1	-0.4
6	Average	1.5	1 : 1.5	26.4	54.8	5.3	1 : 2.1	-0.4
7	1	3.0	1 : 2	27.1	55.0	5.0	1 : 2.0	-0.4
8	2	3.0	1 : 2	28.8	55.9	5.1	1 : 1.9	-0.4
9	Average	3.0	1 : 2	28.0	55.5	5.1	1 : 2.0	-0.4
10	1	4.5	1 : 2.5	26.6	54.3	3.8	1 : 2.0	-0.4
11	2	4.5	1 : 2.5	28.9	54.0	3.5	1 : 1.9	-0.4
12	Average	4.5	1 : 2.5	27.8	54.2	3.7	1 : 1.9	-0.4
13	1	9.0	1 : 4	24.8	48.4	2.5	1 : 2.0	-0.4
14	2	9.0	1 : 4	27.7	50.4	1.7	1 : 1.8	-0.3
15	Average	9.0	1 : 4	26.2	49.4	2.1	1 : 1.9	-0.4

[a]Reactions were conducted according to the General Procedure for GC-scale reactions. GC yields calibrated against undecane as an internal standard. [b]Difference in free energies of activation for reaction at C4 versus C2 calculated from the experimental product ratios using the Eyring equation at 298.15 K.

Effect of [Pd]

The effect of catalyst loading on on the selectivity of the Suzuki coupling using (η^3-1-^{t}Bu-indenyl)Pd(IPr)(Cl) and (η^3-1-^{t}Bu-indenyl)Pd(IMes)(Cl) was evaluated. If multinuclear species are involved in the C4-selective pathway, then changes in selectivity would be expected upon changing initial precatalyst concentration, since multinuclear species would form more rapidly at higher [Pd]. However, using (η^3-1-^{t}Bu-indenyl)Pd(IPr)(Cl), selectivity remains essentially constant from 0.5–10 mol % catalyst loading:

Table B3. Influence of [Pd] on Selectivity using IPr[a]

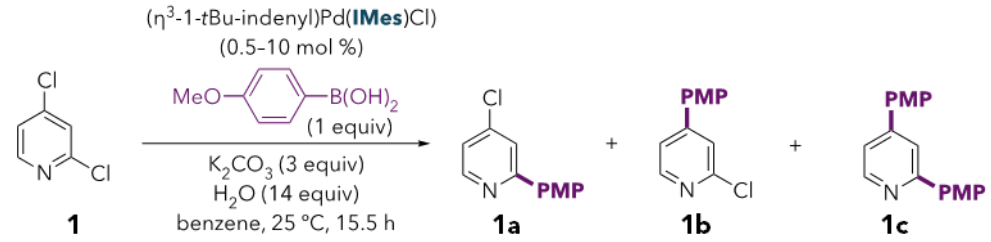


entry	trial	Pd mol %	**1a** (%)	**1b** (%)	**1c** (%)	**1a** : **1b**	$\Delta\Delta G^{\ddagger}_{(C4\text{-}C2)}$ (kcal/mol)[b]
1	1	0.5	4.2	32.9	1.1	1 : 7.8	
2	2	0.5	5.0	40.6	1.8	1 : 8.1	
3	Average	0.5	4.6	36.8	1.5	1 : 8.0	-1.2
4	1	1	4.4	36.0	1.5	1 : 8.2	
5	2	1	5.6	46.5	3.0	1 : 8.3	
6	Average	1	5.0	41.3	2.3	1 : 8.3	-1.3
7	1	3	8.1	69.0	6.0	1 : 8.5	
8	2	3	8.6	70.5	6.4	1 : 8.2	
9	Average	3	8.3	69.7	6.2	1 : 8.4	-1.3
10	1	5	8.6	69.9	4.3	1 : 8.1	
11	2	5	8.5	71.7	5.3	1 : 8.4	
12	Average	5	8.6	70.8	4.8	1 : 8.2	-1.2
13	1	10	8.0	67.4	3.8	1 : 8.4	
14	2	10	8.2	71.3	5.0	1 : 8.7	
15	Average	10	8.1	69.4	4.4	1 : 8.6	-1.3

[a]Reactions were conducted according to the General Procedure for GC-scale reactions. GC yields calibrated against undecane as an internal standard. [b]Difference in free energies of activation for reaction at C4 versus C2 calculated from the experimental product ratios using the Eyring equation at 298.15 K.

With (η^3-1-^{t}Bu-indenyl)Pd(IMes)(Cl) (below) the reaction is slightly less selective (more reaction at C2) at low catalyst loadings. This is consistent with our observation that, with Pd/IMes, more reaction at C2 is observed at higher 2,4-dichloropyridine concentration (*vide supra*). At lower catalyst loadings, the effective substrate:Pd concentration is higher, which can explain the slight influence of catalyst loading on selectivity.

Table B4. Influence of [Pd] on Selectivity using IMes[a]



entry	trial	Pd mol %	**1a** (%)	**1b** (%)	**1c** (%)	**1a** : **1b**	$\Delta\Delta G^{\ddagger}_{(C4\text{-}C2)}$ (kcal/mol)[b]
1	1	0.5	4.7	5.7	0.3	1 : 1.2	
2	2	0.5	4.4	5.9	0.2	1 : 1.3	
3	Average	0.5	4.6	5.8	0.3	1 : 1.3	-0.1
4	1	1	6.0	8.3	0.3	1 : 1.4	
5	2	1	10.1	14.0	0.4	1 : 1.4	
6	Average	1	8.1	11.2	0.4	1 : 1.4	-0.2
7	1	3	21.1	35.3	2.7	1 : 1.7	
8	2	3	24.3	44.0	3.0	1 : 1.8	
9	Average	3	22.7	39.6	2.9	1 : 1.7	-0.3
10	1	5	25.3	43.5	2.4	1 : 1.7	
11	2	5	29.2	48.7	3.3	1 : 1.7	
12	Average	5	27.3	46.1	2.9	1 : 1.7	-0.3
13	1	10	26.1	40.2	2.5	1 : 1.5	
14	2	10	24.5	43.4	2.5	1 : 1.8	
15	Average	10	25.3	41.8	2.5	1 : 1.7	-0.3

[a]Reactions were conducted according to the General Procedure for GC-scale reactions. GC yields calibrated against undecane as an internal standard. [b]Difference in free energies of activation for reaction at C4 versus C2 calculated from the experimental product ratios using the Eyring equation at 298.15 K.

B10. Computational Methods

Calculations were performed with Gaussian 16.[10] An ultrafine integration grid and the keyword 5d were used for all calculations. Geometry optimizations of stationary points were carried out in implicit solvent using the CPCM continuum solvation model[11] (THF) with MN15L,[12] LANL2DZ[13] for Pd, and 6-31+G(d) for all other atoms ("BS1"). Frequency analyses were carried out at the same level to evaluate the zero-point vibrational energy and thermal corrections at 298.15 K. The nature of the stationary points was determined in each case according to the appropriate number

of negative eigenvalues of the Hessian matrix. Forward and reverse intrinsic reaction coordinate (IRC) calculations were carried out on the optimized transition structures to ensure that the TSs indeed connect the appropriate reactants and products.[14] Multiple conformations were considered for all structures, and the lowest energy conformations are reported. It is worth noting that the lowest-energy π-complexes are not necessarily directly connected to the oxidative addition transition structures on the potential energy surfaces (i.e., in some cases the IRC calculations, in particular for reaction at C2, lead to different higher-energy π complexes than the lowest-energy structures reported). This factor is unimportant to the overall energetics, assuming that the barrier to interconverting π-complexes is low (e.g., by palladium ring-walking). Unless otherwise indicated, the final reported energies were obtained from single point energy calculations on the optimized geometries using MN15,[15] the CPCM solvation model (THF), and a larger basis set (SDD[16] for Pd and 6-311++G(2d,p) for all other atoms, "BS2"). Gibbs free energy values are reported after applying Cramer and Truhlar's anharmonic correction to frequencies that are less than 100 cm^{-1}.[17] All thermodynamic quantities were computed with the GoodVibes code[18] at 298.15 K, applying corrections for initial concentrations consistent with the optimized experimental conditions ([Pd] = 0.0075 *M* and [**2**] = 0.25 *M*). 3D images of optimized structures were generated with CYLview.[19] 3D images of molecular orbitals were generated with Avogadro.[20]

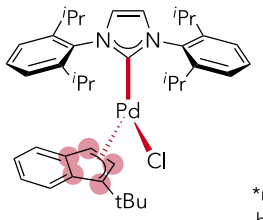
B11. Benchmarking Calculations and Method-Dependence of TS13a-IMes Energetics

Geometry Optimizations

The functional used for geometry optimizations (MN15L) was selected for several reasons. First, benchmarking calculations performed on (η^3-1-^{t}Bu-indenyl)Pd(NHC)(Cl) showed that, out

of four functionals (MN15L, M06, B3LYP, and B3LYP-D3BJ), MN15L gave the lowest root mean square deviation (RMSD) for several key bond distances when compared to the published crystal structure.[21]

Table B5. MN15L gives the lowest error in bond distances when compared to a crystal structure.



functional	RMSD*
MN15L	0.10
M06	0.15
B3LYP	0.35
B3LYP-D3BJ	0.27

*root mean squared error for the 7 distances highlighted in red (includes Pd–C distances for each of the carbons of the 5-membered ring)

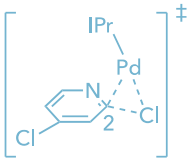
Furthermore, recent benchmarking studies on the performance of DFT functionals for computing bond energies of 3d transition metals concluded that "*...Overall, the best performing functionals are PW6B95, the MN15 and MN15-L functionals, and the double hybrid B2PLYP*."[22]

Finally, in recent work on related systems (oxidative addition of chloroaryl triflates at $Pd(0)L_n$), we found that MN15L gave the best correlation to experiment.[23] Based on all of these considerations, MN15L was chosen as the functional for geometry optimizations.

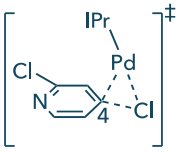
Single Point Energy Calculations

In choosing a functional for single-point energy calculations using a larger basis set, we first compared the predicted selectivity of Pd-IPr using four different functionals for single point energy calculations (MN15L, MN15, M06, and B3LYP-D3). All four functionals led to similar predictions (Table B15).

Table B6. Effect of Functional on Predicted C2:C4 Selectivity with Pd(IPr)



TS10a-IPr



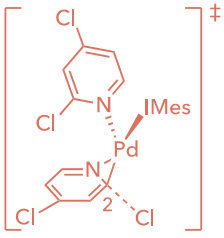
TS10b-IPr

functional	TS10a-IPr	TS10b-IPr	$\Delta\Delta G^{\ddagger}_{(\textbf{TS10b-TS10a})}$	predicted C2 : C4
MN15L	11.5	10.4	-1.1	1 : 6
MN15	13.8	12.1	-1.7	1 : 17
M06	10.0	8.7	-1.3	1 : 9
B3LYP-D3BJ	8.6	7.9	-0.7	1 : 3

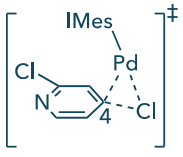
ΔG‡ values in kcal/mol, measured from preceding pi complex. Calculations at the [functional]/6-311++G(2d,p)/SDD(Pd) // MN15L/6-31+G(d)/LANL2DZ(Pd) level of theory.

We next evaluated several functionals for single point energy calculations on the lowest-energy TSs for reaction at C4 (monoligated, **TS10b-IMes**) and at C2 (bisligated, **TS13a-IMes**) using the ligand IMes. The numbers below are adjusted for initial concentration. Although the single point energy functional does not seem to matter very much when comparing **TS10a-IPr** and **TS10b-IPr** (Table B15 above), the relative energies of **TS10b-IMes** and **TS13a-IMes** were found to vary enormously with functional (Table B16). This is likely due to the crowdedness of **TS13a-IMes** and differences in how the functionals handle dispersion interactions.

Table B7. Effect of Functional on Predicted C2:C4 Selectivity with Pd(IMes)



TS13a-IMes



TS10b-IMes

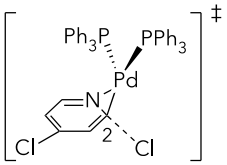
functional	$\Delta\Delta G^{\ddagger}_{(\textbf{TS10b-TS13a})}$	predicted C2 : C4
MN15L	+3.5	368 : 1
MN15	+1.4	11 : 1
M06L	+3.7	516 : 1
M06	-4.2	1 : 1,199
B3LYP-D3BJ	+7.1	160,277 : 1
wB97XD	+3.6	436 : 1

ΔΔG‡ values in kcal/mol. Calculations at the [functional]/6-311++G(2d,p)/SDD(Pd) // MN15L/6-31+G(d)/LANL2DZ(Pd) level of theory.

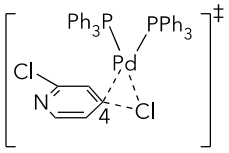
As shown above, most functionals predict that, with IMes, the C2 product should be favored, although the predicted selectivies with those functionals span five orders of magnitude. On the other hand, M06 predicts that the C4 product should be exclusively observed. Overall, the selectivity predicted with the hybrid functional MN15 provides results that are most consistent with the near 1:1 selectivity observed experimentally.

We next further evaluated some of these functionals in another crowded system where dispersion interactions would also be important. The energies of the minimum-energy transition structures for reaction at C2 and C4 with $Pd(PPh_3)_2$ were calculated (Table B18). Experimentally, the use of PPh_3 leads exclusively to the C2-functionalized product. As shown below, both MN15 and M06 provide predictions consistent with experiment for this system. However, MN15L fails to predict the very high experimental selectivity (predicted C2:C4 ~ 13:1, experimental >99:1).

Table B8. Effect of Functional on Predicted C2:C4 Selectivity with $Pd(PPh_3)_2$.



C2



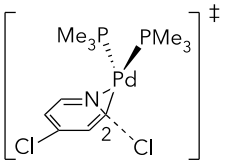
C4

functional	$\Delta\Delta G^{\ddagger}_{(\mathbf{C4-C2})}$	predicted C2 : C4
MN15L	+1.5	13 : 1
MN15	+5.0	4,628 : 1
M06	+4.2	1,199 : 1

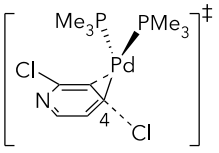
ΔΔG‡ values in kcal/mol. Calculations at the [functional]/6-311++G(2d,p)/SDD(Pd) // MN15L/6-31+G(d)/LANL2DZ(Pd) level of theory.

Notably, MN15 and MN15L give identical predictions for selectivity with $Pd(PMe_3)_2$, a much smaller system in which dispersion interactions are significantly less important (Table B19). The predicted ratio of C2:C4 = 3:1 is similar to the experimentally observed selectivity of ~11:1.

Table B9. Effect of Functional on Predicted C2:C4 Selectivity with $Pd(PMe_3)_2$.



C2



C4

functional	$\Delta\Delta G^{\ddagger}_{(\mathbf{C4-C2})}$	predicted C2 : C4
MN15L	+0.6	3 : 1
MN15	+0.6	3 : 1

ΔΔG‡ values in kcal/mol. Calculations at the [functional]/6-311++G(2d,p)/SDD(Pd) // MN15L/6-31+G(d)/LANL2DZ(Pd) level of theory.

Based on all of these benchmarking calculations, MN15 was chosen for the single point energy calculations in Chapter 3, and is expected to provide the best accuracy especially when comparing structures with very different degrees of crowdedness.

B12. Frontier Molecular Orbital Calculations (Figure 3.1, Figure 3.2, Scheme 3.3B)

MO calculations were performed at the CPCM(THF)-MN15L/BS1 level of theory using the "pop=regular" keyword. The percent contribution of individual atoms to a given molecular orbital was calculated from the molecular orbital coefficients provided in the Gaussian output file. For a given MO, the absolute values of the coefficients for each atomic orbital of the carbon in question were summed. This sum was divided by the sum of the absolute values of the coefficients for each atomic orbital of all atoms in the molecule, and the result was multiplied by 100% to arrive at the % contribution of an individual carbon to that MO.

Graphical depictions of the LUMOs of **45**, **1, 29**, and **24** from Scheme 3.3B are provided in Figure B3 below. Figure B3 illustrates the HOMOs of monoligated Pd(IPr) and bisligated Pd(IPr)(2,4-dichloropyridine). The latter is distorted into the bent geometry that it adopts during oxidative addition (structure was obtained from **TS13b-IPr**). Analogous to the simple model

complexes $Pd(PMe_3)$ and $Pd(PMe_3)_2$, the HOMO of monoligated Pd(IPr) has σ-symmetry while the HOMO of bisligated Pd(IPr)(2,4-dichloropyridine) has π-symmetry.

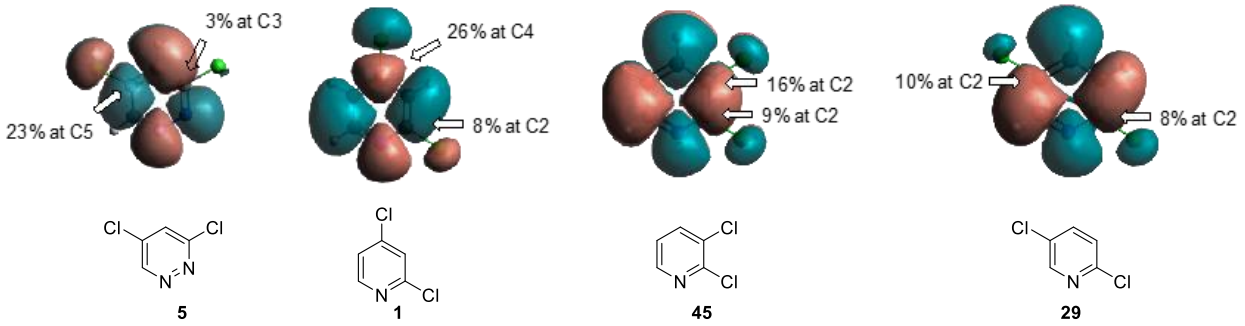


Figure B2. LUMOs of dichloroheteroarene substrates from Figure 3.2.

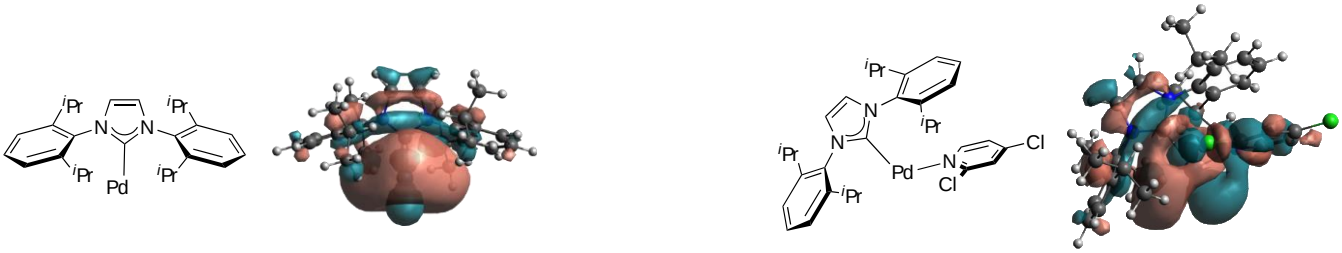


Figure B3. HOMOs of mono and bisligated Pd(IPr) complexes.

B13. Higher Energy Transition Structures with Pd/IPr

With monoligated Pd(IPr), only 3-centered mechanisms were located for oxidative addition at C4 of **1** (**TS10b-IPr**). Three different conformations were found, and the lowest energy one is reported in the manuscript. Attempts to find displacement mechanisms were unsuccessful, as the geometries optimized to 3-centered concerted structures instead. For reaction at C2, three different conformations of a 3-centered mechanism were located, and the lowest energy one is reported in the manuscript (**TS10a-IPr**). In addition, one structure representing a displacement-type

mechanism was found (**STS10a2-IPr**, below). Its energy is higher than any of the conformations of the 3-centered mechanism ($\Delta G‡$ = 17.8 kcal/mol relative to π-complex **9-IPr**). Seven conformations of bisligated transition structures were located each for reaction at both C2 and C4, and the lowest energy conformation for reaction at each site is reported in the manuscript (**TS13a-IPr** and **TS13b-IPr**). All of the bisligated conformations represent displacement mechanisms, and no 3-centered concerted structures could be found at the level of theory used in this work.

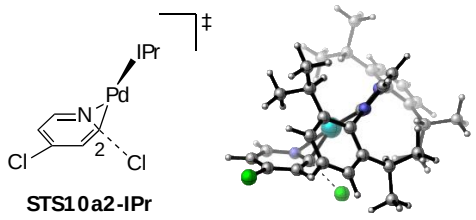


Figure B4. Structure of a higher-energy nucleophilic displacement mechanism for oxidative addition of C2-Cl at monoligated Pd(IPr).

B14. Higher Energy Pd(0) Structures with IPr and IMes

As shown below, the lowest calculated coordination mode for Pd(0)(NHC) is the pre-oxidative addition π-complex.

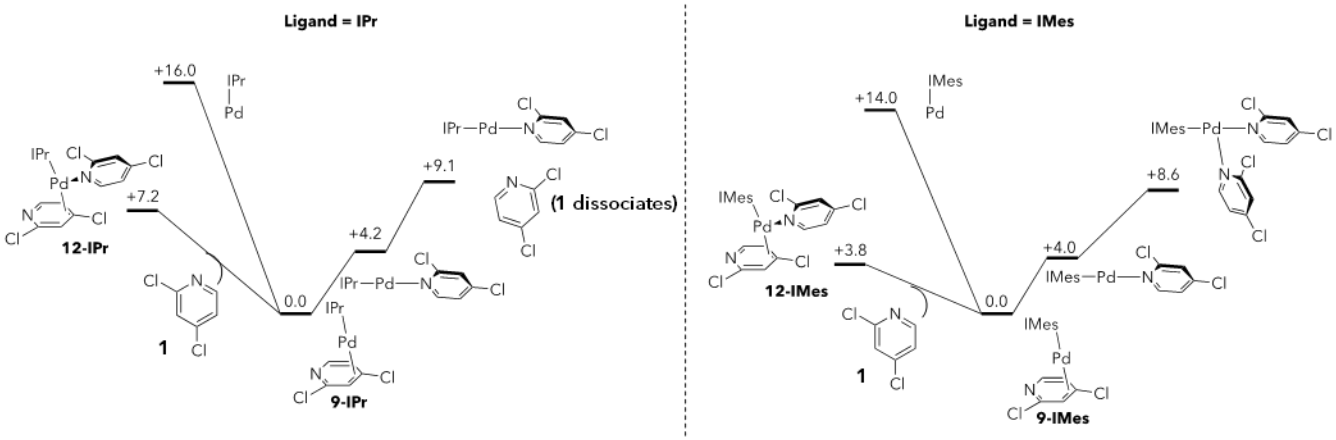


Figure B5. Other coordination environments for Pd(NHC) are higher-energy than Pd(NHC)(η^2-**2**).

B15. Discussion About Selectivity-Influencing Factors Beyond PdL vs. PdL_2

Although L_2Pd vs. LPd seems to be the critical determining factor between a C2 vs C4 preference, there are also more subtle factors that influence the magnitude of that preference. Additional calculations were completed with phosphine ligands involving oxidative addition at monoligated $Pd(PMe_3)$, $Pd(PMe_3)_2$, $Pd(PPh_3)$, $Pd(PPh_3)_2$, and $Pd(P^tBu_3)$. Reaction at PdL is unlikely for PMe_3 and probably also PPh_3 (but see ref 24, in which monoligated $Pd(PPh_3)$ is implicated during oxidative addition of PhBr). However, our calculations on (hypothetical) PdL illustrate some interesting differences between triarylphosphines, trialkylphosphines, and *N*-heterocyclic carbene ligands. The more nuanced factors that influence the magnitude of C2 vs C4 preference seem to include:

(1) The nucleophilicity of PdL. This is related to the σ-donicity of L, and is somewhat correlated with the energy of the HOMO for PdL. As shown in the table below, the predicted C4 selectivity of PdL trends with its HOMO energy.

(2) Whether a concerted or displacement mechanism is favored at C4 for PdL_2. This seems to be related to both the sterics and the electronics of L, and is a topic of ongoing detailed research in our group. Maseras et al. have shown that the mechanism of oxidative addition of PhBr varies with ligand,[25] and similarly we have found that the lowest-energy mechanism of oxidative addition at C4—Cl of 2,4-dichloropyridine varies with ligand. For $Pd(PMe_3)_2$ and $Pd(PPh_3)_2$, a displacement mechanism is favored for reaction at C2—Cl. However, although $Pd(PMe_3)_2$ also favors a displacement mechanism at C4—Cl, $Pd(PPh_3)_2$ reacts through a concerted mechanism at this position. This mechanistic

difference may explain the exceedingly high C2-selectivity of $Pd(PPh_3)_2$, although the reason for this mechanistic difference is still under investigation.

Table B10. Correlation between Calculated Selectivity of PdL and HOMO Energy.

PdL	calc. $\Delta\Delta G_{(C4-C2)}^{\ddagger}$ (considering only PdL, kcal/mol)[a]	calc. selectivity (considering only PdL, C2 : C4)[a]	exp. selectivity of PdL (C2 : C4)	HOMO (eV)
$Pd(PPh_3)$	+0.3	2 : 1	N/A[b]	-0.218[c]
$Pd(P^tBu_3)$	-0.9	1 : 5	1 : 2	-0.215
$Pd(PMe_3)$	-1.4	1 : 11	N/A[b]	-0.208
Pd(IPr)	-1.7	1 : 18	1 : 10	-0.207
Pd(IMes)	-2.3	1 : 49	N/A[b]	-0.206

[a]Calculations performed at the CPCM(THF)-MN15/6-311++G(2d,p)/SDD(Pd) //CPCM(THF)-MN15L-6-31+G(d)/LANL2DZ(Pd) level of theory. [b]Under experimental conditions, reaction most likely occurs partly or completely through a bisligated Pd species, so it is not possible to assess the experimental selectivity of monoligated PdL. [c]Geometry optimization of $Pd(PPh_3)$ failed to converge, so a single point energy calculation was performed on a $Pd(PPh_3)$ fragment taken from a $Pd(PPh_3)$(**1**) π-complex.

Table B11. Comparison of Preferred Mechanisms for Oxidative Addition with PdL_2 (L = PMe_3 or PPh_3).

PdL_2	mechanism at C2	mechanism at C4	calc. $\Delta\Delta G_{(C4-C2)}^{\ddagger}$ (considering only PdL_2, kcal/mol)	calc. selectivity (considering only PdL_2, C2 : C4)	exp. selectivity of PdL_2 (C2 : C4)
$Pd(PMe_3)_2$	displacement	displacement	+0.6	3 : 1	11 : 1
$Pd(PPh_3)_2$	displacement	concerted	+5.0	436 : 1	>99 : 1

Calculations performed at the CPCM(THF)-MN15/6-311++G(2d,p)/SDD(Pd)//CPCM(THF)-MN15L-6 31+G(d)/LANL2DZ(Pd) level of theory.

The partial charges at Pd were computed for **TS13a-IPr** and **TS13b-IPr**. Palladium is *less positive* during the SN-type mechanism at C2 (**TS13a-IPr**) compared to at C4 (**TS13b-IPr**). This is consistent with nitrogen being more effective than carbon at stabilizing the building positive charge at Pd, and suggests that the reason for conventional C2-selectivity is more complicated than a simple comparison of C2—Cl vs C4—Cl bond strengths. This observation is consistent with a

recent report by Leitch et al., in which conventional selectivity was found to correlate with more positive electrostatic potentials at the *ipso* carbon and with more negative potentials at an *ortho* carbon.[26]

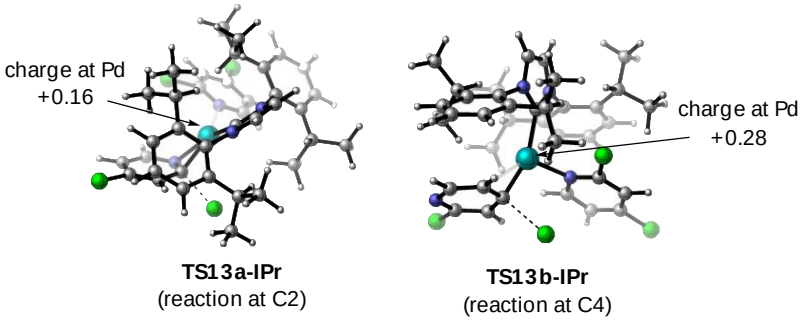


Figure B6. Partial charges at Pd during displacement-type oxidative addition at C2 versus C4 with Pd(IPr)(**1**).

B16. Energies, Entropies, and Lowest Frequencies of Minimum Energy Structures

Table B12. Energies, Entropies, and Lowest Frequencies of Minimum Energy Structures[a]

Structure	E_{elec} (Hartree)	E_{elec} + ZPE (Hartree)	H (Hartree)	S (cal mol^{-1} K^{-1})	G[b] (Hartree)	$G_{corrected}$[c] (Hartree)	Lowest freq. (cm^{-1})	# of imag freq.
TS7a	-1280.102315	-1279.898129	-1279.881899	126.1	-1279.941812	-1279.939842	-181.5	1
TS7b	-1280.098858	-1279.894876	-1279.878312	130.7	-1279.940397	-1279.936888	-235.7	1
TS7c	-1280.084978	-1279.881161	-1279.864742	126.9	-1279.92503	-1279.923424	-221.5	1
TS8a	-1741.005607	-1740.687459	-1740.663099	163.3	-1740.740705	-1740.737083	-281.9	1
TS8b	-1741.011908	-1740.693341	-1740.669092	162.4	-1740.746256	-1740.743024	-201.9	1
2	-1167.119851	-1167.050102	-1167.042657	82.9	-1167.08032	-1167.08032	161.6	0
9-IPr	-2453.730783	-2453.090513	-2453.049859	236.9	-2453.164034	-2453.155668	17.7	0
TS10a-IPr	-2453.707733	-2453.068584	-2453.028051	238.4	-2453.142927	-2453.133659	-135.7	1
TS10b-IPr	-2453.710919	-2453.071466	-2453.031003	238.0	-2453.145702	-2453.13641	-67.2	1
11a-IPr	-2453.759276	-2453.117221	-2453.076806	235.8	-2453.19044	-2453.182122	18.6	0
11b-IPr	-2453.761652	-2453.119249	-2453.07897	234.4	-2453.191948	-2453.184179	20.7	0
12-IPr	-3620.866219	-3620.154355	-3620.106041	272.8	-3620.237269	-3620.226248	13.0	0
TS13a-IPr	-3620.849928	-3620.138432	-3620.090361	274.3	-3620.222277	-3620.210275	-210.2	1
TS13b-IPr	-3620.838787	-3620.127124	-3620.079188	268.4	-3620.208319	-3620.199264	-97.8	1
14a-IPr	-3620.887865	-3620.175356	-3620.126318	281.3	-3620.261591	-3620.247962	12.9	0
14b-IPr	-3620.893594	-3620.179807	-3620.131447	273.8	-3620.263159	-3620.252016	14.3	0
9-IMes	-2218.108449	-2217.641368	-2217.606774	218.2	-2217.712036	-2217.701551	15.6	0
TS10a-IMes	-2218.086513	-2217.61977	-2217.585916	211.1	-2217.687806	-2217.679412	-125.2	1
TS10b-IMes	-2218.090094	-2217.623379	-2217.589502	213.0	-2217.692295	-2217.683132	-69.1	1
11a-IMes	-2218.146487	-2217.677853	-2217.643676	212.7	-2217.746342	-2217.73791	15.1	0
11b-IMes	-2218.1467	-2217.678158	-2217.643855	214.0	-2217.747152	-2217.738397	18.1	0
12-IMes	-3385.24802	-3384.710021	-3384.667679	250.7	-3384.788405	-3384.777506	18.6	0
TS13a-IMes	-3385.236174	-3384.698285	-3384.656419	248.5	-3384.776068	-3384.76572	-219.3	1
TS13b-IMes	-3385.225136	-3384.686139	-3384.644748	243.6	-3384.762106	-3384.753188	-138.5	1
14a-IMes	-3385.299441	-3384.757995	-3384.71694	238.1	-3384.831658	-3384.824454	22.6	0
14b-IMes	-3385.279344	-3384.738809	-3384.697088	247.2	-3384.816127	-3384.805721	10.2	0
9-PtBu3	-2109.127974	-2108.686909	-2108.658464	177.2	-2108.744242	-2108.74063	25.2	0
TS10a-PtBu3	-2109.107486	-2108.666821	-2108.638888	175.0	-2108.723628	-2108.720074	-94.2	1
TS10b-PtBu3	-2109.109484	-2108.66843	-2108.640664	172.9	-2108.724422	-2108.721519	-34.0	1
11a-PtBu3	-2109.149996	-2108.707225	-2108.678913	176.0	-2108.764127	-2108.760791	22.1	0
11b-PtBu3	-2109.149804	-2108.705979	-2108.677991	174.0	-2108.762247	-2108.759133	31.5	0

Table B12 Continued

12-PtBu3	-3276.258264	-3275.746426	-3275.709597	220.8	-3275.816112	-3275.807834	15.9	0
TS13a-PtBu3	-3276.236964	-3275.72466	-3275.688599	216.5	-3275.793088	-3275.785727	-218.9	1
TS13b-PtBu3	-3276.221176	-3275.709307	-3275.673113	216.2	-3275.77742	-3275.770766	-43.5	1
14a-PtBu3	-3276.282445	-3275.767875	-3275.731461	216.8	-3275.836078	-3275.829157	14.3	0
14b-PtBu3	-3276.280225	-3275.76592	-3275.72932	220.2	-3275.835525	-3275.827204	16.9	0

[a]Energy values calculated at the CPCM(THF)-MN15/BS2//CPCM(THF)-MN15L/BS1 level of theory. 1 Hartree = 627.51 kcal mol^{-1}. Thermal corrections at 298.15 K based on [Pd] = 0.0075 M and [**1**] = 0.25 M. [b]Solvent-corrected free energy given by $G = E_{elec} + G_{corr}$, where G_{corr} is the thermal correction to Gibbs free energy. [c]Solvent-corrected free energy given by $G = E_{elec} + G_{corr*}$, where G_{corr*} is the thermal correction to Gibbs free energy obtained after applying Cramer and Truhlar's anharmonic correction.[17]

B17. References

1. Norman, J. P.; Larson, N. G.; Entz, E. D.; Neufeldt, S. R. *J. Org. Chem.* **2022**, *87*, 7414-7421.

2. (a) Amatore, C.; Jutand, A.; M'Barki, M. A. *Organometallics* **1992**, *11*, 3009-3013; (b) Amatore, C.; Carré, E.; Jutand, A.; M'Barki, M. A. *Organometallics* **1995**, *14*, 1818-1826; (c) Wagschal, S.; Perego, L. A.; Simon, A.; Franco-Espejo, A.; Tocqueville, C.; Albaneze-Walker, J.; Jutand, A.; Grimaud, L. *Chem.-Eur. J.* **2019**, *25*, 6980-6987.

3. (a) Mitchell, E. A.; Jessop, P. G.; Baird, M. C. A *Organometallics* **2009**, *28*, 6732-6738; (b) Barrios-Landeros, F.; Carrow, B. P.; Hartwig, J. F. *J. Am. Chem. Soc.* **2009**, *131*, 8141-8154; (c) McMullin, C. L.; Jover, J.; Harvey, J. N.; Fey, N. *Dalton Trans.* **2010**, *39*, 10833-10836.

4. Gensch, T.; dos Passos Gomes, G.; Friederich, P.; Peters, E.; Gaudin, T.; Pollice, R.; Jorner, K.; Nigam, A.; D'Addario, M. L.; Sigman, M. S.; Aspuru-Guzik, A. *J. Am. Chem. Soc.* **2022**, *144*, 1205-1217.

5. Clavier, H.; Nolan, S. P. *Chem. Commun.* **2010**, *46*, 841-861.

6. Dai, X.; Chen, Y.; Garrell, S.; Liu, H.; Zhang, L.-K.; Palani, A.; Hughes, G.; Nargund, R. *J. Org. Chem.* **2013**, *78*, 7758-7763.

7. Gao, Q.; Yan, H.; Wu, M.; Sun, J.; Yan, X.; Wu, A. *Org. Biomol. Chem.* **2018**, 16, 2342-2348.

8. Petersen, T. P.; Becker, M. R.; Knochel, P. *Angew. Chem. Int. Ed.* **2014**, *53*, 7933-7937.

9. (a) Scott, N. W. J.; Ford, M. J.; Jeddi, N.; Eyles, A.; Simon, L.; Whitwood, A. C.; Tanner, T.; Willans, C. E.; Fairlamb, I. J. S. *J. Am. Chem. Soc.* **2021**, *143*, 9682-9693. (b) Appleby, K. M.; Dzotsi, E.; Scott, N. W. J.; Dexin, G.; Jeddi, N.; Whitwood, A. C.; Pridmore, N. E.; Hart, S.; Duckett, S. B.; Fairlamb, I. J. S. *Organometallics* **2021**, *40*, 3560-3570.

10. Gaussian 16, Revision C.01, Frisch, M. J.; Trucks, G. W.; Schlegel, H. B.; Scuseria, G. E.; Robb, M. A.; Cheeseman, J. R.; Scalmani, G.; Barone, V.; Petersson, G. A.; Nakatsuji, H.; Li, X.; Caricato, M.; Marenich, A. V.; Bloino, J.; Janesko, B. G.; Gomperts, R.; Mennucci, B.; Hratchian, H. P.; Ortiz, J. V.; Izmaylov, A. F.; Sonnenberg, J. L.; Williams-Young, D.; Ding, F.; Lipparini, F.; Egidi, F.; Goings, J.; Peng, B.; Petrone, A.; Henderson, T.; Ranasinghe, D.; Zakrzewski, V. G.; Gao, J.; Rega, N.; Zheng, G.; Liang, W.; Hada, M.; Ehara, M.; Toyota, K.; Fukuda, R.; Hasegawa, J.; Ishida, M.; Nakajima, T.; Honda, Y.; Kitao, O.; Nakai, H.; Vreven, T.; Throssell, K.; Montgomery, J. A., Jr.; Peralta, J. E.; Ogliaro, F.; Bearpark, M. J.; Heyd, J. J.; Brothers, E. N.; Kudin, K. N.; Staroverov, V. N.;

Keith, T. A.; Kobayashi, R.; Normand, J.; Raghavachari, K.; Rendell, A. P.; Burant, J. C.; Iyengar, S. S.; Tomasi, J.; Cossi, M.; Millam, J. M.; Klene, M.; Adamo, C.; Cammi, R.; Ochterski, J. W.; Martin, R. L.; Morokuma, K.; Farkas, O.; Foresman, J. B.; Fox, D. J. Gaussian, Inc., Wallingford CT, 2016.

11. Cossi, M.; Rega, N.; Scalmani, G.; Barone, V. *J. Comput. Chem.* **2003**, *24*, 669-681.

12. Yu, H. S.; He, X.; Truhlar, D. G. MN15-L: *J. Chem. Theory Comput.* **2016**, *12*, 1280-1293.

13. Hay, P. J.; Wadt, W. R. Ab initio effective core potentials for molecular calculations. Potentials for K to Au including the outermost core orbitals. *J. Chem. Phys.* **1985**, *82*, 299-310.

14. (a) Gonzalez, C.; Schlegel, H. B. *J. Chem. Phys.* **1989**, *90*, 2154-2161; (b) Gonzalez, C.; Schlegel, H.B. *J. Phys. Chem.* **1990**, *94*, 5523-5527; (c) Fukui, K. *Acc. Chem. Res.* **1981**, *14*, 363-368.

15. Yu, H. S.; He, X.; Li, S. L.; Truhlar, D. G. *Chem. Sci.* **2016**, *7*, 5032-5051.

16. (a) Dolg, M.; Wedig, U.; Stoll, H.; Preuss, H. *J. Chem. Phys.* **1987**, *86*, 866-872; (b) Andrae, D.; Haussermann, U.; Dolg, M.; Stoll, H. Preuss, H. *Theor. Chim. Acta* **1990**, *77*, 123-141.

17. Ribeiro, R. F.; Marenich, A. V.; Cramer, C. J.; Truhlar, D. G. *J. Phys. Chem. B.* **2011**, *115*, 14556-14562.

18. G. Luchini, J. V. Alegre- Requena, I. Funes-Ardoiz and R. S. Paton, GoodVibes: Automated Thermochemistry for Heterogeneous Computational Chemistry Data, *F1000Research*, **2020**, *9*, 291

19. CYLview20; Legault, C. Y., Université de Sherbrooke, 2020 (http://www.cylview.org)

20. (a) Avogadro: an open-source molecular builder and visualization tool. Version 1. http://avogadro.cc/ (b) Hanwell, M. D.; Curtis, D. E.; Lonie, D. C.; Vandermeersch, T.; Zurek, E.; Hutchison; G. R. *J. Cheminformatics* **2012**, *4*, 17.

21. Melvin, P. R.; Nova, A.; Balcells, D.; Dai, W.; Hazari, N.; Hruszkewycz, D. P.; Shah, H. P.; Tudge, M. T. *ACS Catal.* **2015**, *5*, 3680-3688.

22. Moltved, K. A.; Kepp, K. P. *J. Chem. Theory Comput.* **2018**, *14*, 3479-3492.

23. Elias, E. K.; Rehbein, S. M.; Neufeldt, S. R. *Chem. Sci.* **2022**, *13*, 1618-1628.

24. Joshi, C.; Macharia, J. M.; Izzo, J. A.; Wambua, V.; Kim, S.; Hirschi, J. S.; Vetticatt, M. J. *ACS Catal.* **2022**, *12*, 2959-2966.

25. Besora, M.; Maseras, F. *Dalton Trans.* **2019**, *48*, 16242-16248.

26. Lu, J.; Donnecke, S.; Paci, I.; Leitch, D. C. *Chem. Sci.* **2022**, *13*, 3477-3488.

APPENDIX C

CHAPTER FOUR EXPERIMENTAL

C1. General Materials and Methods:

NMR spectra were recorded at 298 K on a Bruker DRX 500 MHz (500.233 MHz for ^{1}H, 125.795 MHz for ^{13}C, 470.639 MHz for ^{19}F) or a Bruker Ascend 400 MHz (400.130 MHz for ^{1}H NMR, 100.613 for ^{13}C). ^{1}H and ^{13}C NMR chemical shifts are reported in parts per million (ppm) relative to TMS, with the residual solvent peak used as an internal reference [^{1}H NMR: $CHCl_3$ (7.26 ppm)]. Multiplicities are reported as follows: singlet (s), doublet (d), doublet of doublets (dd), and multiplet (m). GC data were collected using a Shimadzu GC-2010 Plus with a flame ionization detector equipped with a SH-Rxi-5ms capillary column (15 m x 0.25 mm ID x 0.25 μm df). GCMS data were collected with a Shimadzu GC-2030 paired with a Shimadzu GCMS-QP2020 NX and equipped with a SH-Rxi-5ms capillary column (30 m x 0.25 mm ID x 0.25 μm df). All commercially-obtained chemicals were used as received. (η^3-1-^{t}Bu-indenyl)Pd(IPent)(Cl) was obtained from Umicore. 2,4-Dichloropyrimidine, 4-chloro-2-(methylthio)pyrimidine, phenylboronic acid, pentanethiol, Cu(I) thiophene-2-carboxylate, and Cu(I) 3-methylsalicylate were obtained from Ambeed. Other aryl boronic acids and alkylthio-pyrimidines were obtained from Ambeed or Oakwood chemical. Triphenylphosphine, tri-*tert*-butylphosphine, and 1,3,5-triaza-7-phosphaadamantane were obtained from Alfa Aesar. All other phosphine and imidazolium ligands were obtained from Ambeed, Oakwood Chemical, or Strem Chemical. $Pd(CH_2SiMe_3)_2(cod)$ was stored at -25 °C prior to use (note: this complex decomposes within minutes at ambient temperatures). THF, toluene, acetonitrile, potassium carbonate, and potassium phosphate tribasic were obtained from Fisher Scientific. Deuterochloroform was obtained from Cambridge Isotopes and stored over molecular sieves prior to use. Manual flash column chromatography was performed on SiliCycle silica gel 60 (40-63 μm particle size) and thin layer

chromatography was performed on SiliCycle TLC plates pre-coated with extra hard silica gel 60 F254.

C2. General Procedure for Suzuki-Miyaura Couplings with 2,4-Dichloropyrimidine (Table 4.1)

Inside an N_2-atmosphere glovebox, the specified solids required in the Suzuki-Miyaura reactions were added to a 1-dram reaction vial in order of increasing mass: palladium catalyst (palladium source and free ligand) or Pd precatalyst, 2,4-dichloropyrimidine (14.9 mg, 0.1 mmol, 1 equiv), phenylboronic acid (12.8 mg, 0.105 mmol, 1.05 equiv), potassium carbonate or potassium phosphate tribasic, and then a stir bar. THF, (0.4 mL, 0.25 M) was added via 1-mL syringe. Outside the glovebox, N_2-sparged deionized water (9 μL, 5 equiv) was administered through the septum screwcap via 25-μL syringe, and the puncture was sealed with vacuum grease. The reaction was stirred vigorously at ambient temperature for 14 h. Reaction vials were opened to air, diluted with ~3.5 mL ethyl acetate, and a dodecane internal standard (7.5 μL) was added via 25-μL syringe. Vials were sealed and shaken, then an aliquot (~200 μL) was collected for GC analysis.

C3. General Procedure for Liebeskind-Srogl Couplings with 4-Chloro-(2-methylthio)-pyrimidine (Tables 4.2 and 4.3)

The specified solids required in the Liebeskind-Srogl Coupling were added to a 1-dram reaction vial under air in the order: Pd(II) precatalyst (when specified), phenylboronic acid, then the Cu(I) carboxylate, followed by a stir bar. When specified, Pd(0) catalyst, $Pd(CH_2SiMe_3)_2(cod)$, and unbound phosphine, were added to reaction vials inside an N_2-atmosphere glovebox, followed by 4-chloro-2-(methylthio)pyrimidine (16.1 mg, 0.1 mmol, 1 equiv) administered via 1-mL syringe as a stock solution in the specified reaction solvent. Reactions lacking air-sensitive

reagents were treated outside the glovebox with 4-chloro-2-(methylthio)pyrimidine (16.1 mg, 0.1 mmol, 1 equiv) administered via 1-mL syringe as a stock solution in the specified reaction solvent. A septum cap equipped with an argon-ingas and outgassing needle was fastened to the 1-dram reaction vial and the headspace was sparged for 30-45 seconds. With continuous sparging, the vial was unscrewed from the septum cap and lowered while the cap was replaced with a PTFE-lined cap. The reaction was stirred vigorously under argon at the specified temperature for the specified duration. The reaction vial was opened to air, quenched with ~1.5 mL ethyl acetate, and an undecane internal standard (7.5 μL) was added via 25-μL syringe. The contents of the reaction vial were treated with ~1.5 mL saturated, aqueous sodium carbonate solution, and the sealed vial was shaken vigorously. An aliquot (~100 μL) was collected from the supernatant, diluted in ethyl acetate, and filtered through a short plug of magnesium sulfate layered over Celite, then analyzed by GC.

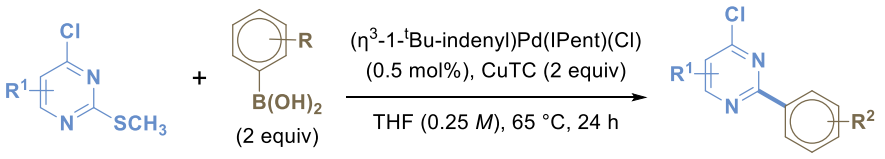
C4. Methods and Analysis of Reactions in Scheme 4.7

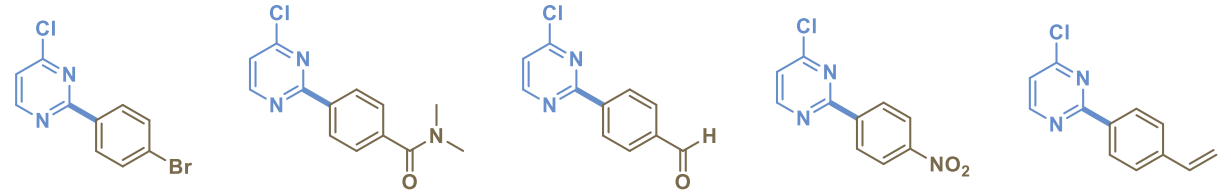
Procedure

All solids were weighed by order of increasing mass into 1-dram reaction vials followed by stir bars. Vials were treated one at a time during addition of liquid(s): THF was dispensed via 1-mL syringe into the reaction vial followed promptly by 4-chloro-2-(methylthio)pyrimidine substrate (if liquid) using a 25-μL syringe. The vial was attached to a septum screwcap containing a 24-gauge N_2-ingas and outgas needle. The vial headspace was sparged for 30 sec—1 min, approximately, prior to quick removal and recapping with a PTF-lined screwcap under continuous N_2-sparging. Sealed vials were stirred at 65 °C for 24 h. Vials were opened to air and treated with a stock solution of 1,3,5-trimethoxybenzene (TMB) in ethyl acetate (4.5 mg, 0.33 equiv TMB per

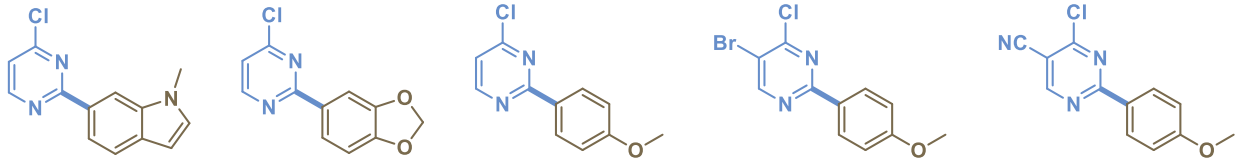
1.5 mL), then vials were recapped and briefly shaken. Approximately 2 mL saturated Na_2CO_3 (aq.) was added to each vial. Vials were shaken once more, and the phases were allowed to separate. An aliquot was collected from the organic layer and filtered through Celite for GC/GCMS analysis. The remaining supernatant was collected via pipette and pressurized through a filter pipette containing layered cotton (bottom), Celite (middle), and anhydrous $MgSO_4$ (top). The filtrate was concentrated under reduced pressure, taken up in deuterochloroform, and analyzed via ^{1}H NMR; yields were calculated based on peak integrations relative to TMB. Reactions were performed in duplicate and are provided in Table C1.

Table C1. Experimental m/z and ^{1}H NMR Yields for C2-Coupled Products in Scheme 4.7

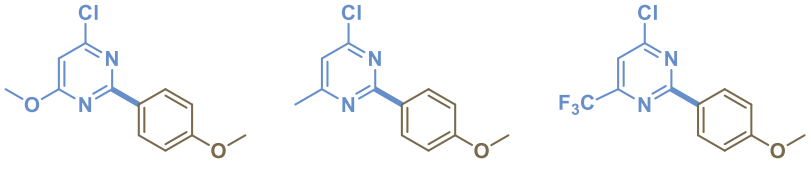




49 (80%) **50** (84%) **51** (94%) **52** (86%) **53** (92%)



54 (59%) **55** (88%) **56** (87%) **57** (76%) **58** (37%)



59 (76%) **60** (86%) **61** (59%)

Table C1 Continued

Product	MW	m/z	% yield (1)	% yield (2)
A	269.5	270	80	79
B	261.7	260	83	84
C	218.6	217	95	92
D	235.6	235	88	84
E	216.6	216	95	89
F	243.7	243	62	55
G	234.6	234	88	87
H	220.7	220	85	89
I	299.6	300	75	76
J	245.7	245	37	36
K	250.7	250	74	78
L	234.7	234	81	90
M	288.7	288	58	59

C5. Description of the Two-Step Protocol in Scheme 4.8

Thiolation protocol

(η^3-1-^{t}Bu-indenyl)Pd(IPent)(Cl) (1.6 mg, 0.002 mmol, 0.02 equiv) was weighed directly into a 1-dram reaction vial, followed by 2,4-dichloropyrimidine (14.9 mg, 0.1 mmol, 1 equiv) and K_3PO_4 (42.5 mg, 0.2 mmol, 2 equiv) using weigh paper, then a stir bar. Inside an N_2-atmosphere glovebox, acetonitrile was added via 1-mL syringe, and the reaction vial was tightly sealed. Outside the glovebox, the vial was submerged (up to the shoulder) in a liquid nitrogen bath for 30 seconds, opened, treated with pentanethiol (12.4 μL, 0.1 mmol, 1 equiv), then the headspace was sparged with argon and tightly sealed using a PTFE-lined screwcap. Vials were transferred to an ice bath and stirring was continued for 3 h.

Liebeskind-Srogl protocol

After thiolation, the vial was opened to air and diluted with 0.5 mL acetonitrile. The suspension was filtered through Celite (four rinses of 0.2 mL acetonitrile were used to complete the transfer of material to the Celite filter), then Celite was washed with four additional rinses of

0.2 mL acetonitrile post-filtration. The filtrate was concentrated under reduced pressure using a rotary evaporator, the residue was dissolved in THF, and a stir bar was added to this solution. (η^3-1-^{t}Bu-indenyl)Pd(IPent)(Cl) (0.4 mg, 0.0005 mmol, 0.005 equiv), Cu(I) thiophene-2-carboxylate (38.1 mg, 0.2 mmol, 2 equiv), and phenylboronic acid (24.4 mg, 0.2 mmol, 2 equiv) were weighed on a single piece of weigh paper and added all at once to the reaction vial. The vial headspace was sparged with argon for 30-45 seconds, then the vial was sealed and heated to 65 °C with vigorous stirring for 17 h.

Workup

The reaction was allowed to cool then opened to air and quenched with ca. 2 mL ethyl acetate. An *n*-undecane internal standard was added, and the resealed vials were shaken. Saturated sodium carbonate (ca. 2 mL) was added, and the vials were shaken once more. Phases were allowed to separate, and an aliquot was drawn from the supernatant, filtered through a layered plug of $MgSO_4$ on Celite, and flushed through the filter with ethyl acetate into a vial for GC/GCMS analysis (86% calibrated GC yield of **47a**).

APPENDIX D

CHAPTER FIVE EXPERIMENTAL

D1. General Materials and Methods

GC data were collected using a Shimadzu GC-2010 Plus with a flame ionization detector equipped with a SH-Rxi-5ms capillary column (15 m x 0.25 mm ID x 0.25 µm df). GCMS data were collected with a Shimadzu GC-2030 paired with a Shimadzu GCMS-QP2020 NX and equipped with a SH-Rxi-5ms capillary column (30 m x 0.25 mm ID x 0.25 µm df). (η^3-1-^{t}Bu-indenyl)Pd(NHC)(Cl) precatalysts were obtained from Umicore. Unless otherwise noted, dichloroarenes and arylboronic acid starting materials were obtained from Ambeed or Oakwood Chemical. Tricyclohexylphosphine was obtained from Oakwood Chemical. Tri-*tert*-butylphosphine was obtained from Alfa Aesar.

D2. General Procedures for Suzuki-Miyaura Cross-Couplings

GC Vial Reactions

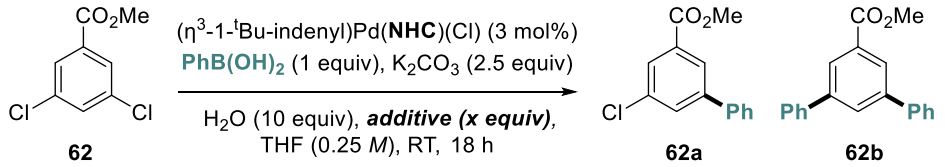
The specified solids were added to a 1-dram reaction vial in order of increasing mass: palladium(II) precatalyst, the specified dichloroarene substrate if solid (0.08 mmol, 1 equiv), arylboronic acid (0.08 mmol, 1.0 equiv), potassium carbonate (0.2 mmol, 2.5 equiv), and then a stir bar. Liquid reagents were pre-measured by syringe and added in quick succession: THF, benzene, or other aromatic solvent (0.32 mL, 0.25 M) via 1-mL syringe, followed by N_2-sparged deionized water (0.8 mmol, 10 equiv) via 50-µL syringe. Note: dichloroarene substrates were added last if liquid, via microliter syringe. A septum cap equipped with an N_2-ingas and outgassing needle was fastened to the 1-dram reaction vial and the headspace was sparged for 30-45 seconds. With continuous sparging, the vial was unscrewed from the septum cap and lowered while the cap was replaced with a PTFE-lined cap. The reaction was stirred vigorously at ambient temperature for the specified duration.

GC Time Studies

The specified solids were added to a 1-dram reaction vial in order of increasing mass: palladium(II) precatalyst (0.012 mmol, 0.03 equiv), the specified dichloroarene substrate if solid (0.4 mmol, 1 equiv), arylboronic acid (0.4 mmol, 1.0 equiv), potassium carbonate (1 mmol, 2.5 equiv), and then a stir bar. Liquid reagents were pre-measured by syringe and added in quick succession: THF (1.6 mL, 0.25 M) via 1-mL syringe, followed by an *n*-undecane internal standard (37.5 µL, 0.178 mmol, 0.44 equiv) via 50-µL syringe, then N_2-sparged deionized water (4 mmol, 10 equiv) via 50-µL syringe. (Note: if liquid, dichloroarene substrates were measured by weight and added via a stock solution in the specified organic solvent prior to the addition of other liquids.) The reaction vial was briefly sealed and shaken vigorously prior to collection of a zero-minute time point (ca. 25-µL aliquot). A septum cap equipped with an N_2-ingas and outgassing needle was fastened to the 1-dram reaction vial and the headspace was sparged for 30-45 seconds. The outgas needle was removed, followed by the ingas needle, and the reaction was stirred vigorously at ambient temperature. At specified time points, stirring was paused, and an N_2-ingas needle was inserted through the septum under positive N_2 pressure. After several seconds, the pressure was released through a one-way oil-bubbler, and an aliquot (ca. 25-µL) was collected through the vial's septum screwcap via syringe for GC analysis. The vial was returned to positive N_2 pressure prior to removal of the ingas needle, and stirring was resumed.

D3. Replicated Entries for GC-Scale Suzuki-Miyaura Couplings

Table D1. Effects of Ligand Additives (Table 5.2)



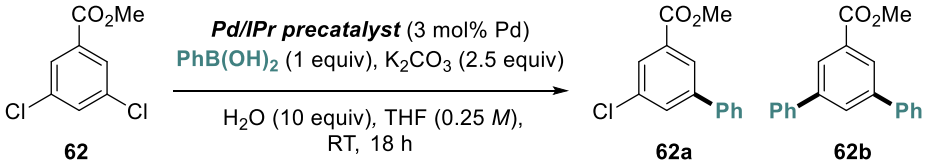
entry	trial	NHC	additive (equiv)	**62a** (%)	**62b** (%)	**a** : **b**
1	1	IPr	--	10	42	1 : 4.3
2	2	IPr	--	10	40	1 : 4.0
3	Average	IPr	--	10	41	1 : 4.2
4	1	IPr	pyridine (0.1)	44	28	1.6 : 1
5	2	IPr	pyridine (0.1)	44	30	1.5 : 1
6	Average	IPr	pyridine (0.1)	44	29	1.5 : 1
7	1	IPr	lutidine (0.1)	35	33	1.1 : 1
8	2	IPr	lutidine (0.1)	36	34	1.1 : 1
9	Average	IPr	lutidine (0.1)	36	34	1.1 : 1
10	1	IPr	indene (0.1)	56	20	2.8 : 1
11	2	IPr	indene (0.1)	61	23	2.7 : 1
12	Average	IPr	indene (0.1)	59	21	2.8 : 1
13	1	IPr	*1-tert*-butylindene (0.1)	23	38	1 : 1.7
14	2	IPr	*1-tert*-butylindene (0.1)	23	40	1 : 1.8
15	Average	IPr	*1-tert*-butylindene (0.1)	23	39	1 : 1.7
16	1	IPr	DMSO (0.1)	61	13	4.7 : 1
17	2	IPr	DMSO (0.1)	64	17	3.8 : 1
18	Average	IPr	DMSO (0.1)	63	15	4.2 : 1
19	1	IPr	DMSO (1)	77	9	8.6 : 1
20	2	IPr	DMSO (1)	81	13	6.2 : 1
21	Average	IPr	DMSO (1)	79	11	7.2 : 1
22	1	IPr	DMSO (10)	79	11	7.2 : 1

Table D1 Continued

23	1	IPr	sulfolane (10)	11	41	1 : 3.7
24	2	IPr	sulfolane (10)	11	41	1 : 3.7
25	Average	IPr	sulfolane (10)	11	41	1 : 3.7
26	1	IPent	DMSO (10)	32	21	1.6 : 1
27	2	IPent	DMSO (10)	31	35	1 : 1.1
28	Average	IPent	DMSO (10)	32	28	1.1 : 1
29	1	IPr	MeCN (10)	62	23	2.7 : 1
30	2	IPr	MeCN (10)	55	17	3.3 : 1
31	Average	IPr	MeCN (10)	58	20	2.9 : 1

[a]Reactions were conducted according to the General Procedure for GC-scale reactions. GC yields calibrated against undecane as an internal standard. Calculated yield values were rounded to the nearest integer. Entries reported as <1 indicate a calibrated GC yield less than 0.5%; nd = not detected.

Table D2. Effect of Precatalyst Structure on Selectivity (Table 5.5).



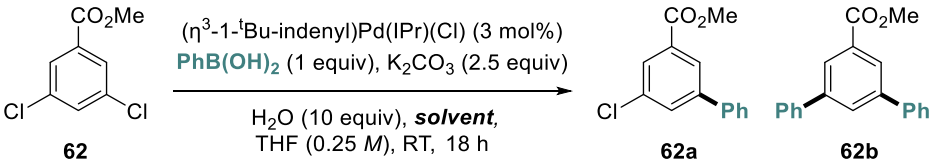
entry	trial	precatalyst	**62a** (%)	**62b** (%)	**a** : **b**
1	1	(η³-1-^{t}Bu-indenyl)Pd(IPr)(Cl)	10	42	1 : 4.3
2	2	(η³-1-^{t}Bu-indenyl)Pd(IPr)(Cl)	10	40	1 : 4
3	Average	(η³-1-^{t}Bu-indenyl)Pd(IPr)(Cl)	10	41	1 : 4.2
4	1	(η³-allyl)Pd(IPr)(Cl)	23	38	1 : 1.7
5	2	(η³-allyl)Pd(IPr)(Cl)	18	33	1 : 1.8
6	Average	(η³-allyl)Pd(IPr)(Cl)	21	36	1 : 1.7
7	1	$Pd(CH_2TMS)_2$(cod)/IPr	15	36	1 : 2.4
8	2	$Pd(CH_2TMS)_2$(cod)/IPr	15	38	2 : 2.5
9	Average	$Pd(CH_2TMS)_2$(cod)/IPr	15	37	1 : 2.5

Table D2 Continued

10	1	Pd-PEPPSI-IPr	15	35	1 : 2.3
11	2	Pd-PEPPSI-IPr	16	38	1 : 2.4
12	Average	Pd-PEPPSI-IPr	16	37	1 : 2.3
13	1	$[Pd(IPr)Cl_2]_2$	10	40	1 : 4
14	2	$[Pd(IPr)Cl_2]_2$	10	41	1 : 4.1
15	Average	$[Pd(IPr)Cl_2]_2$	10	40	1 : 4
16[b]	1	$Pd(IPr)_2$	9	47	1 : 5.4
17[b]	2	$Pd(IPr)_2$	9	46	1 : 4.9
18[b]	Average	$Pd(IPr)_2$	9	47	1 : 5.2
19	1	(η^3-1-^{t}Bu-indenyl)Pd(P^tBu_3)(Cl)	69	18	4 : 1
20	2	(η^3-1-^{t}Bu-indenyl)Pd(P^tBu_3)(Cl)	64	13	5 : 1
21	Average	(η^3-1-^{t}Bu-indenyl)Pd(P^tBu_3)(Cl)	66	15	4.4 : 1
22	1	(P^tBu_3) Pd G4	75	19	3.9 : 1
23	2	(P^tBu_3) Pd G4	73	18	4.2 : 1
24	Average	(P^tBu_3) Pd G4	74	18	4 : 1
25[b]	1	$Pd(P^tBu_3)_2$	70	21	3.4 : 1
26[b]	2	$Pd(P^tBu_3)_2$	68	20	3.4 : 1
27[b]	Average	$Pd(P^tBu_3)_2$	69	20	3.4 : 1

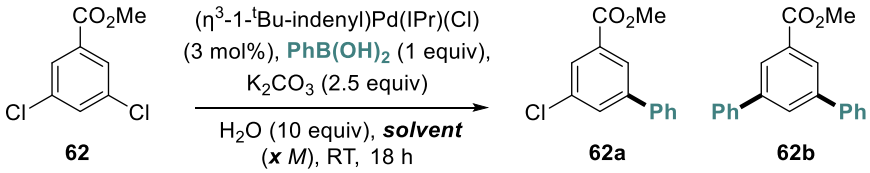
[a]Reactions were conducted according to the General Procedure for GC-scale reactions. GC yields calibrated against undecane as an internal standard. Calculated yield values were rounded to the nearest integer. Entries reported as <1 indicate a calibrated GC yield less than 0.5%; nd = not detected. [b]Reactions were set up inside the glovebox, water was injected through the septum screwcap via outside the glovebox.

Table D3. Effects of Coordinating Aromatic Solvents on Selectivity (Table 5.3).



entry	trial	solvent	**62a** (%)	**62b** (%)	**a** : **b**
1	1	THF	10	42	1 : 4.3
2	2	THF	10	40	1 : 4
3	Average	THF	10	41	1 : 4.2
4	1	benzene	60	16	3.7 : 1
5	2	benzene	60	17	3.5 : 1
6	Average	benzene	60	17	3.6 : 1
7	1	toluene	52	17	3.1 : 1
8	2	toluene	54	19	2.8 : 1
9	Average	toluene	53	18	3 : 1
10	1	xylenes	36	12	2.9 : 1
11	2	xylenes	36	13	2.8 : 1
12	Average	xylenes	36	13	2.8 : 1
13	1	mesitylene	26	29	1 : 1.1
14	2	mesitylene	24	28	1 : 1.2
15	Average	mesitylene	25	28	1 : 1.1
16	1	$PhCF_3$	65	16	4.1 : 1
17	2	$PhCF_3$	66	16	4.3 : 1
18	Average	$PhCF_3$	66	16	4.2 : 1
19	1	anisole	47	26	1.8 : 1
20	2	anisole	43	21	2.1 : 1
21	Average	anisole	45	23	1.9 : 1
22	1	1,3-difluorobenzene	55	19	2.9 : 1
23	2	1,3-difluorobenzene	56	18	3.1 : 1
24	Average	1,3-difluorobenzene	56	19	3 : 1

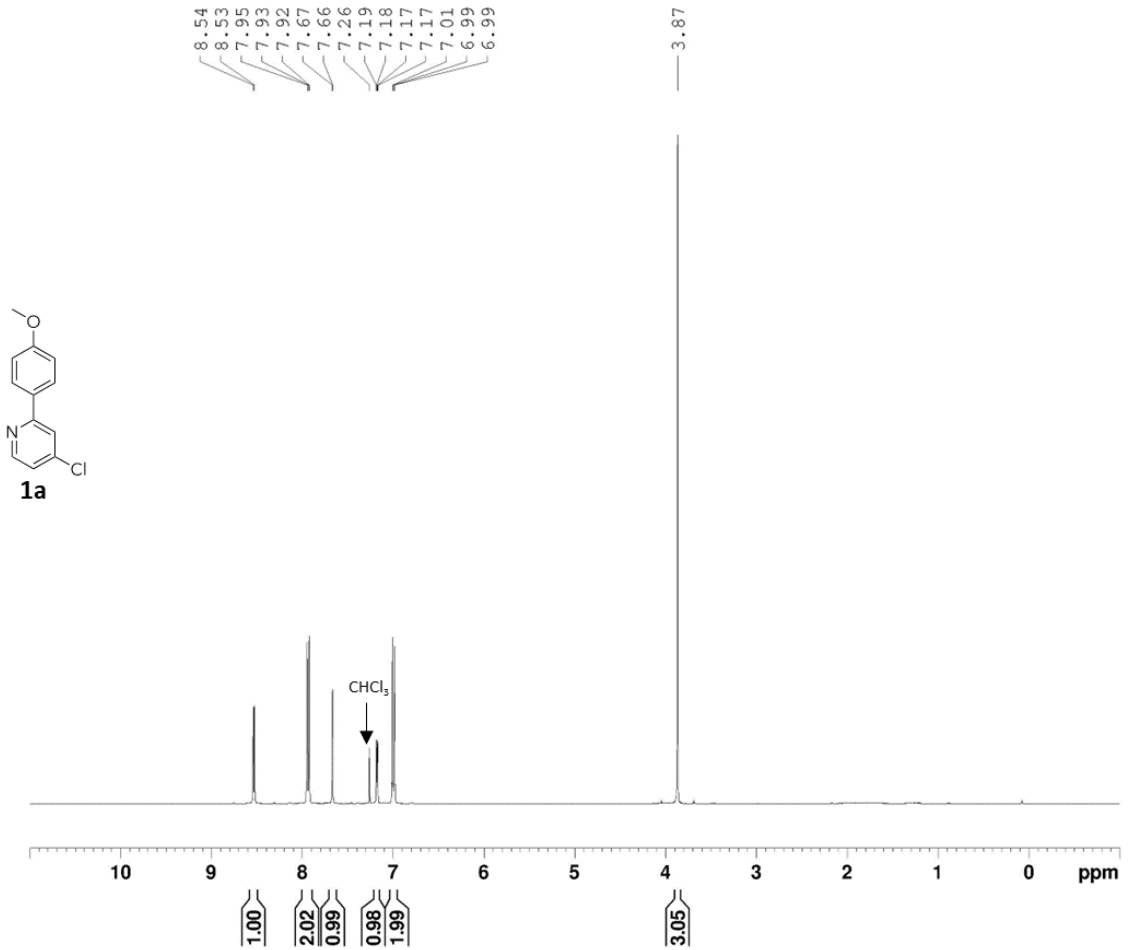
Table D4. Effect of Solvent Molarity on Selectivity (Table 5.4).



entry	trial	solvent	molarity	**62a** (%)	**62b** (%)	**a** : **b**
1	1	THF	0.4	15	40	1 : 2.7
2	2	THF	0.4	14	36	1 : 2.6
3	Average	THF	0.4	14	38	1 : 2.6
4	1	THF	0.25	10	42	1 : 4.3
5	2	THF	0.25	10	40	1 : 4
6	Average	THF	0.25	10	41	1 : 4.2
7	1	THF	0.2	8	41	1 : 5.2
8	2	THF	0.2	7	36	1 : 4.8
9	Average	THF	0.2	8	39	1 : 5
10	1	THF	0.16	7	41	1 : 6.2
11	2	THF	0.16	5	33	1 : 6.1
12	Average	THF	0.16	6	37	1 : 6.2
13	1	benzene	0.4	63	18	3.5 : 1
14	2	benzene	0.4	59	16	3.7 : 1
15	Average	benzene	0.4	61	17	3.6 : 1
16	1	benzene	0.25	60	16	3.7 : 1
17	2	benzene	0.25	60	17	3.5 : 1
18	Average	benzene	0.25	60	17	3.6 : 1
19	1	benzene	0.2	60	18	3.4 : 1
20	2	benzene	0.2	60	17	3.5 : 1
21	Average	benzene	0.2	60	17	3.5 : 1
22	1	benzene	0.16	59	16	3.7 : 1
23	2	benzene	0.16	59	17	3.4 : 1
24	Average	benzene	0.16	59	17	3.6 : 1

APPENDIX E

SPECTRAL DATA

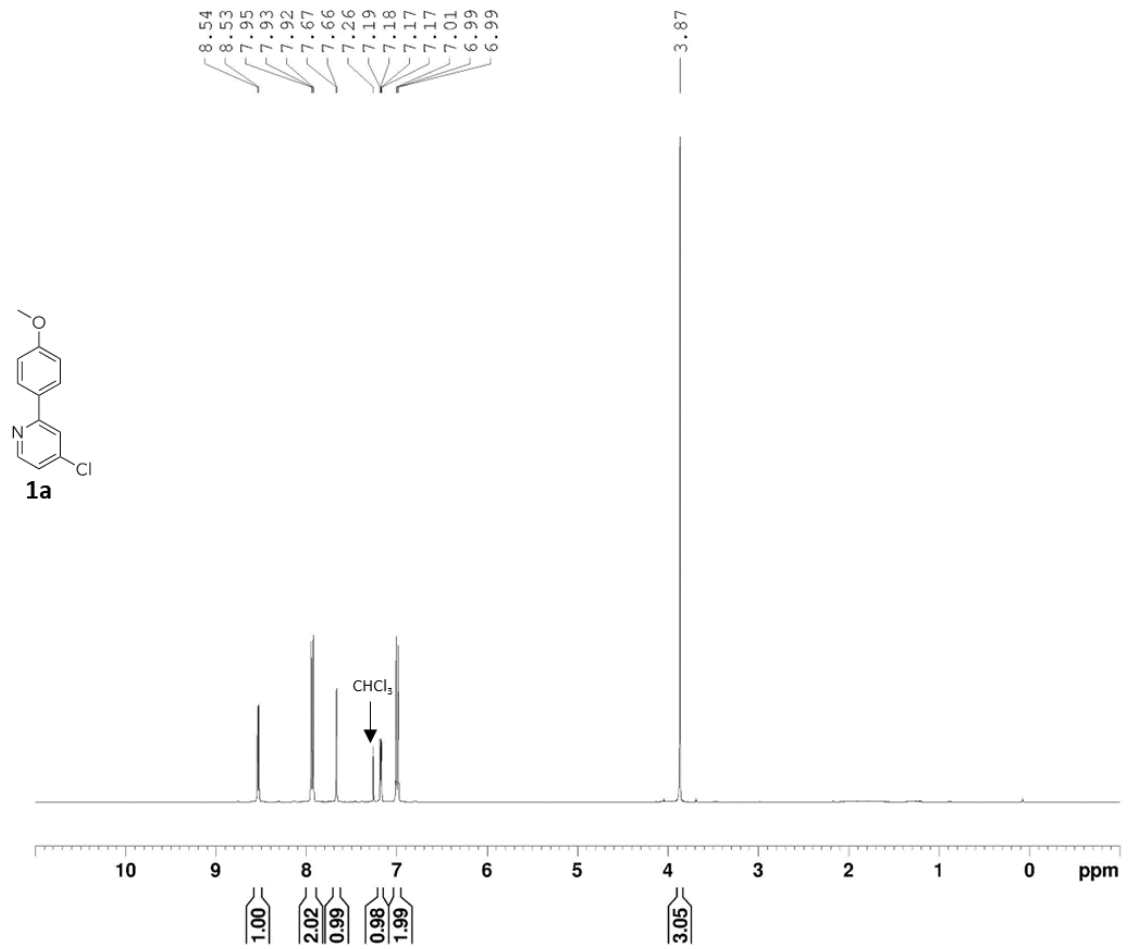


1a

```
Current Data Parameters
NAME          NL-1-96-1H
EXPNO                 12
PROCNO                 1

F2 - Acquisition Parameters
Date_           20210812
Time               14.41 h
INSTRUM       Avance Neo
PROBHD   Z152088_0031 (
PULPROG             zg30
TD                 65536
SOLVENT            CDCl3
NS                    16
DS                     2
SWH             8196.722 Hz
FIDRES          0.250144 Hz
AQ              3.9976959 sec
RG                   101
DW                61.000 usec
DE                13.89 usec
TE                298.2 K
D1           1.00000000 sec
TD0                    1
SFO1        400.1324708 MHz
NUC1                  1H
P0                 2.67 usec
P1                 8.00 usec
PLW1        24.03499985 W

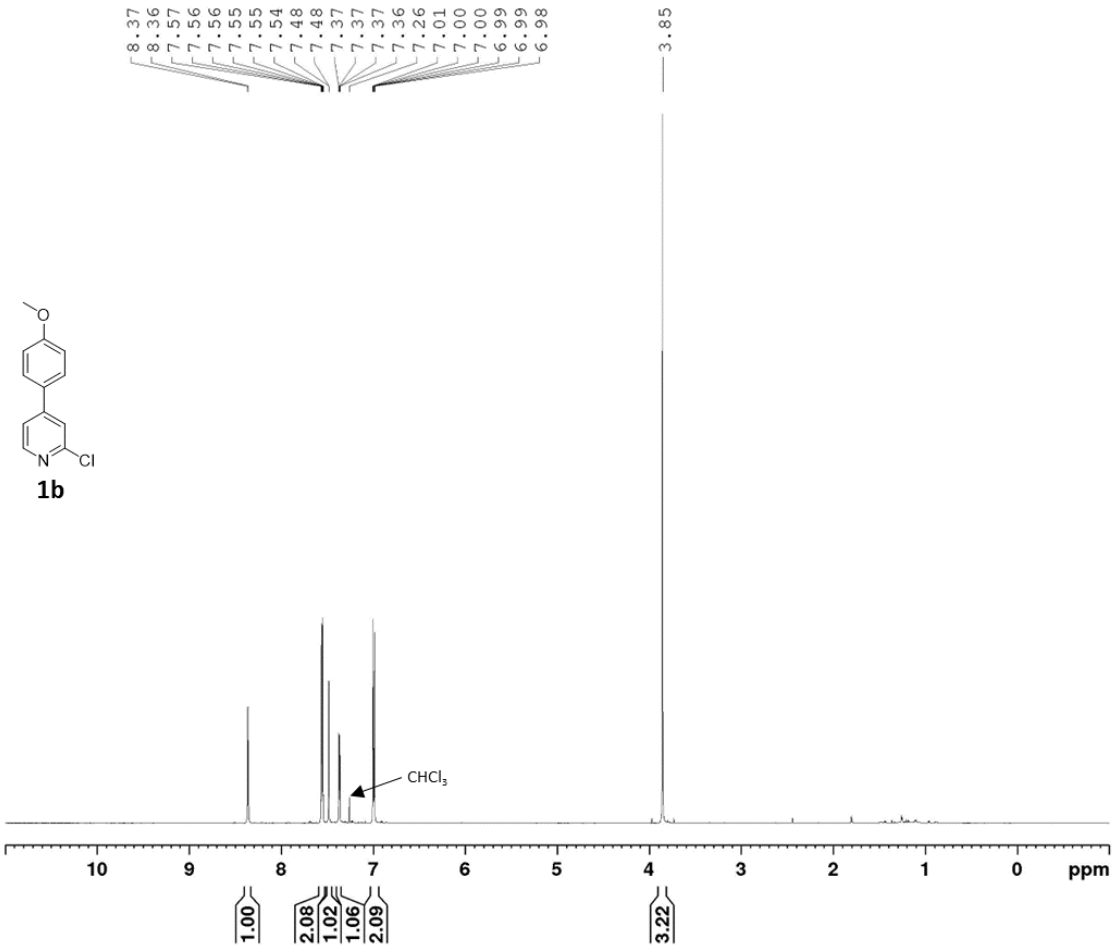
F2 - Processing parameters
SI                 65536
SF          400.1300097 MHz
WDW                   EM
SSB                    0
LB                  0.30 Hz
GB                     0
PC                  1.00
```




```
Current Data Parameters
NAME          NL-1-96-1H
EXPNO                 12
PROCNO                 1

F2 - Acquisition Parameters
Date_           20210812
Time               14.41 h
INSTRUM       Avance Neo
PROBHD   Z152088_0031 (
PULPROG             zg30
TD                 65536
SOLVENT            CDCl3
NS                    16
DS                     2
SWH             8196.722 Hz
FIDRES          0.250144 Hz
AQ              3.9976959 sec
RG                   101
DW                61.000 usec
DE                13.89 usec
TE                298.2 K
D1             1.00000000 sec
TD0                    1
SFO1          400.1324708 MHz
NUC1                  1H
P0                 2.67 usec
P1                 8.00 usec
PLW1          24.03499985 W

F2 - Processing parameters
SI                 65536
SF            400.1300097 MHz
WDW                   EM
SSB                    0
LB                  0.30 Hz
GB                     0
PC                  1.00
```

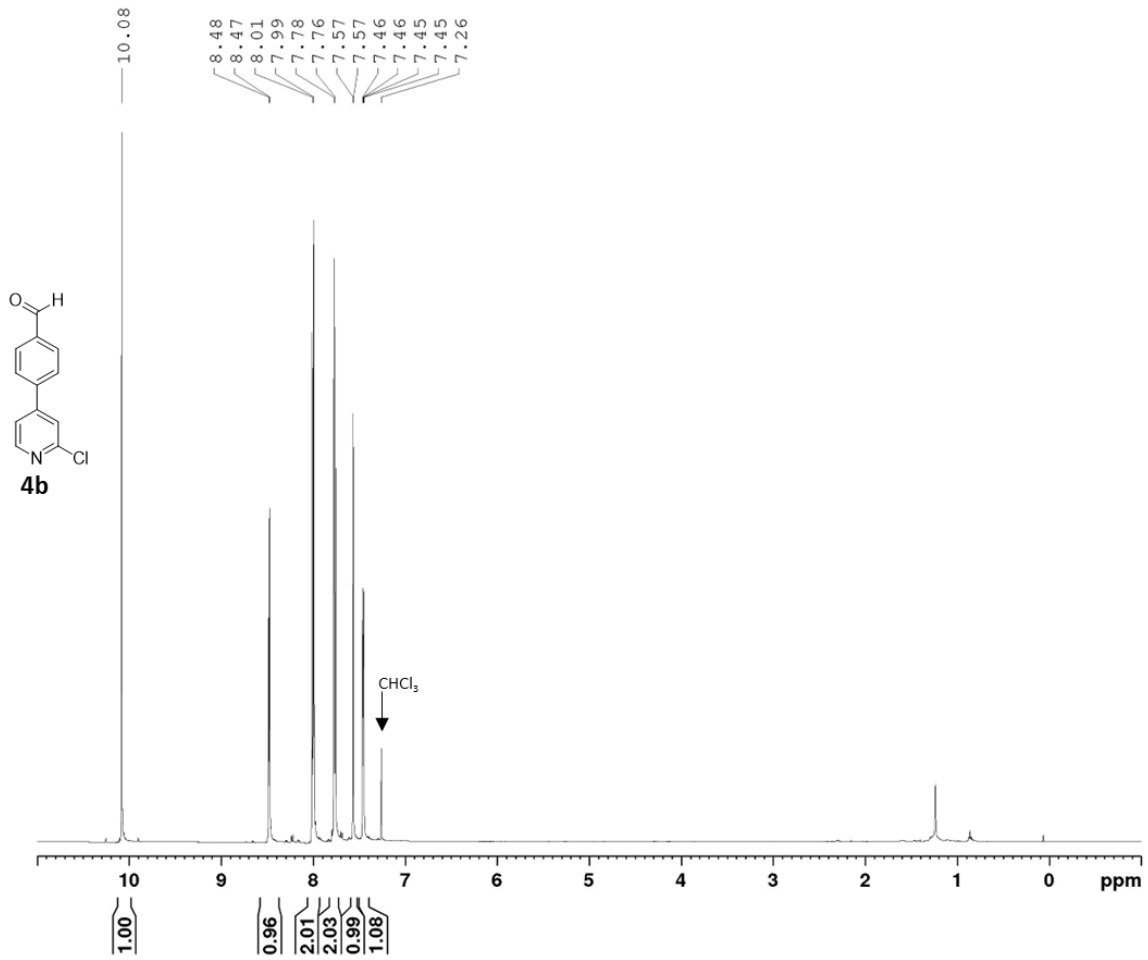


1b

```
Current Data Parameters
NAME      JPN-1-174-7_C4-mono
EXPNO                     10
PROCNO                     1

F2 - Acquisition Parameters
Date_              20200610
Time                 12.30 h
INSTRUM              spect
PROBHD    Z127277_0002 (
PULPROG                zg30
TD                    65536
SOLVENT               CDCl3
NS                       64
DS                        2
SWH              12019.230 Hz
FIDRES            0.366798 Hz
AQ                2.7262976 sec
RG                     4.41
DW                   41.600 usec
DE                   10.00 usec
TE                   300.0 K
D1              1.00000000 sec
TD0                       1
SFO1           600.1337060 MHz
NUC1                    1H
P0                    2.67 usec
P1                    8.00 usec
PLW1            5.59999990 W

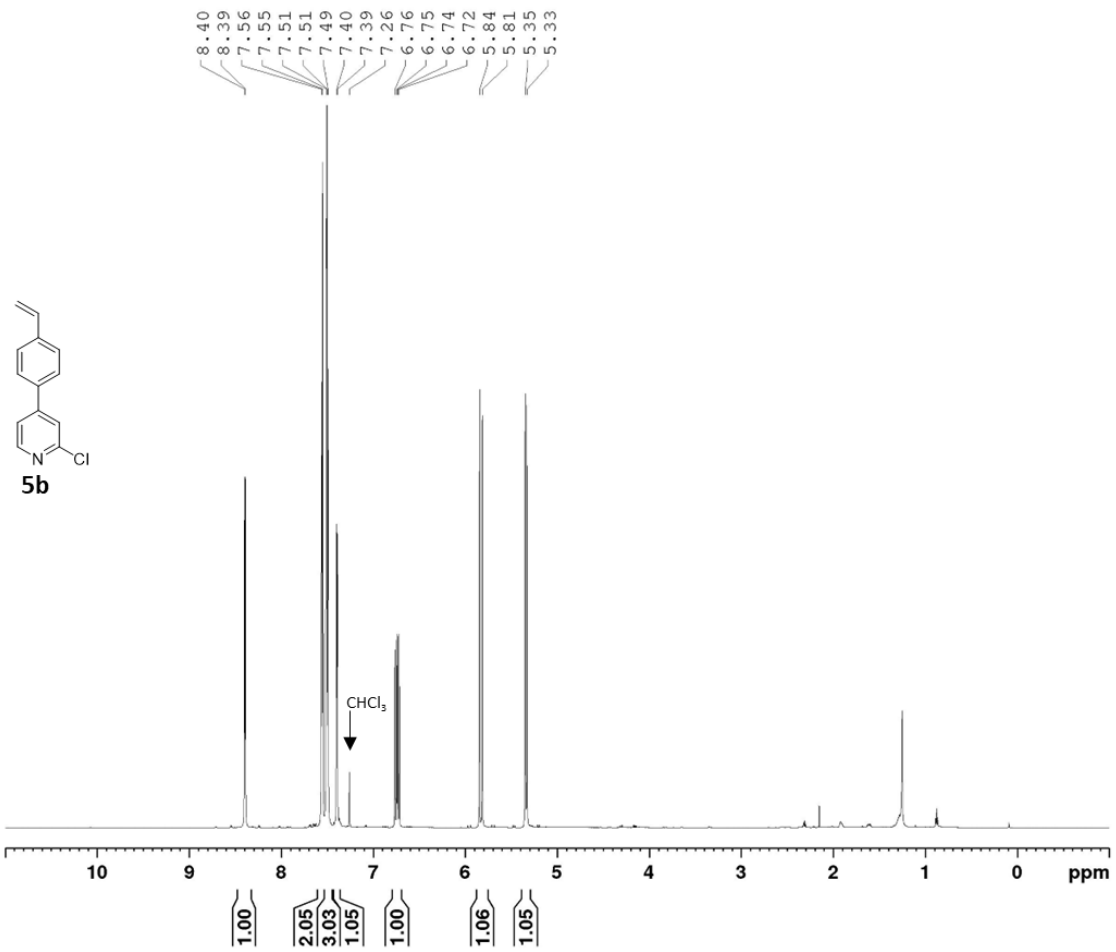
F2 - Processing parameters
SI                    65536
SF             600.1300144 MHz
WDW                     EM
SSB       0
LB                    0.30 Hz
GB        0
PC                    1.00
```




```
Current Data Parameters
NAME         JPN-1-174-5
EXPNO                 17
PROCNO                 1

F2 - Acquisition Parameters
Date_           20211120
Time                5.51 h
INSTRUM            spect
PROBHD   Z125869_0055 (
PULPROG             zg30
TD                 65536
SOLVENT            CDCl3
NS                    64
DS                     2
SWH            10000.000 Hz
FIDRES          0.305176 Hz
AQ             3.2767999 sec
RG                 76.94
DW                 50.000 usec
DE                 16.00 usec
TE                298.0 K
D1             2.00000000 sec
TD0                    1
SFO1         500.2330889 MHz
NUC1                  1H
P0                 4.00 usec
P1                12.00 usec
PLW1         11.44699955 W

F2 - Processing parameters
SI                 65536
SF           500.2300120 MHz
WDW                   EM
SSB       0
LB                 0.30 Hz
GB        0
PC                 1.00
```

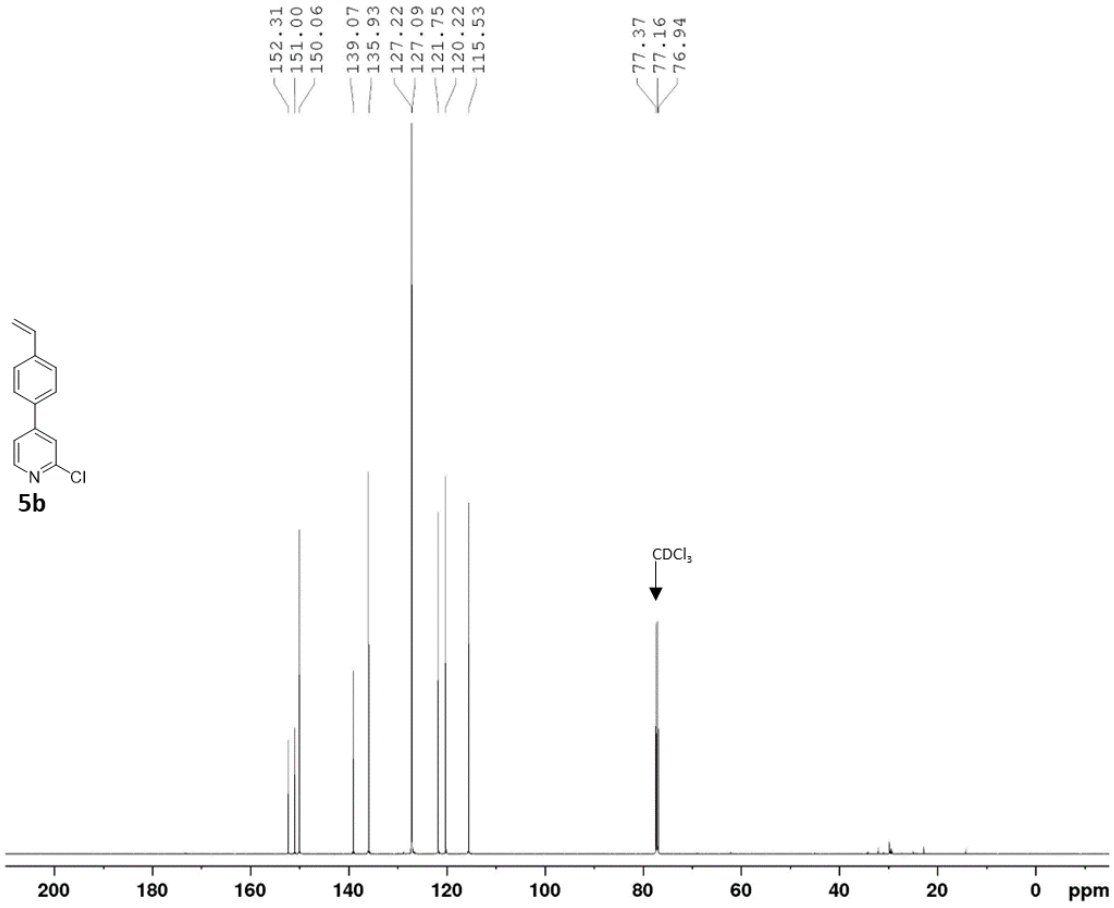


5b

```
Current Data Parameters
NAME      JPN-1-171-3_C4-mono_dried
EXPNO                  10
PROCNO                  1

F2 - Acquisition Parameters
Date_           20200608
Time               16.21 h
INSTRUM            spect
PROBHD   Z127277_0002 (
PULPROG             zg30
TD                 65536
SOLVENT            CDCl3
NS                    64
DS                     2
SWH            12019.230 Hz
FIDRES          0.366798 Hz
AQ             2.7262976 sec
RG                  4.41
DW                41.600 usec
DE                10.00 usec
TE                300.0 K
D1            1.00000000 sec
TD0                    1
SFO1         600.1337060 MHz
NUC1                  1H
P0                 2.67 usec
P1                 8.00 usec
PLW1          5.59999990 W

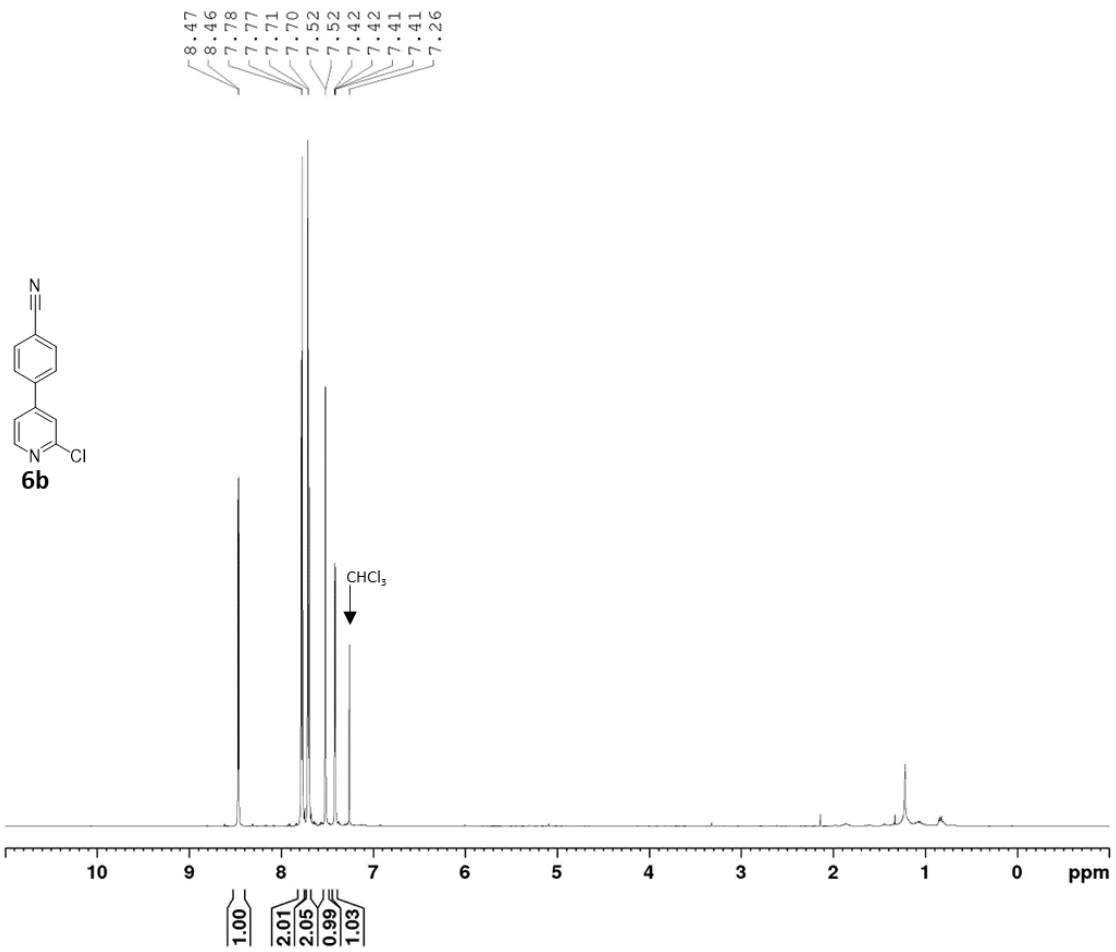
F2 - Processing parameters
SI                 65536
SF           600.1300145 MHz
WDW                   EM
SSB       0
LB                 0.30 Hz
GB        0
PC                 1.00
```




```
Current Data Parameters
NAME      JPN-1-171-3_C4-mono_dried
EXPNO                11
PROCNO                1

F2 - Acquisition Parameters
Date_          20200608
Time               17.13 h
INSTRUM             spect
PROBHD   Z127277_0002 (
PULPROG           zgpg30
TD                65536
SOLVENT           CDCl3
NS                 1024
DS                    4
SWH           36057.691 Hz
FIDRES         1.100393 Hz
AQ            0.9087659 sec
RG                184.4
DW               13.867 usec
DE                18.00 usec
TE                300.0 K
D1           2.00000000 sec
D11          0.03000000 sec
TD0                   1
SFO1        150.9178981 MHz
NUC1                13C
P0                 4.00 usec
P1                12.00 usec
PLW1        91.00000000 W
SFO2        600.1324005 MHz
NUC2                1H
CPDPRG[2         waltz16
PCPD2             70.00 usec
PLW2         5.59999990 W
PLW12        0.07314300 W
PLW13        0.03679000 W

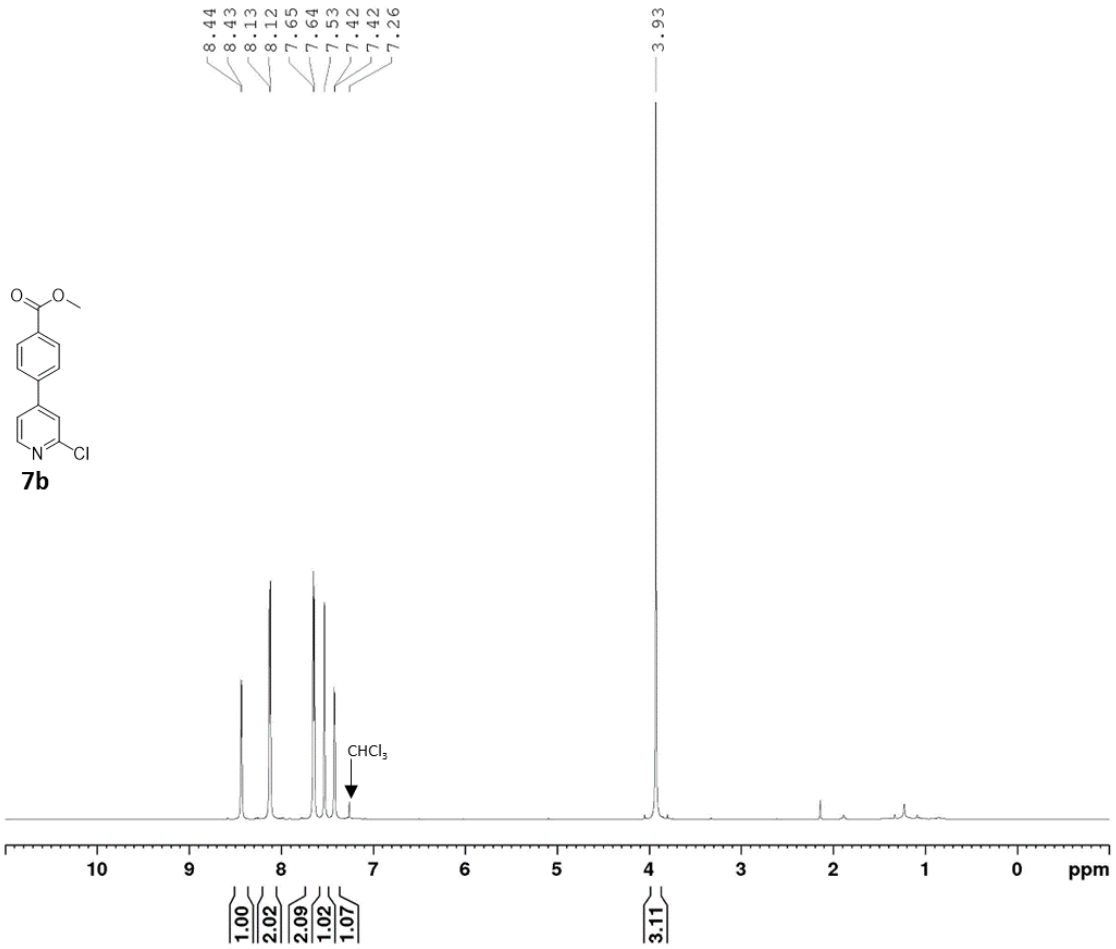
F2 - Processing parameters
SI                32768
SF          150.9028016 MHz
WDW                  EM
SSB       0
LB                1.00 Hz
GB        0
PC                1.40
```




```
Current Data Parameters
NAME      JPN-1-171-2_C4-mono_dried
EXPNO                22
PROCNO                1

F2 - Acquisition Parameters
Date_          20200608
Time              17.21 h
INSTRUM           spect
PROBHD   Z127277_0002 (
PULPROG            zg30
TD                65536
SOLVENT           CDCl3
NS                   64
DS                    2
SWH           12019.230 Hz
FIDRES            0.366798 Hz
AQ             2.7262976 sec
RG                 4.41
DW                41.600 usec
DE                10.00 usec
TE                300.0 K
D1           1.00000000 sec
TD0                   1
SFO1         600.1337060 MHz
NUC1                 1H
P0                2.67 usec
P1                8.00 usec
PLW1          5.59999990 W

F2 - Processing parameters
SI                65536
SF           600.1300145 MHz
WDW                  EM
SSB       0
LB                0.30 Hz
GB        0
PC                1.00
```

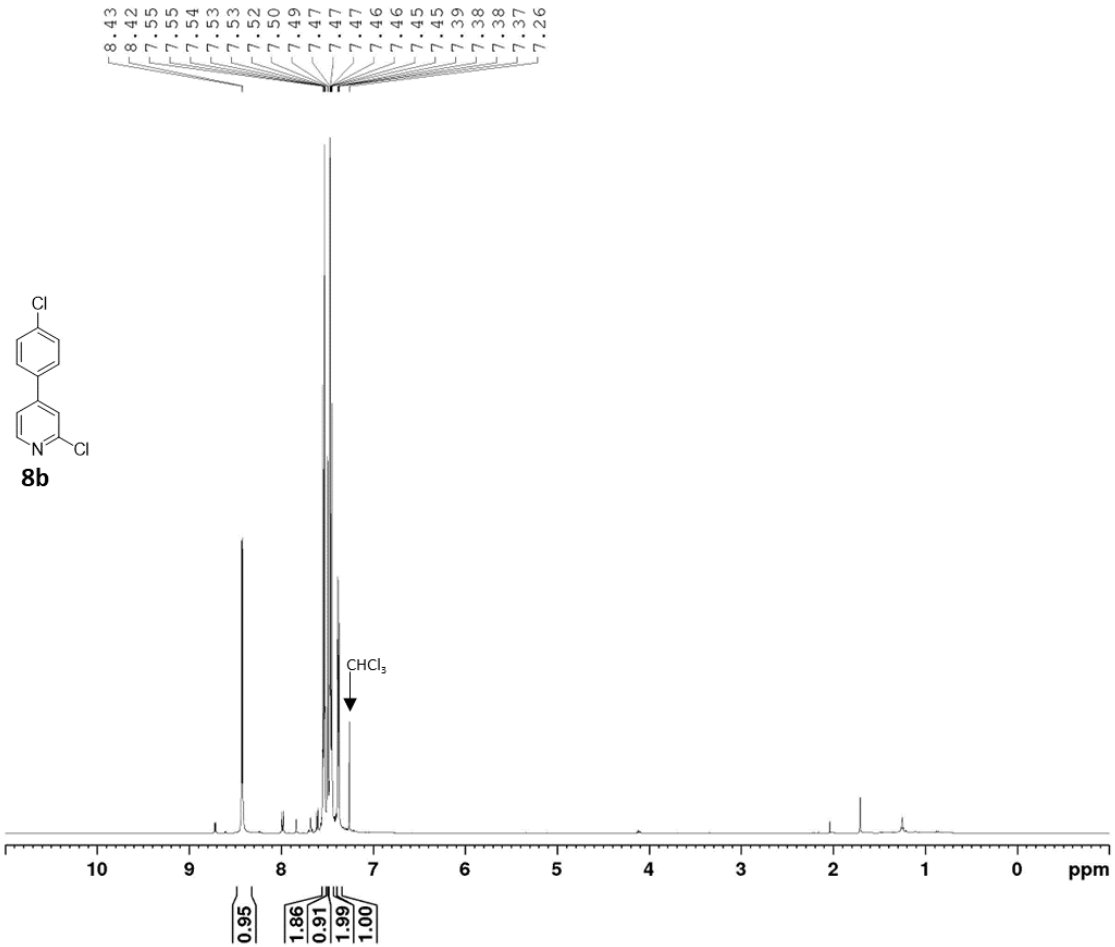


7b

```
Current Data Parameters
NAME      JPN-1-174-4_C4-mono
EXPNO                      10
PROCNO                      1

F2 - Acquisition Parameters
Date_              20200610
Time                  12.06 h
INSTRUM               spect
PROBHD    Z127277_0002 (
PULPROG                 zg30
TD                     65536
SOLVENT                CDCl3
NS                        64
DS                         2
SWH               12019.230 Hz
FIDRES             0.366798 Hz
AQ                2.7262976 sec
RG                     4.41
DW                   41.600 usec
DE                   10.00 usec
TE                   300.0 K
D1              1.00000000 sec
TD0                        1
SFO1           600.1337060 MHz
NUC1                    1H
P0                    2.67 usec
P1                    8.00 usec
PLW1            5.59999990 W

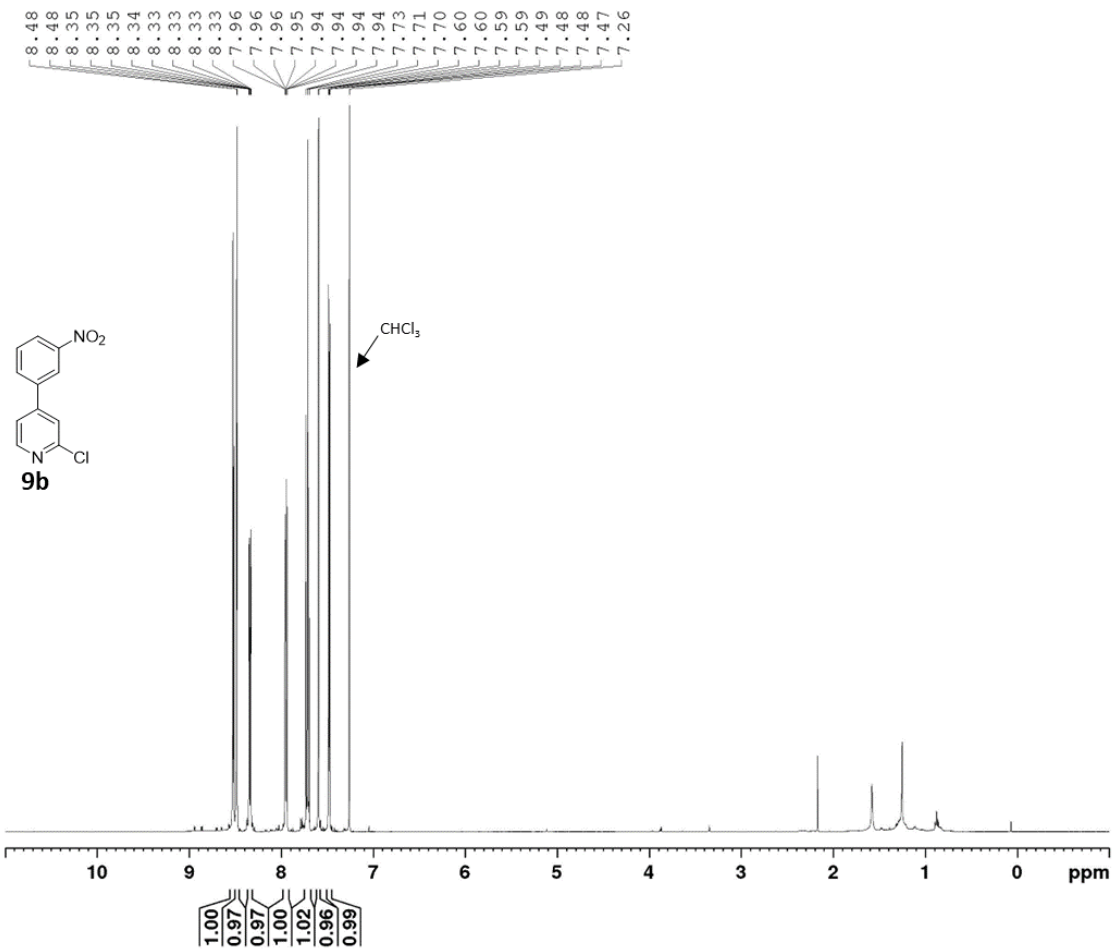
F2 - Processing parameters
SI                     65536
SF             600.1300144 MHz
WDW                       EM
SSB          0
LB                    0.30 Hz
GB           0
PC                    1.00
```




```
Current Data Parameters
NAME      JPN-1-174-3a_C4-mono
EXPNO                      10
PROCNO                      1

F2 - Acquisition Parameters
Date_            20200811
Time                23.22 h
INSTRUM             spect
PROBHD   Z125869_0055 (
PULPROG               zg30
TD                   65536
SOLVENT              CDCl3
NS                      64
DS                       2
SWH             10000.000 Hz
FIDRES              0.305176 Hz
AQ                3.2767999 sec
RG                   86.13
DW                  50.000 usec
DE                  16.00 usec
TE                  300.0 K
D1               2.00000000 sec
TD0                      1
SFO1           500.2330889 MHz
NUC1                    1H
P0                   4.00 usec
P1                  12.00 usec
PLW1           11.44699955 W

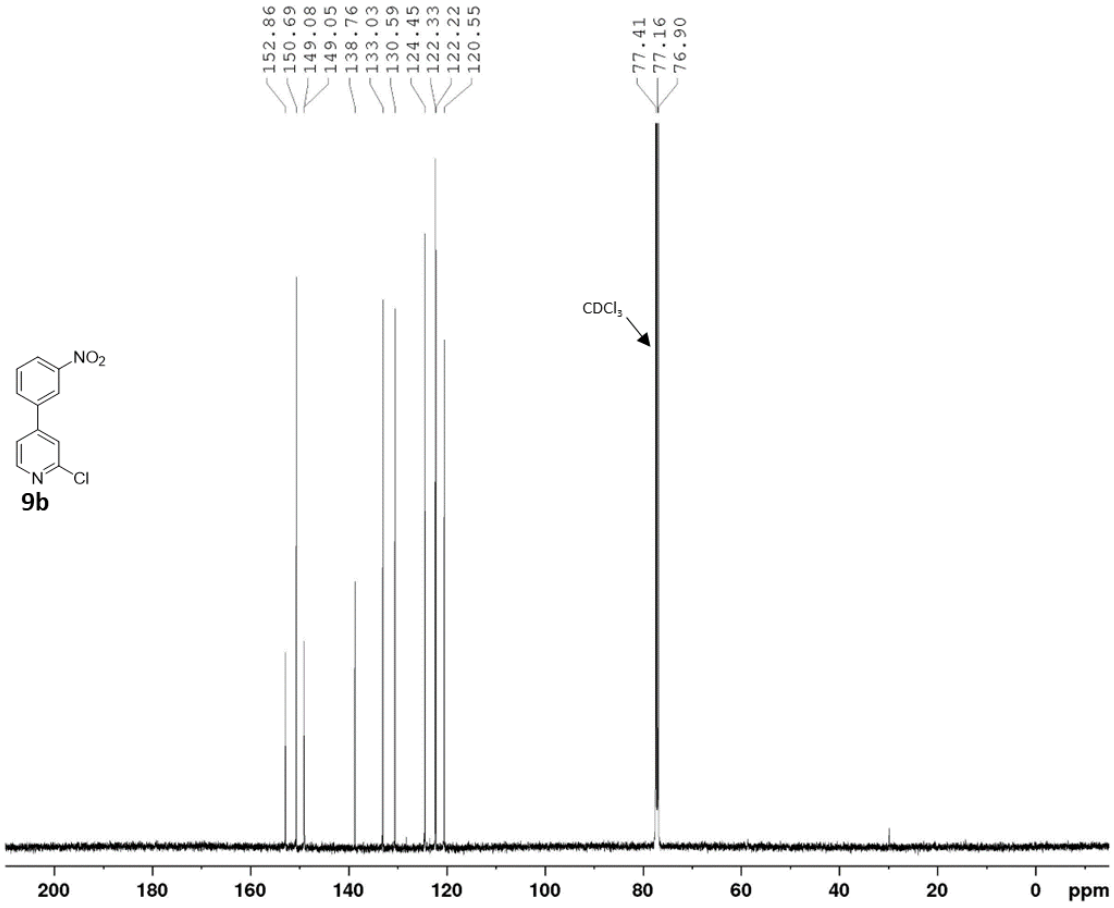
F2 - Processing parameters
SI                   65536
SF             500.2300122 MHz
WDW                     EM
SSB       0
LB                   0.30 Hz
GB        0
PC                   1.00
```




```
Current Data Parameters
NAME         JPN-1-193-1
EXPNO                 10
PROCNO                 1

F2 - Acquisition Parameters
Date_           20211121
Time                1.47 h
INSTRUM             spect
PROBHD   Z125869_0055 (
PULPROG             zg30
TD                 65536
SOLVENT            CDCl3
NS                    64
DS                     2
SWH           10000.000 Hz
FIDRES         0.305176 Hz
AQ            3.2767999 sec
RG               151.18
DW               50.000 usec
DE               16.00 usec
TE               298.0 K
D1            2.00000000 sec
TD0                    1
SFO1         500.2330889 MHz
NUC1                  1H
P0                4.00 usec
P1               12.00 usec
PLW1         11.44699955 W

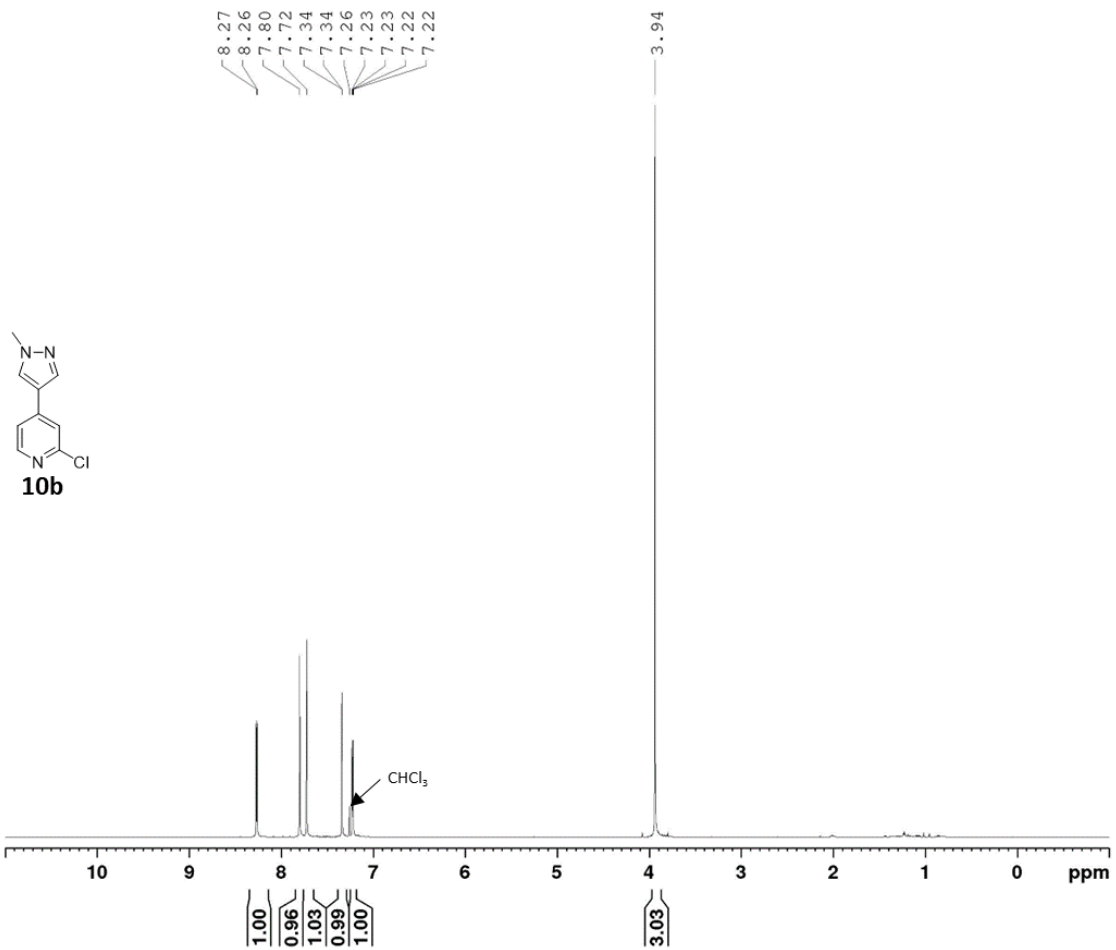
F2 - Processing parameters
SI                 65536
SF           500.2300121 MHz
WDW                   EM
SSB       0
LB                0.30 Hz
GB        0
PC                1.00
```




```
Current Data Parameters
NAME         JPN-1-193-1
EXPNO                 11
PROCNO                 1

F2 - Acquisition Parameters
Date_           20211121
Time              2.43 h
INSTRUM             spect
PROBHD   Z125869_0055 (
PULPROG           zgpg30
TD                 65536
SOLVENT            CDCl3
NS                  1024
DS                     4
SWH           29761.904 Hz
FIDRES         0.908261 Hz
AQ            1.1010048 sec
RG               190.44
DW               16.800 usec
DE               18.00 usec
TE               298.0 K
D1            2.00000000 sec
D11           0.03000000 sec
TD0                    1
SFO1        125.7955118 MHz
NUC1                13C
P0                3.33 usec
P1               10.00 usec
PLW1         56.90299988 W
SFO2        500.2320009 MHz
NUC2                1H
CPDPRG[2         waltz16
PCPD2            80.00 usec
PLW2         11.44699955 W
PLW12         0.25756001 W
PLW13         0.12955000 W

F2 - Processing parameters
SI                 32768
SF          125.7829172 MHz
WDW                   EM
SSB       0
LB                1.00 Hz
GB        0
PC                1.40
```

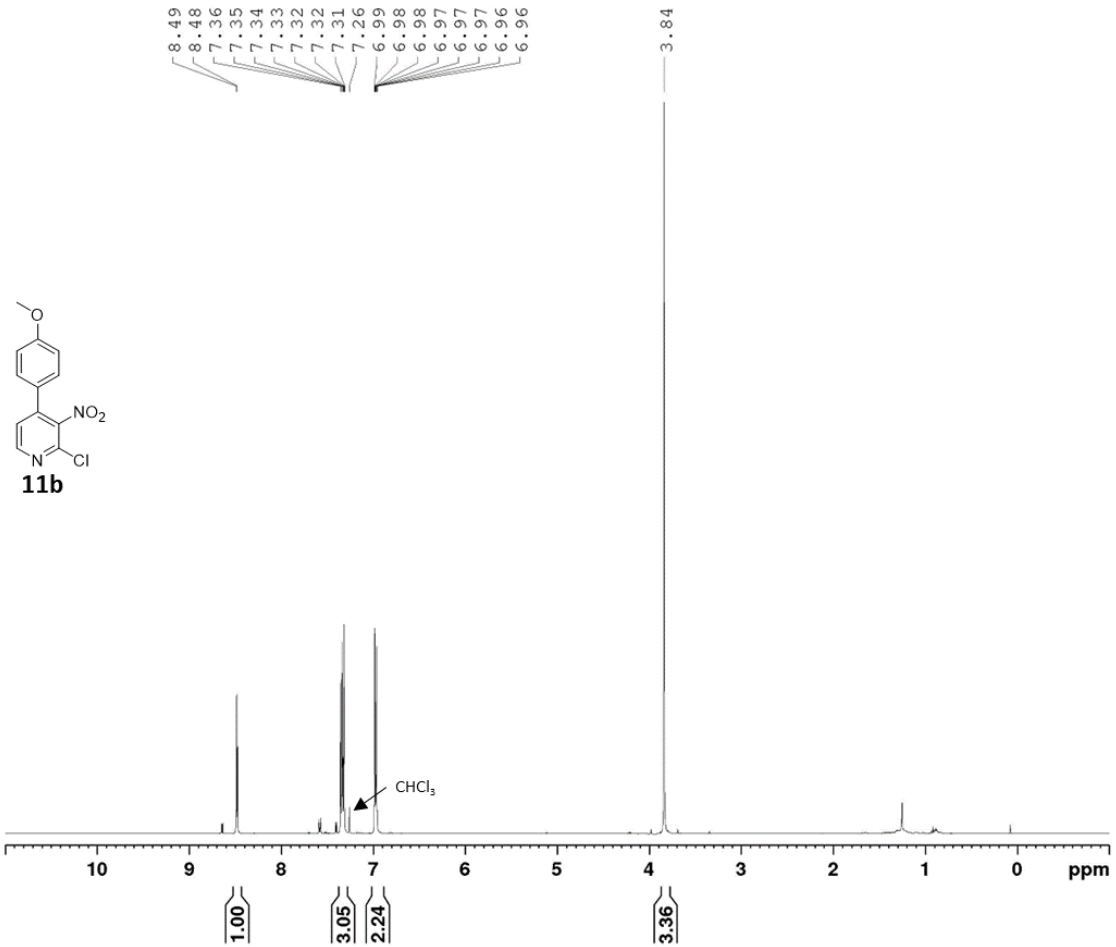


10b

```
Current Data Parameters
NAME      JPN-2-11a_C4-mono_MeOH_column_c
EXPNO                 10
PROCNO                 1

F2 - Acquisition Parameters
Date_           20200829
Time              17.06 h
INSTRUM             spect
PROBHD    Z125869_0055 (
PULPROG             zg30
TD                 65536
SOLVENT            CDCl3
NS                    64
DS                     2
SWH           10000.000 Hz
FIDRES         0.305176 Hz
AQ             3.2767999 sec
RG                37.93
DW               50.000 usec
DE               16.00 usec
TE                300.0 K
D1            2.00000000 sec
TD0                    1
SFO1         500.2330889 MHz
NUC1                  1H
P0                4.00 usec
P1               12.00 usec
PLW1         11.44699955 W

F2 - Processing parameters
SI                 65536
SF           500.2300122 MHz
WDW                   EM
SSB       0
LB                0.30 Hz
GB        0
PC                1.00
```

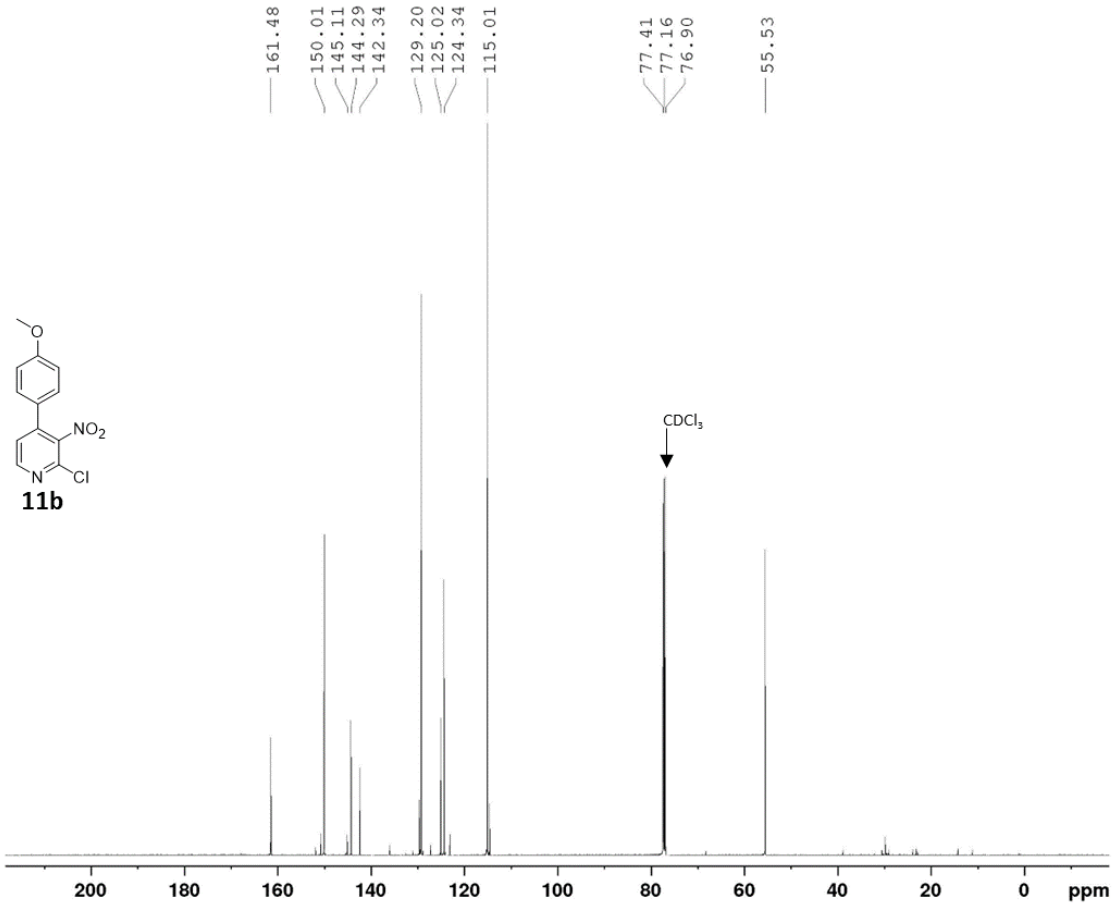


11b

```
Current Data Parameters
NAME         JPN-1-163-3
EXPNO                 16
PROCNO                 1

F2 - Acquisition Parameters
Date_           20211119
Time                2.34 h
INSTRUM            spect
PROBHD   Z125869_0055 (
PULPROG             zg30
TD                 65536
SOLVENT            CDCl3
NS                    64
DS                     2
SWH            10000.000 Hz
FIDRES             0.305176 Hz
AQ             3.2767999 sec
RG                 37.93
DW                 50.000 usec
DE                 16.00 usec
TE                 298.0 K
D1             2.00000000 sec
TD0                    1
SFO1          500.2330889 MHz
NUC1                  1H
P0                 4.00 usec
P1                12.00 usec
PLW1          11.44699955 W

F2 - Processing parameters
SI                 65536
SF            500.2300119 MHz
WDW                   EM
SSB       0
LB                 0.30 Hz
GB        0
PC                 1.00
```

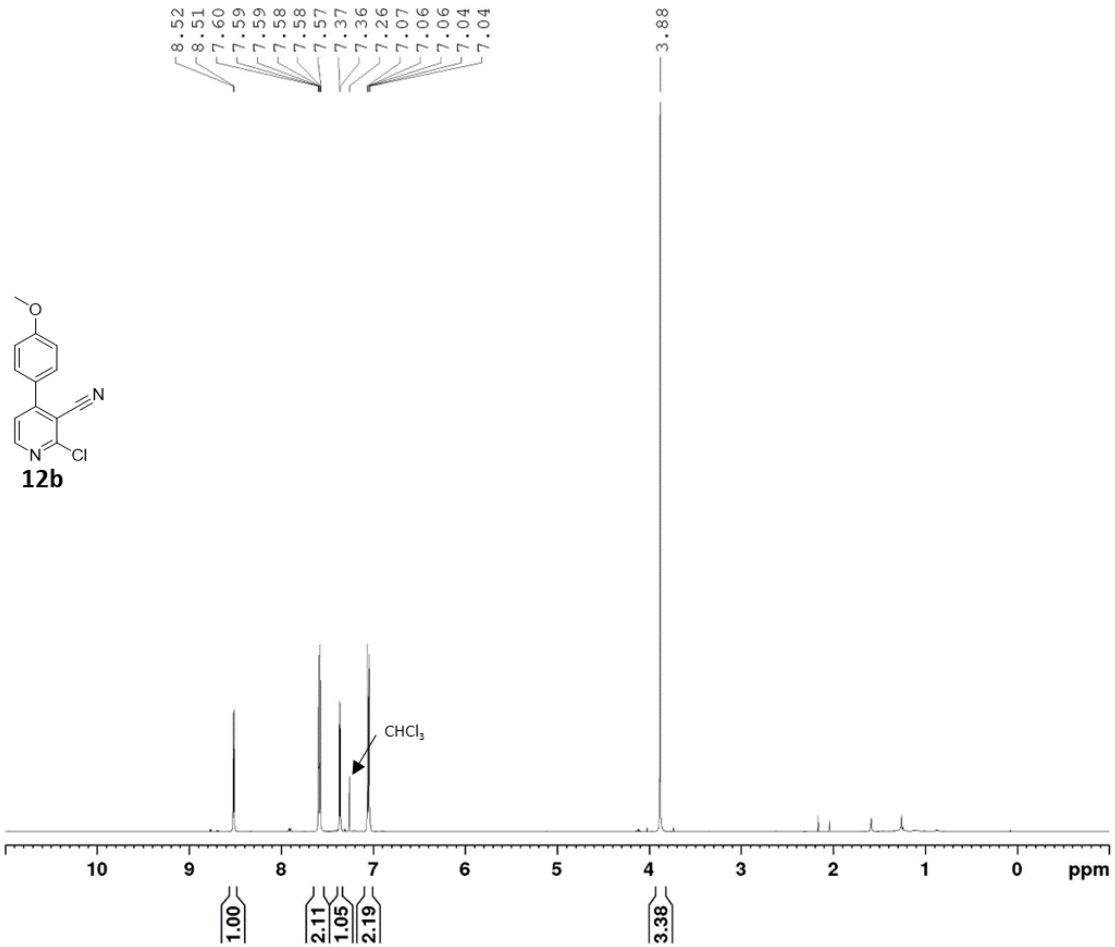


11b

```
Current Data Parameters
NAME         JPN-1-163-3
EXPNO                 17
PROCNO                 1

F2 - Acquisition Parameters
Date_           20211119
Time                3.30 h
INSTRUM            spect
PROBHD   Z125869_0055 (
PULPROG          zgpg30
TD                65536
SOLVENT           CDCl3
NS                 1024
DS                    4
SWH           29761.904 Hz
FIDRES         0.908261 Hz
AQ            1.1010048 sec
RG               190.44
DW               16.800 usec
DE               18.00 usec
TE               298.0 K
D1            2.00000000 sec
D11           0.03000000 sec
TD0                   1
SFO1        125.7955118 MHz
NUC1                13C
P0                3.33 usec
P1               10.00 usec
PLW1         56.90299988 W
SFO2        500.2320009 MHz
NUC2                1H
CPDPRG[2         waltz16
PCPD2            80.00 usec
PLW2         11.44699955 W
PLW12         0.25756001 W
PLW13         0.12955000 W

F2 - Processing parameters
SI                32768
SF          125.7829219 MHz
WDW                  EM
SSB       0
LB                1.00 Hz
GB        0
PC                1.40
```

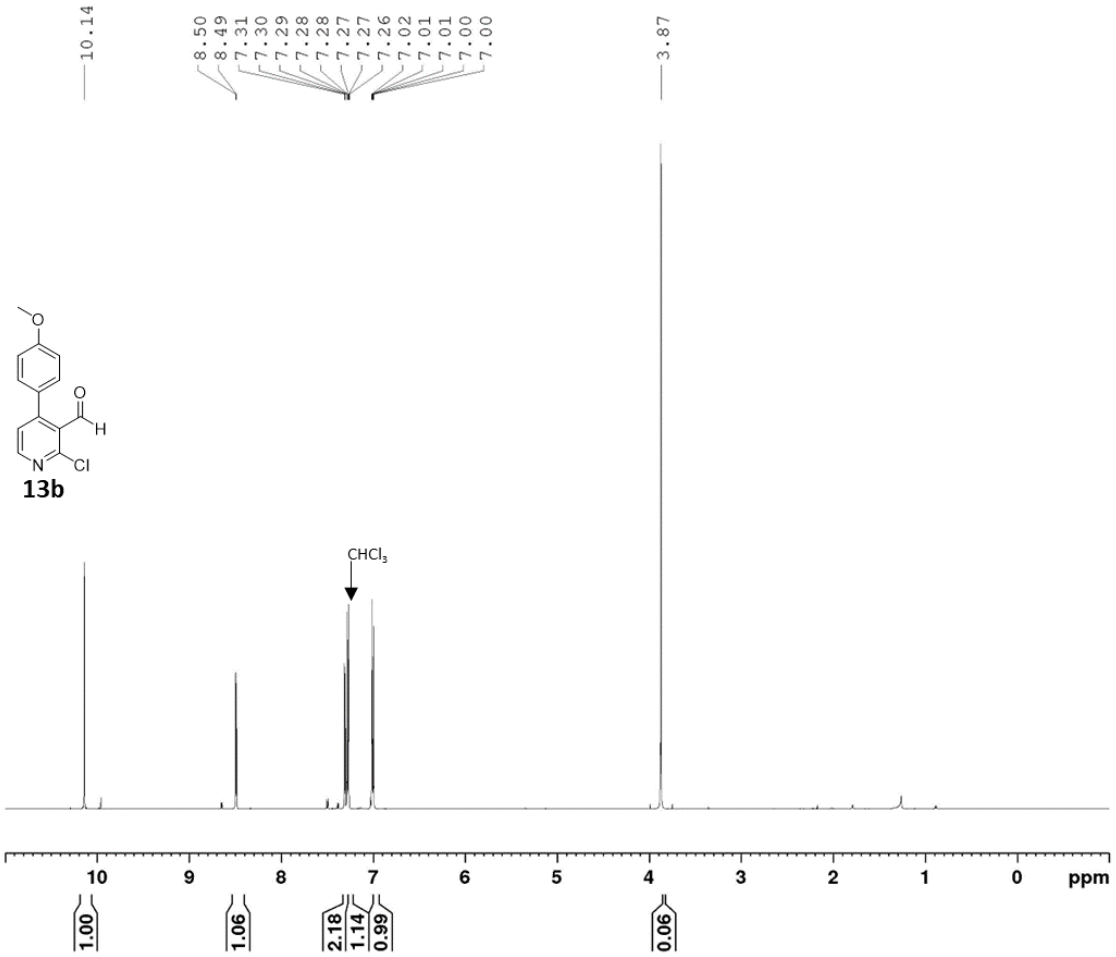


12b

```
Current Data Parameters
NAME      JPN-1-166-1_repeat_c4-mono
EXPNO                 10
PROCNO                 1

F2 - Acquisition Parameters
Date_           20200601
Time                9.25 h
INSTRUM            spect
PROBHD   Z119470_0370 (
PULPROG             zg30
TD                 65536
SOLVENT            CDCl3
NS                    64
DS                     2
SWH            10000.000 Hz
FIDRES             0.305176 Hz
AQ              3.2767999 sec
RG                 137.36
DW                  50.000 usec
DE                   6.50 usec
TE                  300.0 K
D1            1.00000000 sec
TD0                    1
SFO1         500.2330889 MHz
NUC1                  1H
P0                  3.13 usec
P1                  9.38 usec
PLW1         20.00000000 W

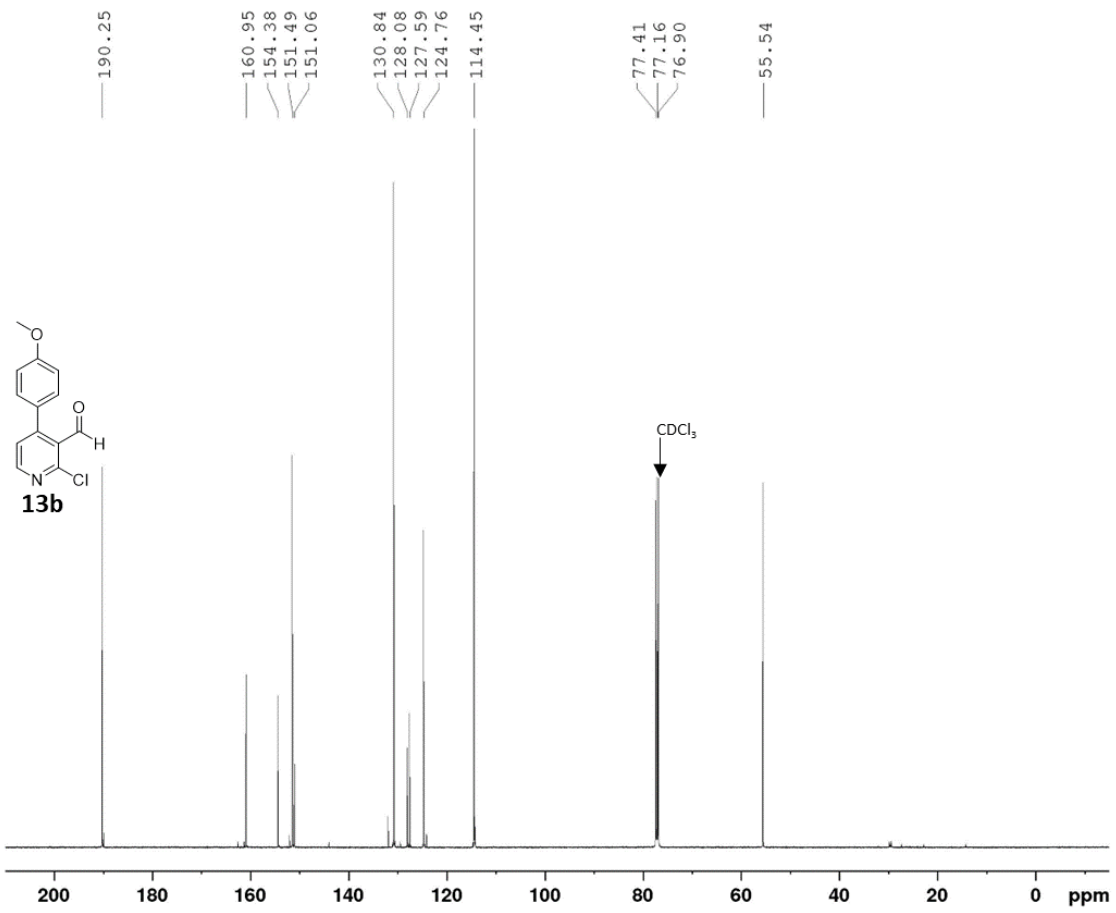
F2 - Processing parameters
SI                 32768
SF           500.2300128 MHz
WDW                  EM
SSB       0
LB                  0.30 Hz
GB        0
PC                  1.00
```




```
Current Data Parameters
NAME      JPN-1-167-1_C4-Mono
EXPNO                     24
PROCNO                     1

F2 - Acquisition Parameters
Date_              20200608
Time                 20.22 h
INSTRUM              spect
PROBHD    Z127277_0002 (
PULPROG                zg30
TD                    65536
SOLVENT               CDCl3
NS                       64
DS                        2
SWH              12019.230 Hz
FIDRES            0.366798 Hz
AQ                2.7262976 sec
RG                     4.41
DW                   41.600 usec
DE                   10.00 usec
TE                   300.0 K
D1              1.00000000 sec
TD0                       1
SFO1           600.1337060 MHz
NUC1                    1H
P0                    2.67 usec
P1                    8.00 usec
PLW1            5.59999990 W

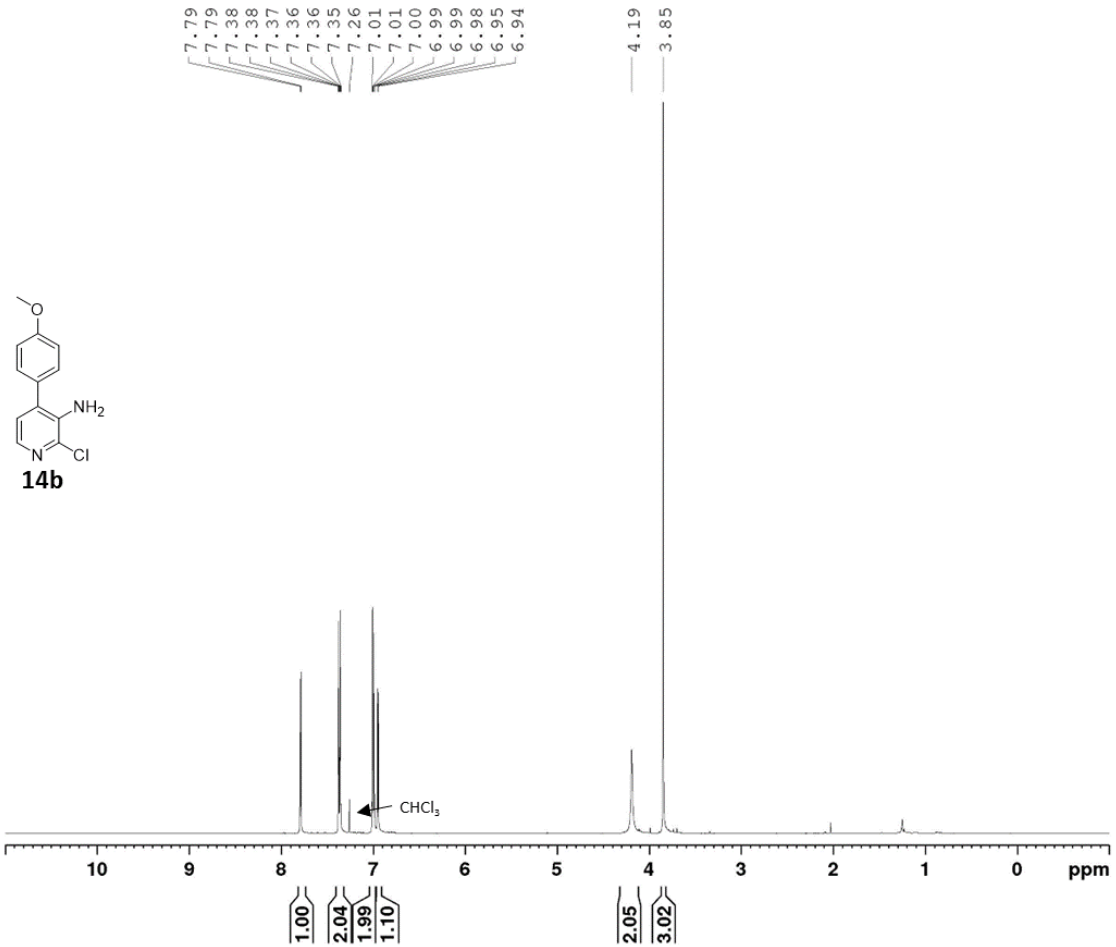
F2 - Processing parameters
SI                    65536
SF             600.1300000 MHz
WDW                     EM
SSB       0
LB                    0.30 Hz
GB        0
PC                    1.00
```




```
Current Data Parameters
NAME      JPN-1-167-1_C4-Mono
EXPNO                     10
PROCNO                     1

F2 - Acquisition Parameters
Date_           20200811
Time                21.16 h
INSTRUM             spect
PROBHD   Z125869_0055 (
PULPROG           zgpg30
TD                 65536
SOLVENT            CDCl3
NS                  1024
DS                     4
SWH            29761.904 Hz
FIDRES          0.908261 Hz
AQ             1.1010048 sec
RG                190.44
DW                16.800 usec
DE                18.00 usec
TE                300.0 K
D1            2.00000000 sec
D11           0.03000000 sec
TD0                    1
SFO1         125.7955118 MHz
NUC1                13C
P0                 3.33 usec
P1                10.00 usec
PLW1         56.90299988 W
SFO2         500.2320009 MHz
NUC2                1H
CPDPRG[2         waltz16
PCPD2             80.00 usec
PLW2         11.44699955 W
PLW12         0.25756001 W
PLW13         0.12955000 W

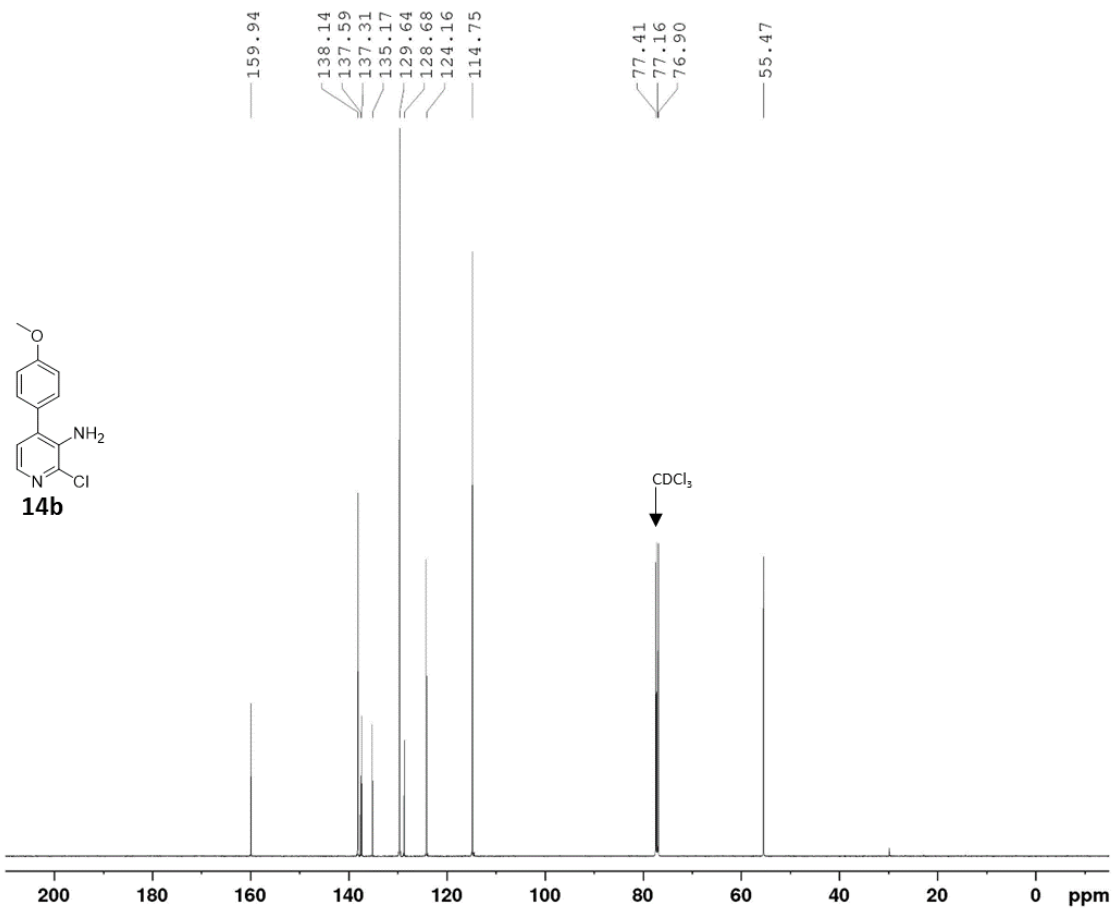
F2 - Processing parameters
SI                 32768
SF           125.7829218 MHz
WDW                   EM
SSB       0
LB                 1.00 Hz
GB        0
PC                 1.40
```




```
Current Data Parameters
NAME      JPN-2-17-1_C4-mono
EXPNO                   10
PROCNO                   1

F2 - Acquisition Parameters
Date_            20200914
Time               10.52 h
INSTRUM             spect
PROBHD    Z125869_0055 (
PULPROG              zg30
TD                  65536
SOLVENT             CDCl3
NS                     64
DS                      2
SWH            10000.000 Hz
FIDRES          0.305176 Hz
AQ             3.2767999 sec
RG                 30.54
DW                50.000 usec
DE                16.00 usec
TE                300.0 K
D1            2.00000000 sec
TD0                     1
SFO1         500.2330889 MHz
NUC1                  1H
P0                  4.00 usec
P1                 12.00 usec
PLW1         11.44699955 W

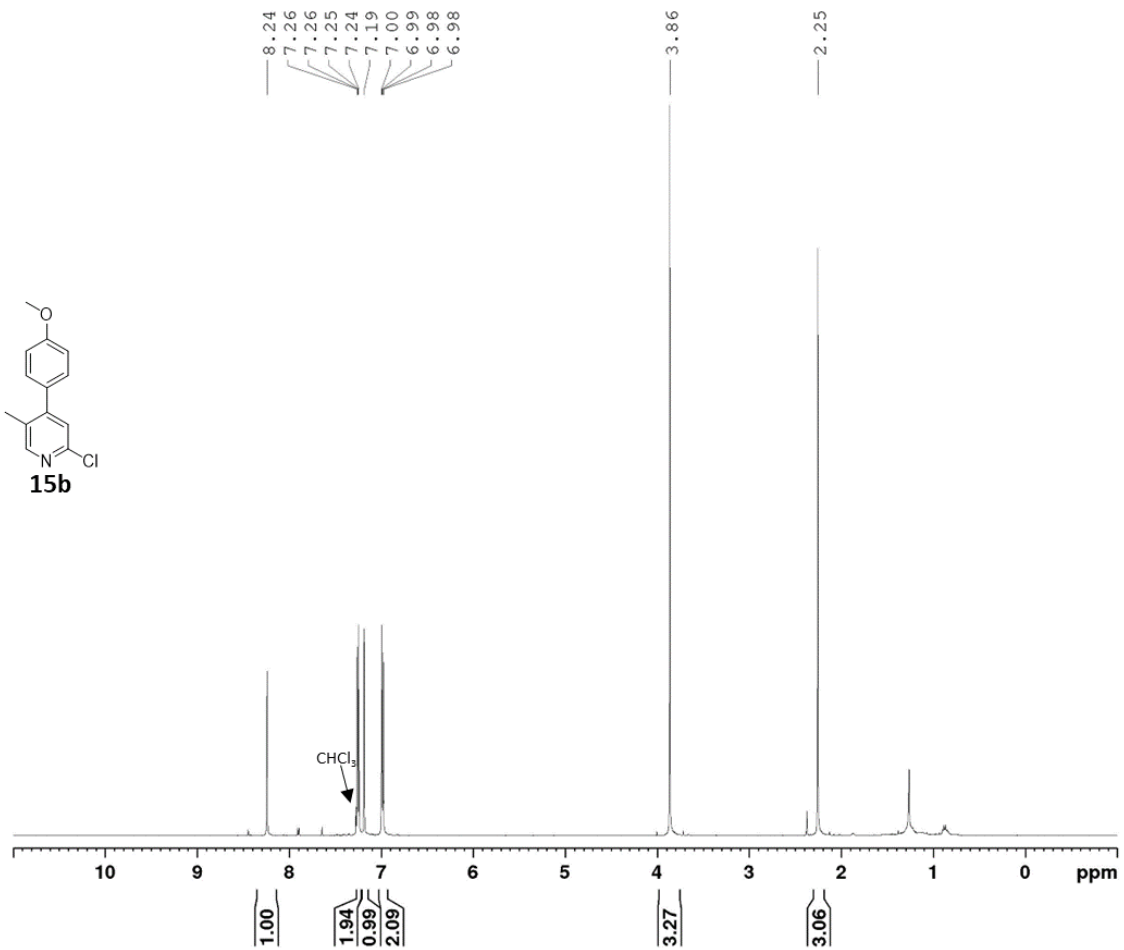
F2 - Processing parameters
SI                  65536
SF           500.2300120 MHz
WDW                   EM
SSB       0
LB                  0.30 Hz
GB        0
PC                  1.00
```




```
Current Data Parameters
NAME          JPN-2-17-1
EXPNO                 17
PROCNO                 1

F2 - Acquisition Parameters
Date_           20211119
Time                9.19 h
INSTRUM            spect
PROBHD   Z125869_0055 (
PULPROG          zgpg30
TD                65536
SOLVENT           CDCl3
NS                 1024
DS                    4
SWH           29761.904 Hz
FIDRES         0.908261 Hz
AQ            1.1010048 sec
RG               190.44
DW               16.800 usec
DE               18.00 usec
TE               298.0 K
D1            2.00000000 sec
D11           0.03000000 sec
TD0                   1
SFO1         125.7955118 MHz
NUC1                 13C
P0                3.33 usec
P1               10.00 usec
PLW1         56.90299988 W
SFO2         500.2320009 MHz
NUC2                 1H
CPDPRG[2          waltz16
PCPD2            80.00 usec
PLW2         11.44699955 W
PLW12         0.25756001 W
PLW13         0.12955000 W

F2 - Processing parameters
SI                32768
SF           125.7829236 MHz
WDW                  EM
SSB       0
LB                1.00 Hz
GB        0
PC                1.40
```

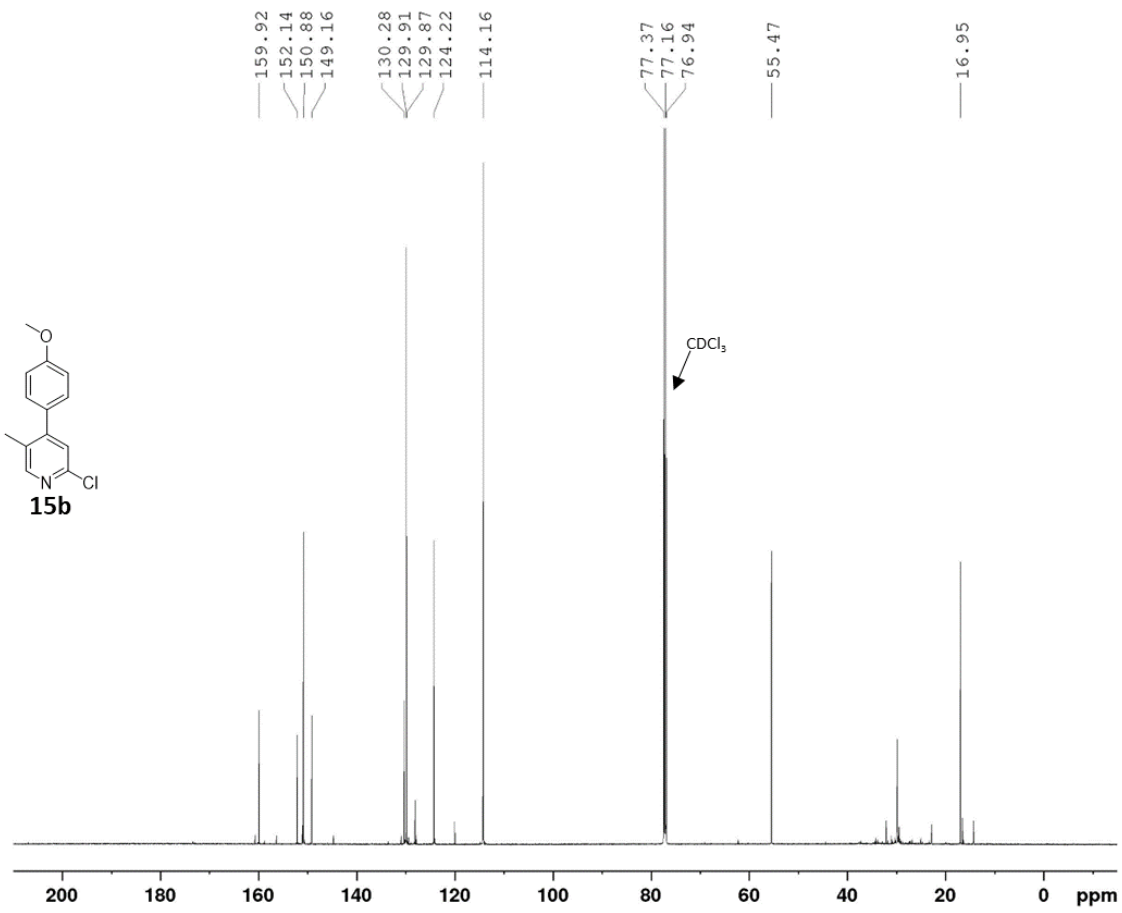


15b

```
Current Data Parameters
NAME      JPN-2-17-2_C4-mono
EXPNO                    10
PROCNO                    1

F2 - Acquisition Parameters
Date_              20200914
Time                  4.30 h
INSTRUM               spect
PROBHD    Z125869_0055 (
PULPROG                zg30
TD                    65536
SOLVENT               CDCl3
NS                       64
DS                        2
SWH              10000.000 Hz
FIDRES               0.305176 Hz
AQ                3.2767999 sec
RG                   25.21
DW                   50.000 usec
DE                   16.00 usec
TE                   300.0 K
D1               2.00000000 sec
TD0                       1
SFO1           500.2330889 MHz
NUC1                     1H
P0                    4.00 usec
P1                   12.00 usec
PLW1          11.44699955 W

F2 - Processing parameters
SI                    65536
SF             500.2300047 MHz
WDW                      EM
SSB       0
LB                    0.30 Hz
GB        0
PC                    1.00
```

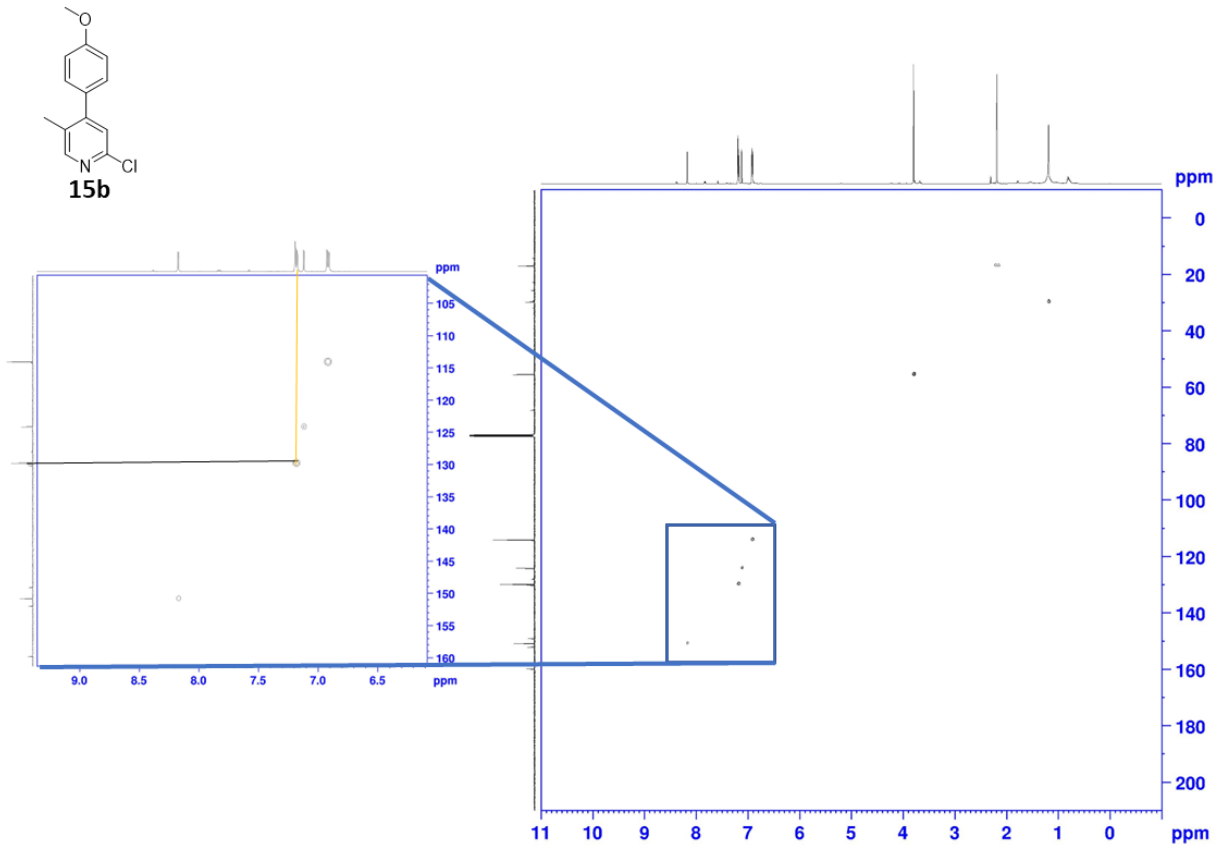


15b

```
Current Data Parameters
NAME          JPN-2-17-2
EXPNO                 11
PROCNO                 1

F2 - Acquisition Parameters
Date_           20200519
Time              16.32 h
INSTRUM             spect
PROBHD   Z127277_0002 (
PULPROG          zgpg30
TD                65536
SOLVENT           CDCl3
NS                 1024
DS                    4
SWH           36057.691 Hz
FIDRES         1.100393 Hz
AQ            0.9087659 sec
RG                184.4
DW               13.867 usec
DE                18.00 usec
TE                300.0 K
D1           2.00000000 sec
D11          0.03000000 sec
TD0                   1
SFO1        150.9178981 MHz
NUC1                13C
P0                 4.00 usec
P1                12.00 usec
PLW1        91.00000000 W
SFO2        600.1324005 MHz
NUC2                1H
CPDPRG[2         waltz16
PCPD2             70.00 usec
PLW2         5.59999990 W
PLW12        0.07314300 W
PLW13        0.03679000 W

F2 - Processing parameters
SI                32768
SF          150.9027914 MHz
WDW                  EM
SSB       0
LB                1.00 Hz
GB        0
PC                1.40
```



Current Data Parameters
NAME JPN-2-1-167-4
EXPNO 12
PROCNO 1

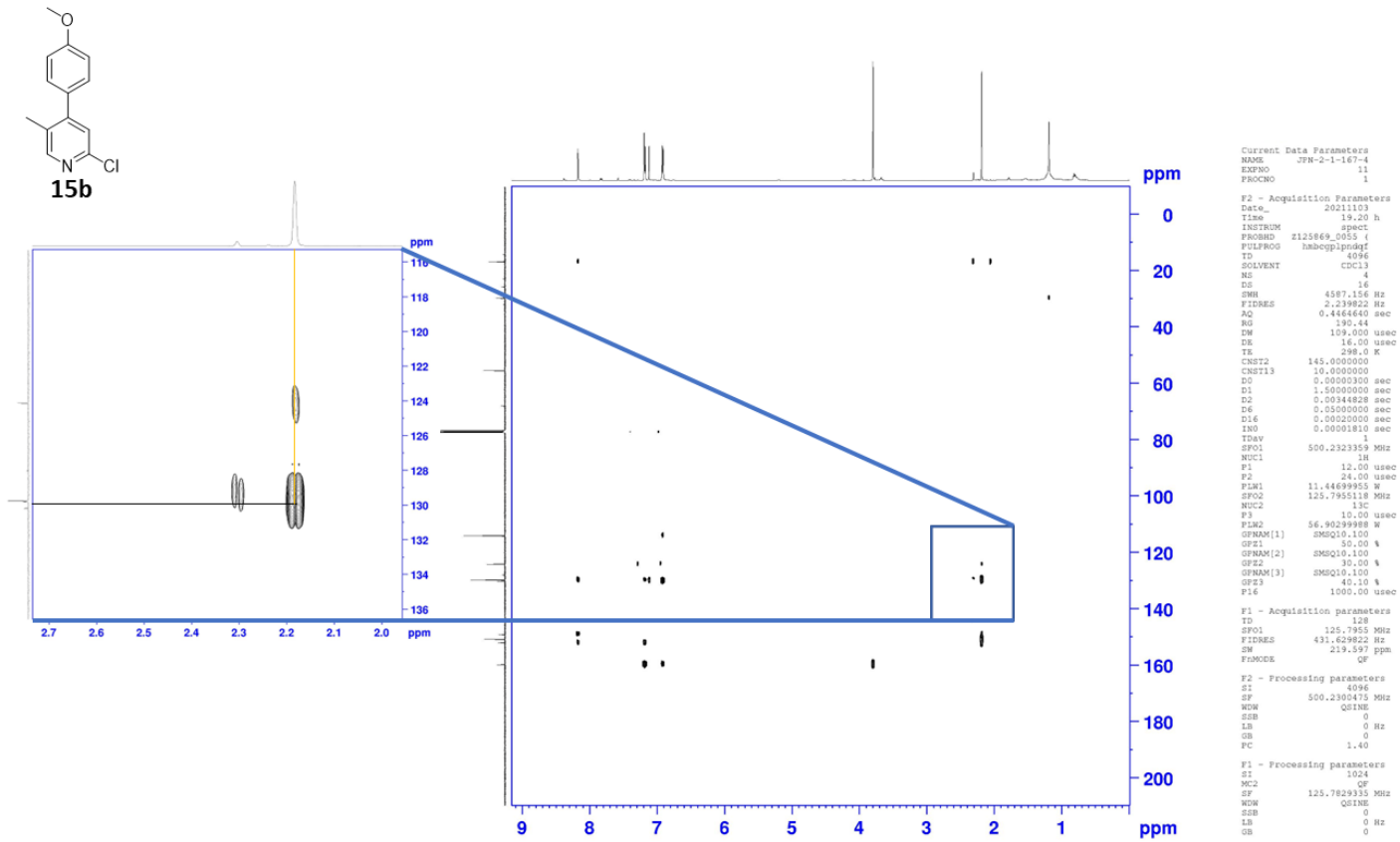
F2 - Acquisition Parameters
Date_ 20211103
Time 20.15 h
INSTRUM spect
PROBHD Z125869_0055 (
PULPROG hsqcetgp
TD 1024
SOLVENT CDCl3
NS 8
DS 16
SWH 7002.801 Hz
FIDRES 13.677346 Hz
AQ 0.07311136 sec
RG 190.44
DW 71.400 usec
DE 16.00 usec
TE 298.0 K
CNST2 145.0000000
D0 0.00000300 sec
D1 1.50000000 sec
D4 0.00172414 sec
D11 0.03000000 sec
D16 0.00020000 sec
IN0 0.00001990 sec
TDav 1
ZGOPTNS
SFO1 500.2330889 MHz
NUC1 1H
P1 12.00 usec
P2 24.00 usec
PLW1 11.44699955 W
SFO2 125.7948829 MHz
NUC2 13C
CPDPRG[2 garp
P3 10.00 usec
P4 20.00 usec
PCPD2 70.00 usec
PLW2 56.90299988 W
PLW12 1.16129994 W
GPNAM[1] SMSQ10.100
GPZ1 80.00 %
GPNAM[2] SMSQ10.100
GPZ2 20.10 %
P16 1000.00 usec

F1 - Acquisition parameters
TD 256
SFO1 125.7949 MHz
FIDRES 196.293976 Hz
SW 199.735 ppm
FnMODE Echo-Antiecho

F2 - Processing parameters
SI 1024
SF 500.2300477 MHz
WDW QSINE
SSB 2
LB 0 Hz
GB 0
PC 1.40

F1 - Processing parameters
SI 1024
MC2 echo-antiecho
SF 125.7829335 MHz
WDW QSINE
SSB 2
LB 0 Hz
GB 0

^{13}C at 130 ppm correlated to the *meta* C-H protons



Meta C-H protons correlate to methyl on the C5 carbon

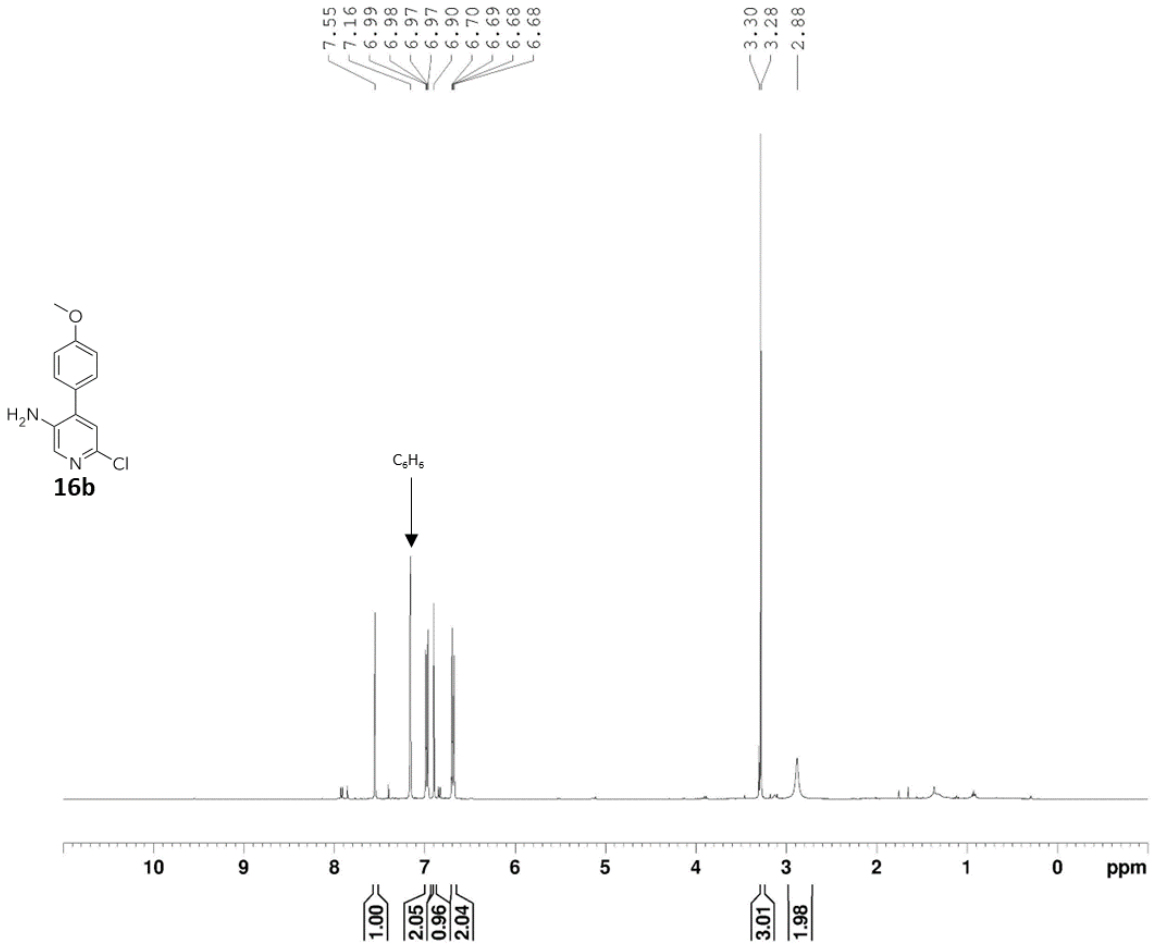
```
Current Data Parameters
NAME        JPN-2-1-167-4
EXPNO                  11
PROCNO                  1

F2 - Acquisition Parameters
Date_            20211103
Time                19.20 h
INSTRUM              spect
PROBHD   Z125869_0055 (
PULPROG     hmbcgplpndqf
TD                  4096
SOLVENT             CDCl3
NS                     4
DS                    16
SWH              4587.156 Hz
FIDRES           2.239822 Hz
AQ               0.4464640 sec
RG                 190.44
DW                109.000 usec
DE                 16.00 usec
TE                 298.0 K
CNST2          145.0000000
CNST13          10.0000000
D0              0.00000300 sec
D1              1.50000000 sec
D2              0.00344828 sec
D6              0.05000000 sec
D16             0.00020000 sec
IN0             0.00001810 sec
TDav                   1
SFO1           500.2323359 MHz
NUC1                  1H
P1                 12.00 usec
P2                 24.00 usec
PLW1           11.44699955 W
SFO2           125.7955118 MHz
NUC2                  13C
P3                 10.00 usec
PLW2           56.90299988 W
GPNAM[1]       SMSQ10.100
GPZ1               50.00 %
GPNAM[2]       SMSQ10.100
GPZ2               30.00 %
GPNAM[3]       SMSQ10.100
GPZ3               40.10 %
P16              1000.00 usec

F1 - Acquisition parameters
TD                   128
SFO1           125.7955 MHz
FIDRES         431.629822 Hz
SW                219.597 ppm
FnMODE                QF

F2 - Processing parameters
SI                  4096
SF             500.2300475 MHz
WDW                 QSINE
SSB                    0
LB                     0 Hz
GB                     0
PC                  1.40

F1 - Processing parameters
SI                  1024
MC2                   QF
SF             125.7829335 MHz
WDW                 QSINE
SSB                    0
LB                     0 Hz
GB                     0
```

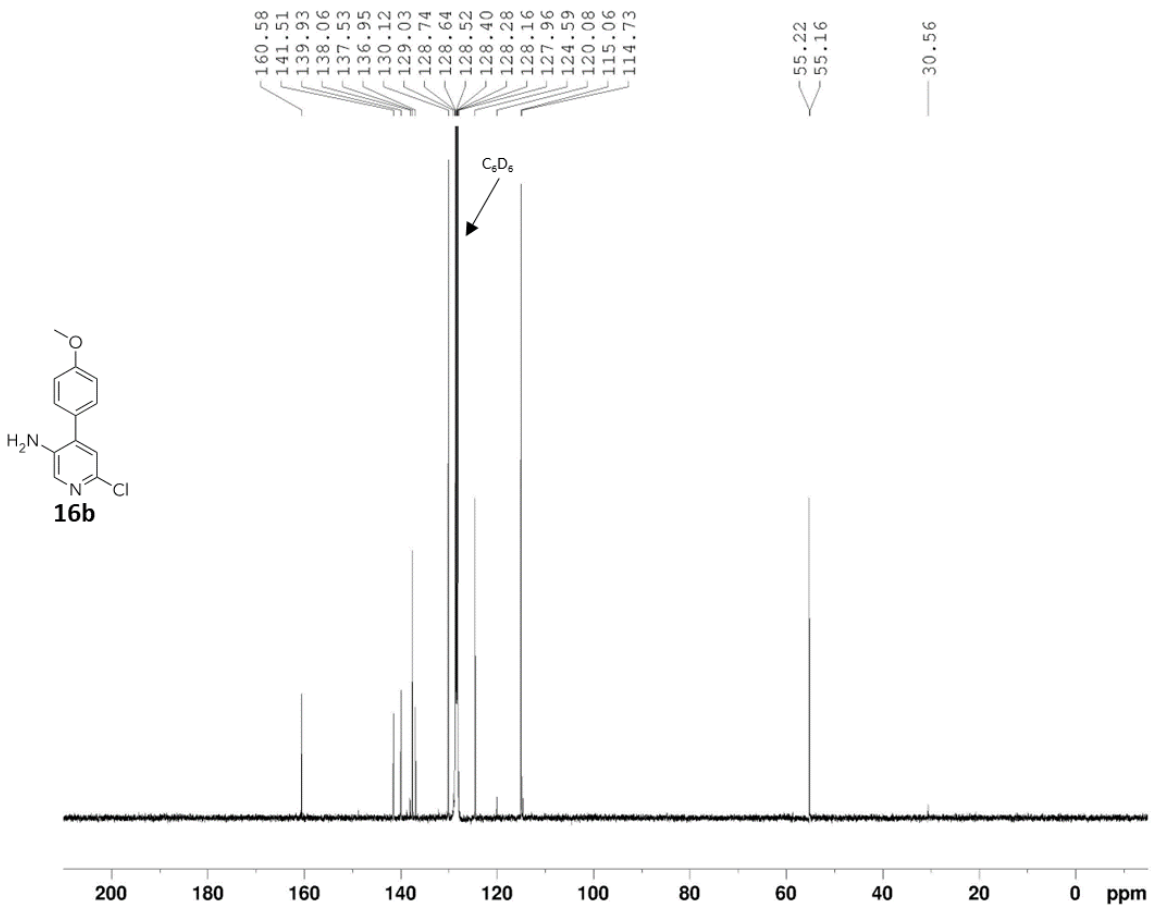


16b

```
Current Data Parameters
NAME        NL-1-94-1Hx2
EXPNO                 10
PROCNO                 1

F2 - Acquisition Parameters
Date_           20210807
Time              12.32 h
INSTRUM       Avance Neo
PROBHD   Z152088_0031 (
PULPROG             zg30
TD                 65536
SOLVENT             C6D6
NS                    16
DS                     2
SWH             8196.722 Hz
FIDRES          0.250144 Hz
AQ              3.9976959 sec
RG                   101
DW                61.000 usec
DE                13.89 usec
TE                298.1 K
D1             1.00000000 sec
TD0                    1
SFO1          400.1324708 MHz
NUC1                  1H
P0                 2.67 usec
P1                 8.00 usec
PLW1          24.03499985 W

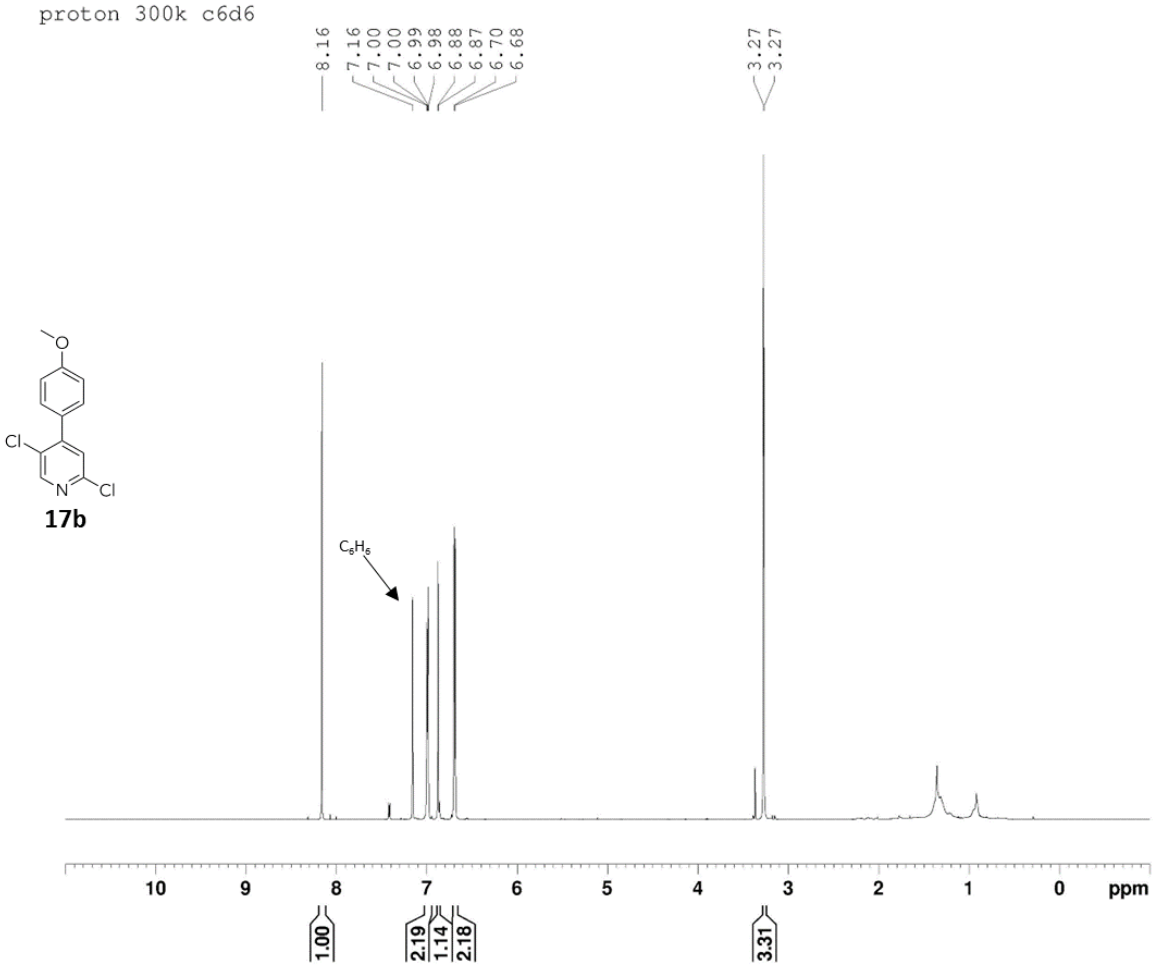
F2 - Processing parameters
SI                 65536
SF            400.1299967 MHz
WDW                   EM
SSB                    0
LB                  0.30 Hz
GB                     0
PC                  1.00
```




```
Current Data Parameters
NAME        NL-1-94-1Hx2
EXPNO                 11
PROCNO                 1

F2 - Acquisition Parameters
Date_           20210807
Time               19.40 h
INSTRUM       Avance Neo
PROBHD   Z152088_0031 (
PULPROG          zgpg30
TD                65536
SOLVENT             C6D6
NS                  1024
DS                     4
SWH            23809.523 Hz
FIDRES          0.726609 Hz
AQ              1.3762560 sec
RG                 8.125
DW                21.000 usec
DE                 6.50 usec
TE                298.1 K
D1           2.00000000 sec
D11          0.03000000 sec
TD0                    1
SFO1         100.6228298 MHz
NUC1                13C
P0                 2.67 usec
P1                 8.00 usec
PLW1         86.55400085 W
SFO2         400.1316005 MHz
NUC2                1H
CPDPRG[2         waltz65
PCPD2             90.00 usec
PLW2         24.03499985 W
PLW12         0.18990999 W
PLW13         0.09552100 W

F2 - Processing parameters
SI                 32768
SF           100.6126977 MHz
WDW                   EM
SSB                    0
LB                  1.00 Hz
GB                     0
PC                  1.40
```

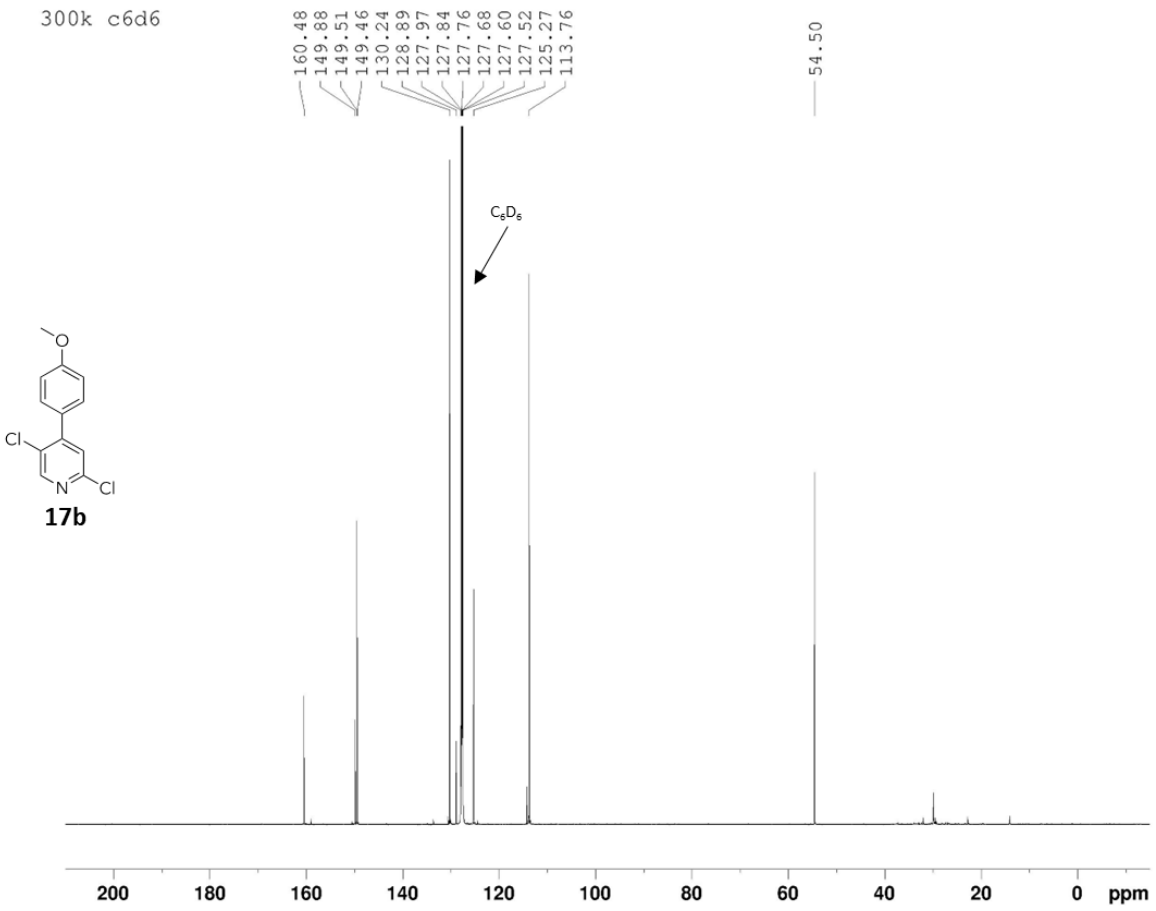


17b

```
Current Data Parameters
NAME      NL-1-93-1n-inadequate-08-27-2
EXPNO                 1
PROCNO                1

F2 - Acquisition Parameters
Date_          20210827
Time              12.31 h
INSTRUM           spect
PROBHD   Z127277_0002 (
PULPROG           zg30
TD               65536
SOLVENT           C6D6
NS                  16
DS                   2
SWH           12019.230 Hz
FIDRES         0.366798 Hz
AQ             2.7262976 sec
RG                6.41
DW               41.600 usec
DE               10.00 usec
TE               300.0 K
D1            1.00000000 sec
TD0                  1
SFO1         600.1337060 MHz
NUC1                 1H
P0                2.67 usec
P1                8.00 usec
PLW1          5.59999990 W

F2 - Processing parameters
SI               65536
SF           600.1299970 MHz
WDW                 EM
SSB                  0
LB                0.30 Hz
GB                   0
PC                1.00
```

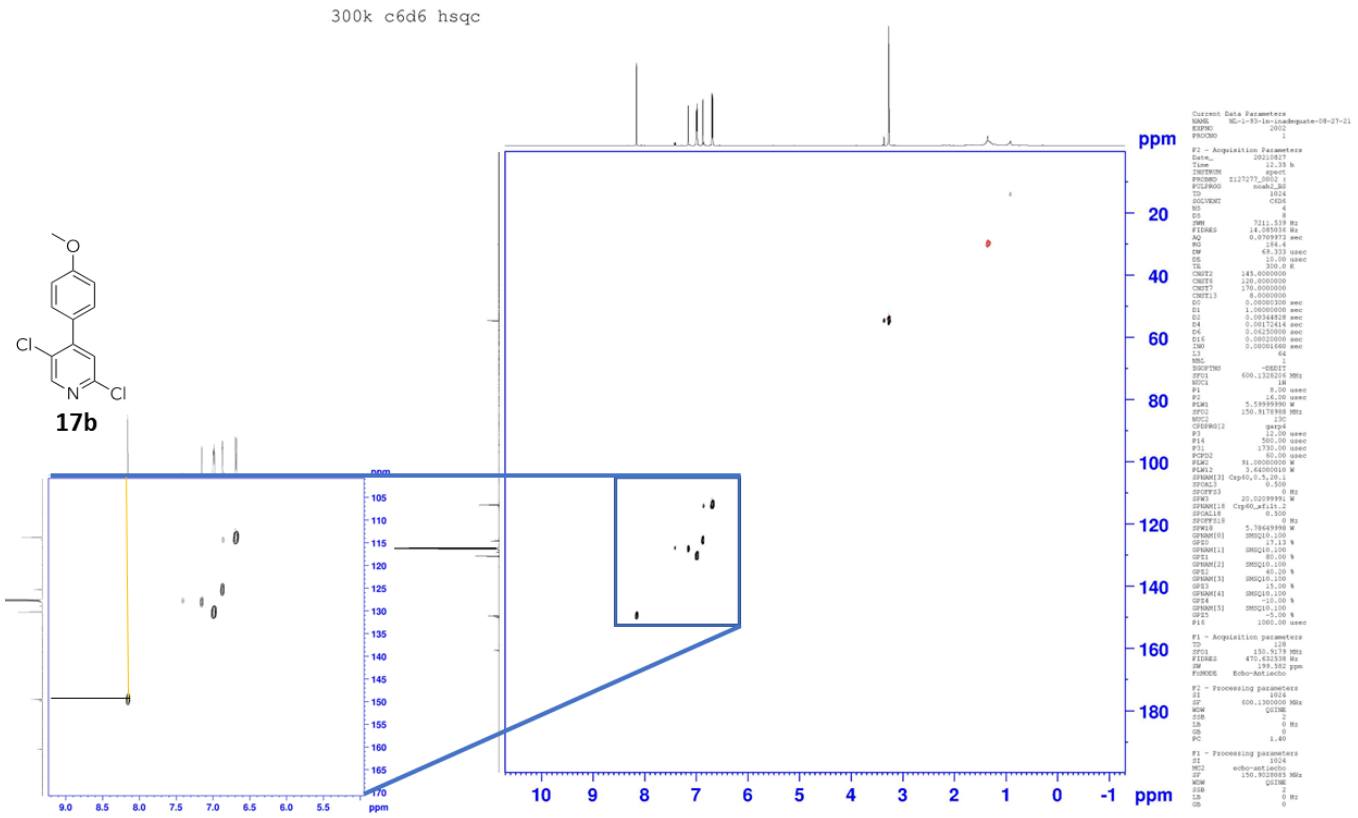


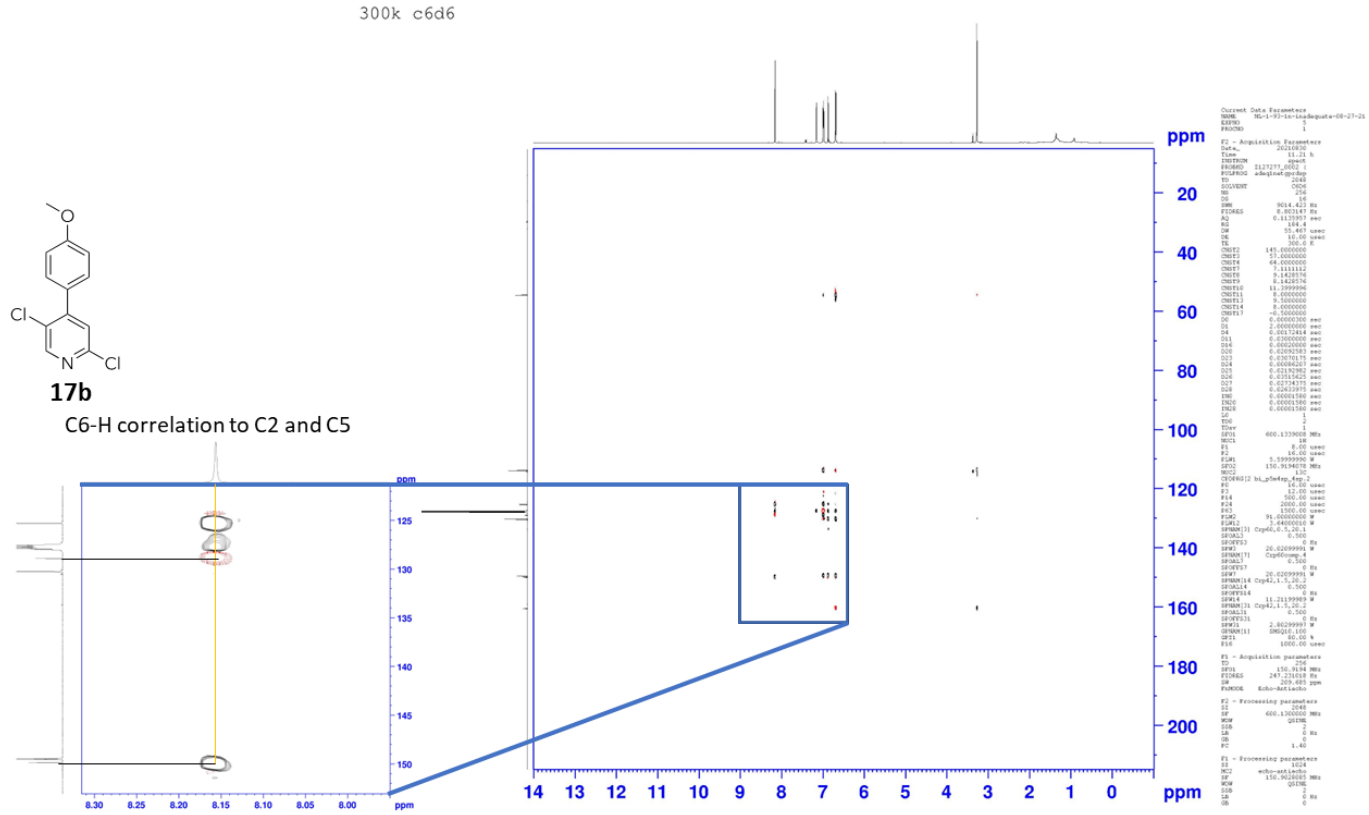
17b

```
Current Data Parameters
NAME      NL-1-93-1n-inadequate-08-27-2
EXPNO                 4
PROCNO                1

F2 - Acquisition Parameters
Date_          20210830
Time               9.42 h
INSTRUM           spect
PROBHD   Z127277_0002 (
PULPROG          zgpg30
TD                65536
SOLVENT             C6D6
NS                  1024
DS                     4
SWH            36057.691 Hz
FIDRES          1.100393 Hz
AQ              0.9087659 sec
RG                184.4
DW               13.867 usec
DE                18.00 usec
TE                300.0 K
D1            2.00000000 sec
D11           0.03000000 sec
TD0                    1
SFO1         150.9178981 MHz
NUC1                 13C
P0                 4.00 usec
P1                12.00 usec
PLW1         91.00000000 W
SFO2         600.1324005 MHz
NUC2                 1H
CPDPRG[2         waltz16
PCPD2             70.00 usec
PLW2           5.59999990 W
PLW12          0.07314300 W
PLW13          0.03679000 W

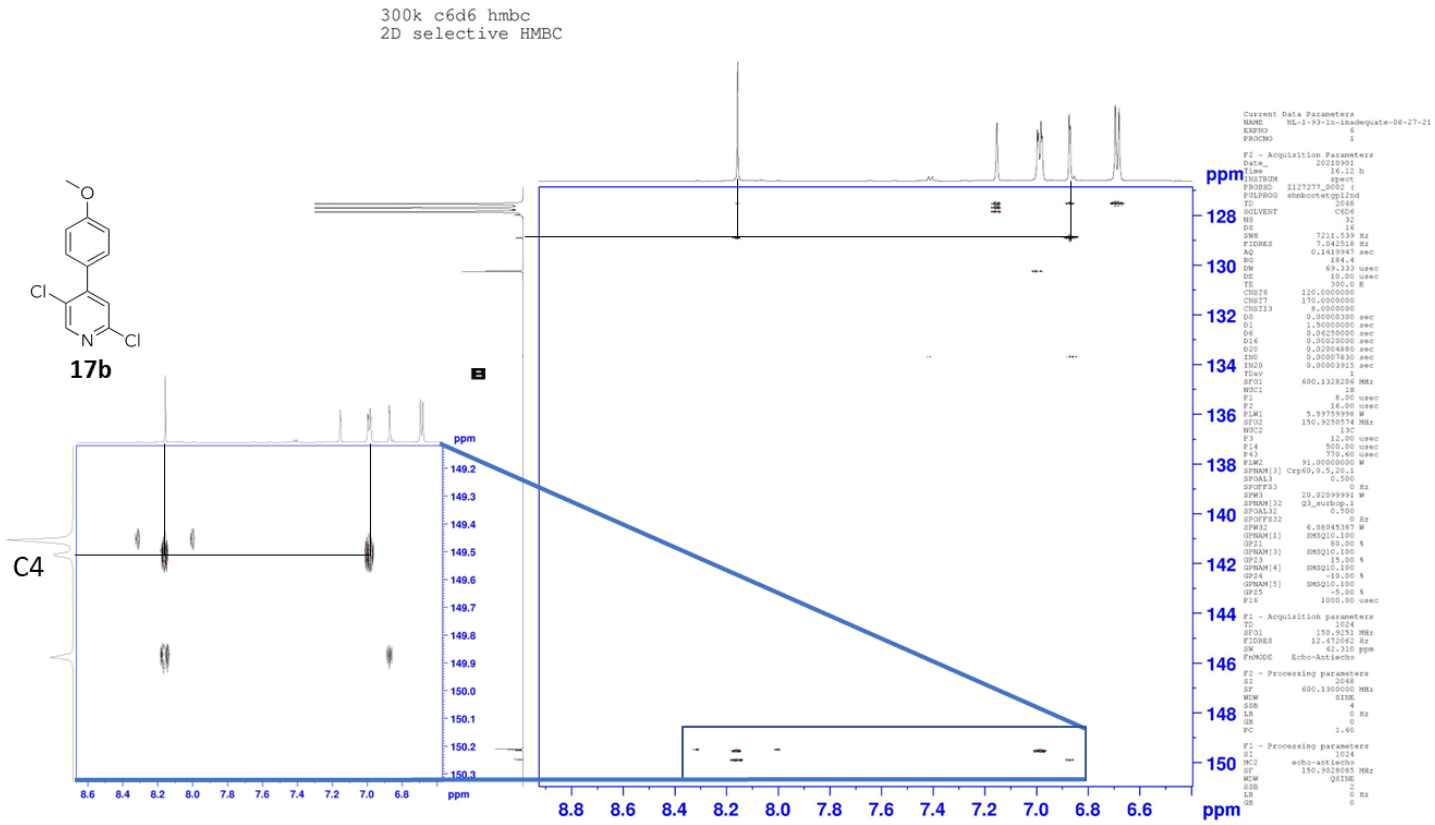
F2 - Processing parameters
SI                 32768
SF           150.9028090 MHz
WDW                   EM
SSB                    0
LB                  1.00 Hz
GB                     0
PC                  1.40
```


300k c6d6 hsqc
17b
Cl
Cl
N
O
ppm
10 9 8 7 6 5 4 3 2 1 0 -1 ppm
20 40 60 80 100 120 140 160 180
9.0 8.5 8.0 7.5 7.0 6.5 6.0 5.5 ppm
105 110 115 120 125 130 135 140 145 150 155 160 165 170 ppm

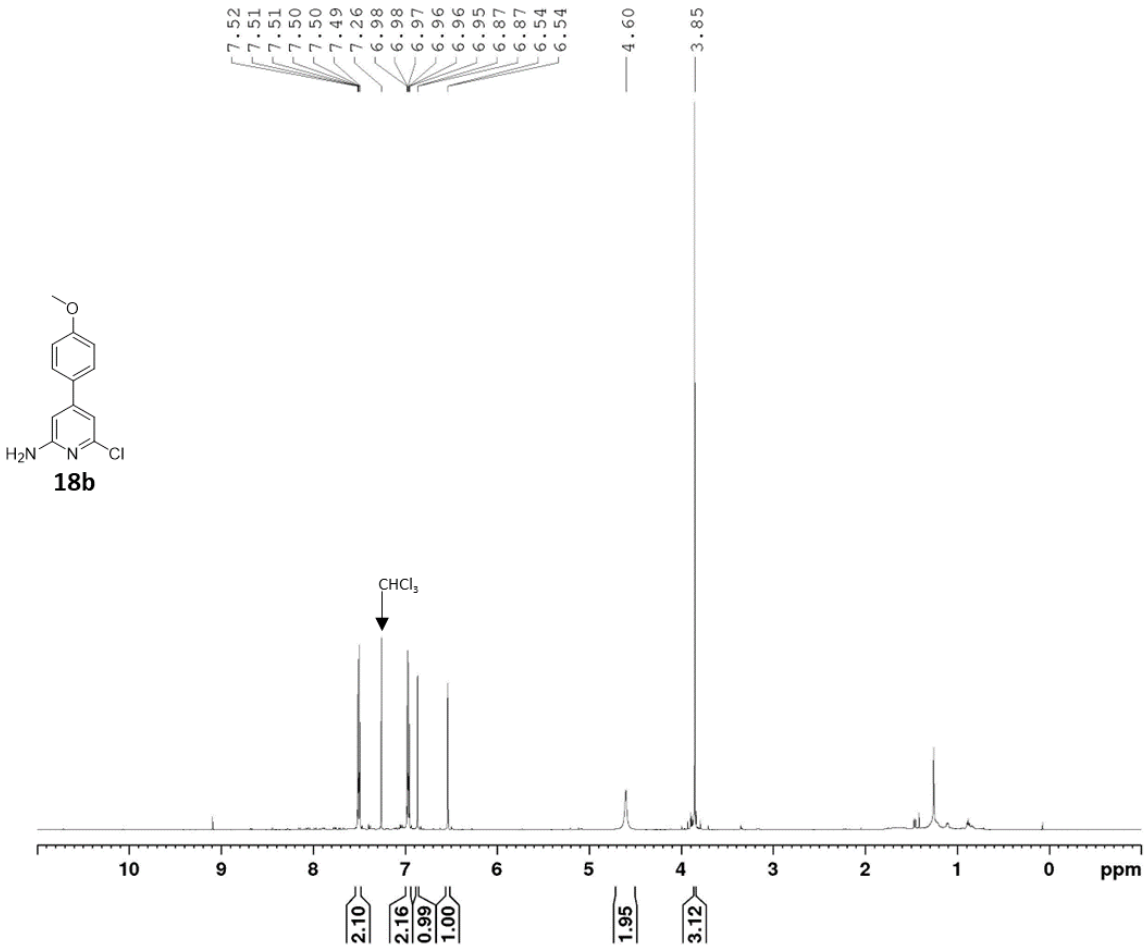


17b

C6-H correlation to C2 and C5



C4 reasoned by process of elimination, HMBC correlations, and chemical shift. Optimized 3-bond correlations. C(129ppm) weak correlation to C6-H, and a strong correlation to C3-H results in identification as C5. Absence of correlation from C(149.5) to C3-H and strong correlation to C6-H results in identification of C4.

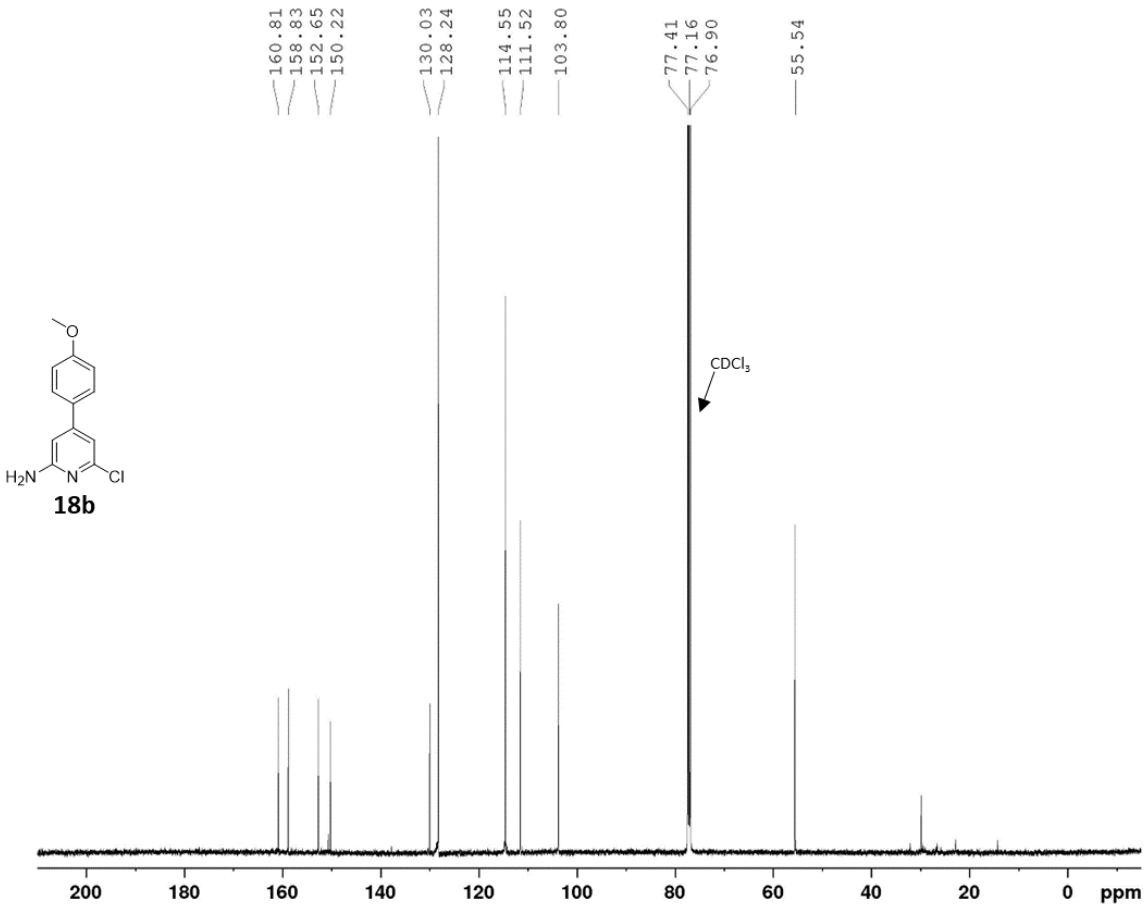


18b

```
Current Data Parameters
NAME          JPN-2-16-2
EXPNO                 16
PROCNO                 1

F2 - Acquisition Parameters
Date_           20211120
Time                1.49 h
INSTRUM            spect
PROBHD   Z125869_0055 (
PULPROG             zg30
TD                 65536
SOLVENT            CDCl3
NS                    64
DS                     2
SWH           10000.000 Hz
FIDRES         0.305176 Hz
AQ             3.2767999 sec
RG                151.18
DW                50.000 usec
DE                16.00 usec
TE                298.0 K
D1            2.00000000 sec
TD0                    1
SFO1          500.2330889 MHz
NUC1                  1H
P0                 4.00 usec
P1                12.00 usec
PLW1         11.44699955 W

F2 - Processing parameters
SI                 65536
SF          500.2300121 MHz
WDW                   EM
SSB       0
LB                 0.30 Hz
GB        0
PC                 1.00
```

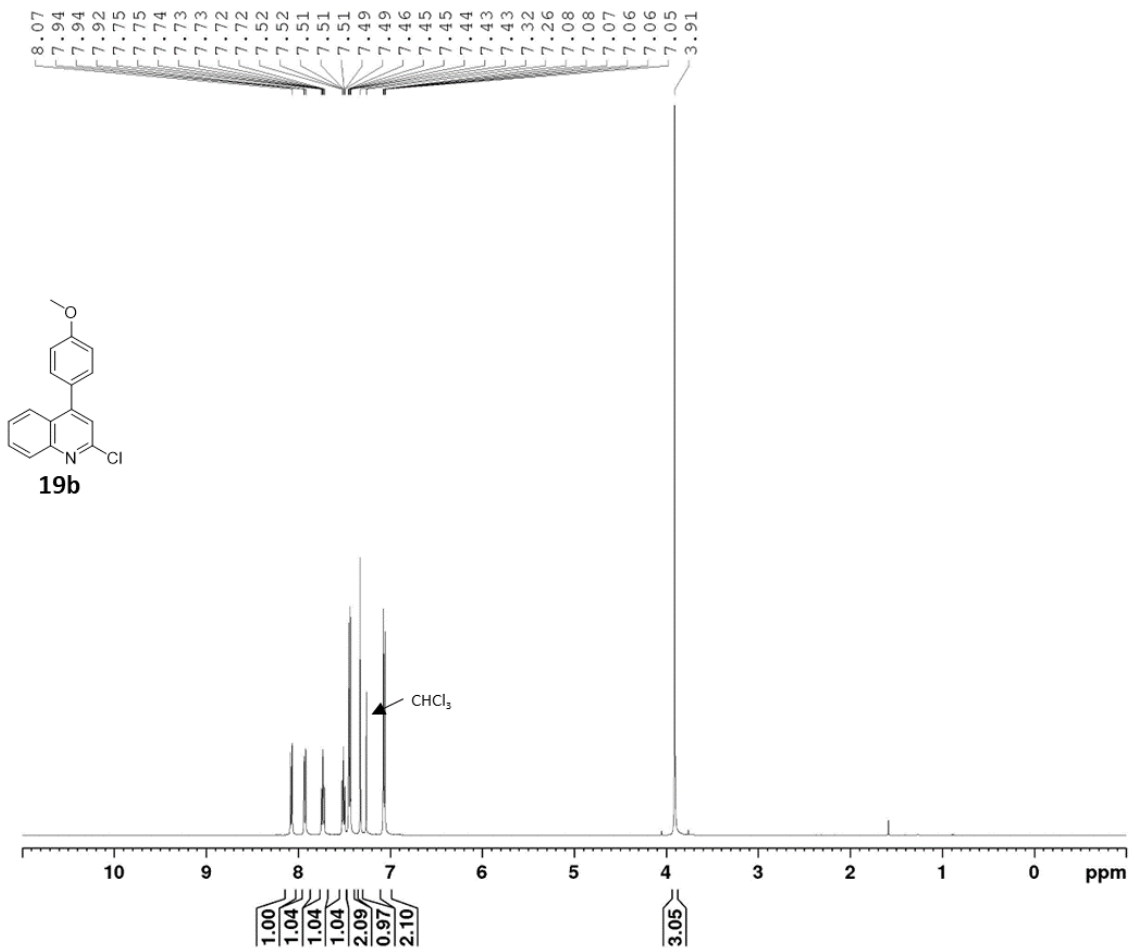


18b

```
Current Data Parameters
NAME          JPN-2-16-2
EXPNO                 17
PROCNO                 1

F2 - Acquisition Parameters
Date_           20211120
Time                2.45 h
INSTRUM            spect
PROBHD   Z125869_0055 (
PULPROG           zgpg30
TD                 65536
SOLVENT            CDCl3
NS                  1024
DS                     4
SWH            29761.904 Hz
FIDRES          0.908261 Hz
AQ             1.1010048 sec
RG                190.44
DW                16.800 usec
DE                18.00 usec
TE                298.0 K
D1             2.00000000 sec
D11            0.03000000 sec
TD0                    1
SFO1         125.7955118 MHz
NUC1                13C
P0                 3.33 usec
P1                10.00 usec
PLW1          56.90299988 W
SFO2         500.2320009 MHz
NUC2                1H
CPDPRG[2         waltz16
PCPD2             80.00 usec
PLW2          11.44699955 W
PLW12          0.25756001 W
PLW13          0.12955000 W

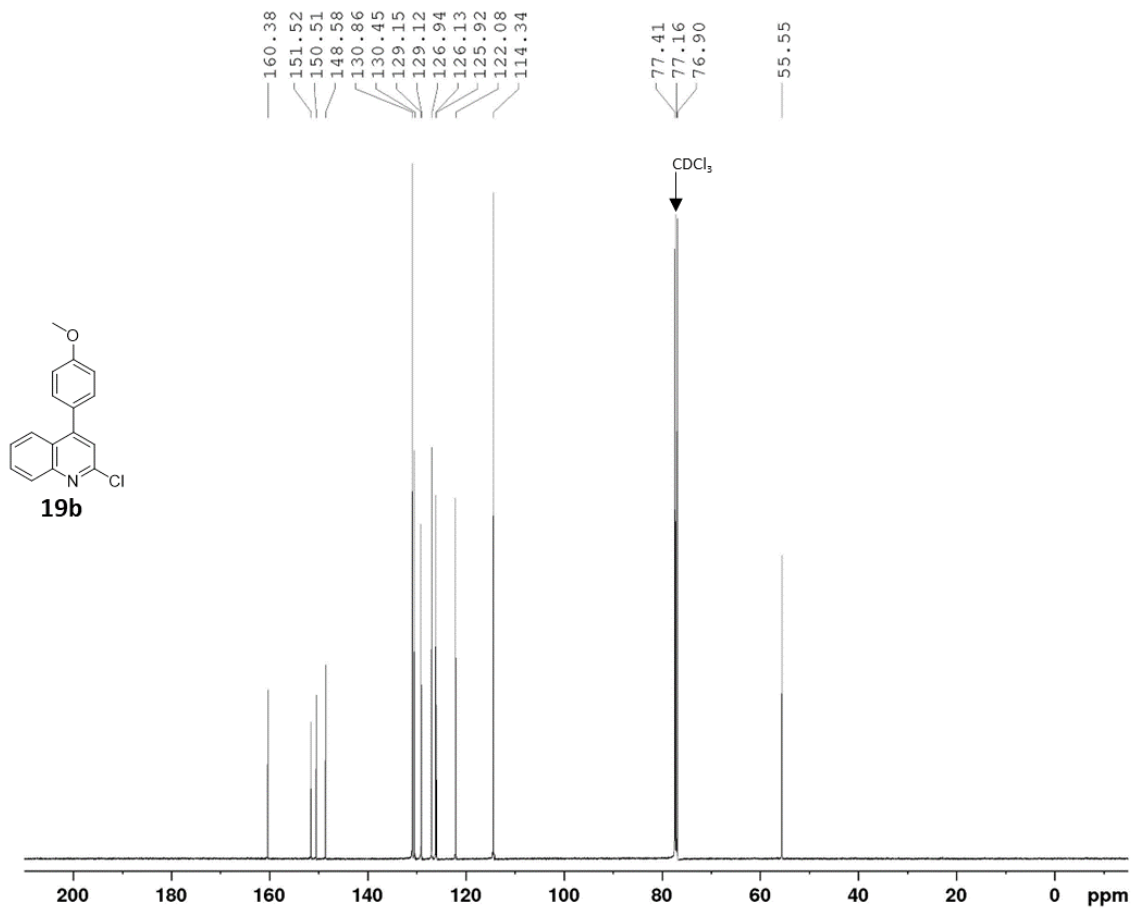
F2 - Processing parameters
SI                 32768
SF           125.7829170 MHz
WDW                   EM
SSB       0
LB                 1.00 Hz
GB        0
PC                 1.40
```




```
Current Data Parameters
NAME      JPN-2-8_repeat_C4-mono_crop
EXPNO                  10
PROCNO                  1

F2 - Acquisition Parameters
Date_           20201130
Time               17.10 h
INSTRUM             spect
PROBHD   Z125869_0055 (
PULPROG              zg30
TD                  65536
SOLVENT             CDCl3
NS                     64
DS                      2
SWH            10000.000 Hz
FIDRES          0.305176 Hz
AQ              3.2767999 sec
RG                 122.05
DW                 50.000 usec
DE                 16.00 usec
TE                 300.0 K
D1             2.00000000 sec
TD0                     1
SFO1         500.2330889 MHz
NUC1                   1H
P0                  4.00 usec
P1                 12.00 usec
PLW1         11.44699955 W

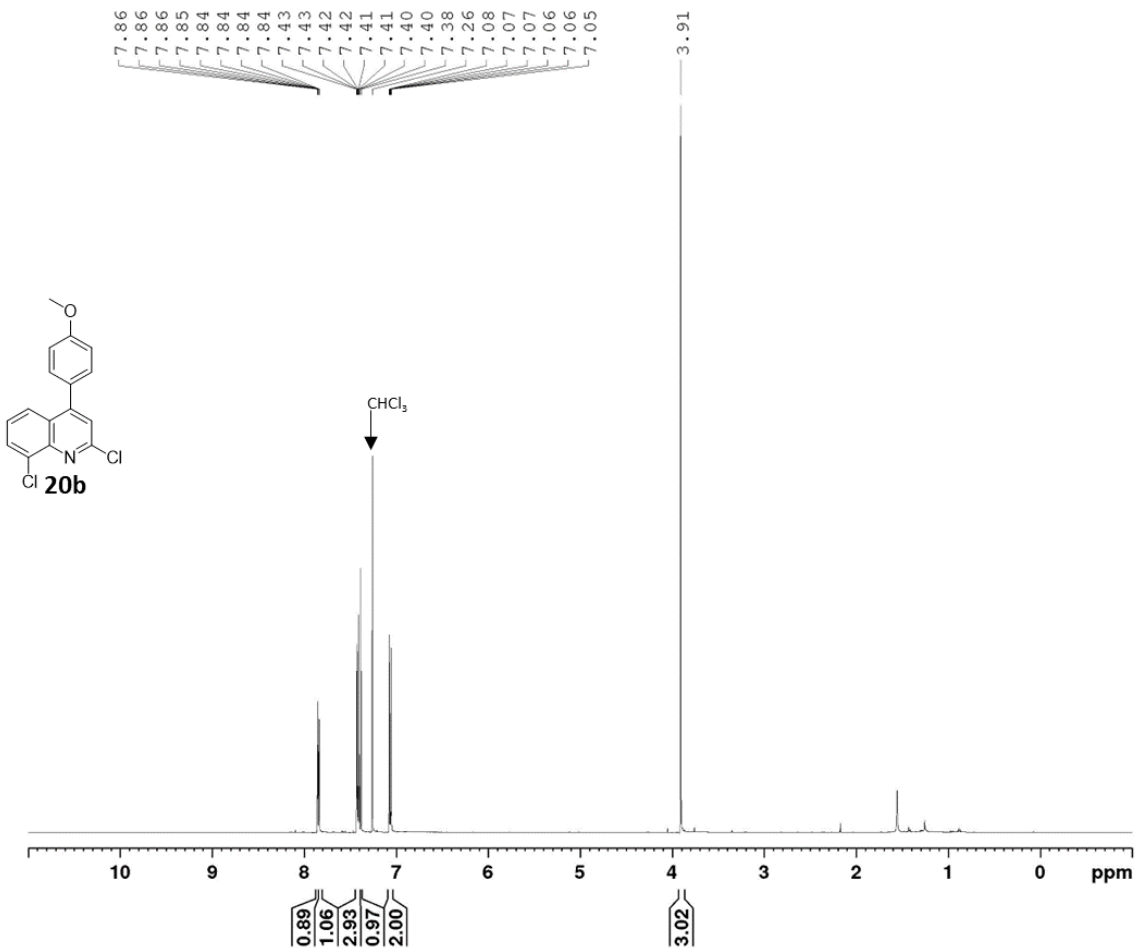
F2 - Processing parameters
SI                  65536
SF           500.2300120 MHz
WDW                    EM
SSB       0
LB                  0.30 Hz
GB        0
PC                  1.00
```




```
Current Data Parameters
NAME      JPN-2-8_repeat
EXPNO                 17
PROCNO                 1

F2 - Acquisition Parameters
Date_           20211119
Time               6.24 h
INSTRUM           spect
PROBHD   Z125869_0055 (
PULPROG         zgpg30
TD               65536
SOLVENT          CDCl3
NS                1024
DS                   4
SWH           29761.904 Hz
FIDRES         0.908261 Hz
AQ            1.1010048 sec
RG               190.44
DW               16.800 usec
DE               18.00 usec
TE               298.0 K
D1           2.00000000 sec
D11          0.03000000 sec
TD0                  1
SFO1        125.7955118 MHz
NUC1               13C
P0                3.33 usec
P1               10.00 usec
PLW1        56.90299988 W
SFO2        500.2320009 MHz
NUC2               1H
CPDPRG[2        waltz16
PCPD2            80.00 usec
PLW2        11.44699955 W
PLW12        0.25756001 W
PLW13        0.12955000 W

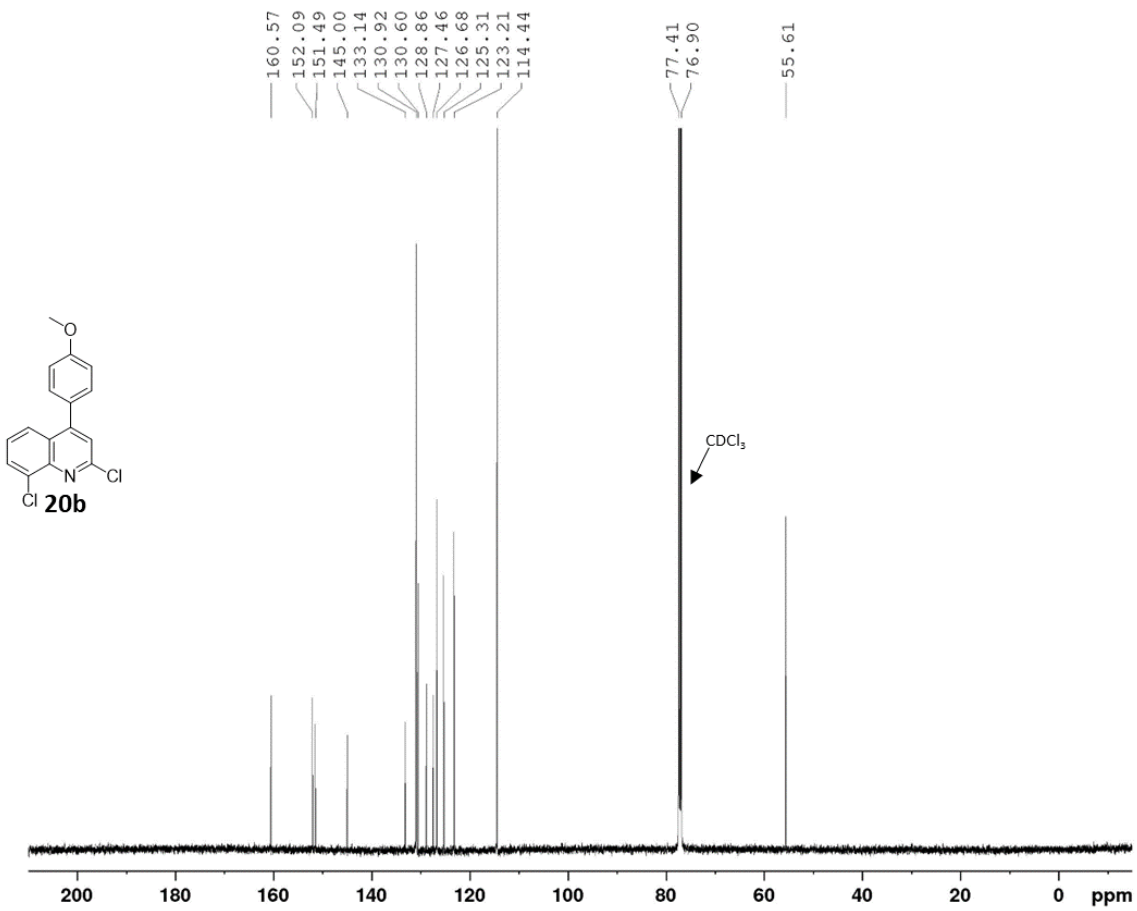
F2 - Processing parameters
SI               32768
SF          125.7829201 MHz
WDW                EM
SSB       0
LB               1.00 Hz
GB        0
PC               1.40
```




```
Current Data Parameters
NAME      JPN-2-47-3_20-Nov-2021
EXPNO                 10
PROCNO                 1

F2 - Acquisition Parameters
Date_           20211120
Time               21.51 h
INSTRUM            spect
PROBHD   Z125869_0055 (
PULPROG             zg30
TD                 65536
SOLVENT            CDCl3
NS                    64
DS                     2
SWH            10000.000 Hz
FIDRES          0.305176 Hz
AQ              3.2767999 sec
RG                151.18
DW                 50.000 usec
DE                 16.00 usec
TE                 298.0 K
D1             2.00000000 sec
TD0                    1
SFO1         500.2330889 MHz
NUC1                  1H
P0                 4.00 usec
P1                12.00 usec
PLW1         11.44699955 W

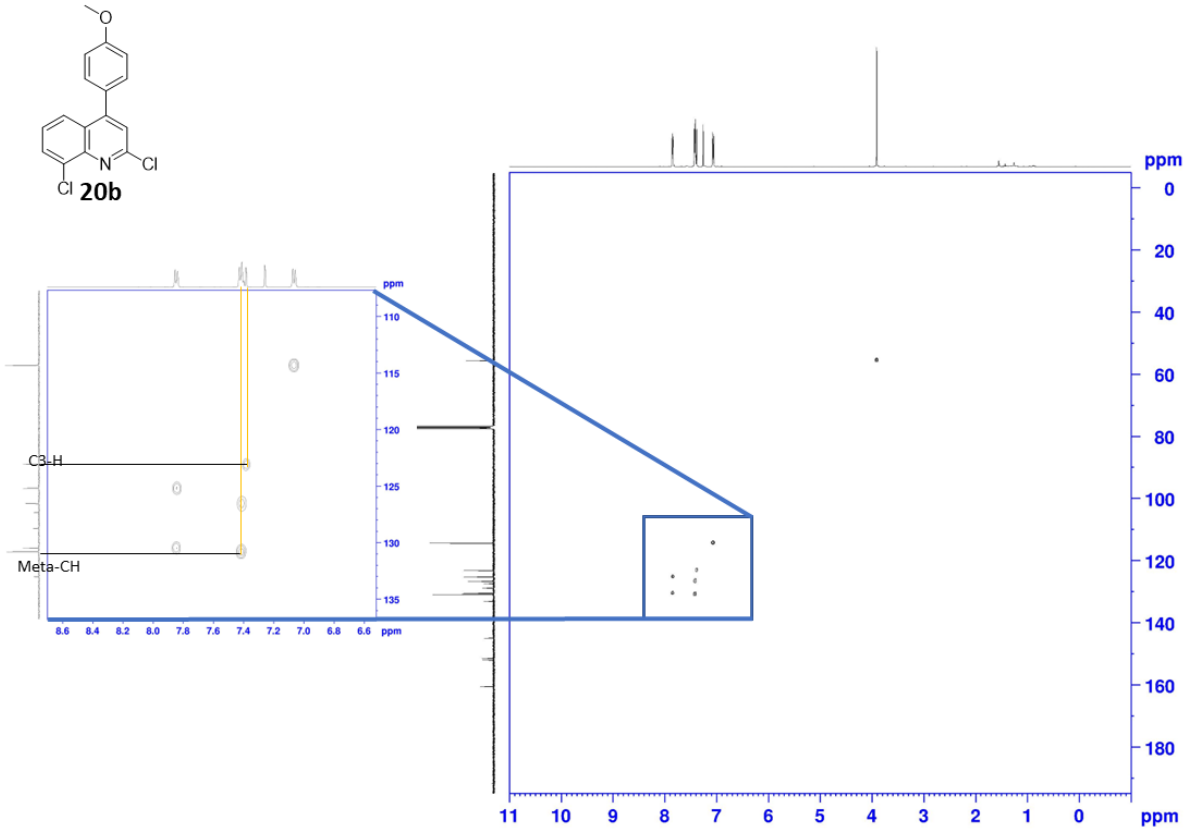
F2 - Processing parameters
SI                 65536
SF           500.2300121 MHz
WDW                   EM
SSB       0
LB                 0.30 Hz
GB        0
PC                 1.00
```




```
Current Data Parameters
NAME      JPN-2-47-3_20-Nov-2021
EXPNO                    11
PROCNO                    1

F2 - Acquisition Parameters
Date_            20211120
Time                22.47 h
INSTRUM             spect
PROBHD    Z125869_0055 (
PULPROG            zgpg30
TD                  65536
SOLVENT             CDCl3
NS                   1024
DS                      4
SWH              29761.904 Hz
FIDRES            0.908261 Hz
AQ               1.1010048 sec
RG                  190.44
DW                 16.800 usec
DE                 18.00 usec
TE                 298.0 K
D1              2.00000000 sec
D11             0.03000000 sec
TD0                     1
SFO1           125.7955118 MHz
NUC1                  13C
P0                   3.33 usec
P1                  10.00 usec
PLW1           56.90299988 W
SFO2           500.2320009 MHz
NUC2                  1H
CPDPRG[2           waltz16
PCPD2               80.00 usec
PLW2           11.44699955 W
PLW12           0.25756001 W
PLW13           0.12955000 W

F2 - Processing parameters
SI                   32768
SF             125.7829164 MHz
WDW                     EM
SSB       0
LB                   1.00 Hz
GB        0
PC                   1.40
```



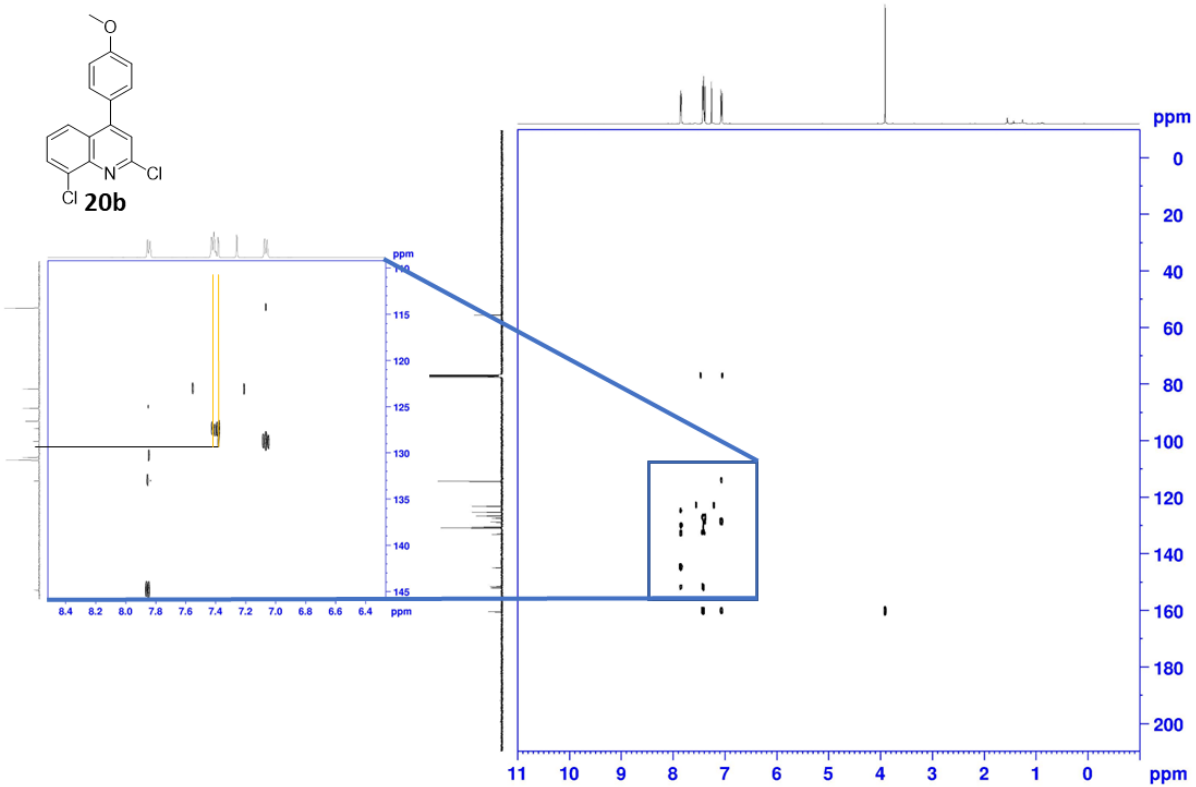

```
Current Data Parameters
NAME              JPN-2-47-3
EXPNO                     13
PROCNO                     1

F2 - Acquisition Parameters
Date_           20211103
Time                 10.57 h
INSTRUM              spect
PROBHD     Z125869_0055 (
PULPROG          hsqcetgp
TD                   1024
SOLVENT              CDCl3
NS                      8
DS                     16
SWH               7002.801 Hz
FIDRES           13.677346 Hz
AQ                0.07311136 sec
RG                   190.44
DW                   71.400 usec
DE                   16.00 usec
TE                   298.0 K
CNST2           145.0000000
D0                0.00000300 sec
D1                1.50000000 sec
D4                0.00172414 sec
D11               0.03000000 sec
D16               0.00020000 sec
IN0               0.00001990 sec
TDav                       1
ZGOPTNS
SFO1           500.2330889 MHz
NUC1                     1H
P1                   12.00 usec
P2                   24.00 usec
PLW1          11.44699955 W
SFO2          125.7948829 MHz
NUC2                     13C
CPDPRG[2                 garp
P3                   10.00 usec
P4                   20.00 usec
PCPD2                70.00 usec
PLW2          56.90299988 W
PLW12          1.16129994 W
GPNAM[1]       SMSQ10.100
GPZ1                 80.00 %
GPNAM[2]       SMSQ10.100
GPZ2                 20.10 %
P16                1000.00 usec

F1 - Acquisition parameters
TD                       256
SFO1           125.7949 MHz
FIDRES        196.293976 Hz
SW                199.735 ppm
FnMODE     Echo-Antiecho

F2 - Processing parameters
SI                      1024
SF            500.2300122 MHz
WDW                   QSINE
SSB                        2
LB                         0 Hz
GB                         0
PC                      1.40

F1 - Processing parameters
SI                      1024
MC2          echo-antiecho
SF            125.7829335 MHz
WDW                   QSINE
SSB                        2
LB                         0 Hz
GB                         0
```



Current Data Parameters
NAME JPN-2-47-3
EXPNO 11
PROCNO 1

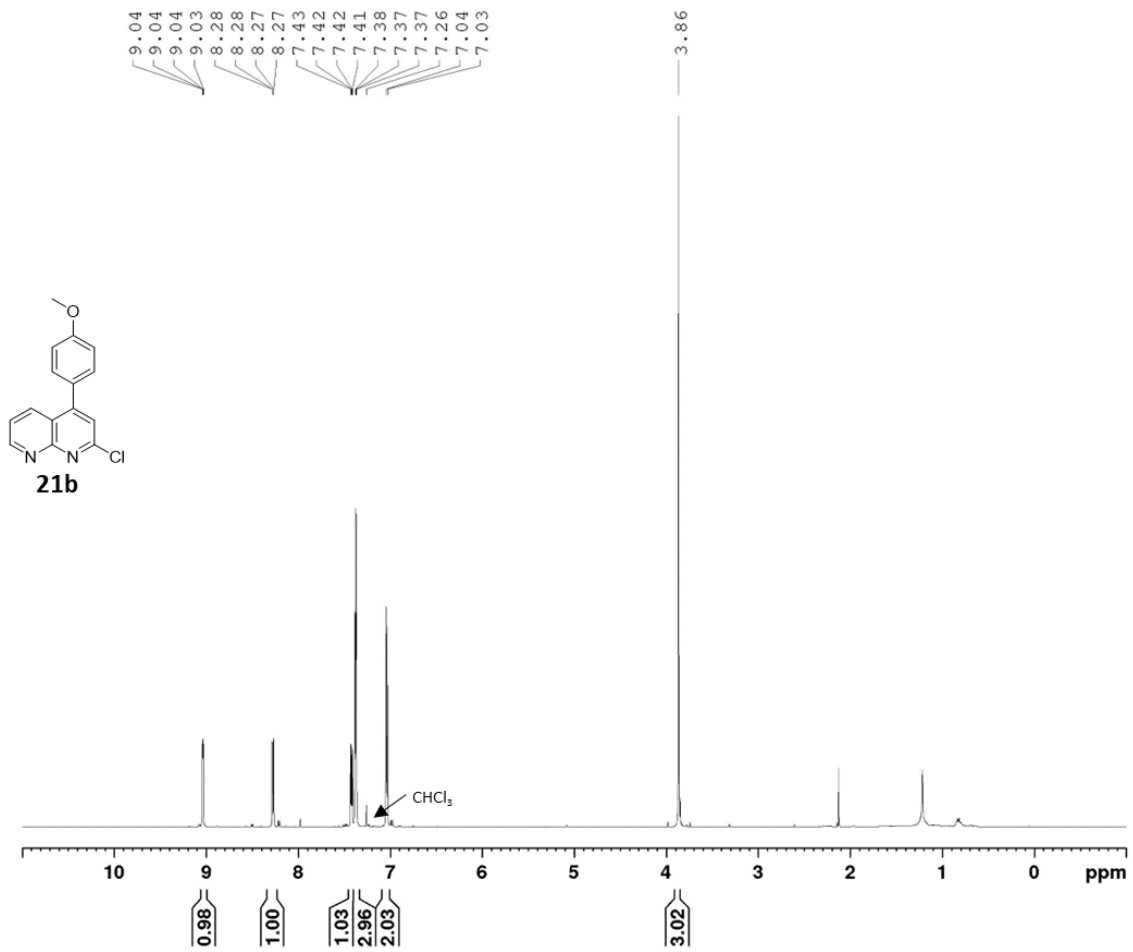
F2 - Acquisition Parameters
Date_ 20211103
Time 18.01 h
INSTRUM spect
PROBHD Z125869_0055 (
PULPROG hmbcgplpndqf
TD 4096
SOLVENT CDCl3
NS 4
DS 16
SWH 4201.681 Hz
FIDRES 2.051602 Hz
AQ 0.4874240 sec
RG 190.44
DW 119.000 usec
DE 16.00 usec
TE 298.0 K
CNST2 145.0000000
CNST13 10.0000000
D0 0.00000300 sec
D1 1.50000000 sec
D2 0.00344828 sec
D6 0.05000000 sec
D16 0.00020000 sec
IN0 0.00001810 sec
TDav 1
SFO1 500.2321971 MHz
NUC1 1H
P1 12.00 usec
P2 24.00 usec
PLW1 11.44699955 W
SFO2 125.7955118 MHz
NUC2 13C
P3 10.00 usec
PLW2 56.90299988 W
GPNAM[1] SMSQ10.100
GPZ1 50.00 %
GPNAM[2] SMSQ10.100
GPZ2 30.00 %
GPNAM[3] SMSQ10.100
GPZ3 40.10 %
P16 1000.00 usec

F1 - Acquisition parameters
TD 128
SFO1 125.7955 MHz
FIDRES 431.629822 Hz
SW 219.597 ppm
FnMODE QF

F2 - Processing parameters
SI 4096
SF 500.2300126 MHz
WDW QSINE
SSB 0
LB 0 Hz
GB 0
PC 1.40

F1 - Processing parameters
SI 1024
MC2 QF
SF 125.7829432 MHz
WDW QSINE
SSB 0
LB 0 Hz
GB 0

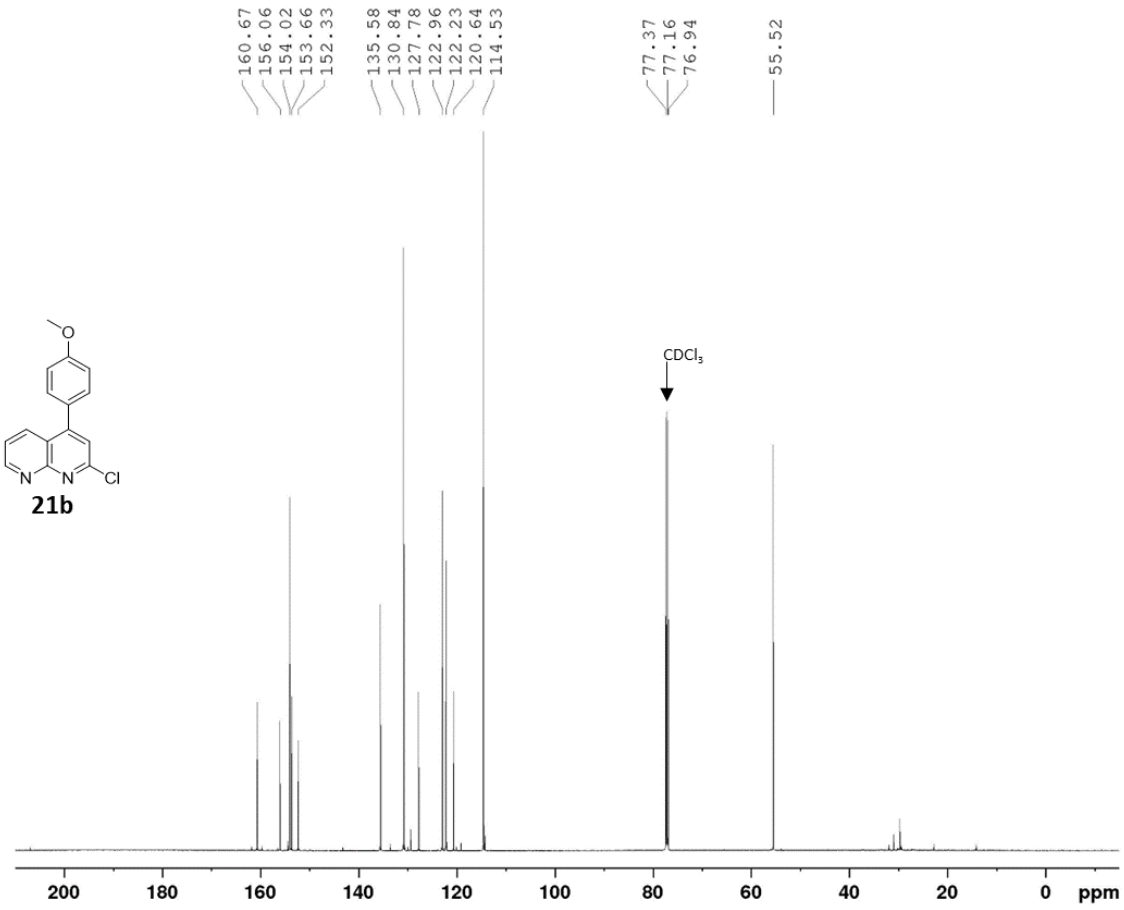
C9 correlation to *meta* C-H and C3-H




```
Current Data Parameters
NAME      JPN-1-169-2_C4-monoaryl
EXPNO                 22
PROCNO                 1

F2 - Acquisition Parameters
Date_           20200527
Time              10.24 h
INSTRUM            spect
PROBHD    Z127277_0002 (
PULPROG             zg30
TD                 65536
SOLVENT            CDCl3
NS                    64
DS                     2
SWH           12019.230 Hz
FIDRES         0.366798 Hz
AQ            2.7262976 sec
RG                  4.41
DW                41.600 usec
DE                10.00 usec
TE                300.0 K
D1           1.00000000 sec
TD0                    1
SFO1        600.1337060 MHz
NUC1                  1H
P0                 2.67 usec
P1                 8.00 usec
PLW1          5.59999990 W

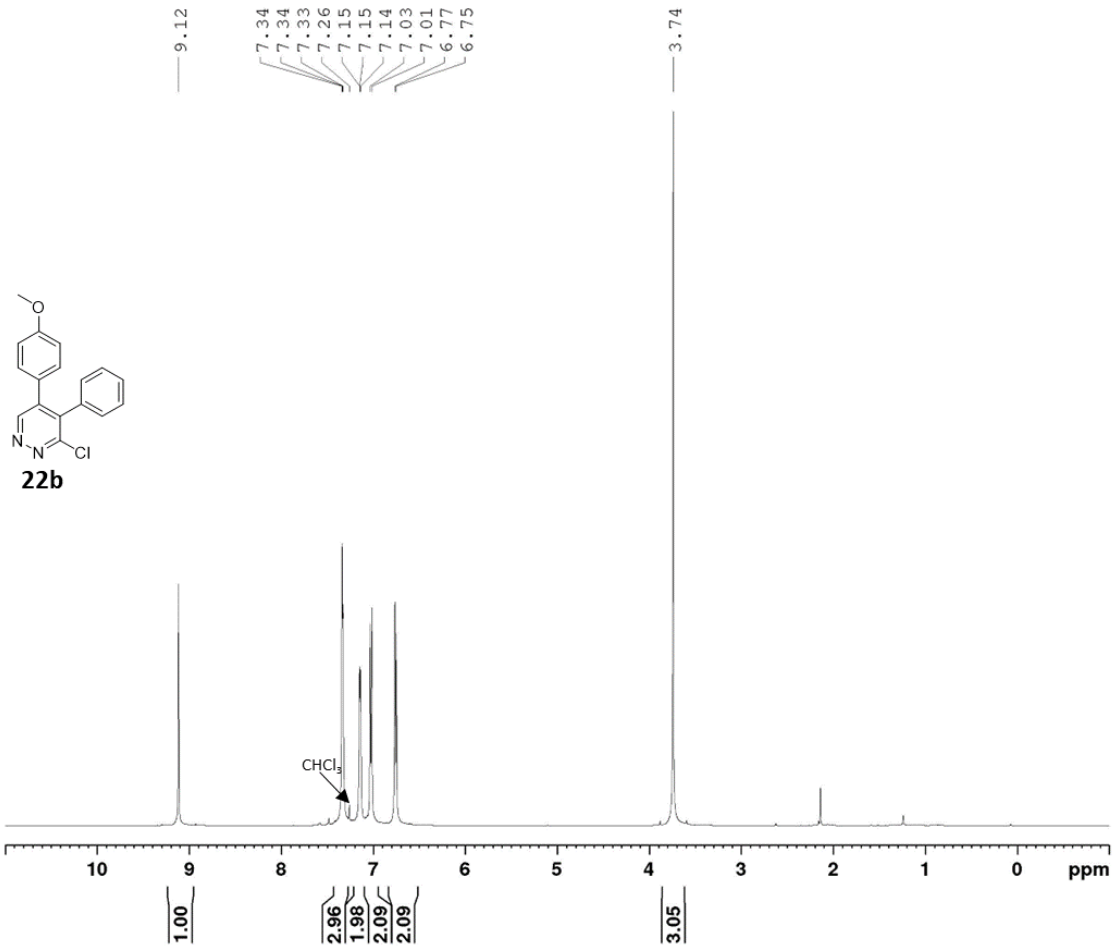
F2 - Processing parameters
SI                 65536
SF          600.1300147 MHz
WDW                   EM
SSB       0
LB                 0.30 Hz
GB        0
PC                 1.00
```




```
Current Data Parameters
NAME      JPN-1-169-2_C4-monoaryl
EXPNO                 23
PROCNO                 1

F2 - Acquisition Parameters
Date_           20200527
Time              11.16 h
INSTRUM             spect
PROBHD   Z127277_0002 (
PULPROG           zgpg30
TD                 65536
SOLVENT            CDCl3
NS                  1024
DS                     4
SWH            36057.691 Hz
FIDRES          1.100393 Hz
AQ             0.9087659 sec
RG                 184.4
DW                13.867 usec
DE                 18.00 usec
TE                 300.0 K
D1           2.00000000 sec
D11          0.03000000 sec
TD0                    1
SFO1         150.9178981 MHz
NUC1                13C
P0                 4.00 usec
P1                12.00 usec
PLW1         91.00000000 W
SFO2         600.1324005 MHz
NUC2                1H
CPDPRG[2         waltz16
PCPD2             70.00 usec
PLW2          5.59999990 W
PLW12         0.07314300 W
PLW13         0.03679000 W

F2 - Processing parameters
SI                 32768
SF           150.9028026 MHz
WDW                   EM
SSB       0
LB                 1.00 Hz
GB        0
PC                 1.40
```

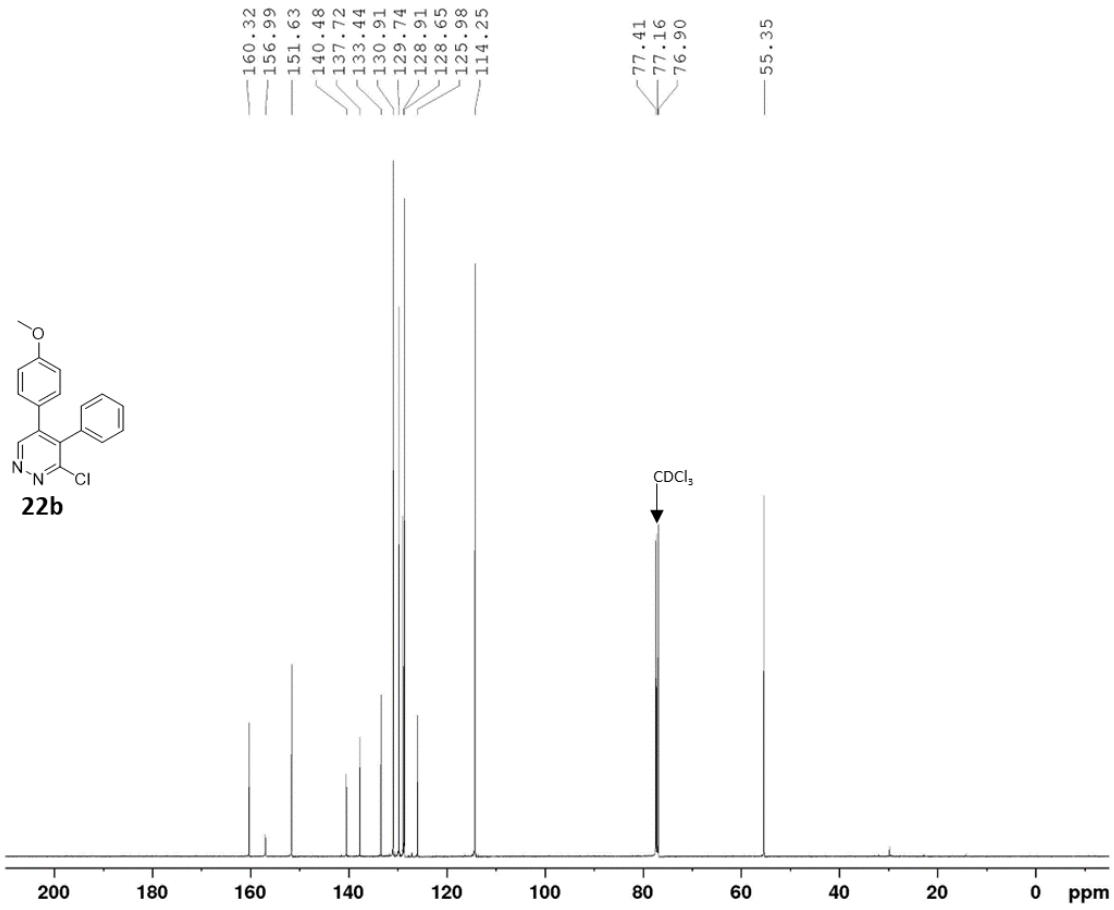


22b

```
Current Data Parameters
NAME      JPN-2-27-1_repeat_C5-mono
EXPNO                10
PROCNO                1

F2 - Acquisition Parameters
Date_          20201130
Time              17.40 h
INSTRUM           spect
PROBHD   Z125869_0055 (
PULPROG             zg30
TD                65536
SOLVENT           CDCl3
NS                   64
DS                    2
SWH           10000.000 Hz
FIDRES            0.305176 Hz
AQ             3.2767999 sec
RG                22.16
DW               50.000 usec
DE               16.00 usec
TE               300.0 K
D1            2.00000000 sec
TD0                   1
SFO1         500.2330889 MHz
NUC1                 1H
P0                4.00 usec
P1               12.00 usec
PLW1         11.44699955 W

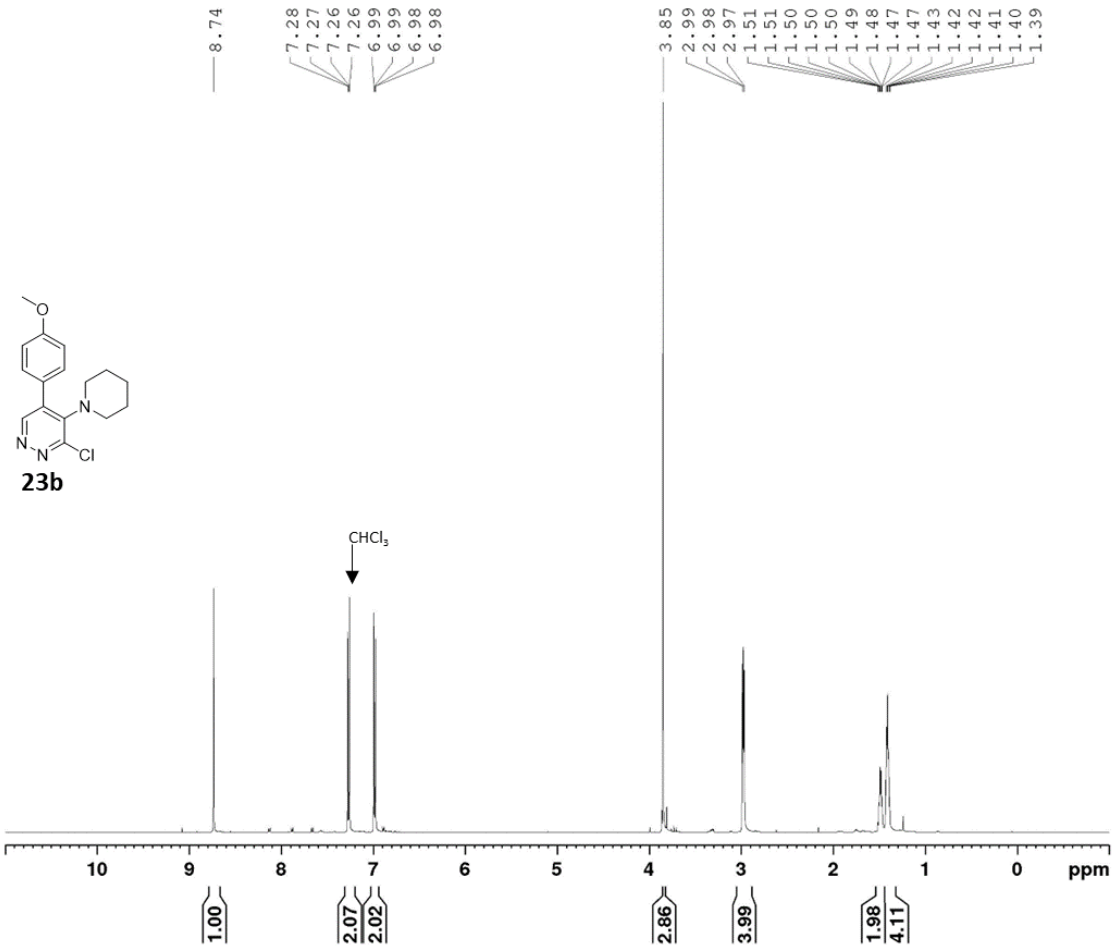
F2 - Processing parameters
SI                65536
SF           500.2300118 MHz
WDW                  EM
SSB       0
LB                0.30 Hz
GB        0
PC                1.00
```




```
Current Data Parameters
NAME      JPN-2-27-1_repeat
EXPNO                   17
PROCNO                   1

F2 - Acquisition Parameters
Date_              20211119
Time                  4.28 h
INSTRUM               spect
PROBHD    Z125869_0055 (
PULPROG             zgpg30
TD                   65536
SOLVENT              CDCl3
NS                    1024
DS                       4
SWH              29761.904 Hz
FIDRES            0.908261 Hz
AQ                1.1010048 sec
RG                   190.44
DW                   16.800 usec
DE                   18.00 usec
TE                   298.0 K
D1               2.00000000 sec
D11              0.03000000 sec
TD0                      1
SFO1           125.7955118 MHz
NUC1                   13C
P0                    3.33 usec
P1                   10.00 usec
PLW1            56.90299988 W
SFO2           500.2320009 MHz
NUC2                   1H
CPDPRG[2           waltz16
PCPD2                80.00 usec
PLW2            11.44699955 W
PLW12            0.25756001 W
PLW13            0.12955000 W

F2 - Processing parameters
SI                   32768
SF             125.7829267 MHz
WDW                     EM
SSB       0
LB                    1.00 Hz
GB        0
PC                    1.40
```

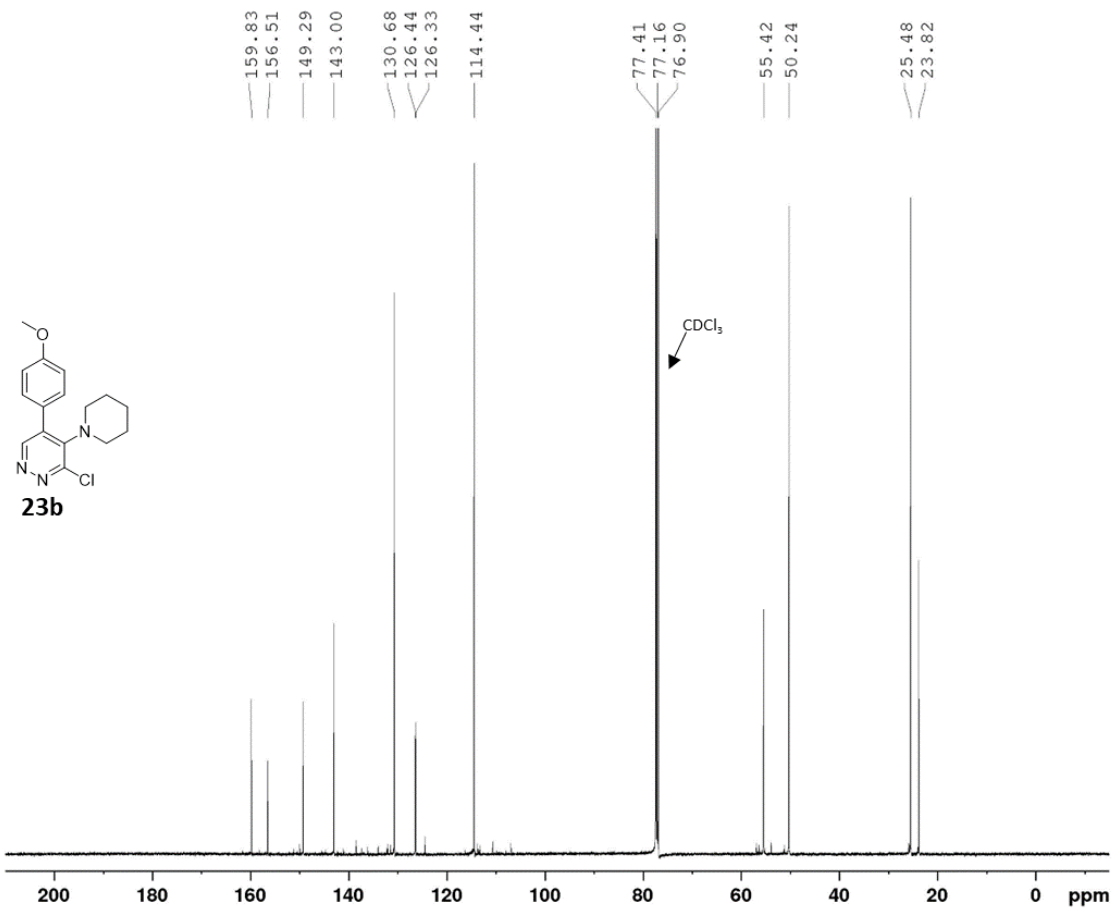


23b

```
Current Data Parameters
NAME      JPN-2-27-2_C5-mono
EXPNO                    10
PROCNO                    1

F2 - Acquisition Parameters
Date_              20201130
Time                 18.00 h
INSTRUM              spect
PROBHD    Z125869_0055 (
PULPROG              zg30
TD                  65536
SOLVENT             CDCl3
NS                     64
DS                      2
SWH            10000.000 Hz
FIDRES             0.305176 Hz
AQ               3.2767999 sec
RG                   35.18
DW                  50.000 usec
DE                  16.00 usec
TE                  300.0 K
D1              2.00000000 sec
TD0                     1
SFO1           500.2330889 MHz
NUC1                   1H
P0                  4.00 usec
P1                 12.00 usec
PLW1           11.44699955 W

F2 - Processing parameters
SI                  65536
SF             500.2300119 MHz
WDW                    EM
SSB       0
LB                  0.30 Hz
GB        0
PC                  1.00
```

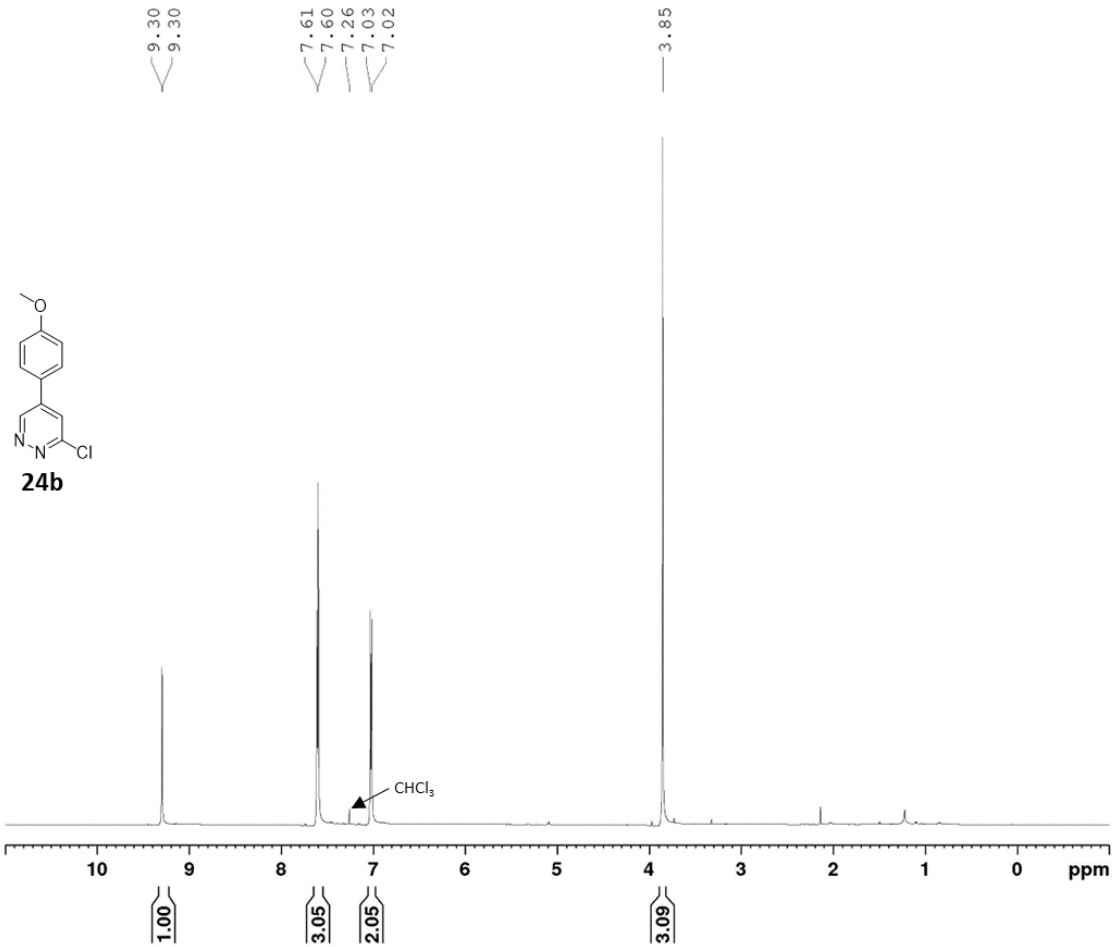


23b

```
Current Data Parameters
NAME          JPN-2-27-2
EXPNO                 17
PROCNO                 1

F2 - Acquisition Parameters
Date_           20211119
Time                5.26 h
INSTRUM            spect
PROBHD   Z125869_0055 (
PULPROG         zgpg30
TD                 65536
SOLVENT            CDCl3
NS                  1024
DS                     4
SWH            29761.904 Hz
FIDRES          0.908261 Hz
AQ             1.1010048 sec
RG                190.44
DW                16.800 usec
DE                18.00 usec
TE                298.0 K
D1             2.00000000 sec
D11            0.03000000 sec
TD0                    1
SFO1         125.7955118 MHz
NUC1                13C
P0                 3.33 usec
P1                10.00 usec
PLW1         56.90299988 W
SFO2         500.2320009 MHz
NUC2                1H
CPDPRG[2         waltz16
PCPD2             80.00 usec
PLW2         11.44699955 W
PLW12         0.25756001 W
PLW13         0.12955000 W

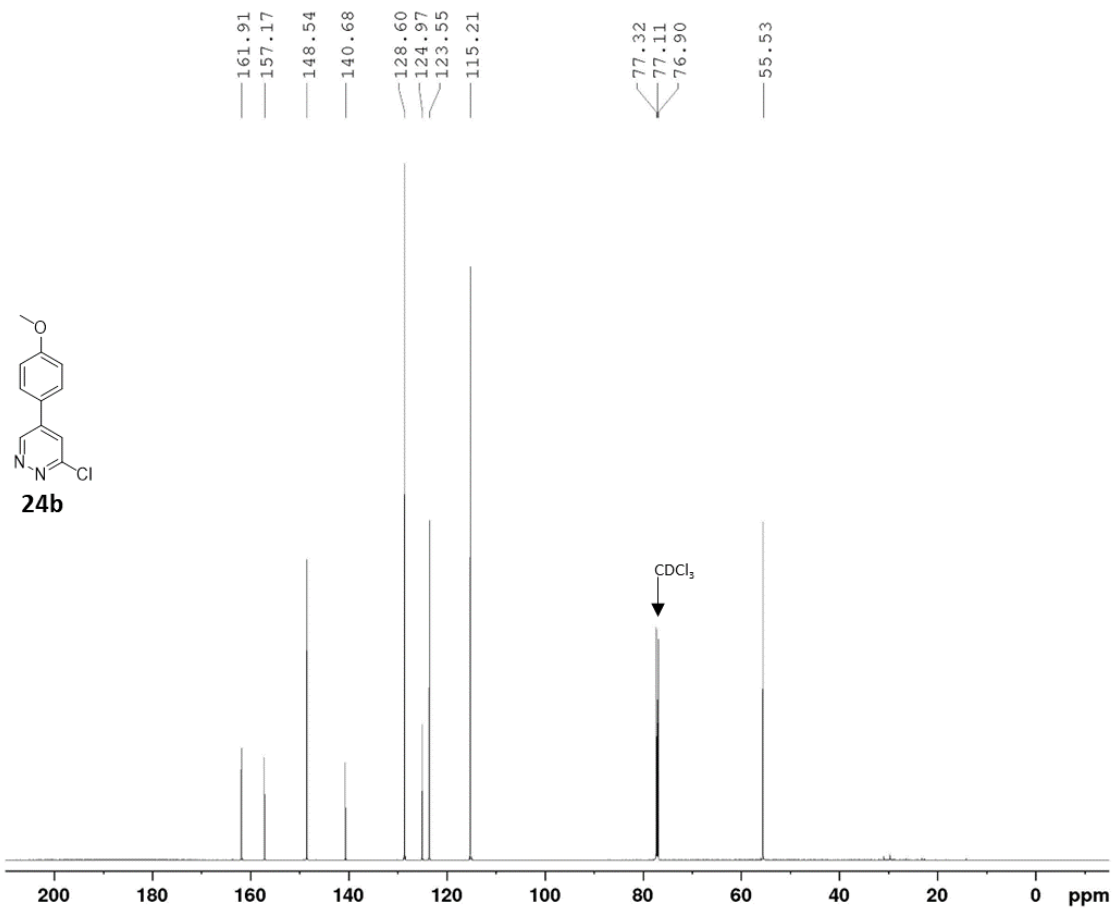
F2 - Processing parameters
SI                 32768
SF           125.7829191 MHz
WDW                   EM
SSB       0
LB                 1.00 Hz
GB        0
PC                 1.40
```




```
Current Data Parameters
NAME      JPN-1-166-2_C5-Mono
EXPNO                     10
PROCNO                     1

F2 - Acquisition Parameters
Date_              20200519
Time                 13.52 h
INSTRUM              spect
PROBHD    Z127277_0002 (
PULPROG              zg30
TD                  65536
SOLVENT             CDCl3
NS                     64
DS                      2
SWH             12019.230 Hz
FIDRES           0.366798 Hz
AQ               2.7262976 sec
RG                    4.41
DW                  41.600 usec
DE                  10.00 usec
TE                  300.0 K
D1              1.00000000 sec
TD0                     1
SFO1          600.1337060 MHz
NUC1                   1H
P0                   2.67 usec
P1                   8.00 usec
PLW1           5.59999990 W

F2 - Processing parameters
SI                  65536
SF            600.1300144 MHz
WDW                    EM
SSB       0
LB                   0.30 Hz
GB        0
PC                   1.00
```

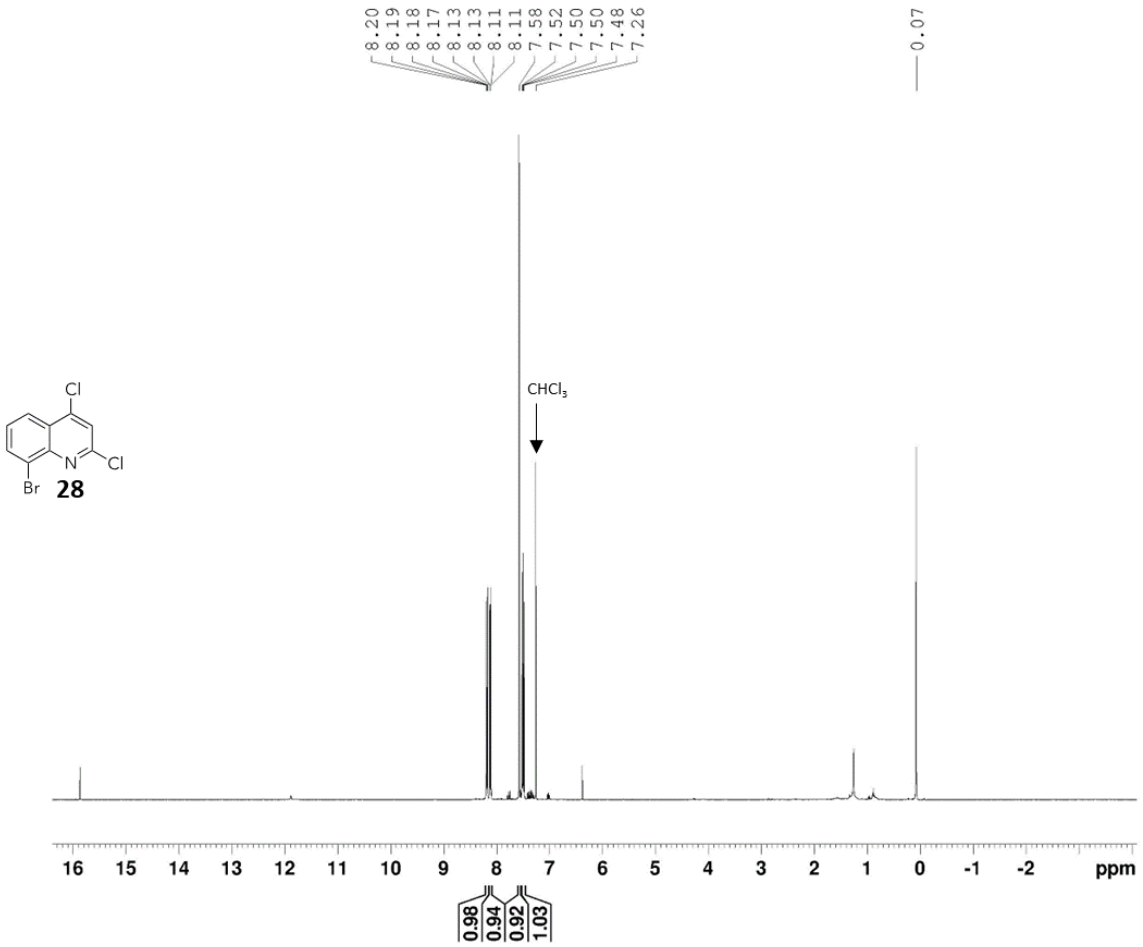


24b

```
Current Data Parameters
NAME      JPN-1-166-2_C5-Mono
EXPNO                     11
PROCNO                     1

F2 - Acquisition Parameters
Date_              20200519
Time                  15.36 h
INSTRUM                spect
PROBHD    Z127277_0002 (
PULPROG             zgpg30
TD                      65536
SOLVENT                 CDCl3
NS                       1024
DS                          4
SWH               36057.691 Hz
FIDRES             1.100393 Hz
AQ                0.9087659 sec
RG                    184.4
DW                   13.867 usec
DE                   18.00 usec
TE                   300.0 K
D1               2.00000000 sec
D11              0.03000000 sec
TD0                         1
SFO1           150.9178981 MHz
NUC1                     13C
P0                    4.00 usec
P1                   12.00 usec
PLW1           91.00000000 W
SFO2           600.1324005 MHz
NUC2                     1H
CPDPRG[2            waltz16
PCPD2                70.00 usec
PLW2            5.59999990 W
PLW12           0.07314300 W
PLW13           0.03679000 W

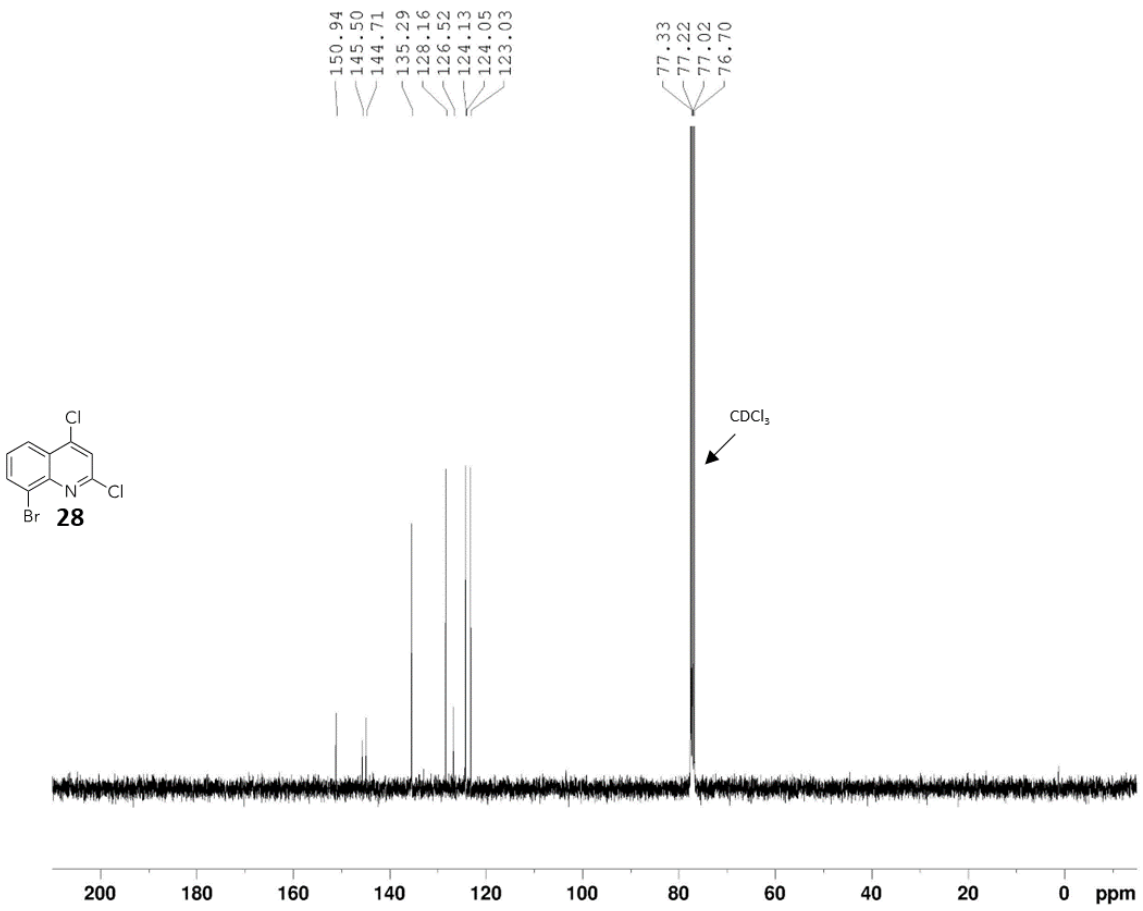
F2 - Processing parameters
SI                      32768
SF             150.9028090 MHz
WDW                        EM
SSB       0
LB                    1.00 Hz
GB        0
PC                    1.40
```




```
Current Data Parameters
NAME         NL-1-117-1H
EXPNO                 10
PROCNO                 1

F2 - Acquisition Parameters
Date_           20211208
Time               14.16 h
INSTRUM       Avance Neo
PROBHD    Z152088_0031 (
PULPROG            zg30
TD                65536
SOLVENT           CDCl3
NS                   16
DS                    2
SWH             8196.722 Hz
FIDRES          0.250144 Hz
AQ              3.9976959 sec
RG                  101
DW                61.000 usec
DE                13.89 usec
TE                298.0 K
D1             1.00000000 sec
TD0                   1
SFO1          400.1324708 MHz
NUC1                 1H
P0                 2.67 usec
P1                 8.00 usec
PLW1          24.03499985 W

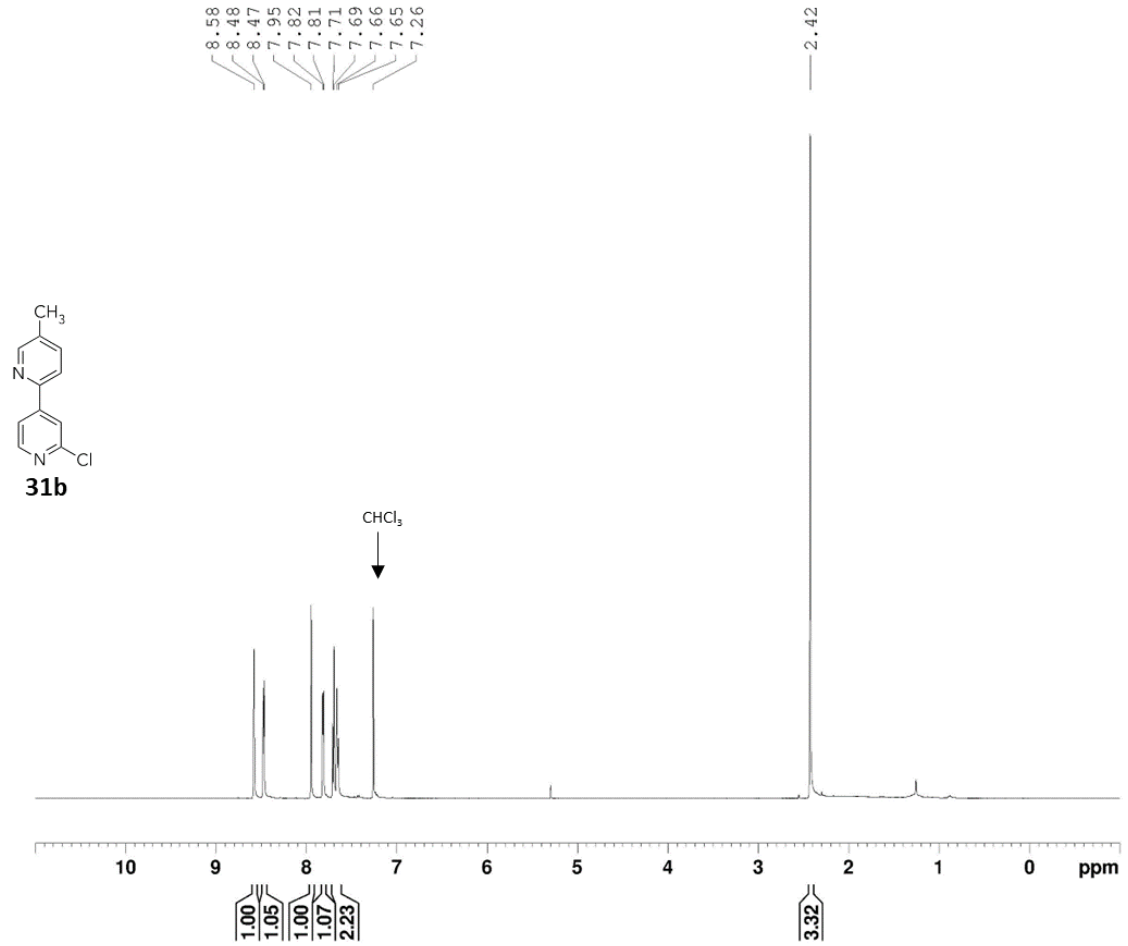
F2 - Processing parameters
SI                65536
SF            400.1300098 MHz
WDW                  EM
SSB                   0
LB                 0.30 Hz
GB                    0
PC                 1.00
```




```
Current Data Parameters
NAME                  NL-1-117
EXPNO                       14
PROCNO                       1

F2 - Acquisition Parameters
Date_                 20211127
Time                     14.39 h
INSTRUM              Avance Neo
PROBHD   Z152088_0031 (
PULPROG                 zgpg30
TD                       65536
SOLVENT                  CDCl3
NS                        1024
DS                           4
SWH                  23809.523 Hz
FIDRES                0.726609 Hz
AQ                    1.3762560 sec
RG                        8.125
DW                       21.000 usec
DE                        6.50 usec
TE                       298.0 K
D1                 2.00000000 sec
D11                0.03000000 sec
TD0                          1
SFO1               100.6228298 MHz
NUC1                        13C
P0                        2.67 usec
P1                        8.00 usec
PLW1               86.55400085 W
SFO2               400.1316005 MHz
NUC2                        1H
CPDPRG[2                waltz65
PCPD2                    90.00 usec
PLW2               24.03499985 W
PLW12               0.18990999 W
PLW13               0.09552100 W

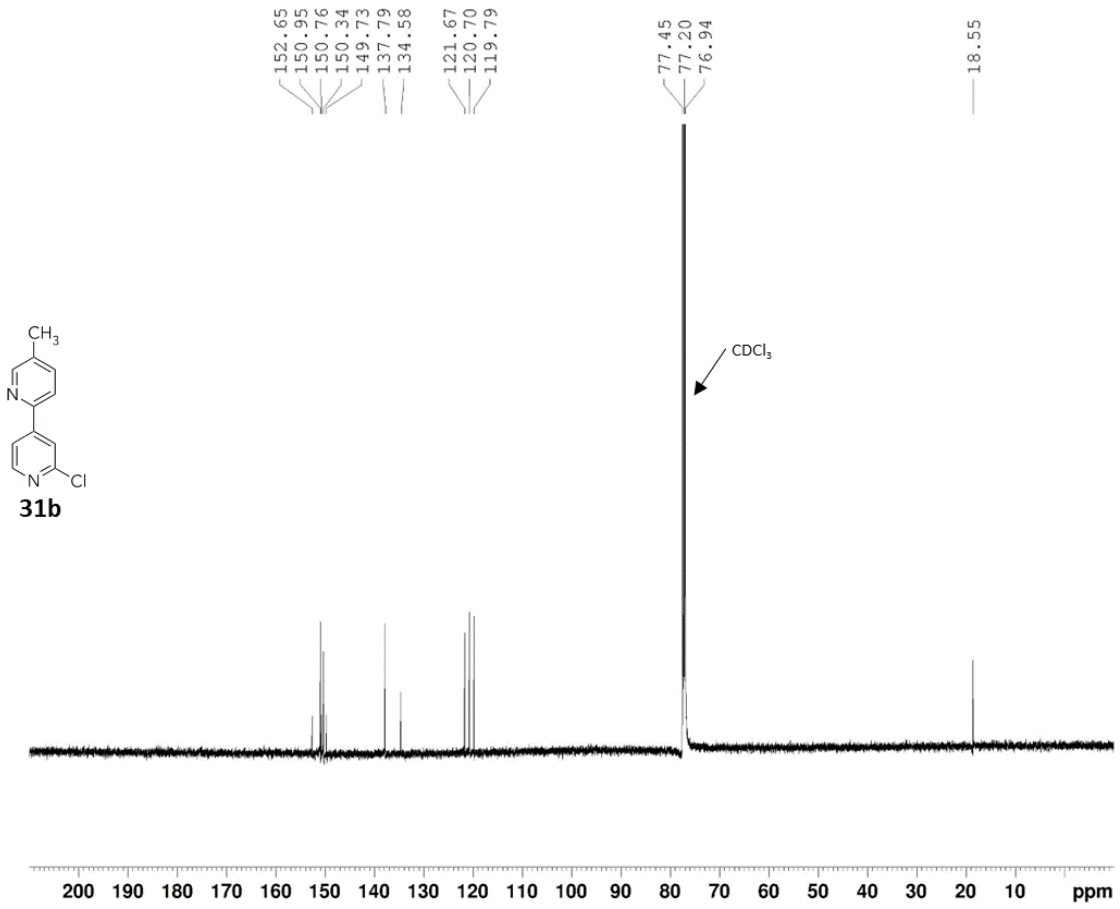
F2 - Processing parameters
SI                       32768
SF                 100.6127505 MHz
WDW                         EM
SSB                          0
LB                        1.00 Hz
GB                           0
PC                        1.40
```




```
Current Data Parameters
NAME           NL-1-6-2d
EXPNO                 11
PROCNO                 1

F2 - Acquisition Parameters
Date_           20210701
Time               17.05 h
INSTRUM            spect
PROBHD   Z125869_0055 (
PULPROG             zg30
TD                 65536
SOLVENT            CDCl3
NS                    16
DS                     2
SWH            10000.000 Hz
FIDRES         0.305176 Hz
AQ             3.2767999 sec
RG                137.36
DW                50.000 usec
DE                16.00 usec
TE                300.0 K
D1            1.00000000 sec
TD0                    1
SFO1          500.2330889 MHz
NUC1                  1H
P0                  4.00 usec
P1                 12.00 usec
PLW1          11.44699955 W

F2 - Processing parameters
SI                 65536
SF            500.2300121 MHz
WDW                   EM
SSB                    0
LB                  0.30 Hz
GB                     0
PC                  1.00
```

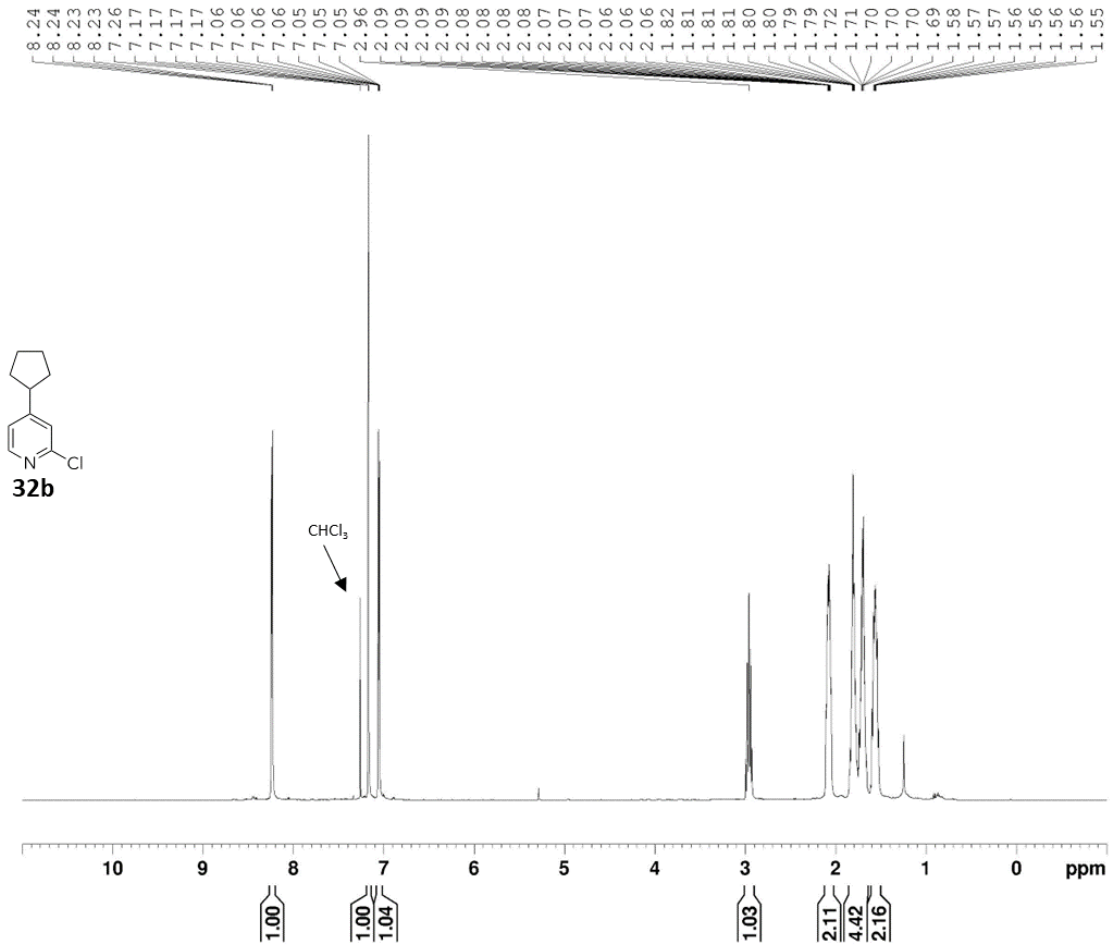


31b

```
Current Data Parameters
NAME        NL-1-6-13Cx2
EXPNO                 10
PROCNO                 1

F2 - Acquisition Parameters
Date_           20211028
Time              23.54 h
INSTRUM             spect
PROBHD   Z125869_0055 (
PULPROG           zgpg30
TD                65536
SOLVENT           CDCl3
NS                 1024
DS                    4
SWH           29761.904 Hz
FIDRES         0.908261 Hz
AQ            1.1010048 sec
RG               190.44
DW               16.800 usec
DE               18.00 usec
TE               298.0 K
D1           2.00000000 sec
D11          0.03000000 sec
TD0                   1
SFO1        125.7955118 MHz
NUC1                13C
P0                3.33 usec
P1               10.00 usec
PLW1        56.90299988 W
SFO2        500.2320009 MHz
NUC2                1H
CPDPRG[2         waltz16
PCPD2             80.00 usec
PLW2        11.44699955 W
PLW12        0.25756001 W
PLW13        0.12955000 W

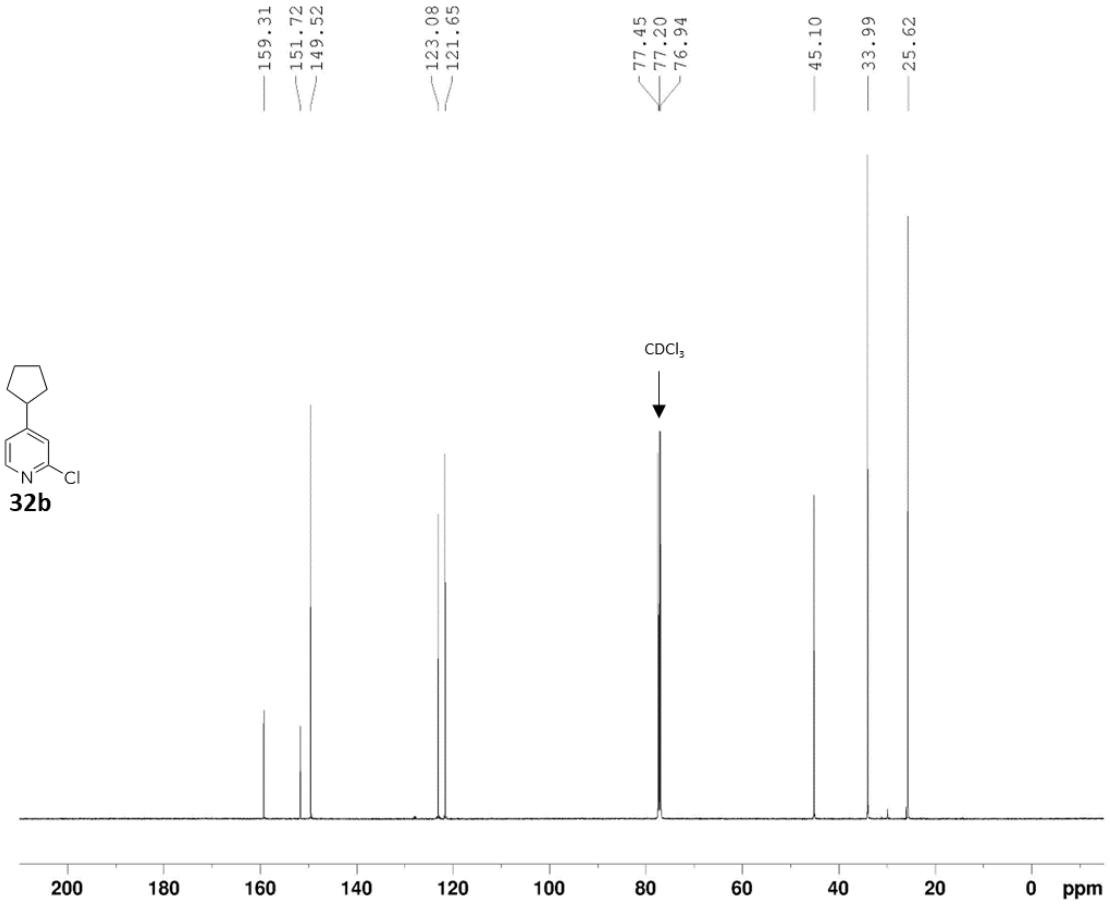
F2 - Processing parameters
SI                32768
SF          125.7829104 MHz
WDW                  EM
SSB                   0
LB                 1.00 Hz
GB                    0
PC                 1.40
```




```
Current Data Parameters
NAME       NL-1-73-C4-1H
EXPNO                 10
PROCNO                 1

F2 - Acquisition Parameters
Date_           20210621
Time              13.29 h
INSTRUM             spect
PROBHD   Z125869_0055 (
PULPROG             zg30
TD                 65536
SOLVENT            CDCl3
NS                    64
DS                     2
SWH           10000.000 Hz
FIDRES         0.305176 Hz
AQ             3.2767999 sec
RG                 37.93
DW                50.000 usec
DE                16.00 usec
TE                300.0 K
D1           2.00000000 sec
TD0                    1
SFO1        500.2330889 MHz
NUC1                  1H
P0                 4.00 usec
P1                12.00 usec
PLW1        11.44699955 W

F2 - Processing parameters
SI                 65536
SF          500.2300123 MHz
WDW                   EM
SSB                    0
LB                  0.30 Hz
GB                     0
PC                  5.00
```

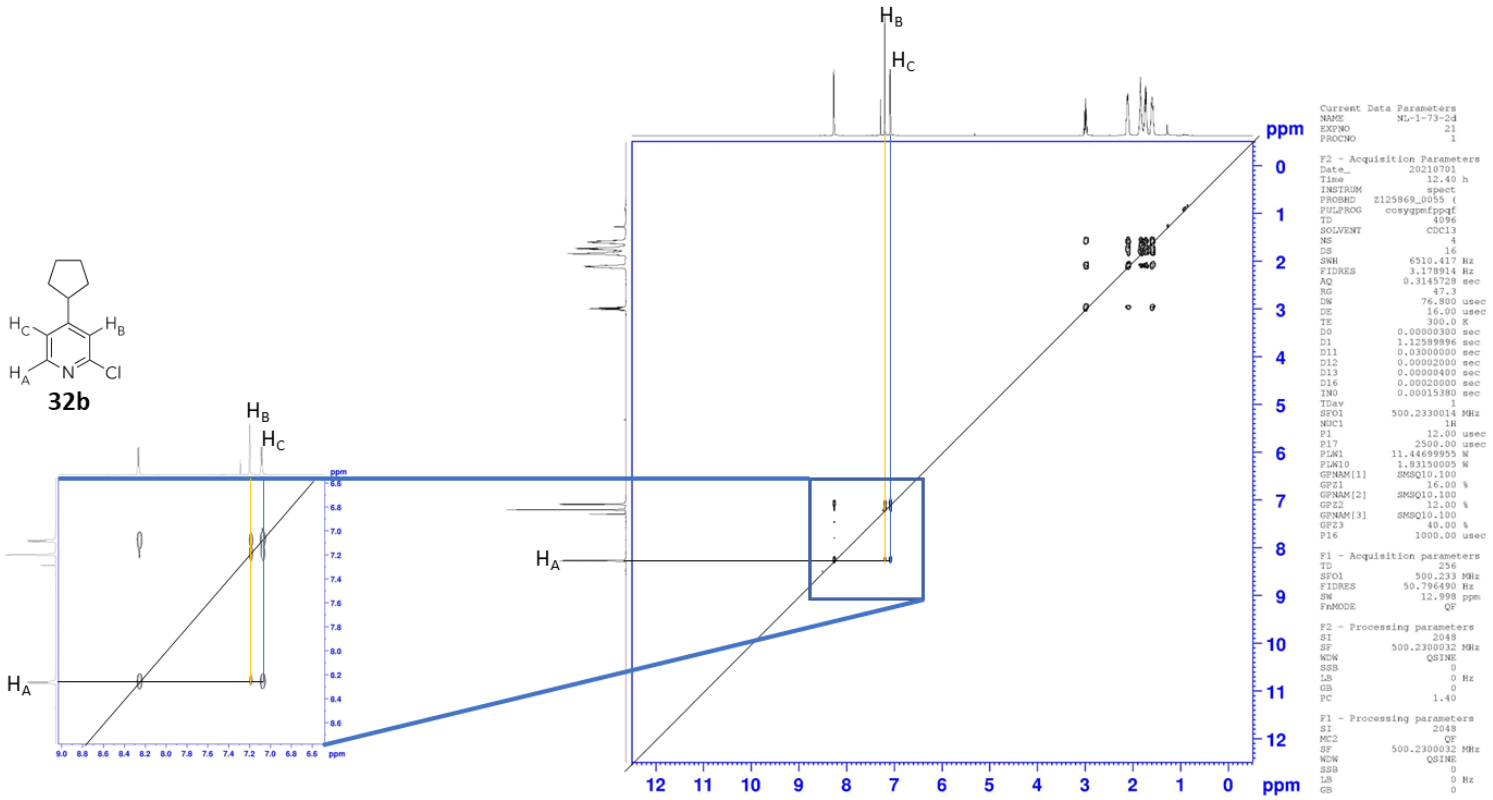


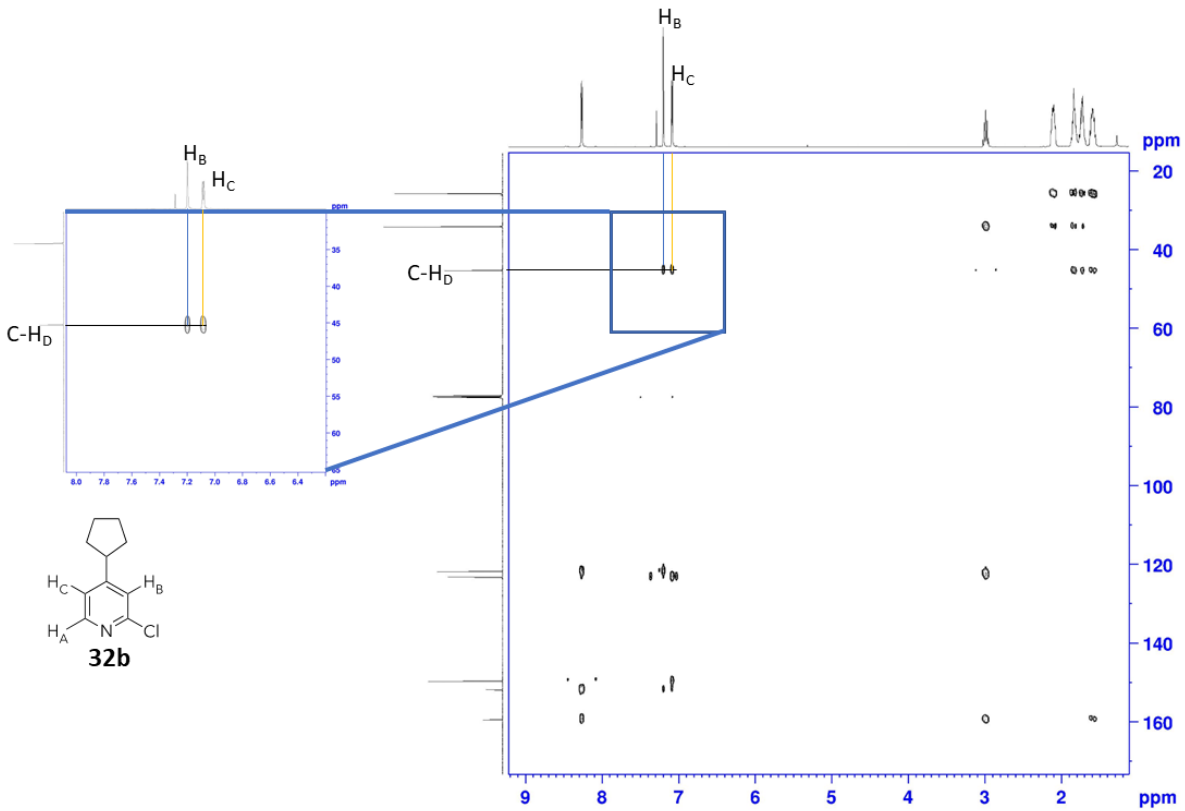
32b

```
Current Data Parameters
NAME          NL-1-73-2d
EXPNO                 20
PROCNO                 1

F2 - Acquisition Parameters
Date_           20210701
Time              12.39 h
INSTRUM             spect
PROBHD   Z125869_0055 (
PULPROG          zgpg30
TD                65536
SOLVENT           CDCl3
NS                 1024
DS                    4
SWH           29761.904 Hz
FIDRES         0.908261 Hz
AQ            1.1010048 sec
RG               190.44
DW               16.800 usec
DE               18.00 usec
TE                300.0 K
D1           2.00000000 sec
D11          0.03000000 sec
TD0                   1
SFO1        125.7955118 MHz
NUC1                13C
P0                3.33 usec
P1               10.00 usec
PLW1        56.90299988 W
SFO2        500.2320009 MHz
NUC2                1H
CPDPRG[2         waltz16
PCPD2            80.00 usec
PLW2        11.44699955 W
PLW12        0.25756001 W
PLW13        0.12955000 W

F2 - Processing parameters
SI                32768
SF          125.7829141 MHz
WDW                  EM
SSB                   0
LB                 1.00 Hz
GB                    0
PC                 1.40
```


H_B
H_C
H_A
H_C
H_B
H_A
N
Cl
32b
ppm
12 11 10 9 8 7 6 5 4 3 2 1 0 ppm



32b

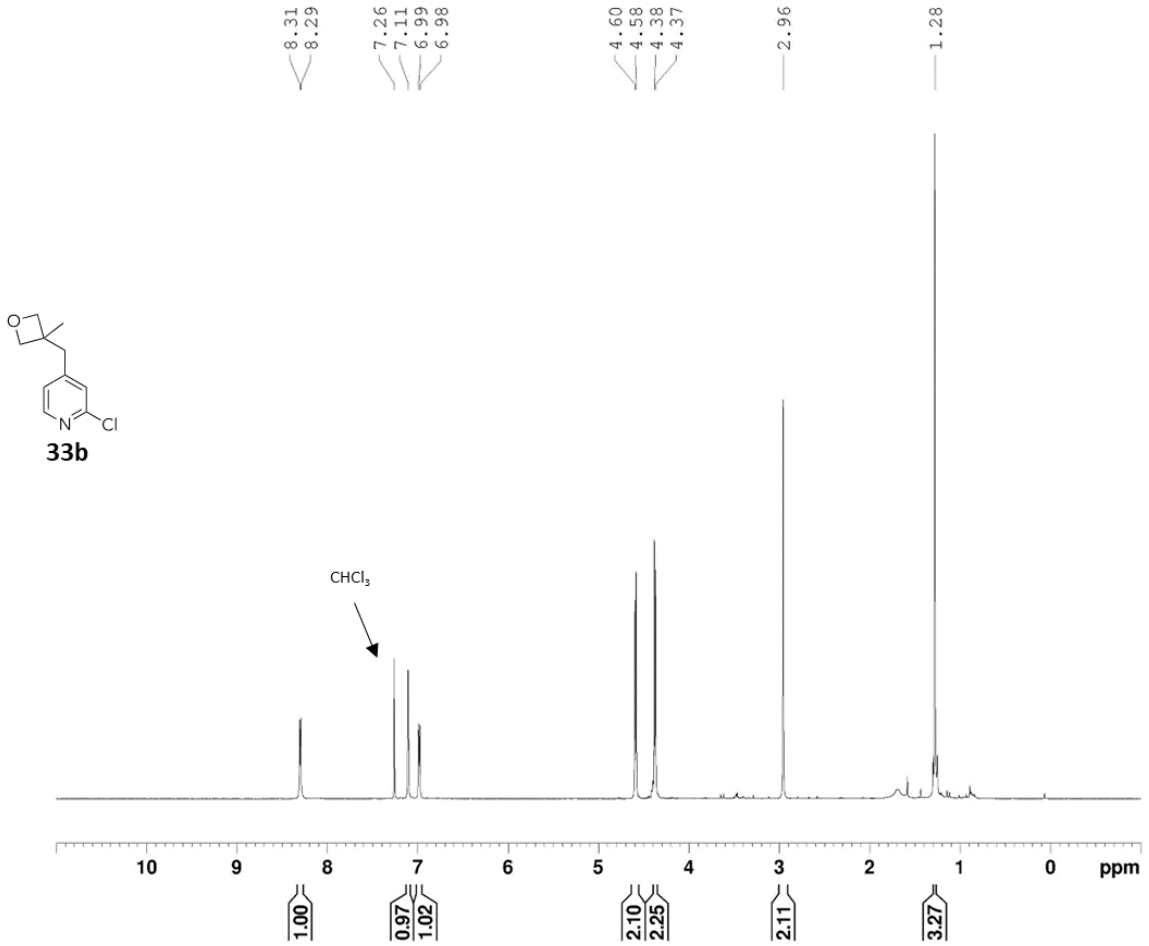
```
Current Data Parameters
NAME              ML-1-73-2d
EXPNO                     23
PROCNO                     1

F2 - Acquisition Parameters
Date_           20210701
Time                 13.09 h
INSTRUM              spect
PROBHD    Z125869_0055 (
PULPROG    hmbcgplpndqf
TD                   2048
SOLVENT              CDCl3
NS                      4
DS                     16
SWH               4716.981 Hz
FIDRES            4.606427 Hz
AQ                0.2170880 sec
RG                  190.44
DW                106.000 usec
DE                 16.00 usec
TE                 300.0 K
CNST2          145.0000000
CNST13          10.0000000
D0              0.00000300 sec
D1              1.50000000 sec
D2              0.00344828 sec
D6              0.05000000 sec
D16             0.00020000 sec
IN0             0.00001810 sec
TDav                    1
SFO1          500.2322599 MHz
NUC1                   1H
P1                  12.00 usec
P2                  24.00 usec
PLW1          11.44699955 W
SFO2          125.7955118 MHz
NUC2                  13C
P3                  10.00 usec
PLW2          56.90299988 W
GPNAM[1]       SMSQ10.100
GPZ1                50.00 %
GPNAM[2]       SMSQ10.100
GPZ2                30.00 %
GPNAM[3]       SMSQ10.100
GPZ3                40.10 %
P16               1000.00 usec

F1 - Acquisition parameters
TD                     128
SFO1            125.7955 MHz
FIDRES         431.629822 Hz
SW                219.597 ppm
FnMODE                  QF

F2 - Processing parameters
SI                     2048
SF            500.2299980 MHz
WDW                  SINE
SSB                     0
LB                      0 Hz
GB                      0
PC                   1.40

F1 - Processing parameters
SI                     1024
MC2                    QF
SF            125.7828890 MHz
WDW                  SINE
SSB                     0
LB                      0 Hz
GB                      0
```

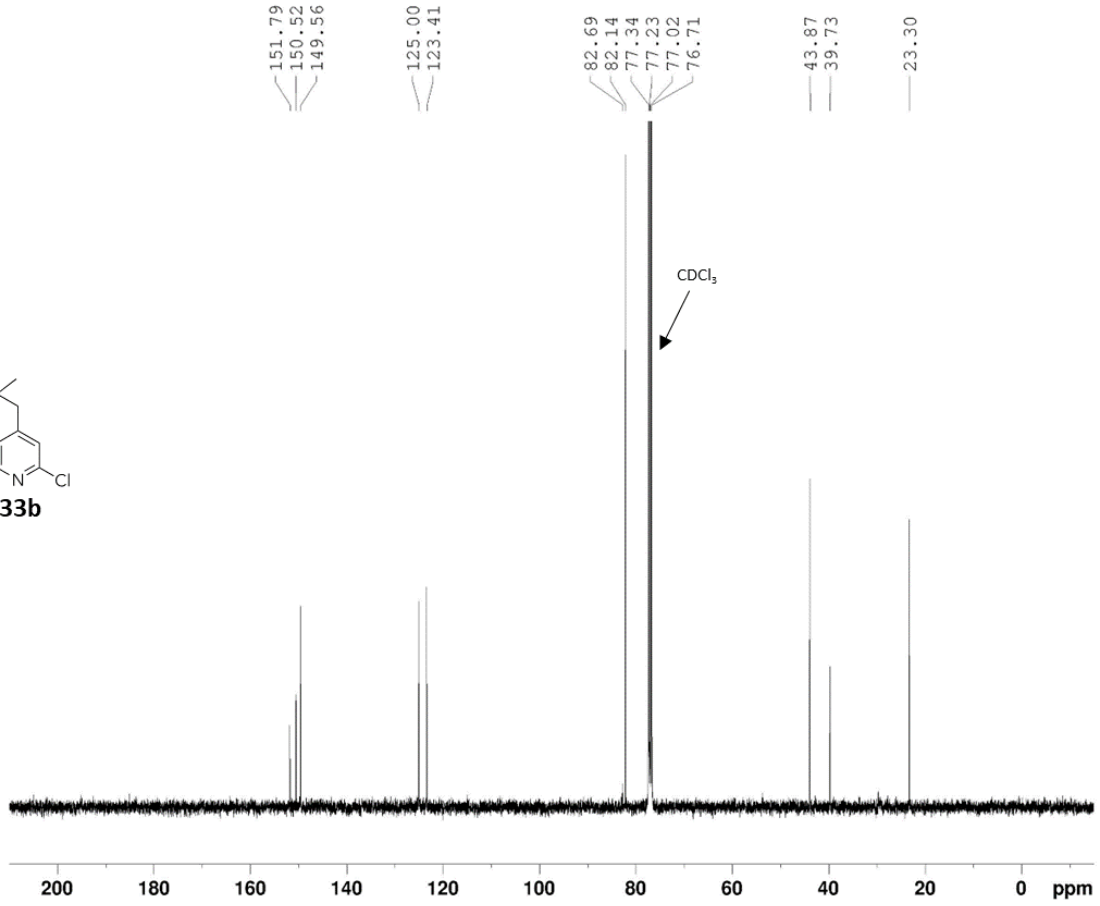


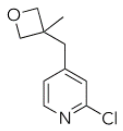
33b

```
Current Data Parameters
NAME      NL-1-89-incconc
EXPNO                  10
PROCNO                  1

F2 - Acquisition Parameters
Date_           20210729
Time              18.10 h
INSTRUM       Avance Neo
PROBHD   Z152088_0031 (
PULPROG             zg30
TD                 65536
SOLVENT            CDCl3
NS                    16
DS                     2
SWH             8196.722 Hz
FIDRES          0.250144 Hz
AQ              3.9976959 sec
RG                   101
DW                61.000 usec
DE                13.89 usec
TE                298.1 K
D1             1.00000000 sec
TD0                    1
SFO1         400.1324708 MHz
NUC1                  1H
P0                 2.67 usec
P1                 8.00 usec
PLW1         24.03499985 W

F2 - Processing parameters
SI                 65536
SF           400.1300099 MHz
WDW                   EM
SSB                    0
LB                  0.30 Hz
GB                     0
PC                  1.00
```





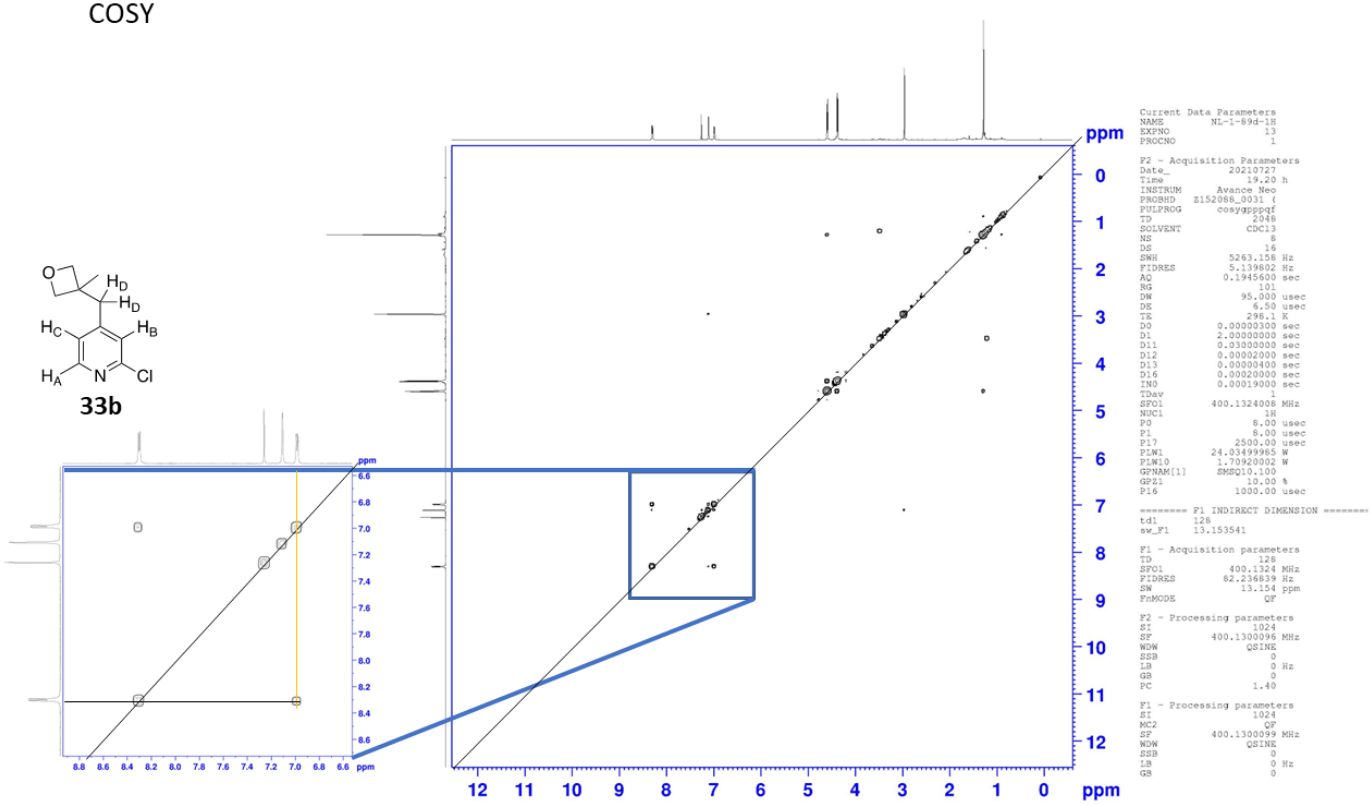
33b

```
Current Data Parameters
NAME      NL-1-89-incconc
EXPNO                 11
PROCNO                 1

F2 - Acquisition Parameters
Date_           20210729
Time              19.12 h
INSTRUM       Avance Neo
PROBHD   Z152088_0031 (
PULPROG          zgpg30
TD                65536
SOLVENT           CDCl3
NS                 1024
DS                    4
SWH           23809.523 Hz
FIDRES         0.726609 Hz
AQ            1.3762560 sec
RG                8.125
DW               21.000 usec
DE                6.50 usec
TE                298.1 K
D1           2.00000000 sec
D11          0.03000000 sec
TD0                   1
SFO1        100.6228298 MHz
NUC1                13C
P0                 2.67 usec
P1                 8.00 usec
PLW1        86.55400085 W
SFO2        400.1316005 MHz
NUC2                1H
CPDPRG[2        waltz65
PCPD2             90.00 usec
PLW2        24.03499985 W
PLW12        0.18990999 W
PLW13        0.09552100 W

F2 - Processing parameters
SI                32768
SF          100.6127685 MHz
WDW                  EM
SSB                   0
LB                 1.00 Hz
GB                    0
PC                 1.40
```

COSY




```
Current Data Parameters
NAME          NL-1-89d-1H
EXPNO                  13
PROCNO                  1

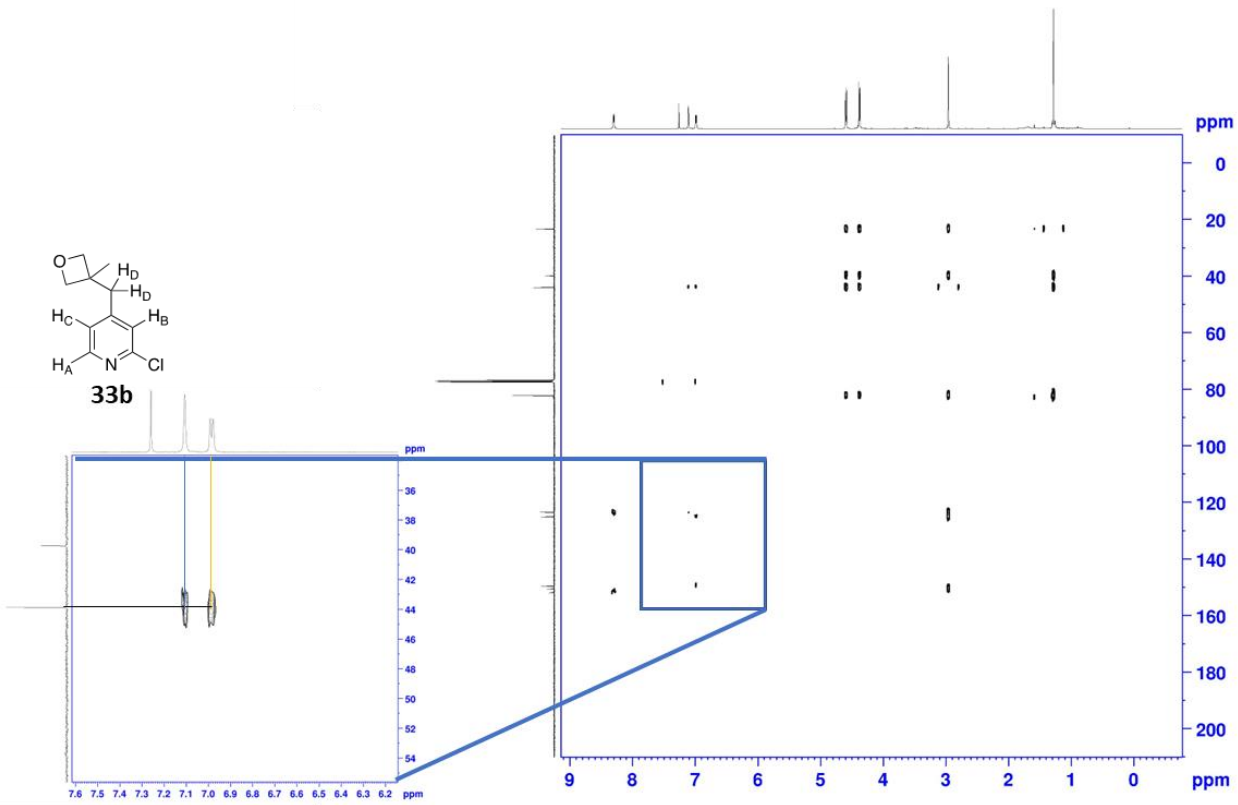
F2 - Acquisition Parameters
Date_            20210727
Time                19.20 h
INSTRUM       Avance Neo
PROBHD    Z152088_0031 (
PULPROG       cosygpppqf
TD                   2048
SOLVENT             CDCl3
NS                      8
DS                     16
SWH              5263.158 Hz
FIDRES           5.139802 Hz
AQ               0.1945600 sec
RG                    101
DW                 95.000 usec
DE                  6.50 usec
TE                298.1 K
D0              0.00000300 sec
D1              2.00000000 sec
D11             0.03000000 sec
D12             0.00002000 sec
D13             0.00000400 sec
D16             0.00020000 sec
IN0             0.00019000 sec
TDav                    1
SFO1          400.1324008 MHz
NUC1                   1H
P0                  8.00 usec
P1                  8.00 usec
P17              2500.00 usec
PLW1          24.03499985 W
PLW10          1.70920002 W
GPNAM[11]      SMSQ10.100
GPZ1                10.00 %
P16               1000.00 usec

======== F1 INDIRECT DIMENSION ========
td1       128
sw_F1     13.153541

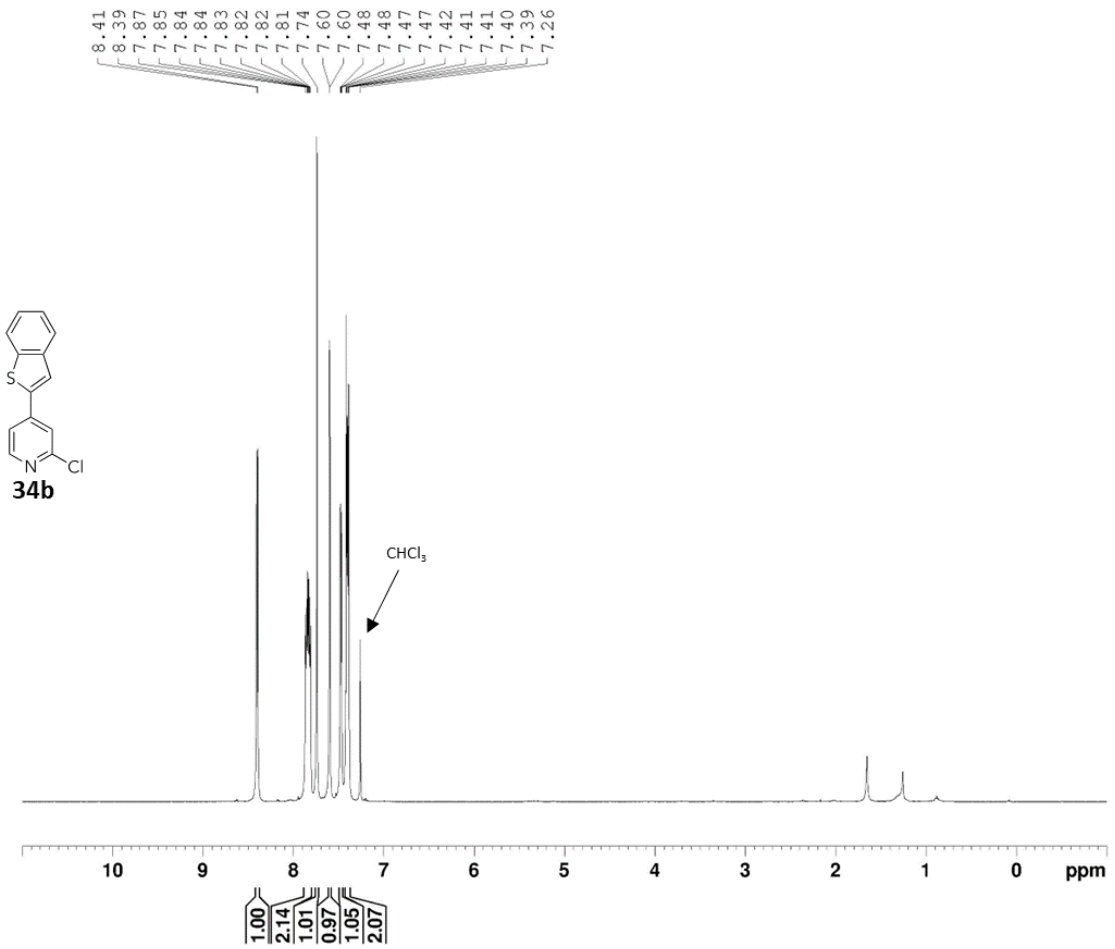
F1 - Acquisition parameters
TD                     128
SFO1          400.1324 MHz
FIDRES         82.236839 Hz
SW                13.154 ppm
FnMODE                  QF

F2 - Processing parameters
SI                    1024
SF            400.1300096 MHz
WDW                 QSINE
SSB                     0
LB                      0 Hz
GB                      0
PC                   1.40

F1 - Processing parameters
SI                    1024
MC2                     QF
SF            400.1300099 MHz
WDW                 QSINE
SSB                     0
LB                      0 Hz
GB                      0
```



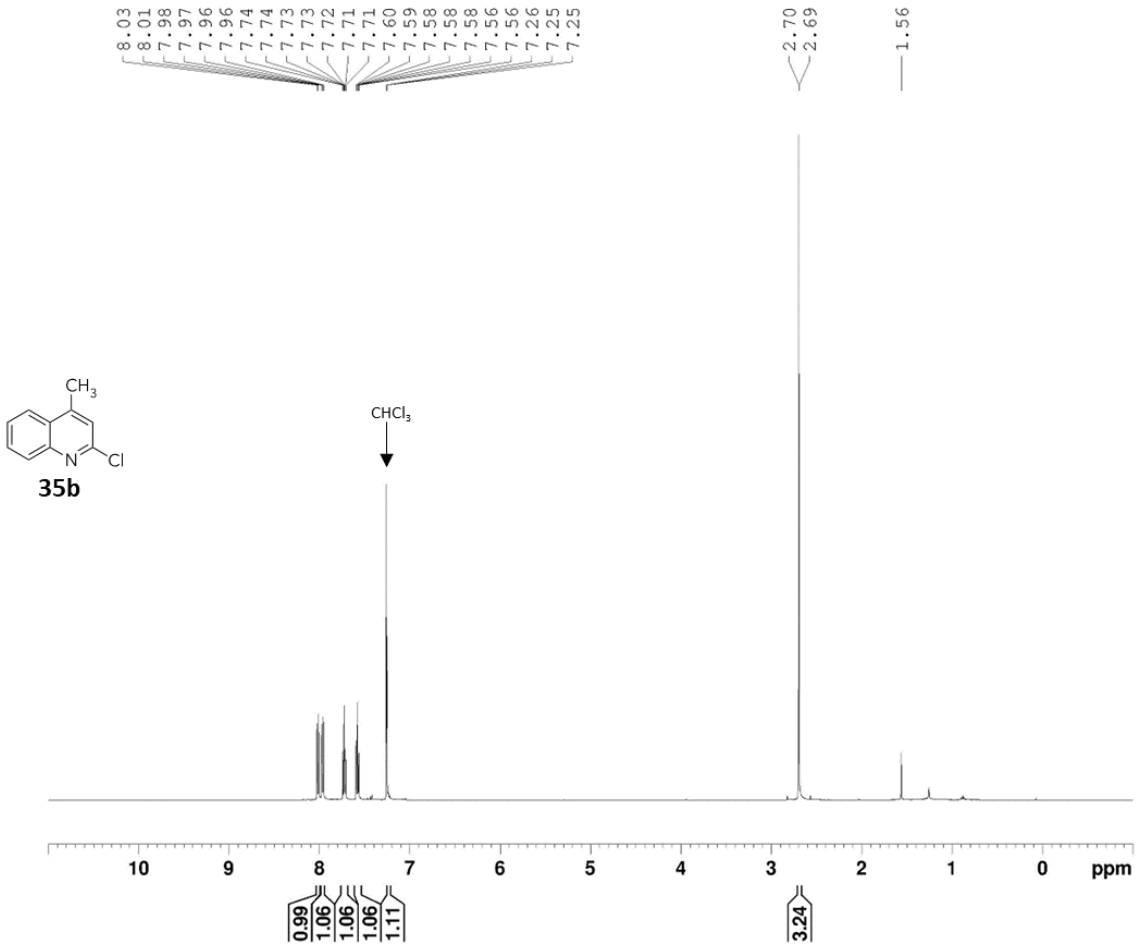

```
Current Data Parameters
NAME      NL-1-89-incconc
F2 - Acquisition Parameters
INSTRUM       Avance Neo
PROBHD    Z152088_0031 (
PULPROG     hmbcgplpndqf
TD                  4096
SOLVENT             CDCl3
NS                     4
DS                    16
SWH             3968.254 Hz
FIDRES          1.937624 Hz
AQ              0.5160960 sec
RG                   101
DW                126.000 usec
DE                  6.50 usec
TE                 298.2 K
CNST2          145.0000000
CNST13          10.0000000
D0               0.00000300 sec
D1               1.50000000 sec
D2               0.00344828 sec
D6               0.05000000 sec
D16              0.00020000 sec
IN0              0.00002259 sec
TDav                    1
SFO1          400.1316847 MHz
NUC1                   1H
P1                   8.00 usec
P2                  16.00 usec
PLW1          24.03499985 W
SFO2          100.6228298 MHz
NUC2                  13C
P3                   8.00 usec
PLW2          86.55400085 W
GPNAM[1]       SMSQ10.100
GPZ1                50.00 %
GPNAM[2]       SMSQ10.100
GPZ2                30.00 %
GPNAM[3]       SMSQ10.100
GPZ3                40.10 %
P16               1000.00 usec
======== F1 INDIRECT DIMENSION =
td1       128
sw_F1     220.000000
F1 - Acquisition parameters
TD                   128
SFO1           100.6228 MHz
FIDRES        345.877136 Hz
SW              219.991 ppm
FnMODE               QF
```




```
Current Data Parameters
NAME         NL-1-38-C4+
EXPNO                 10
PROCNO                 1

F2 - Acquisition Parameters
Date_           20210501
Time              14.01 h
INSTRUM       Avance Neo
PROBHD   Z152088_0031 (
PULPROG             zg30
TD                 65536
SOLVENT            CDCl3
NS                    16
DS                     2
SWH             8196.722 Hz
FIDRES          0.250144 Hz
AQ              3.9976959 sec
RG                   101
DW                61.000 usec
DE                13.89 usec
TE                298.1 K
D1             1.00000000 sec
TD0                    1
SFO1          400.1324708 MHz
NUC1                  1H
P0                 2.67 usec
P1                 8.00 usec
PLW1          24.03499985 W

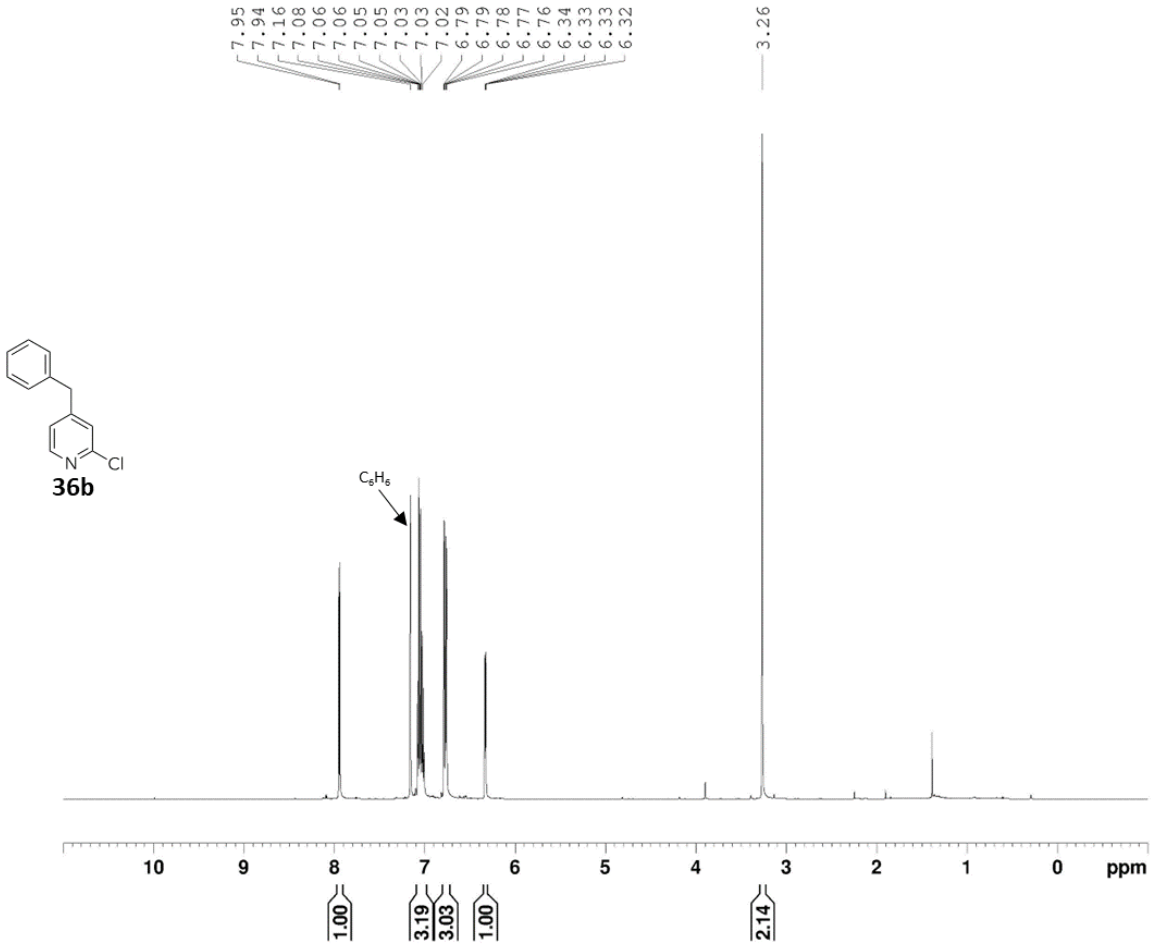
F2 - Processing parameters
SI                 65536
SF            400.1300100 MHz
WDW                   EM
SSB                    0
LB                  0.30 Hz
GB                     0
PC                 10.00
```




```
Current Data Parameters
NAME          NL-1-75-1H
EXPNO                 10
PROCNO                 1

F2 - Acquisition Parameters
Date_           20211028
Time               14.50 h
INSTRUM             spect
PROBHD   Z125869_0055 (
PULPROG             zg30
TD                 65536
SOLVENT            CDCl3
NS                    64
DS                     2
SWH            10000.000 Hz
FIDRES          0.305176 Hz
AQ              3.2767999 sec
RG                151.18
DW                50.000 usec
DE                16.00 usec
TE                298.0 K
D1             2.00000000 sec
TD0                    1
SFO1          500.2330889 MHz
NUC1                  1H
P0                 4.00 usec
P1                12.00 usec
PLW1          11.44699955 W

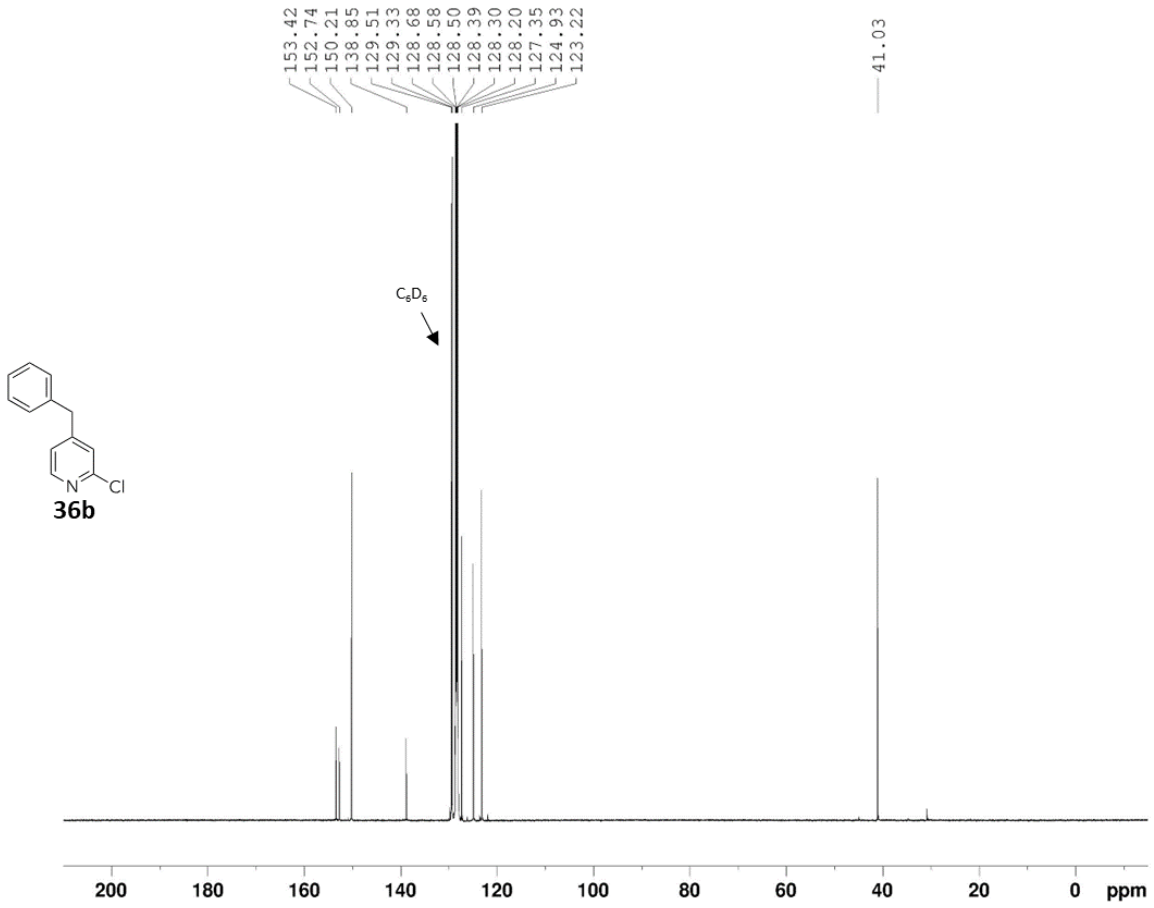
F2 - Processing parameters
SI                 65536
SF            500.2300122 MHz
WDW                   EM
SSB                    0
LB                  0.30 Hz
GB                     0
PC                  1.00
```




```
Current Data Parameters
NAME      NL-1-61-C4-1H-benzene
EXPNO                        10
PROCNO                        1

F2 - Acquisition Parameters
Date_              20210624
Time                  14.01 h
INSTRUM               spect
PROBHD    Z125869_0055 (
PULPROG                 zg30
TD                     65536
SOLVENT                 C6D6
NS                        64
DS                         2
SWH               10000.000 Hz
FIDRES             0.305176 Hz
AQ                3.2767999 sec
RG                    43.72
DW                   50.000 usec
DE                   16.00 usec
TE                   300.0 K
D1               2.00000000 sec
TD0                        1
SFO1           500.2330889 MHz
NUC1                      1H
P0                    4.00 usec
P1                   12.00 usec
PLW1           11.44699955 W

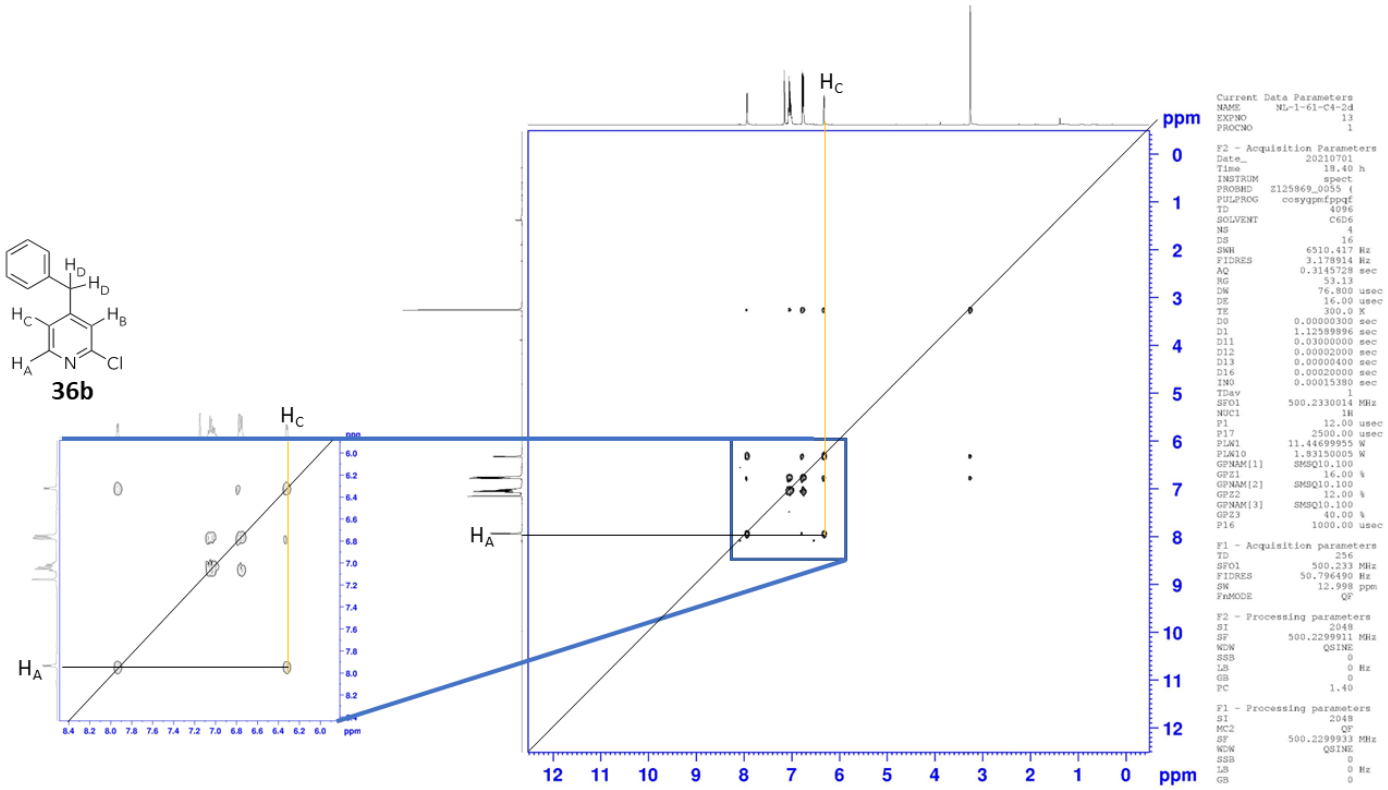
F2 - Processing parameters
SI                     65536
SF             500.2299949 MHz
WDW                       EM
SSB                        0
LB                    0.30 Hz
GB                         0
PC                     1.00
```




```
Current Data Parameters
NAME       NL-1-61-C4-2d
EXPNO                 10
PROCNO                 1

F2 - Acquisition Parameters
Date_           20210701
Time              18.21 h
INSTRUM             spect
PROBHD   Z125869_0055 (
PULPROG           zgpg30
TD                 65536
SOLVENT              C6D6
NS                   1024
DS                      4
SWH            29761.904 Hz
FIDRES          0.908261 Hz
AQ             1.1010048 sec
RG                190.44
DW                16.800 usec
DE                18.00 usec
TE                300.0 K
D1           2.00000000 sec
D11          0.03000000 sec
TD0                    1
SFO1         125.7955118 MHz
NUC1                13C
P0                 3.33 usec
P1                10.00 usec
PLW1         56.90299988 W
SFO2         500.2320009 MHz
NUC2                1H
CPDPRG[2         waltz16
PCPD2             80.00 usec
PLW2         11.44699955 W
PLW12         0.25756001 W
PLW13         0.12955000 W

F2 - Processing parameters
SI                 32768
SF           125.7828447 MHz
WDW                   EM
SSB                    0
LB                  1.00 Hz
GB                     0
PC                  1.40
```



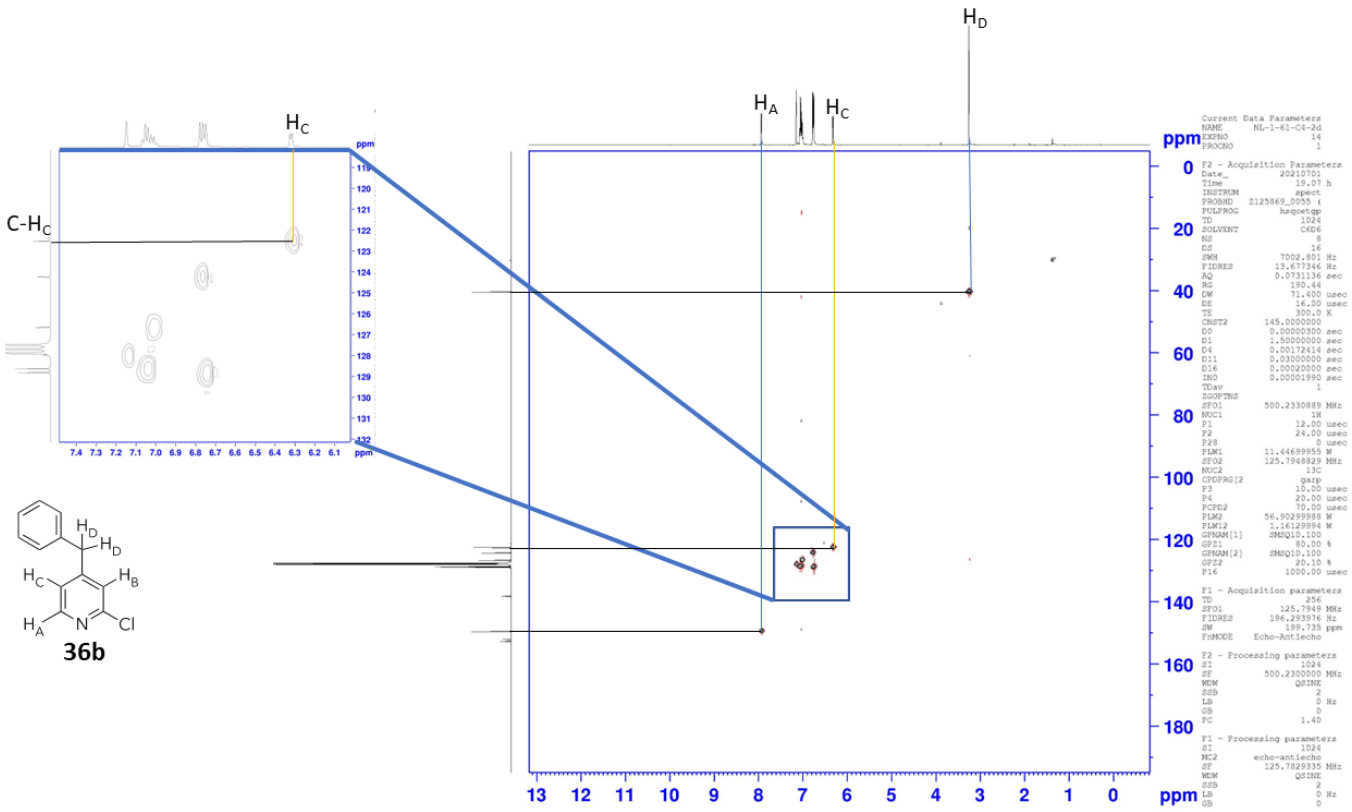
Current Data Parameters
NAME NL-1-61-C4-2d
EXPNO 13
PROCNO 1

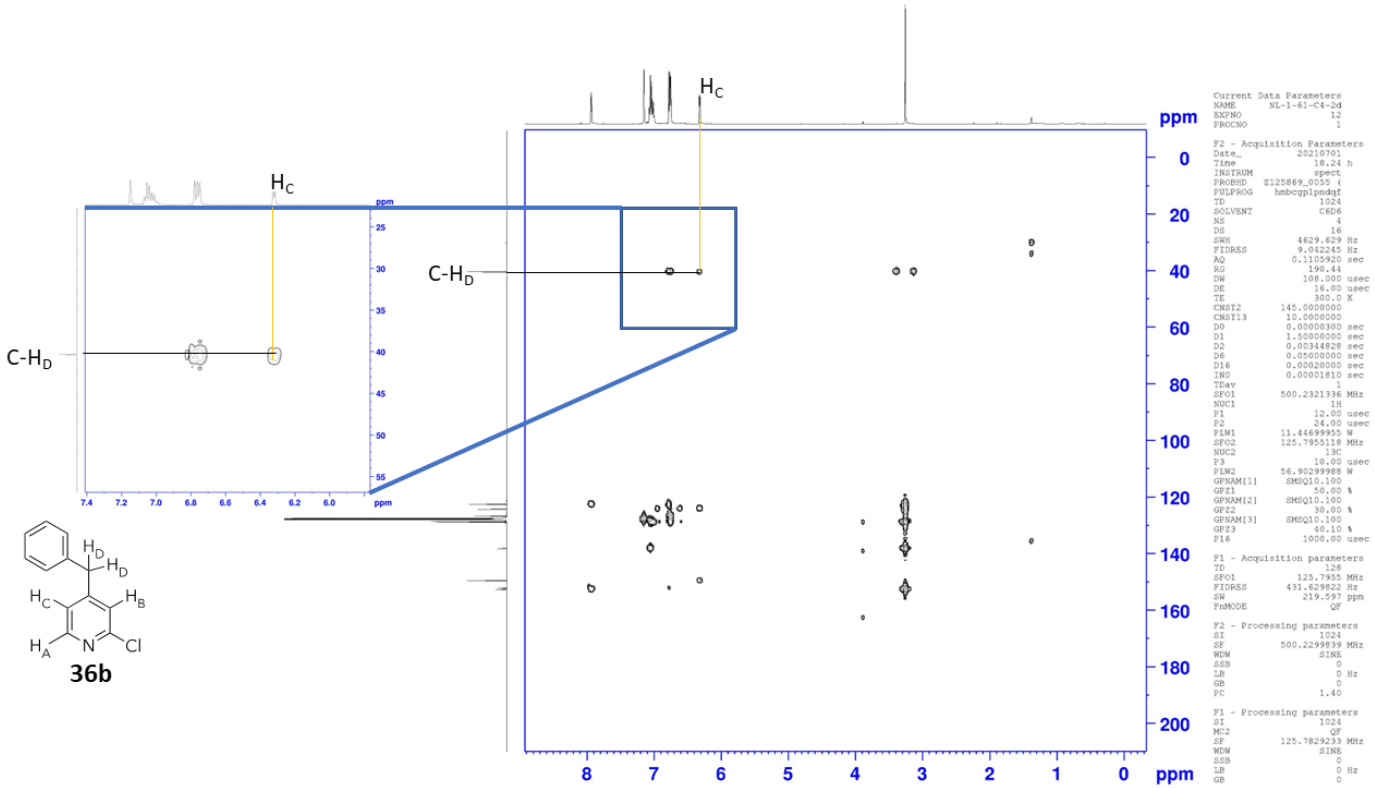
F2 - Acquisition Parameters
Date_ 20210701
Time 18.40 h
INSTRUM spect
PROBHD Z125869_0055 (
PULPROG cosygpmfppqf
TD 4096
SOLVENT C6D6
NS 4
DS 16
SWH 6510.417 Hz
FIDRES 3.178914 Hz
AQ 0.3145728 sec
RG 53.13
DW 76.800 usec
DE 16.00 usec
TE 300.0 K
D0 0.00000300 sec
D1 1.12589896 sec
D11 0.03000000 sec
D12 0.00002000 sec
D13 0.00000400 sec
D16 0.00020000 sec
IN0 0.00015380 sec
TDav 1
SFO1 500.2330014 MHz
NUC1 1H
P1 12.00 usec
P17 2500.00 usec
PLW1 11.44699955 W
PLW10 1.83150005 W
GPNAM[1] SMSQ10.100
GPZ1 16.00 %
GPNAM[2] SMSQ10.100
GPZ2 12.00 %
GPNAM[3] SMSQ10.100
GPZ3 40.00 %
P16 1000.00 usec

F1 - Acquisition parameters
TD 256
SFO1 500.233 MHz
FIDRES 50.796490 Hz
SW 12.998 ppm
FnMODE QF

F2 - Processing parameters
SI 2048
SF 500.2299911 MHz
WDW QSINE
SSB 0
LB 0 Hz
GB 0
PC 1.40

F1 - Processing parameters
SI 2048
MC2 QF
SF 500.2299933 MHz
WDW QSINE
SSB 0
LB 0 Hz
GB 0


H_D
H_A
H_C
C-H_C
H_C
H_D
H_D
H_B
H_A
N
Cl
36b
ppm
13 12 11 10 9 8 7 6 5 4 3 2 1 0 ppm



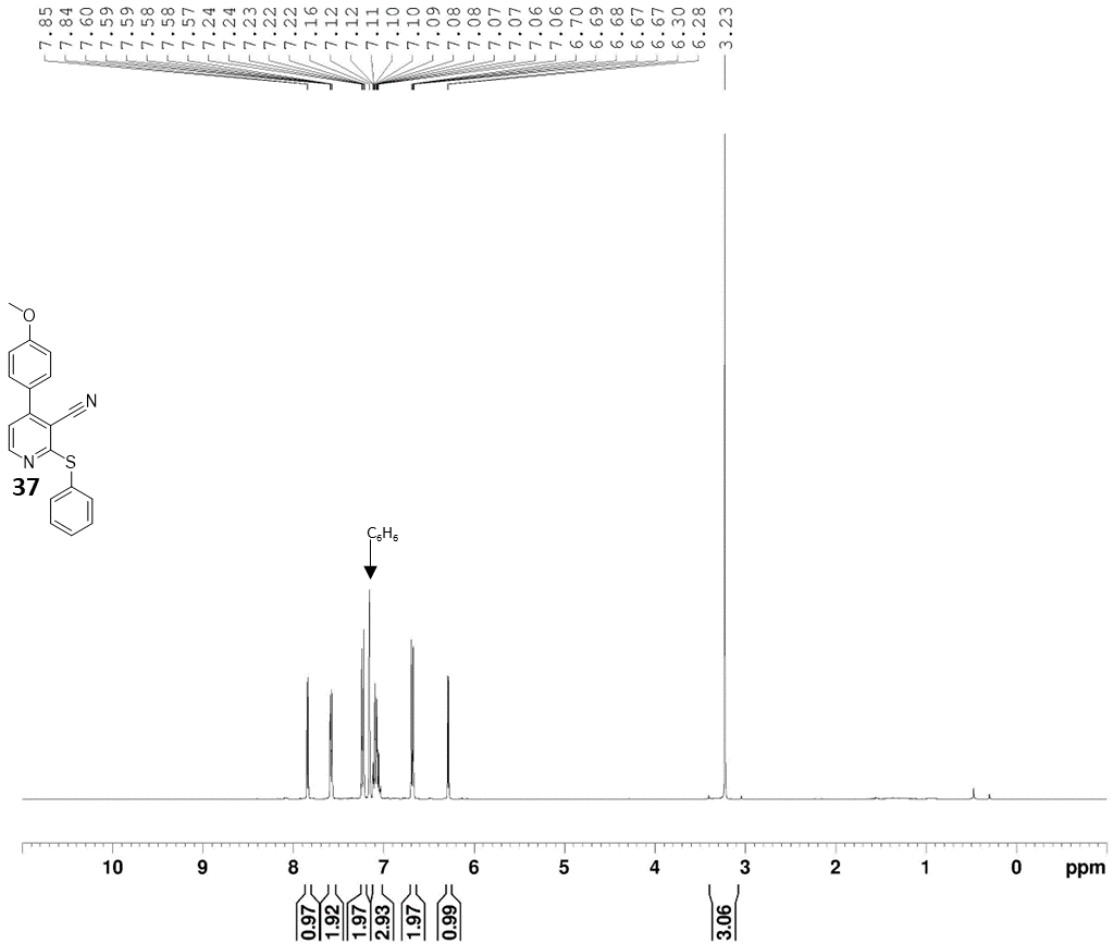
Current Data Parameters
NAME NL-1-61-C4-2d
EXPNO 12
PROCNO 1

F2 - Acquisition Parameters
Date_ 20210701
Time 18.24 h
INSTRUM spect
PROBHD Z125869_0055 (
PULPROG hmbcgplpndqf
TD 1024
SOLVENT C6D6
NS 4
DS 16
SWH 4629.629 Hz
FIDRES 9.042245 Hz
AQ 0.1105920 sec
RG 198.44
DW 108.000 usec
DE 16.00 usec
TE 300.0 K
CNST2 145.0000000
CNST13 10.0000000
D0 0.00000300 sec
D1 1.50000000 sec
D2 0.00344828 sec
D6 0.05000000 sec
D16 0.00020000 sec
IN0 0.00001810 sec
TDav 1
SFO1 500.2321336 MHz
NUC1 1H
P1 12.00 usec
P2 24.00 usec
PLW1 11.44699955 W
SFO2 125.7955118 MHz
NUC2 13C
P3 10.00 usec
PLW2 56.90299988 W
GPNAM[1] SMSQ10.100
GPZ1 50.00 %
GPNAM[2] SMSQ10.100
GPZ2 30.00 %
GPNAM[3] SMSQ10.100
GPZ3 40.10 %
P16 1000.00 usec

F1 - Acquisition parameters
TD 128
SFO1 125.7955 MHz
FIDRES 431.629822 Hz
SW 219.597 ppm
FnMODE QF

F2 - Processing parameters
SI 1024
SF 500.2299839 MHz
WDW SINE
SSB 0
LB 0 Hz
GB 0
PC 1.40

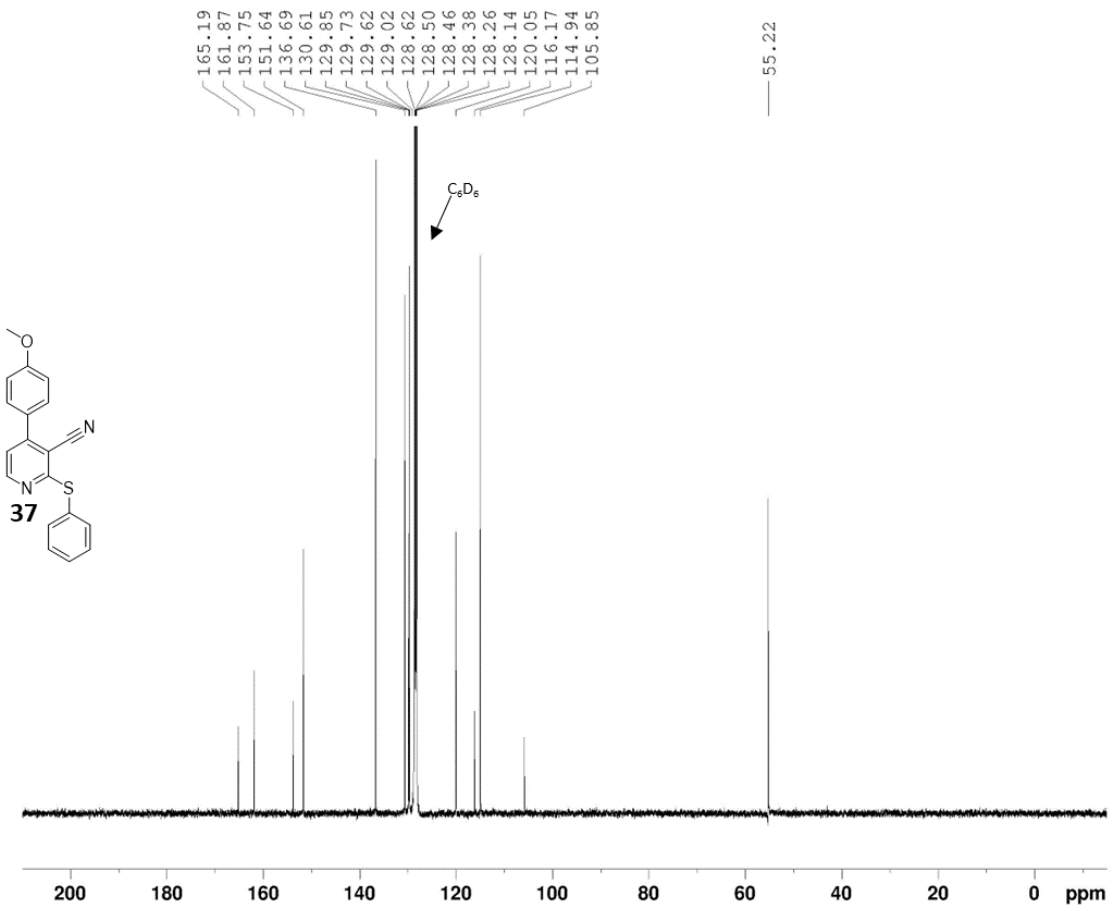
F1 - Processing parameters
SI 1024
MC2 QF
SF 125.7829233 MHz
WDW SINE
SSB 0
LB 0 Hz
GB 0




```
Current Data Parameters
NAME         JPN-1-189-1
EXPNO                 15
PROCNO                 1

F2 - Acquisition Parameters
Date_           20211107
Time               20.23 h
INSTRUM       Avance Neo
PROBHD   Z152088_0031 (
PULPROG             zg30
TD                 65536
SOLVENT             C6D6
NS                    16
DS                     2
SWH             8196.722 Hz
FIDRES          0.250144 Hz
AQ              3.9976959 sec
RG                   101
DW                61.000 usec
DE                13.89 usec
TE                298.0 K
D1             1.00000000 sec
TD0                    1
SFO1          400.1324708 MHz
NUC1                  1H
P0                 2.67 usec
P1                 8.00 usec
PLW1          24.03499985 W

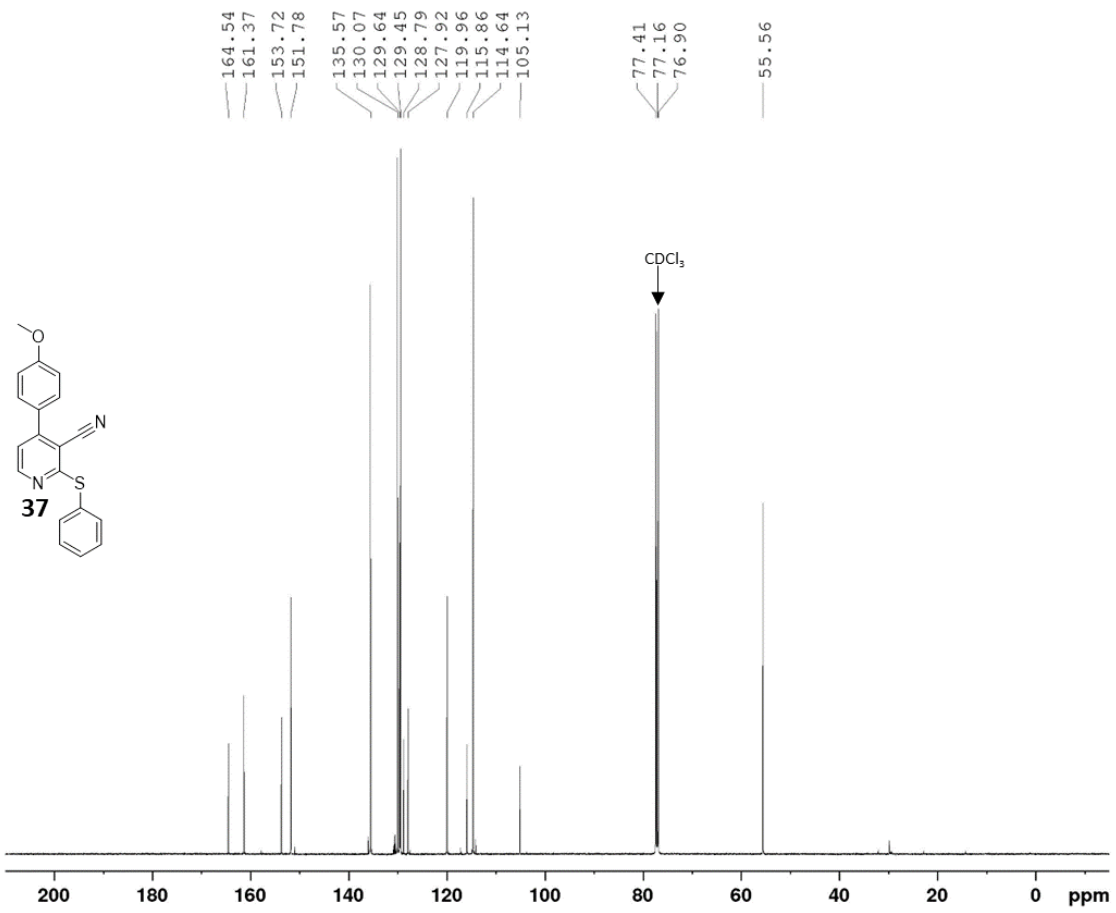
F2 - Processing parameters
SI                 65536
SF            400.1299968 MHz
WDW                   EM
SSB                    0
LB                  0.30 Hz
GB                     0
PC                  1.00
```




```
Current Data Parameters
NAME         JPN-1-189-1
EXPNO                 14
PROCNO                 1

F2 - Acquisition Parameters
Date_           20211107
Time              20.21 h
INSTRUM       Avance Neo
PROBHD   Z152088_0031 (
PULPROG           zgpg30
TD                65536
SOLVENT             C6D6
NS                  1024
DS                     4
SWH           23809.523 Hz
FIDRES         0.726609 Hz
AQ            1.3762560 sec
RG                 8.125
DW                21.000 usec
DE                 6.50 usec
TE                298.0 K
D1           2.00000000 sec
D11          0.03000000 sec
TD0                    1
SFO1        100.6228298 MHz
NUC1                13C
P0                 2.67 usec
P1                 8.00 usec
PLW1        86.55400085 W
SFO2        400.1316005 MHz
NUC2                1H
CPDPRG[2         waltz65
PCPD2             90.00 usec
PLW2        24.03499985 W
PLW12        0.18990999 W
PLW13        0.09552100 W

F2 - Processing parameters
SI                 32768
SF          100.6126995 MHz
WDW                   EM
SSB                    0
LB                  1.00 Hz
GB                     0
PC                  1.40
```

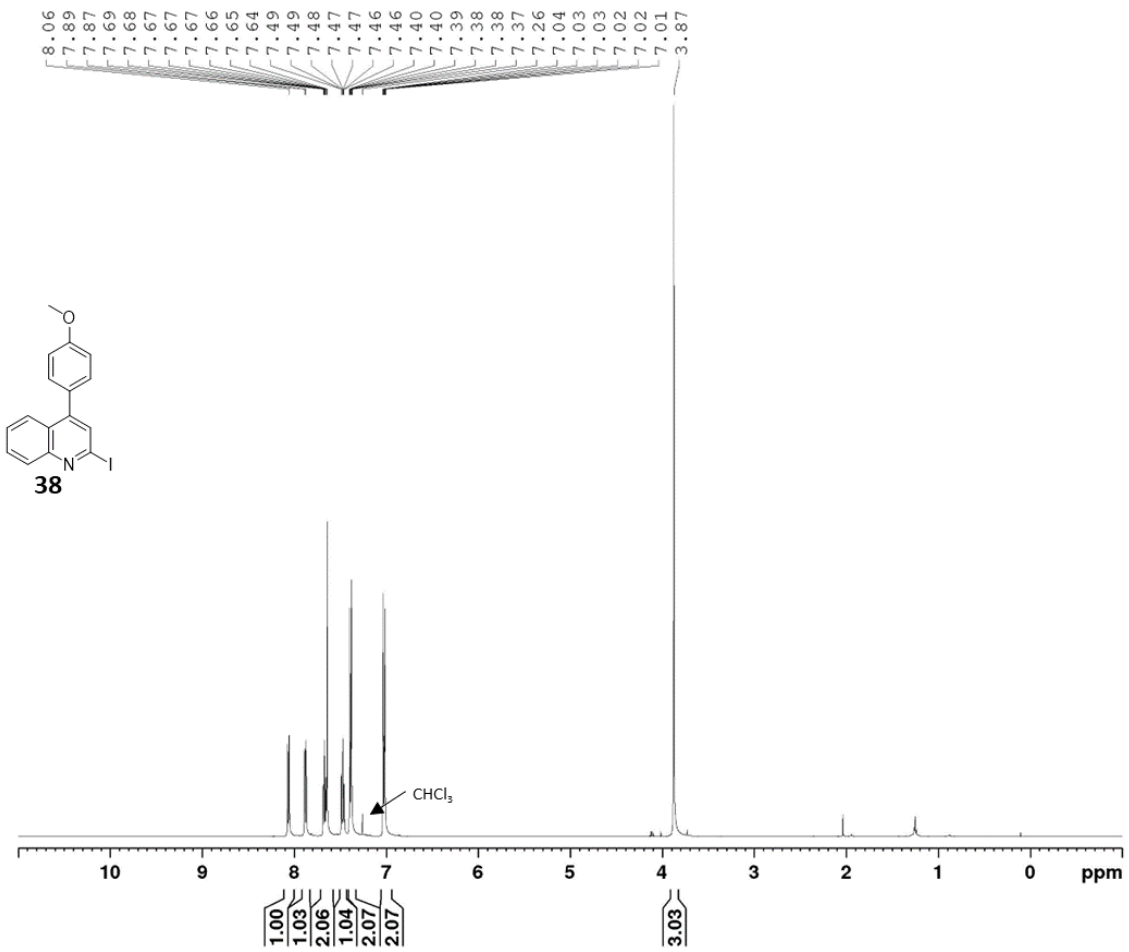


37

```
Current Data Parameters
NAME      JPN-1-189-1_CDCl3
EXPNO                   11
PROCNO                   1

F2 - Acquisition Parameters
Date_              20211209
Time                  0.37 h
INSTRUM               spect
PROBHD    Z125869_0055 (
PULPROG             zgpg30
TD                   65536
SOLVENT              CDCl3
NS                    1024
DS                       4
SWH              29761.904 Hz
FIDRES            0.908261 Hz
AQ               1.1010048 sec
RG                  190.44
DW                  16.800 usec
DE                  18.00 usec
TE                  298.0 K
D1              2.00000000 sec
D11             0.03000000 sec
TD0                      1
SFO1           125.7955118 MHz
NUC1                   13C
P0                    3.33 usec
P1                   10.00 usec
PLW1           56.90299988 W
SFO2           500.2320009 MHz
NUC2                   1H
CPDPRG[2           waltz16
PCPD2                80.00 usec
PLW2           11.44699955 W
PLW12           0.25756001 W
PLW13           0.12955000 W

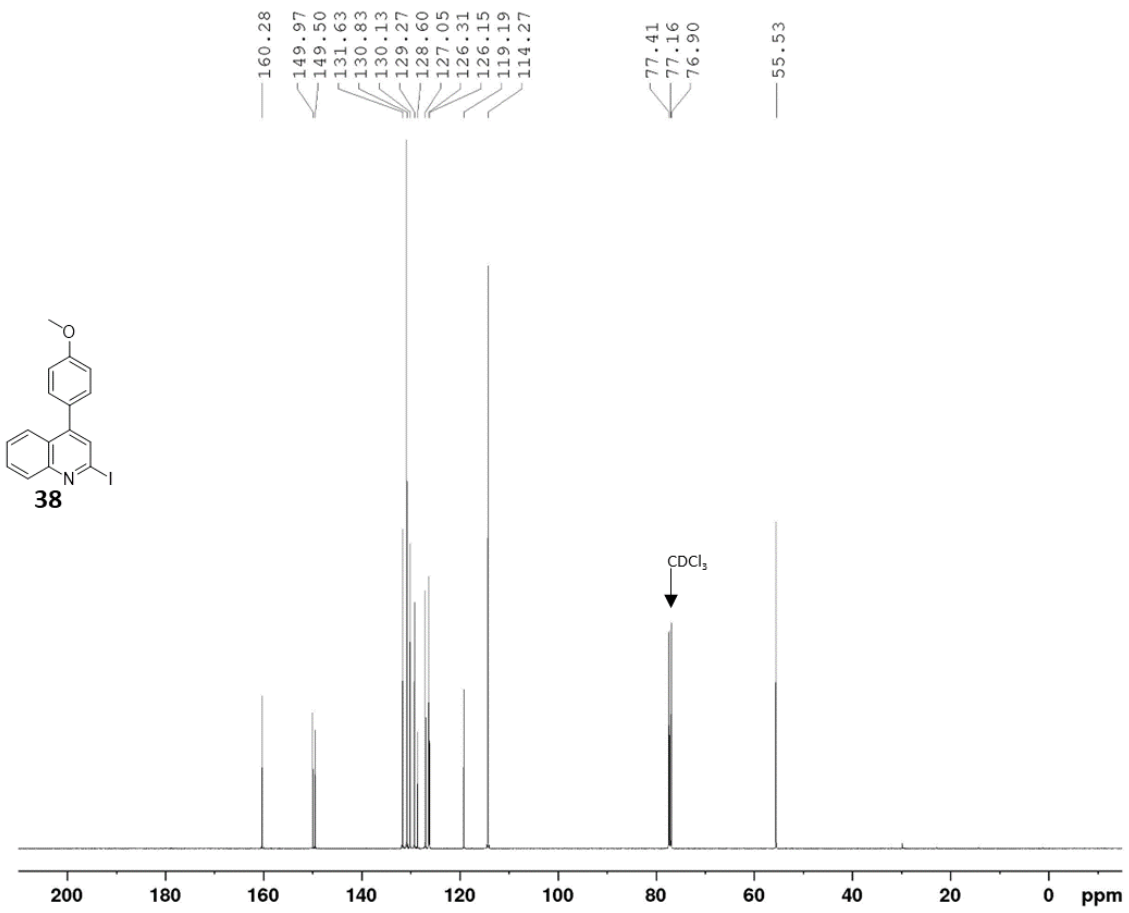
F2 - Processing parameters
SI                   32768
SF             125.7829231 MHz
WDW                     EM
SSB       0
LB                    1.00 Hz
GB        0
PC                    1.40
```




```
Current Data Parameters
NAME            JPN-2-25
EXPNO                 10
PROCNO                 1

F2 - Acquisition Parameters
Date_           20201019
Time               18.36 h
INSTRUM             spect
PROBHD   Z125869_0055 (
PULPROG             zg30
TD                 65536
SOLVENT            CDCl3
NS                    64
DS                     2
SWH            10000.000 Hz
FIDRES          0.305176 Hz
AQ              3.2767999 sec
RG                 22.16
DW                 50.000 usec
DE                 16.00 usec
TE                 300.0 K
D1              2.00000000 sec
TD0                    1
SFO1         500.2330889 MHz
NUC1                  1H
P0                 4.00 usec
P1                 12.00 usec
PLW1         11.44699955 W

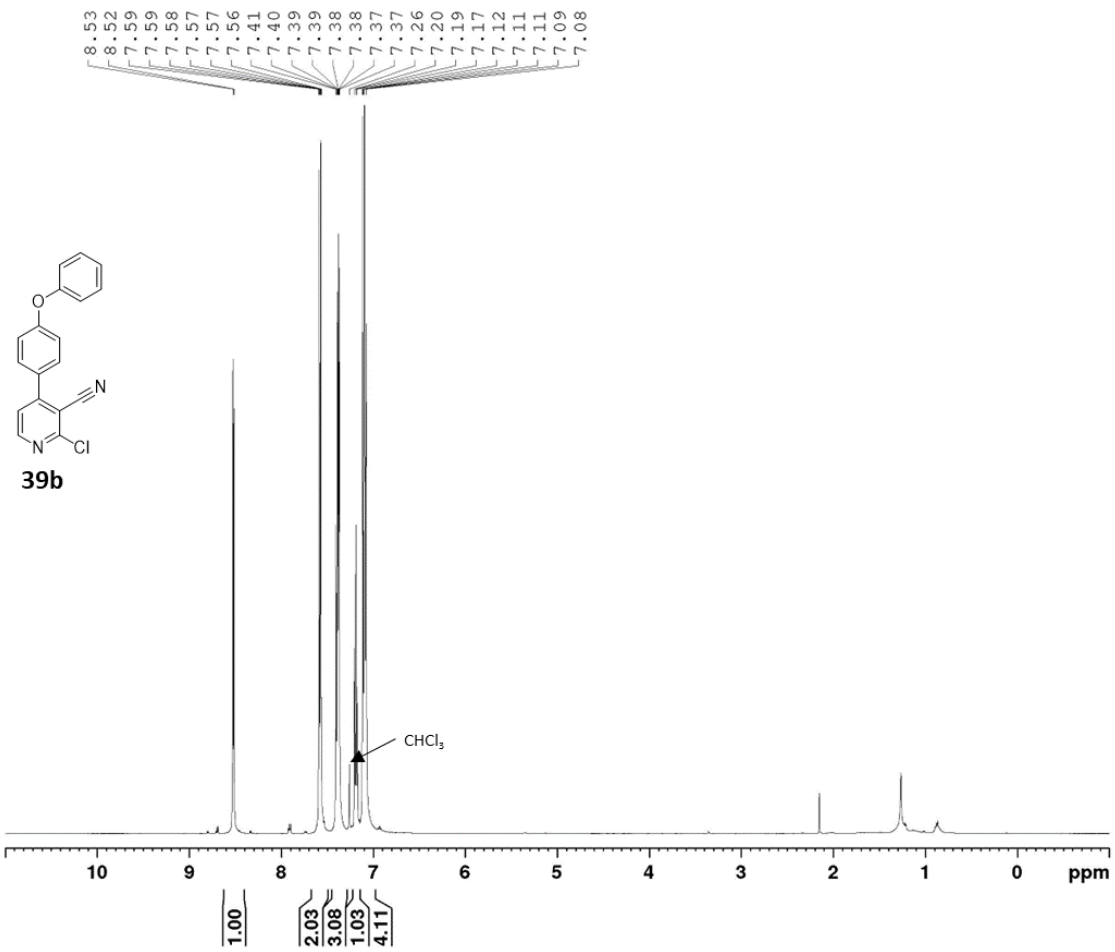
F2 - Processing parameters
SI                 65536
SF           500.2300124 MHz
WDW                   EM
SSB       0
LB                 0.30 Hz
GB        0
PC                 1.00
```




```
Current Data Parameters
NAME          JPN-2-25-1
EXPNO                 17
PROCNO                 1

F2 - Acquisition Parameters
Date_           20211120
Time                4.43 h
INSTRUM            spect
PROBHD   Z125869_0055 (
PULPROG          zgpg30
TD                65536
SOLVENT           CDCl3
NS                 1024
DS                    4
SWH           29761.904 Hz
FIDRES         0.908261 Hz
AQ            1.1010048 sec
RG               190.44
DW               16.800 usec
DE               18.00 usec
TE               298.0 K
D1           2.00000000 sec
D11          0.03000000 sec
TD0                   1
SFO1        125.7955118 MHz
NUC1               13C
P0                3.33 usec
P1               10.00 usec
PLW1        56.90299988 W
SFO2        500.2320009 MHz
NUC2               1H
CPDPRG[2        waltz16
PCPD2            80.00 usec
PLW2        11.44699955 W
PLW12        0.25756001 W
PLW13        0.12955000 W

F2 - Processing parameters
SI                32768
SF          125.7829267 MHz
WDW                EM
SSB       0
LB               1.00 Hz
GB        0
PC               1.40
```

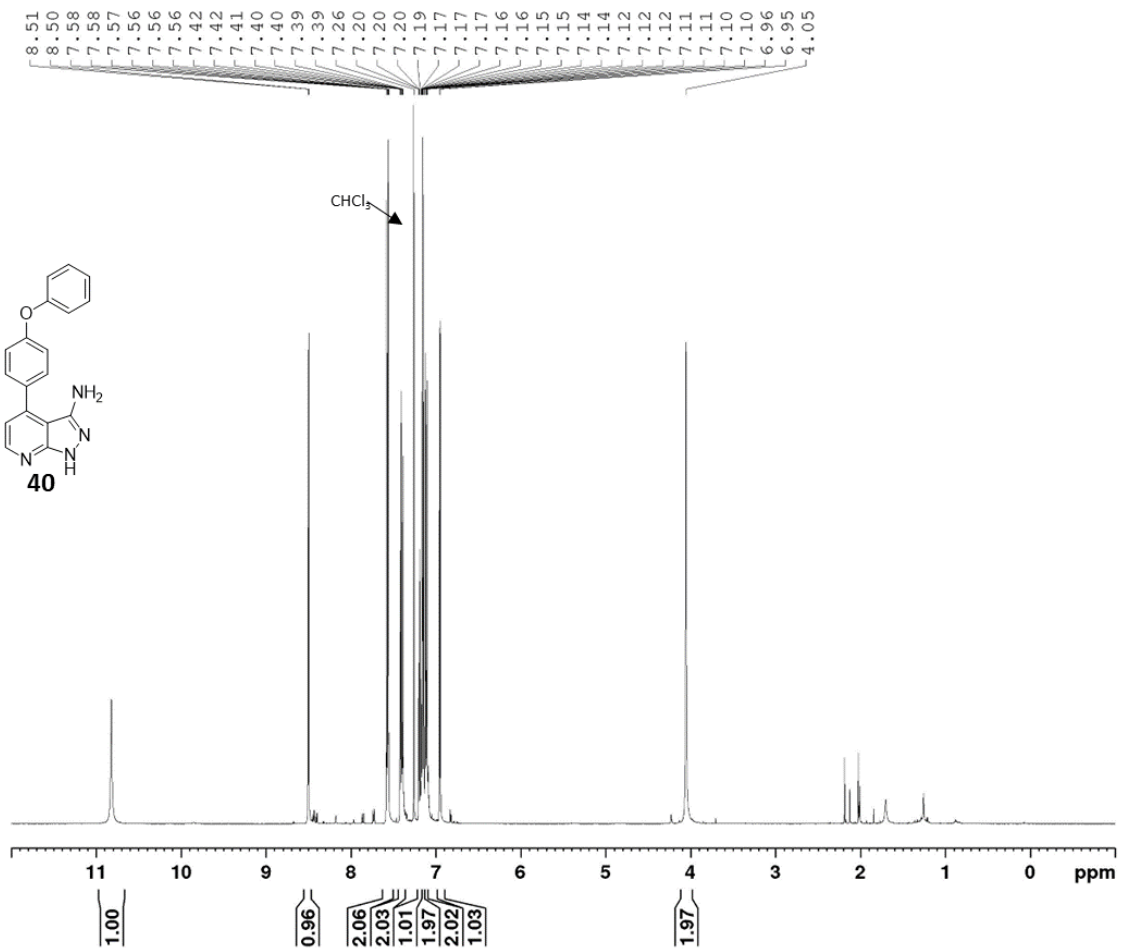


39b

```
Current Data Parameters
NAME      JPN-2-6-C4-mono_dried
EXPNO                        10
PROCNO                        1

F2 - Acquisition Parameters
Date_              20200823
Time                    8.03 h
INSTRUM                 spect
PROBHD    Z125869_0055 (
PULPROG                 zg30
TD                     65536
SOLVENT                CDCl3
NS                        64
DS                         2
SWH                10000.000 Hz
FIDRES             0.305176 Hz
AQ                 3.2767999 sec
RG                      19.46
DW                     50.000 usec
DE                     16.00 usec
TE                     300.0 K
D1                2.00000000 sec
TD0                        1
SFO1            500.2330889 MHz
NUC1                      1H
P0                     4.00 usec
P1                    12.00 usec
PLW1           11.44699955 W

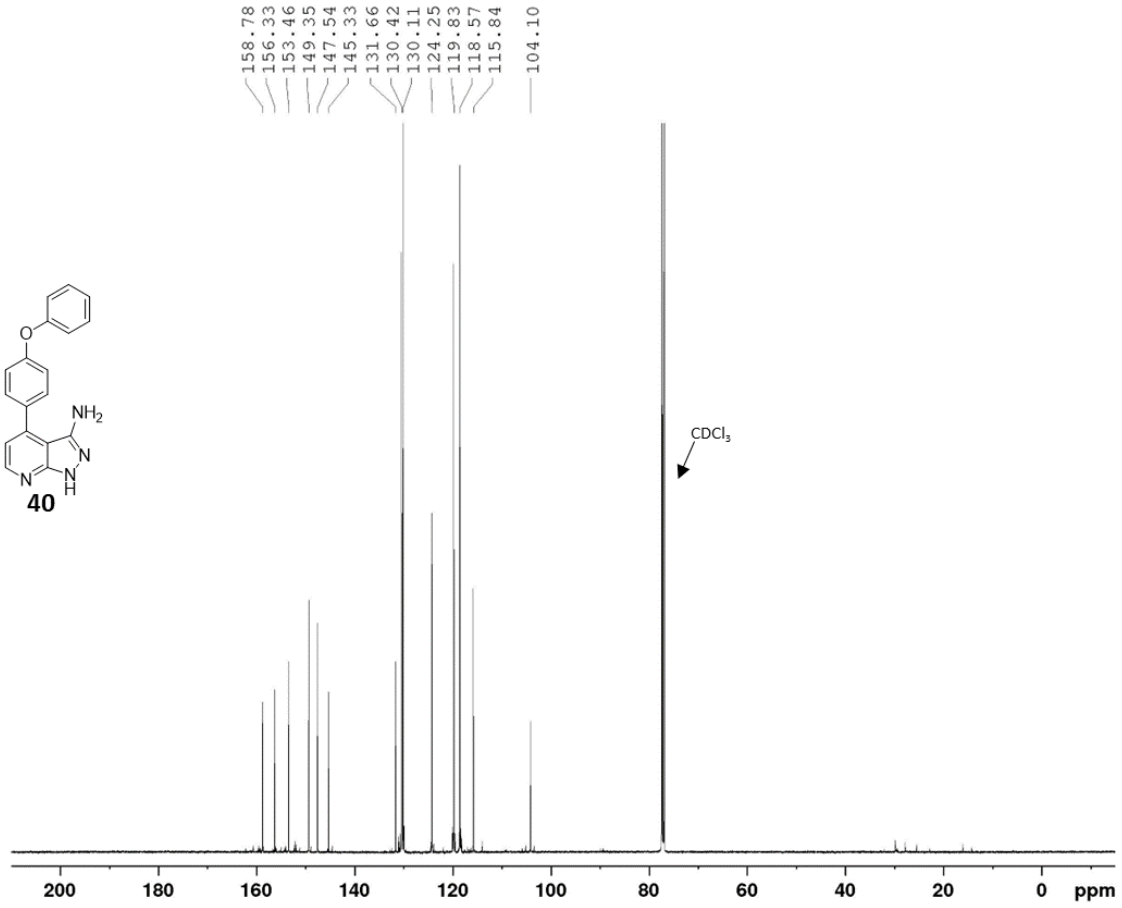
F2 - Processing parameters
SI                     65536
SF              500.2300120 MHz
WDW                       EM
SSB       0
LB                     0.30 Hz
GB        0
PC                     1.00
```




```
Current Data Parameters
NAME      JPN-2-6-2_repeat
EXPNO                   10
PROCNO                   1

F2 - Acquisition Parameters
Date_           20201019
Time               18.27 h
INSTRUM             spect
PROBHD   Z125869_0055 (
PULPROG             zg30
TD                 65536
SOLVENT            CDCl3
NS                    64
DS                     2
SWH            10000.000 Hz
FIDRES          0.305176 Hz
AQ              3.2767999 sec
RG                151.18
DW                 50.000 usec
DE                 16.00 usec
TE                 300.0 K
D1             2.00000000 sec
TD0                    1
SFO1         500.2330889 MHz
NUC1                  1H
P0                 4.00 usec
P1                12.00 usec
PLW1         11.44699955 W

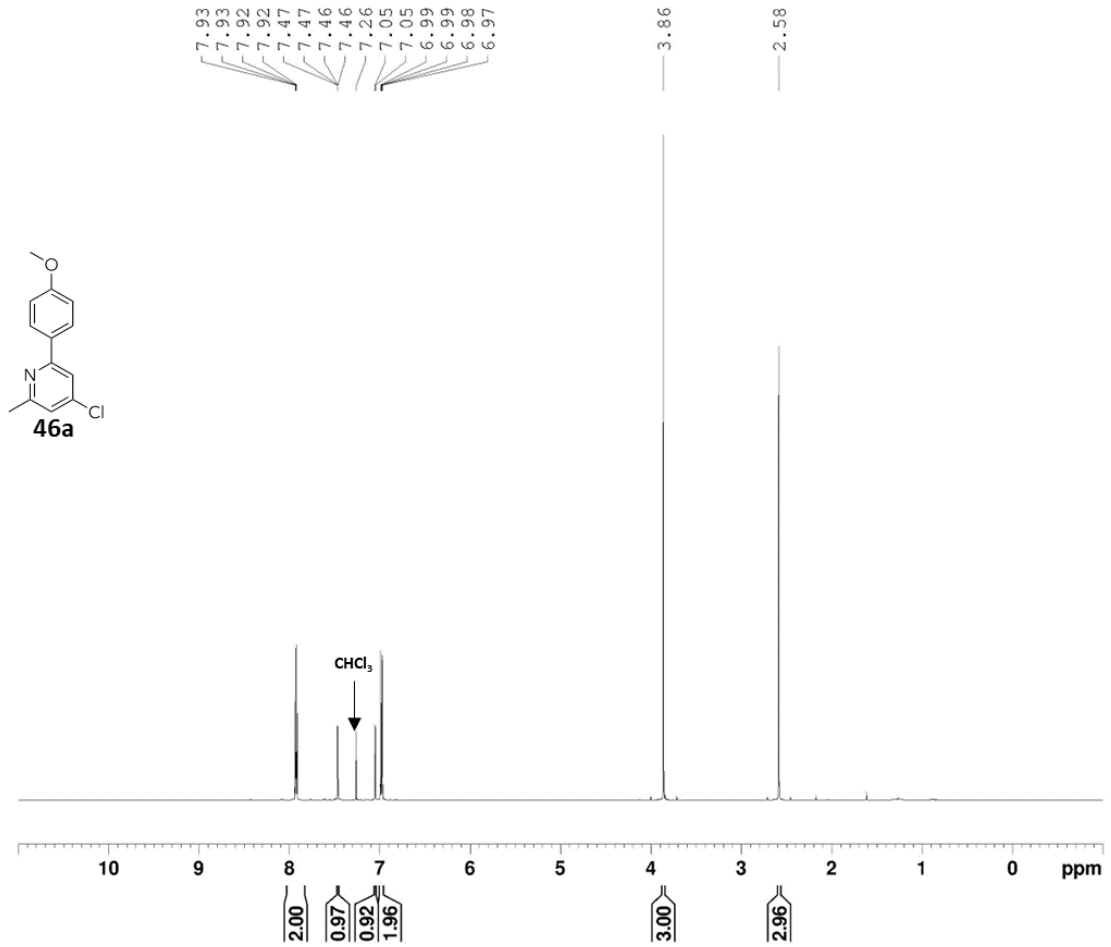
F2 - Processing parameters
SI                 65536
SF           500.2300122 MHz
WDW                   EM
SSB      0
LB                 0.30 Hz
GB       0
PC                 1.00
```




```
Current Data Parameters
NAME           JPN-2-6-2
EXPNO                 17
PROCNO                 1

F2 - Acquisition Parameters
Date_           20211120
Time                5.41 h
INSTRUM            spect
PROBHD    Z125869_0055 (
PULPROG          zgpg30
TD                65536
SOLVENT           CDCl3
NS                 1024
DS                    4
SWH            29761.904 Hz
FIDRES          0.908261 Hz
AQ             1.1010048 sec
RG                190.44
DW                16.800 usec
DE                18.00 usec
TE                298.0 K
D1             2.00000000 sec
D11            0.03000000 sec
TD0                    1
SFO1         125.7955118 MHz
NUC1                 13C
P0                 3.33 usec
P1                10.00 usec
PLW1         56.90299988 W
SFO2         500.2320009 MHz
NUC2                 1H
CPDPRG[2          waltz16
PCPD2             80.00 usec
PLW2         11.44699955 W
PLW12         0.25756001 W
PLW13         0.12955000 W

F2 - Processing parameters
SI                 32768
SF           125.7829211 MHz
WDW                   EM
SSB       0
LB                 1.00 Hz
GB        0
PC                 1.40
```

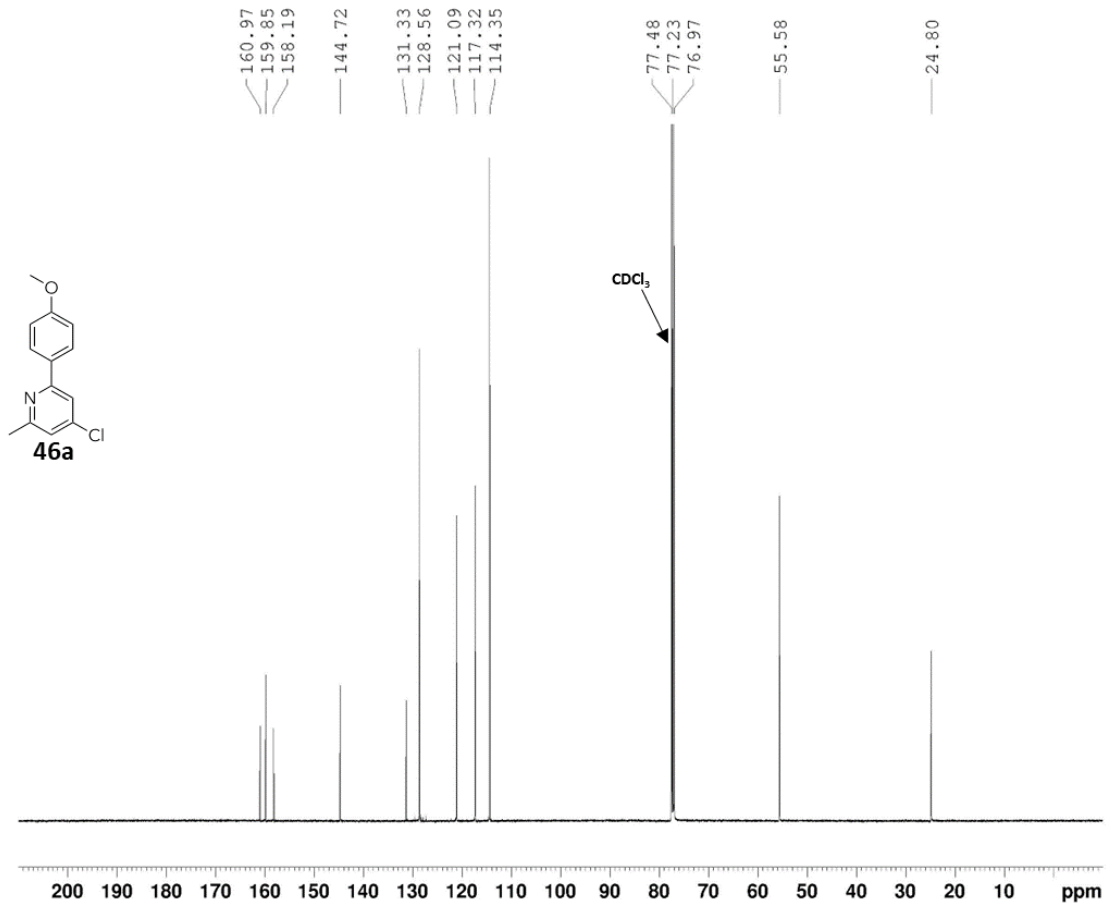


46a

```
Current Data Parameters
NAME      NL-1-171-f11-13
EXPNO                  10
PROCNO                  1

F2 - Acquisition Parameters
Date_           20220214
Time               10.17 h
INSTRUM             spect
PROBHD   Z125869_0055 (
PULPROG             zg30
TD                 65536
SOLVENT            CDCl3
NS                    64
DS                     2
SWH            10000.000 Hz
FIDRES             0.305176 Hz
AQ              3.2767999 sec
RG                 94.51
DW                50.000 usec
DE                16.00 usec
TE                298.0 K
D1             2.00000000 sec
TD0                    1
SFO1          500.2330889 MHz
NUC1                  1H
P0                 4.00 usec
P1                12.00 usec
PLW1          11.44699955 W

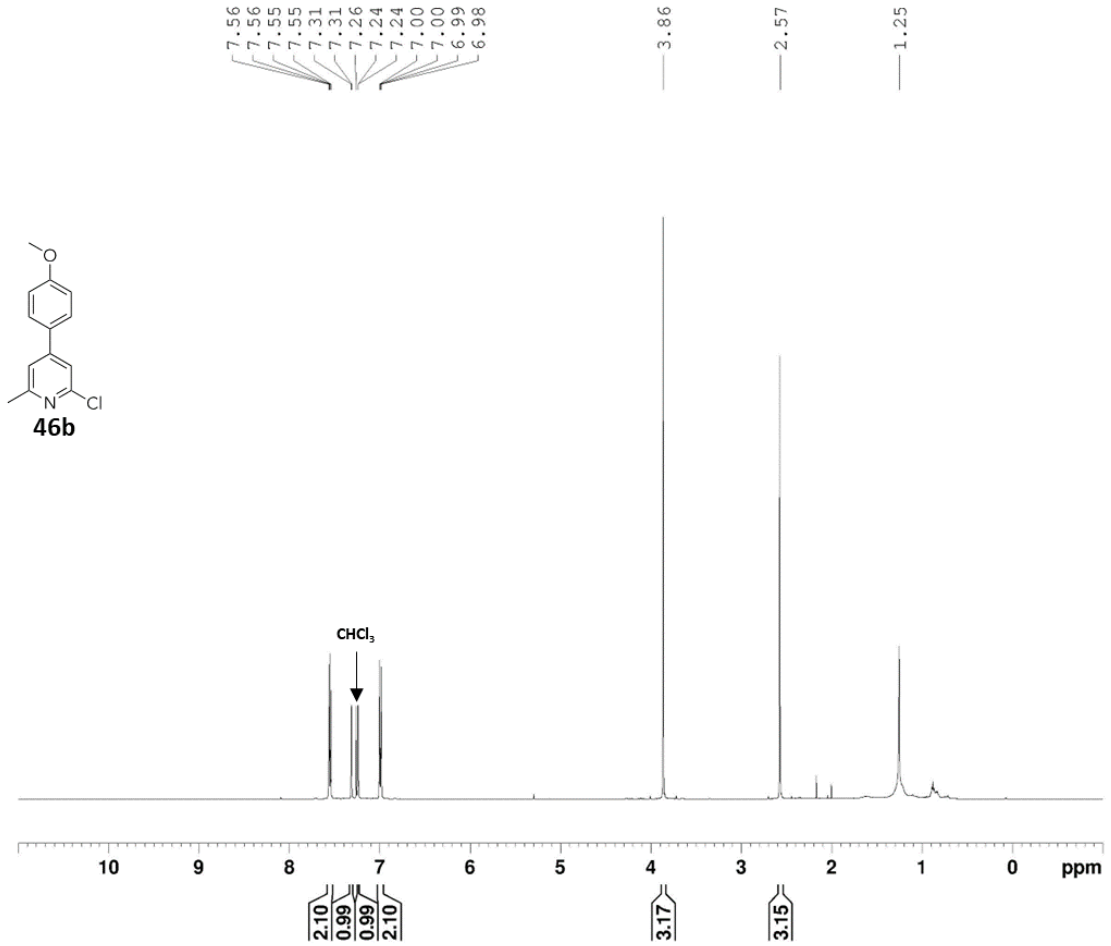
F2 - Processing parameters
SI                 65536
SF            500.2300120 MHz
WDW                   EM
SSB                    0
LB                  0.30 Hz
GB                     0
PC                  1.00
```




```
Current Data Parameters
NAME      NL-1-171-f11-13
EXPNO                  11
PROCNO                  1

F2 - Acquisition Parameters
Date_           20220214
Time               18.57 h
INSTRUM             spect
PROBHD   Z125869_0055 (
PULPROG          zgpg30
TD                65536
SOLVENT           CDCl3
NS                 1024
DS                    4
SWH           29761.904 Hz
FIDRES         0.908261 Hz
AQ            1.1010048 sec
RG               190.44
DW               16.800 usec
DE               18.00 usec
TE               298.0 K
D1           2.00000000 sec
D11          0.03000000 sec
TD0                   1
SFO1        125.7955118 MHz
NUC1                13C
P0                3.33 usec
P1               10.00 usec
PLW1        56.90299988 W
SFO2        500.2320009 MHz
NUC2                1H
CPDPRG[2         waltz16
PCPD2            80.00 usec
PLW2        11.44699955 W
PLW12        0.25756001 W
PLW13        0.12955000 W

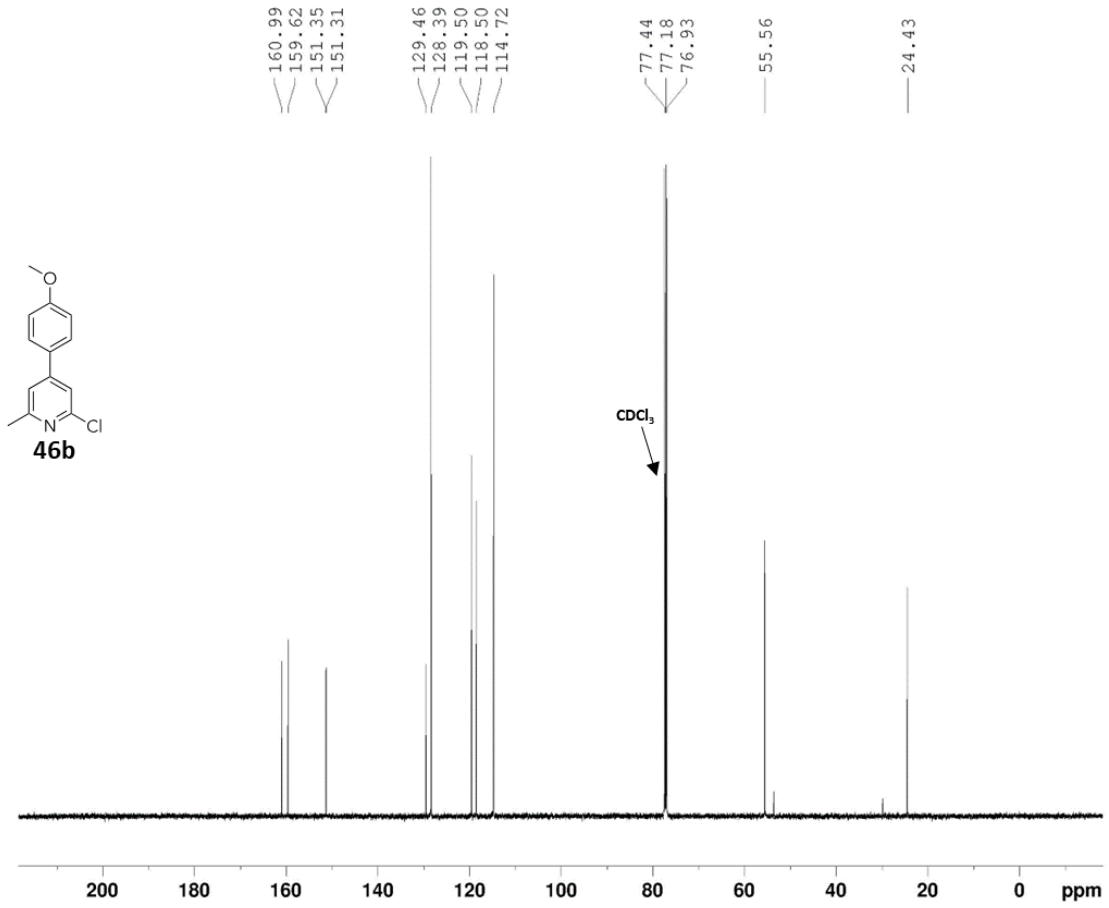
F2 - Processing parameters
SI                32768
SF          125.7829086 MHz
WDW                  EM
SSB                   0
LB                 1.00 Hz
GB                    0
PC                 1.40
```




```
Current Data Parameters
NAME       NL-1-172.1-1H
EXPNO                 10
PROCNO                 1

F2 - Acquisition Parameters
Date_           20220216
Time               12.19 h
INSTRUM             spect
PROBHD   Z125869_0055 (
PULPROG             zg30
TD                 65536
SOLVENT            CDCl3
NS                    64
DS                     2
SWH            10000.000 Hz
FIDRES          0.305176 Hz
AQ              3.2767999 sec
RG                 94.51
DW                50.000 usec
DE                16.00 usec
TE                298.0 K
D1             2.00000000 sec
TD0                    1
SFO1          500.2330889 MHz
NUC1                  1H
P0                 4.00 usec
P1                12.00 usec
PLW1          11.44699955 W

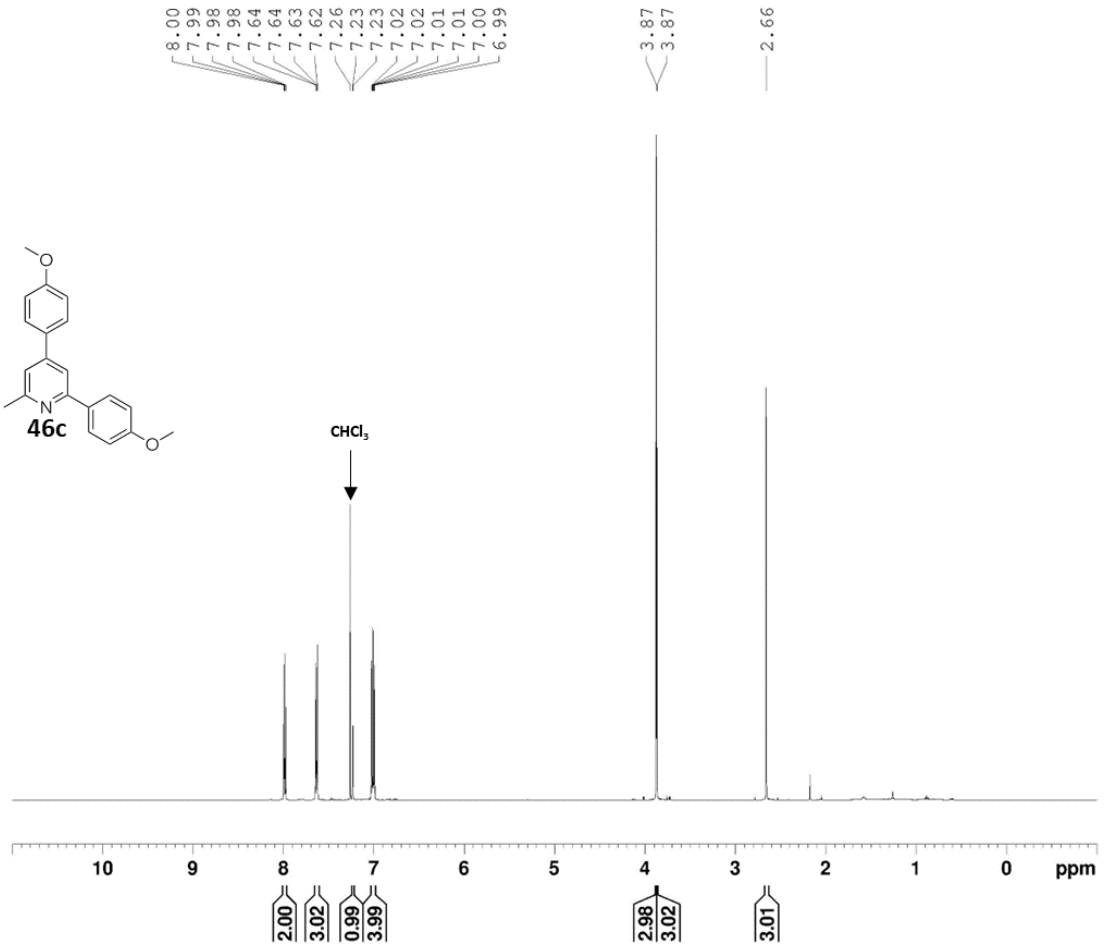
F2 - Processing parameters
SI                 65536
SF            500.2300121 MHz
WDW                   EM
SSB                    0
LB                  0.30 Hz
GB                     0
PC                  1.00
```




```
Current Data Parameters
NAME        NL-1-172-13C
EXPNO                 10
PROCNO                 1

F2 - Acquisition Parameters
Date_           20220216
Time              11.07 h
INSTRUM             spect
PROBHD   Z125869_0055 (
PULPROG          zgpg30
TD                65536
SOLVENT           CDCl3
NS                   64
DS                    4
SWH           29761.904 Hz
FIDRES         0.908261 Hz
AQ            1.1010048 sec
RG               190.44
DW               16.800 usec
DE               18.00 usec
TE               298.0 K
D1           2.00000000 sec
D11          0.03000000 sec
TD0                   1
SFO1        125.7955118 MHz
NUC1                13C
P0                3.33 usec
P1               10.00 usec
PLW1        56.90299988 W
SFO2        500.2320009 MHz
NUC2                1H
CPDPRG[2        waltz16
PCPD2            80.00 usec
PLW2        11.44699955 W
PLW12        0.25756001 W
PLW13        0.12955000 W

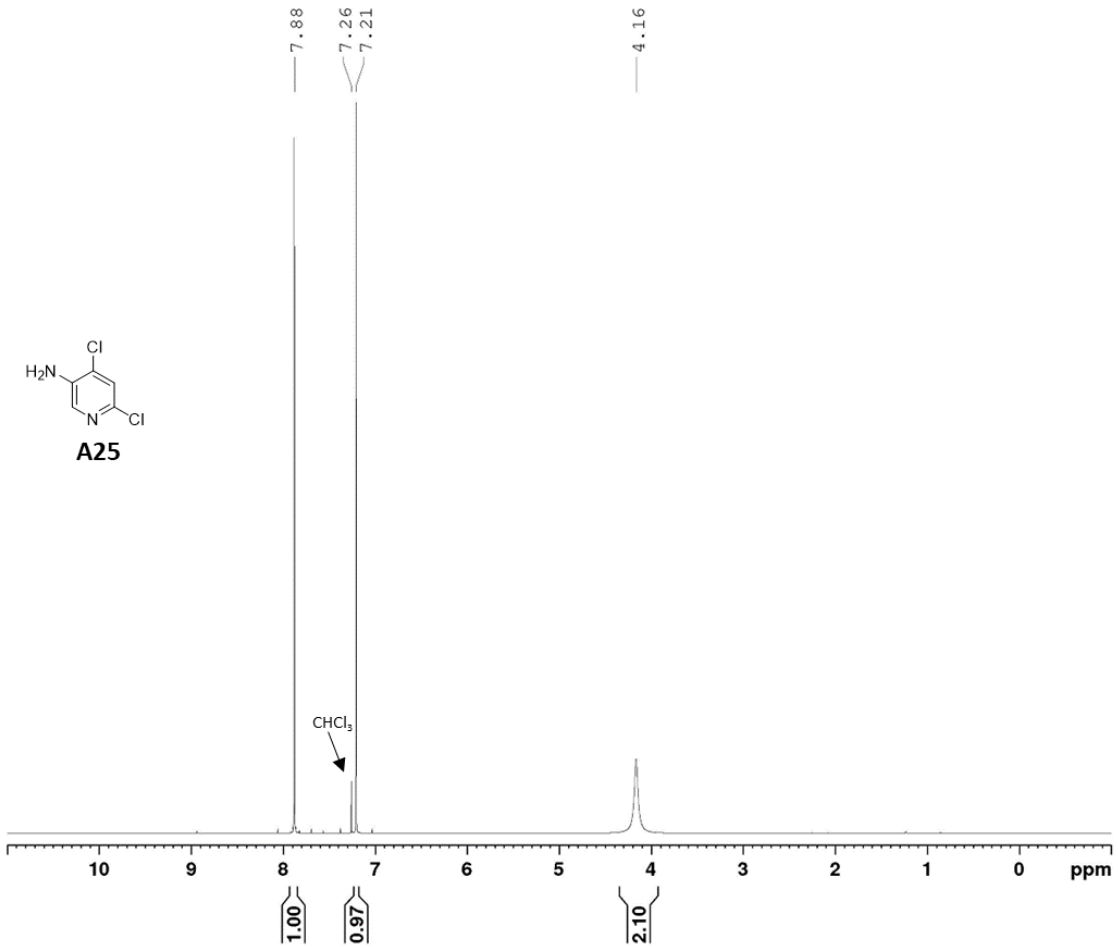
F2 - Processing parameters
SI                32768
SF          125.7829166 MHz
WDW                  EM
SSB                   0
LB                 1.00 Hz
GB                    0
PC                 1.40
```




```
Current Data Parameters
NAME          NL-1-133-2
EXPNO                 11
PROCNO                 1

F2 - Acquisition Parameters
Date_           20220215
Time              21.56 h
INSTRUM            spect
PROBHD   Z125869_0055 (
PULPROG            zg30
TD                65536
SOLVENT           CDCl3
NS                   64
DS                    2
SWH           10000.000 Hz
FIDRES        0.305176 Hz
AQ            3.2767999 sec
RG               151.18
DW               50.000 usec
DE               16.00 usec
TE               298.0 K
D1           2.00000000 sec
TD0                   1
SFO1        500.2330889 MHz
NUC1                 1H
P0                4.00 usec
P1               12.00 usec
PLW1        11.44699955 W

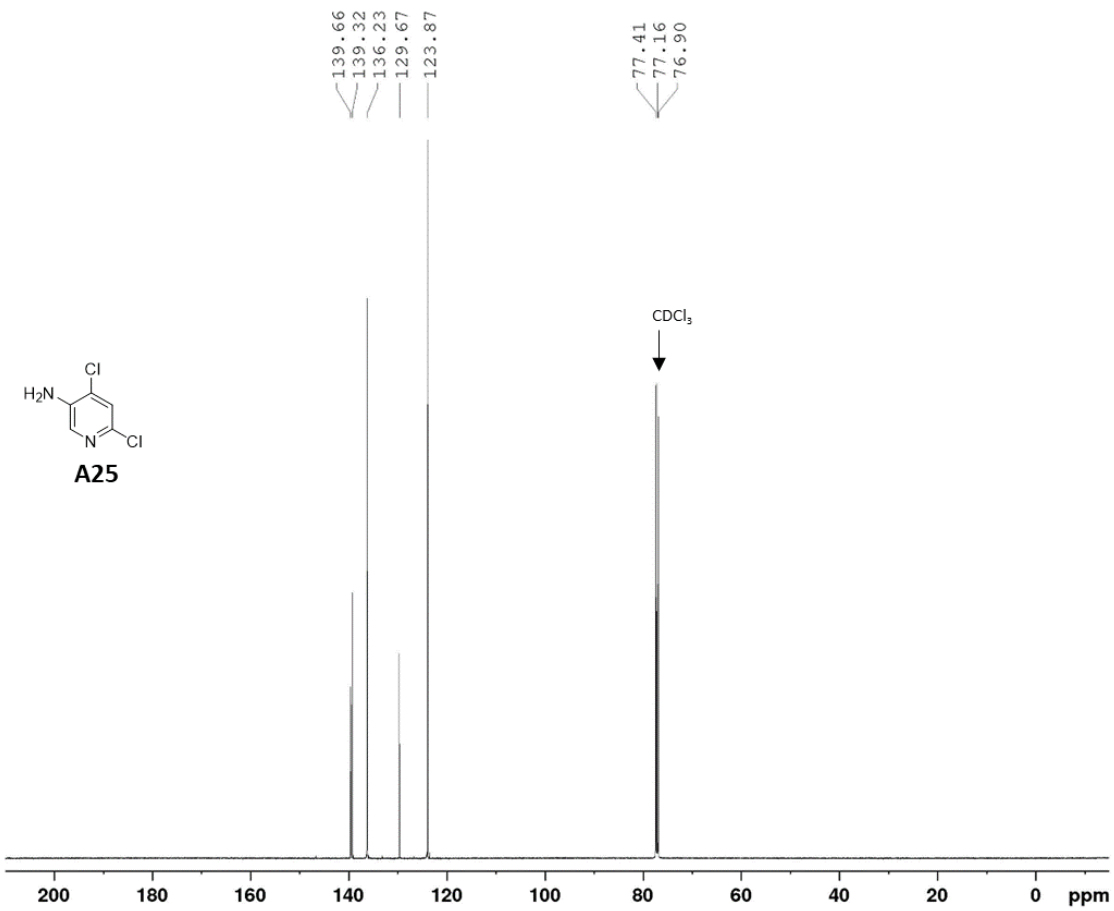
F2 - Processing parameters
SI                65536
SF          500.2300121 MHz
WDW                  EM
SSB                   0
LB                 0.30 Hz
GB                    0
PC                 1.00
```




```
Current Data Parameters
NAME      JPN-2-54_(5-amino-2,4-DCP)
EXPNO                 10
PROCNO                 1

F2 - Acquisition Parameters
Date_           20211127
Time              18.56 h
INSTRUM             spect
PROBHD   Z125869_0055 (
PULPROG             zg30
TD                 65536
SOLVENT            CDCl3
NS                    64
DS                     2
SWH           10000.000 Hz
FIDRES            0.305176 Hz
AQ             3.2767999 sec
RG                  47.3
DW                50.000 usec
DE                16.00 usec
TE                298.0 K
D1            2.00000000 sec
TD0                    1
SFO1         500.2330889 MHz
NUC1                  1H
P0                 4.00 usec
P1                12.00 usec
PLW1         11.44699955 W

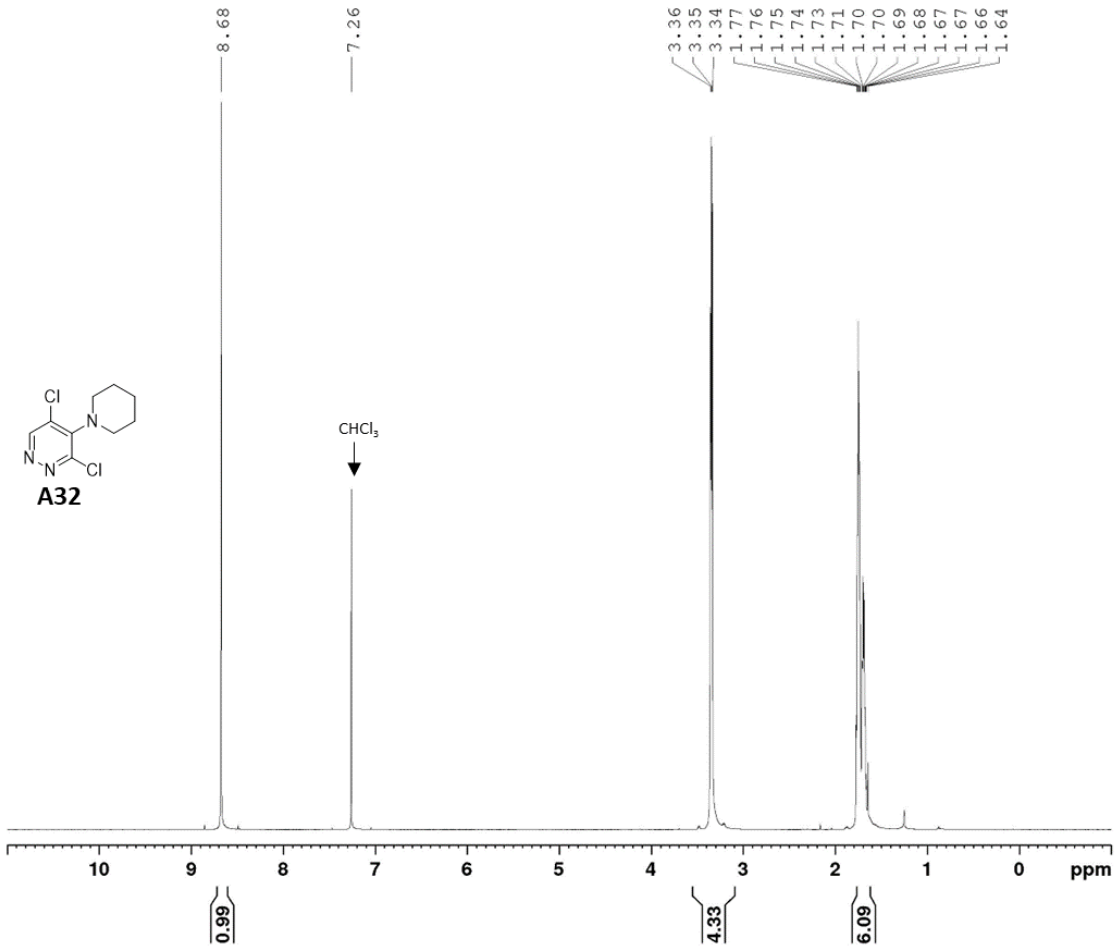
F2 - Processing parameters
SI                 65536
SF           500.2300120 MHz
WDW                   EM
SSB       0
LB                0.30 Hz
GB        0
PC                1.00
```




```
Current Data Parameters
NAME      JPN-2-54_(5-amino-2,4-DCP)
EXPNO                 11
PROCNO                 1

F2 - Acquisition Parameters
Date_           20211127
Time              19.52 h
INSTRUM           spect
PROBHD   Z125869_0055 (
PULPROG          zgpg30
TD                65536
SOLVENT           CDCl3
NS                 1024
DS                    4
SWH           29761.904 Hz
FIDRES         0.908261 Hz
AQ             1.1010048 sec
RG               190.44
DW                16.800 usec
DE                18.00 usec
TE                298.0 K
D1            2.00000000 sec
D11           0.03000000 sec
TD0                   1
SFO1         125.7955118 MHz
NUC1                13C
P0                 3.33 usec
P1                10.00 usec
PLW1         56.90299988 W
SFO2         500.2320009 MHz
NUC2                1H
CPDPRG[2         waltz16
PCPD2             80.00 usec
PLW2         11.44699955 W
PLW12         0.25756001 W
PLW13         0.12955000 W

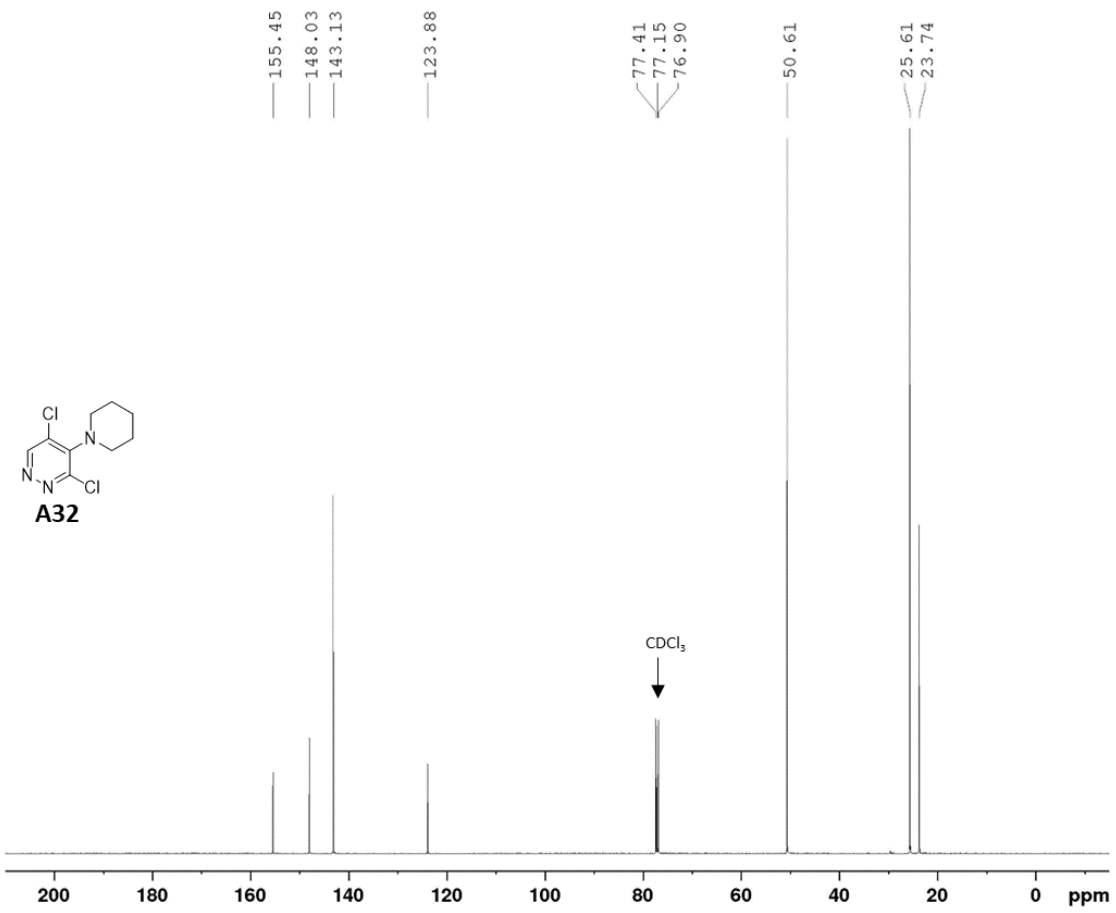
F2 - Processing parameters
SI                32768
SF           125.7829244 MHz
WDW                  EM
SSB      0
LB                1.00 Hz
GB       0
PC                1.40
```




```
Current Data Parameters
NAME      JPN-2-14-1_C4-subst%2E
EXPNO                 10
PROCNO                 1

F2 - Acquisition Parameters
Date_           20200914
Time                3.42 h
INSTRUM            spect
PROBHD    Z125869_0055 (
PULPROG             zg30
TD                 65536
SOLVENT            CDCl3
NS                    64
DS                     2
SWH            10000.000 Hz
FIDRES             0.305176 Hz
AQ              3.2767999 sec
RG                 122.05
DW                 50.000 usec
DE                 16.00 usec
TE                 300.0 K
D1             2.00000000 sec
TD0                    1
SFO1          500.2330889 MHz
NUC1                  1H
P0                 4.00 usec
P1                12.00 usec
PLW1          11.44699955 W

F2 - Processing parameters
SI                 65536
SF            500.2300122 MHz
WDW                   EM
SSB       0
LB                 0.30 Hz
GB        0
PC                 1.00
```

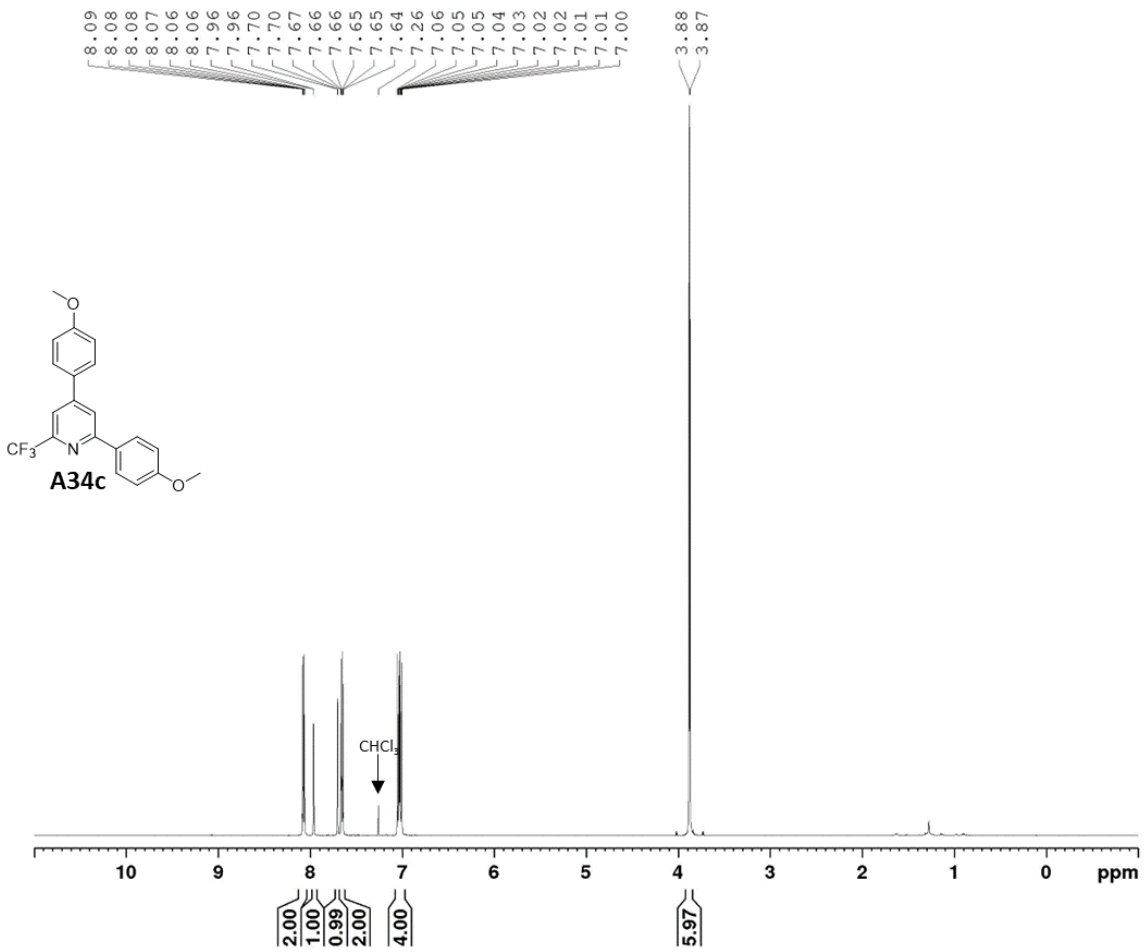


A32

```
Current Data Parameters
NAME      JPN-2-14-1_(C4-subst.)
EXPNO                 10
PROCNO                 1

F2 - Acquisition Parameters
Date_           20211127
Time              20.52 h
INSTRUM           spect
PROBHD    Z125869_0055 (
PULPROG          zgpg30
TD                65536
SOLVENT           CDCl3
NS                 1024
DS                    4
SWH           29761.904 Hz
FIDRES         0.908261 Hz
AQ            1.1010048 sec
RG               190.44
DW               16.800 usec
DE               18.00 usec
TE               298.0 K
D1            2.00000000 sec
D11           0.03000000 sec
TD0                   1
SFO1         125.7955118 MHz
NUC1                 13C
P0                3.33 usec
P1               10.00 usec
PLW1         56.90299988 W
SFO2         500.2320009 MHz
NUC2                 1H
CPDPRG[2         waltz16
PCPD2             80.00 usec
PLW2         11.44699955 W
PLW12         0.25756001 W
PLW13         0.12955000 W

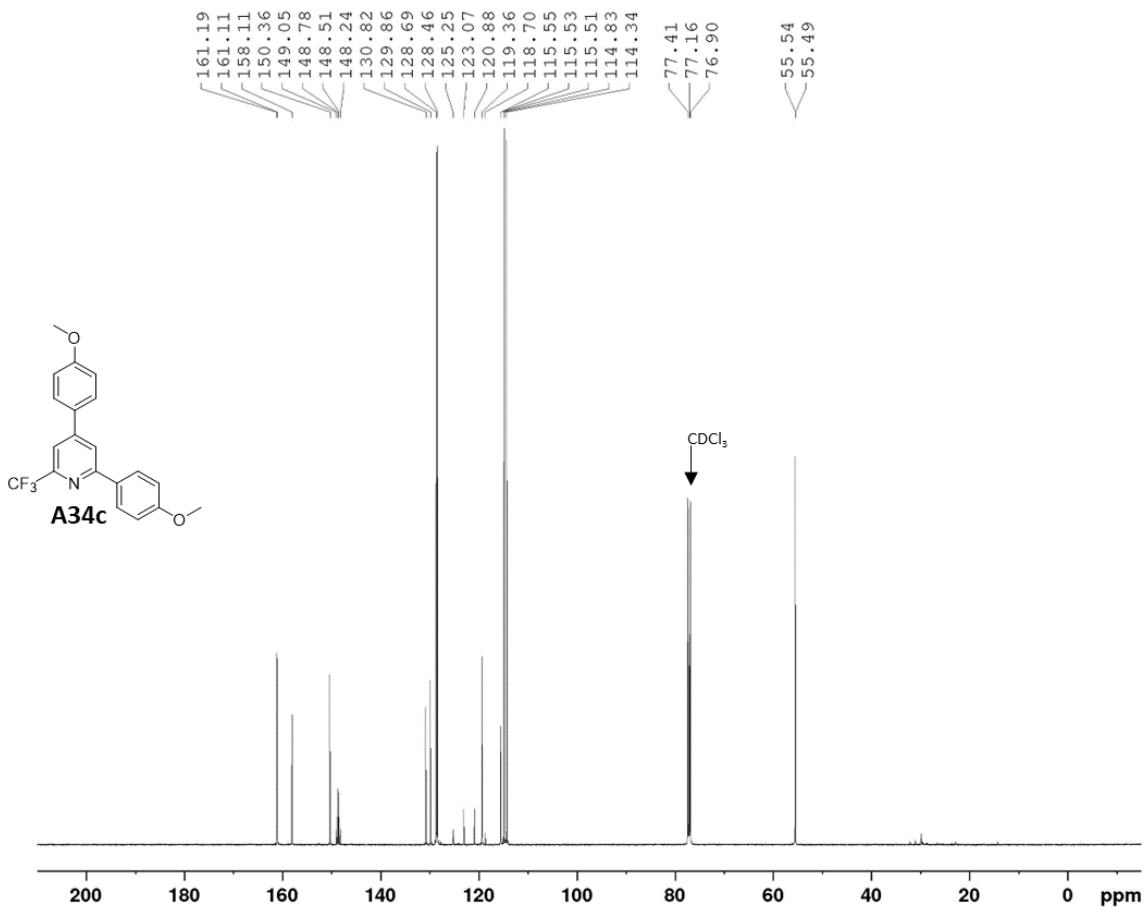
F2 - Processing parameters
SI                32768
SF           125.7829371 MHz
WDW                  EM
SSB       0
LB                1.00 Hz
GB        0
PC                1.40
```




```
Current Data Parameters
NAME      JPN-1-187-2_20-Nov-2021
EXPNO                 20
PROCNO                 1

F2 - Acquisition Parameters
Date_           20211121
Time              1.37 h
INSTRUM           spect
PROBHD   Z125869_0055 (
PULPROG           zg30
TD               65536
SOLVENT          CDCl3
NS                  64
DS                   2
SWH          10000.000 Hz
FIDRES           0.305176 Hz
AQ             3.2767999 sec
RG                30.54
DW               50.000 usec
DE               16.00 usec
TE               298.0 K
D1            2.00000000 sec
TD0                  1
SFO1         500.2330889 MHz
NUC1                 1H
P0                4.00 usec
P1               12.00 usec
PLW1         11.44699955 W

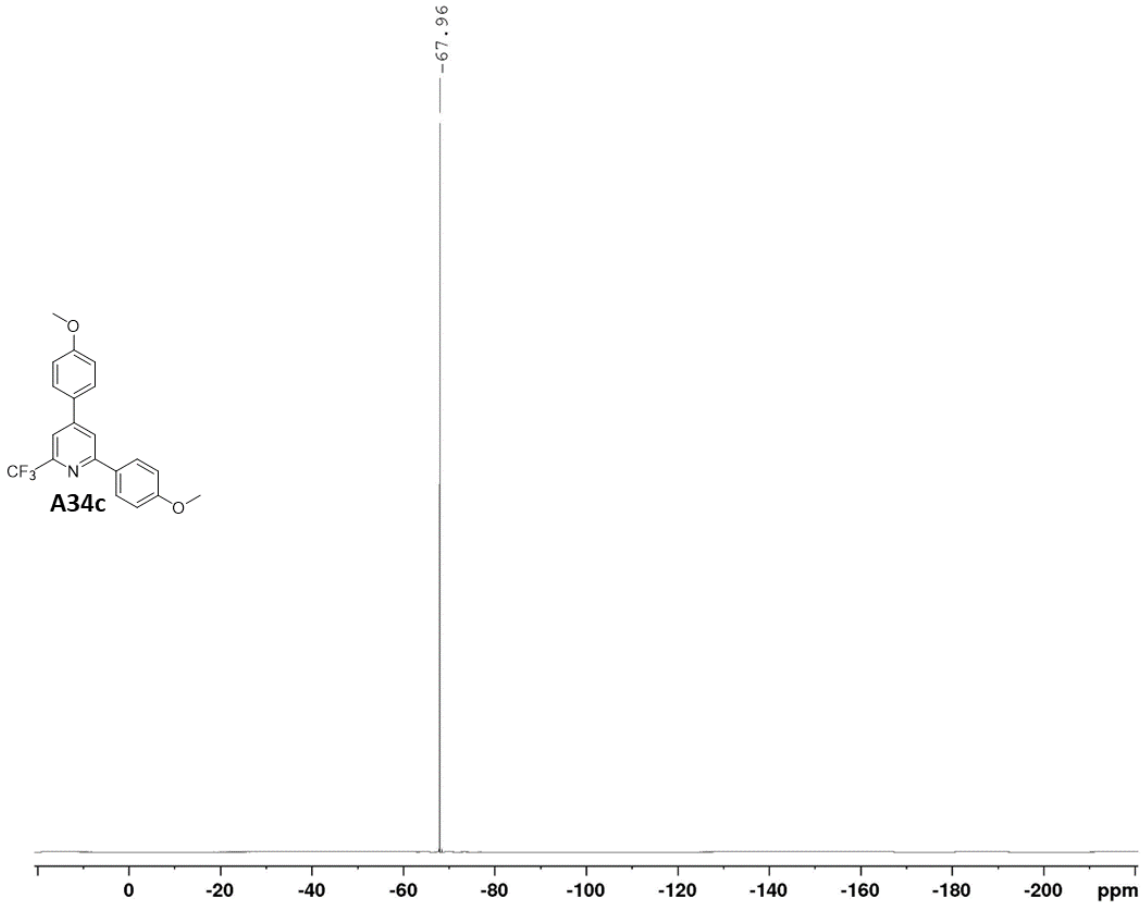
F2 - Processing parameters
SI               65536
SF           500.2300119 MHz
WDW                  EM
SSB       0
LB              0.30 Hz
GB        0
PC                1.00
```




```
Current Data Parameters
NAME      JPN-1-187-2_DA
EXPNO                 10
PROCNO                 1

F2 - Acquisition Parameters
Date_           20200812
Time               3.15 h
INSTRUM             spect
PROBHD   Z125869_0055 (
PULPROG           zgpg30
TD                 65536
SOLVENT            CDCl3
NS                  1024
DS                     4
SWH            29761.904 Hz
FIDRES          0.908261 Hz
AQ             1.1010048 sec
RG                190.44
DW                16.800 usec
DE                18.00 usec
TE                300.0 K
D1            2.00000000 sec
D11           0.03000000 sec
TD0                    1
SFO1         125.7955118 MHz
NUC1                 13C
P0                 3.33 usec
P1                10.00 usec
PLW1         56.90299988 W
SFO2         500.2320009 MHz
NUC2                 1H
CPDPRG[2          waltz16
PCPD2             80.00 usec
PLW2         11.44699955 W
PLW12         0.25756001 W
PLW13         0.12955000 W

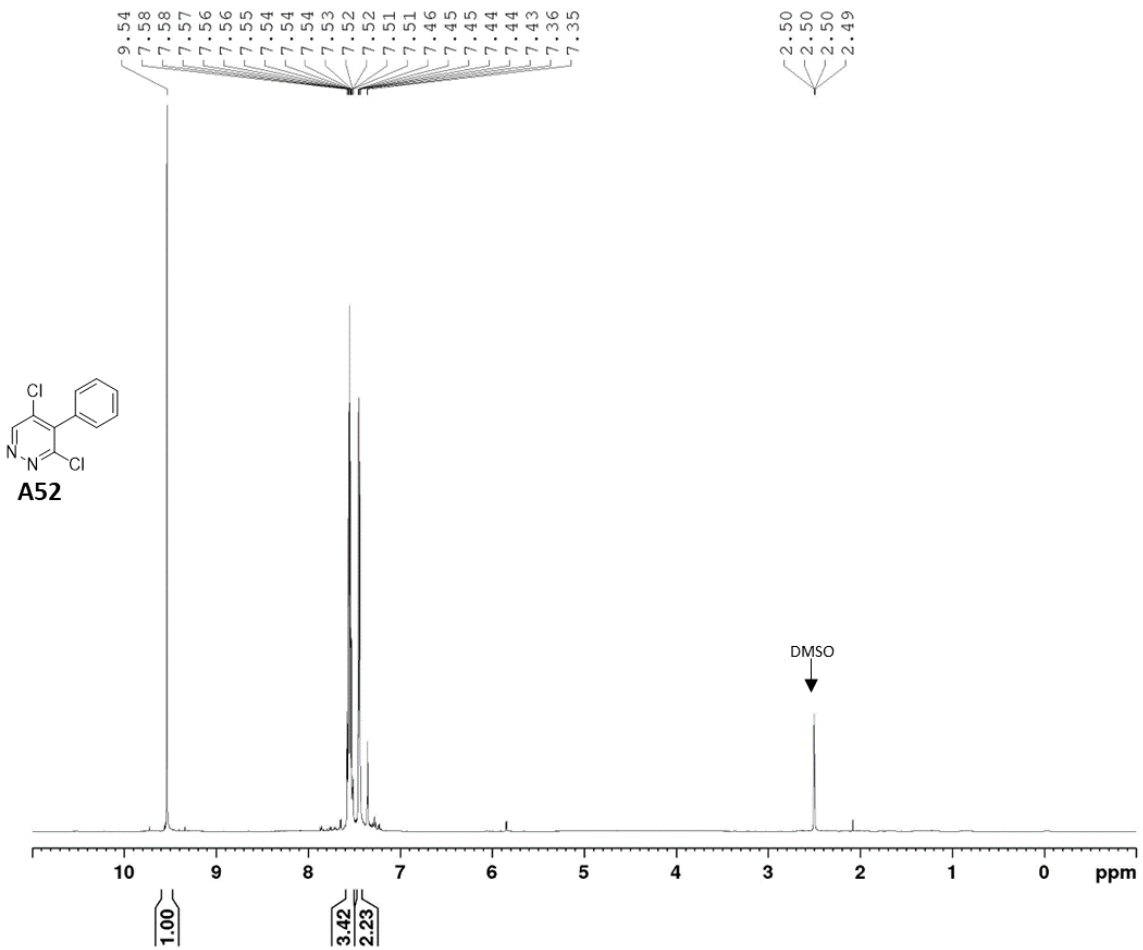
F2 - Processing parameters
SI                 32768
SF           125.7829205 MHz
WDW                   EM
SSB       0
LB                 1.00 Hz
GB        0
PC                 1.40
```




```
Current Data Parameters
NAME         JPN-1-187-2
EXPNO                 18
PROCNO                 1

F2 - Acquisition Parameters
Date_           20211120
Time                3.44 h
INSTRUM            spect
PROBHD   Z125869_0055 (
PULPROG           zgflqn
TD                131072
SOLVENT            CDCl3
NS                    16
DS                     4
SWH          113636.367 Hz
FIDRES         1.733953 Hz
AQ           0.5767168 sec
RG                 15.61
DW                 4.400 usec
DE                18.00 usec
TE                298.0 K
D1           1.00000000 sec
TD0                    1
SFO1         470.6394024 MHz
NUC1                 19F
P1                 15.00 usec
PLW1         11.70800018 W

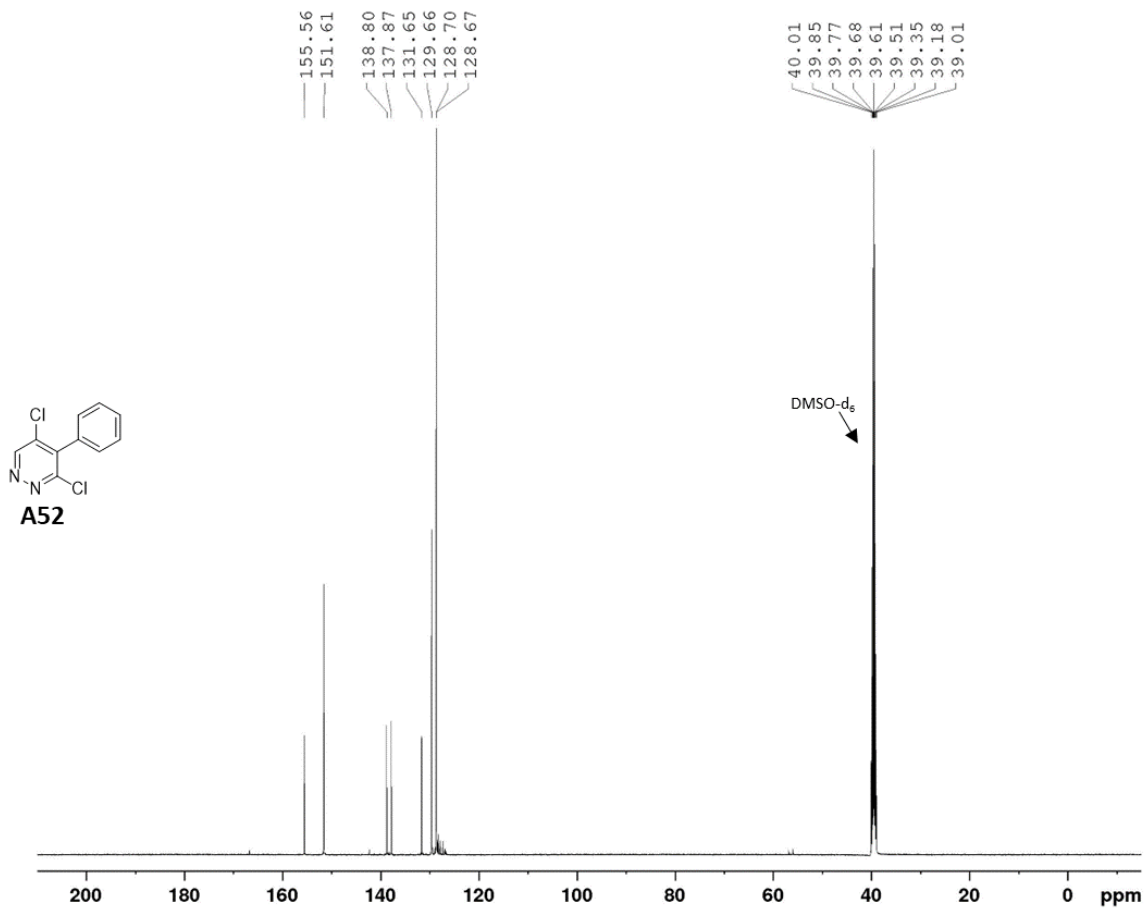
F2 - Processing parameters
SI                 65536
SF           470.6864712 MHz
WDW                   EM
SSB       0
LB                 0.30 Hz
GB        0
PC                 1.00
```




```
Current Data Parameters
NAME      JPN-2-22-2_dried
EXPNO                  10
PROCNO                  1

F2 - Acquisition Parameters
Date_           20201010
Time               10.30 h
INSTRUM             spect
PROBHD   Z125869_0055 (
PULPROG              zg30
TD                  65536
SOLVENT              DMSO
NS                     64
DS                      2
SWH            10000.000 Hz
FIDRES          0.305176 Hz
AQ             3.2767999 sec
RG                 69.97
DW                50.000 usec
DE                16.00 usec
TE                300.0 K
D1            2.00000000 sec
TD0                     1
SFO1         500.2330889 MHz
NUC1                   1H
P0                  4.00 usec
P1                 12.00 usec
PLW1         11.44699955 W

F2 - Processing parameters
SI                  65536
SF           500.2300035 MHz
WDW                    EM
SSB       0
LB                  0.30 Hz
GB        0
PC                  1.00
```

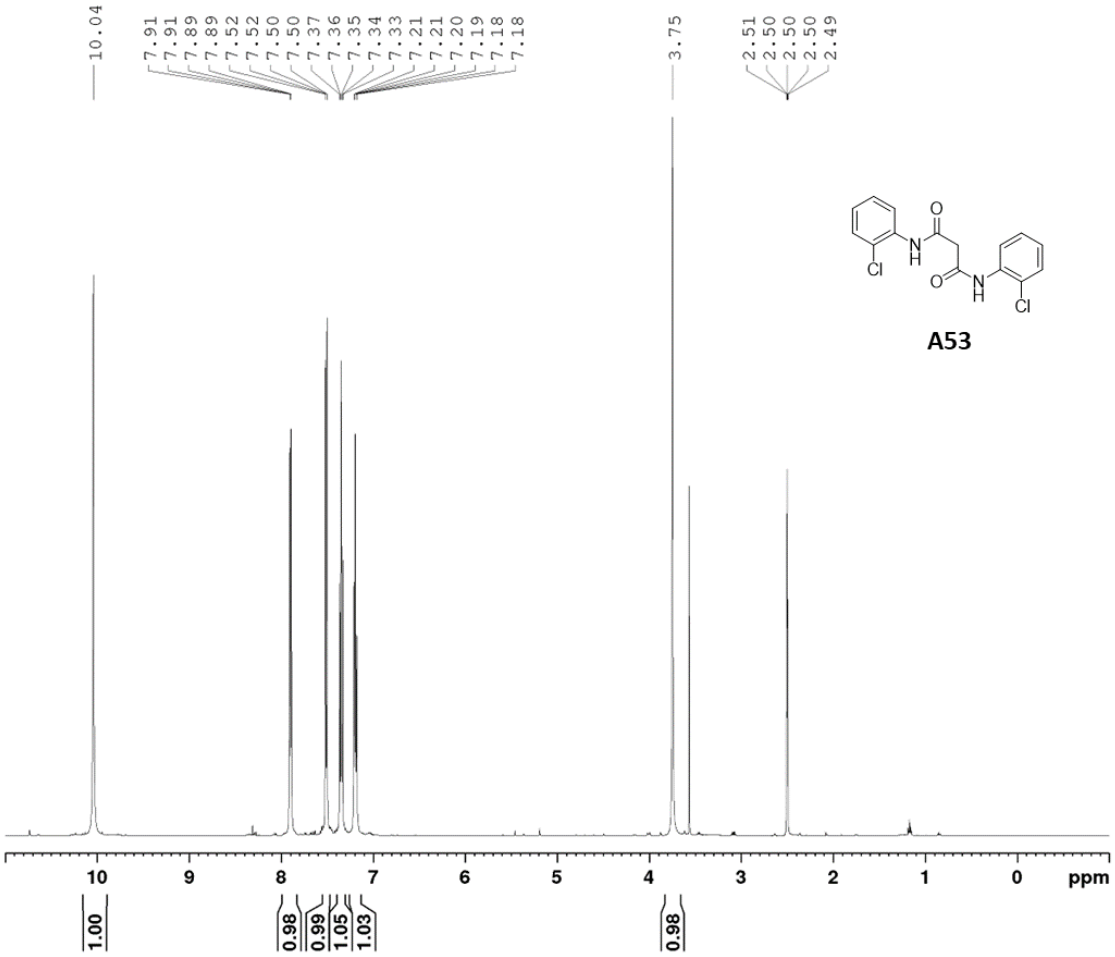


A52

```
Current Data Parameters
NAME      JPN-2-22-2_dried
EXPNO                  11
PROCNO                  1

F2 - Acquisition Parameters
Date_           20201010
Time               12.37 h
INSTRUM             spect
PROBHD   Z125869_0055 (
PULPROG           zgpg30
TD                 65536
SOLVENT              DMSO
NS                    1024
DS                       4
SWH            29761.904 Hz
FIDRES          0.908261 Hz
AQ             1.1010048 sec
RG                190.44
DW                16.800 usec
DE                18.00 usec
TE                300.0 K
D1           2.00000000 sec
D11          0.03000000 sec
TD0                    1
SFO1         125.7955118 MHz
NUC1                13C
P0                 3.33 usec
P1                10.00 usec
PLW1         56.90299988 W
SFO2         500.2320009 MHz
NUC2                1H
CPDPRG[2         waltz16
PCPD2             80.00 usec
PLW2         11.44699955 W
PLW12         0.25756001 W
PLW13         0.12955000 W

F2 - Processing parameters
SI                 32768
SF           125.7829976 MHz
WDW                   EM
SSB       0
LB                 1.00 Hz
GB        0
PC                 1.40
```

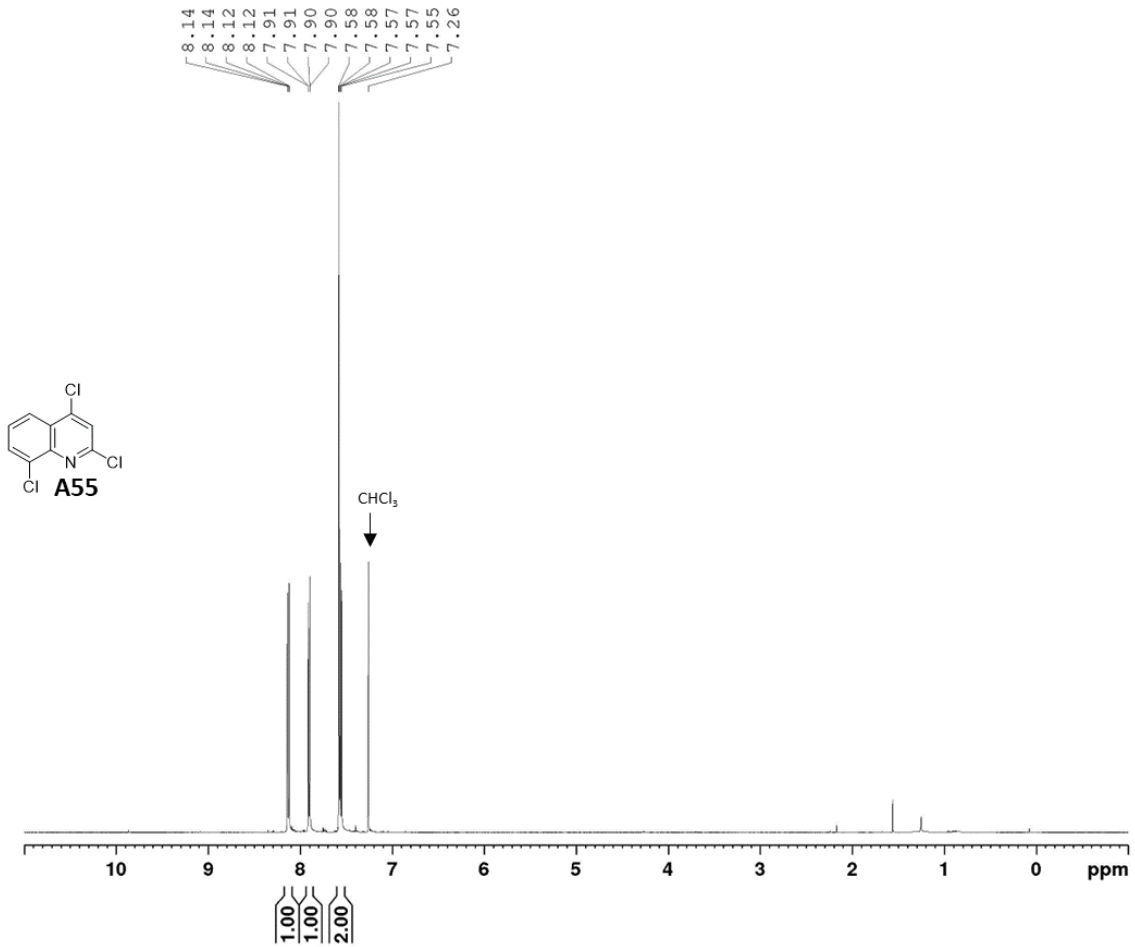


A53

```
Current Data Parameters
NAME      JPN-2-143_DMSO-D6
EXPNO                   10
PROCNO                   1

F2 - Acquisition Parameters
Date_              20220211
Time                 14.25 h
INSTRUM              spect
PROBHD    Z125869_0055 (
PULPROG              zg30
TD                  65536
SOLVENT              DMSO
NS                     32
DS                      2
SWH            10000.000 Hz
FIDRES             0.305176 Hz
AQ               3.2767999 sec
RG                   86.13
DW                   50.000 usec
DE                   16.00 usec
TE                   298.0 K
D1             2.00000000 sec
TD0                     1
SFO1          500.2330889 MHz
NUC1                   1H
P0                   4.00 usec
P1                  12.00 usec
PLW1          11.44699955 W

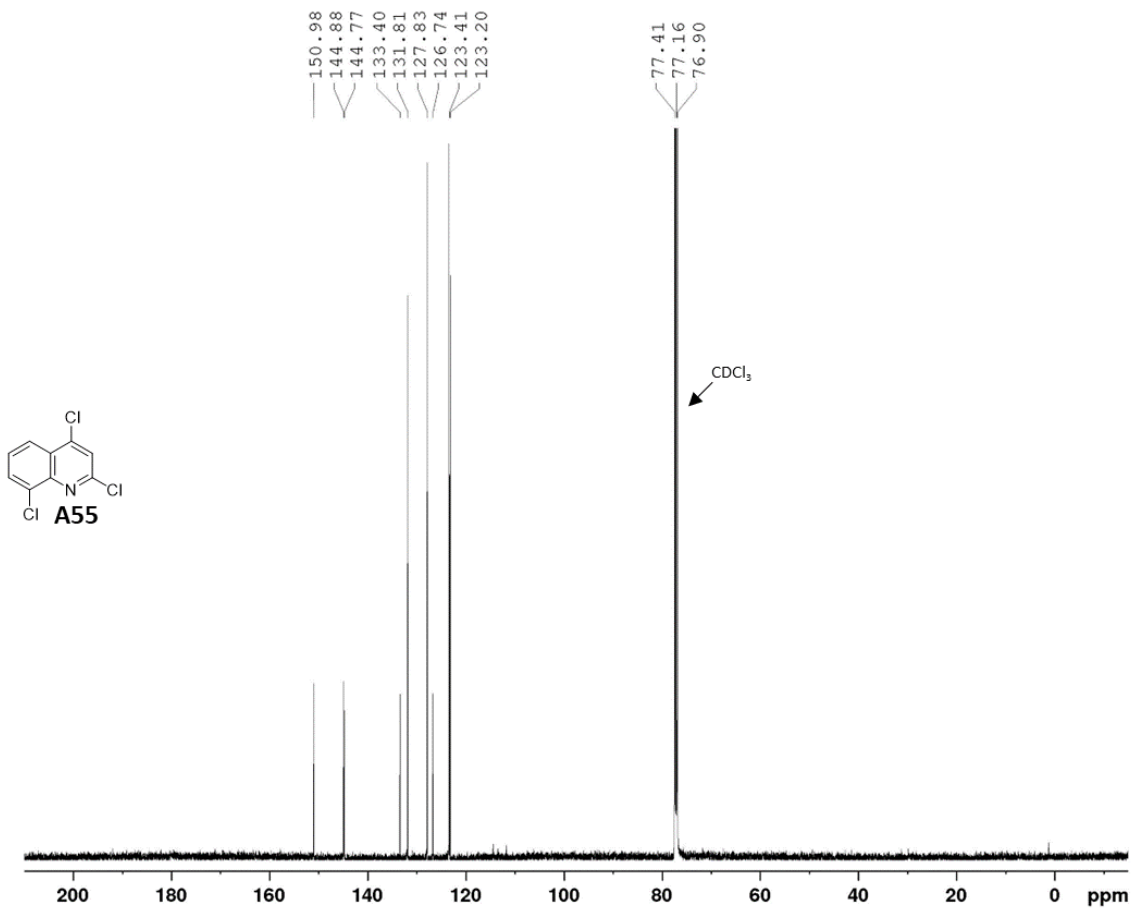
F2 - Processing parameters
SI                  65536
SF            500.2300032 MHz
WDW                    EM
SSB       0
LB                   0.30 Hz
GB        0
PC                   1.00
```




```
Current Data Parameters
NAME          JPN-2-42-3
EXPNO                 10
PROCNO                 1

F2 - Acquisition Parameters
Date_           20210209
Time               10.24 h
INSTRUM            spect
PROBHD   Z125869_0055 (
PULPROG             zg30
TD                 65536
SOLVENT            CDCl3
NS                    64
DS                     2
SWH            10000.000 Hz
FIDRES             0.305176 Hz
AQ              3.2767999 sec
RG                151.18
DW                50.000 usec
DE                16.00 usec
TE                300.0 K
D1             2.00000000 sec
TD0                    1
SFO1         500.2330889 MHz
NUC1                  1H
P0                 4.00 usec
P1                12.00 usec
PLW1         11.44699955 W

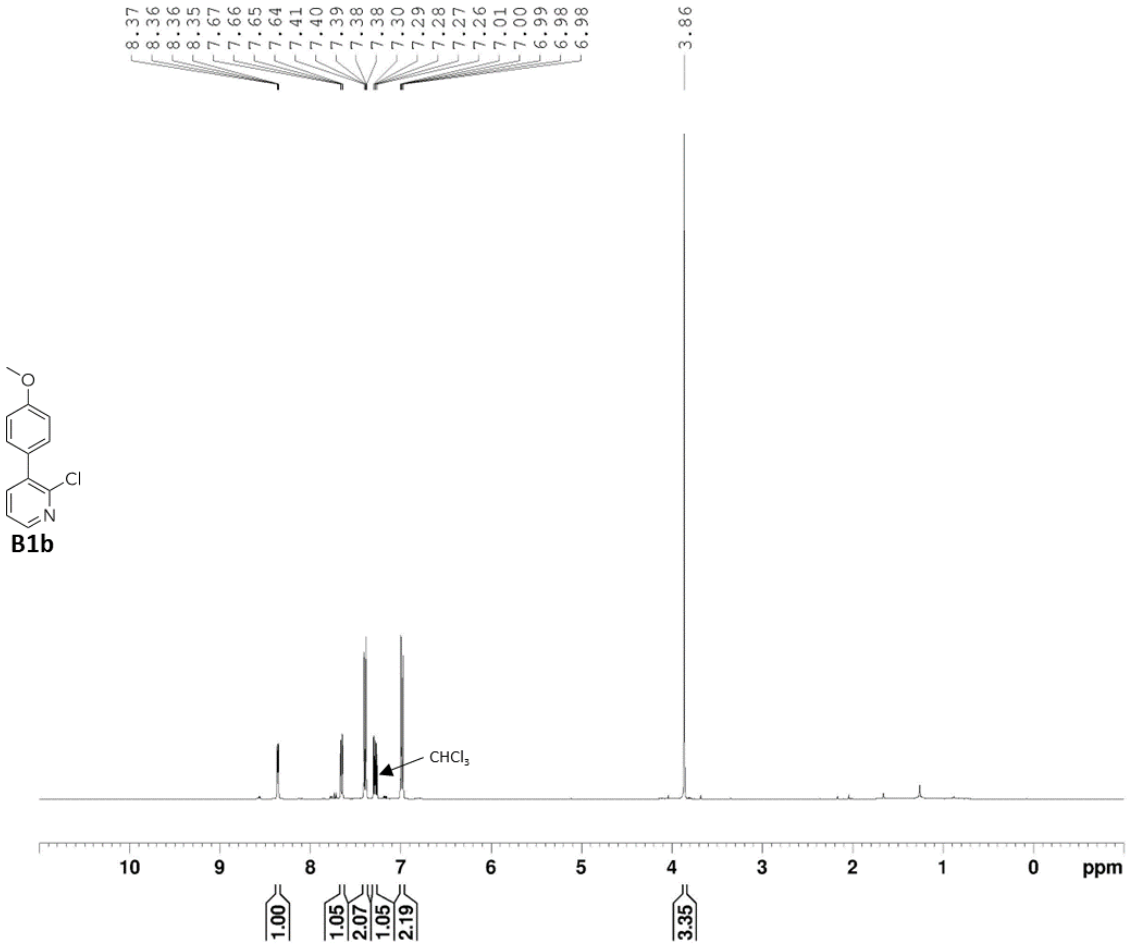
F2 - Processing parameters
SI                 65536
SF           500.2300121 MHz
WDW                   EM
SSB       0
LB                 0.30 Hz
GB        0
PC                 1.00
```




```
Current Data Parameters
NAME      JPN-2-42-3_(2)
EXPNO                11
PROCNO                1

F2 - Acquisition Parameters
Date_          20211128
Time              21.42 h
INSTRUM           spect
PROBHD   Z125869_0055 (
PULPROG          zgpg30
TD                65536
SOLVENT           CDCl3
NS                 1024
DS                    4
SWH           29761.904 Hz
FIDRES         0.908261 Hz
AQ            1.1010048 sec
RG               190.44
DW               16.800 usec
DE               18.00 usec
TE               298.0 K
D1           2.00000000 sec
D11          0.03000000 sec
TD0                   1
SFO1        125.7955118 MHz
NUC1               13C
P0                3.33 usec
P1               10.00 usec
PLW1        56.90299988 W
SFO2        500.2320009 MHz
NUC2               1H
CPDPRG[2        waltz16
PCPD2             80.00 usec
PLW2        11.44699955 W
PLW12        0.25756001 W
PLW13        0.12955000 W

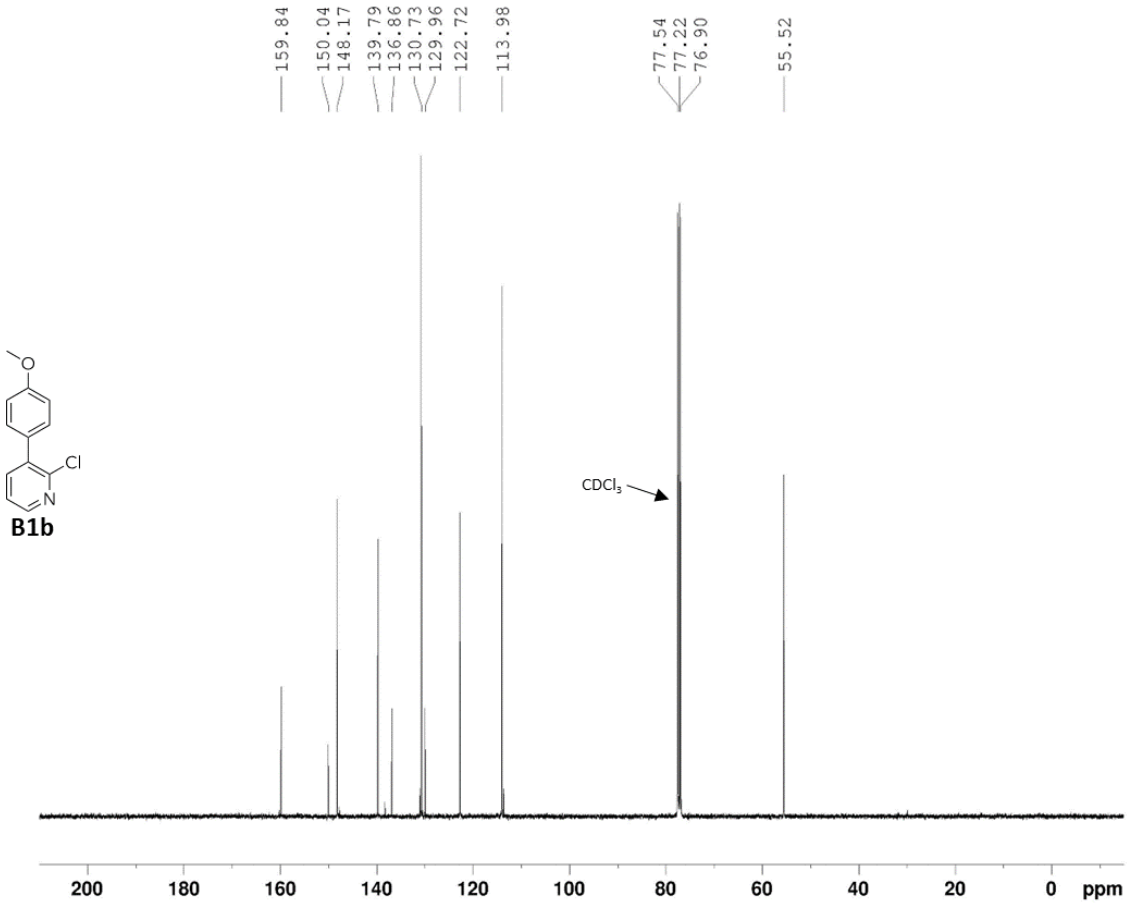
F2 - Processing parameters
SI                32768
SF          125.7829163 MHz
WDW                EM
SSB       0
LB                1.00 Hz
GB        0
PC                1.40
```




```
Current Data Parameters
NAME       NL-2-2-f12-14
EXPNO                 13
PROCNO                 1

F2 - Acquisition Parameters
Date_           20220331
Time              17.57 h
INSTRUM       Avance Neo
PROBHD   Z152088_0031 (
PULPROG             zg30
TD                 65536
SOLVENT            CDCl3
NS                    16
DS                     2
SWH             8196.722 Hz
FIDRES          0.250144 Hz
AQ              3.9976959 sec
RG                   101
DW                61.000 usec
DE                13.89 usec
TE                298.0 K
D1           1.00000000 sec
TD0                    1
SFO1         400.1324708 MHz
NUC1                  1H
P0                 2.67 usec
P1                 8.00 usec
PLW1         24.03499985 W

F2 - Processing parameters
SI                 65536
SF           400.1300096 MHz
WDW                   EM
SSB                    0
LB                  0.30 Hz
GB                     0
PC                  1.00
```



B1b

```
Current Data Parameters
NAME       NL-2-2-f12-14
EXPNO                 14
PROCNO                 1

F2 - Acquisition Parameters
Date_           20220331
Time              19.17 h
INSTRUM       Avance Neo
PROBHD   Z152088_0031 (
PULPROG           zgpg30
TD                65536
SOLVENT           CDCl3
NS                 1024
DS                    4
SWH           23809.523 Hz
FIDRES         0.726609 Hz
AQ            1.3762560 sec
RG                8.125
DW               21.000 usec
DE                6.50 usec
TE               298.0 K
D1            2.00000000 sec
D11           0.03000000 sec
TD0                   1
SFO1         100.6228298 MHz
NUC1                 13C
P0                2.67 usec
P1                8.00 usec
PLW1         86.55400085 W
SFO2         400.1316005 MHz
NUC2                 1H
CPDPRG[2         waltz65
PCPD2             90.00 usec
PLW2         24.03499985 W
PLW12         0.18990999 W
PLW13         0.09552100 W

F2 - Processing parameters
SI                32768
SF           100.6127503 MHz
WDW                  EM
SSB                   0
LB                 1.00 Hz
GB                    0
PC                 1.40
```

REFERENCES CITED

Chapter One

1. Tamura, M.; Kochi, J. K. Vinylation of Grignard Reagents. Catalysis by Iron. *J. Am. Chem. Soc.* **1971**, *93*, 1487−1489.

2. Vavon and Mottez, *Bull. Soc. Chim.,* **1994**, *5*, 11, 196.

3. Kharasch, M. S.; Reinmuth, O. *Grignard Reactions of Nonmetallic Substances*; Constable: London, 1954.

4. Gomberg, M.; Bachmann, W. E. *J. Am. Chem. Soc.* **1924**, *46*, 10, 2339–2343.

5. (a) Wolf, W.; Kharasch, N. *J. Org. Chem.* **1965**, *30*, 8, 2493—2498 (b) Bunnett, J. F.; Wamser, C. C. *J. Am. Chem. Soc.* **1966**, *88*, 23, 5534-5537.

6. Taylor, E. C.; Kienzle, F.; McKillop, A. *J. Am. Chem. Soc.* **1970**, *92*, 20, 6088—6089.

7. Dieck, H. A.; Heck, R. F. *J. Am. Chem. Soc.* **1974**, *96*, 4, 1133—1136.

8. Tamao, K.; Minato, A.; Miyake, N.; Matsuda, T.; Kiso, Y.; Kumada, M. *Chem. Lett.* **1975**, *4*, 133– 136.

9. Sonogashira, K.; Tohda, Y.; Hagihara, N. *Tetrahedron Lett.* **1975**, *16*, 4467–4470.

10. Murahashi, S.; Yamamura, M.; Yanagisawa, K.; Mita, N.; Kondo, K. *J. Org. Chem.* **1979**, *44*, 2408—2417.

11. (a) Kosugi, M.; Sasazawa, K.; Shikizu, Y.; Migita, T. *Chem. Lett*., **1977**, *6*, 301–302. (b) Kosugi, M.; Shimizu, Y.; Migita, T. *J. Organomet. Chem.*, **1977**, *129*, C36-C38. (c) Milstein, D.; Stille, J. K. *J. Am. Chem. Soc.*, **1978**, *100*, 3636–3638.

12. King, A. O.; Okukado, N.; Negishi, E. *J. Chem. Soc.*, *Chem. Commun.* **1977**, 683– 684.

13. Miyaura, N.; Yanagi, T.; Suzuki, A. *Synth. Commun.* **1981**, *11*, 513—519.

14. Not all Pd-catalyzed C—C bond-forming reactions require an organometallic nucleophile. For instance, the Mizoroki-Heck reaction enables cross-coupling of alkenes with aryl halide electrophiles and does not involve a transmetalation step.

15. For Nobel Lecture, see: E. Negishi, *Angew. Chem.* **2011**, *123*, 6870–6897; *Angew. Chem. Int. Ed.* **2011**, *50*, 6738–6764.

16. A. Suzuki, *Angew. Chem.* **2011**, *123*, 6854–6869; *Angew. Chem. Int. Ed*. **2011**, *50*, 6722–6737.

17. Roughley, S. D.; Jordan, A. M. *J. Med. Chem.* **2011**, *54*, 3451– 3479.

18. Lovering, F.; Bikker, J.; Humblet, C. *J. Med. Chem.* **2009**, *52*, 6752– 6756.

19. Campeau, J.-L.; Hazari, N. *Organometallics* **2019**, *38*, 3– 35.

20. (a) Farina, V.; Krishnamurthy, V.; Scott, W. *J. Org. React.* **1997**, *50*, 1-652. (b) Mitchell, T. N. In *Metal-catalyzed Cross-coupling Reactions*; Diederich, F., Stang, P. J., Eds.; Wiley-VCH: New York, 1998; Chapter 4. (c) Gribble, G. W. *Palladium in Heterocyclic Chemistry*; Pergamon: New York, 2000.

21. (a) van Leeuwen, P. W. N. M. *Appl. Catal., A* **2001**, *212*, 61−81. (b) Widegren, J. A.; Finke, R. G. J. *Mol. Catal. A* **2003**, *198*, 317−341. (c) de Vries, J. G. When Does Catalysis with Transition Metal Complexes Turn into Catalysis by Nanoparticles? In *Selective Nanocatalysts and Nanoscience*; Zecchina, A., Bordiga, S., Groppo, E., Eds.; Wiley-VCH, 2011; pp 73−103.

22. Beller, M.; Fischer, H.; Herrmann, W. A.; Öfele, K.; Brossmer, C. *Angew. Chem., Int. Ed.* **1995**, *34*, 1848– 1849.

23. Nicholas, P. P. *J. Org. Chem.* **1987**, *52* (23), 5266– 5272.

24. F. Paul, J. Pratt, J. F. Hartwig, *J. Am. Chem. Soc*. **1994**, *116*, 5969 – 5970. (b) J. F. Hartwig, F. Paul, *J. Am. Chem. Soc.* **1995**, *117*, 5373 – 5374. (c) J. F. Hartwig, *Angew. Chem.* **1998**, *110*, 2154 –2177; *Angew. Chem. Int. Ed.* **1998**, *37*, 2046 – 2067.

25. (a) Nishiyama, M.; Yamamoto, T.; Koie, Y. *Tetrahedron Lett.* **1998**, *39*, 617– 620. (b) Yamamoto, T.; Nishiyama, M.; Koie, Y. *Tetrahedron Lett.* **1998**, *39*, 2367.

26. G. C. Fu, *Acc. Chem. Res.* **2008**, *41*, 1555 – 1564, and references cited therein.

27. Shen, W. *Tetrahedron Letters*, **1997**, *38*, 32, 5575-5578.

28. Littke, A. F.; Schwarz, L.; Fu, G. C. *J. Am. Chem. Soc.* **2002**, *124*, 6343-6348.

29. Stürmer, R. *Angew. Chem. Int. Ed.* **1999**, *38*, 22, 3307-3308.

30. (a) Huang, J.; Grasa, G. *Org. Lett.*, **1999** *1*, 8, 1307-1309. (b) Grasa, G. A.; Nolan, S. P. *Org. Lett.*, **2001**, *3*, 1, 119-122.

31. Caddick, S.; Cloke, F. G. N.; Hitchcock, P. B.; Leonard, J.; Lewis, A. K. d. Ks.; McKerrecher, D.; Titcomb, L. R. *Organometallics* **2002**, *21*, 4318– 4319. (b) Lewis, A. K.; Caddick, S.; Cloke, F. G.; Billingham, N. C.; Hitchcock, P. B.; Leonard, J. *J. Am. Chem. Soc.* **2003**, *125*, 10066–10073.

32. (a) Christmann, U.; Vilar, R. *Angew. Chem. Int. Ed.* **2005**, *44*, 366 –374. (b) Molander, G. A.; Canturk, B. *Angew. Chem. Int. Ed.* **2009**, *48*, 9240 – 9261.

33. Newman-Stonebraker, S. H.; Smith, S. R.; Borowski, J. E.; Peters, E.; Gensch, T.; Johnson, H. C.; Sigman, M. S.; Doyle, A. G. *Science* **2021**, *374* (6565), 301– 308.

34. See also: Zhao, S.; Gensch, T.; Murray, B.; Niemeyer, Z. L.; Sigman, M. S.; Biscoe, M. R. *Science* **2018**, *362*, 670– 674.

35. See: Stambuli, J. P.; Stauffer, S. R.; Shaughnessy, K. H.; Hartwig, J. W. *J. Am. Chem. Soc.* **2001,** *123*, 2677-2678.

36. Borowski, J. E.; Newman-Stonebraker, S. H.; Doyle, A. G. *ACS Catal*. **2023**, *13*, 7966–7977.

37. For selected exceptions where chemoselective cross-coupling results at the site of a smaller halide, see: (a) Cheng, J.; Trudell, M. L. *Org. Lett.* **2001**, *3*, 1371–1374. (b) Ji, J.; Bunnelle, W. H. *Org. Lett.* **2003**, *5*, 4611–4614. (c) Keylor, M. G.; Niemeyer, Z. L.; Sigman, M. S.; Tan, K. L. *J. Am. Chem. Soc.* **2017**, *139*, 10613–10616. (d) Qiu, Y. L.; Wang, C.; Peng, X.; Cao, H.; Ying, L.; Gao, X.; Wang, B.; Or, Y. S. WO2013052369 A1, **2013**. (e) Ashcroft, C. P.; Fussell, S. J.; Wilford, K. *Tetrahedron Lett.* **2013**, *54*, 4529–4532. (f) Ishikawa, S.; Manabe, K.; *Tetrahedron* **2011**, *67*, 10156–10163.

38. (a) Reeves, E. K.; Entz, E. D.; Neufeldt, S. R. *Chem. Eur. J.* **2021**, *27*, 6161– 6177 (b) Ng, S. S.; Pang, W. H.; Yuen, O. Y.; So, C. M. *Org. Chem. Front.*, **2023**, *10*, 4408-4436.

39. Littke, A. F.; Dai, C. Y.; Fu, G. C. *J. Am. Chem. Soc.* **2000**, *122*, 4020–4028.

40. Schoenebeck, F.; Houk, K. N. *J. Am. Chem. Soc.* **2010**, *132*, 2496–2497.

41. Manabe, K.; Ohba, M.; Matsushima, Y. *Org. Lett.* **2011**, *13*, 2436–2439.

42. Niemeyer, Z. L. ; Milo, A.; Hickey, D. P.; Sigman, M. S. *Nature Chem.* **2016**, *8*, 610–617.

43. Reeves, E. K. ; Humke, J. J.; Neufeldt, S. R. *J. Org. Chem.* **2019**, *84*, 11799–11812.

44. (a) Chen, Z.; Gu, C.; Yuen, O. Y.; So, C. M. *Chem. Sci.* **2022**, *13*, 4762– 4769. (b) Wang, M.; Yuen, O. Y.; So, C. M. *Chin. J. Chem*. **2023**, *41*, 909—914.

45. Cardoza, S.; Shrivash, M. K.; Das, P.; Tandon, V. *J. Org. Chem.*, **2021**, *86*, 1330—1356.

46. (a) Colacot, T. J. Platinum Met. Rev. 2011, 55, 84–90. (b) Johansson Seechurn, C. C. C.; Deangelis, A.; Colacot, T. J.; Introduction to *New Trends in Cross Coupling, Theory*

and Applications; RSC Catalysis Series *No. 21*; Colacot, T. J.; The Royal Society of Chemistry: Cambridge, UK, 2015; pp. 1-19

47. For reviews on site-selectivity in cross-couplings of multiply halogenated heteroarenes, see: (a) Schröter, S.; Stock, C.; Bach, T. *Tetrahedron* **2005**, *61*, 2245−2267. (b) Fairlamb, I. J. S. *Chem. Soc. Rev.* **2007**, *36*, 1036−1045. (c) Bellina, F.; Rossi, R. Adv. Synth. Catal. 2010, 352, 1223−1276. (d) Rossi, R.; Bellina, F.; Lessi, M. 2012, 354, 1181−1255. (e) Manabe, K.; Yamaguchi, M. *Catalysts* **2014**, *4*, 307−320. (f) Kapdi, A. R.; Prajapati, D. *RSC Adv.* **2014**, *4*, 41245−41259. (g) Almond-Thynne, J.; Blakemore, D. C.; Pryde, D. C.; Spivey, A. C. *Chem. Sci.* **2017**, *8*, 40−62. (h) Palani, V.; Perea, M. A.; Sarpong, R. *Chem. Rev.* **2022**, *122*, 10126−10169.

48. (a) Handy, S. T.; Zhang, Y. *Chem. Commun.* **2006**, *3*, 299−301. See also (b) Zhang, Y.; Handy, S. T. *Open Org. Chem. J.* **2008**, *2*, 58−64. (c) Kashihara, M.; Gordon, C. P.; Copéret, C. *Org. Lett.* **2020**, *22*, 8910−8915.

49. Abraham, R. J.; Reid, M. ^{1}H chemical shifts in NMR. Part 18. Ring currents and p-electron effects in hetero-aromatics. *J. Chem. Soc., Perkin Trans. 2* **2002**, 1081−1091.

50. (a) Legault, C. Y.; Garcia, Y.; Merlic, C. A.; Houk, K. N. *J. Am. Chem. Soc.* **2007**, *129*, 12664−12665. (b) Garcia, Y.; Schoenebeck, F.; Legault, C. Y.; Merlic, C. A.; Houk, K. N. *J. Am. Chem. Soc.* **2009**, *131*, 6632−6639.

51. (a) de Jong, G. T.; Bickelhaupt, F. M. *ChemPhysChem* **2007**, *8*, 1170—1181. (b) de Jong, G. T.; Bickelhaupt, F. M. *J. Chem. Theory Comput.* **2007**, *3*, 514—529.

52. Lu, J.; Donnecke, S.; Paci, I.; Leitch, D. C. *Chem. Sci.* **2022**, *13*, 3477−3488.

53. For noteworthy examples of unconventional site-selectivity, see: (a) Strotman, N. A.; Chobanian, H. R.; He, J.; Guo, Y.; Dormer, P. G.; Jones, C. M.; Steves, J. E. *J. Org. Chem.* **2010**, *75*, 1733−1739. (b) Dai, X.; Chen, Y.; Garrell, S.; Liu, H.; Zhang, L.-K.; Palani, A.; Hughes, G.; Nargund, R. *J. Org. Chem.* **2013**, *78*, 7758−7763. (c) Fowler, J. M.; Britton, E.; Pask, C. M.; Willans, C. E.; Hardie, M. J. *Dalton Trans.* **2019**, *48*, 14687−14695. (d) Palani, V.; Hugelshofer, C. L.; Kevlishvili, I.; Liu, P.; Sarpong, R. *J. Am. Chem. Soc.* **2019**, *141*, 2652– 2660 (e) Yang, M.; Chen, J.; He, C.; Hu, X.; Ding, Y.; Kuang, Y.; Liu, J.; Huang, Q. *J. Org. Chem.* **2020**, *85*, 6498−6508. (f) Scott, N. W. J.; Ford, M. J.; Jeddi, N.; Eyles, A.; Simon, L.; Whitwood, A. C.; Tanner, T.; Willans, C. E.; Fairlamb, I. J. S. *J. Am. Chem. Soc.* **2021**, *143*, 9682−9693. (g) Norman, J. P.; Larson, N. G.; Entz, E. D.; Neufeldt, S. R. *J. Org. Chem.* **2022**, *87*, 7414−7421. (h) Kim, G.; Lee, G.; Kim, G.; Seo, Y.; Jarhad, D. B.; Jeong, L. S. *Org. Chem. Front.* **2022**, *9*, 5536– 5543.

54. Norman, J. P.; Neufeldt, S. R. *ACS Catal.* **2022**, *12*, 12014– 12026.

Chapter Two

1. Roughley, S. D.; Jordan, A. M. *J. Med. Chem.* **2011**, *54*, 3451.

2. Smith, B. R.; Eastman, C. M.; Njardarson, J. T. *J. Med. Chem.* **2014**, *57*, 9764−9773.

3. Reviews: (a) Schröter, S.; Stock, C.; Bach, T. *Tetrahedron* **2005**, *61*, 2245− 2267. (b) Fairlamb, I. J. S. *Chem. Soc. Rev.* **2007**, *36*, 1036−1045. (c) Manabe, K.; Yamaguchi, M. *Catalysts* **2014**, *4*, 307− 320. (d) Almond-Thynne, J.; Blakemore, D. C.; Pryde, D. C.; Spivey, A. C. *Chem. Sci.* **2017**, *8*, 40−62. (e) Palani, V.; Perea, M. A.; Sarpong, R. *Chem. Rev.* **2021**, DOI: 10.1021/acs.chemrev.1c00513

4. Cross-coupling examples of 2,4-dichloropyridines: (a) Cruskie, M. P. J., Jr.; Zoltewicz, J. A.; Abboud, K. A. *J. Org. Chem.* **1995**, *60*, 7491−7495. (b) Norman, M. H.; Chen, N.; Chen, Z.; Fotsch, C.; Hale, C.; Han, N.; Hurt, R.; Jenkins, T.; Kincaid, J.; Liu, L.; Lu, Y.; Moreno, O.; Santora, V. J.; Sonnenberg, J. D.; Karbon, W. *J. Med. Chem.* **2000**, *43*, 4288−4312. (c) Murray, J. I.; Woscholski, R.; Spivey, A. C. *Chem. Commun*. **2014**, *50*, 13608−13611. (d) Young, I. S.; Glass, A.-L.; Cravillion, T.; Han, C.; Zhang, H.; Gosselin, F. *Org. Lett.* **2018**, *20*, 3902−3906.

5. Cross-coupling examples of 2,4-dichloroquinoline: (a) Shiota, T.; Yamamori, T. *J. Org. Chem.* **1999**, *64*, 453−457. (b) Legros, J.-Y.; Primault, G.; Fiaud, J.-C. *Tetrahedron* **2001**, *57*, 2507−2514.

6. Cross-coupling example with 3,5-dichloropyridazine, which also favors reaction adjacent to nitrogen at C3: Blaise, E.; Kümmerle, A. E.; Hammoud, H.; de Araujo-Ju´nior, J. X.; Bihel, F.; Bourguignon, J.-J.;´ Schmitt, M. *J. Org. Chem.* **2014**, *79*, 10311−10322.

7. Isolated reports of exceptions to C2-selectivity: (a) Dai, Y.; Hartandi, K.; Ji, Z.; Ahmed, A. A.; Albert, D. H.; Bauch, J. L.; Bouska, J. J.; Bousquet, P. F.; Cunha, G. A.; Glaser, K. B.; Harris, C. M.; Hickman, D.; Guo, J.; Li, J.; Marcotte, P. A.; Marsh, K. C.; Moskey, M. D.; Martin, R. L.; Olson, A. M.; Osterling, D. J.; Pease, L. J.; Soni, N. B.; Stewart, K. D.; Stoll, V. S.; Tapang, P.; Reuter, D. R.; Davidsen, S. K.; Michaelides, M. R. *J. Med. Chem.* **2007**, *50*, 1584−1597. (b) Khoje, A. D.; Gundersen, L.-L. Reactivity and regioselectivity in Stille couplings of 3-substituted 2,4-dichloropyridines. *Tetrahedron Lett.* **2011**, *52*, 523− 525.

8. (a) Legault, C. Y.; Garcia, Y.; Merlic, C. A.; Houk, K. N. *J. Am. Chem. Soc.* **2007**, *129*, 12664−12665. (b) Garcia, Y.; Schoenebeck, F.; Legault, C. Y.; Merlic, C. A.; Houk, K. N. *J. Am. Chem. Soc.* **2009**, *131*, 6632−6639.

9. Dai, X.; Chen, Y.; Garrell, S.; Liu, H.; Zhang, L.-K.; Palani, A.; Hughes, G.; Nargund, R. *J. Org. Chem.* **2013**, *78*, 7758−7763.

10. Reeves, E. K.; Humke, J. N.; Neufeldt, S. R. *J. Org. Chem.* **2019**, *84*, 11799−11812.

11. Yang, M.; Chen, J.; He, C.; Hu, X.; Ding, Y.; Kuang, Y.; Liu, J.; Huang, Q. *J. Org. Chem.* **2020**, *85*, 6498−6508.

12. Melvin, P. R.; Nova, A.; Balcells, D.; Dai, W.; Hazari, N.; Hruszkewycz, D. P.; Shah, H. P.; Tudge, M. T. *ACS Catal.* **2015**, *5*, 3680−3688.

13. We hypothesize that polar solvents can promote a more polar "displacement" mechanism for oxidative addition, compared to a 3-centered mechanism in nonpolar solvents. These two different mechanisms are biased toward C2 versus C4 selectivity, respectively (a detailed mechanistic study is forthcoming).

14. Pd/IPent has been shown to promote exhaustive arylation in other contexts. Although the origin of IPent's effect has not been studied, it is likely that its steric bulk disfavors dissociation of Pd from the product after reductive elimination: Groombridge, B. J.; Goldup, S. M.; Larrosa, I. *Chem. Commun.* **2015**, *51*, 3832−3834.

15. Cook, X. A. F.; Gombert, A.; McKnight, J.; Pantaine, L. R. E.; Willis, M. C. *Angew. Chem., Int. Ed.* **2021**, *60*, 11068− 11091.

16. Examples: (a) Banks, R. E.; Burgess, J. E.; Cheng, W. M.; Haszeldine, R. N. 93. Heterocyclic polyfluoro-compounds. Part IV. Nucleophilic substitution in pentafluoropyridine: the preparation and properties of some 4-substituted 2,3,5,6-tetrafluoropyridines. *J. Chem. Soc.* **1965**, 575−581. (b) Mittelbach, M. *Synthesis* **1988**, *1988*, 479−480. (c) Schlosser, M.; Rausis, T.; Bobbio, C. *Org. Lett*. **2005**, *7*, 127−129. (d) Schlosser, M.; Bobbio, C.; Rausis, T. *J. Org. Chem.* **2005**, *70*, 2394−2502.

17. Duan, J.; Jian, B.; Lu, Z. Azaindoles as BTK Kinase Modulators and Use Thereof. WO 2011019780 A1, February 17, 2011; pp 63− 64.

18. (a) Scott, N. W. J.; Ford, M. J.; Jeddi, N.; Eyles, A.; Simon, L.; Whitwood, A. C.; Tanner, T.; Willans, C. E.; Fairlamb, I. J. S. A *J. Am. Chem. Soc.* **2021**, *143*, 9682−9693. (b) Appleby, K. M.; Dzotsi, E.; Scott, N. W. J.; Dexin, G.; Jeddi, N.; Whitwood, A. C.; Pridmore, N. E.; Hart, S.; Duckett, S. B.; Fairlamb, I. J. S. *Organometallics* **2021**, *40*, 3560−3570.

19. Fairlamb's conditions employ PPh_3 in a low ligand:Pd ratio, which promote formation of clusters and nanoparticles. These conditions were shown to effect C4-selective cross-coupling of 2,4-dibromopyridine (C2/C4 ~ 1:10). Notably, Fairlamb's conditions are not effective for C4-selective cross-coupling of 2,4-dichloropyridine (Appendix A).

20. (a) Jeffery, T. *J. Chem. Soc., Chem. Commun.* **1984**, 1287−1289. (b) Jeffery, T. *Tetrahedron Lett.* **1985**, *26*, 2667− 2670. (c) Jeffery, T. *Tetrahedron* **1996**, *52*, 10113−10130.

21. Chernyshev, V. M.; Khazipov, O. V.; Eremin, D. B.; Denisova, E. A.; Ananikov, V. P. *Coord. Chem. Rev.* **2021**, *437*, 213860.

22. de Vries, J. G. When Does Catalysis with Transition Metal Complexes Turn into Catalysis by Nanoparticles?. *Selective Nanocatalysts and Nanoscience*, 2011; Wiley:VCH, pp 73−103.

23. For selected examples of typical selectivity with 2,5- dihalopyrimidine see: (a) Hughes, G.; Wang, C.; Batsanov, A. S.; Fern, M.; Frank, S.; Bryce, M. R.; Perepichka, I. F.; Monkman, A. P.; Lyons, B. P. *Org. Biomol. Chem.* **2003**, *1*, 3069−3077. (b) Malik, I.; Ahmed, Z.; Reimann, S.; Ali, I.; Villinger, A.; Langer, P. *Eur. J. Org. Chem.* **2011**, *2011*, 2088−2093.

24. For selected examples of typical selectivity with 2,5- dichloropyridines see: (a) Brumfield, S.; Matasi, J. J.; Tulshian, D.; Czarniecki, M.; Greenlee, W.; Garlisi, C.; Qiu, H.; Devito, K.; Chen, S.-C.; Sun, Y.; Bertorelli, R.; Ansell, J.; Geiss, W.; Le, V.-D.; Martin, G. S.; Vellekoop, S. A.; Haber, J.; Allard, M. L. *Bioorg. Med. Chem. Lett.* **2011**, *21*, 7287−7290. (b) Curreli, F.; Ahmed, S.; Benedict Victor, S. M.; Iusupov, I. R.; Belov, D. S.; Markov, P. O.; Kurkin, A. V.; Altieri, A.; Debnath, A. K. *J. Med. Chem*. **2020**, *63*, 1724−1749.

25. For reported exceptions to conventional selectivity of 2,5-dichloropyridine and -pyrimidine in direct arylations and Sonogashira couplings, albeit without spectroscopic support for structural assignment of the products, see (a) Zheng, L.-L.; Yin, B.; Tian, X.- C.; Yuan, M.-Y.; Li, X.-H.; Gao, F. *Tetrahedron Lett.* **2019**, *60*, 151316. (b) Al-Khawaldeh, I.; Al Yasiri, M. J.; Aldred, G. G.; Basmadjian, C.; Bordoni, C.; Harnor, S. J.; Heptinstall, A. B.; Hobson, S. J.; Jennings, C. E.; Khalifa, S.; Lebraud, H.; Martin, M. P.; Miller, D. C.; Shrives, H. J.; de Souza, J. V.; Stewart, H. L.; Temple, M.; Thomas, H. D.; Totobenazara, J.; Tucker, J. A.; Tudhope, S. J.; Wang, L. Z.; Bronowska, A. K.; Cano, C.; Endicott, J. A.; Golding, B. T.; Hardcastle, I. R.; Hickson, I.; Wedge, S. R.; Willmore, E.; Noble, M. E. M.; Waring, M. J. *J. Med. Chem*. **2021**, *64*, 10001−10018.

Chapter Three

1. Pennington, L. D.; Moustakas, D. T. *J. Med. Chem.* **2017**, *60*, 3552−3579.

2. For reviews, see: (a) Schröter, S.; Stock, C.; Bach, T. *Tetrahedron* **2005**, *61*, 2245−2267. (b) Fairlamb, I. J. S. *Chem. Soc. Rev.* **2007**, *36*, 1036−1045. (c) Manabe, K.; Yamaguchi, M. *Catalysts* **2014**, *4*, 307−320. (d) Almond-Thynne, J.; Blakemore,

D. C.; Pryde, D. C.; Spivey, A. C. *Chem. Sci.* **2017**, *8*, 40−62. (e) Palani, V.; Perea, M. A.; Sarpong, R. *Chem. Rev.* **2022**, *122*, 10126−10169.

3. (a) Legault, C. Y.; Garcia, Y.; Merlic, C. A.; Houk, K. N. *J. Am. Chem. Soc.* **2007**, *129*, 12664−12665. (b) Garcia, Y.; Schoenebeck, F.; Legault, C. Y.; Merlic, C. A.; Houk, K. N. *J. Am. Chem. Soc.* **2009**, *131*, 6632−6639.

4. Lu, J.; Donnecke, S.; Paci, I.; Leitch, D. C. *Chem. Sci.* **2022**, *13*, 3477−3488.

5. Dai, X.; Chen, Y.; Garrell, S.; Liu, H.; Zhang, L.-K.; Palani, A.; Hughes, G.; Nargund, R. *J. Org. Chem.* **2013**, *78*, 7758−7763.

6. Fowler, J. M.; Britton, E.; Pask, C. M.; Willans, C. E.; Hardie, M. J. *Dalton Trans.* **2019**, *48*, 14687−14695.

7. Norman, J. P.; Larson, N. G.; Entz, E. D.; Neufeldt, S. R. *J. Org. Chem.* **2022**, *87*, 7414−7421.

8. Yang, M.; Chen, J.; He, C.; Hu, X.; Ding, Y.; Kuang, Y.; Liu, J.; Huang, Q. *J. Org. Chem.* **2020**, *85*, 6498−6508.

9. (a) The precatalysts used in ref 7 are of the type (η^3-1-*t* Bu-indenyl)Pd(NHC)(Cl) and were designed to release monoligated PdL: Melvin, P. R.; Nova, A.; Balcells, D.; Dai, W.; Hazari, N.; Hruszkewycz, D. P.; Shah, H. P.; Tudge, M. T. *ACS Catal.* **2015**, *5*, 3680−3688. (b) Espinosa, M. R.; Doppiu, A.; Hazari, N. *Adv. Synth. Catal.* **2020**, *362*, 5062−5078.

10. (a) Multinuclear clusters are implicated in C4-selective cross-coupling of 2,4-dibromopyridine at low ligand loadings in a Pd/PPh_3 system, although the reason for a C4-preference of multinuclear clusters is not yet known: Scott, N. W. J.; Ford, M. J.; Jeddi, N.; Eyles, A.; Simon, L.; Whitwood, A. C.; Tanner, T.; Willans, C. E.; Fairlamb, I. J. S. *J. Am. Chem. Soc.* **2021**, *143*, 9682−9693. (b) Appleby, K. M.; Dzotsi, E.; Scott, N. W. J.; Dexin, G.; Jeddi, N.; Whitwood, A. C.; Pridmore, N. E.; Hart, S.; Duckett, S. B.; Fairlamb, I. J. S. *Organometallics* **2021**, *40*, 3560−3570.

11. (a) For examples of the use of Pd(COD)(CH_2SiR_3)$_2$ + free ligand "L" as a precursor to putative PdL_n see: Fors, B. P.; Watson, D. A.; Biscoe, M. R.; Buchwald, S. L. *J. Am. Chem. Soc.* **2008**, *130*, 13552−13554. (b) Watson, D. A.; Su, M.; Teverovskiy, G.; Zhang, Y.; Garcia-Fortanet, J.; Kinzel, T.; Buchwald, S. L. Formation of ArF from LPdAr(F): Catalytic Conversion of Aryl Triflates to Aryl Fluorides. *Science* **2009**, *325*, 1661−1664. (c) Sergeev, A. G.; Schulz, T.; Torborg, C.; Spannenberg, A.; Neumann, H.; Beller, M. *Angew. Chem., Int. Ed.* **2009**, *48*, 7595−7599. (d) Larini, P.; Kefalidis, C. E.; Jazzar, R.; Renaudat, A.; Clot, E.; Baudoin, O. *Chem.−Eur. J.* **2012**, *18*, 1932−1944. (e) Andersen, T. L.; Friis, S. D.; Audrain, H.; Nordeman, P.; Antoni, G.; Skrydstrup, T. *J. Am. Chem. Soc.* **2015**, *137*, 1548−1555. (f) Milner, P. J.; Yang, Y.;

Buchwald, S. L. *Organometallics* **2015**, 34, 4775−4780. (g) Elias, E. K.; Rehbein, S. M.; Neufeldt, S. R. *Chem. Sci.* **2022**, *13*, 1618−1628.

12. Gensch, T.; dos Passos Gomes, G.; Friederich, P.; Peters, E.; Gaudin, T.; Pollice, R.; Jorner, K.; Nigam, A.; Lindner-D'Addario, M.; Sigman, M. S.; Aspuru-Guzik, A. *J. Am. Chem. Soc.* **2022**, *144*, 1205−1217.

13. Clavier, H.; Nolan, S. P. *Chem. Commun.* **2010**, *46*, 841−861.

14. (a) Vummaleti, S. V. C.; Nelson, D. J.; Poater, A.; Gómez-Suárez, A.; Cordes, D. B.; Slawin, A. M. Z.; Nolan, S. P.; Cavallo, L. *Chem. Sci.* **2015**, *6*, 1895−1904. (b) Lummiss, J. A. M.; Higman, C. S.; Fyson, D. L.; McDonald, R.; Fogg, D. E. *Chem. Sci.* **2015**, *6*, 6739−6746. (c) Back, O.; Henry-Ellinger, M.; Martin, C. D.; Martin, D.; Bertrand, G. *Angew. Chem., Int. Ed.* **2013**, *52*, 2939−2943. (d) Morán-González, L.; Pedregal, J. R.-G.; Besora, M.; Maseras, F. *App. Eur. J. Inorg. Chem.* **2022**, No. e202100932.

15. (a) For examples of nitrogen-containing substrates/products acting as ligands for Pd during cross-couplings, see: Alcazar-Roman, L. M.; Hartwig, J. F.; Rheingold, A. L.; Liable-Sands, L. M.; Guzei, I. A. *J. Am. Chem. Soc.* **2000**, *122*, 4618−4630. (b) Singh, U. K.; Strieter, E. R.; Blackmond, D. G.; Buchwald, S. L. *J. Am. Chem. Soc.* **2002**, *124*, 14104−14114. (c) Jutand, A.; Négri, S.; Principaud, A. *Eur. J. Inorg. Chem.* **2005**, *2005*, 631−635. (d) Tougerti, A.; Negri, S.; Jutand, A. *Chem.-Eur. J.* **2007**, *13*, 666−676. (e) Perego, L. A.; Grimaud, L.; Bellina, F. *Adv. Synth. Catal.* **2016**, *358*, 597−609.

16. (a) Evidence has been reported for oxidative addition of aryl halides at both bisligated $Pd(PPh_3)_2$ and monoligated $Pd(PPh_3)$: Amatore, C.; Jutand, A.; Khalil, F.; M'Barki, M. A.; Mottier, L. *Organometallics* **1993**, *12*, 3168−3178. (b) Joshi, C.; Macharia, J. M.; Izzo, J. A.; Wambua, V.; Kim, S.; Hirschi, J. S.; Vetticatt, M. J. *ACS Catal.* **2022**, *12*, 2959− 2966.

17. Newman-Stonebraker, S. H.; Smith, S. R.; Borowski, J. E.; Peters, E.; Gensch, T.; Johnson, H. C.; Sigman, M. S.; Doyle, A. G. *Science* **2021**, *374*, 301−308.

18. (a) Evidence suggests that PCy_3 can support oxidative addition at both $Pd(PCy_3)$ and $Pd(PCy_3)_2$: Mitchell, E. A.; Jessop, P. G.; Baird, M. C. *Organometallics* **2009**, *28*, 6732−6738. (b) Barrios-Landeros, F.; Carrow, B. P.; Hartwig, J. F. *J. Am. Chem. Soc.* **2009**, *131*, 8141−8154. (c) McMullin, C. L.; Jover, J.; Harvey, J. N.; Fey, N. *Dalton Trans.* **2010**, *39*, 10833−10836.

19. (a) Portnoy, M.; Milstein, D. *Organometallics* **1993**, *12*, 1665−1673. (b) Maes, B. U. W.; Verbeeck, S.; Verhelst, T.; Ekomie, A.; von Wolff, N.; Lefevre, G.; Mitchell, E. A.; Jutand, A. *Chem. Eur. J.* **2015**, *21*, 7858−7865. (c) Besora, M.; Maseras, F. *Dalton Trans.* **2019**, *48*, 16242−16248.

20. Senn, H. M.; Ziegler, T. *Organometallics* **2004**, *23*, 2980−2988.

21. Relative free energies are reported after applying Cramer and Truhlar's quasi-harmonic approximation to vibrational entropy: Ribeiro, R. F.; Marenich, A. V.; Cramer, C. J.; Truhlar, D. G. *Phys. Chem. B* **2011**, *115*, 14556−14562.

22. (a) 3D images of optimized structures were generated with CYLview: Legault, C. Y. CYLview20; Universitéde Sherbrooke, 2020 (http://www.cylview.org). (b) 3D images of molecular orbitals were generated with Avogadro: Hanwell, M. D; Curtis, D. E; Lonie, D. C; Vandermeersch, T.; Zurek, E.; Hutchison, G. R Avogadro: An advanced semantic chemical editor, visualization, and analysis platform. *J. Cheminformatics* **2012**, *4*, 17.

23. For previous experimental studies supporting a displacement mechanism for PdL_2 during reaction of PhCl, see ref 19a.

24. For previous computational studies showing that PdL and PdL_2 can favor different mechanisms during reaction with PhBr, see ref 19c.

25. (a) For seminal examples of computational studies showing a 3-centered concerted mechanism for oxidative addition of ArCl at PdL (L = P^tBu_3), see: Ahlquist, M.; Norrby, P.-O. *Organometallics* **2007**, *26*, 550−553. (b) Schoenebeck, F.; Houk, K. N. *J. Am. Chem. Soc.* **2010**, *132*, 2496−2497.

26. The LUMO and LUMO + 1 of PhCl are nearly isoenergetic (∼1 kcal/mol difference). In contrast, the LUMO and LUMO + 1 of **1** differ by about 9 kcal/mol.

27. Entz, E. D.; Russell, J. E. A.; Hooker, L. V.; Neufeldt, S. R. *J. Am. Chem. Soc.* **2020**, *142*, 15454−15463.

28. We also find that the preferred mechanism of oxidative addition of the C4−Cl bond of 2,4-dichloropyridine at PdL_2 depends on L. Ligand-dependent mechanistic differences might explain the variable magnitude of C2-selectivity with small triaryl vs trialkyl phosphines (see Appendix B).

29. For prior evidence supporting a displacement mechanism for PdL_2 (L = PPh_3) during reaction of 2-chloropyridine, see ref 19b.

30. (a) Huang, J.; Schanz, H.-J.; Stevens, E. D.; Nolan, S. P. *Organometallics* **1999**, *18*, 2370−2375. (b) Hopkinson, M. N.; Richter, C.; Schedler, M.; Glorius, F. *Nature* **2014**, *510*, 485−496.

31. A recent publication demonstrates that a C6-substituent can also slow the rate of oxidative addition at C2 due to sterics, although the effect of C6-sterics on C4−X oxidative addition was not examined: see ref 4.

32. Notably, LUMO differences are not the only variable that trends with selectivity. The most selective substrate (pyridazine) also has the smallest difference in bond dissociation energies. Additionally, pyridazines are worse ligands than pyridines, which could further disfavor bisligated Pd.

33. With 2,4-dibromopyridine **26**, over-arylation is observed (see ref 7).

34. All thermodynamic quantities were computed with the GoodVibes code (298.15 K) applying corrections for initial concentrations ([Pd] = 0.0075 M and [2] = 0.25 M): Luchini, G.; Alegre- Requena, J. V.; Funes-Ardoiz, I.; Paton, R. S. GoodVibes: Automated Thermochemistry for Heterogeneous Computational Chemistry Data. F1000Research **2020**, *9*, 291.

Chapter Four

1. For selected examples of 2,4-disubstituted pyrimidines in medicinal chemistry, see: (a) Manley, P. J.; Balitza, A. E.; Bilodeau, M. T.; Coll, K. E.; Hartman, G. D.; McFall, R. C.; Rickert, K. W.; Rodman, L. D.; Thomas, K. A. *Bioorg. Med. Chem. Lett.* **2003**, *13*, 1673– 1677. (b) Mohamed, T.; Rao, P. P. *Bioorg. Med. Chem. Lett.* **2010**, *20*, 3606–3609. (c) Mohamed, T.; Zhao, X.; Habib, L. K.; Yang, J.; Rao, P. P. N. *Bioorg. Med. Chem.* **2011**, *19*, 2269– 2281. (d) Mohamed, T.; Yeung, J. C. K.; Vasefi, M. S.; Beazely, M. A.; Rao, P. P. N. *Bioorg. Med. Chem. Lett.* **2012**, *22*, 4707– 4712. (e) Mukherjee, P.; Li, H.; Sevrioukova, I.; Chrei, G.; Marta, P.; Roman, L. J.; Poulos, T. L.; Silverman, R. B. *J. Med. Chem.* **2015**, *58*, 3, 1067– 1088. (f) Kim, J.; Kim, Y. J.; Londhe, A. M.; Pae, A. N.; Choo, H.; Kim, H. J.; Min, S. J. *Molecules* **2019**, *24.* (g) Hopfner, S. M.; Lee, B. S.; Kalia, N. P.; Miller, M. J.; Pethe, K.; Moraski, G. C. *Applied Sciences* **2021**, *11*, 19, 9092. DOI:10.3390/app11199092. (h) Zhang, X.; Wang, J.; Xu, J.; Pang, Q.; Liu, D.; Zhang, G. *J. Org. Chem.* **2023**, *88*, 10266−10276. (i) Kim, G.; Hou, X.; Byun, W. S.; Kim, G.; Jarhad, D. B.; Lee, G.; Hyun, Y. E.; Yu, J.; Lee, C. S.; Qu, S.; Warnick, E.; Gao, Z.-G.; Kim, J. Y.; Ji, S.; Shin, H.; Choi, J.-R.; Jacobson, K. A.; Lee, H. W.; Lee, S. K.; Jeong, L. S. *J. Med. Chem.* **2023**, *66*, 17, 12249–12265.

2. Williams, R. E.; Top 200 Small Molecule Drugs by Retail Sales in 2022; https://njardarson.lab.arizona.edu/sites/njardarson.lab.arizona.edu/files/NjardarsonGroup2022SmallMoleculeTopPosterV3.pdf (poster accessed online November 28, 2023); *see:* McGrath, N. A.; Brichacek, M.; Njardarson, J. T. *J. Chem. Educ*. **2010**, *87*, 12, 1348–1349.

3. (a) Singh, K.; Kaur, H.; Smith, P.; de Kock, C.; Chibale, K.; Balzarini, J. *J. Med. Chem.* **2014**, *57*, 435– 448. (b) Gehringer, M.; Forster, M.; Pfaffenrot, E.; Bauer, S. M.; Laufer, S. A. *Chemmedchem* **2014**, *9*, 11, 2516– 2527. (c) Manzoor, S.; Gabr, M. T.; Rasool, B.; Pal K.; Hoda, N. *Bioorg. Chem.*, **2021**, *116*, 105354.

4. Almond-Thynne, J.; Blakemore, D. C.; Pryde, D. C.; Spivey, A. C. *Chem. Sci.* **2017**, *8*, 40−62., See also: reference 6.

5. Dvorak, C.A. (**2008**). 2,4-Dichloropyrimidine. In Encyclopedia of Reagents for Organic Synthesis, (Ed.). https://doi.org/10.1002/047084289X.rn00879

6. Norman, J. P.; Neufeldt, S. R. *ACS Catal.* **2022**, *12*, 12014– 12026

7. F Garcia, Y.; Schoenebeck, F.; Legault, C. Y.; Merlic, C. A.; Houk, K. N. *J. Am. Chem. Soc.* **2009**, *131*, 6632– 6639.

8. For selected examples of C4- followed by C2-substitution, see: (a) Solberg, J.; Undheim, K. *Acta Chem. Scand.* **1989**, *43*, 62–68. (b) Mangalagiu, I.; Benneche, T.; Undheim, K. *Acta Chem. Scand.* **1996**, *50*, 914. (c) Duan, S.; Widlicka, D. W.; Burns, M. P.; Kumar, R.; Hotham, I.; Desrosiers, J. N.; Bowles, P.; Jones, K. N.; Nicholson, L. D.; Buetti-Weekly, M. T.; Han, L.; Steflik, J.; Hansen, E.; Hayward, C. M.; Strohmeyer, H.; Monfette, S.; Sutton, S. C.; Morris, C. *Org. Process Res. Dev.* **2022**, *26*, 3, 879– 890.
9. Marcella, B. P.; Housseman, C. G.; Daugan, A.; Dumoulin, A.; Laugeois; M.; Denis; A.; Faucher, N.; Botez, I.; Le Tiran, A.; Christensen K.; Lamotte, Y. New Macrocyclic LRRK2 Kinase Inhibitors. WO 2021/224320, November 11, 2021, A1;—pp 284.

10. (a) Mosrin, M.; Petrera, M.; Knochel, P. *Synthesis* **2008**, 3697– 3702. (b) Mosrin, M.; Knochel, P. *Org. Lett.* **2008**, *10*, 12, 2497–2500.

11. Ceide, S. C.; Montalban, A. G. *Tetrahedron Lett.* **2006**, *47*, 4415– 4418.

12. Li, C.; Haeffner, F.; Wang, S.; Yuan, C.; Shang, D.; Shi, X.; Ma, B.; Hopkins, B. T.; OBrien, E. M. *Org. Process Res. Dev.* **2022**, *26*, 137– 143.

13. Smith, S. M.; Buchwald, S. L. *Org. Lett.* **2016**, *18*, 9, 2180– 2183.

14. Strotman, N. A.; Chobanian, H. R.; He, J.; Guo, Y.; Dormer, P. G.; Jones, C. M.; Steves, J. E. *J. Org. Chem.* **2010**, *75*, 1733−1739.

15. (a) Abdel-Rahman, A. A. H.; Abdel-Megied, A. E. S.; Goda, A. E. S.; Zeid, I. F.; El Ashry, E. S. H. *Nucleosides Nucleotides* **2003**, *22*, 2027. (b) Tibiletti, F.; Simonetti, M.; Nicholas, K. M.; Palmisano, G.; Parravicini, M.; Imbesi, F.; Tollari, S.; Penoni, A. *Tetrahedron* **2010**, *66*, 1280– 1288. (c) Werner, M.; Pampel, J.; Pham, T. L.; Thomas, F. *Chem. Eur. J.* **2022**, *28*, e202201339.

16. Davey, D. D.; Adler, M.; Arnaiz, D.; Eagen, K.; Erickson, S.; Guilford, W.; Kenrick, M.; Morrissey, M. M.; Ohlmeyer, M.; Pan, G.; Paradkar, V. M.; Parkinson, J.; Polokoff, M.; Saionz, K.; Santos, C.; Subramanyam, B.; Vergona, R.; Wei, R. G.; Whitlow, M.; Ye, B.; Zhao, Z.; Devlin, J. J.; Phillips, G. *J. Med. Chem.* **2007**, *50*, 1146– 1157. (b) Abdel-Mohsen, H. T.; Omar, M. A.; El Kerdawy, A. M.; Mahmoud, A. E. E.; Ali, M. M.; El Diwani, H. I. *Eur. J. Med. Chem.* **2019**, *179*, 707– 722.

17. (a) Liebeskind, L. S.; Srogl, J. *J. Am. Chem. Soc*. **2000**, *122*, 45, 11260–11261. (b) Liebeskind, L. S.; Srogl, J. *Org. Lett.* **2002**, *4*, 6, 979–981. (c) Djamaladdin G. Musaev and Lanny S. Liebeskind. *Organometallics* **2009**, *28*, 16, 4639-4642.

18. For examples of chemoselective LSCs where aryl chlorides or bromides are tolerated, see: (a) Kusturin, C.; Liebeskind, L. S.; Rahman, H.; Sample, K.; Schweitzer, B.; Srogl, J.; Neumann, W.; *Org. Lett.* **2003**, *5*, 4349-4352. (b) Fausett, B. W.; Liebeskind, L. S.; *J. Org. Chem.* **2005**, *69*, 4851-4853. (c) Mehta, V. P.; Sharama, A.; Van der Eycken, E. *Org. Lett.* **2008**, *10*, 1147-1150. (c) Mehta, V. P.; Modha, S. G.; Van der Eycken, E.; *J. Org. Chem*. **2009**, *74*, 6870-6873. (d) Creech, G. S.; Kwon, O. *Chem. Sci.*, **2013**, *4*, 2670–2674. (e) Quan, Z. J.; Lv, Y.; Jing, F. Q.; Jia, X. D.; Huo, C. D.; Wang, X. C. *Adv. Synth. Catal.* **2014**, *356*, 325-332.

19. Prieur, V.; Pujol, M. D.; Guillaumet, G.; *Eur. J. Org. Chem.* **2015**, 6547-6556.

20. Cheng, H.-G.; Chen, H.; Liu, Y.; Zhou, Q. *Asian J. Org. Chem.* **2018**, *7*, 490.

21. Jackson, O. D.; Reyes, A.; Stein, C. D.; Andrews, C. T.; Neufeldt, S. R. C2-Selective Palladium-Catalyzed C—S Cross-Coupling of 2,4-Dihalopyrimidines [manuscript in preparation].

22. Zhang, Z.; Lindale, M. G.; Liebeskind, L. S. *J. Am. Chem. Soc.* **2011**, *133*, 6403– 6410.

23. (a) Villalobos, J. M.; Srogl, J.; Liebeskind, L. S. *J. Am. Chem. Soc.* **2007**, *129*, 15734–15735. (b) Adrián Varela-Álvarez, Lanny S. Liebeskind, and Djamaladdin G. Musaev *Organometallics* **2012**, *31*, 22, 7958-7968.

Chapter Five

1. For selected examples of stepwise functionalization of polyhalo(hetero)arenes, see: (a) Garg, N. K., Sarpong, R. and Stoltz, B. M. *J. Am. Chem. Soc.* **2002**, *124*, 131794 (b) Fisher, T. J.; Dussault, P. H. *Eur. J. Org. Chem.* **2012**, 2831–2836 and references therein. (b) Ceide, S. C.; Montalban, A. G. *Tetrahedron Lett.* **2006**, *47*, 4415– 4418. (c) Young, I. S.; Glass, A.-L.; Cravillion, T.; Han, C.; Zhang, H.; Gosselin, F. *Org. Lett.* **2018**, *20*, 3902– 3906.

2. Prajapati, D.; Schulzke, C.; Kindermann, M. K.; Kapdi, A. R. *RSC Adv.* **2015**, *5*, 53073−53085.

3. Examples of monosubstitution with traditional catalysts and symmetrical substrates: (a) Bunz, U. H. F.; Roidl, G.; Adams, R. D. *J. Organometallic Chem.* **2000**, *600*, 56-62. (b) Guillén, E.; Hirrezuelo, J.; Martínez-Mallorquín, R.; López-Romero, J. M.; Rico, R. *Tetrahedron* **2011**, *67*, 2555– 2561. Doebelin, C.; Wagner, P.; Bertin, I.; Simonin, F.; Schmitt, M.; Bihel, F.; Bourguignon, J.-J. *RSC Adv.* **2013**, *3*, 10296–10300.

4. For PPh_3, examples of selective diarylation are largely limited to diiodoarenes: (a) Tsvetkov, A. V.; Latyshev, G. V.; Lukashev, N. V.; Beletskaya, I. P. *Tetrahedron Lett*. **2000**, *41*, 3987-3990. (b) Sinclair, D. J.; Sherburn, M. S. J. *Org. Chem.* **2005**, *70*, 9, 3730–3733.

5. See ref. 2a. Note, in some scenarios, difunctionalization cannot be mitigated by using an excess of dihaloarene: Tietze, L. F.; Nordmann, G. *Synlett* **2001**, 337-340.

6. (a) Dong, C.-G.; Hu, Q.-S. *J. Am. Chem. Soc.* **2005**, *127,* 28, 10007. (b) Weber, S. K., Galbrecht, F., and Scherf, U. *Org. Lett*. **2006**, *8*, 4039– 4041.

7. For examples of difunctionalization or polymerization with RuPhos, see: (a) Dai, X.; Chen, Y.; Garrell, S.; Liu, H.; Zhang, L.-K.; Palani, A.; Hughes, G.; Nargund, R. *J. Org. Chem.* **2013**, *78*, 7758−7763, see Table 1, entry 16. (b) Lee, J.; Park, H.; Hwang, S.-H.; Lee, I.-H.; Choi, T.-L. *Macromolecules* **2020**, *53*, 3306– 3314. (c) Lee, J. Ryu, H.; Park, S.; Cho, M.; Choi, T.-L. *J. Am. Chem. Soc*. **2023**, *145,* 28, 15488-15495.

8. For an example of difunctionalization with the ligands SIPr, IPr, and IPent, see: Norman, J. P.; Larson, N. G.; Entz, E. D.; Neufeldt, S. R. *J. Org. Chem.* **2022**, *87*, 7414−7421.

9. Zhu, Y. X.; Li, E. C.; Shen, K.; Hang, X.; Bonnesen, P. V.; Hong, K.; Zhang, H. H.; Huang, W. Intramolecular Catalyst Transfer over Sterically Hindered Arenes in Suzuki Cross-Coupling Reactions, *Asian J. Org. Chem.*, **2019**, *8* , 1506 —1512. See also: ref. 18.

10. Groombridge, B. J.; Goldup, S. M.; Larrosa, I. Selective and general exhaustive cross-coupling of dichloroarenes with a deficit of nucleophiles mediated by a Pd–NHC complex. *Chem. Commun.* **2015**, *51*, 3832– 3834.

11. Leone, A. K.; Goldberg, P. K.; McNeil, A. J. Ring-Walking in Catalyst-Transfer Polymerization. *J. Am. Chem. Soc*. **2018**, *140,* 25, 7846– 7850.

12. (a) Strawser, D.; Karton, A.; Zenkina, O. V.; Iron, M. A.; Shimon, L. J. W.; Martin, J. M. L.; van der Boom, M. E. *J. Am. Chem. Soc*. **2005**, *127*, 9322– 9323, DOI: 10.1021/ja050613h (b) Zenkina, O. V.; Karton, A.; Freeman, D.; Shimon, L. J. W.; Martin, J. M. L.; van der Boom, M. E. *Inorg. Chem.* **2008**, *47*, 5114– 5121, DOI: 10.1021/ic702289n (c) Sontag, S. K.; Bilbrey, J. A.; Huddleston, N. E.; Sheppard, G. R.; Allen, W. D.; Locklin, J. *J. Org. Chem*. **2014**, *79*, 1836– 1841, DOI: 10.1021/jo402259z (d) Smith, J. A.; Schouten, A.; Wilde, J. H.; Westendorff, K. S.; Dickie, D. A.; Ess, D. H.; Harman, W. D. *J. Am. Chem. Soc.* **2020**, *142*, 16437– 16454, DOI: 10.1021/jacs.0c08032.

13. (a) Sheina, E. E.; Liu, J.; Iovu, M. C.; Laird, D. W.; McCullough, R. D. Chain Growth Mechanism for Regioregular Nickel-Initiated Cross-Coupling Polymerizations. *Macromolecules* **2004**, *37*, 3526−3528. (b) Yokoyama, A.; Miyakoshi, R.; Yokozawa, T. *Macromolecules* **2004**, *37*, 1169−1171. (c) Yokoyama, A.; Yokozawa, T. *Macromol. Rapid Commun*. **2004**, *25*, 1663−1666. For notable papers describing CTP mechanism, see: (d) Zhao, Y.; Nett, A. J.; McNeil, A. J.; Zimmerman, P. M *Macromolecules* **2016**, *49*, 7632– 7641.

14. (a) Adachi, I.; Miyakoshi, R.; Yokoyama, A.; Yokozawa, T. *Macromolecules*, **2006**, *39*, 7793-7795. Yokozawa, T.; Ohta, Y. *Chem. Rev.* **2016**, *116*, 1950−1968.

15. Bryan, Z. J.; Smith, M. L.; McNeil, A. J. *Macromol. Rapid Commun.* **2012**, *33*, 842–847, DOI: 10.1002/marc.201200096

16. Leone, A. K.; Mueller, E. A.; McNeil, A. J. *J. Am. Chem. Soc.* **2018**, *140*, 15126–15139, DOI: 10.1021/jacs.8b09103

17. (a) Mao, Y.; Wang, Y.; Lucht, B. L. *J. Polymer Sci.: Part A: Polymer Chem.* **2004**, *42*, 5538 –5547 (b) Bhatt, M. P.; Magurudeniya, H. D.; Sista, P.; Sheina, E. E.; Jeffries-EL, M.; Janesko, B. G.; McCullough, R. D.; Stefan, M. C. *J. Mater. Chem. A* **2013**, *1*, 12841– 12849.

18. Deem, M. C.; Derasp, J. S.; Malig, T. C.; Legard, K.; Berlinguette, C. P.; Hein, J. E. *Nat. Commun*. **2022**, *13*, 2869, DOI: 10.1038/s41467-022-30255-1

19. Norman, J. P.; Larson, N. G.; Entz, E. D.; Neufeldt, S. R. *J. Org. Chem.* **2022**, *87*, 7414−7421.

20. Norman, J. P.; Larson, N. G.; Neufeldt, S. R. *ACS Catal*. **2022**, *12*, 15, 8822–8828.

21. Larrosa, I.; Somoza, C.; Banquy, A.; Goldup, S. M. *Org. Lett.* **2011**, *13*, 1, 146-149. *See also: Ref 18 and 9.*

22. Newman-Stonebraker, S. H.; Smith, S. R.; Borowski, J. E.; Peters, E.; Gensch, T.; Johnson, H. C.; Sigman, M. S.; Doyle, A. G. *Science* **2021**, *374*, 301−308.

23. Bryan, Z. J.; Hall, A. O.; Zhao, C. T.; Chen, J.; McNeil, A. J. *ACS Macro Lett*. **2016**, *5*, 69–72.

24. Mikami, K.; Nojima, M.; Masumoto, Y.; Mizukoshi, Y.; Takita, R.; Yokozawa, T.; Uchiyama, M. *Polym. Chem*. **2017**, *8*, 1708– 1713, DOI: 10.1039/C6PY01934J

25. 1-*tert*-butyl-3-phenylindene was detected in the product mixture by GCMS. Formation of this byproduct by reduction of (η^3-1-^{t}Bu-indenyl)Pd(NHC)(Cl) has been reported previously: Melvin, P. R.; Balcells, D.; Hazari, N.; Nova, A. *ACS Catal*. **2015**, *5*, 5596–5606, DOI: 10.1021/acscatal.5b01291

26. Reduction of $[Pd(IPr)Cl_2]_2$ by phenylboronic acid generates biphenyl which is arguably a (weak) "throw-away" ligand in this context.

27. For the dissociation of Pd(IPr)(**62a**) → Pd(IPr) + **62a**, DFT calculations indicate the products are 20 kcal/mol higher in energy than the reactant: Larson, N. G.; Norman, J. P.; Neufeldt, S. R. (manuscript in preparation).

28. Note that unlike PdL_2, NiL_2 is well known for its ability to ring-walk, thus the mechanistic findings of this study do not apply to Ni-catalyzed processes.

Appendix A

1. Melvin, P. R.; Nova, A.; Balcells, D.; Dai, W.; Hazari, N.; Hruszkewycz, D. P.; Shah, H. P.; Tudge, M. T. *ACS Catal.* **2015**, *5*, 3680−3688.

2. Jiang, X.; Hu, F. *Synlett.* **2018**, *29*, 1207-1210.

3. Baranov, A. B.; Tsypin, V. G.; Malin, A. S.; Laskin, B. M. *Russ. J. Appl. Chem.* **2004**, *77*, 1997-2000.

4. Krasovskiy, A.; Knochel, P. *Synthesis* **2006**, 5, 0890-0891.

5. Tran, T.-A.; Shin, Y.-J.; Kramer, B.; Choi, J.; Zou, N.; Vallar, P.; Martens, P.; Boatman, P. D.; Adams, J. W.; Ramirez, J.; Shi, Y.; Morgan, M.; Unett, D. J.; Chang, S.; Shu, H.-H.; Tung, S.-F.; Semple, G. *Bioorg. Med. Chem. Lett.* **2015,** *25*, 1030–1035.

6. Habash, M.; Taha, M. O. *Bioorg. Med. Chem.* **2011**, *19*, 4746–4771.

7. Yahyazadeh, A.; Yousefi, H. *Spectrochim. Acta A Mol. Biomol. Spectrosc.* **2014**, 1*17*, 696–701.

8. Rossiter, S.; Péron J. M.; Whitfield P. J.; Jones, K.; *Bioorganic Med. Chem Lett.* **2005**, 15, 4806-4808.

9. Su, Z.; Yeagley, A. A.; Su, R.; Peng, L.; Melander, C. *ChemMedChem*. **2012**, 7, 2030-2039.

10. Dai, X.; Chen, Y.; Garrell, S.; Liu, H.; Zhang, L.-K.; Palani, A.; Hughes, G.; Nargund, R. *J. Org. Chem.* **2013**, *78*, 7758– 7763.

11. Reeves, E. K.; Humke, J. N.; Neufeldt, S. R. *J. Org. Chem.* **2019**, *84*, 11799–11812.

12. Thapa, S.; Gurung, S. K.; Dickie, D. A.; Giri, R.; *Angew. Chem. Int. Ed*. **2014**, *53*, 11620−11624.

13. Sicre, C.; Alonso-Gómez, J. L.; Cid, M. M. *Tetrahedron* **2006**, *62*, 11063-11072.

14. Crouse, G. D.; Sparks, T. C.; McLead, C. L.; Demeter, D. A.; Bryan, K.; Brown, A. V.; Dent III W. H.; Cudworth, D. P.; Nugent, J. S.; Hunter R.; Samaritoni, J. G. Pesticidal Compositions. U.S. Patent US 2009/0209476 A1, August 20, **2009**.

15. Yang, M.; Chen, J.; He, C.; Hu, X.; Ding, Y.; Kuang, Y.; Liu, J. Huang, Q. *J. Org. Chem.* **2020**, *85*, 6498–6508.

16. Minxing, X.; Feng, T.; Wei, H.; Jun, W.; Han, S.; Zhaoyu, L.; Chongxing, Tu.; Xinge, Z. Pyrimidinamine and pyridinamine Hedgehog signal conduction inhibitors. International Patent CN103864770 (A), June 18, **2014**. (paragraph 1443).

17. Duan, Jingwu; Jian, Bing; Lu, Zhonghui. Azaindoles as BTK Kinase Modulators and Use Thereof. International Patent WO 2011/019780 A1, February 17, **2011**. (pages 63-64).

18. Scott, N. W. J.; Ford, M. J.; Jeddi, N.; Eyles, A.; Simon, L.; Whitwood, A. C.; Tanner, T.; Willans, C. E.; Fairlamb, I. J. S. *J. Am. Chem. Soc.* **2021**, *143*, 9682-9693.

19. Louërat, F.; Gros, P.C. *Tetrahedron* **2010,** *51*, 3558-3560.

20. Baloch, M.; Roy, D.; Bensaid, S.; Guerchais, V.; Doucet, H. *Eur. J of Inorg. Chem.* **2012**, *28*, 4454-4462.

21. Levy, J. N.; Alegre-Requena, J. V.; Liu, R.; Paton, R. S.; McNally, A. *J. Am. Chem. Soc.* **2020**, *142*, 11295-11305.

22. Corcoran, R. C.; Bang, S. H. *Tetrahedron Lett.* **1990**, *31*, 6757-6758.

23. Gurung, S. K.; Thapa, S.; Vangala, A. S.; Giri, R. *Org. Lett.* **2013**, *15*, 20, 5378-5381.

24. Mosquera, Á.; Riveiros, R.; Sestelo, J. P.; Sarandeses, L. A. *Org. Lett.* **2008** *10*, 17, 3745-3748.

Appendix B

1. Norman, J. P.; Larson, N. G.; Entz, E. D.; Neufeldt, S. R. *J. Org. Chem.* **2022**, *87*, 7414-7421.

2. (a) Amatore, C.; Jutand, A.; M'Barki, M. A. *Organometallics* **1992**, *11*, 3009-3013; (b) Amatore, C.; Carré, E.; Jutand, A.; M'Barki, M. A. *Organometallics* **1995**, *14*, 1818-1826; (c) Wagschal, S.; Perego, L. A.; Simon, A.; Franco-Espejo, A.; Tocqueville, C.; Albaneze-Walker, J.; Jutand, A.; Grimaud, L. *Chem.-Eur. J.* **2019**, *25*, 6980-6987.

3. (a) Mitchell, E. A.; Jessop, P. G.; Baird, M. C. A. *Organometallics* **2009**, *28*, 6732-6738; (b) Barrios-Landeros, F.; Carrow, B. P.; Hartwig, J. F. *J. Am. Chem. Soc.* **2009**, *131*, 8141-8154; (c) McMullin, C. L.; Jover, J.; Harvey, J. N.; Fey, N. *Dalton Trans.* **2010**, *39*, 10833-10836.

4. Gensch, T.; dos Passos Gomes, G.; Friederich, P.; Peters, E.; Gaudin, T.; Pollice, R.; Jorner, K.; Nigam, A.; D'Addario, M. L.; Sigman, M. S.; Aspuru-Guzik, A. *J. Am. Chem. Soc.* **2022**, *144*, 1205-1217.

5. Clavier, H.; Nolan, S. P. *Chem. Commun.* **2010**, *46*, 841-861.

6. Dai, X.; Chen, Y.; Garrell, S.; Liu, H.; Zhang, L.-K.; Palani, A.; Hughes, G.; Nargund, R. *J. Org. Chem.* **2013**, *78*, 7758-7763.

7. Gao, Q.; Yan, H.; Wu, M.; Sun, J.; Yan, X.; Wu, A. *Org. Biomol. Chem.* **2018**, 16, 2342-2348.

8. Petersen, T. P.; Becker, M. R.; Knochel, P. *Angew. Chem. Int. Ed.* **2014**, *53*, 7933-7937.

9. (a) Scott, N. W. J.; Ford, M. J.; Jeddi, N.; Eyles, A.; Simon, L.; Whitwood, A. C.; Tanner, T.; Willans, C. E.; Fairlamb, I. J. S. *J. Am. Chem. Soc.* **2021**, *143*, 9682-9693. (b) Appleby, K. M.; Dzotsi, E.; Scott, N. W. J.; Dexin, G.; Jeddi, N.; Whitwood, A. C.; Pridmore, N. E.; Hart, S.; Duckett, S. B.; Fairlamb, I. J. S. *Organometallics* **2021**, *40*, 3560-3570.

10. Gaussian 16, Revision C.01, Frisch, M. J.; Trucks, G. W.; Schlegel, H. B.; Scuseria, G. E.; Robb, M. A.; Cheeseman, J. R.; Scalmani, G.; Barone, V.; Petersson, G. A.; Nakatsuji, H.; Li, X.; Caricato, M.; Marenich, A. V.; Bloino, J.; Janesko, B. G.; Gomperts, R.; Mennucci, B.; Hratchian, H. P.; Ortiz, J. V.; Izmaylov, A. F.; Sonnenberg, J. L.; Williams-Young, D.; Ding, F.; Lipparini, F.; Egidi, F.; Goings, J.; Peng, B.; Petrone, A.; Henderson, T.; Ranasinghe, D.; Zakrzewski, V. G.; Gao, J.; Rega, N.; Zheng, G.; Liang, W.; Hada, M.; Ehara, M.; Toyota, K.; Fukuda, R.; Hasegawa, J.; Ishida, M.; Nakajima, T.; Honda, Y.; Kitao, O.; Nakai, H.; Vreven, T.; Throssell, K.; Montgomery, J. A., Jr.; Peralta, J. E.; Ogliaro, F.; Bearpark, M. J.; Heyd, J. J.; Brothers, E. N.; Kudin, K. N.; Staroverov, V. N.; Keith, T. A.; Kobayashi, R.; Normand, J.; Raghavachari, K.; Rendell, A. P.; Burant, J. C.; Iyengar, S. S.; Tomasi, J.; Cossi, M.; Millam, J. M.; Klene, M.; Adamo, C.; Cammi, R.; Ochterski, J. W.; Martin, R. L.; Morokuma, K.; Farkas, O.; Foresman, J. B.; Fox, D. J. Gaussian, Inc., Wallingford CT, 2016.

11. Cossi, M.; Rega, N.; Scalmani, G.; Barone, V. *J. Comput. Chem.* **2003**, *24*, 669-681.

12. Yu, H. S.; He, X.; Truhlar, D. G. MN15-L: *J. Chem. Theory Comput.* **2016**, *12*, 1280-1293.

13. Hay, P. J.; Wadt, W. R. Ab initio effective core potentials for molecular calculations. Potentials for K to Au including the outermost core orbitals. *J. Chem. Phys.* **1985**, *82*, 299-310.

14. (a) Gonzalez, C.; Schlegel, H. B. *J. Chem. Phys.* **1989**, *90*, 2154-2161; (b) Gonzalez, C.; Schlegel, H.B. *J. Phys. Chem.* **1990**, *94*, 5523-5527; (c) Fukui, K. *Acc. Chem. Res.* **1981**, *14*, 363-368.

15. Yu, H. S.; He, X.; Li, S. L.; Truhlar, D. G. *Chem. Sci.* **2016**, *7*, 5032-5051.

16. (a) Dolg, M.; Wedig, U.; Stoll, H.; Preuss, H. *J. Chem. Phys.* **1987**, *86*, 866-872; (b) Andrae, D.; Haussermann, U.; Dolg, M.; Stoll, H. Preuss, H. *Theor. Chim. Acta* **1990**, *77*, 123-141.

17. Ribeiro, R. F.; Marenich, A. V.; Cramer, C. J.; Truhlar, D. G. *J. Phys. Chem. B.* **2011**, *115*, 14556-14562.

18. G. Luchini, J. V. Alegre- Requena, I. Funes-Ardoiz and R. S. Paton, GoodVibes: Automated Thermochemistry for Heterogeneous Computational Chemistry Data, *F1000Research*, **2020**, *9*, 291

19. CYLview20; Legault, C. Y., Université de Sherbrooke, 2020 (http://www.cylview.org)

20. (a) Avogadro: an open-source molecular builder and visualization tool. Version 1. http://avogadro.cc/ (b) Hanwell, M. D.; Curtis, D. E.; Lonie, D. C.; Vandermeersch, T.; Zurek, E.; Hutchison; G. R. *J. Cheminformatics* **2012**, *4*, 17.

21. Melvin, P. R.; Nova, A.; Balcells, D.; Dai, W.; Hazari, N.; Hruszkewycz, D. P.; Shah, H. P.; Tudge, M. T. *ACS Catal.* **2015**, *5*, 3680-3688.

22. Moltved, K. A.; Kepp, K. P. *J. Chem. Theory Comput.* **2018**, *14*, 3479-3492.

23. Elias, E. K.; Rehbein, S. M.; Neufeldt, S. R. *Chem. Sci.* **2022**, *13*, 1618-1628.

24. Joshi, C.; Macharia, J. M.; Izzo, J. A.; Wambua, V.; Kim, S.; Hirschi, J. S.; Vetticatt, M. J. *ACS Catal.* **2022**, *12*, 2959-2966.

25. Besora, M.; Maseras, F. *Dalton Trans.* **2019**, *48*, 16242-16248.

26. Lu, J.; Donnecke, S.; Paci, I.; Leitch, D. C. *Chem. Sci.* **2022**, *13*, 3477-3488.